GENERAL DYNAMICS | ASTRONAUTICS

CONTRACT AF 04(645)-4

FLIGHT SUMMARY REPORT SERIES D ATLAS MISSILES

DIVISION REPORT AE60-0131-2

PREPARED BY TEST EVALUATION GROUP

Approved by _____

W. F. MILLER, *Assistant Chief Engineer, Test*

Approved by _____

W. W. WITHEE *Vice-President, Research and Engineering*

[redacted]

UNCLASSIFIED

SECURITY NOTICE

This document contains information affecting the national defense of the United States within the meaning of the Espionage Laws, Title 18, U.S.C., Sections 793 and 794. The transmission or the revelation of its contents in any manner to an unauthorized person is prohibited by law.

UNCLASSIFIED

[redacted]

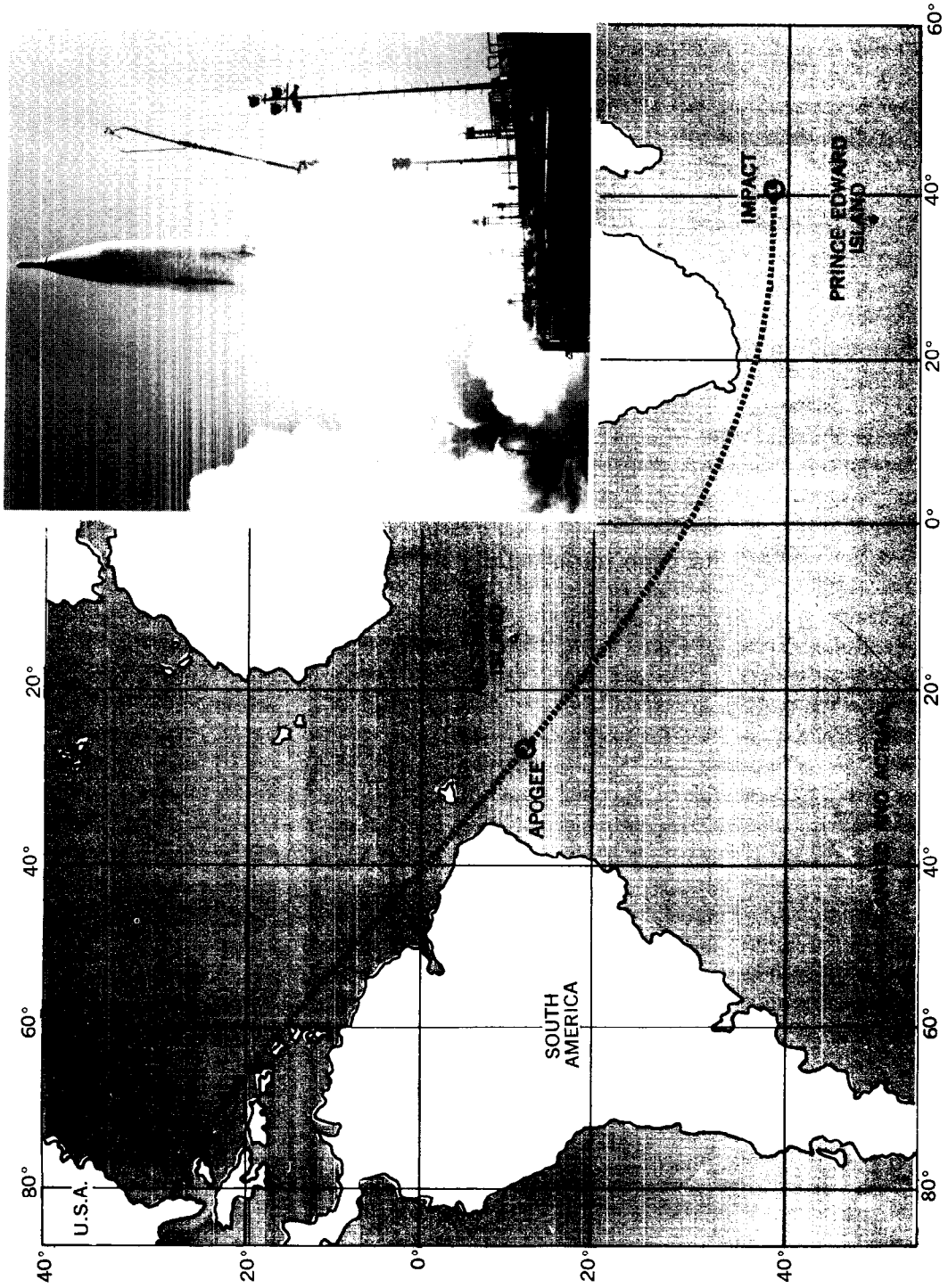

SERIES D ATLAS, 9,000 MILE CAPABILITY

This page intentionally left blank.

TABLE OF CONTENTS

This page intentionally left blank.

SECTION 1 INTRODUCTION

The purpose of this report is to present a performance analysis of the Atlas weapon system and subsystems based upon data obtained from Series D research and development (R&D) flights subsequent to the flight of Missile 51D and including the flight tests of all D/AIG missiles. The analysis includes data obtained from Series D R&D flights using radio-inertial guidance (RIG) and all-inertial guidance (AIG) systems. The last vehicle considered is Missile 90D, the last Series D R&D missile, launched on 23 January 1961. Series D/RIG R&D flights up to and including Missile 51D are reported in summary form in Report No. AE60-0131-1.

Test results from Series D data are compared with data from Series A, B and C flights, as well as from captive tests, where applicable. General trends, average values, and one standard deviation values (which are a measure of repeatability, shown on graphs as a shaded area) are presented and discussed.

Details of individual flights are available in the individual Flight Test Evaluation reports that are issued immediately after each flight. In addition, Series A flights are summarized in Report No. ZC-7-201, Series B flights are summarized in Report No. ZC-7-214 and Series C flights are summarized in Report No. ZC-7-224.

FIRST FOUR PHASES IN THE DEVELOPMENT OF THE OPERATIONAL ATLAS

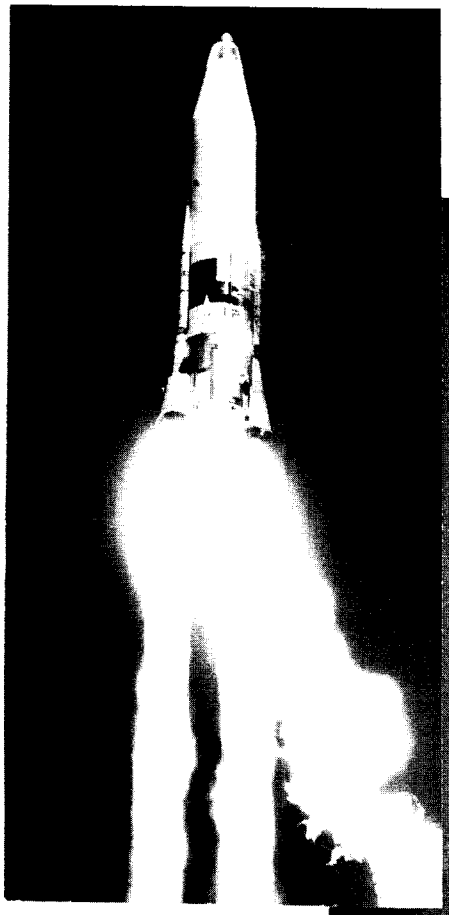

TYPICAL SERIES A
MISSILE

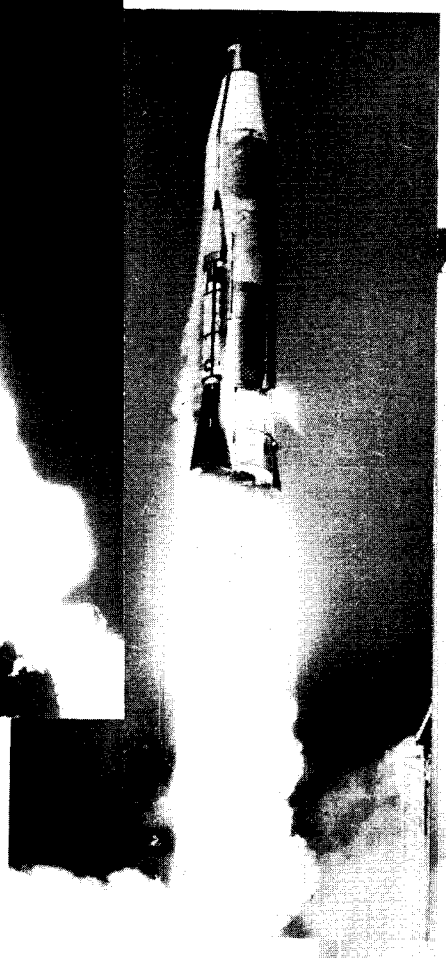

TYPICAL SERIES B
MISSILE

TYPICAL SERIES C
MISSILE

TYPICAL SERIES D
MISSILE

SECTION 2 SUMMARY

Flight testing of the Series D Atlas intercontinental ballistic missile is the fourth phase in a program of progressive flight tests of six missile groups: Series A, B, C, D, E, and F. Each succeeding group represents an improved configuration leading toward the operational version of the 107A-1 Weapon System.

The Series A missiles consisted of a minimum configuration capable of flight. The Series B missile configuration was the first to incorporate essentially all of the airborne systems planned for use on the operational version of the Atlas. A lightweight tank section having a thinner skin was incorporated on the Series C missiles in addition to missile system design improvements reflecting the results of previous tests. Major Series D design improvements include use of the MA-2 propulsion system, use of lighter weight steel in some areas of the tank section and system components, and changes in thrust section and pod configuration.

A total of 32 Series D research and development (R&D) missiles were flight tested in a continuing effort to evaluate missile configuration changes effected in the transition from the Series C configuration; to improve the performance, reliability, and simplicity of the Atlas weapon system; and to demonstrate initial operational performance capabilities. Included in the 32 Series D R&D test flights are 25 missiles which used radio-inertial guidance (RIG) and 7 missiles which had the all-inertial guidance (AIG) system installed. Series D/AIG missiles provided initial flight testing of a self-contained inertial guidance system installed on a ballistic missile and tested over full intercontinental range. Installation of an all-inertial guidance system on a ballistic missile provides salvo launch capability, guidance jamming immunity and weapon system cost reduction through elimination of ground guidance facilities, all of which are desirable for missile operational status. Major differences between Series D research and development RIG and AIG missiles are:

1. The flight attitude of the D/AIG missile is rotated 90 degrees from the attitude of the RIG missile. (i.e., the plane through the vernier engine coincides with the pitch plane.)

2. The B2 equipment pod is redesigned to accommodate the missile guidance set of the D/AIG system.

3. The D/AIG autopilot is redesigned electronically and repackaged in a square canister.

SUMMARY

4. The D/AIG Convair propellant utilization (PU) system is repackaged to the Series E configuration and uses a 400-cps PU valve position feedback transducer excitation.

5. The D/AIG Acoustica propellant utilization system is repackaged to the Series E configuration. However, the Acoustica loading control capability is retained.

The first portion of the Series D R&D test program, involving 17 test flights employing the RIG system, was summarized in Report No. AE60-0131-1, "Flight Test Summary, Atlas Series D Missiles", dated 1 July 1960. The remaining 15 missiles (42D, 48D, 56D, 54D, 62D, 27D, 60D, 32D, 66D, 76D, 79D, 71D, 55D, 83D, and 90D) of the 32 Series D R&D test flights are considered in the quantitative discussions presented in this report. Major accomplishments in the development of the Atlas weapon system during the portion of the Series D flight test program reported here were:

1. First planned and successful open-loop flight of the all-inertial guidance system on 8 March 1960. (Missile 42D)

2. First planned and successful flight of a missile over a range of 9,000 statute miles on 20 May 1960. (Missile 56D)

3. First successful closed-loop flight of the all-inertial guidance system on 11 June 1960. (Missile 54D)

4. First planned and successful flight with the Mark 3 Mod IIB ablation re-entry vehicle on 22 June 1960. (Missile 62D)

5. First planned and successful recovery of an RVX-2A re-entry vehicle carrying biospecimens and special instrumentation on 13 October 1960. (Missile 71D)

6. First planned and successful flight with the Mark 4 Mod I re-entry vehicle on 15 November 1960. (Missile 83D)

In addition, development tests of techniques to minimize the possibility of detection of the re-entry vehicle by enemy defense systems were continued. This included testing of various decoy devices to confuse enemy detection systems.

A number of modified Series D/RIG missiles successfully carried special equipment and payloads for special investigations or projects not pertaining directly to the development of the Atlas weapon system. The special assignments included:

1. The National Aeronautics and Space Administration (NASA) Project Mercury "man-in-space" capsule and associated equipment development experiments.

2. USAF lunar probe project for NASA (Atlas-Able).

3. USAF program for a satellite early warning system against ballistic missiles, using infrared detection and other techniques (Midas).

4. USAF program for a reconnaissance satellite (Samos).

5. Radiometer and ionization studies for the Air Force Cambridge Research Center (AFCRC).

6. Upper atmosphere studies for the Air Force Special Weapons Center (AFSWC).

7. Equipment development investigations for the STL Advanced Guidance System.

8. Upper atmospheric and equipment development experiments for the General Electric Missile and Space Vehicle Department.

A total of 29 Series D Atlas missiles were launched during the portion of the Series D flight test program covered by this report. Of these 29 flights, 14 were flown for the following special purposes and are not considered in the quantitative discussions presented in this report.

1. To demonstrate the initial operational capability in launches from Vandenberg Air Force Base (VAFB), Missiles 25D and 23D were launched to impact into the Wake Island splash net at a range of 3,900 nautical miles and Missiles 74D, 47D, 33D, 81D and 99D were launched to impact into the Eniwetok Lagoon target area at a range of 4,380 nautical miles. Missiles 25D and 99D satisfactorily demonstrated this capability.

2. Missiles 50D and 67D were launched from the Atlantic Missile Range (AMR) with the Project Mercury capsule aboard to allow evaluation of the Mercury capsule re-entry

SUMMARY

characteristics and behavior. Missile 67D successfully accomplished this objective. The Missile 50D flight was unsatisfactory, but the reason for failure has not been fully determined.

3. Missiles 80D and 91D were launched from AMR with an Able payload aboard to establish a lunar satellite. The Atlas portion of Missile 80D flight was satisfactory. The over-all mission was not accomplished due to a failure which occurred at separation of the Able vehicle from the Atlas. The Missile 91D flight was unsatisfactory, but the reason for the failure has not been fully determined.

4. Missile 45D was successfully launched from AMR and placed a Midas satellite into the planned orbit.

5. Missiles 57D and 70D were launched from VAFB to place a Samos satellite into orbit. The Atlas portion of both flights was satisfactory.

A tabular history of the Atlas flight test program covering all Atlas missiles flown up to the time of the preparation of this report is shown at the end of this section.

TRAJECTORY

Of the 15 Series D R&D flights discussed, seven, including three closed-loop D/AIG missiles, had assigned targets in the Ascension Island splash net area. All but one, 62D, impacted within 3.5 nautical miles of the target. Missile 62D impacted 15 to 18 nautical miles long, due to failure of the guidance vernier cutoff discrete command to effect vernier cutoff. Vernier cutoff was effected by the autopilot flight programmer vernier cutoff back-up signal approximately eight seconds after the guidance discrete command.

Two flight tests were successfully completed to targets in the South Atlantic Ocean near Capetown at a range of 6,350 nautical miles (Missiles 32D and 55D). Two tests were successfully completed to assigned targets in the Indian Ocean at a range of 7,859 nautical miles (Missiles 56D and 79D).

The initial four D/AIG flight tests of the subject group, (42D, 48D, 54D and 60D) were assigned targets in the open ocean area. Missile 42D was successfully flown over a range of 4,396 nautical miles to evaluate the AIG system in the open-loop configuration. The flight test of 48D, with the AIG system in closed-loop operation, was terminated before liftoff because of a failure in the booster propulsion system. Missile 54D successfully reached its assigned target over a range of 4,306 nautical miles and represented the first successful flight of an ICBM guided over an intercontinental range by a self-contained inertial guidance

system. Missile 60D (AIG closed-loop) impacted approximately 40 nautical miles short of its target due to an electrical short which resulted in abnormal propulsion system operation.

Two additional flight tests have been included in this report for use in trajectory performance evaluation. These were special projects using the Atlas missile as booster for an Able lunar probe (80D) and a Midas surveillance satellite (45D). The Atlas performance in both cases was satisfactory.

A circular probable error (CEP) of 1.70 nautical miles has been calculated for all Series D R&D missiles assigned to the Ascension Island splash net and which suffered no major subsystem failures.

Following is a brief summary of test results based upon analysis of all data obtained from the 15 Series D R&D missiles reported here.

AIRFRAME

Structural Integrity

The structural integrity of the Atlas missile was successfully demonstrated on the 14 flights achieved with the 15 Series D R&D missiles discussed.

The flight test of Missile 48D was terminated prior to liftoff due to a failure in the booster propulsion system which resulted in an explosion in the engine compartment and subsequent total loss of the missile. High frequency combustion instability in the B2 thrust chamber immediately after engine ignition, similar to that in the B1 thrust chamber that led to the failure of Missile 51D, was the cause of the propulsion system failure. This failure, however, does not reflect upon the structural integrity of the Atlas missile.

Engine Compartment Temperatures

On several early Series D/RIG flights, engine compartment ambient temperature data exhibited abnormal temperature increases of a random nature beginning at about 80 seconds of flight. Ambient temperatures in the engine compartment were expected to remain at a reasonable constant level during powered flight. Subsequent investigation revealed the most probable cause of these temperature increases was hot exhaust gases entering the engine compartment through openings which developed between the engines and engine boots. Aerodynamic conditions create a force on the aft surface of the missile, thereby causing the boots to move forward on the engines. This forward movement creates openings which vary in

size and orientation, thus explaining the random nature of the temperatures recorded.

A vernier hydraulic system failure, which occurred during the flight of D/AIG Missile 42D, was attributed to an abnormal engine compartment temperature environment. The Series D/AIG missiles incorporate a redesigned and enlarged B2 equipment pod to accommodate the

AIG system. A low pressure area in the vicinity of the B2 nacelle was considered responsible for the abnormal temperature increase on this missile. This low pressure area tended to evacuate the engine compartment and apparently caused a large differential pressure to exist across the boots. This created openings (similar to D/RIG missiles) and allowed entry of hot gases into the engine compartment.

To insure against the recurrence of abnormal temperature increases, the booster boots were more securely attached to the engines and, on D/AIG missiles, a shield was installed between the nacelle area and the engine compartment.

Vibration And Acoustic Studies

Landline vibration and acoustic measurements were monitored until missile liftoff to evaluate booster and sustainer engine combustion stability and the acoustic environment within the AIG pod. Generally, the AIG equipment operated satisfactorily within the launch vibration and acoustic environment.

No booster engine combustion stability problems or structural problems were apparent for the launchings of Missiles 56D through 90D. Sustainer rough combustion on Missile 32D resulted in a rough combustion cutoff prior to liftoff. The engine was subsequently replaced and the missile was satisfactorily flight tested. Generally, thrust chamber vibration was normal and displayed maximum steady-state levels between 4 and 10 g(rms). Major energy contributions were within a frequency band of 500 to 1,200 cps. High frequency vibration measurements made on the booster propellant lines showed levels ranging between 8 and 40 g(rms) at predominant frequencies between 1,000 and 1,700 cps.

The acoustic environment within the AIG pod was established for an Atlas launch from an AMR launching pad. The resulting over-all maximum sound pressure level, for a frequency band of 10 to 10,000 cps, was 143.5 decibels.

Flight vibration measurements made within the AIG pod and the Number 1 equipment pod, displayed moderate levels throughout powered flight. Generally, the maximum vibratory response was exhibited at launch and through the Mach 1 and maximum q region, as was also experienced on Atlas missiles flight tested prior to the Series D configuration.

The all-inertial guidance equipment was exposed to vibration levels ranging between 0.2 and 3 g(rms). Predominant frequency components prevailed within a band of 110 to 550 cps.

Vibration measurements made on the instrumentation beacon equipment (radial direction) in equipment pod No. 1 also exhibited maximum vibration levels through the Mach 1 - maximum q period. The resulting vibration environment was within the specified design allowable limits. The maximum level observed at the rate beacon package was 3.0 g(rms) with predominant frequency components of 250 and 500 cps. The maximum level indicated at the rate beacon waveguide was 8.8 g(rms) with predominant frequency components of 525 and 710 cps.

Exhaust Flame Study System

A radiometer package was installed on four missiles. The Air Force Cambridge Research Center (AFCRC) radiometer was installed on Missiles 27D and 32D and the Lockheed radiometer was used on Missiles 55D and 56D. In addition, the Lockheed spectrometer package was flown on Missiles 79D, 83D and 90D. These tests were conducted to provide data on the characteristics of infrared radiation emanating from engine exhaust plumes during the flight of an Atlas missile. Useful data were recovered on all seven flights. Complete test data analysis and system analysis is the responsibility of AFCRC and Lockheed/Burbank.

PROPULSION SYSTEM

Engine Performance

Propulsion system operation was generally satisfactory on thirteen of the fifteen Series D R&D flights. The two incidents of unsatisfactory performance occurred on Missiles 48D and 60D. Booster engine combustion instability ultimately led to the destruction of Missile 48D prior to liftoff. On Missile 60D, a severe deterioration in sustainer and vernier engine performance after staging was instrumental in causing the missile to impact 40 nautical miles short of the target. The 60D problem was attributed to a malfunctioning vernier engine propellant pressurization circuit.

As a result of the failure of Missile 48D, a number of changes were made in the prelaunch and countdown procedures including a holddown delay ranging from 1.50 to 4.25 seconds and use of a wet start on several missiles. No prelaunch booster propulsion system malfunction was observed after initiation of the changes.

Sustainer lox pump net positive suction head (NPSH) during the staging interval was satisfactory on all flights except 71D, in which an apparent obstruction in the main low pressure

lox duct adversely affected the sustainer lox pump inlet pressure. This condition was evident between 115.4 seconds and booster cutoff. Despite evidence of partial pump cavitation immediately after booster cutoff, sustainer engine performance was not significantly affected and the flight was successful.

The calculated thrust decay impulse (from the cutoff signal to the 10 percent thrust level) for the booster and sustainer engines averaged 179,000 and 12,600 lb-secs, respectively. These values are consistent with those calculated for earlier Series D flights.

Propellant Utilization

Open and closed-loop testing of both Convair and Acoustica propellant utilization systems was continued. However, the ability of the propellant utilization system to properly control the propellant residuals could be evaluated on only ten missiles. Test results for the Convair system were satisfactory, with all five applicable closed-loop flights being successful in achieving, at theoretical propellant depletion, a burnable excess less than the Convair design tolerance of 500 pounds. The excess at theoretical propellant depletion was outside the Acoustica design tolerance of 125 lbs on all five applicable Acoustica closed-loop flights. Only two of the five Acoustica flights were within the Convair design tolerance of 500 pounds. The average propellant excess at theoretical depletion was 247 pounds for the Convair PU system and 880 pounds for the Acoustica PU system.

Test results were satisfactory on the one Convair system open-loop flight and three of four Acoustica system open-loop flights.

Missile tanking was satisfactorily accomplished on all flight articles. The Acoustica propellant loading control monitor (PLCM) was employed as the primary tanking monitor on fourteen missiles and the Convair propellant loading control unit (PLCU) on the remaining one. Agreement among the various propellant weight monitoring devices (PLCU, PLCM, load cells, fuel totalizer) was generally excellent.

FLIGHT CONTROL

Autopilot

Operation of the autopilot was satisfactory throughout all flights, with the exception of Missiles 54D and 66D. On the latter two flights, autopilot performance was marginal.

A malfunction of the "square" type electronic flight programmer on 54D resulted in failure of the retrorockets to fire at vernier cutoff plus 17 seconds, as required. The programmer malfunction was attributed to ringing of the 28 vdc programmer filter, which subsequently caused the programmer to advance from subroutine 3 (during which time the retrorockets are fired) to subroutine 1, thus bypassing the "fire retrorockets" function. Redesign of the 28 vdc programmer filter successfully prevented recurrence of this problem on subsequent Series D/AIG flights.

On Missile 66D, excessive missile bending in the yaw plane began at 80 seconds. A peak maximum rate gyro output of 4.67 degrees/second at a frequency of 4.8 cps was reached at 112.3 seconds, and subsequently caused one of the re-entry vehicle latches to break. The initial buildup of yaw bending was attributed to the RVX-2A re-entry vehicle configuration, and the associated latch clearances. Recurrence of this problem was successfully prevented on Missiles 71D and 76D, which also flew with RVX-2A re-entry vehicles, by reducing the latch clearances, and incorporating Series E type quadratic-lead triple-lag stabilization filters in the pitch and yaw channels.

The "square" type autopilot system, flown for the first time on the Series D/AIG missiles, satisfactorily demonstrated the ability to stabilize the missile throughout powered flight, to properly execute the pitch and roll programs, to accept and respond correctly to all-inertial guidance (AIG) system steering and discrete commands, and to perform numerous preset switching functions. Data for flight control system reliability analysis were obtained for the "round" type autopilot, which was flown on all subject D/RIG missiles except 83D and 90D. Satisfactory performance of a "square" type autopilot system with a D/RIG missile was indicated on the latter two missiles.

Shorting of the retrorockets wiring during the flights of Missile 54D and 66D resulted in burnout of a flight programmer printed circuit board, and premature resetting of the programmer. The above malfunctions had no adverse effect on flight performance. In order to isolate the programmer from possible shorting of high power switching functions, current limiters will be added to all programmer high power switch outputs on all Series E operational missiles, and all Series E/R&D missiles beginning with 18E.

Radio-Inertial Guidance

The precision of the Mod III system in providing both a guidance and an instrumentation function has been capably demonstrated by the 14 Series D R&D missile flight tests. Eight of the 14 missiles utilized the Radio Command Guidance provided by the Mod III system, while the remaining 6 missiles carried the all-inertial guidance (AIG) system. The Mod III system provided range safety and instrumentation data on the AIG flights.

SUMMARY

The operation of the track subsystem was satisfactory. All missiles launched were tracked off the pad in the monopulse mode and in general, the tracker remained in this mode throughout all phases of flight until well after vernier engine cutoff, with final loss of lock attributable to below specification signal level (due to missile attitude) or to reaching the range limit of the tracker. Received signal levels were as expected, with adequate surplus at all points on the trajectory.

The operation of the rate subsystem was satisfactory. Performance was, in general, similar to that occurring on previous RIG flights; i.e., a noisy interval with periods of unlock through booster cutoff and staging, followed by solid lock and good data to termination of tracking. Signal levels as in the case of the track subsystem were adequate, with signal surplus.

Impact Predictor

The downrange impact prediction system, located at San Salvador, provided satisfactory instantaneous impact prediction for range safety purposes on all eight vehicles on which it was installed. Although minor discrepancies were noted on several flights the system provided the necessary data for real-time impact prediction through vernier cutoff. There was no indication of any relationship between the discrepancies noted on the various flights. Modifications made as a result of problems noted on earlier flights accomplished their purpose of making the system more reliable.

All-Inertial Guidance

Flight testing of the Series D/AIG missiles marked the first time that the Atlas missiles were guided over full intercontinental range by a self-contained inertial guidance system (IGS).

A total of six D/AIG missiles were successfully launched from the Atlantic Missile Range (AMR) during the period covered by this report; a seventh (48D) developed a malfunction which caused its destruction on the launch pad. All D/AIG guidance test objectives for the program were achieved and virtually complete data were obtained on all flights.

Performance of the all-inertial guidance system was satisfactory on all flights except Missile 60D. IGS performance on 60D was considered marginal because of a computer malfunction.

SUPPORTING SYSTEMS

Hydraulic

Hydraulic system performance was satisfactory in all but one of the fifteen Series D R&D flight tests.

Lack of hydraulic pressure after sustainer cutoff during the flight of Missile 42D resulted in the loss of missile attitude control during the vernier solo phase. Hydraulic system performance was satisfactory prior to this time. At 97.2 seconds of flight an unusual pressure transient appeared in the sustainer/vernier hydraulic system. This transient was simulated on a static test vehicle by abruptly venting a pneumatic charge line leading to the accumulator. Consequently, it appears as though the pneumatic charge line to the vernier solo accumulator, on Missile 42D, had ruptured at 97.2 seconds of flight, resulting in loss of GN_2 pressure and subsequent malfunctioning of the accumulator.

Beginning at 80 seconds, engine compartment temperature data indicated an abnormal increase to approximately 400°F at the time of the pressure transient. Thus, it appears that the failure of the GN_2 charge line is partially attributed to an excessively high temperature environment in the engine compartment.

Booster hydraulic pressures were adequate, maintaining an average of 3,090 psig over 14 long duration flights. No problems were experienced in booster system operation. An indicated ground supply pressure of 2,860 psig on Missile 71D was considered erroneous. The normal setting of 2,000 psig on the hydraulic pumping unit was substantiated by switch activations, confirming that, prior to booster start, hydraulic pressure had been less than 2,500 psig.

Sustainer hydraulic pressures were adequate on all flights, averaging 3,070 psig.

With the exception noted above, adequate vernier solo hydraulic pressure (680 psig and above) was provided for periods ranging from 17.4 to 42.6 seconds after sustainer cutoff. The vernier solo accumulator system is planned for use on all future vehicles. Some vehicles will have accumulator installations with a volume of 50 cubic-inches, as contrasted to the 25 cubic-inch accumulator generally used.

Pneumatic

Steady-state lox and fuel tank pressures were maintained at an average 24.6 and 59.1 psig, respectively, during booster stage operation; well within the nominal design range of 23.4 to 26 and 55 to 60 psig, respectively. During the interval between booster staging and sustainer

cutoff, an average pressure drop of only 2.0 psig in the lox tank and 10.9 psi in the fuel tank was indicated.

During the booster phase of the Missile 60D flight, difficulties with the missileborne electrical system caused repeated pressurization and venting of the vernier engine tanks, resulting in depletion of the controls bottle helium supply and subsequent abnormal operation of both the sustainer and vernier engines. This was not considered to reflect on the adequacy of the pneumatic system.

Controls helium bottle pressure on Missile 42D exhibited an abnormal decay after vernier engine tanks repressurization and again after vernier cutoff. This anomaly had no detrimental effect and all control functions were performed properly. Subsequent analysis of the data indicated a leak had developed downstream of the ISS regulator in the area of the vernier engine tanks.

Booster separation bottle pressure exhibited an abnormal pressure drop, between liftoff and staging, of 545 psid and 910 psid on Missiles 56D and 90D, respectively. During the same interval, bottle pressure drops averaging 198 psid were indicated on the twelve remaining long duration flights. The minimum pneumatic pressure required to actuate the separation fittings is approximately 1,200 psig. This specification was not exceeded in either case and the booster separation function was properly effected. Analysis of the data indicated that the high decay rates were caused by a leak which existed in the separation system or in the booster portion of the controls system.

The integrated start system (ISS) pneumatic regulator did not perform as expected after vernier engine tanks repressurization on six flights. (Missiles 56D, 62D, 32D, 66D, 79D, and 83D.) Regulator discharge pressure failed to return to the proper level after the normal overpressurization transient and exhibited a gradual increase to a pressure of approximately 700 psig. The pressure remained at this level until sustainer cutoff when it abruptly returned to its nominal level of 600 psig. There were no apparent detrimental effects. This anomaly is assumed to be either the result of a piston O-ring modification incorporated in the regulator by Rocketdyne or a malfunctioning of the vernier solo oxidizer tank helium check valve in the ISS manifold. The new O-ring, having tighter dimensions and tolerances, could bind against the cylinder wall causing the piston to stick and to move erratically, thereby causing the pressure buildup condition. A malfunctioning check valve could permit vernier lox tank pressure (approximately 670 psig) to be reflected at the discharge side of the ISS pneumatic regulator. At the time of this writing, neither possibility can be firmly established as the cause of this anomaly. Investigation of this problem is being continued.

Hadley Series D main propellant tank pneumatic regulators, used on all missiles discussed in this report, exhibited good stability under conditions of heaviest demand; i.e., at main engines start. Maximum and minimum pressures during the main engine start transient

averaged, respectively, 26.1 and 23.8 psig in the lox tank and 61.0 and 58.2 psig in the fuel tank. No other pressure transients of any significance were noted during flight.

Electrical

Electrical system performance was satisfactory on all flight test vehicles with the exception of Missiles 62D and 60D. On these two flights, electrical system anomalies adversely affected missile systems performance. The main missile battery and the rotary inverter provided 400-cycle frequency, phase A voltage and missile systems d-c input at average values of 400 cps, 114.6 vac and 27.4 vdc, respectively.

On Missile 60D, an intermittent short circuit, possibly in or near engine relay box plug J-13 caused repeated activation of the pressurize vernier tanks (PVT) relay (K32C) during the booster phase of flight. The subsequent premature depletion of helium supply to the vernier engine propellant tanks adversely affected propulsion system operation and missile impact accuracy. Electrical circuitry was reoriented on subsequent missiles such that the pressurize vernier tanks sequence was initiated by the booster cutoff discrete. Previously the PVT sequence was a separate programmer function. No recurrence of this problem has been observed on flights subsequent to Missile 60D.

Missile guidance on 62D was adversely affected by an apparent open circuit in the electrical harness between the guidance decoder output and the input to the flight programmer. This resulted in failure of the vernier cutoff discrete, generated by the ground guidance computer at 299.7 seconds, to initiate vernier cutoff (VCO). The verniers were eventually cut off by the flight programmer at 307.7 seconds. Following the flight, an analysis of preflight checkout data revealed that there was no continuity through this circuit at any time prior to launch.

The Leland rotary inverter, developed as a backup item for the similar Bendix inverter was successfully flight tested during this period. Electrical outputs of the Leland units were particularly stable and relatively free of the power fluctuations usually noted as a result of acceleration and load changes at major event times; i.e., booster cutoff, sustainer cutoff, vernier cutoff and retrorockets firing.

Azusa

Azusa tracking was confined primarily to the Mark I system during this portion of the Atlas Series D test program. However, two missiles (83D and 90D) were tracked with the new Azusa Mark II system. Comparisons between the Mark II tracking data of 90D and the Mark I tracking data of 54D clearly indicate the expected improvement in data quality obtained with the Mark II system.

SUMMARY

The operation of the Azusa system as a real-time impact predictor was satisfactory. Two criteria are used to determine if satisfactory operation has been accomplished: (1) maintenance of radio frequency lock throughout powered flight, and (2) maintenance of nonambiguous tracking during at least part of the free-fall period. Of the 14 subject Series D flights, the Azusa system completely satisfied range safety requirements on ten. These were: 42D, 56D, 54D, 60D, 66D, 76D, 79D, 71D, 55D, and 83D. Of the remaining four flights, the Azusa system partially met range safety requirements on 62D and failed to meet range safety requirements on 27D, 32D and 90D.

Two antennas were flown during the subject test program; the elliptical horn and the tilted beam. The tilted beam antenna was used on Missiles 83D and 90D, and the elliptical horn was used on the remainder of the flights. The elliptical horn has the advantage of a higher gain. However, the pattern of the antenna is such as to yield lobing effects on the data during the early portion of a flight (0 to 60 seconds). Lobes are inherent to antennas of this type due to interference from reflected energy, and cause phase disturbances in the received radiated data. The tilted beam antenna was designed to produce a broader beamwidth and to tilt the radiation away from the booster fairing, thus reducing reflection. Lobing effects on the data have been reduced to a period of 30 seconds by using the tilted beam antenna; however, the antenna has the disadvantage of a lower gain. Both antennas have demonstrated the ability to satisfy the range safety requirements for the Azusa system.

Range Safety Command

The performance of the range safety command (RSC) system was satisfactory for all missiles discussed in this report. All commands sent to the missile were properly received and decoded. The resulting cutoff signals were properly generated in the missile circuitry. During all flights, except for the five of the AIG configuration, range safety signals were sent for either test or backup purposes only. During the D/AIG flights of Missiles 66D, 76D and 71D, the automatic sustainer fuel cutoff signal, sent from Cape Canaveral, slightly preceded the AIG sustainer cutoff signal by 0.12, 0.004 and 0.015 seconds, respectively. These results indicate a slight, but not serious, difference between the AIG and RIG computers. Ordinarily, the automatic sustainer fuel cutoff (ASFCO) signal lags the corresponding guidance signal by approximately 0.18 seconds. For Missile 42D the ASFCO signal was used to cut off the sustainer engine, since the AIG system was operating in open-loop configuration. For Missile 60D, the ASFCO signal effected an early sustainer cutoff because of abnormally low missile velocity and velocity limiting features of the RIG computer.

Launcher

Operation of the launcher system was satisfactory for all fifteen missiles discussed in this report. One missile, 48D, was destroyed prior to liftoff due to a propulsion system failure; however, the operation of the launcher system was satisfactory during the incident. Complete data was obtained during ten of the fourteen actual launches to verify the satisfactory performance of the launcher holddown cylinders.

The only significant problem indicated was the magnitude of the holddown cylinder residual pressures, which were marginal on the high side during five launches. While this condition did not cause any malfunctions, reduction in the residual pressures and the resulting load on the engine nacelles was desirable for safety reasons. A new release valve, known as the Benbow valve, was installed for Missiles 83D and 90D to accomplish this objective. Test data shows that the installation of the new release valve produced the desired result. Residual pressures were reduced by a factor of four during the launchings of Missiles 83D and 90D, where the new valve was used.

Film coverage of all launches showed satisfactory operation of the launcher system.

Facility and Site

Compatibility of missile systems and ground facilities was demonstrated for all Series D R&D missiles.

Instrumentation

For the 15 missiles discussed in this report, 2,172 measurements were instrumented for telemetry. Fifty-nine measurements did not yield satisfactory data for a percentage recovery of 97.3 percent. Vibration type instrumentation yielded the least reliable recovery with a percentage failure of 21.1 percent, based upon the number of measurements of that type attempted.

Landline system operation was satisfactory with 48 unsatisfactory measurements resulting from the 2,814 measurements attempted. Percentage recovery was 98.3 percent. Vibration instrumentation yielded the least reliable recovery with a percentage failure of 17.6 percent based upon the number of measurements of that type attempted.

SUMMARY

PAYLOAD

Re-Entry Vehicle

Twelve of the fifteen re-entry vehicles carried by the Series D missiles, included in this report, were equipped with warhead instrumentation in order to verify the proper occurrence of arming and fuzing functions. These re-entry vehicles, eleven Mk 3 and one Mk 4, were capable of delivering a nuclear warhead to an assigned target. Ten of the eleven Mk 3 re-entry vehicles satisfied their planned flight mission. Only one, the re-entry vehicle installed on Missile 48D, was prevented from accomplishing its objective due to an explosion that destroyed the missile prior to liftoff.

The Mk 4 Mod 1 re-entry vehicle flown by Missile 83D successfully ejected its data cassette, which was recovered shortly after impact.

Three RVX-2A vehicles, extensively instrumented, were flown by Missiles 66D, 67D and 71D. Of these three vehicles, which carried a series of environmental experiments and recovery subsystems, only one (flown on Missile 71D) was recovered. The testing of RVX-2A vehicles permitted obtaining valuable data for further refinement of present designs and materials particularly through the successful recovery and postflight analysis of the R/V carried by 71D.

Separation was satisfactory on 13 flights. Failure of the inflight disconnect to eject properly on the R/V aboard Missile 76D restrained and imparted abnormal motions to the vehicle. Performance was otherwise satisfactory. Missile 90D carried a Mk 3 Mod 1B re-entry vehicle equipped with special flashing beacons on its aft face for the purpose of obtaining optical terminal tracking data. No General Electric data on this R/V was available at the time of the preparation of this report.

Decoy

The decoy system was installed on four flight test articles. Missiles 55D, 62D and 83D carried the 4-tube R&D pod and 90D carried the single tube Mod 1 pod. System operation was satisfactory on Missiles 55D and 83D although telemetry was lost on the latter. Arming and timing functions were properly generated on Missiles 62D and 90D but apparent malfunctions in the tube latching mechanism caused failure to eject decoys from two of the four tubes on 62D and from the single tube on 90D.

Abort Sensing and Implementation System

Components proposed for the Project Mercury abort sensing and implementation system (ASIS) were installed and tested on five Series D R&D Atlas missiles (56D, 62D, 32D, 79D and 55D). During a Mercury flight, the ASIS is designed to monitor selected critical parameters in five missile subsystems of the Mercury/Atlas booster, sense the development of any possible catastrophic failure and, if conditions warrant, generate an "Abort Command" such that Mercury capsule escape can be effected prior to the development of a condition which would be hazardous to the capsule occupant. The components consist of rate gyros for monitoring pitch, yaw and roll rates, sensors for monitoring critical pressures in the performance of the tank pressurization system, propulsion system and hydraulic system, and sensors for monitoring the electrical system 115-volt, 400-cycle supply voltage and Atlas/capsule interface continuity.

Operation of the ASIS components was satisfactory during the flights of two of the five aforementioned Series D R&D missiles. Abort parameters were not exceeded and with few exceptions, no abort conditions were indicated by ASIS sensors during powered flight.

During the flight of Missile 56D, the first missile flown with ASIS components aboard, erroneous abort conditions were indicated by 3 of the 7 pressure sensors installed. The two lox tank pressure monitor switches (prestaging and post-staging) both indicated an abort condition. This was attributed to inadvertent capping of the atmospheric pressure sensing ports on these transducers which effectively introduces a transducer bias and results in switch activation (abort indication) at pressures higher than the normal setting. The sustainer hydraulic switch also indicated an abort condition. This was attributed to freezing of the hydraulic oil in the sensing line due to the close proximity of this sensing line to the sustainer gas generator lox line; a configuration peculiar to Missile 56D. Under a normal Mercury configuration this problem would not occur since the sensing line to the pressure switch is routed differently.

During the flights of Missiles 62D and 79D, the switches which monitor the intermediate bulkhead differential pressure indicated erroneous abort conditions. This condition was resolved to be the result of a momentary pressure surge resulting from lox being forced into the sensing line at liftoff and flashing into vapor as a result of contact with the relatively warmer sensing line. A modification has been satisfactorily accomplished on Atlas/Mercury missiles to eliminate these spurious abort signals as evidenced by satisfactory performance of ASIS on Atlas/Mercury Missiles 50D and 67D flown during the test period discussed in this report.

Countdown

A planned 150-minute countdown procedure was used on 14 of the 15 missiles discussed. Missile 48D, the one exception had a planned 180-minute countdown. Of the 15 flight countdowns conducted, three were performed without holds. The total hold and recycle time required to complete the countdowns as planned was 1778 minutes. There were 17 flight countdowns aborted prior to launch.

FLIGHT TEST OBJECTIVES FOR ATLAS SERIES D RESEARCH AND DEVELOPMENT MISSILES

KEY:
RED — FIRST PRIORITY (MANDATORY)
BLUE — SECOND PRIORITY (REQUIRED)
GREEN — THIRD PRIORITY (DESIRED)

● ACCOMPLISHED
O PARTIALLY ACCOMPLISHED
▲ NOT ACCOMPLISHED

	OBJECTIVE	MISSILE (IN CHRONOLOGICAL FIRING ORDER) 42D	48D	56D	54D	62D	27D	60D	32D	66D	76D	79D	71D	55D	83D	90D
	TRAJECTORY															
OD18	Evaluate missile system accuracy in terms of impact error, separating the effects of guidance and non-guidance errors.		▲		●			O								
OD19	Evaluate missile guidance gross accuracy in terms of CEP, separating the effects of guidance and non-guidance errors.									ABA	ABA					
OD20	Obtain data for statistical determination of CEP.					▲	●								●	●
OD21	Demonstrate weapon system performance at a range approaching the maximum.			●								●				
	AIRFRAME															
	Aerodynamic Heating															
AD77	Obtain aerodynamic heating data on the forward portion of the Mark 3 adapter.														●	
	Engine Compartment Temperature															
MD42	Obtain data on the engine compartment temperature environment.	●	O		●			●	●	●	●	●	●	●	●	●
	Structural Integrity															
MD45	Obtain data to measure deflections of the AIG pod cover in flight.		▲		●											
AD13	Demonstrate the structural integrity of the airframe.	●	O													
AD78	Obtain data to analyze the 5 cps longitudinal oscillations that develop during the first 20 seconds of flight.			●										●		
AD80	Obtain data to determine the feasibility of removing the insulation bulkhead.													●		
	Booster Separation															
AD19	Demonstrate the performance of the booster jettison system.	●	▲		●			●								
	AFCRC Radiometer Package															
OD16	Determine radiation spectrum of the propulsion system exhaust plume.															
	Advanced Guidance System															
MD53	Evaluate the components of the advanced guidance system.															
	PROPULSION SYSTEM															
	Engine Performance															
PD30	Determine the performance of the propulsion system.	●	O		●			O								
PD57	Determine the effects of dry starts on propulsion system performance.		●													
PD69	Determine NPSH at the inlet of the liquid oxygen pump during and immediately after staging.					●	●									
PD71	Obtain data for propulsion system reliability analysis.			●		●	●		●			●		●		
PD75	Obtain data on propulsion system operating parameters.									●			●			
PD78	Obtain data for booster propulsion system stability analysis from ignition start to missile 2-inch motion.			●	●	●	●	●	●	●	●	●	●	●	●	●
	Propellant Utilization Convair Manometer PU System															
UD16	Determine closed-loop performance of the Convair propellant utilization system.	O	▲													
UD18	Obtain open-loop data on the Convair PU system.						●									●
	Acoustica PU System															
UD17	Determine closed-loop performance of the Acoustica propellant utilization system.				●		●	O			●		O		●	
UD19	Determine open-loop performance of the Acoustica propellant utilization system.								●							●

FLIGHT TEST OBJECTIVES FOR ATLAS SERIES D RESEARCH AND DEVELOPMENT MISSILES (Continued)

	OBJECTIVE	(MISSILE (IN CHRONOLOGICAL FIRING ORDER) 42D	48D	56D	54D	62D	27D	60D	32D	66D	76D	79D	71D	55D	83D	90D
	General															
UD34	Obtain data for propellant utilization system reliability analysis.			●		●				●		◍		●		
	Propellant Loading															
WD02	Determine the ability of the Convair propellant loading system to provide propellant level indications for accurate loading control.	◉	◉							◍			◍			
WD03	Determine the ability of the Acoustica propellant loading system to provide propellant level indications for accurate loading control.			●	●	●	●	●	●			●		●	●	●
	FLIGHT CONTROL															
	Autopilot															
SD18	Evaluate the ability to properly execute pitch and roll programs. (D AIG missiles)	●	▲		●			●								
SD20	Evaluate the ability to accept and properly execute D/AIG guidance steering commands. (Roll correction only for 42D.)	●	▲		●			○								
SD23	Evaluate the ability to accept and execute D/AIG guidance discrete commands and associated subroutines.		▲		○			○								
SD26	Evaluate the ability to maintain attitude stability throughout powered flight (D/AIG missiles.)	○	▲		●			○								
SD38	Evaluate the ability to accept and execute commands and associated subroutines.	●														
SD43	Obtain data for flight control system reliability analysis.			●		●	◍		◍			◍		●		
SD48	Evaluate the performance and reliability of the autopilot system on the D series AIG configuration missile.									●	●		●			
SD49	Determine performance of the square autopilot.														●	●
SD51	Obtain data to determine the effectiveness of the isolation diodes between the square autopilot programmer and the engine relay box.									◍	◍		◍			
MD44	Obtain data on missile bending effects on the autopilot rate gyro as may be caused by the AIG hardware.	●	▲		●											
	Radio Guidance - GE															
GD16	Determine the effects of antenna radiation characteristics and radar look-angles on system operation.			GE DSD		GE DSD	GE DSD		GE DSD			GE DSD		GE DSD		
GD19	Evaluate the performance and operation of the Mod III-E instrumentation and tracking system.	GE DSD	GE DSD		GE DSD			GE DSD		GE DSD	GE DSD		GE DSD			
GD27	Determine the performance of angle memory and range memory circuitry under varied conditions of acceleration and tracking rate.			GE DSD										GE DSD		
GD31	Obtain data for radio guidance system reliability analysis.			GE DSD		GE DSD								GE DSD		
GD35	Determine guidance system performance using operational guidance equations.					GE DSD	GE DSD		GE DSD					GE DSD		
GD11	Evaluate radio tracking accuracy in terms of impact dispersion separating the effects of guidance and non-guidance errors.					GE DSD	GE DSD		GE DSD					GE DSD		
	ARMA INERTIAL GUIDANCE															
	AIG Test Objectives															
ID01	Determine performance of MGS in generation of proper guidance signals during flight.	ABA	ABA		ABA			ABA								
ID03	Demonstrate MGS compatibility with all associated airborne systems.	ABA	ABA		ABA			ABA								
ID06	Demonstrate compatibility of IGS with the entire weapons system under test conditions at AMR launch complexes.	ABA	ABA		ABA			ABA								
ID08	Evaluate the ability of the MGS computer to accurately compute missile position and velocity during flight.	ABA	ABA		ABA			ABA								
ID10	Evaluate accuracy of preflight accelerometer calibration and platform leveling performed by ACS (Lot II and Lot III). (Alignment-Countdown Set.)	ABA	ABA		ABA			ABA								
ID11	Evaluate accuracy of optical alignment.	ABA	ABA		ABA			ABA								
ID12	Evaluate accuracy of prism servo system.	ABA	ABA		ABA			ABA								
ID13	Obtain data on the flight environment of MGS components.	ABA	ABA		ABA											
ID14	Obtain data on operation of computer redundancy feature during flight.	ABA	ABA		ABA			ABA								
ID16	Obtain data regarding reliability of the MGS platform, computer and control.	ABA	ABA		ABA			ABA								

FLIGHT TEST OBJECTIVES FOR ATLAS SERIES D RESEARCH AND DEVELOPMENT MISSILES (Continued)

	OBJECTIVE	MISSILE (IN CHRONOLOGICAL FIRING ORDER) 42D	48D	56D	54D	62D	27D	60D	32D	66D	76D	79D	71D	55D	83D	90D
ID17	Evaluate MGS performance in generating roll correction and pitch steering signals to the autopilot during flight.	ABA	ABA		ABA			ABA								
ID18	Determine error components attributable to platform, computer, and A-CS in terms of target miss, utilizing best available range instrumentation.	ABA	ABA		ABA			ABA								
ID19	Evaluate computer ability to compute reference and accuracy in generating the necessary discrete commands to the autopilot during flight.	ABA	ABA		ABA			ABA								
ID20	Evaluate MGS computer performance in generating warhead prearm during flight (including OFS circuitry).	ABA	ABA		ABA			ABA								
	Cross-Range Error Function															
ID21	Evaluate MGS computer ability to compute CEF and accuracy in generating yaw steering signals to the autopilot during flight.	ABA	ABA		ABA			ABA								
ID22	Evaluate accelerometer performance and sum frequency stability during flight.	ABA	ABA		ABA			ABA								
ID23	Evaluate MGS gyro and platform servo performance during flight.	ABA	ABA		ABA			ABA								
	Analog Signal Converter															
ID24	Evaluate compatibility of ASC with airborne and ground equipment associated with transmitting, receiving, and recording telemetry data during flight.	ABA	ABA		ABA			ABA								
	Digital Signal Converter															
ID25	Evaluate compatibility of DSC with airborne and ground equipment associated with transmitting, receiving, and recording telemetry data during flight.	ABA	ABA		ABA			ABA								
ID26	Evaluate the performance of the AIG system.									ABA	ABA		ABA			
ID27	Obtain data to ascertain the effect of preflight and flight environment on the AIG system.				ABA			ABA		ABA						
ID28	Evaluate the AIG system compatibility with all associated missile subsystems.									ABA						
	SUPPORTING SYSTEMS															
	Hydraulic System															
HD47	Demonstrate performance of the hydraulic system.															
HD55	Obtain data for hydraulic system reliability analysis.			●		●				●			●	●		
HD60	Demonstrate performance of the vernier solo hydraulic accumulator.	▲														
HD61	Obtain data on the temperature environment of the airborne hydraulic rise-off valve.															
	Pneumatic System															
FD27	Demonstrate performance of the pneumatic pressurization system.															
FD47	Determine pressure history of booster jettison supply bottle during booster stage operation and initiation of booster separation.	●	▲													
FD59	Demonstrate performance of the controls pneumatic system.	●	○		●			○								
FD64	Obtain data for pneumatic system reliability analysis.			●		●				●			●	●		
FD70	Evaluate the performance of the Convair propellant tank pressurization regulators.			●												
FD71	Evaluate the performance of the F and G propellant tank pressure regulators.															
FD73	Determine the effect of removal of the insulation bulkhead on lox boiloff, tank pressure decays and helium requirements.													●		
	Electrical System															
ED13	Determine the performance of the battery-inverter electrical power supply. (Remotely activated battery.)	●	○		●											
ED24	Obtain data for electrical system reliability analysis.			●		●				●			●	●		
ED26	Determine characteristics of the 28vdc at the autopilot programmer input from vernier cutoff on.									●	●		●			
	Range Safety and Tracking Systems															
	Azusa															
DD11	Determine the accuracy of the Azusa tracking and impact predictor system.									●			●			
ZD04	Obtain data on Azusa Mark II performance.														●	●

FLIGHT TEST OBJECTIVES FOR ATLAS SERIES D RESEARCH AND DEVELOPMENT MISSILES (Continued)

	OBJECTIVE	MISSILE (IN CHRONOLOGICAL FIRING ORDER) 42D	48D	56D	54D	62D	27D	60D	32D	66D	76D	79D	71D	55D	83D	90D
	Range Safety Command															
DD17	Determine the capability of the range safety command system to fulfill range safety requirements.	●	▲													
	Strobe Light Beacon System															
DD22	Determine the performance of the strobe light/ ballistic camera tracking system.				▲	o	o	▲						●	●	o
DD24	Determine strobe light beacon system performance.		▲													
	Launcher															
LD21	Obtain data on the performance of the Benbow release valves during operations.														●	
	Facility and Site															
MD15	Demonstrate compatibility of the MD21 blockhouse and launch control equipment.	●	●		●									●		
	Procedures															
MD20	Establish checkout of pre-launch and launch procedures. (AIG missiles.)	●	●		●											
	Instrumentation															
TD12	Demonstrate the performance of the telemetry system.(AIG missiles.)	●	o		●			●		●			●			
	PAYLOAD															
	Re-Entry Vehicle (GE Mark 3)															
YD70	Demonstrate the performance of the Mark 3 re-entry vehicle.	GE MSVD	GE MSVD		GE MSVD		GE MSVD	GE MSVD								
YD78	Evaluate the internal environment with respect to its effect on the warhead.			GE MSVD								GE MSVD		GE MSVD		
YD79	Evaluate the performance of the heat protection subsystem.			GE MSVD								GE MSVD		GE MSVD		
YD80	Evaluate the performance of the re-entry vehicle and each of its subsystems.			GE MSVD					GE MSVD			GE MSVD		GE MSVD		GE MSVD
	Warhead															
YD77	Evaluate the arming, fuzing, and warhead firing subsystems with particular emphasis on the fuzing altitude.			GE MSVD		GE MSVD						GE MSVD		GE MSVD		
	Re-entry Vehicle (GE RVX - 2A)															
YD90	Demonstrate the performance of the GE RVX-2A re-entry vehicle.									GE MSVD	GE MSVD		GE MSVD			
	Re-entry Vehicle (AVCO Mark 4 Mod I)															
YD97	Evaluate the performance of the AVCO Mark 4 Mod I re-entry vehicle.														AVCO	
	Special Experiments															
YD03	Obtain data on the special experiments carried in the re-entry vehicle.															
	Decoy System															
YD68	Demonstrate the performance of the ADF penetration system. (Research tube.)															ADF
YD88	Demonstrate the performance of the ADF penetration system. (Four-tube pod.)					ADF								ADF	ADF	
	MISCELLANEOUS															
MD27	Obtain data on the concentration of free electrons at altitudes above one million feet. (AFSWC pkg).			LMSD		LMSD										
MD28	Evaluate the performance of the Mercury abort sensing and implementation system when operating open-loop.					●			●			●				
MD49	Evaluate the performance of the components of the Mercury program abort sensing and implementation system.			●										●		
MD22	Obtain data on Atlas Systems for gross system performance and reliability analysis.										●		●		●	●
MD46	Determine the axial acceleration of the AIG missile.	●	▲		●			o		●			●			

KEY: OBJECTIVE RESPONSIBILITY

ABA	AMERICAN BOSCH ARMA CORPORATION
AFCRC	AIR FORCE CAMBRIDGE RESEARCH CENTER
STL	SPACE TECHNOLOGY LABS
GE DSD	GENERAL ELECTRIC DEFENSE SYSTEMS DEPARTMENT
GE MSVD	GENERAL ELECTRIC MISSILE AND SPACE VEHICLE DIVISION
ADF	AERONUTRONICS DIVISION OF FORD
AVCO	AVCO INDUSTRIAL
LMSD	LOCKHEED MISSILE AND SPACE DIVISION

HISTORY OF ATLAS FLIGHT TESTS

MISSILE	ERECTION PAD	ERECTION DATE	TEST DATES FRF	TEST DATES LAUNCH	FLIGHT COUNTDOWN TIME (MINUTES) NOMINAL	FLIGHT COUNTDOWN TIME (MINUTES) ACTUAL	HOLD & RECYCLE TIME (MINUTES)	COMMENTS ON FLIGHT PERFORMANCE
4A	14	3/22/57	5/28/57*					Range safety command destruct at 50.72 seconds. Propulsion failure at 24.7 seconds due to engine compartment heating and 17.5 cps missile bending.
			6/3/57	6/7/57*				
				6/11/57	390	667	277	
6A	14	8/2/57	9/18/57*					Range safety command destruct at 63 seconds. Propulsion failure at 32.7 seconds due to engine compartment heating and 17.5 cps missile bending.
			9/20/57	9/25/57	390	686	296	
12A	14	11/20/57	12/11/57	12/17/57	400	679	279	Full duration booster phase achieved as planned. Booster cutoff occurred after approximately 127 seconds of powered flight.
10A	12	9/27/57(1)						First Atlas flight tested with vernier engines installed. Full duration booster phase achieved as planned. Propulsion system cutoff occurred after approximately 127 seconds of powered flight.
		10/27/57(2)	11/25/57*					
			11/27/57*					
		12/3/57	12/10/57*	12/16/57*				
			1/4/58	1/7/58*				
				1/10/58	400	417	17	
13A	14	1/17/58	1/31/58	2/7/58	400	676	276	First Atlas flight tested with gimbaling vernier engines installed. Flight terminated prematurely at 118 seconds due to vernier feedback transducer being shorted by aerodynamic heating.
11A	12	1/25/58	2/8/58	2/15/58*				Flight terminated prematurely at 125 seconds due to vernier feedback transducer being shorted by aerodynamic heating.
				2/20/58	400	445	45	
15A	14	2/26/58	3/17/58*					Flight terminated prematurely at 105 seconds due to failure of the B1 turbopump.
			3/18/58*					
			3/22/58	3/28/58*				
				4/1/58*				
				4/5/58	215	215	0	
16A	12	3/17/58	4/18/58*					Full duration booster phase achieved as planned. Propulsion system cutoff occurred after approximately 127 seconds of powered flight.
			5/22/58*	5/29/58*				
				6/3/58	215	483	268	
3B	11	4/29/58	6/18/58*					First Atlas flight tested with booster, sustainer and vernier engines installed. Flight terminated prematurely at 41 seconds due to malfunction of yaw rate gyro.
			6/23/58*					
			6/27/58*					
			7/8/58	7/12/58*				
				7/15/58*				
				7/18/58*				
				7/19/58	180	216	36	
4B	13	6/13/58	7/16/58	7/29/58*				Booster, sustainer and vernier solo phases and reentry vehicle separation accomplished as planned. Propulsion system cutoff properly effected after 260 seconds of powered flight.
				8/1/58*	180	255	75	
				8/2/58				
5B	11	7/22/58	8/19/58*					First Atlas flight tested with closed-loop guidance and propellant utilization systems. Booster, sustainer and vernier solo phases and re-entry vehicle separation accomplished as planned. Missile radial miss distance was 0.59 NM. Planned range was 2,853 NM.
			8/20/58	8/28/58	240	264	24	
8B	14	8/4/58	9/6/58	9/11/58*				Booster, sustainer and vernier solo phases and reentry vehicle separation accomplished as planned. Missile radial miss distance was 0.52 NM. Planned range was 3,151 NM.
				9/14/58	240	323	83	
6B	13	8/14/58	9/10/58	9/18/58	180	327	147	Flight prematurely terminated at 82.9 seconds due to malfunction of B1 turbopump at 80.8 seconds.

Notes on last page of table.

HISTORY OF ATLAS FLIGHT TESTS (Continued)

MISSILE	ERECTION PAD	ERECTION DATE	TEST DATES FRF	TEST DATES LAUNCH	FLIGHT COUNTDOWN TIME (MINUTES) NOMINAL	FLIGHT COUNTDOWN TIME (MINUTES) ACTUAL	HOLD & RECYCLE TIME (MINUTES)	COMMENTS ON FLIGHT PERFORMANCE
9B	11	9/12/58(3) 9/30/58	10/14/58* 10/24/58 10/27/58	11/12/58* 11/14/58* 11/17/58	180	210	30	Flight prematurely terminated at 227.6 seconds as a result of fuel depletion. Expedited flight testing of modified booster turbopumps required that the vehicle be flown without matching the turbopumps with the chambers. This resulted in excessive fuel consumption during booster stage.
12B	14	11/8/58	11/21/58* 11/24/58	11/28/58	180	207	27	First flight of an Atlas missile over a 5,500 NM range. Inflight operation of all missile systems was satisfactory. Missile radial miss distance was less than 5 NM. Planned range was 5,506 NM.
10B	11	11/20/58	12/9/58* 12/10/58* 12/12/58	12/18/58	180	182	2	Entire missile (Satellite 1958 Zeta), minus the booster section, was placed into an orbit around the earth as planned. All systems operated satisfactorily throughout powered flight with exception of the autopilot system which permitted an excessive roll during booster phase. Deviation from planned azimuth was corrected by guidance system during sustainer phase. No telemetry was aboard the missile.
3C	12	11/4/58(4) 11/25/58	12/17/58	12/23/58	210	255	45	First flight test in which booster engines were operated for 146 seconds. No indications of problems as result of extended operating duration. Missile radial miss distance was 0.41 NM. Planned range of 3,803 NM.
13B	14	12/8/58	12/22/58	12/30/58* 1/15/59	240	240	0	Flight terminated prematurely at 108 seconds due to autopilot and propulsion problems. Complete analysis could not be performed due to removal of the airborne telemetry system.
11B	11	12/23/58	1/20/59	2/4/59	180	420	240	First missile flown without helium pressurization to lox tank during sustainer phase. Satisfactory pressures were maintained in lox tank. Missile radial miss distance was 0.87 NM. Planned range was 3,100 NM.
4C	12	1/6/59	1/19/59	1/22/59* 1/27/59	160	183	23	Planned range was 4,268 NM. Guidance system failed early in flight. Propulsion system shut down occurred at 234.5 seconds as result of lox depletion. Missile impacted 43 NM long and 53 NM to left of planned target.
5C	12	2/5/59		2/20/59	150	248	98	Due to failure of fuel disconnect valve and/or associated plumbing during staging sequence, fuel tank pressurization was lost. Subsequent reversal of intermediate bulkhead resulted in missile destruction at 172.6 seconds.
7C	12	2/23/59		3/18/59	150	150	0	Premature booster cutoff occurred at 130 seconds. Autopilot incapable of gimbaling sustainer engine at this time which resulted in missile instability throughout remainder of powered flight.
3D	13	2/27/59	3/27/59	4/14/59	150	254	104	Due to failure of the lox fill and drain valve to close prior to launch, the missile was destroyed after 36 seconds of flight by range safety command.
7D	14	4/14/59	5/8/59	5/15/59* 5/18/59	150	150	0	Propellant tank pressurization system was affected by a launcher system malfunction. Low tank pressures caused the intermediate bulkhead to reverse, resulting in final destruction of the missile after approximately 65 seconds of flight.

Notes on last page of table.

HISTORY OF ATLAS FLIGHT TESTS (Continued)

MISSILE	ERECTION PAD	ERECTION DATE	TEST DATES FRF	TEST DATES LAUNCH	FLIGHT COUNTDOWN TIME (MINUTES) NOMINAL	FLIGHT COUNTDOWN TIME (MINUTES) ACTUAL	HOLD & RECYCLE TIME (MINUTES)	COMMENTS ON FLIGHT PERFORMANCE
5D	13	4/29/59	5/15/59	6/2/59* 6/4/59* 6/6/59	150	189	39	Due to failure of the fuel disconnect valve and/or associated plumbing during the staging sequence, fuel tank pressurization was lost. Subsequent reversal of the intermediate bulkhead resulted in missile destruction at 157.3 seconds.
8C	12	5/11/59	5/22/59 7/9/59	7/14/59* 7/15/59* 7/19/59* 7/21/59	150	230	80	All systems operated satisfactorily throughout the flight. Missile radial miss distance was less than 1.5 NM. Planned range was 4,385 NM.
11D	11	5/12/59	7/14/59* 7/16/59* 7/22/59	7/28/59	150	160	10	Operation of all missile systems was satisfactory, with the exception of the pneumatic system. A malfunction at approximately 108 seconds caused helium flow to the fuel tank to cease abruptly with no detrimental effects. Minor difficulties were also experienced in the propulsion and hydraulic systems. This was the first missile planned to impact in the Ascension Island Splash Net. Missile radial miss distance was less than 1.5 NM.
14D	13	6/10/59	7/24/59* 7/28/59	8/11/59	150	151	1	All missile systems operated satisfactorily. Missile radial miss distance was 0.72 NM. Planned range was 4,389 NM.
11C	12	7/25/59	8/14/59	8/21/59* 8/24/59	150	203	53	Data indicated that residual thrust after vernier cutoff caused an additional range increment prior to the time of retrorockets firing. Data also indicated excess of usable lox and near depletion of fuel at sustainer cutoff. Missile radial miss distance was less than 4.5 NM. Planned range was 4,385 NM.
10D	14	6/2/59[5] 7/23/59	9/1/59* 9/3/59	9/9/59	180	199	19	First Atlas missile designated to support NASA Mercury Project. The booster section failed to jettison, resulting in premature propellant depletion. Planned velocity and range were not achieved. NASA Mercury capsule recovered in satisfactory condition.
12D	576-A2	7/30/59	8/23/59	9/9/59	20	124.5	104.5	First Atlas IOC launched from VAFB. Planned impact area was the Wake Island Splash Net. Missile radial miss distance was 1.57 NM.
17D	13	8/17/59	9/8/59* 9/9/59	9/15/59* 9/16/59	150	159	9	Failure of the vernier solo hydraulic power system to activate at sustainer cutoff resulted in loss of missile attitude control during vernier solo phase. Missile radial miss distance was less than 5.5 NM. Planned range was 4,389 NM.
18D	11	9/2/59		9/22/59* 9/30/59* 10/1/59* 10/6/59	150	415	265	Operation of all missile systems was satisfactory. Missile radial miss distance was 0.3 NM. Planned range was 4,389 NM.
22D	13	9/21/59		10/9/59	150	310	160	Satisfactory operation of all airborne systems except the decoy and instrumentation systems. Missile radial miss distance was 0.43 NM. Planned range was 4,389 NM.
26D	11	10/8/59		10/29/59	150	440	290	Interference from photoflash system resulted in loss of guidance rate lock during vernier solo phase. Missile radial miss distance was less than 13 NM. Planned range was 4,389 NM.

Notes on last page of table.

HISTORY OF ATLAS FLIGHT TESTS (Continued)

MISSILE	ERECTION PAD	ERECTION DATE	TEST DATES FRF	TEST DATES LAUNCH	FLIGHT COUNTDOWN TIME (MINUTES) NOMINAL	FLIGHT COUNTDOWN TIME (MINUTES) ACTUAL	HOLD & RECYCLE TIME (MINUTES)	COMMENTS ON FLIGHT PERFORMANCE
28D	13	10/14/59		11/4/59	150	307	157	Failure of the primary airborne impact predictor system required a range safety manual fuel cutoff at 274.06 seconds. The resultant impact point was 250 to 300 miles short of the target.
15D	11	8/1/59(6)						Operation of all airborne systems, with the exception of the re-entry vehicle, was satisfactory. There was no indication of re-entry vehicle arming and fuzing or separation prior to re-entry into the atmosphere. Missile radial miss distance was 1.37 NM. Planned range was 4,389 NM.
	14	9/23/59(7)		10/13/59*				
	14			10/15/59*				
	13	11/9/59		11/24/59	150	198	48	
20D	14	10/20/59		11/26/59	240	240	0	First booster vehicle flown for the Able 4 mission. Atlas performance was satisfactory for accomplishing the mission objectives.
31D	13	11/28/59		12/8/59	150	160	10	All airborne systems operated satisfactorily. Missile radial miss distance was 0.55 NM. Planned range was 4,389 NM.
40D	13	12/10/59		12/18/59	150	168	18	All airborne systems operated satisfactorily. Missile radial miss distance was 3.26 NM. Planned range was 5,504 NM.
43D	13	12/22/59		1/6/60	150	220	70	Performance of the missile systems was satisfactory with the exception of discrepancies in the electrical, photo-flash and decoy systems. Missile radial miss distance was 0.81 NM. Planned range was 5,504 NM.
6D(9)	576A-2	3/6/59(10)						A ground guidance problem resulted in an erroneous premature vernier cutoff signal being sent; however, due to discontinuity in the missile circuitry, the signal was not received. Vernier cutoff was initiated by the flight programmer backup. Missile radial miss distance was 9.56 NM. Planned range was 3,899 NM.
	576A-2	4/18/59(11)						
	576A-3	11/6/59(12)						
	576A-3	12/11/59		1/22/60*				
				1/25/60*				
				1/26/60	20	34	19(16)	
44D	13	1/11/60		1/22/60*				First Atlas missile to fly an AVCO RVX4A-2 re-entry vehicle. Missile radial miss distance was 1.02 NM. Planned range was 4,389 NM.
				1/26/60	150	241	91	
49D	13	1/28/60		2/9/60*				Third Series D missile to be flown over 5,500 NM range. Missile radial miss distance was 1.31 NM.
				2/11/60	150	161	11	
29D	14	1/18/60		2/26/60	315	460	145	First Atlas missile designated to support AFBMD project MIDAS. Atlas performance was satisfactory for accomplishing the mission objectives.
42D	11	12/21/59	2/4/60(8)					First Atlas to test the all-inertial guidance (AIG) system. AIG system flown in open-loop configuration. Planned range was 4,396 NM without guidance. Impact was within 20 NM of target.
			2/23/60	3/2/60*				
				3/4/60*				
				3/8/60	180	190	10	
51D	13	2/15/60		3/10/60	150	156	6	Flight terminated shortly after liftoff due to combustion instability in the B1 thrust chamber.
48D	11	3/3/60		4/7/60	150	156	6	Flight terminated prior to liftoff due to combustion instability in the B2 thrust chamber. Missile exploded on the stand 60.29 seconds after sustainer flight lockin.
25D(9)	576B-2	8/21/59(13)						Operation of all airborne systems was satisfactory, although minor difficulties were encountered in the flight control and hydraulic systems. Missile radial miss distance was 0.1 NM. Planned range was 3,899 NM.
	576B-2	11/28/59(14)						
	576B-2	3/10/60		4/6/60*				
				4/7/60*				
				4/22/60	15	23:39.3		

Notes on last page of table.

HISTORY OF ATLAS FLIGHT TESTS (Continued)

MISSILE	ERECTION PAD	ERECTION DATE	TEST DATES FRF	TEST DATES LAUNCH	FLIGHT COUNTDOWN TIME (MINUTES) NOMINAL	FLIGHT COUNTDOWN TIME (MINUTES) ACTUAL	HOLD & RECYCLE TIME (MINUTES)	COMMENTS ON FLIGHT PERFORMANCE
23D[9]	576B-2	4/24/60		5/6/60	15	15:56**	8:39.3	The missile was destroyed by the Flight Safety Officer after 25.63 seconds of flight due to a failure of the pitch displacement gyro.
56D	12	4/11/60	5/10/60*	5/10/60* 5/12/60* 5/20/60	150	150	0	First Atlas missile flown over an extended range of 7,860 NM or 9,040 statute miles. Missile radial miss distance was 1.18 NM.
45D	14	3/2/60		5/24/60	300	456	156	Second Atlas missile designated to support AFBMD project MIDAS. Atlas performance was satisfactory for accomplishing the mission objectives.
54D	11	5/13/60		6/11/60	150	390	240***	First Atlas missile flown with closed-loop all-inertial guidance (AIG) system. Retrorockets failed to fire. Missile radial miss distance was 1.5 NM. Planned range was 4,306 NM.
62D	14	5/26/60		6/20/60[17] 6/22/60	150	199	49	First Atlas to fly a GE Mark 3 Mod IIB re-entry vehicle. Re-entry vehicle overshot target 15 to 18 NM due to failure of the guidance vernier cutoff discrete command to effect vernier engine cutoff. Planned range was 4,389 NM.
27D	576B-1 12	8/6/59[18] 6/4/60		6/24/60[19] 6/27/60	150	150	0	A converted IOC missile carrying a Mark 3 Mod IIB re-entry vehicle. Missile radial miss distance was 0.77 NM. Planned range was 4,389 NM.
60D	11	6/14/60		6/30/60[20] 7/2/60	150	328	178***	Second Atlas to be flown with a closed-loop all-inertial guidance system. Planned range was not achieved due to an electrical short which caused depletion of the controls helium pressure and resulted in abnormal sustainer and vernier engine performance. Impact was approximately 40 nautical miles short of the target. Planned range was 4,306 NM.
74D[9]	576B-1	7/5/60		7/22/60	15	238[21]	223	The missile was self-destructed at 69.18 seconds as a result of excessive aerodynamic forces when the planned pitchover program was exceeded. This malfunction was the result of high torquer amplifier gain due to component failure. Fifth IOC missile to be flight tested.
50D	14	6/30/60	7/21/60	7/29/60	215	257	42	The second Atlas to support the NASA Project Mercury program and the first to boost a McDonnell capsule. The planned trajectory was not achieved due to an incident, as yet unexplained, which culminated in missile destruction at 58.995 seconds.
32D	12	7/1/60		8/2/60[22]	150	219	69	A converted IOC missile carrying a Mark 3 Mod IB re-entry vehicle. First missile flown to a 6,350 NM target. All airborne systems operated satisfactorily. Missile radial miss distance was 4.2 NM.
66D	11	7/7/60		7/22/60[23] 7/25/60[24] 8/8/60[25] 8/12/60	150	156	0	Third closed-loop all-inertially guided missile. Minor discrepancies were noted in the propulsion, PU, flight control, and re-entry vehicle systems. Also, excessive missile bending was noted during the booster phase of flight. The planned range of 4,387 NM was achieved. Missile radial miss distance was 1.9 NM.
47D[9]	576B-1 576B-3	2/17/60[26] 7/17/60		9/12/60	15	24:32	9:32	Impact was approximately 535 NM short of target as result of gradual decrease in sustainer engine thrust beginning at 222 seconds. The anomaly was result of a controls bottle helium leak which began at the time of vernier tanks repressurization, downstream of the ISS regulator. Planned range was 4,384 NM. Telemetry transducer power supply failed at 109.90 seconds resulting in extensive loss of data. This was sixth IOC Atlas to be flown.

Notes on last page of table.

HISTORY OF ATLAS FLIGHT TESTS (Continued)

MISSILE	ERECTION PAD	ERECTION DATE	TEST DATES FRF	TEST DATES LAUNCH	FLIGHT COUNTDOWN TIME (MINUTES) NOMINAL	FLIGHT COUNTDOWN TIME (MINUTES) ACTUAL	HOLD & RECYCLE TIME (MINUTES)	COMMENTS ON FLIGHT PERFORMANCE
76D	11	8/15/60[27] 9/11/60		9/16/60	150	328	178***	Fourth Atlas missile flown with closed-loop AIG system. Missile radial miss distance was 2.8 NM. Planned range was 4,387 NM. An RVX-2A re-entry vehicle was carried.
79D	14	8/26/60[27] 9/11/60		9/15/60[28] 9/19/60	150	481	331***	Second Atlas missile flown over an extended range of 9,030 statute miles (7,860 NM). All missile systems functioned satisfactorily. Missile radial miss distance was less than 4 NM.
80D	12	9/2/60[27] 9/11/60		9/25/60	180	240	60[29]	Second booster vehicle assigned to the Able lunar mission. Atlas performance was satisfactory for accomplishing the mission objectives.
33D[9]	576B-2	6/3/60		9/20/60[30] 9/23/60[31] 9/29/60	15	31:12.7	16:12.7***	Missile impact was approximately 1,200 miles short due to an inadvertent separation of an electrical disconnect plug which caused premature booster shutdown and failure to jettison the booster section. This was the seventh IOC Atlas to be flown. Planned range was 4,385 NM.
3E	13	7/29/60[27] 9/12/60	9/23/60[32] 10/3/60	10/11/60	150	345	195***	First Series E Atlas to be flight tested. The planned range of 4,387 NM was not achieved because of loss of sustainer hydraulic pressure during booster stage resulting in missile instability at booster cutoff, and subsequent explosion of the missile at 154 seconds. Closed-loop autopilot instability existed at various times during booster stage. An AVCO Mark 4 Mod I vehicle was aboard.
57D	PALS-1	6/2/60	8/10/60[33] 8/23/60	10/11/60	30	32:51.9	2:51.8	First SAMOS booster. Atlas performance was satisfactory for the mission. Loss of guidance early in the flight was not detrimental to accomplishment of the mission.
81D[9]	576B-3	9/29/60		10/12/60[34] 10/12/60	20	74:20.7	54:20.7	The planned range of 4,380 NM was not achieved. A malfunction in the lox tank pressurization system became apparent at 40 seconds, resulting in overpressurization of the missile lox tank, subsequent reversal of the intermediate bulkhead and missile self-destruction at 71.58 seconds. This was the eighth IOC Atlas to be launched.
71D	11	9/26/60		10/7/60[35] 10/13/60	150	304	154***	Fifth Series D flight with AIG system in the closed-loop configuration. Planned range was 4,387 NM. Missile radial miss distance was 1.25 NM. An RVX-2A re-entry vehicle was aboard. Recovery of the re-entry vehicle with biospecimens and associated special instrumentation was accomplished.
55D	12	3/7/60[36] 5/24/60[37] 10/3/60		10/22/60	150	403	253***	A Mark 3 Mod IIB re-entry vehicle was delivered over a 6,350 NM range. Operation of all missile systems was satisfactory. Missile radial miss distance was 1.27 NM.
83D	12	10/27/60		11/10/60[38] 11/15/60	150	444	294***	First Series D missile to carry a Mark 4 Mod I re-entry vehicle. All airborne systems operated satisfactorily. Missile radial miss distance was 0.27 NM. Planned range was 4,389 NM.
4E	13	10/21/60		11/26/60[39] 11/29/60	150	191:30	41:30	Second Series E Atlas to be flight tested. Planned range of 4,385 NM was not fulfilled due to loss of sustainer hydraulic pressure after 41 seconds of flight. The missile became unstable at booster cutoff and sustainer thrust was lost at 149.3 seconds.
91D	12			12/14/60[40] 12/15/60	180	270	90	Third Series D Atlas used as a booster for the Able lunar mission. The planned trajectory was not achieved due to an incident, as yet unexplained, which culminated in missile destruction at 73.95 seconds.

Notes on last page of table.

HISTORY OF ATLAS FLIGHT TESTS (Continued)

MISSILE	ERECTION PAD	ERECTION DATE	TEST DATES FRF	TEST DATES LAUNCH	FLIGHT COUNTDOWN TIME (MINUTES) NOMINAL	FLIGHT COUNTDOWN TIME (MINUTES) ACTUAL	HOLD & RECYCLE TIME (MINUTES)	COMMENTS ON FLIGHT PERFORMANCE
99D[9]	576B-3	11/25/60		12/16/60	15	30:19.5	15:19.5	First IOC Atlas to deliver a re-entry vehicle to the Eniwetok Lagoon target area. Performance of all systems was satisfactory. Planned range was 4,388 NM. Missile radial miss distance was 0.52 NM.
90D	12	12/20/60		1/11/61[41] 1/12/61 1/13/61 1/16/61 1/23/61	150	167	17	The 32nd and final Series D R&D Atlas missile launched from AMR. First Atlas missile to flight test the Aeronutronics Mod I decoy pod system. The planned range of 4,394 NM was accomplished. Missile radial miss distance was 1 NM.
8E	13	12/5/60[42] 12/21/60	1	1/19/61[43] 1/23/61[44] 1/24/61	150	446:10	296:10***	Third Series E Atlas to be flight tested. The planned range of 4,387 NM was not fulfilled due to loss of stability at 160.9 seconds. A short in the V2 engine pitch servovalve wiring at 114.27 seconds, due to aerodynamic heating, caused instability. An AVCO Mark 4 Mod IV re-entry vehicle was aboard.
70D	PALS-1	10/14/60		12/21/60[45] 12/30/60 1/14/61 1/31/61	30	96:41	66:41	Second SAMOS booster vehicle launched from PALS-1. Atlas performance was satisfactory for accomplishing the mission objectives.
67D	14	11/4/60	11/19/60	2/21/61	250	320	70	Third Atlas missile used in support of the NASA project Mercury. Atlas performance was satisfactory for accomplishing the mission objectives.
9E	13	1/30/61		2/24/61	150	419	269***	First Atlas flight test to provide data on a full duration firing of the MA-3 propulsion system. Performance of all systems was satisfactory, with the exception of minor discrepancies in the PU and instrumentation beacon systems. Missile radial miss distance was 0.18 NM. Planned range was 6,350 NM over a "dog-leg" course.
13E	13	2/27/61		3/10/61[46] 3/13/61	150	316	166	A failure in the PU system resulted in excessive fuel consumption and premature sustainer engine shutdown at 251 seconds. Planned range was 7,863 NM with impact in the Indian Ocean.
16E	13	3/14/61		3/24/61	150	168	18	Flight plan not fulfilled due to failure to jettison the booster section. Premature depletion of controls bottle pressure was caused by a fault in the propulsion system wiring which resulted in reversal of the vernier engine ignition and vernier solo tanks pressurization events. The vernier tanks pressurized at 2.7 seconds and the vernier engines ignited at booster cutoff. Planned range was 7,863 NM.
100D	14	3/27/61		4/25/61	250	385	135	Fourth Atlas to support the NASA Project Mercury program. Failure of the autopilot programmer to generate the pitch and roll program, necessitated destruction of the missile by range safety command.
12E	11	2/16/61		5/11/61[47] 5/12/61	150	150	0	First Atlas flight tested with a Mark 5 Mod I (Minuteman) re-entry vehicle, with a ballasted transition section to simulate the CG and weight of MK 4 vehicles. All systems operated satisfactorily. Missile radial miss distance was 0.31 NM. Planned range was 4,388 NM with impact in the Ascension Island Splash Net.
95D	576B-2	3/28/61		5/24/61	25	33:17.6	8:17.6	Performance of all systems was satisfactory. The re-entry vehicle impacted in the Eniwetok Lagoon target area. Missile radial miss distance was 0.73 NM. Planned range was 4,385 nautical miles.

Notes on last page of table.

SUMMARY

HISTORY OF ATLAS FLIGHT TESTS (Continued)

MISSILE	ERECTION PAD	ERECTION DATE	TEST DATES FRF	TEST DATES LAUNCH	FLIGHT COUNTDOWN TIME (MINUTES) NOMINAL	FLIGHT COUNTDOWN TIME (MINUTES) ACTUAL	HOLD & RECYCLE TIME (MINUTES)	COMMENTS ON FLIGHT PERFORMANCE

NOTES:

(1) Removed on 4 October 1957 for modifications required as a result of Missile 6A flight test analysis.

(2) Removed from launcher on 27 November 1957 to replace damaged components.

(3) Removed on 19 September 1958 from the launcher to install a Series C turbopump.

(4) Returned to hangar K on 18 November 1958 and demated to replace the power package with original power package.

(5) Removed from stand on 1 July 1959 and demated for modifications and to change booster engines.

(6) Removed from stand on 28 August 1959 for required rework.

(7) Removed from stand on 16 October 1959 due to high priority of Missile 20D.

(8) Unsuccessful due to ARMA guidance system difficulties.

(9) Launcher uses horizontal-readiness concept.

(10) Removed on 14 April 1959 to complete validation of the launcher and pad.

(11) Removed on 27 July 1959 and returned to San Diego.

(12) Removed on 1 December 1959 to facilitate launcher validation.

(13) Removed on 24 November 1959 for cleanup and inspection of lox tank baffles.

(14) Removed on 3 March 1960 to replace holddown and release cylinders on launcher and align and level the heads.

(15) Erected as Venus probe. Removed from stand on 5/5/59 and placed in temporary storage.

(16) Including 5 minutes planned hold.

(17) Aborted when difficulties with the San Salvador IP station could not be resolved.

(18) Returned to the squadron maintenance area on 1 February 1960 to be cleaned and to receive a protective coating. Shipped to San Diego on 6 February 1960 for conversion to an R&D configuration, and subsequently airlifted to AMR on 27 May 1960.

(19) Scrubbed due to a re-entry vehicle problem.

(20) Terminated because an improper frequency output was noted on Channel 5 of the analog signal converter for accelerometer string 1 of the inertial guidance system.

(21) A number of difficulties were encountered with the fuel transfer system.

(22) Engine cutoff occurred 1.53 seconds after sustainer flight lockin due to an accumulation of RCC count on the sustainer engine.

(23) Cancelled at T-70 minutes due to a discrepancy in the sustainer RCC accelerometer circuitry.

(24) Cancelled at T-7 minutes due to a spurious engine tank pressurization signal.

(25) Cancelled at T-7 minutes when re-entry vehicle telemetry failed.

(26) Removed from launcher due to contamination of missile fuel system on 4 July 1960.

(27) Removed from complex on 10 September 1960 because of hurricane Donna.

(28) Test terminated due to absence of a release signal.

(29) This was a planned hold.

(30) Aborted during ignition stage when vernier No. 1 pressure switch failed.

(31) Terminated during transition to main stage by mainstage timer.

(32) Terminated by an observer cutoff at 13.06 seconds due to the B2 lube oil pump shaft shearing. The B2 engine was replaced.

(33) Two FRF's were conducted on 19 August 1960, both were unsatisfactory.

(34) Terminated due to failure of the B1 fuel manifold pressure switch to complete the B1 thrust "OK" logic.

(35) Cancelled due to loss of modulation on GE re-entry vehicle telemetry link four.

(36) Removed from complex on 7 April 1960 due to a contamination problem.

(37) Removed from launcher on 3 June 1960 and demated (booster and sustainer) for work on the bulkhead seam.

(38) Cancelled at T-40 minutes due to F&G regulator problems at MSTS Test Stand 1-4. The F&G regulators were replaced with Hadicy D regulators.

(39) Aborted at T-7 minutes due to a leak in the 3-inch lox topping line swivel joint.

(40) Scrubbed at T-7 minutes because of a spurious reset of the autopilot programmer.

(41) First four launch attempts were cancelled due to inclement downrange weather conditions.

(42) Lowered from tower on 19 December 1960 for hydraulic work.

(43) Terminated at T-15 minutes due to loss of commutation on RF-1 Channel 11.

(44) Terminated at T-100 minutes because of a hydraulic leak at the V2 engine gimbal joint.

(45) The first three were simulated flights. The first test was unsuccessful. The second and third were successful.

(46) Aborted because of repeated problems with telemetry RF No. 2.

(47) Aborted because of lack of sufficient time to resolve problems prior to cutoff time of countdown necessitated by night re-entry mission.

* Aborted or prematurely terminated.

** Discrepancy in timing (human error).

*** See Summary of Holds & Aborts.

SECTION 3. TRAJECTORY

External tracking systems data defining the powered flight trajectory of an Atlas 107A-1 weapon system permit evaluation of the over-all performance of the Atlas missile system and subsystems. The values of certain trajectory parameters at the end of powered flight completely determine subsequent free-fall missile flight performance and success in fulfilling mission objectives. The manner in which the trajectory data are utilized to determine missile system and subsystem performance is outlined in Table 3-1.

This section of the report summarizes the more important results of these data as compiled for the individual Series D tests discussed in this report. At the end of this section a performance summary of the external tracking systems used to obtain trajectory data is included to indicate their usefulness, reliability and accuracy.

Table 3-2 lists the principal trajectory parameters of the Series D flight tests discussed in this section. The tests are tabulated in chronological order. The nominal or planned parameter values given in this table, and elsewhere in this section, were obtained from preflight computer simulations prepared for each test. These simulations, prepared by the Convair flight performance and analysis group, are based on nominal engine test data, missile factory weights, re-entry vehicle parameters, and specific guidance equations and target data for each test. A standard tropical atmosphere and Sissenwine wind profile are used to permit dynamic pressure and Mach number calculations.

TABLE 3-1 APPLICABILITY OF TRAJECTORY DATA TO MISSILE SYSTEM EVALUATION

TRAJECTORY PARAMETER OBSERVED		MISSILE SYSTEM PERFORMANCE INDICATED		
1.	Altitude as a function of range	1.	a)	Flight control system pitch program prior to booster engine cutoff.
			b)	Guidance system pitch control, if required, after booster cutoff.
			c)	Guidance system accuracy with respect to booster cutoff criterion.
2.	Crossrange as a function of range	2.	a)	Flight control system roll program during booster phase (all RIG missiles plus 54D, 60D and 66D AIG missiles).
			b)	Guidance system roll program control for 71D and 76D AIG missiles.
			c)	Guidance system yaw steering control after booster engine cutoff.
3.	Resultant velocity as a function of time	3.	a)	Propulsion system thrust performance. (Since resultant velocity is also dependent upon missile attitude the indicated velocity may not completely reflect propulsion performance.)
			b)	Guidance system accuracy with respect to sustainer and vernier engine cutoff criteria.
4.	Component velocities and range as functions of time	4.	a)	Flight control and/or guidance system control of flight path angle.
			b)	Flight control and/or guidance system control of pitch over angle. (Approximately only since actual angle of attack can not be determined.)
5.	Acceleration as a function of time	5.	a)	Propulsion system: over-all performance and thrust variations.
			b)	Airframe: weight and/or drag changes reflecting abnormalities. Retrorocket firing time.
			c)	Guidance system: engine cutoff event times.

TABLE 3.1 APPLICABILITY OF TRAJECTORY DATA TO MISSILE SYSTEM EVALUATION (CONTINUED)

TRAJECTORY PARAMETER OBSERVED	MISSILE SYSTEM PERFORMANCE INDICATED
6. Position and attitude as a function of time, liftoff to 20 seconds (Optical Tracking)	6. a) Launch control system: satisfactory control at missile release function. b) Flight control system: missile stability during vertical flight. c) Functions (a) and (b) above affect operational launch site design problems.
7. Resultant velocity and altitude as functions of time	7. Aerodynamic parameters: mach number and dynamic pressure. Requires correlation with ambient upper air meteorological conditions.
8. Impact location	8. a) Weapon system: over-all performance of co-ordinated sub-systems to meet re-entry vehicle target impact requirements. b) Flight control and guidance systems: accuracy of steering control; velocity magnitude control; and flight path angle control. Also reflects adequate performance of hydraulic and electrical systems. c) Propulsion system: adequate thrust to satisfy range and velocity requirements, including propellant utilization control. Also reflects adequate performance of hydraulic and pneumatic systems. d) Airframe: reflects integrity of airframe and satisfactory separation functions for booster engines and re-entry vehicle. Also reflects adequate performance of pneumatic pressurization system. e) Re-entry vehicle: separation function; re-entry stability control; adequate heat shield performance to maintain integrity of vehicle and payload. f) Impact predictor systems: impact data supplies a measure to evaluate the relative accuracy of the various IP systems and indicate bias, if any. Especially valuable if independent spash net and/or Sofar data are available.

TABLE 3-2 FLIGHT PERFORMANCE SUMMARY

	MISSILE 48D	MISSILE 56D	MISSILE 45D	MISSILE 54D	MISSILE 62D	MISSILE 27D	MISSILE 60D
Date of Launch	4/7/60	5/20/60	5/24/60	6/11/60	6/22/60	6/27/60	7/2/60
Zero Time (EST)	(1)	1000:26.98	1236:4575	0130:18.46	0949:33.24	2130:54.05	0158:22.19
Range Test Number	301	1885	619	615	801	1002	803
Base and Complex	AMR 11	AMR 12	AMR 14	AMR 11	AMR 14	AMR 12	AMR 11
Pitchover Azimuth	98.626°T	113°T	107°T	98.626°T	105°T	105°T	98.627°T
Re-Entry Vehicle Type	GE MK 3 MOD IA	GE MK 3 MOD IB	Agena Satellite	GE MK 3 MOD IB	GE MK 3 MOD IIB	GE MK 3 MOD IB	GE MK 3 MOD IB
Guidance System	GE-RIG	GE-RIG	GE-RIG	ARMA-AIG	GE-RIG	GE-RIG	ARMA-AIG
FLIGHT PHASE AND PARAMETER							
LAUNCH PHASE							
Total Launch Weight (lbs)							
Planned	265,046	262,080	270,986	258,625	242,517	257,166	258,695
Actual	266,496	261,000	269,734	256,401	239,851	256,437	257,888
Booster Thrust (lbs)							
Planned	308,366	308,406	307,886	308,007	308,439	308,411	308,007
Actual	(1)	313,400	303,850	307,750	308,400	303,000	308,400
Sustainer Thrust (lbs)							
Planned	56,259	56,156	56,569	56,124	56,117	56,091	56,124
Actual	(1)	56,700	55,650	56,500	53,400	54,400	54,000
Vernier Thrust (Axial, lbs)							
Planned	1,720	1,719	1,722	1,718	1,719	1,719	1,718
Actual	(1)	1,700	1,680	1,650	1,700	1,600	1,700
Total Axial Thrust (lbs)							
Planned	367,315	367,281	367,177	366,849	367,275	367,221	366,849
Actual	(1)	372,800	362,180	366,900	364,500	360,000	365,100
Thrust to Weight Ratio							
Planned	1,386	1,401	1,355	1,418	1,514	1,428	1,418
Actual	(1)	1,428	1,343	1,431	1,520	1,418	1,416
BOOSTER CUTOFF							
Time (sec)							
Planned	142.47	138.96	148.78	140.12	119.04	130.98	140.12
Actual	(1)	136.57	146.78	137.62	117.77	131.94	141.03
Altitude Above Earth (ft)							
Planned	254,212	232,232	251,659	262,515	213,429	230,317	262,515
Actual	(1)	236,979	249,359	275,284	215,907	232,485	285,333
Range Along Earth (NM)							
Planned	59.03	55.86	65.72	57.86	35.0	43.75	57.86
Actual	(1)	55.63	63.42	56.20	34.22	45.27	56.85
Velocity (ft/sec)							
Planned	11,226	10,683	11,710	11,362	8,501	9,350	11,362
Actual	(1)	10,871	11,527	11,581	8,523	9,595	11,684
SUSTAINER CUTOFF							
Time (sec)							
Planned	251.19	279.50	238.89	246.21	258,888	282.95	246.21
Actual	(1)	271.06	238.52	235.55	284.265	278.68	307.55
Altitude Above Earth (ft)							
Planned	860,527	957,756	664,821	882,933	1,122,338	1,063,659	882,993
Actual	(1)	940,579	675,525	901,170	1,144,004	1,048,296	1,372,447
Range Along Earth (NM)							
Planned	299.32	382.76	266.01	291.58	340.15	340.33	291.58
Actual	(1)	370.59	265.46	271.20	336.81	335.29	434.86
Velocity (ft/sec)							
Planned	20,364	23,613	18,474	20,335	20,109	20,167	20,335
Actual	(1)	23,601	18,428	20,300	20,071	20,151	19,604
VERNIER CUTOFF							
Time (sec)							
Planned	265.74	294.72	256.74	259.20	305.29	302.35	259.20
Actual	(1)	285.00	257.59	242.79	307.69	292.03	277.45
Altitude Above Earth (ft)							
Planned	940,561	1,085,010	749,726	982,612	1,288,326	1,222,830	982,612
Actual	(1)	1,059,910	762,263	958,535	1,339,446	1,173,199	1,140,873
Range Along Earth (NM)							
Planned	342.65	435.29	316.57	329.99	393.94	395.77	330.00
Actual	(1)	418.67	317.90	292.73	403.46	379.62	351.05
Velocity							
Planned	20,244	23,521	18,372	20,225	19,936	20,000	20,225
Actual	(1)	23,554	18,344	20,265	19,893	20,066	19,346
IMPACT (2)							
Latitude (deg)							
Planned	1.383°S	38.0°S	NA	1.383°S	8.0762°S	8.0762°S	1.383°S
Actual	(1)	37.9826°S(3)	NA	1.3921°S(3)	8.2009°S	8.0642°S	1.0967°S(4)
Longitude (deg)							
Planned	12.167°W	41.0°E	NA	12.1667°W	14.745°W	14.745°W	12.167°W
Actual	(1)	40.9885°E(3)	NA	12.1908°W(3)	14.5322°W	14.7501°W	12.7708°W(4)
Range (NM)							
Planned	4306	7859	NA	4306	4389	4389	4306
Actual	(1)	7858(3)	NA	4305(3)	4404	4388	4267(4)

TABLE 3.2 FLIGHT PERFORMANCE SUMMARY (CONTINUED)

MISSILE 32D	MISSILE 66D	MISSILE 76D	MISSILE 79D	MISSILE 80D	MISSILE 71D	MISSILE 55D	MISSILE 83D	MISSILE 90D
8/9/60	8/12/60	9/16/60	9/19/60	9/25/60	10/13/60	10/22/60	11/15/60	1/11/61
1309:33.77	0800:10.46	0458:06.26	1331:27.10	1013:16.92	0434:48.64	0013:20.67	0054:07.56	1602:05.60
1003	1004	2817	802	2801	1502	613	3503	3505
AMR 12	AMR 11	AMR-11	AMR-14	AMR-12	AMR-11	AMR-12	AMR-12	AMR-12
112°T	106.263°T	106.263°T	112°T	98°T	106.263°T	112°T	105°T	106.3°T
GE MOD 3 MK 1B	GE RVX-2A	GE-RVX-2A	GE-MK 3 MOD 1B	ABLE V	GE-RVX-2A	GE-MK 3 MOD IIB	AVCO-MK 4 MOD I	GE-MK 3 MOD 1B
GE-RIG	ARMA-AIG	ARMA-AIG	GE-RIG	GE-RIG	ARMA-AIG	GE-RIG	GE-RIG	GE-RIG
257,769	261,148	264,316	262,817	263,665	265,389	264,550	265,785	264,277
259,150	260,855	263,896	262,269	262,222	263,725	263,273	264,788	263,810
308.419	308.012	308,080	308,109	307,531	308,088	308,406	308,368	308,393
311,500	311,000	308,000	305,800	302,000	305,300	311,000	308,000	305,500
56,075	56,150	56,050	56,051	57,413	56,049	56,159	56,807	56,232
55,500	54,000	51,500	53,200	54,000	(6)	55,000	56,000	52,200
1,719	1,718	1,718	1,717	1,732	1,718	1,720	1,720	1,720
1,660	1,700	1,700	1,680	1,700	1,670	1,700	1,960	1,970
367,213	366,880	366,848	365,877	366,676	365,855	366,285	366,895	366,345
369,660	367,700	362,200	361,680	358,700	(6)	367,700	365,960	360,700
1,422	1,405	1.388	1.392	1.391	1.379	1.385	1.382	1.386
1,426	1,410	1.373	1.379	1.368	(6)	1.397	1.382	1.367
133.27	137.62	139.12	138.08	140.0	139.62	138.06	138.76	136.27
131.55	136.45	138.59	138.59	140.11	139.56	135.86	137.75	137.66
229,284	241,879	238,650	225,446	252,025	237,508	229,269	242,305	222,020
230,888	261,268	243,040	230,888	246,037	255,678	231,617	242,735	224,370
48.18	52.60	53.25	53.96	53.60	53.46	51.96	51.0	50.80
46.25	50.33	51.64	55.19	53.84	52.52	51.65	51.05	53.6
98,43	10,380	10,324	10,342	10,505	10,302	10,096	10,066	9,898
97,26	10,566	10,303	10,622	10,592	10,419	10,204	10,250	10,206
285.49	267.52	272.02	286.53	275.40	273.59	287.69	276.58	277.67
288.09	259.24	274.89	282.48	271.22	266.73	283.04	269.91	271.93
1,040,916	929,780	923,449	960,809	1,073,628	921,001	996,963	1,006,195	892,255
1,105,832	1,002,540	960,008	947,856	987,509	983,704	1,025,568	979,815	ND
373.66	327.72	335.23	394.15	341.24	337.80	379.47	333.90	347.9
373.03	304.80	337.59	387.04	339.09	317.4	372.37	324.80	ND
22,398	20,399	20,409	23,558	21,558	20,408	22,387	20,257	20,450
22,346	20,271	20,334	23,482	21,484	20,309	22,395	20,294	ND
301.16	280.52	285.08	302.29	277.40	288.52	306.60	293.78	294.43
302.00	274.43	290.91	295.22	273.53	280.71	298.3	286.34	389.77
1,174,509	1,025,034	1,017,448	1,088,539	1,092,696	1,207,644	1,149,838	1,143,575	1,005,208
1,233,428	1,124,060	1,075,452	1,051,148	993,486	1,094,895	1,155,594	1,110,570	ND
424.13	366.47	374.31	448.58	347.28	382.50	440.87	383.8	398.5
417.41	349.84	386.0	431.05	340.36	358.40	420.42	278.7	ND
22,288	20,296	20,307	23,467	21,539	20,294	21,248	20,103	20,330
22,301	20,170	20,228	23,509	21,506	20,309	22,323	20,108	ND
33.50°S(3)	8.1548°S	8.1467S	38.5S	NA	8.1467S	33.5S	8.0762S	8.2S
33.50°S(3)	8.1278°S	8.1922S	38.4987S(2)	NA	8.1082S	33.4863S(3)	8.0720S	8.1963S(5)
10.31°E	14.7775°W	14.7900W	41.0E	NA	14.7900W	10.31E	14.7450W	14.7W
10.3912°E(3)	14.7925°W	14.8024W	41.0808D(3)	NA	14.8350W	10.3237E(3)	14.7467W	14.6960W(5)
6350	4388	4,387	7,863	NA	4,387	6,350	4,389	4,395
6354(3)	4390	4,388	7,867(3)	NA	4,385	6,350(3)	4,389	4,395(5)

NOTES: (1) Liftoff not achieved.
(2) Actual impact location according to MILS splash net data unless otherwise indicated.
(3) According to San Salvador Impact Predictor data.
(4) According to Cape GE Instrumentation Beacon data.
(5) According to SOFAR data.
(6) Sustainer chamber pressure instrumentation malfunctioned.
NA Not applicable.
ND No data.

DISCUSSION

Impact

Over-all performance of a ballistic missile as a weapon system component is best evaluated by the location of its actual impact point with respect to the assigned test target. The Area 12 Ascension Island splash net system, by providing a direct physical measurement of re-entry vehicle impact, permits direct correlation of impact data for tests with assigned targets in that area. Data for comparison of the impact prediction systems calculations are also made available when the splash net is used.

Table 3-3 lists the assigned target point for each subject Series D missile with the geodetic coordinates and miss distance for each as actually determined by the various location systems. Miss distances are given in nautical miles in downrange and crossrange components from the assigned target using the nominal re-entry flight azimuth as the downrange axis. Table 3-4 lists the actual radial miss distances from the assigned targets. The radial miss distances listed are based on MILS splash net data if the target was in that area and the data were valid. Otherwise the data from the System 4 Impact Predictor at San Salvador were used.

TABLE 3-3 IMPACT PREDICATION (LATITUDE AND LONGITUDE, NAUTICAL MILES FROM TARGET)

DATE OF LAUNCH	MISSILE NO.	ASSIGNED TARGET	MILS		GE SYSTEMS			FPS/16
			SPLASH	SOFAR	CAPE CANAVARAL	SAN SALAVADOR	AZUSA	RADAR 12.16
4-7-60	48D	1.383°S 12.167°W			LIFTOFF NOT ACHIEVED			
5-20-60	56D	38.0°S 41.0°E	NA	NA	37.9814°S 40.9445°E 2.64 short 1.10 left	37.9826°S 40.9885°E 0.55 short 1.04 left	37.9728°S 40.8335°E 7.90 short 1.61 left	NA
5-24-60	45D	Atlas used as booster for Midas orbital vehicle. Objectives placed accuracy requirements for Atlas apogee altitude of 291.9 NM and inertial velocity of 18,393 ft/sec. These requirements met with +0.03% and zero error, respectively.						
6-11-60	54D	1.383°S 12.167°W	NA	NA	1.3864°S 12.1787°W 0.50 short 0.54 right	NA	1.3823°S 12.2035°W 1.88 short 1.12 right	NA
6-22-60	62D	8.0762°S 14.7450°W	8.2009°S 14.5322°W 14.75 long 0.72 left	ND	8.2367°S 14.4941°W 17.80 long 0.13 left	8.2355°S 14.4991°W 17.52 long 0.06 left	8.2095°S 14.5113°W 16.1 long 0.98 left	ND
6-27-60	27D	8.0762°S 14.7450°W	8.0642°S 14.7501°W 0.64 short 0.43 left	NA	8.0733°S 14.7536°W 0.52 short 0.15 right	8.0813°S 14.7295°W 0.93 long 0.25 left	ND	ND
7-2-60	60D	1.3833°S 12.1667°W	NA	NA	1.0967°S 12.7708°W 39.08 short 4.26 right	NA	1.0489°S 12.7939°W 42.48 short 2.55 right	1.1250°S 12.7393°W 37.26 short 4.68 right
8-9-60	32D	33.50°S 10.31°F	NA	NA	33.5048°S 10.3326°E 1.15 long 0.21 left	33.50°S 10.3912°E 3.84 long 1.70 left	33.471°S 10.268°E 2.51 short 0.73 left	NA
8-12-60	66D	8.1548°S 14.7775°W	8.1278°S 14.7925°W 1.64 short 0.87 left	8.1399°S 14.7602°W 0.40 long 1.31 left	8.1470°S 14.7536°W 0.96 long 1.17 left	NA	8.1936°S 14.8199°W 0.83 short 3.31 right	ND
9-16-60	76D	8.1467°S 14.7900°W	8.1922°S 14.8024°W 0.86 long 2.69 right	8.1279°S 14.9179°W 6.98 short 3.19 right	8.2236°S 14.7703°W 3.47 long 3.21 right	NA	8.1716°S 14.8055°W 0.01 long 1.74 right	ND
9-19-60	79D	38.50°S 41.0°E	NA	NA	38.5108°S 40.9878°E 0.58 short 0.64 right	38.4987°S 41.0808°E 3.81 long 0.05 left	38.5068°S 41.1187°E 5.58 long 0.45 right	NA
9-25-60	80D	ATLAS USED AS BOOSTER FOR ORBITING VEHICLE						
10-13-60	71D	8.1467°S 14.7900°W	8.1082°S 14.8350°W 3.50 short 0.47 left	8.1154°S 14.8039°W 1.70 short 1.12 left	8.1255°S 14.7885°W 0.61 short 1.10 left	NA	8.0955°S 14.8141°W 2.87 short 1.79 left	8.1113°S 14.8006°W 1.67 short 1.43 left
10-22-60	55D	33.50°S 10.31°E	NA	NA	33.5003°S 10.3237°E 0.68 long 0.25 left	33.4836°S 10.3237°E 0.42 long 1.20 left	33.4858°S 10.3687°E 2.73 long 1.88 left	NA
11-15-60	83D	8.0762°S 14.7450°W	8.0720°S 14.7467°W 0.22 short 0.16 left	8.0722°S 14.7473°W 0.24 short 0.12 left	8.0842°S 14.7495°W 0.03 long 0.55 right	8.0767°S 14.7395°W 0.28 long 0.17 left	8.0758°S 14.7680°W 1.18 short 0.72 right	8.0785°S 14.7371°W 0.46 long 0.14 left
1-23-61	90D	8.20°S 14.70°W	8.1839°S 14.7013°W 0.62 short 0.77 left	8.1963°S 14.6960°W 0.08 long 0.32 left	8.2062°S 14.7076°W 0.18 short 0.55 right	8.1973°S 14.7090°W 0.57 short 0.15 right	8.1870°S 14.7030°W 0.54 short 0.53 left	ND

NOTE:

NA - Not applicable
ND - No data
Miss distances given in nautical miles.

TABLE 3-4 RADIAL MISS DISTANCE

MISSILE NUMBER	TARGET RANGE (NM)	RADIAL MISS DISTANCE (NM)	DOWNRANGE	CROSSRANGE
56D	7,859	1.18	-0.55	1.04 L
54D	4,306	1.54	-0.94	1.22 R
62D	4,390	14.77 (1)	+14.75	0.72 L
27D	4,390	0.77	-0.64	0.43 L
60D	4,306	39.31 (2)	-39.08	4.26 R
32D	6,350	4.20	+3.84	1.7 L
66D	4,390	1.86	-1.64	0.87 L
76D	4,390	2.82	+0.86	2.69 R
79D	7,859	3.81	+3.81	0.05 L
71D	4,390	3.53	-3.50	0.47 L
55D	6,350	1.27	+0.42	1.2 L
83D	4,390	0.27	-0.22	0.16 L
90D	4,390	0.99	-0.62	0.77 L

(1) Overshoot due to failure of guidance discrete to effect vernier engine cutoff.

(2) Abnormal propulsion system operation caused by electrical short.

NOTE: Impact location system data used in following order according to availability and/or validity; MILS Splash Net data and GE San Salvador Impact Predictor (System 4).

Figure 3-1 is a graphic presentation of the miss distance data listed in Table 3-3. The intersection of the zero-miss axes represents the assigned target for each case regardless of its actual location on the earth. Data for Missiles 60D and 62D are not shown due to the limited scale of the plot.

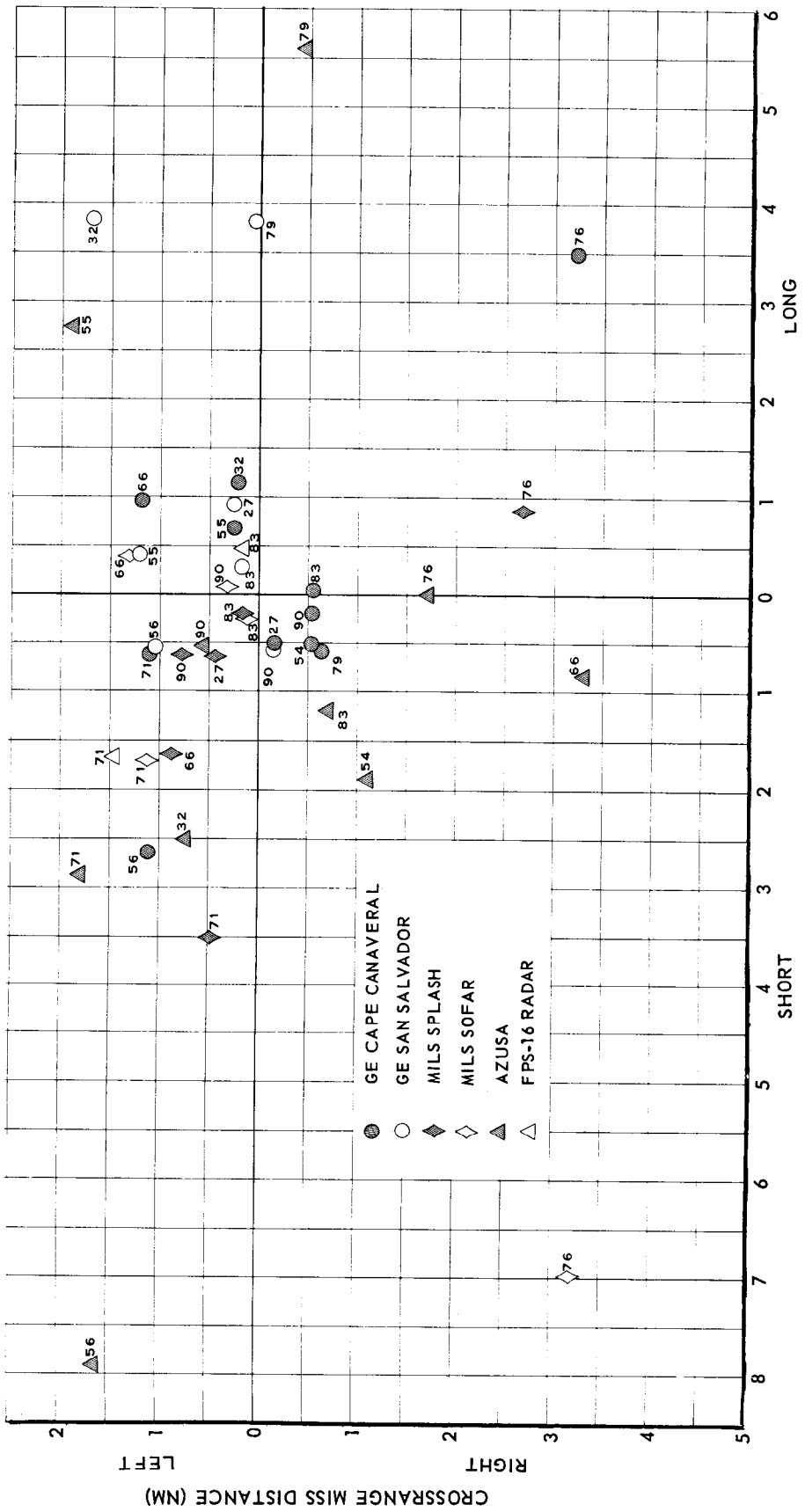

FIGURE 3-1 DEVIATION OF IMPACT POINTS FROM ASSIGNED TARGET

A study of the distribution of the plotted data of Figure 3-1 shows that, of the readings obtained by all systems, 56.25% indicate the impact point was short, and 64.58% indicate the impact point was to the left with respect to the assigned target. However, on only 6 of the 13 applicable tests did all systems agree as to the direction of the miss, i.e., long or short, left or right. It is of further interest to note that, when the directions most often indicated by each system are compared separately, the following results are obtained.

System	Direction of Miss Most Often Indicated
MILS Splash Net	Short and to left
MILS Sofar	Short and to left
GE System 1 (Cape Canaveral)	Short and to right
GE System 4 (San Salvador)	Long and to left
Azusa	Short with even crossrange distribution
FPS-16 Radar	Short and to left

The above table indicates that, in general, the two GE systems disagree on one count each with all other systems, and that the two GE systems generally disagree with each other on both counts.

Seven of the subject Series D missiles were assigned targets in the Ascension Island splash net area. Six of these tests impacted within the sensing area of the splash net although two were on a marginal basis. Figure 3-2 is an outline of the Ascension Island splash net hydrophone array showing the impact points and assigned targets for the six successful tests. The accuracy of the data for Missiles 90D, 71D and 76D has been diluted by the location of the targets outside of or bordering the hydrophone array.

The maximum miss distance shown in Figure 3-2 is 3.53 nautical miles for Missile 71D. The average miss distance for the six tests is 1.71 nautical miles.

A useful measure of the accuracy of a missile system to strike the assigned target is that of the circular probable error, commonly designated CEP. This parameter defines the radius of a circle within which 50% of the missiles will impact if a normal circular distribution function is applicable. The pattern of impact points of long range ballistic missile re-entry vehicles and/or warheads is considered to be of this form.

$$CEP = 1.1774 \sqrt{\frac{\sum_{i=1}^{n} (\bar{R} - R_i)^2}{n}} \qquad (1)$$

where:

n = number of tests in sample

$\bar{R}$ = the average radial miss distance

R_i = the radial miss distance of the i^{th} test

Applying the CEP concept to all successful Series D missiles having assigned targets in the Ascension Island splash net area, where "success" is arbitrarily defined as impact within 10 nautical miles of the target, a CEP of 1.70 nautical miles is obtained. The "success" limitation of 10 nautical miles has been selected as compatible with the effective damage radius of thermonuclear warheads.

An over-all performance record of the principal impact location systems is given in Table 3-5. Relative accuracy of the various systems is not reflected in these results.

TABLE 3-5 PERFORMANCE OF IMPACT LOCATION SYSTEMS

MISSILE NUMBER	IMPACT PREDICTORS			MILS SYSTEM	
	GE SYSTEM 1 (CAPE CANAVERAL)	GE SYSTEM 4 (SAN SALVADOR)	AZUSA	SPLASH NET	SOFAR
56D	X	X	X	NA	NA
54D	X	NA	X	NA	NA
62D	X	X	X	X	
27D	X	X		X	
60D	X	NA	X	NA	NA
32D	X	X	X	NA	NA
66D	X	NA	X	X	X
76D	X	NA	X	X	X
79D	X	X	X	NA	NA
71D	X	NA	X	X	X
55D	X	X	X	NA	NA
83D	X	X	X	X	X
90D	X	X	X	X	X

X Indicates data obtained NA Not applicable

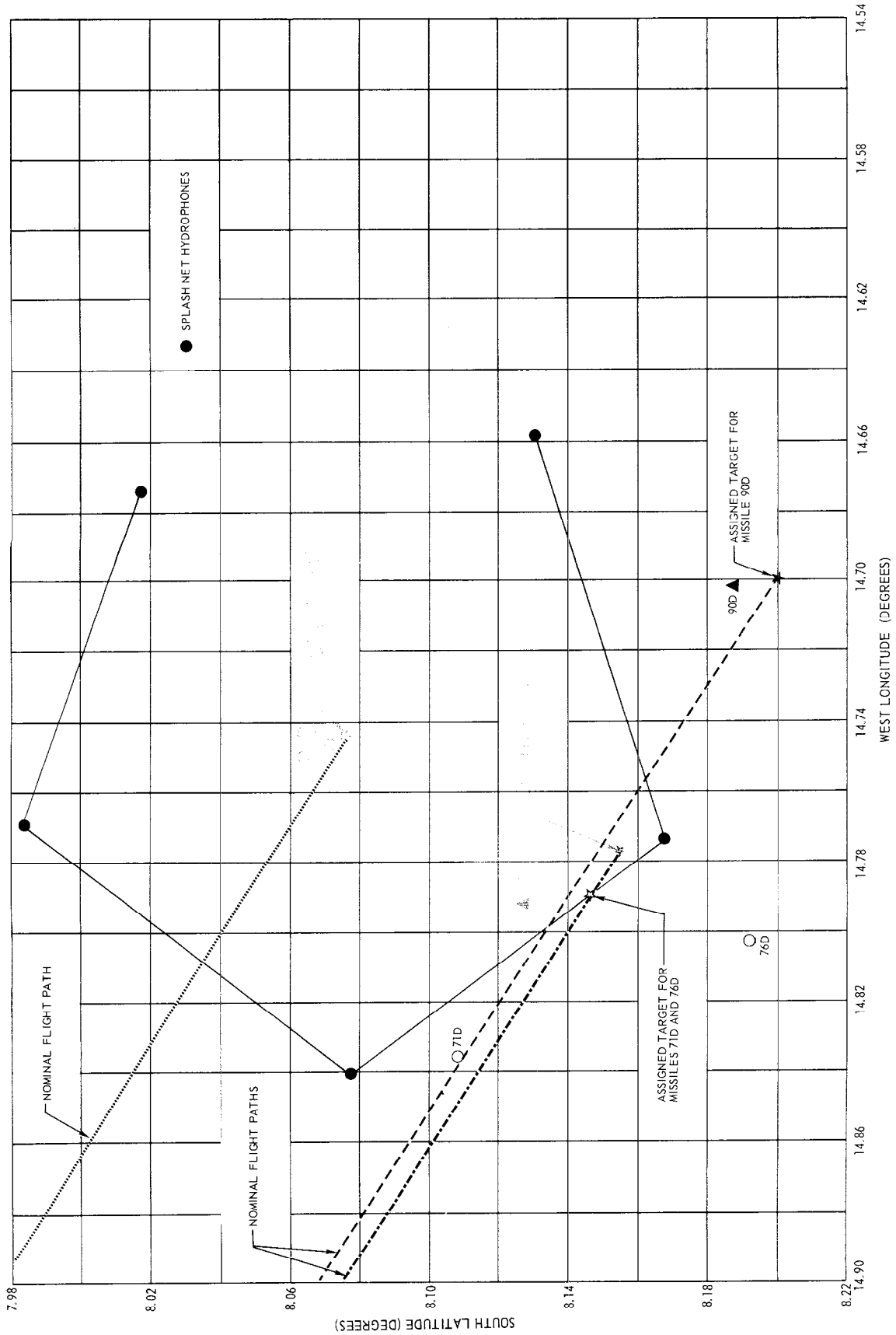

FIGURE 3-2 IMPACT DESPERSION ACCORDING TO MILS SPLASH NET DATA

General Flight Parameters

The free-fall trajectory of a ballistic missile is completely determined by the space position and the velocity vector parameters at the end of powered flight. For a given mission, variation of these parameters will yield a different range to target or, within limits, variations of these parameters can be made to yield the same range to target by following elliptical paths of different eccentricities.

Table 3-6 illustrates this point for four sub-groups of Series D R&D missiles, each of the four sub-groups having a common target range. Within each group, the tests are listed in order of ascending altitude at vernier engine cutoff. It will be seen that, as the altitude at vernier engine cutoff for a given range is increased, the required velocity magnitude decreases and the flight path angle increases. The flight path angle is the angle the velocity vector makes with the local horizontal and, together with the velocity magnitude, is considered to completely define the velocity vector since the yaw steering error should be zero at this time.

TABLE 3-6 VARIATION OF RANGE WITH FLIGHT PARAMETERS AT VCO

MISSILE NO.	RANGE TO IMPACT (NM)	ALTITUDE (ft)	PERCENT INCREASE	VELOCITY (ft/sec)	PERCENT CHANGE	FLIGHT PATH ANGLE (deg)	PERCENT CHANGE	PROPELLANTS CONSUMED (lbs)	PERCENT CHANGE	ENGINE CUTOFF TIMES BOOST	SUST	VERN	RATIO OF DURATION OF SUSTAINER PHASE TO BOOSTER PHASE
56D	7859	1,085,010		23,521		20.85		243,764		138.96	279.50	294.72	1.0114
54D	4306	982,612		20,225		22.13		236,178		140.12	246.21	259.20	0.7571
62D	4390	1,288,326	5.36	19,936	-0.32	25.16	+4.92	221,034	-5.88	119.04	285.89	305.29	1.4016
27D	4390	1,222,830	6.93	20,000	-0.51	23.98	+3.36	234,846	-3.25	130.98	282.95	302.35	1.1602
60D	4306	982,612	0	20,225	0	22.13	0	236,178	0	140.12	246.21	259.20	0.7571
32D	6350	1,174,509	2.14	22,288	+4.89	22.45	+5.65	238,382	+0.08	133.27	285.49	301.16	1.1422
66D	4390	1,025,034	0.74	20,296	-0.05	21.04	+1.99	238,549	-1.23	137.62	267.52	280.52	0.9439
76D	4390	1,017,448	1.22	20,307	-0.13	20.63	+4.61	241,513	-0.08	139.12	272.02	285.08	0.9553
71D	4390	1,027,644	0.25	20,294	-0.01	20.45	-2.80	242,498	+1.66	139.62	273.59	288.52	0.9595
55D	6350	1,149,838		21,248		21.25		238,185		138.06	287.70	306.60	1.0839
83D	4390	1,143,575	11.28	20,103	-0.94	23.20	+13.45	242,727	+0.09	138.76	276.58	293.78	0.9932
79D	7859	1,088,539	0.32	23,467	-0.23	20.23	-2.97	244,331	+0.23	138.08	286.53	302.29	1.0751
90D	4390	1,005,208		20,330		19.73		241.717		136.27	277.67	294.43	1.0376

Slight deviations from this general statement occur with respect to the increase in flight path angle. However, in such cases the duration of powered flight will be noted to vary also such that the range of the missile from the launch site at cutoff time is greater for cases where the flight path angle is lower (e.g., 71D). Conversely, where the range is shorter, the flight path angle is greater.

The initial phase of a ballistic missile trajectory is designed to get the missile out of the atmosphere as soon as possible, compatible with heating and acceleration limitations, and to roughly establish the missile on the desired elliptical trajectory. For Atlas missile tests this initial phase is considered to extend to booster engines cutoff and staging.

Various criteria have been used on Atlas Series D tests for determining when the guidance system should transmit the booster cutoff discrete signal. Flight articles employing the GE radio inertial guidance system (RIG) have used two criteria, namely, the attainment of a specified altitude, or the attainment of a specified slant range from the guidance system tracker. Flight articles guided by the Arma inertial guidance system (AIG) have used as a criterion the attainment of a specified value of the downrange component of inertial velocity.

Figure 3-3 is a graphical presentation showing the performance of the subject Series D missiles with respect to the applicable booster cutoff criterion. The intersection of the zero deviation axes represents perfect adherence to the planned cutoff criterion. The axis of abscissas has two scales, one for the RIG criteria and one for the AIG velocity criterion.

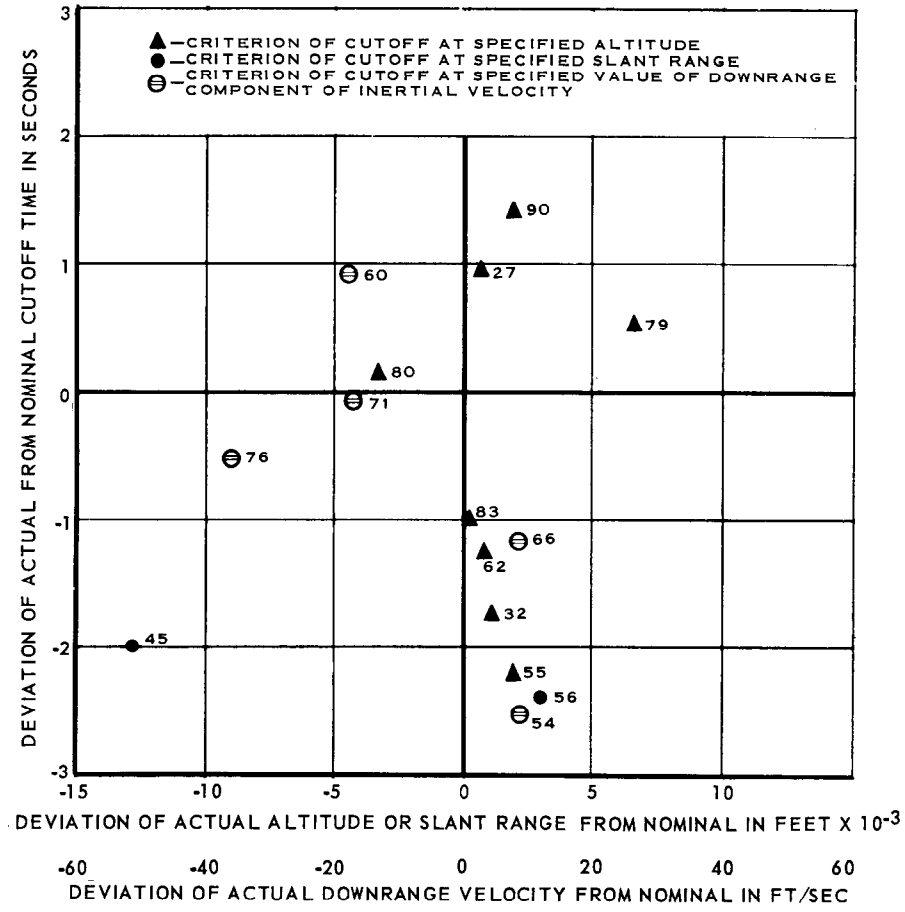

FIGURE 3-3 FLIGHT PERFORMANCE WITH RESPECT TO BOOSTER CUTOFF CRITERION

Table 3-7 lists planned versus actual time and velocity data at the three successive cutoff events for all subject tests. Whereas velocity only serves as the booster cutoff criterion for AIG tests, it is the sustainer and vernier engine cutoff criterion for all tests. Both RIG and AIG guidance systems continuously monitor the real-time missile position and velocity data. The RIG ground based computer receives these data from its tracker while the AIG missile-borne computer integrates accelerometer data. Both systems compute the velocity vector required to effect impact on the assigned target (stored in the computer) from the instantaneous space position of the missile. When the achieved velocity differs from the required velocity by a predetermined amount the sustainer engine cutoff discrete signal is transmitted.

TABLE 3-7 COMPARISON OF CUTOFF TIMES AND VELOCITIES

MISSILE NUMBER	BOOSTER CUTOFF TIME (sec) PLAN	BOOSTER CUTOFF TIME (sec) ACTUAL	BOOSTER CUTOFF VELOCITY (ft/sec) PLAN	BOOSTER CUTOFF VELOCITY (ft/sec) ACTUAL	SUSTAINER CUTOFF TIME (sec) PLAN	SUSTAINER CUTOFF TIME (sec) ACTUAL	SUSTAINER CUTOFF VELOCITY (ft/sec) PLAN	SUSTAINER CUTOFF VELOCITY (ft/sec) ACTUAL	VERNIER CUTOFF TIME (sec) PLAN	VERNIER CUTOFF TIME (sec) ACTUAL	VERNIER CUTOFF VELOCITY (ft/sec) PLAN	VERNIER CUTOFF VELOCITY (ft/sec) ACTUAL
56D	138.96	136.57	10,683	10,871	279.50	271.06	23,613	23,601	294.72	285.00	23,521	23,554
54D	140.12	137.62	11,527	11,362	246.21	235.55	20,335	20,300	259.20	242.79	20,225	20,265
62D	119.04	117.77	8,501	8,523	285.89	284.26	20,109	20,071	305.29	307.69	19,936	19,893
27D	130.98	131.94	9,350	9,595	282.95	278.68	20,167	20,151	302.35	292.03	20,000	20,066
60D(1)	140.12	141.03	11,362	11,684	246.21	307.55	20,335	19,604	259.20	277.45	20,225	19,346
32D	133.27	131.55	9,843	9,726	285.49	288.09	22,398	22,346	301.16	302.00	22,288	22,301
66D	137.62	136.45	10,380	10,566	267.52	259.24	20,399	20,271	280.52	274.43	20,296	20,170
76D	139.12	138.59	10,503	10,497	272.02	274.89	20,409	20,334	285.08	290.91	20,307	20,228
79D	138.08	138.59	10,342	10,622	286.53	282.47	23,558	23,482	302.29	295.22	23,467	23,509
71D	139.62	139.56	10,302	10,419	273.59	266.73	20,408	20,309	288.52	280.71	20,309	21,248
55D	138.06	135.86	10,096	10,204	287.69	283.04	22,387	22,395	306.60	298.13	21,248	22,323
83D	138.76	137.75	10,060	10,250	276.58	269.91	20,257	20,294	293.78	286.34	20,103	20,108
90D	136.27	137.66	9,898	10,206	277.67	271.93	20,450	ND	294.43	289.77	20,330	ND
45D	148.78	146.78	11,710	11,527	238.89	238.52	18,474	18,428	256.74	257.59	18,372	18,344
80D	140.00	140.11	10,505	10,592	275.40	271.22	21,558	21,484	277.40(2)	273.53(2)	21,539(2)	21,506(2)

(1) Vernier shutdown during sustainer phase and abnormal propulsion system operation.

(2) Value at upper stage ignition start.

ND No data

The velocity decreases on a very slight gradient during vernier solo allowing fine adjustment of the final cutoff velocity to the required magnitude. The required velocity, which is continuously being determined by the computer, is also falling off as the attained range and altitude of the missile increases. In this manner the actual and required velocities approach each other very gradually during vernier phase. When the difference between the two becomes zero the vernier engine cutoff discrete signal is initiated.

Reference to the data of Table 3-7 shows that, when the actual velocity at booster cutoff exceeds the nominal value, the duration of the sustainer phase is shortened. Conversely, when booster cutoff velocity is less than nominal, sustainer phase duration is lengthened. The exceptions to this statement were Missiles 60D and 54D. The former suffered abnormal propulsion system operation. Missile 54D had an unplanned additional holddown before launch which lightened the propellant load and permitted high acceleration and early cutoff times.

Table 3-8 compares nominal and actual values of the flight path angle, previously defined. The actual flight path angles were computed from velocity components along the coordinate system axes used for tracking data reference and are corrected to the local horizontal as reference. The average deviation of the actual flight path angle from the nominal is seen to decrease with the successive cutoff events. The standard deviation increases with successive cutoff events, however, which seems to reflect greater differences in velocity vector requirements between later portions of the various tests and, to a small extent, increasing inaccuracy in the metric tracking data as the missile range from the tracker increases.

TABLE 3-8 COMPARISON OF FLIGHT PATH ANGLES AT CUTOFF TIMES

MISSILE NO.		NOMINAL TIME (sec)	NOMINAL ANGLE (deg)	ACTUAL TIME (sec)	ACTUAL ANGLE (deg)	DEVIATION FROM NOMINAL ANGLE (deg)
56D	(1)	138.96	23.66	126.57	23.93	-0.56
	(2)	279.50	20.86	271.06	21.06	+0.20
	(3)	294.72	20.85	285.00	20.86	+0.01
45D	(1)	148.78	22.80	146.78	23.31	+0.51
	(2)	238.89	15.34	238.52	15.18	-0.16
	(3)	256.74	14.69	257.59	14.56	-0.13
54D	(1)	140.12	26.81	137.62	28.22	+1.41
	(2)	246.21	22.38	235.55	22.96	+0.58
	(3)	259.20	22.13	242.79	22.83	+0.70
62D	(1)	119.04	32.87	117.77	34.00	+1.13
	(2)	285.89	25.52	284.26	25.75	+0.23
	(3)	305.29	25.16	307.69	25.37	+0.21
27D	(1)	130.98	29.92	131.94	29.36	-0.56
	(2)	282.95	24.35	278.68	24.39	+0.04
	(3)	302.35	23.98	292.03	24.15	+0.17
60D	(1)	140.12	26.81	141.03	30.03	+3.22
	(2)	246.21	22.39	307.55	22.74	+0.35
	(3)	259.20	22.13	277.45	21.32	-0.81
32D	(1)	133.27	26.97	131.55	28.68	+1.71
	(2)	285.49	22.56	288.09	24.03	+1.47
	(3)	301.16	22.45	302.00	24.16	+1.71
66D	(1)	137.62	26.90	136.45	30.40	+3.50
	(2)	267.52	21.29	259.24	23.29	+2.00
	(3)	280.52	21.04	274.43	23.17	+2.13
76D	(1)	139.12	26.31	138.59	27.43	+1.12
	(2)	272.02	20.89	274.89	21.03	+0.14
	(3)	285.08	20.63	290.91	20.81	+0.18
79D	(1)	138.08	22.79	138.59	23.61	+0.82
	(2)	286.53	20.25	282.47	19.95	-0.30
	(3)	302.29	20.23	295.22	19.95	-0.28
80D	(1)	140.00	27.73	140.11	27.62	-0.11
	(2)	275.40	26.29	271.22	22.70	-3.59
	(3)	277.40	26.27	273.53	22.44	-3.83
71D	(1)	139.62	76.11	139.56	29.13	+3.02
	(2)	273.59	20.74	266.73	22.62	+1.88
	(3)	288.52	20.45	280.71	22.22	+1.77
55D	(1)	138.06	25.39	135.86	25.96	+0.57
	(2)	287.70	21.39	283.04	22.67	+1.28
	(3)	306.60	21.25	298.13	22.62	+1.37
83D	(1)	138.76	28.09	137.75	27.89	-0.20
	(2)	276.58	23.53	269.91	22.94	-0.59
	(3)	293.78	23.20	286.34	23.00	-0.20
90D	(1)	136.27	25.12	137.66	24.44	-0.68
	(2)	277.67	20.04	271.93	No Data	No Data
	(3)	294.43	19.73	289.77	No Data	No Data

Standard Deviation of Flight Path Angle = (1) 1.29 degrees
(2) 1.32 degrees
(3) 1.41 degrees

Average Deviation of Flight Path Angle = (1) 1.05 degrees
(2) +0.25 degrees
(3) +0.21 degrees

Code: (1) Value at Booster Cutoff.
(2) Value at Sustainer Cutoff.
(3) Value at Vernier Cutoff.

Table 3-9 compares actual and nominal peak acceleration data for the three phases of powered flight. Acceleration data for the missiles guided by the Arma inertial system flying closed-loop, namely, 54D, 60D, 66D, 71D and 76D, were obtained from the guidance system accelerometers. Acceleration data for all other tests discussed in this section were obtained by telemetry from a single accelerometer sensing only axial acceleration. Data from the guidance system reflects the resultant of accelerations along the three accelerometer axes. The table contains, in addition, the average and standard deviations from the nominal for both time and acceleration at the booster and sustainer peak values. These were not calculated for vernier engine cutoff data because of the small accelerations encountered at that time. General high acceleration performance is evident from the table as is indicated in the earlier than nominal average cutoff time and the higher than nominal average acceleration. These points are graphically emphasized in Figure 3-4 where the time and acceleration deviations of Table 3-9 are plotted for booster and sustainer engines cutoff.

TABLE 3-9 COMPARISON OF MISSILE ACCELERATION AT CUTOFF TIMES

MISSILE NUMBER	BOOSTER CUTOFF				SUSTAINER CUTOFF				VERNIER CUTOFF			
	TIME (sec)		ACCELERATION (g's)		TIME (sec)		ACCELERATION (g's)		TIME (sec)		ACCELERATION (g's)	
	PLAN	ACTUAL	PLAN	ACTUAL	PLAN	ACTUAL	PLAN	ACTUAL	PLAN	ACTUAL	PLAN	ACTUAL
48D	EXPLODED ON PAD											
56D	138.96	136.57	8.056	8.303	279.50	271.06	7.330	7.443	294.72	285.00	0.138	0.05
54D	140.12	137.62	8.869	9.430	246.21	235.55	5.289	5.563	259.20	242.79	0.0836	0.100
62D	119.04	117.77	6.79	6.67	285.89	284.26	5.69	5.59	305.29	307.68	0.107	0.100
27D	130.98	131.94	7.129	7.264	282.95	278.68	5.374	5.393	302.35	294.03	0.1	0.125
60D	140.12	141.03	8.87	9.261	246.50	307.55	5.31	(1)	259.20	277.45	0.084	(1)
32D	133.27	131.549	7.479	7.473	285.49	288.09	6.680	6.887	301.16	301.997	0.125	0.126
66D	137.62	136.45	7.86	8.28	267.52	259.24	5.25	5.40	280.52	274.43	0.083	0.054
76D	139.12	138.59	7.72	7.78	272.02	274.89	5.19	5.18	285.08	290.91	0.08	0.07
79D	138.08	138.59	7.72	7.92	286.53	282.47	7.25	7.27	302.29	295.22	0.136	0.14
71D	139.62	139.56	7.68	7.54	273.59	266.73	5.17	5.34	288.52	280.71	0.08	0.12
55D	138.06	135.86	7.51	7.81	287.7	283.04	6.47	6.76	306.60	298.13	0.103	0.11
83D	138.76	137.75	7.49	7.74	276.58	269.91	5.19	5.36	293.78	286.34	0.081	0.11
90D	136.27	137.66	7.38	7.57	277.67	271.93	5.30	5.24	294.43	289.77	0.084	0.1
45D(2)	148.78	146.78	8.67	8.60	238.89	238.52	3.98	3.97	256.74	257.59	0.063	0.08
80D(3)	140.0	140.11	7.89	8.09	275.4	271.22	6.23	6.05	280.4	290.90	NA	0.18
	Average Δt = -0.73 Standard Deviation = 1.264		Average ΔA = +0.17 Standard Deviation = 0.196		Average Δt = -4.31 Standard Deviation = 3.870		Average ΔA = +0.075 Standard Deviation = 0.137					

(1) Values for SCO and VCO not quoted due to abnormal propulsion performance.

(2) Booster for the Midas satellite vehicle.

(3) Booster for the Able lunar probe upper stage.

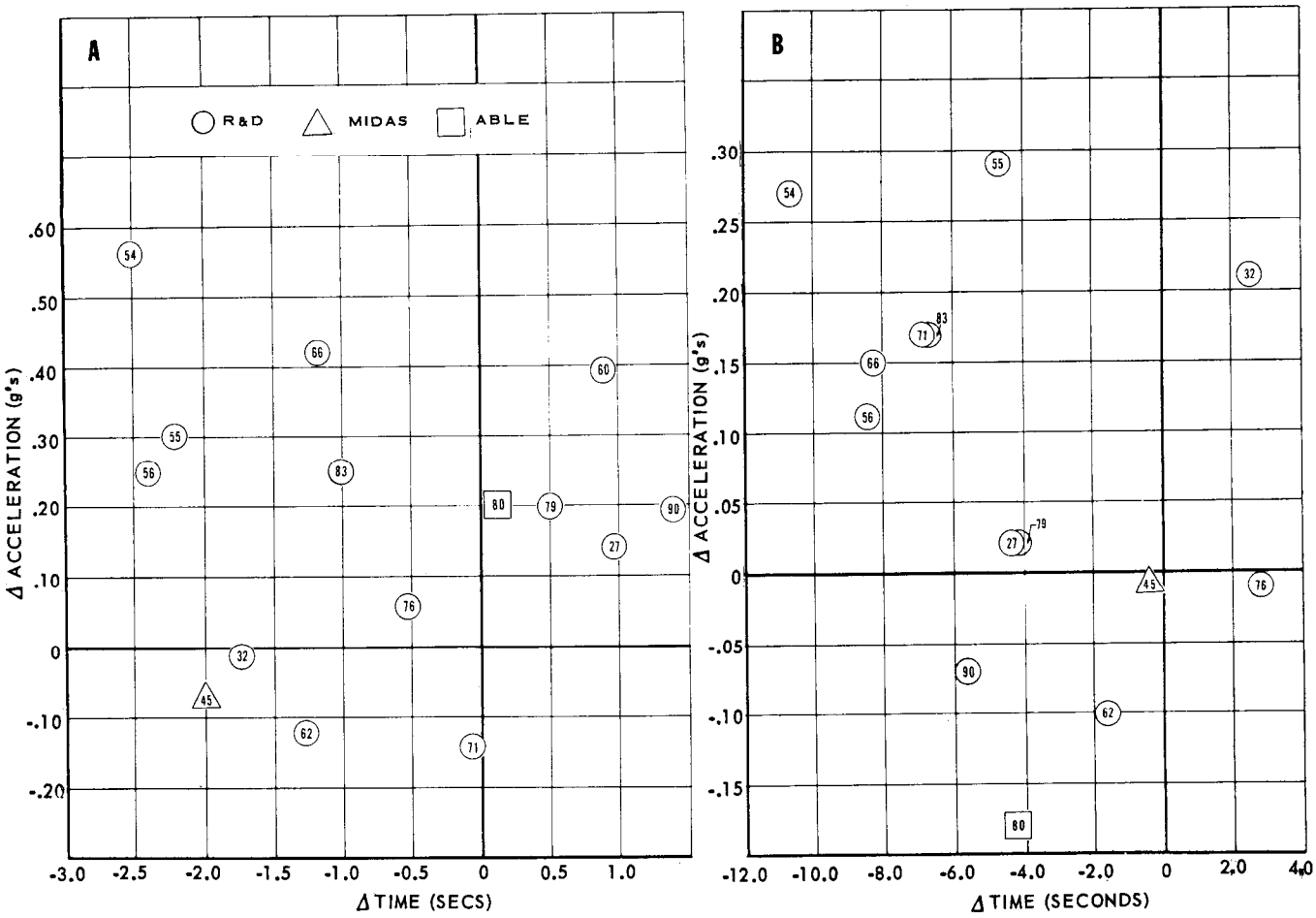

FIGURE 3-4 DEVIATIONS OF TIME AND ACCELERATION

Dynamic Pressure and Mach Number

Dynamic pressure is the pressure of the environmental medium, per unit area of surface, experienced by an object by virtue of its motion through that medium. For a ballistic missile the dynamic pressure is generated by the passage of the missile through the atmosphere, and is a direct function of the velocity of the missile with respect to the atmosphere and the density of the latter at the point in question. In treating dynamic pressures associated with supersonic vehicles the relationship

$$q = 0.7\ P_a M^2 \qquad (1)$$

is used, where:

q = dynamic pressure

P_a = ambient pressure

M = Mach number = ratio of velocity of vehicle to local velocity of sound.

Table 3-10 lists the nominal and actual values of altitude and ambient pressure at which maximum dynamic pressure occurred, together with the maximum dynamic pressure and corresponding Mach number. Average values of each tabulated item are given, also, the standard deviations for both nominal and actual maximum "q". The averaged actual values of all items are seen to exceed the corresponding nominal values. These increases are partially attributable to high missile velocities and partially to deviations of the actual atmospheric temperature and pressure from the standard model used to compute nominal M and q.

In the determination of Mach number, the missile velocity should be taken as the velocity with respect to the atmosphere rather than the earth-relative velocity as measured by the tracking system. The effects of the motion of the atmosphere with respect to the earth must be taken into account if they are of significant magnitude and direction to affect the calculated results. By coincidence, the altitude region at which the maximum winds are encountered at AMR includes the altitude interval at which maximum dynamic pressure occurs so that, with with an adverse combination of wind speed and direction, the dynamic pressure on the missile may be significantly increased at a critical time.

TABLE 3-10 CONDITIONS OF MAXIMUM DYNAMIC PRESSURE

	NOMINAL					ACTUAL				
MISSILE	TIME	ALT	MACH #	PSTD.	MAX Q	TIME	ALT	MACH #	P_A (PSI)	MAX Q
56D	65.5	41,332	1.83	2.6	951	65.0	42,968	1.953	2.58	991
54D	65	42,042	1.87	2.5	957	62.5	41,047	1.851	2.81	969
62D	58.5	40,180	1.83	2.7	978	59.0	41,818	1.89	2.65	1,010
27D	64	41,865	1.83	2.65	928	65	42,566	1.892	2.67	963
60D	65	42,042	1.87	2.5	957	64.6	41,219	1.83	2.85	963
32D	65	42,799	1.89	2.37	939	65	43,650	1.96	2.52	974
66D	66	42,325	1.88	2.4	953	65	43,100	1.926	2.57	963
76D	66	40,812	1.81	2.62	952	67.8	42,711	1.917	2.64	980
79D	66	44,351	1.82	2.22	948	67	42,436	1.90	2.75	996
71D	65	38,963	1.77	2.9	952	65	39,481	1.783	2.99	960
55D	67	42,444	1.87	2.4	931	67.5	44,693	2.04	2.36	992
83D	66	40,500	1.80	2.6	937	67.5	42,850	1.92	2.57	954
90D	66	40,931	1.81	2.61	1,002	66	41,037	1.83	2.77	968
TOTAL	845	540,586	23.88	33.07	12,385	846.9	549,576	24.692	34.73	12,683
AVERAGE	65.0	41,584	1.84	2.54	953	65.2	42,275	1.899	2.67	976
Nominal standard deviation of q max = 18.9 (R&D test)						Actual standard deviation of q max = 16.2 (R&D test)				
Special Vehicles										
45 (Midas)	65	36,631	1.65	3.21	886	70.0	43,702	1.970	2.44	954
80 (Able)	64	38,760	1.73	2.90	874	69	44,851	2.0	2.44	969
TOTAL	974	615,977	27.26	39.18	14,145	985.9	638,129	28.662	39.61	14,606
AVERAGE	64.9	41,065	1.82	2.61	943	65.7	42,542	1.911	2.64	974

Figure 3-5 shows a typical curve of dynamic pressure as a function of time. Superimposed on this plot are the time interval limits for the occurrence of maximum dynamic pressure and the time interval limits within which maximum winds existed with respect to the Series D missiles time in flight.

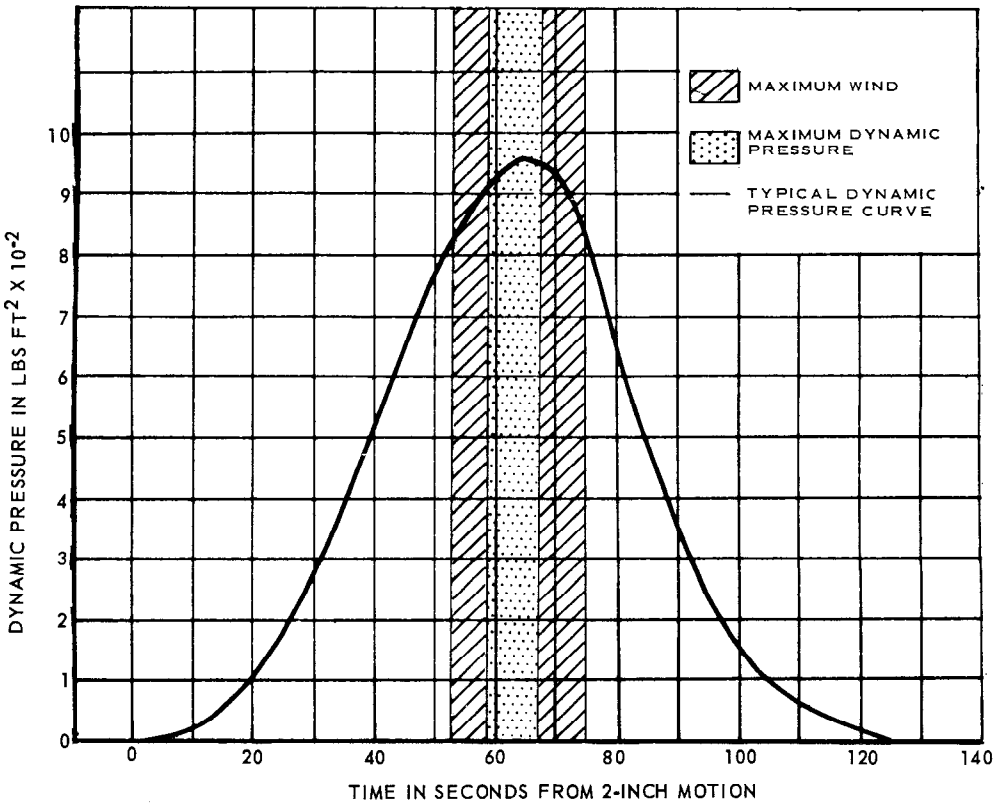

FIGURE 3-5 TYPICAL BUILDUP AND DECAY OF DYNAMIC PRESSURE

Figure 3-6 represents a "wind-rose" type graph showing at once the direction, speed, altitude of occurrence, time of year and missile concerned for the maximum winds in the region of maximum dynamic pressure at AMR.

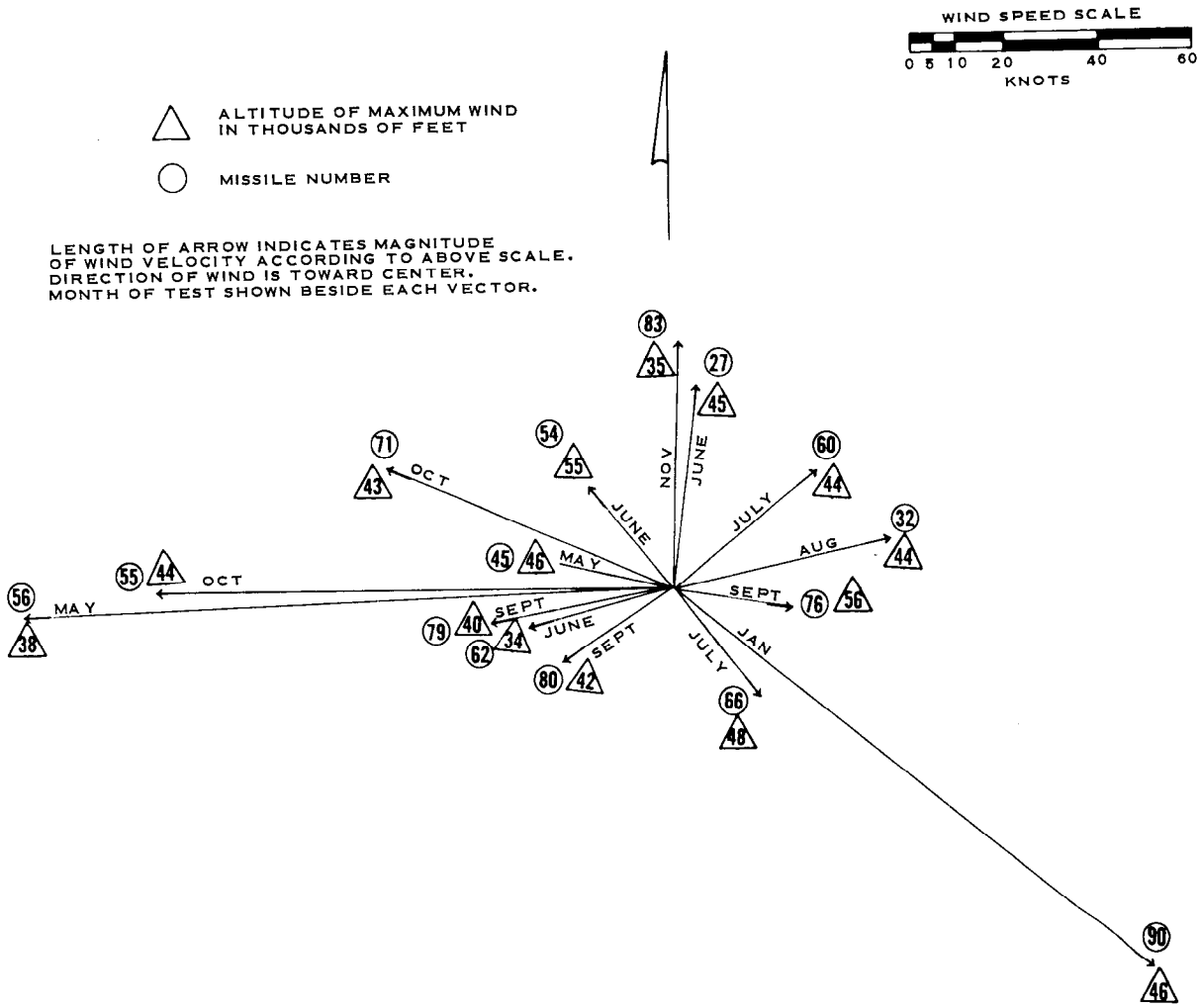

FIGURE 3-6 ALTITUDE, MAGNITUDE AND DIRECTION OF MAXIMUM WINDS DURING LAUNCH

Optical Beacon Trajectory Data

The Atlas missileborne high-intensity optical beacon system was designed for the specific application of obtaining precision position and velocity data during the vernier solo phase of flight, for performance evaluation of the guidance system.

The system consists essentially of a strobe lamp (gas-filled hollow-tube filament) with a luminous energy of 1,200 candle-seconds per flash at the center of the beam, a programmer, battery and associated circuitry. Reference Figure 3-7. The sustainer engine cutoff signal activates the optical beacon battery which, though a programmer and a capacitor, causes the strobe lamp to flash for approximately one millisecond at the rate of two flashes per second. Advantages of the strobe optical beacon over the previously used photoflash cartridge beacon are as follows:

1. Allows for a greater accuracy in the determination of missile position because of the consistency of the image size and known location of the light flash.

2. Eliminates the possibility of damage to the missile structure that might result from the use of pyrotechnic devices.

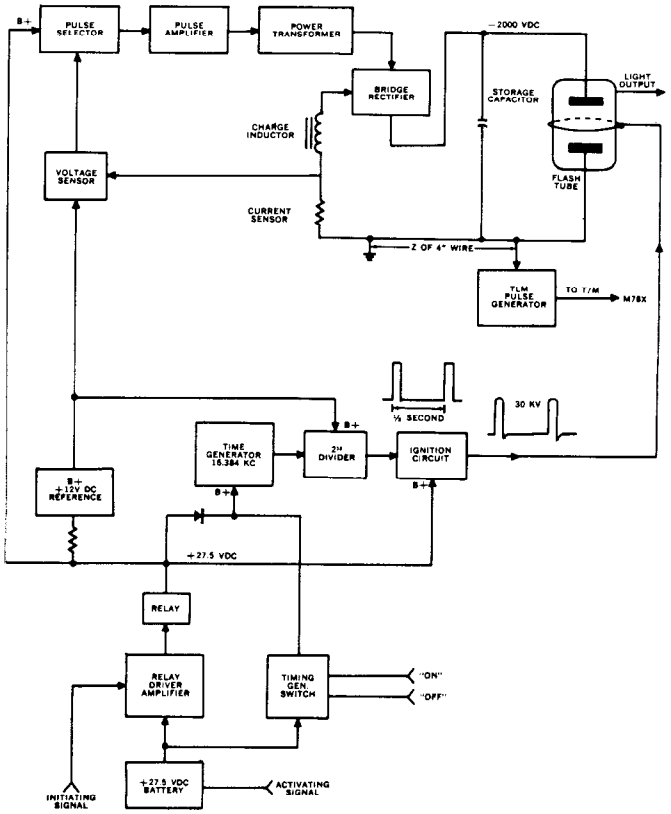

FIGURE 3-7 ATLAS OPTICAL BEACON SYSTEM

The light energy emitted from the strobe light, conditions permitting, is recorded on the photographic plates of ballistic cameras strategically located in the Bahama Islands.

The occurrence of each flash is telemetered to ground where it is recorded as a function of range timing. Each ballistic camera plate is exposed to a star-grid background for precise camera orientation determination. Angular position data of each flash with respect to the different camera locations are reduced to missile space position data by triangulation techniques.

Table 3-11 is a summary of the over-all performance of the strobe light-ballistic camera systems combination in Series D test program. Of nine tests on which the strobe light was carried, six were satisfactory, one partially so, and two were unsatisfactory. Data was recorded on only three (55D, 71D, 83D) of the six successful tests, however. Cloud cover or daylight operation precluded photographic recording of the flashes on the other three.

TABLE 3-11 OPTICAL BEACON/BALLISTIC CAMERA PERFORMANCE

MISSILE NUMBER	STROBE CARRIED	OPERATION AS INDICATED BY TELEMETRY DATA	NUMBER OF FLASHES INDICATED BY TELEMETRY DATA	FLASH SPACING	PHOTO COVERAGE OBTAINED	NUMBER OF DATA POINTS OBTAINED BY PHOTO COVERAGE	REMARKS
54D	Yes	Satisfactory	86	Satisfactory	No		No data was recorded by the ballistic cameras due to cloud cover and rain.
62D	Yes	Satisfactory	77	Satisfactory	No		Daylight flight precluded photographic recording. Operation was otherwise satisfactory.
27D	Yes	Unsatisfactory		Unsatisfactory			Ballistic camera plates showed sustainer engine flame but no indication of flashes. Telemetry data indicate abnormal operation of either or both systems (telemetry and/or beacon).
60D	Yes	Satisfactory	60+	Satisfactory	No		Strobe system was not activated until initiation of manual fuel cutoff, thus being 90 seconds late. Cameras were not oriepted for this portion of flight. Operation was otherwise satisfactory.
32D	No						
66D	No						
76D	Yes	Satisfactory	64	Satisfactory	No		Ballistic cameras could not pick-up flashes due to cloud cover.
79D	No						
71D	Yes	Unsatisfactory		Unsatisfactory	Yes	29	Data was recorded by ballistic cameras although timing of flashes was erratic due to spurious timing bursts in telemetry records. Some data was obtained.
55D	Yes	Satisfactory	77	Satisfactory	Yes	79	Operation was satisfactory.
83D	Yes	Satisfactory	65	Satisfactory	Yes	49	Operation was satisfactory.
90D	Yes	Satisfactory	67	Satisfactory	No		Daylight flight precluded photographic recording. Operation was otherwise satisfactory.

Table 3-12 indicates the accuracy of the position data obtained by the ballistic cameras recording the strobe light flashes. These estimates were made by the data reduction group of RCA acting as AMR range contractor.

TABLE 3-12 ESTIMATES OF OPTICAL BEACON/BALLISTIC CAMERA ACCURACY

MISSILE NO.	FLIGHT TIME INTERVAL (SEC FROM LIFTOFF)	STANDARD DEVIATIONS (FT) X	Y	Z	TOTAL	NUMBER OF EFFECTIVE CAMERA STATIONS
55D	284.132 to 324.132	38.08	53.76	86.08	108.40	4 to 5
71D	268.0683 to 282.0671	19.31	33.16	39.40	55.00	4
83D	277.528 to 299.527	14.96	20.16	22.24	33.54	3
	300.027 to 303.027	32.66	70.99	70.02	104.92	
	277.528 to 303.027	17.49	26.74	29.07	43.21	

Terminal Trajectory

The performance details of all aspects of re-entry are treated in a special section of this report. Figure 3-8 is included here for reference on typical terminal trajectory data. The effect of atmospheric drag on the terminal trajectory are shown by the greater decrease in velocity from re-entry to impact experienced by the longer range vehicle passing through a greater range of atmosphere.

Tracking systems coverage of the terminal trajectory is greatly complicated by the vehicle acquisition problem, high initial re-entry velocities and excessive angular tracking rate requirements. Both the Mod II and FPS-16 radar systems at Ascension Island have obtained some data during the subject tests. The time of flight intervals covered by these data are listed in Table 3-13. A comparison of the final tracking interval time with the time of impact for each test shows that in no case was it possible to track all the way to impact.

	FLIGHT PATH ANGLES (γ)		VELOCITIES (FT/SEC)	
	7859 NM RANGE	4389 NM RANGE	7859 RANGE	4389 RANGE
REENTRY	-21.06°	-26.11°	24,500	21,333
IMPACT	-43.87°	-82.77°	768	1,310
γ CHANGE DURING ATMOSPHERIC FLIGHT	-22.81°	- 6.66°	VELOCITY DECREASE THROUGH ATMOSPHERE. -23,832	-20,023

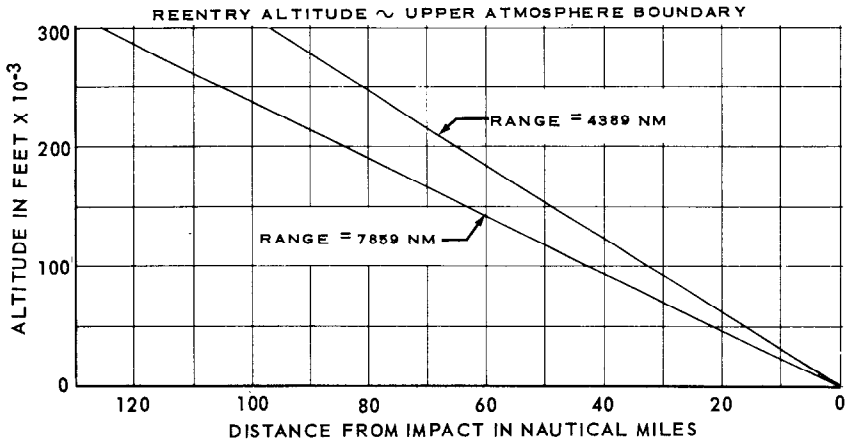

FIGURE 3-8 TYPICAL TERMINAL TRAJECTORY CURVES

TABLE 3-13 TERMINAL TRAJECTORY TRACKING COVERAGE

(AMR Tests - Ascension Island Area)

MISSILE NO.	TRACKING SYSTEM	TIME OF COVERAGE (sec) FROM	TO	TIME OF IMPACT (sec)
45D(1)	Mod II Radar, Station 12.2	1483.75	1487.75	NA
		1496.25	1543.75	
60D	FPS-16 Radar, Station 12.16	1712.81	1734.01	1890
		1735.81	1799.71	
32D	FPS-16 Radar, Station 12.16	1864.83	2059.43	2769
66D	FPS-16 Radar, Station 12.16	1631.54	1669.02	1945
		1775.04	1812.44	
		1828.24	1887.54	
76D	FPS-16 Radar, Station 12.16	1782.24	1819.64	1880
71D	FPS-16 Radar, Station 12.16	1768.36	1796.16	1918
83D	FPS-16 Radar, Station 12.16	1819.44	1895.84	1939

NOTE: (1) Although 45D was a Midas vehicle booster with no planned impact the trajectory followed permitted tracking as indicated.

Range Instrumentation

Data for the evaluation of missile trajectory performance may be obtained from a variety of tracking systems, impact predictors and impact location systems. The systems available for use at the AMR are listed in Table 3-14 together with a short functional description of each. Information on some non-metric systems is included for reference.

Actual performance of the principal metric data tracking systems is shown by the time of coverage listings of Table 3-15. The relative period of flight capable of coverage by each system is evident from the table, as well as the comparative reliability of each. It should be noted that the coverage intervals listed include only the metric data officially released by the AMR range contractor and do not necessarily represent all data originally available for any given test.

Table 3-16 showing estimated accuracies of the principal trajectory measurement systems was compiled from figures supplied with the data by the range contractor. In some cases a breakdown between random and systematic errors was not made and the published accuracies were assumed to reflect both types.

TABLE 3-14 ATLANTIC MISSILE RANGE INSTRUMENTATION

NAME	TYPE AND USE	FUNCTION	LOCATION
Azusa (FRW-1)	Electronic; Range Safety	Track the missileborne transponder to obtain position and velocity data. Predict impact point in real-time from trajectory data by use of the IBM-709 computer.	Cape Canaveral (ground station)
AN/FPS-16 Radar (XN-1)	Electronic; Range Safety	Same function as above except no transponder involved. Skin track the missile for data. Constitutes backup to Azusa as input to impact prediction calculation.	Cape Canaveral (XN-1) Note: FPS-16 radar (XN-2) is located at Grand Bahama Island
AN/ARW-59 and KY-55; Receiver-Decoder	Electronic; Range Safety Command System	Receives and decodes r-f transmissions of engine cutoff and/or missile destruct commands sent out by the range safety commands system.	Missileborne
RSC Transmitters	Electronic	Serve to transmit range safety commands to the missileborne unit.	As specified by AFMTC; presently at Cape Canaveral, San Salvador and Grand Turk
Mod II "S" Band Radar	Electronic; Re-entry phase trajectory data	Obtains position and velocity trajectory data by tracking beacon in re-entry vehicle during terminal phase.	Ascension Island and/or San Salvador as applicable
Azusa	Electronic; Trajectory data	Obtains missile position and velocity data for trajectory performance evaluation by tracking missileborne transponder.	Ground station at Cape Canaveral. Missileborne transponder
AN/FPS-16 Radar	Electronic; Trajectory data, powered and terminal flight phases.	Obtains missile position and velocity data for trajectory performance evaluation by "skin track" of missile and/or re-entry vehicle.	Cape Canaveral, Grand Bahama Island, Ascension Island, and San Salvador
Mod IV "X" Band Radar	Electronic; Trajectory data	Tracks missile during the first 500 feet of flight for trajectory performance purposes.	Cape Canaveral and Grand Bahama Island
BC-4 Ballistic Cameras	Optical; Trajectory data	Records space position of strobe light flashing on missile during the vernier phase of powered flight. Intended to yield highly accurate metric trajectory data for guidance tracker evaluation.	Cape Canaveral, Grand Bahama Island, Eleuthera, San Salvador, Grand Turk, Magaguana Antigua, and Ascension
Splash Net Hydrophone System	Acoustical; To locate actual impact point	To provide accurate measurement of actual impact point of re-entry vehicle for tests terminating at Ascension Island (Area 12) splash net.	Approximately 25 NM WSW of Ascension Island (Station 12) Antigua (Area 9)
SOFAR Bomb System	Acoustical; To locate actual point of bomb detonation.	Basic principle similar to splash net except a special bomb is used as signal source. Has greater effective range than splash system but is less accurate. Utilizes many scattered hydrophones.	Various locations in open ocean areas as well as near Antigua, Fernando de Noronha and Ascension Island stations.
Millstone Radar	Electronic; Trajectory data	Skin track the missile during flight to provide position data; tracking on engineering test basis by Lincoln Laboratories of MIT.	Millstone Hill, Mass
Telemetry Receivers	Electronic; Internal data	Track missile and/or re-entry vehicle to receive and record internal (missileborne) systems data during flight as transmitted by missileborne telemetry system.	TLM #2 at Cape Canaveral; others at Spruce Creek, Vero Beach, Jupiter (Sta. 2), Grand Bahama Is. (Sta. 3), Grand Turk (Sta. 7), San Salvador (Sta. 5), Antigua (Sta. 9), and Ascension Is. (Sta. 12)
Cinetheodolite system	Optical; Trajectory	35 mm pulse operated tracking cameras with azimuth and elevation angles recording on film. Supplies trajectory position and velocity data when data from two or more cameras are combined in solution.	Cape Canaveral; Patrick AFB
CZR-1 cameras	Optical; Trajectory data	Fixed orientation cameras supplying accurate position, velocity and acceleration data during initial launch period. Data from two or more cameras are combined in data reduction process.	Cape Canaveral
Recording Optical Tracking Instrument, ROTI	Optical; Trajectory data	500-inch focal length, long range Recording Optical Tracking Instrument. Supplies visual information on missile attitude and flight details. No quantitative tracking data at present.	Melbourne Beach, Vero Beach, and San Salvador
IGOR	Optical; Trajectory data	Long focal length tracking telescope with film recording. Not used for quantitative data.	Cape Canaveral; Patrick AFB and Melbourne Beach

TABLE 3-15 INTERVALS OF EXTERNAL TRAJECTORY DATA COVERAGE

MISSILE	AZUSA FROM	AZUSA TO	THEODOLITE FROM	THEODOLITE TO	RADAR FROM	RADAR TO	CZR FROM	CZR TO	OTHER FROM	OTHER TO	GRAND TOTAL (sec)	CUTOFF OR SHUTDOWN TIMES (sec)
56D	34.82	139.72	1.27	98.52	No Data		0.049	24.742	None			BCO 136.57
	140.32	208.42										SCO 271.06
	208.92	320.02										VCO 285.00
Total Seconds		284.10		97.25				24.693			406.043	
45D	41.75	57.95	2.50	147.00	34.25	238.55(1)	-0.029	26.780	None			BCO 146.78
												SCO 238.52
												VCO 257.59
Total Seconds		271.80		144.50		255.80		26.809			698.909	
54D	39.54	137.64	2.29	130.29	No Data		2.573	25.468				BCO 137.62
	141.64	257.64										SCO 235.55
	258.44	324.74										VCO 242.79
Total Seconds		280.40		128.00				22.895			431.295	
62D	57.76	116.76	1.51	68.01	No Data		-0.015	22.799	None	-		BCO 117.77
	119.36	283.26										SCO 264.26
	285.86	306.86										VCO 307.69
	309.46	336.86										
Total Seconds		271.30		66.50				22.814		-	360.614	
27D	37.07	250.97	1.22	19.72	No Data		-0.026	24.969	None	-		BCO 131.94
			21.97	57.22								SCO 278.68
			59.47	94.97								VCO 294.03
Total Seconds		213.90		89.25				24.995		-	328.145	
60D	46.51	343.01	2.06	142.56	1712.81	1734.01(3)	0.928	26.239		-		BCO 141.03
					1735.81	1799.71(3)						SCO 307.55
												VCO 277.45
Total Seconds		296.50		140.50		85.10		25.311		-	547.411	
32D	34.33	289.03	1.73	131.73	322.03	386.23(4)	0.142	24.531	None	-		BCO 131.55
	300.23	304.03			1864.83	2059.43(3)						SCO 288.09
	305.43	351.03										VCO 302.00
Total Seconds		304.10		130.00		258.80		24.389		-	717.289	
66D	33.84	62.44	1.29	84.54	1631.54	1669.04(3)	0.055	24.846	None	-		BCO 136.45
	65.24	139.24			1775.04	1812.44(3)						SCO 259.24
	140.84	343.34			1828.24	1887.54(3)						VCO 274.43
Total Seconds		305.10		83.25		134.20		24.791		-	547.341	
76D	44.54	331.84	0.99	100.74	1782.24	1819.64(3)	0.283	26.278	None	-		BCO 138.59
												SCO 274.89
												VCO 290.91
Total Seconds		287.30		99.75		37.40		25.995		-	450.445	
79D	27.70	339.60	1.65	69.90	No Data		0.025	25.630	None			BCO 138.59
												SCO 282.48
												VCO 295.22
Total Seconds		311.90		68.25				25.605		-	405.755	
80D	6.38	294.38	1.08	31.83	No Data		-0.004	17.480	None			BCO 140.11
			37.33	47.58			17.680	22.774				SCO 271.22
			49.33	68.33			22.794	26.081				VCO 290.90
Total Seconds		288.00		60.00				25.865			373.865	
71D	35.16	149.66	4.11	67.86	33.46	124.36(1)	0.864	26.449	267.428	281.427(6)		BCO 139.56
	151.66	321.06			124.46	190.46(5)						SCO 266.73
					216.36	269.26(5)						VCO 280.71
					269.36	417.36(4)						
					1768.36	1796.16(3)						
Total Seconds		283.90		63.75		385.60		25.585		13.999	772.834	
55D	39.33	139.03	1.58	22.33	No Data		0.044	25.434	284.132	301.132(6)		BCO 135.86
	139.63	341.33	37.08	46.08					303.132	324.132		SCO 283.04
												VCO 298.13
Total Seconds	301.40		29.75					25.390		38.00	394.54	
83D	4.44	266.44	2.69	33.94	249.44	366.84(5)	0.071	26.646	277.528	303.027(6)		BCO 137.75
			46.19	79.19	1819.44	1895.84(3)						SCO 269.91
												VCO 286.34
Total Seconds		262.0		64.25		193.8		26.575		25.499	572.124	
90D	10.6	293.50	0.65	124.40	No Data		0.025	25.908	None			BCO 137.66
												SCO 271.93
												VCO 289.77
Total Seconds		282.9		123.75				25.883			432.533	

NOTES: (1) FPS/16 Radar, Cape Canaveral (1.16).
(2) Mod II Radar, Ascension Island (Station 12.2).
(3) FPS/16 Radar, Ascension Island (12.16).
(4) FPS/16 Radar, San Salvador (5.16).
(5) FPS/16 Radar, Grand Bahama (3.16).
(6) Ballistic Camera

TABLE 3-16 ESTIMATED ACCURACIES OF METRIC TRAJECTORY DATA COVERAGE

SYSTEM	PARAMETER	TYPE OF ERROR	STANDARD DEVIATION
CZR-1 (fixed camera)	POSITION 0-25 sec = 0-18,000 ft	All	X = 0.6 to 1.5 ft; y = 0.9 to 2.0 ft; z = 0.6 to 2.5 ft Point in Space = 1.24 to 3.54 ft
	VELOCITY	All	V_x = 0.2 to 0.3 ft/sec; V_y = 0.3 to 0.4 ft/sec; V_z = 0.2 to 0.5 ft/sec; V_r = 0.4 to 0.7 ft/sec
	ACCELERATION	All	A_x = 0.26 to 0.39 ft/sec^2; A_y = 0.39 to 0.55 ft/sec^2; A_z = 0.26 to 0.68 ft/sec^2; A_x = 0.54 to 0.96 ft/sec^2
CINETHEODOLITE (tracking camera)	POSITION 0-80 sec = 0-78,000 ft	Random Systematic All	x = 0.4 to 1.9 ft; y = 0.4 to 1.3 ft; z = 0.3 to 3.1 ft x = 1.2 to 19 ft; y = 1.2 to 13 ft; z = 0.9 to 31 ft Point in Space = 2.6 to 42 ft
	VELOCITY	All	V_x = 0.5 to 2.5 ft/sec; V_y = 0.6 to 1.7 ft/sec; V_z = 0.4 to 4.2 ft/sec; V_r = 0.88 to 5.2 ft/sec
	ACCELERATION	All	A_x = 0.64 to 4.5 ft/sec^2; A_y = 0.64 to 20 ft/sec^2; A_z = 0.64 to 4.5 ft/sec^2; A_x = 1.1 to 4.9 ft/sec^2
AZUSA	POSITION 45-210 sec = 26,000 to 1.2 X 10^6 ft	All	x = 0.66 ft; y = 0.62 ft; z = 0.93 ft Point in Space = 1.3 ft
	210 to 300 sec = 1.2 X 10^6 to 2.7 X 10^6 ft	All	x = 1.75 ft; y = 1.63 ft; z = 4.43 ft Point in Space = 5.0 ft
	VELOCITY 45-210 sec	All	V_x = 0.06 ft/sec; V_y = 0.06 ft/sec; V_z = 0.09 ft/sec; V_r = 0.12 ft/sec
	210-300 sec	All	V_x = 0.14 ft/sec; V_y = 0.13 ft/sec; V_z = 0.36 ft/sec; V_r = 0.41 ft/sec
	ACCELERATION	All (to 300 sec)	A_x = 0.02 to 0.1 ft/sec^2; A_y = 0.03 to 0.1 ft/sec^2; A_z = 0.03 to 0.2 ft/sec^2; A_x = 0.05 to 0.2 ft/sec^2
FPS-16 RADAR	POSITION 0-200 sec = 0-1. X 10^6 ft	Random Systematic	X = 1.0 ft; Y = 0.6 ft; Z = 1.0 ft X = 10 ft; Y = 6 ft; Z = 10 ft Point in Space = 17 ft
	200 to 270 sec 10^6 to 2 X 10^6 ft	Random Systematic	X = 6 ft; Y = 1.5 ft; Z = 3 ft X = 60 ft; Y = 15 ft; Z = 20 ft Point in Space = 75 ft
	270 to 300 sec 2 X 10^6 to 2.7 X 10^6 ft	Random Systematic	X = 13 ft; Y = 4 ft; Z = 12 ft X = 100 ft; Y = 40 ft; Z = 100 ft Point in Space = 165 ft
	VELOCITY 0-300 sec	All	V_x = 0.8 to 2.0 ft/sec; V_y = 0.7 to 1.5 ft/sec; V_z = 0.9 to 1.2 ft/sec; V_r = 1.4 to 2.6 ft/sec
	ACCELERATION 0-300 sec	All	A_x = 0.2 to 3.0 ft/sec^2; A_y = 0.15 to 0.5 ft/sec^2; A_z = 0.5 to 2.5 ft/sec^2; A_r = 0.6 to 4.0 ft/sec^2

SPECIAL PROJECTS

Two special project tests are included in this section of the report. These tests utilized the Atlas missile as a first stage or booster for placing space vehicles in their initial orbit positions. On such flights the requirements placed on the Atlas missile with respect to trajectory performance are that the upper stage vehicle be placed at a specified altitude with a specified inertial velocity at the time of separation.

Figure 3-9 shows a comparison of the powered flight profiles for the two special project tests with a typical R&D, 4,390 nautical mile range, flight test. The profile of the latter is seen to fall between the other two and to have the greatest range at the end of powered flight. The booster engine cutoff points of all three are quite close although considerable variation occurs between the sustainer and vernier engine cutoff relationships.

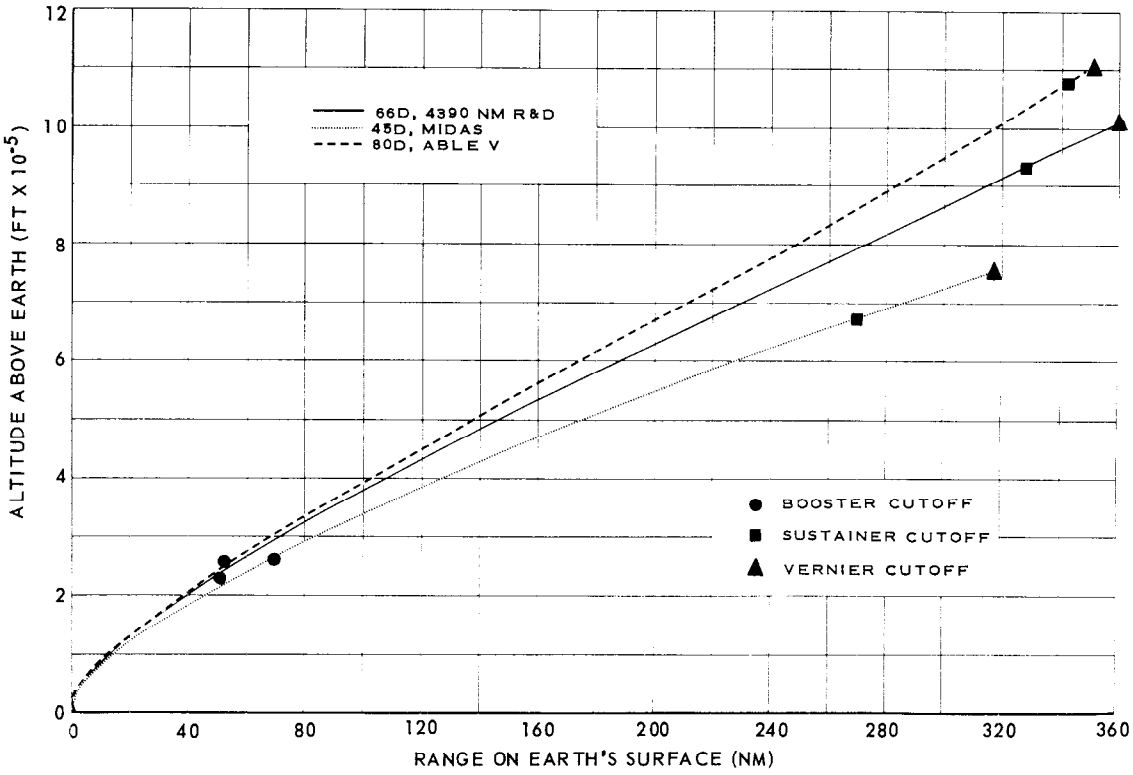

FIGURE 3-9 COMPARISON OF FLIGHT PROFILES

Atlas-Able

Missile 80D, carrying an Able lunar probe as the upper stage, was required to be at a range of 22,003,760 feet from the center of the earth with an inertial velocity of 22,807 feet per second at the time of vernier engines cutoff in order that the upper stage propulsion systems could place the Able payload on the proper lunar transfer orbit. The mission was not accomplished. Atlas missile position and velocity were within satisfactory limits at the end of powered flight.

Project Midas

Missile 45D acted as the booster for a Midas satellite vehicle. The Midas satellite is intended to orbit the earth at an altitude of approximately 260 nautical miles, for the purpose of observation as an early warning system. In this case the requirements for the Atlas booster were to achieve a specified coast apogee altitude and velocity of 292 nautical miles and 18,393 feet per second, respectively. These requirements were successfully fulfilled within acceptable limits and the mission was successfully accomplished.

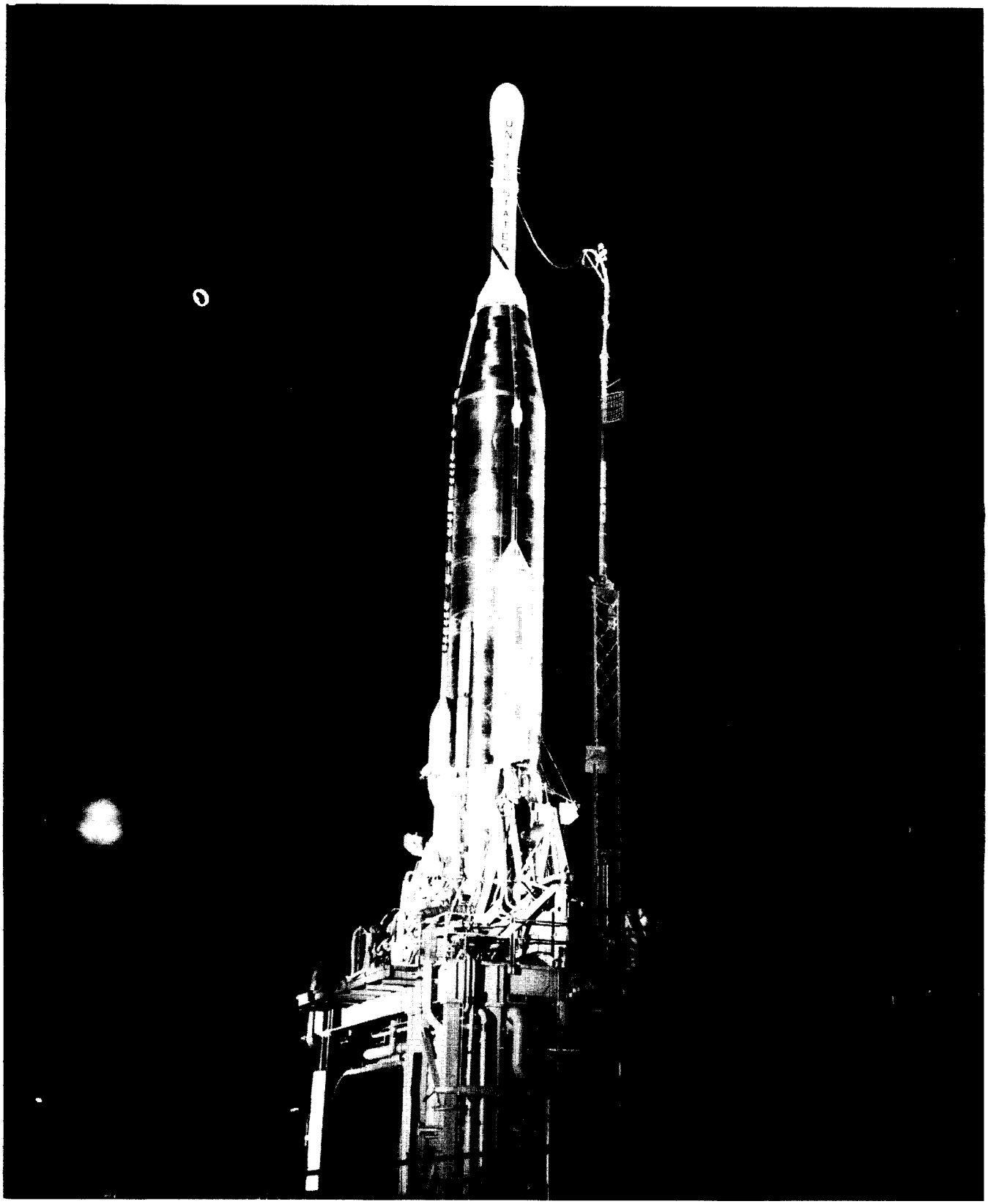

MISSILE 91D ATLAS-ABLE

SECTION 4. AIRFRAME

SECTION 4.1 - VIBRATION AND ACOUSTIC STUDIES

PURPOSE OF TESTING

Landline vibration and acoustic measurements were made within the missile thrust section and AIG pod, respectively, during launch to determine the vibration and acoustic environment at specific missile component installations. The resulting information was utilized in establishing criteria for design and qualification test considerations and also provided sufficient test data coverage to aid in determining the adequacy of the respective systems operation. Flight vibration measurements were made within the missile equipment pods to determine the flight vibration characteristics of AIG guidance and instrumentation beacon system components.

Rough combustion cutoff accelerometers on the booster and sustainer engine propellant lines and vibration pickups on the booster engine propellant lines were monitored during launch to facilitate the evaluation of booster and sustainer engine combustion stability. The study stemmed from the rough combustion problem evidenced at launch on Missiles 51D and 48D. Extended holddown periods were utilized to assure the adequacy of propulsion system operation prior to launch.

The sound pressure measurements were obtained from within the AIG pod section to aid in determining the cause for operational difficulties encountered at the AIG computer, and more generally, to provide data for environmental qualification test specifications. Knowledge of the specific sound pressure levels within the pod was lacking, therefore, action was taken to determine the acoustic environment. During the flight readiness firing of Missile 42D, the AIG airborne computer displayed erroneous outputs. The results of environmental tests on that same computer showed that the malfunction could be reproduced under an acoustic environment. The fault in the computer was traced to an open clamp diode in the sequence counter portion of the computer. The open diode closed intermittently when it was exposed to the acoustic environment. The details of the investigation are reported in Arma's Progress Report Number DAG 6783.

TEST CONDITIONS

All of the special launch vibration and acoustic data were recorded by utilizing the site FM landline recording system. The duration of the recording periods varied between 3 and 7 seconds, depending on the length of the holddown period prior to launch (Reference the Propulsion Section for holddown periods). Generally, the vibration analysis was conducted within a frequency band of 10 to 2,000 cps, while the sound pressure levels were determined within a band of 10 to 10,000 cps.

A rough combustion cutoff accelerometer was located on the lox dome of each thrust chamber with the accelerometer output fed to the cutoff device. Figure 4.1-1 shows a typical installation of the crystal type high frequency accelerometer. The cutoff parameters were set at 60 g(rms) for 20 milliseconds on the sustainer engine and 30 g(rms) for 40 milliseconds on the booster engines. The binary counter of the cutoff device was also monitored.

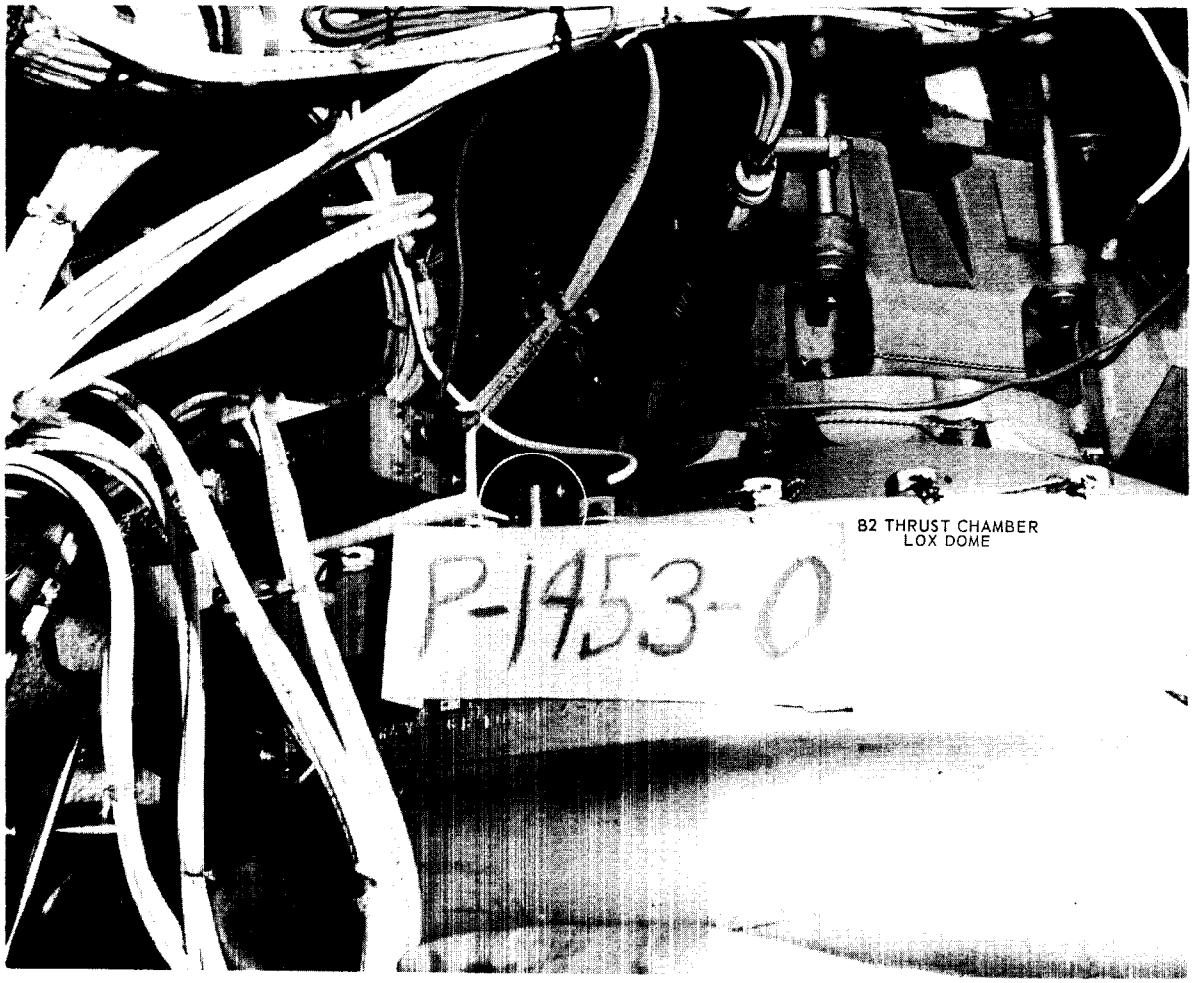

FIGURE 4.1-1 HIGH FREQUENCY ACCELEROMETER INSTALLATION

The vibration measurements on the booster engine propellant ducts were made on a total of 10 Series D missiles. High frequency accelerometers were utilized on each missile. Figure 4.1-2 shows the general location of these measurements while Figures 4.1-3 through 4.1-5, inclusive, show the details of each accelerometer installation. The measurement number and location of each measurement is shown below.

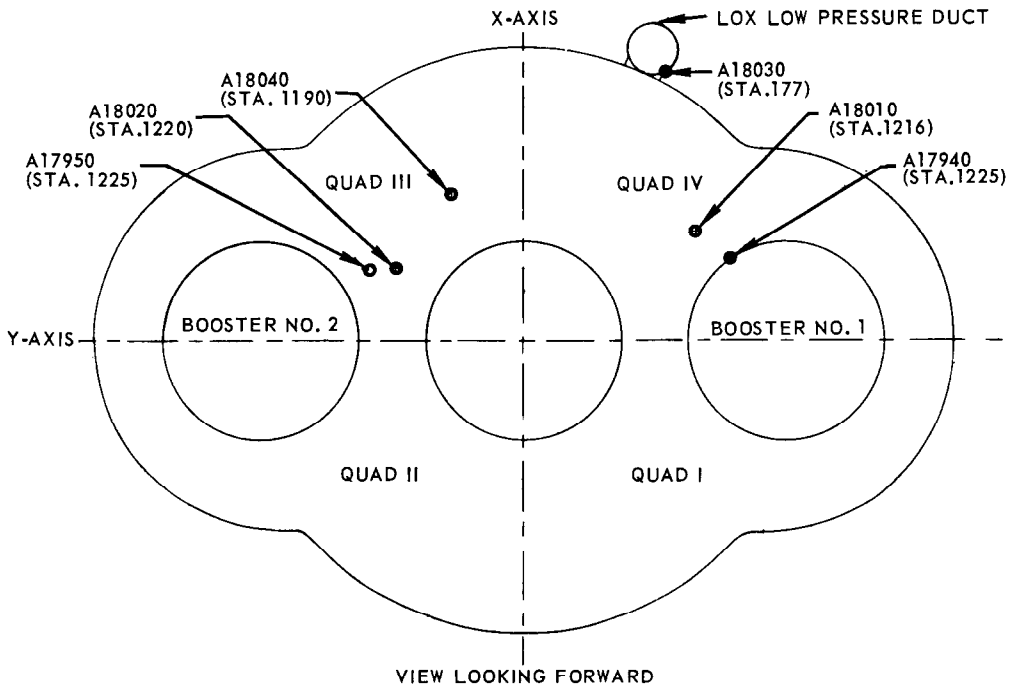

FIGURE 4.1-2 LOCATION OF PROPELLANT LINE ACCELEROMETERS

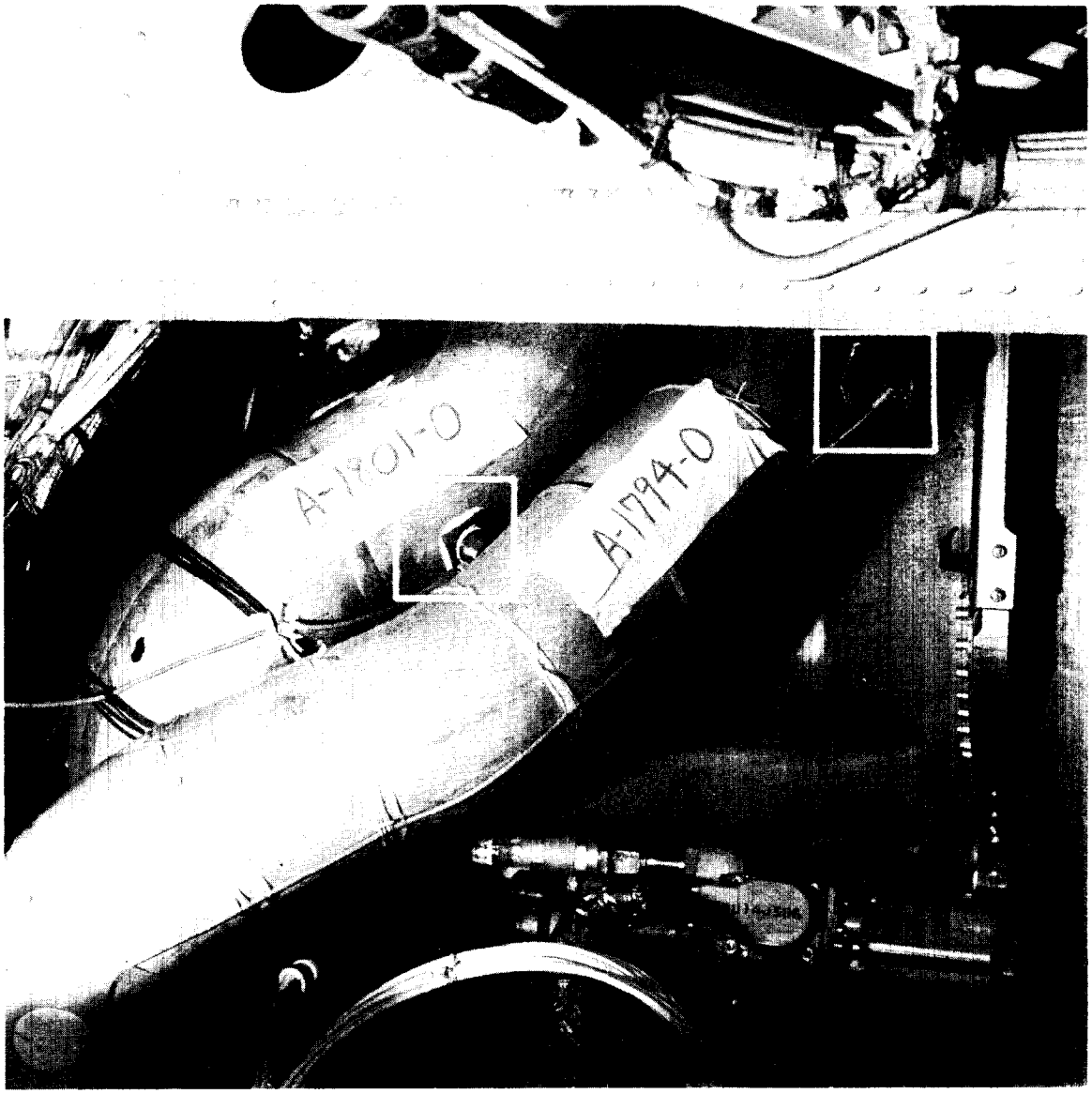

FIGURE 4.1-3 DETAILED INSTALLATION OF PROPELLANT LINE ACCELEROMETER

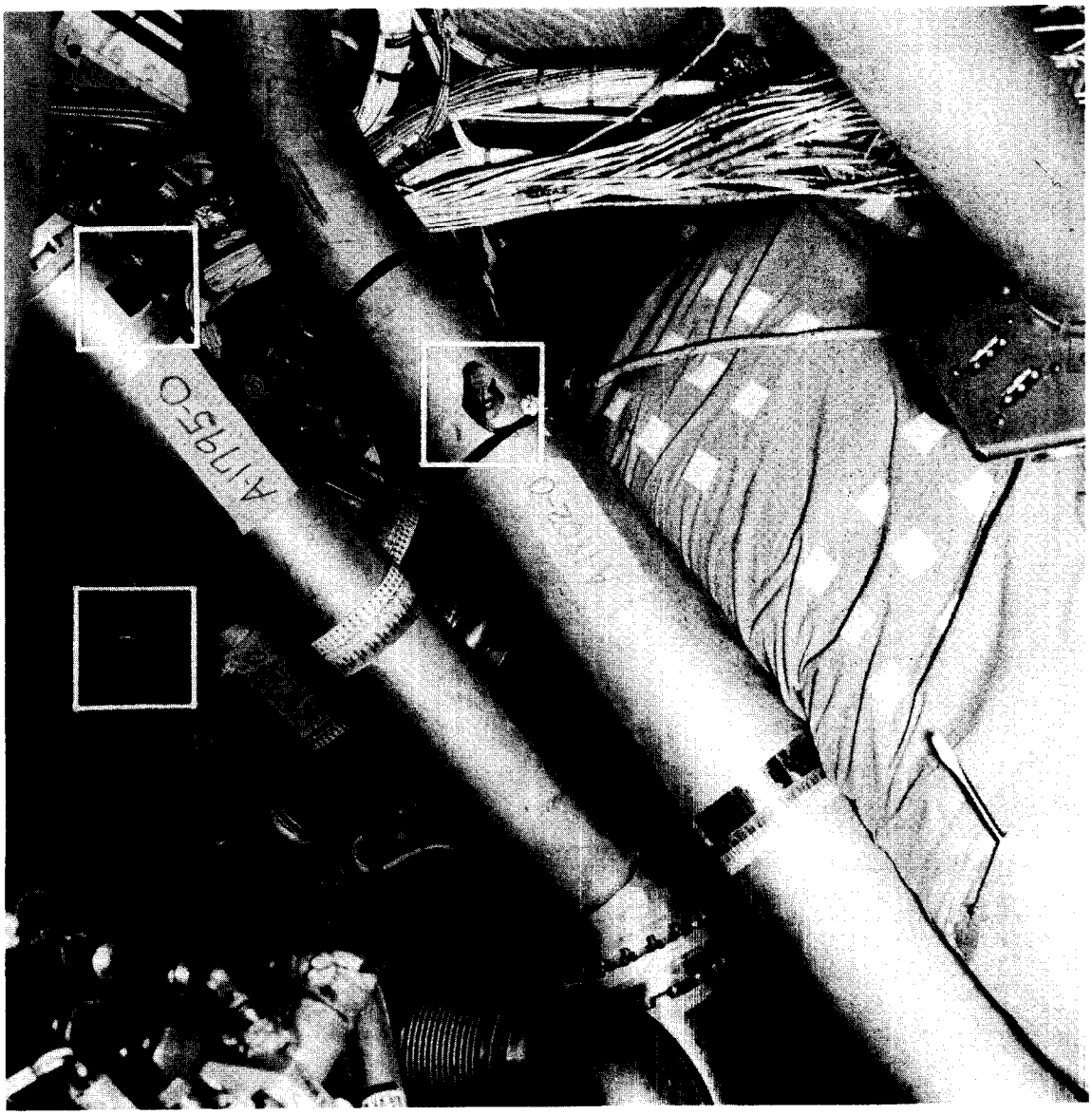

FIGURE 4.1-4 DETAILED INSTALLATION OF PROPELLANT LINE ACCELEROMETER

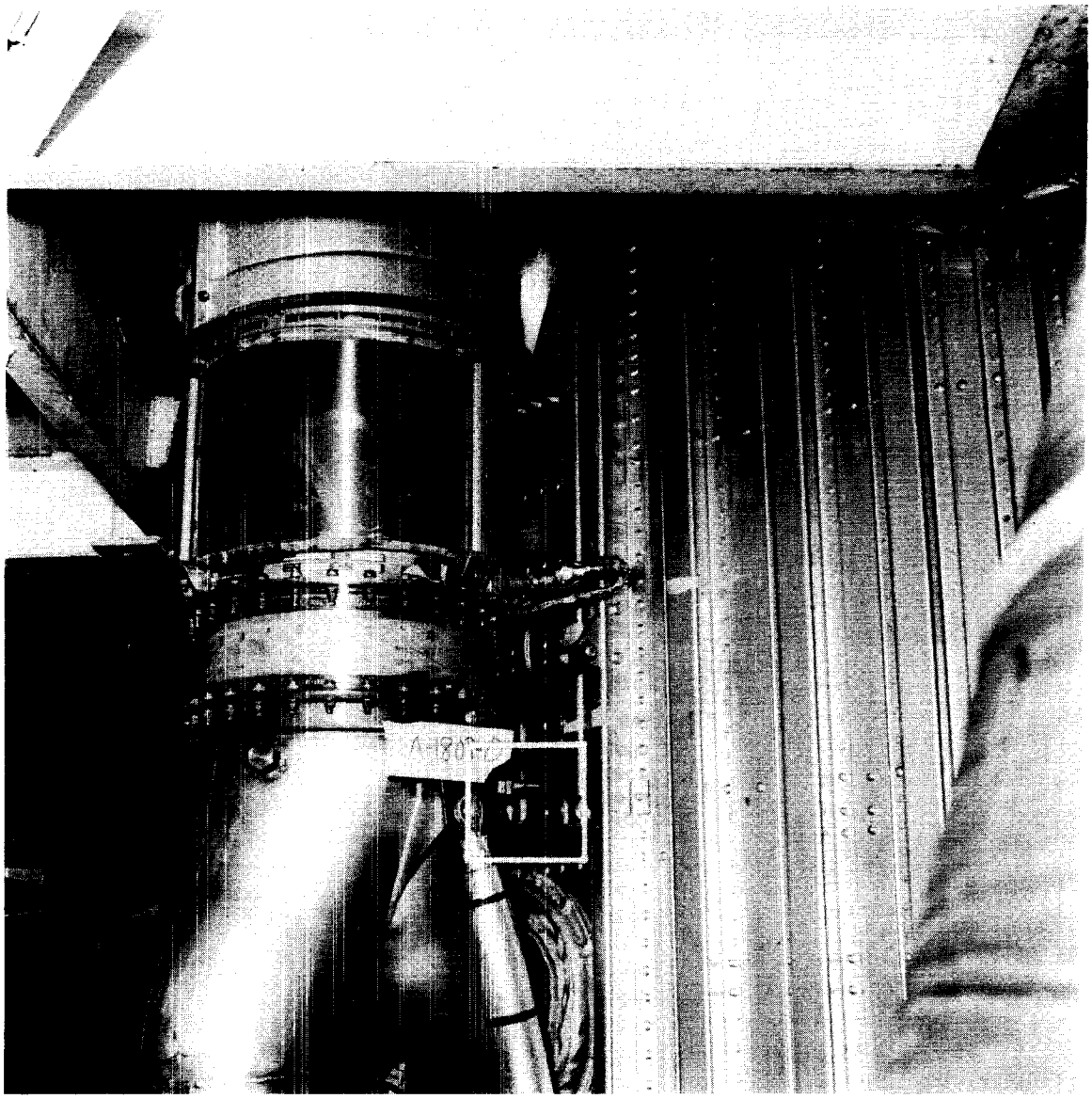

FIGURE 4.1-5 DETAILED INSTALLATION OF PROPELLANT LINE ACCELEROMETER

Measurement Number	Location
A1794O	B1 High Pressure Fuel Line
A1795O	B2 High Pressure Fuel Line
A1801O	B1 High Pressure Lox Line
A1802O	B2 High Pressure Lox Line
A1803O	Booster Low Pressure Lox Line
A1804O	Booster Low Pressure Fuel Line

The AIG pod acoustic measurements were recorded during the flight readiness firing on Missile 42D and during launch on Missiles 54D and 60D. The locations of the microphones inside the pod are shown in Figures 4.1-6, 4.1-7 and 4.1-8. The site 70KC (±15 percent deviation) FM recording system was utilized in recording sound on Missile 42D. The sound recording equipment was changed for Missile 54D and 60D tests, wherein a special wide-band 54KC (±40 percent deviation) FM system was utilized. Both an end to end and a synthetic electrical calibration were conducted on each microphone system prior to the test. The microphone, Model NM125, was manufactured by the Chesapeake Instrument Corp. and set to a sound pressure level range of 120 to 160 db. The end to end calibration was accomplished with a B and K artificial voice unit, adapted for use with the NM125 microphone.

Approximately 30 flight vibration measurements were planned for installation on Missiles 42D through 90D. Valid flight data was obtained from only 15 of the measurements. These were located within the equipment pods. In most cases the high frequency vibration data was analyzed within a frequency band of 10 to 2,000 cps.

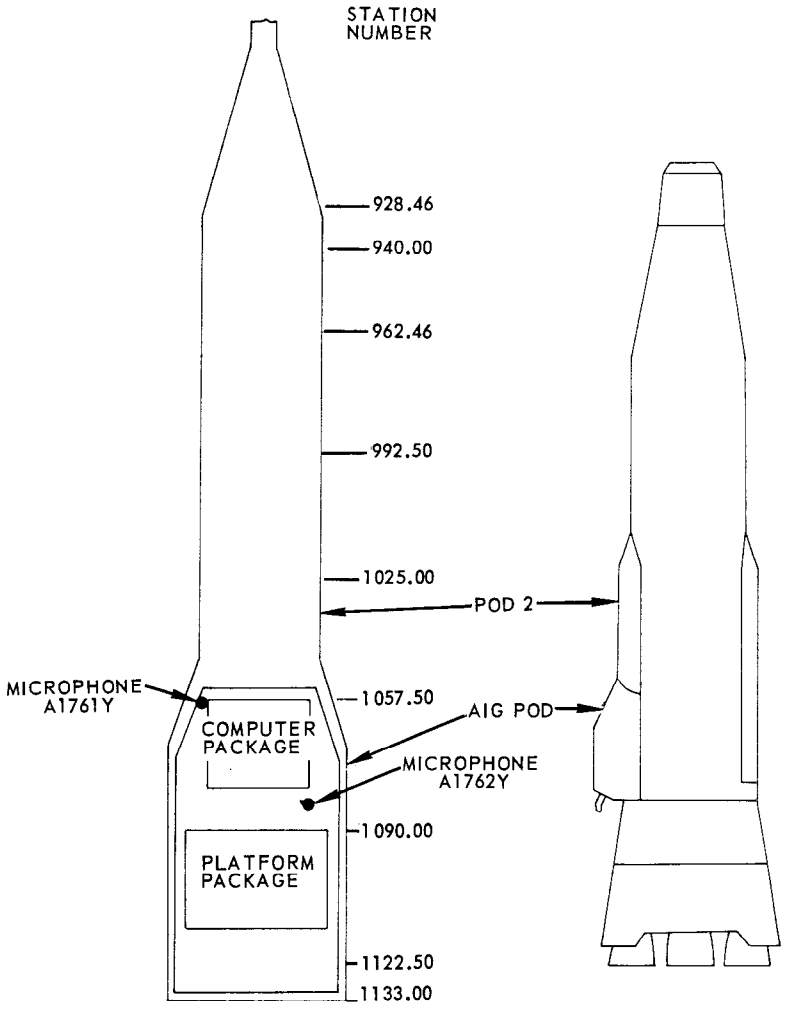

FIGURE 4.1-6 LOCATION OF AIG POD ACOUSTIC MICROPHONES

FIGURE 4.1-7 DETAILED INSTALLATION OF AIG POD ACOUSTIC MICROPHONE

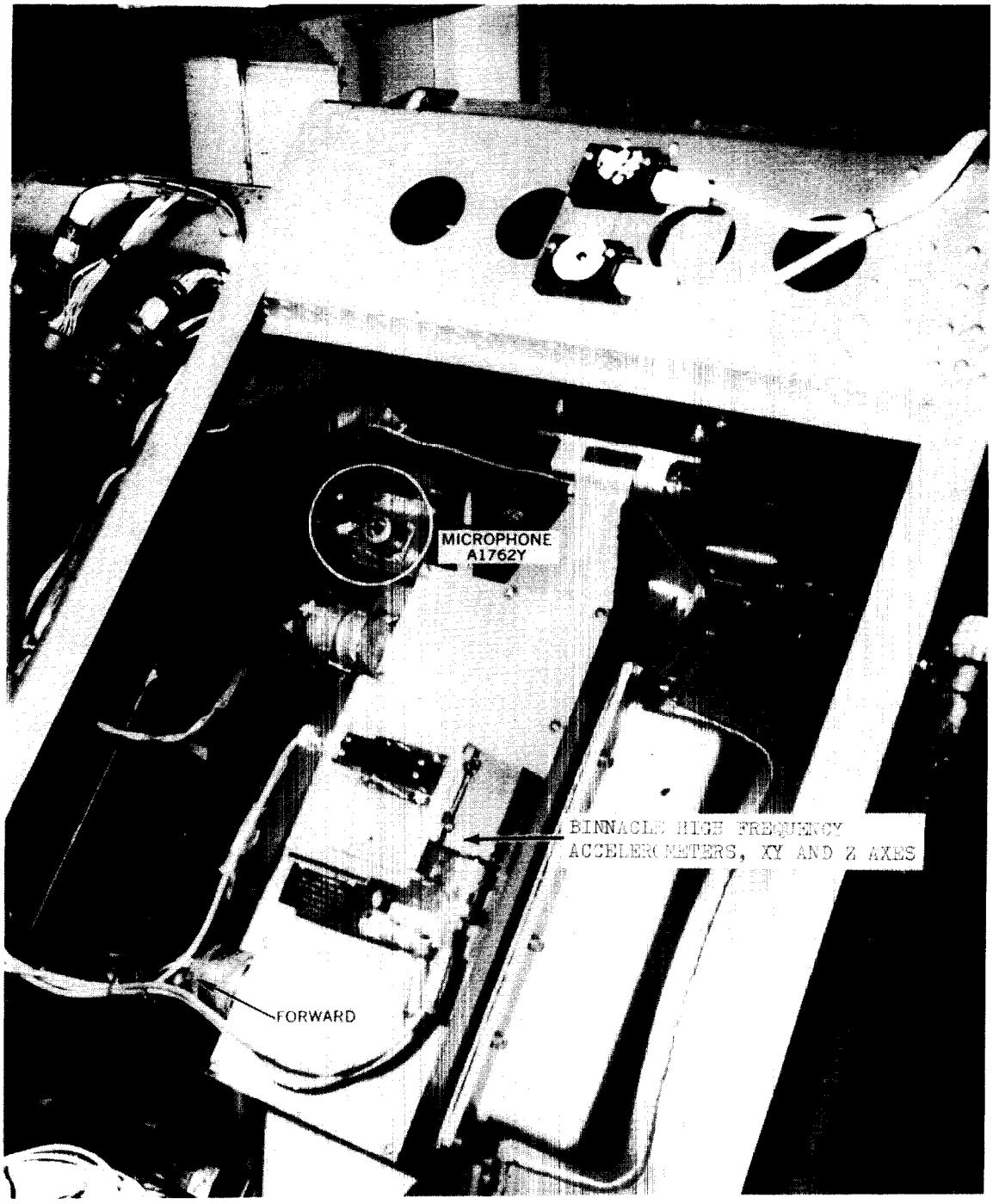

FIGURE 4.1-8 DETAILED INSTALLATION OF AIG POD ACOUSTIC MICROPHONE

The AIG computer and platform binnacle were instrumented with high frequency accelerometers for measurement of vibration. Each provided vibration data along the X, Y and Z axes. The outboard portion of the AIG pod frame was instrumented with three low frequency accelerometers that were flat to a frequency of approximately 50 cps. The location of each accelerometer is shown in Figure 4.1-9.

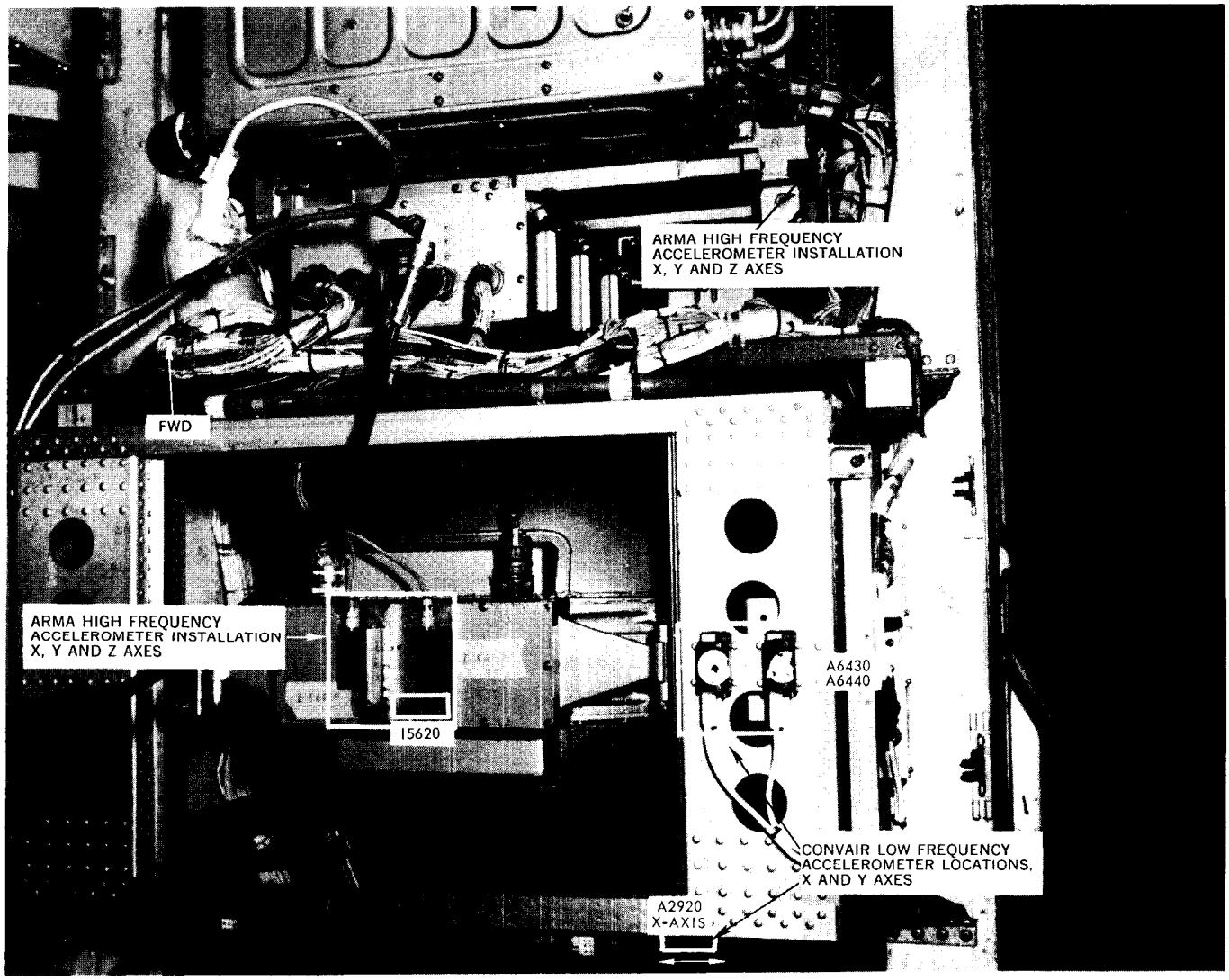

FIGURE 4.1-9 DETAILED INSTALLATION OF AIG POD ACCELEROMETERS

Three high frequency vibration measurements were attempted on the instrumentation beacon equipment during flight. The measurements were on the rate beacon-impact predictor package (radial direction), the rate beacon waveguide (radial direction), and the beacon system boom antenna. However, boom antenna data was not obtained due to faulty instrumentation. The locations of the accelerometers on the rate beacon-impact predictor package and waveguide are shown in Figures 4.1-10 and 4.1-11.

FIGURE 4.1-10 ACCELEROMETER INSTALLATION ON RATE BEACON PACKAGE

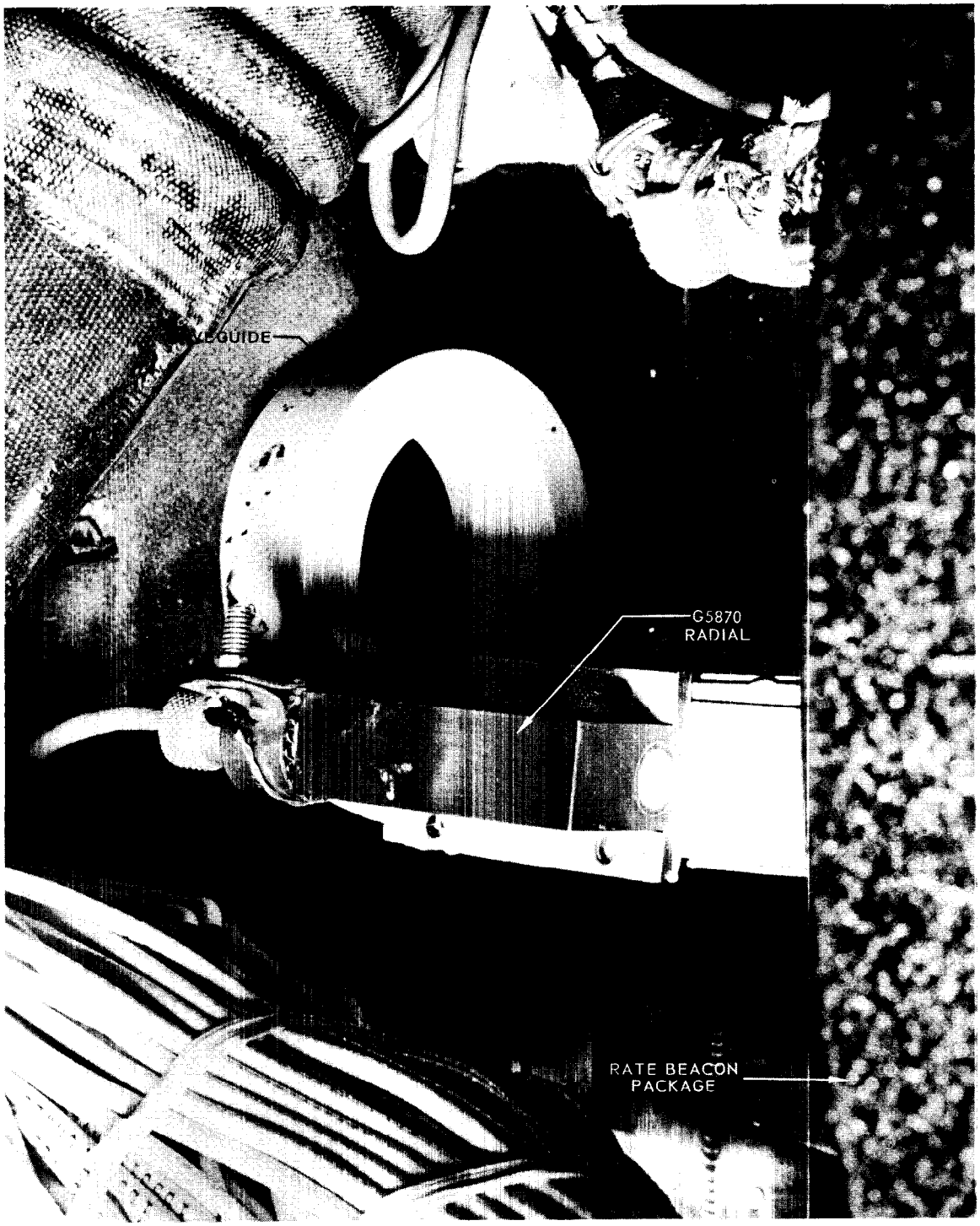

FIGURE 4.1-11 ACCELEROMETER INSTALLATION ON RATE BEACON WAVEGUIDE

Nomenclature and Computational Methods

The power density spectral estimates made on the vibration data were computed by analog methods utilizing a tape loop containing the desired sample. All spectra were computed for a time duration of 0.5 seconds. The data was analyzed to 1,000 cps to 2,000 cps and integrated over intervals of 20 or 50 cps, respectively.

The rms value of the acceleration between two frequencies is derived by taking the square root of the integral of the power density spectra from the lower to the higher frequency. The following is a mathematical presentation of the method.

$$\left[g(\text{rms})\right]_{f_1}^{f_2} = \left[\int_{f_1}^{f_2} \phi(f)\, df\right]^{1/2} \quad (1)$$

where: $\phi = g^2/\text{cps}$ (power density).

Both octave band and constant band analyses were used in analyzing the acoustic data. To compute the sound pressure level spectra, an analog tape loop of a desired sample was utilized in conjunction with an octave band analyzer and/or a wave analyzer. The octave band data presented was analyzed to 10,000 cps with full octave intervals. The constant band data presented was analyzed to 200 cps, 2,000 cps and 10,000 cps over intervals of 5, 50 and 200 cps, respectively. The computing period was 0.5 seconds. A diagram of the data reduction system is shown in Figure 4.1-12.

The sound pressure level plots were computed using the following mathematical expression.

$$\text{Root mean square (rms) sound pressure} = \left[\frac{1}{T}\int_0^T P^2(t)\, dt\right]^{1/2} \quad (2)$$

where: P = existing instantaneous sound pressure

T = data sample period.

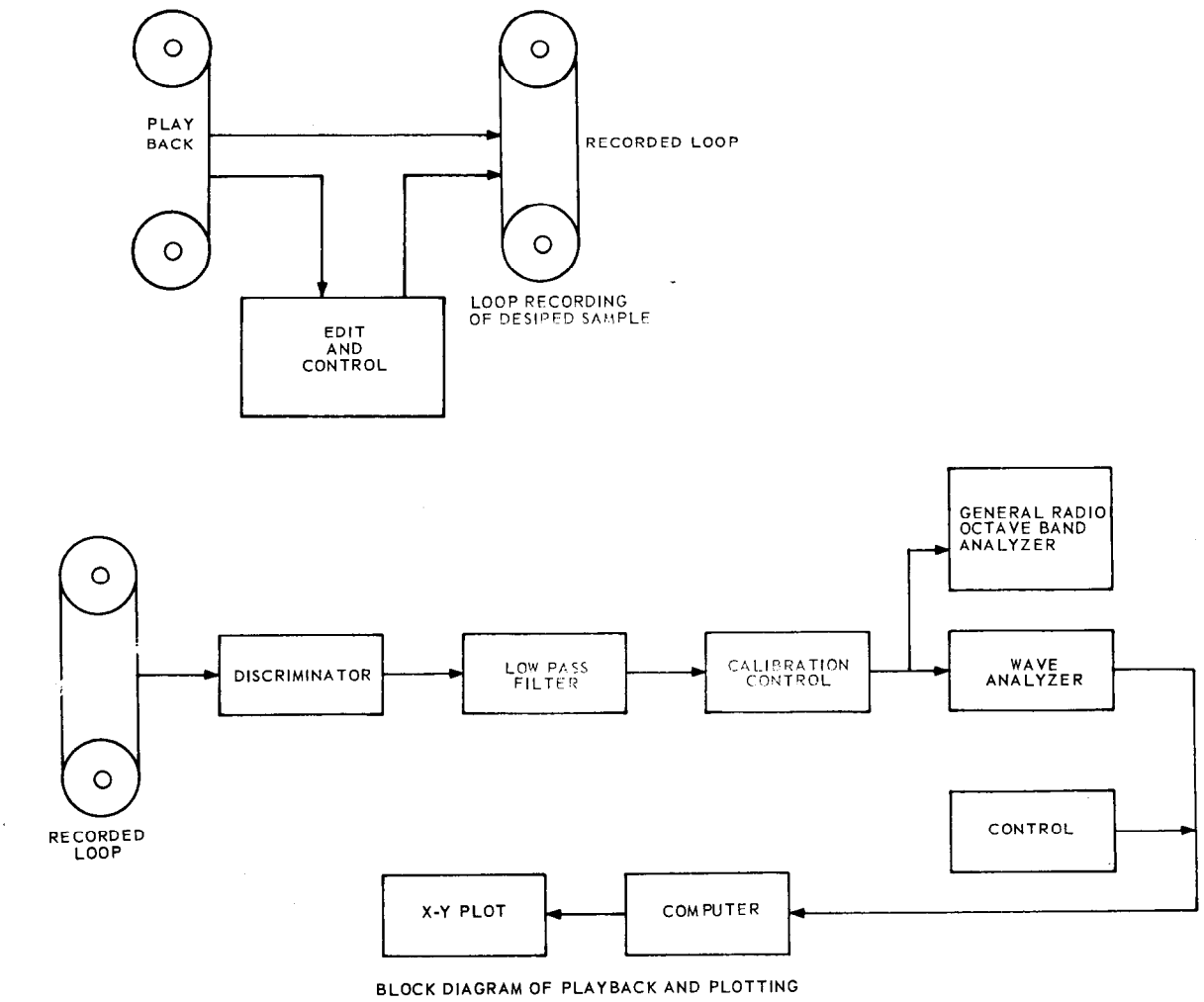

FIGURE 4.1-12 DATA REDUCTION SYSTEM

All decibel levels indicated in this section were based on the generally accepted sound pressure reference of 0.0002 dyne/cm^2 (Po), which is the pressure for the threshold of hearing at approximately 1,000 cps. The sound pressure was converted to sound pressure level in decibels by the following method:

$$\text{Sound Pressure Level} = 20 \log_{10} \frac{P(\text{rms})}{Po} \text{ decibels (db).}$$

~~SECRET~~

TEST RESULTS

Landline Vibration Analysis

The primary purpose of monitoring vibration on the booster engines was to support the evaluation engine combustion stability. The vibration data from the flight tests of Missiles 56D through 90D indicated that booster engine vibration was normal. No significant combustion stability problems were apparent. A summary of propulsion system vibration levels is shown in Table 4.1-1.

TABLE 4.1-1 SUMMARY OF PROPULSION SYSTEM VIBRATION DATA

MEAS. NO.	LOCATION	ACCELERATION g(rms) RANGE	ACCELERATION g(rms) AVERAGE	PREDOMINANT FREQ. BAND cps
P1439O	Sustainer Thrust Chamber	4-8	5.5	1150-1200 and 510-580[2]
P1452O	B_1 Thrust Chamber	5-10	7	1080 and 1950-2000[2]
P1453O	B_2 Thrust Chamber	5-10	7	1110-1200
A1794O	B_1 High Pressure Fuel Line	11-30	19	1200-1600
A1795O	B_2 High Pressure Fuel Line	11-19	15	1000-1500
A1801O	B_1 High Pressure Lox Line	15-40	24	1200-1550
A1802O	B_2 High Pressure Lox Line	15-37	27	1600-1620
A1803O	Booster Low Pressure Lox Line	11-23	14	1200
A1804O	Booster Low Pressure Fuel Line	8-25	17	1200-1700

NOTES:

(1) Includes Missiles 56D, 54D, 62D, 27D, 60D, 32D, 66D, 71D, 83D, and 90D.

(2) Second most predominant frequency band.

All values are maximum steady-state levels during launch.

~~SECRET~~

Thrust chamber vibration steady-state levels ranged between 4 and 10 g(rms). Major energy contributions were within a frequency band of 500 to 1,200 cps. Figure 4.1-13 shows an oscillograph recording that typifies RCC accelerometer outputs during launch. Figure 4.1-14 contains power density spectra computed for each thrust chamber during a steady-state period prior to launch.

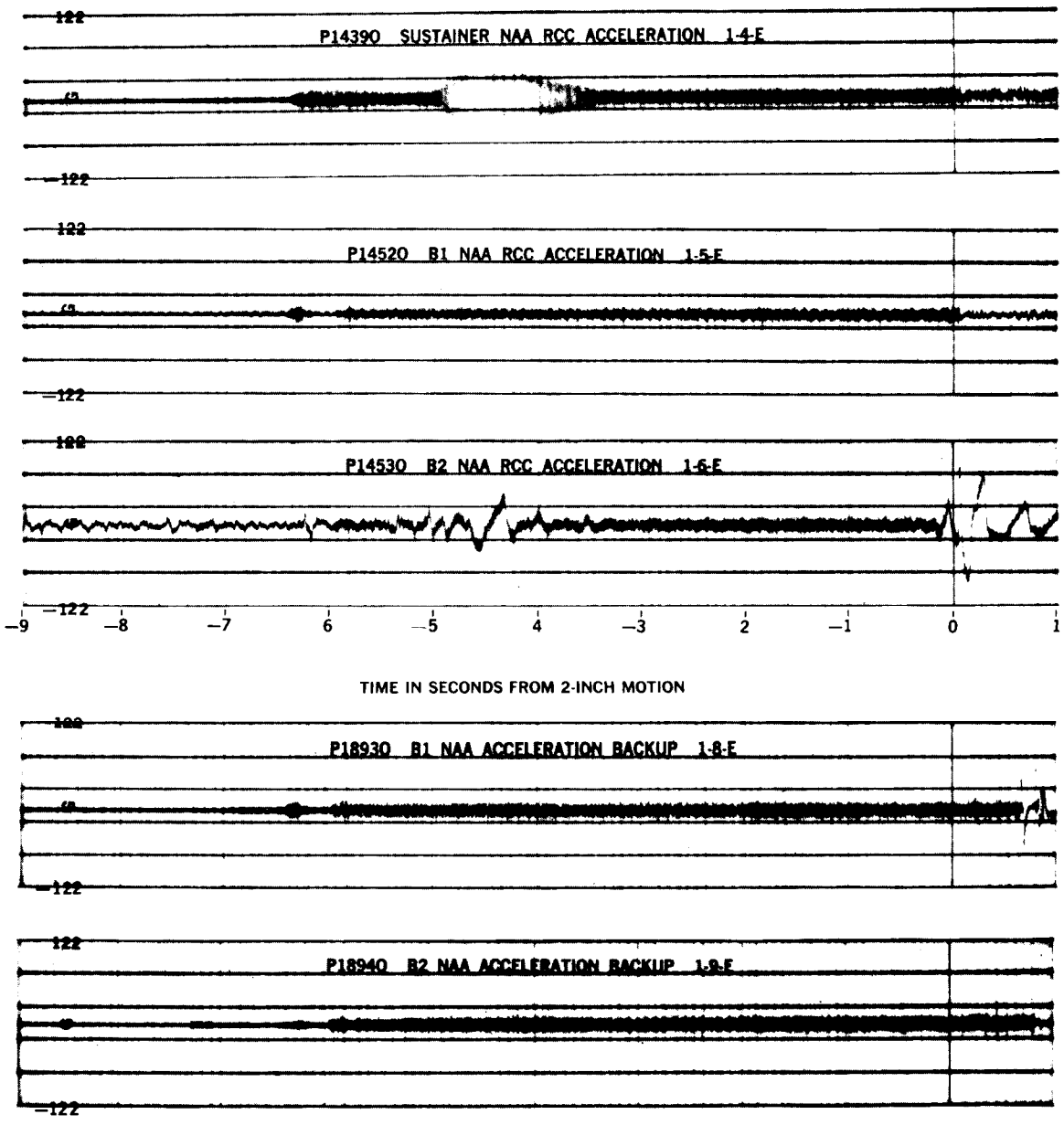

FIGURE 4.1-13 RCC ACCELEROMETER OUTPUTS

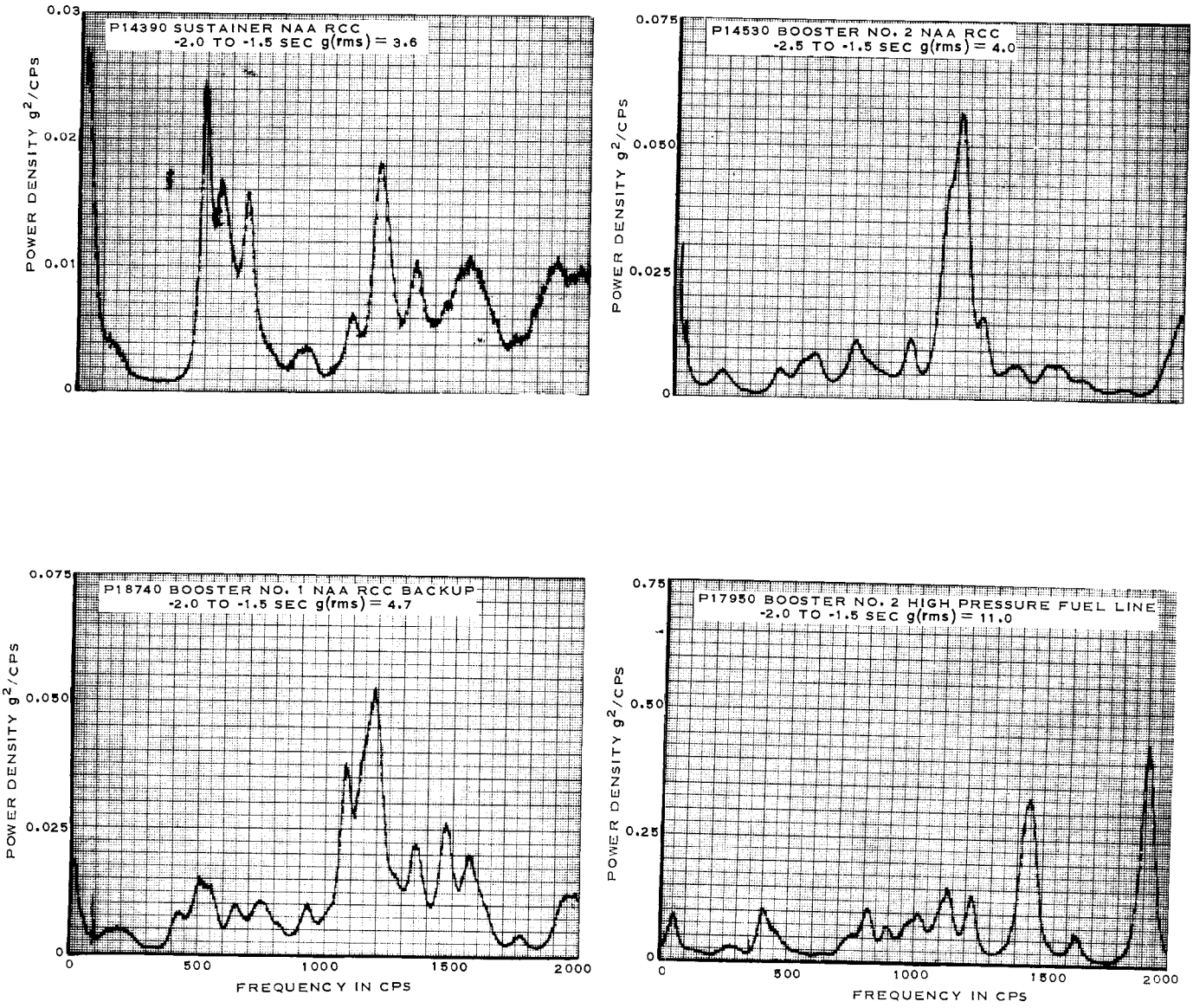

FIGURE 4.1-14 POWER DENSITY SPECTRA

Only one period of significant rough combustion prevailed and that occurred on the sustainer engine during the attempted launch of Missile 32D. An oscillatory burst of energy at a frequency of 1,160 cps occurred between 1.4 and 1.6 seconds and was sustained for a sufficient time in excess of 60 g(rms) (approximately 50 milliseconds) to initiate propulsion system shutdown. The maximum level observed was approximately 80 g(rms). The burst of energy occurred at the time the propellant utilization and the head suppression valves were moving to their nominal position. The sustainer thrust chamber was replaced to ascertain adequate sustainer engine operation for the subsequent launch of Missile 32D.

The 1,160 cps oscillation had occurred at approximately the same time on previous static and flight tests without damaging effects. Static tests had shown burst durations ranging between 2 and 3 seconds with levels ranging between approximately 50 and 100 g(rms). Four Series D flight tests prior to the attempted flight of Missile 32D showed burst durations between 1 and 2 seconds with levels ranging between 25 and 30 g(rms). The cause for the vibration buildup was attributed to an improper propellant mixture ratio initiated at the time the main propellant valves commenced going into control.

The vibration levels on the low and high pressure propellant lines showed a significant variation in magnitude between missiles. Table 4.1-1 shows a summary of the propellant line vibration. The variation in magnitude was probably caused by variation in the mounting of the accelerometers on the lines and/or the differences in line flexibility between engine packages. Of the four high pressure line measurements, the booster No. 2 high pressure lox line consistently displayed the greater magnitude. It was apparent that the longer line lengths on the B2 side were conducive to the slightly higher vibration levels. An oscillograph record displaying a typical waveform of each measurement is shown in Figure 4.1-15. Power density spectra computed for each measurement during a steady-state period are shown in Figure 4.1-16. Generally, the displacements of the propellant lines during engine start and launch were extremely small and showed no indication of structural design problems. Also, no propulsion system combustion stability difficulties were evident.

~~SECRET~~

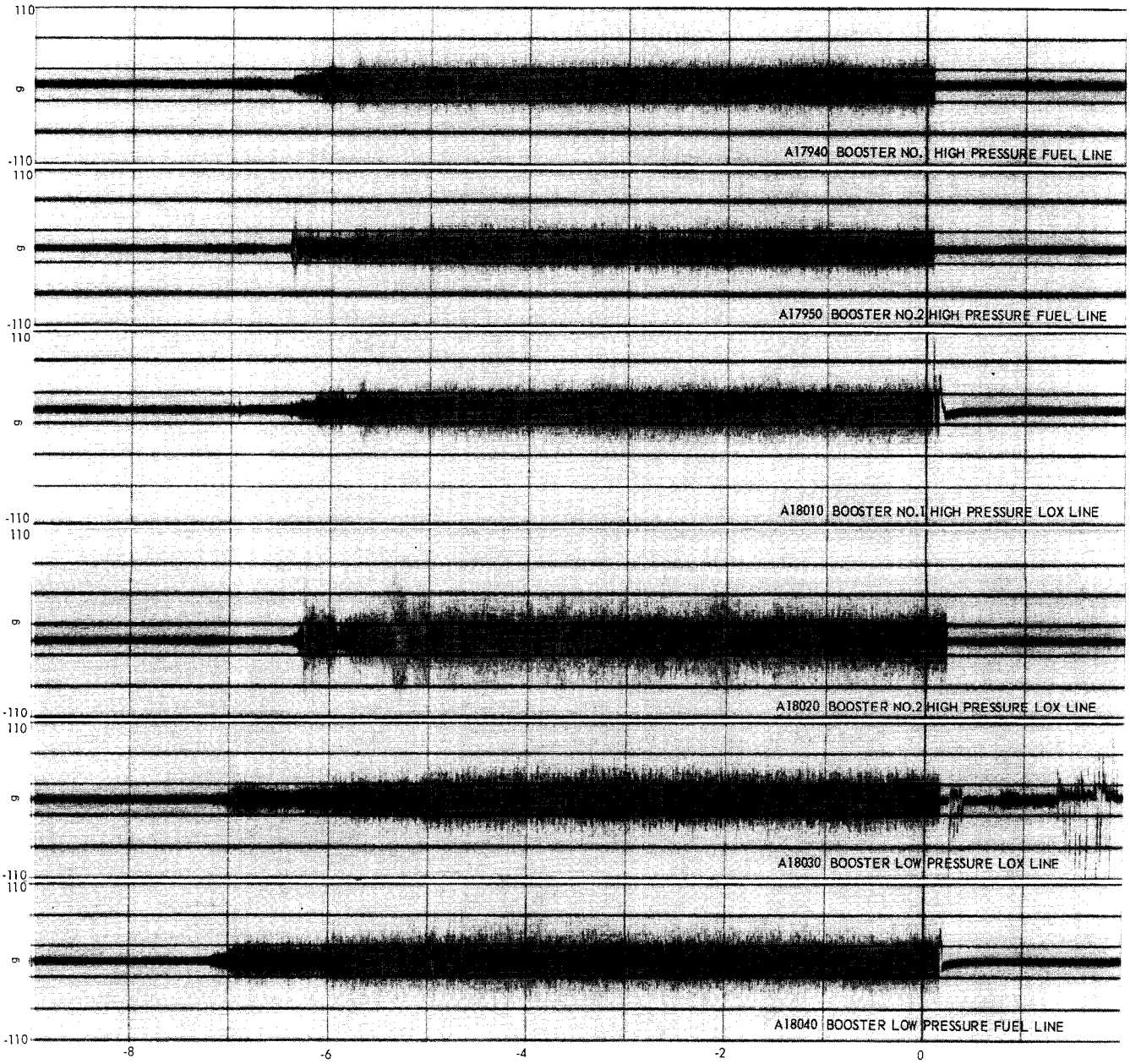

FIGURE 4.1-15 PROPELLANT LINE VIBRATION DATA

~~SECRET~~

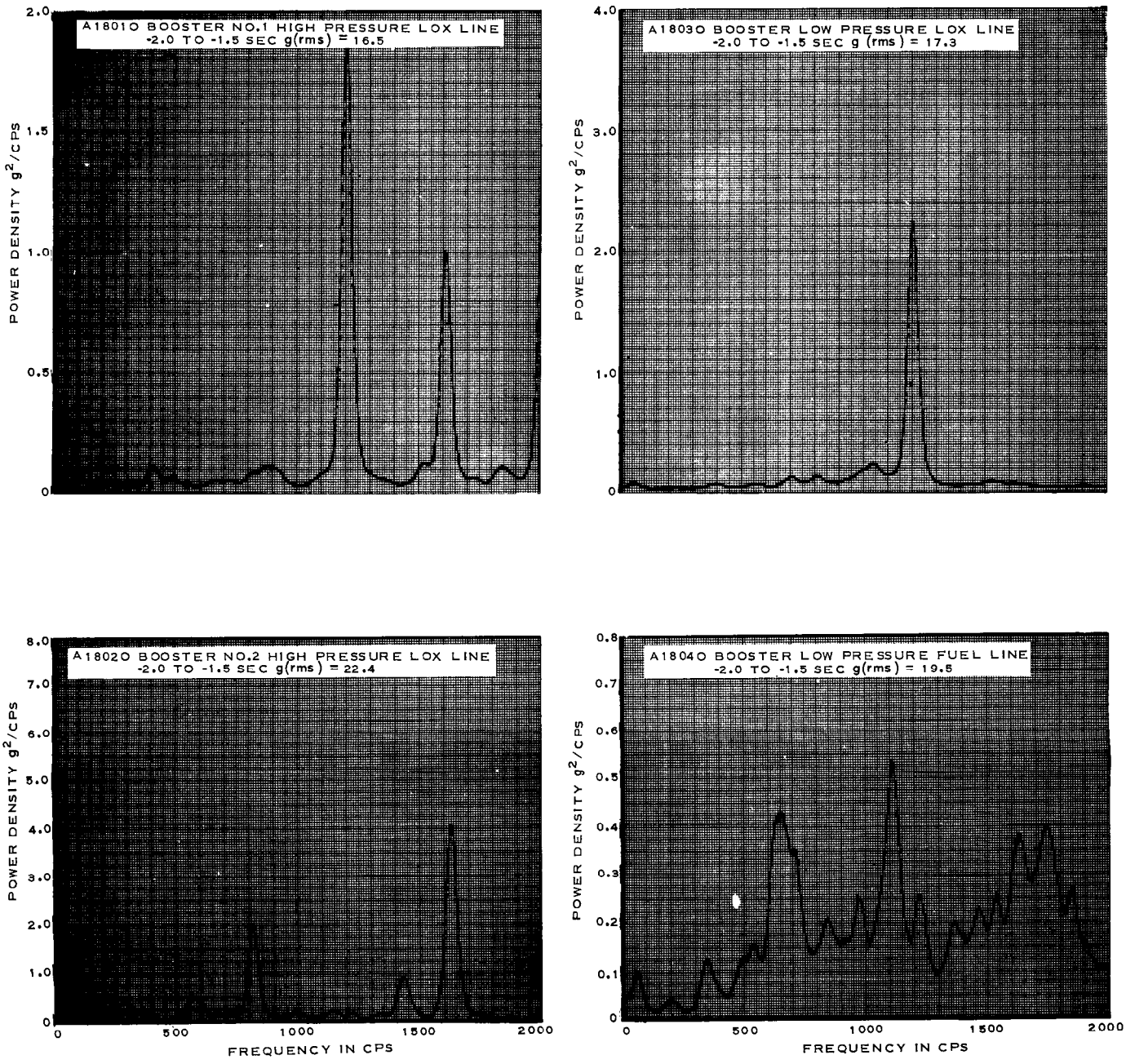

FIGURE 4.1-16 POWER DENSITY SPECTRA

Landline Acoustic Analysis

The acoustic environment was established within the AIG pod during launch as the result of the test data obtained from Missiles 42D, 54D and 60D. The overall maximum sound pressure level, within a frequency band of 10 to 10,000 cps, was 143.5 db. Maximum vibratory energy prevailed within a frequency band of 10 to 1,000 cps. Table 4.1-2 shows a summary of the resulting test data. Laboratory tests were conducted on a specimen AIG computer with the computer exposed to an acoustic environment comparable to that prescribed herein. Computer operation was completely satisfactory during the laboratory tests. The computer diode problem encountered on Missile 42D was found to be a quality control problem in manufacturing the diode.

TABLE 4.1-2 SUMMARY OF AIG POD ACOUSTIC ENVIRONMENT

MISSILE TEST	FORWARD MICROPHONE A1761Y				AFT MICROPHONE A1762Y			
	1	2	3	4	1	2	3	4
42D FRF	143.5	10-2000	50-60 / 127	160-215 / 127				
54D Launch	143.5	10-1000	30-50 / 130	150-170 / 128	143.0	10-1000	30-50 / 117	150-180 / 115
60D Launch	141.0	10-1000	30-60 / 129	110-130 / 122	137.0	10-1000	30-40 / 125	80-120 / 121

Code:

1. Maximum over-all sound pressure level in db (15 to 10,000 cps).
2. Frequency band wherein maximum energy prevailed.
3. Most predominant frequency (cps)/maximum sound pressure level (db) at that frequency.
4. Second most predominant frequency/sound pressure level in db.

Values indicate maximum level during launch phase.

Graphic presentations of the acoustic data are shown in Figures 4.1-17 through 4.1-26. A sound pressure level versus time plot for Missile 54D is displayed, and also octave band plots of the data received from the three test missiles. Constant band width plots are shown only for Missile 54D data.

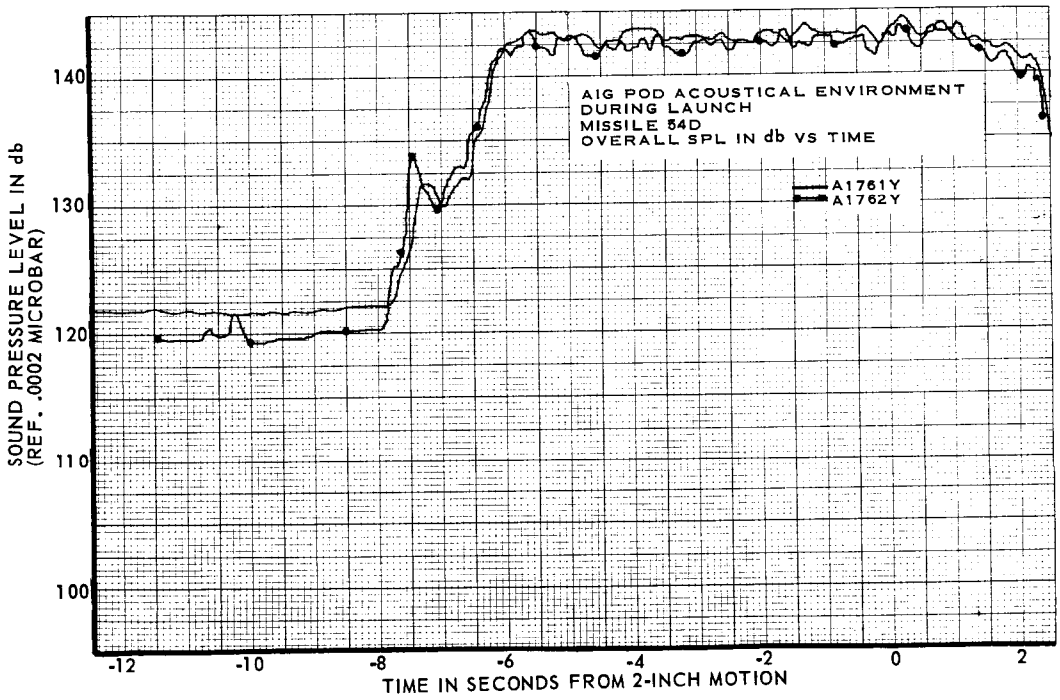

FIGURE 4.1-17 AIG POD ACOUSTICAL ENVIRONMENT, SOUND PRESSURE LEVEL

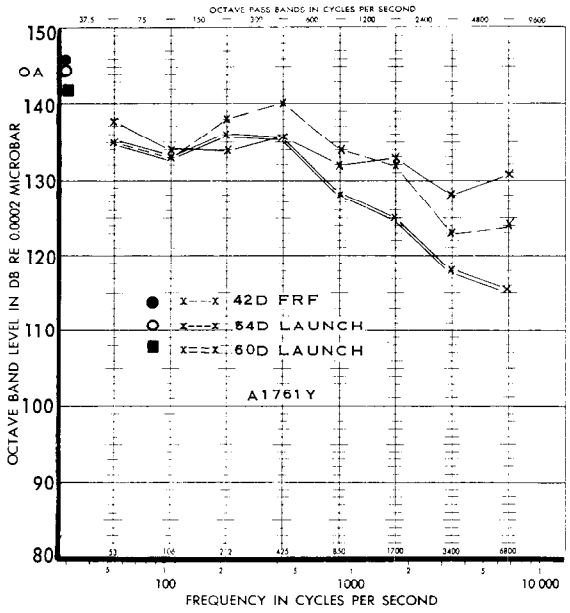

NOTE: EACH PLOT REPRESENTS 0.5 SECOND SAMPLE TAKEN DURING PERIOD OF MAXIMUM STEADY-STATE LEVEL

OA OVERALL SOUND PRESSURE LEVEL (10 TO 10,000 CPS)

FIGURE 4.1-18 AIG POD ACOUSTICAL ENVIRONMENT, COMPOSITE OF SOUND PRESSURE LEVEL (A1761Y)

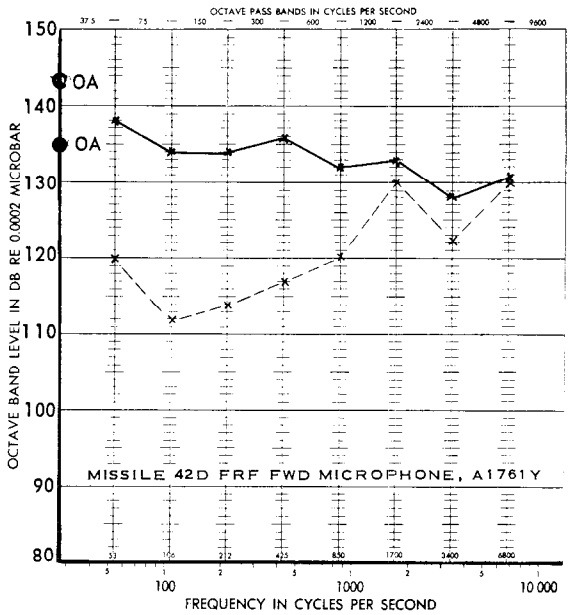

O X—X STEADY-STATE SAMPLE AT 2 SECONDS
● X---X BACKGROUND SAMPLE AT -10 SECONDS

OA OVERALL SOUND PRESSURE LEVEL (10 TO 10,000 CPS) REFERENCE MAIN STAGE IGNITION AS ZERO TIME

FIGURE 4.1-19 AIG POD ACOUSTICAL ENVIRONMENT, FORWARD MICROPHONE

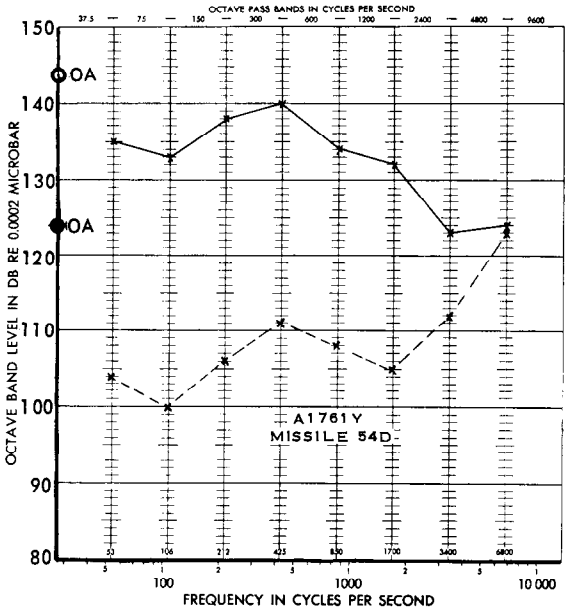

O X——X STEADY-STATE SAMPLE AT -0.5 SECONDS
● X---X BACKGROUND SAMPLE AT -12 SECONDS
OA OVERALL SOUND PRESSURE LEVEL (10 TO 10,000 CPS) REFERENCE 2-INCH MOTION AS ZERO TIME

FIGURE 4.1-20 AIG COMPUTER ACOUSTICAL ENVIRONMENT, AFT MICROPHONE

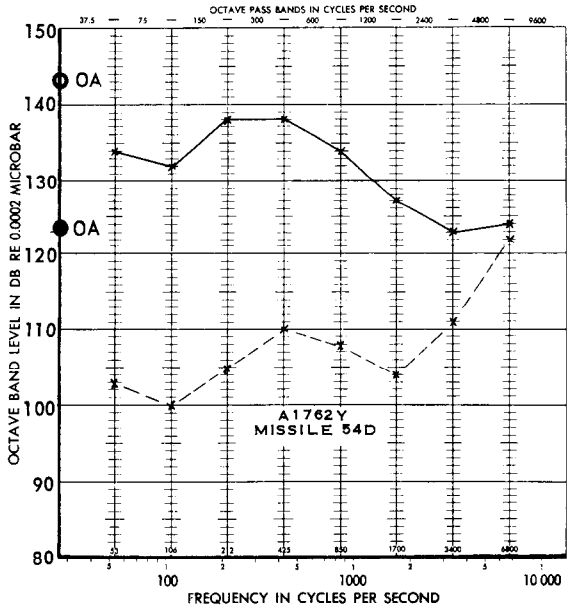

O X——X STEADY-STATE SAMPLE AT -0.5 SECONDS
● X---X BACKGROUND LEVEL AT -12 SECONDS
OA OVERALL SOUND PRESSURE LEVEL (10 TO 10,000 CPS) REFERENCE 2-INCH MOTION AS ZERO TIME

FIGURE 4.1-21 AIG COMPUTER ACOUSTICAL ENVIRONMENT, FORWARD MICROPHONE

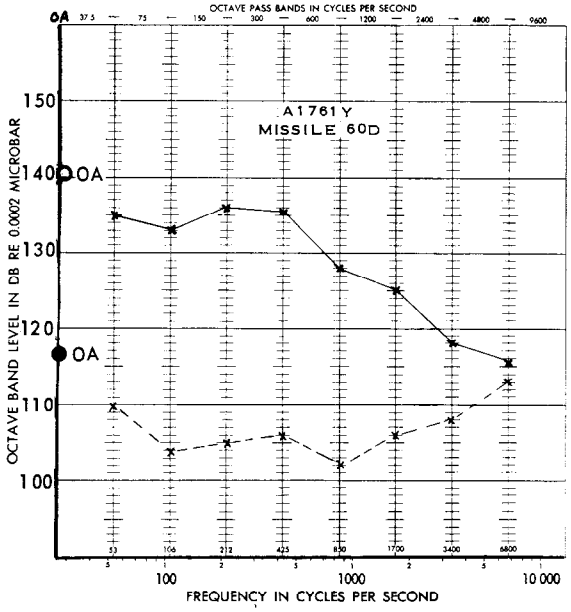

O X——X STEADY-STATE SAMPLE AT -2 SECONDS
● X----X BACKGROUND LEVEL AT -10 SECONDS

OA OVERALL SOUND PRESSURE LEVEL (10 TO 10,000 CPS)
REFERENCE 2-INCH MOTION AS ZERO TIME

FIGURE 4.1-22 AIG POD ACOUSTICAL ENVIRONMENT

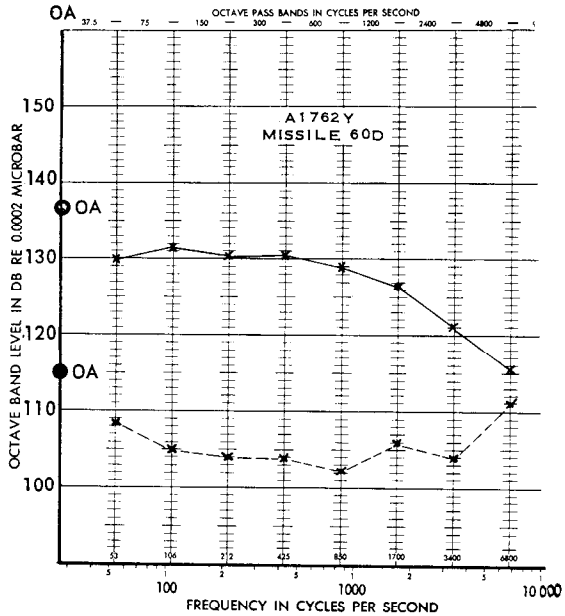

O X——X STEADY-STATE SAMPLE AT -2 SECONDS
● X---X BACKGROUND LEVEL AT -10 SECONDS

OA OVERALL SOUND PRESSURE LEVEL (10 TO 10,000 CPS)
REFERENCE 2-INCH MOTION AS ZERO TIME

FIGURE 4.1-23 AIG POD ACOUSTICAL ENVIRONMENT

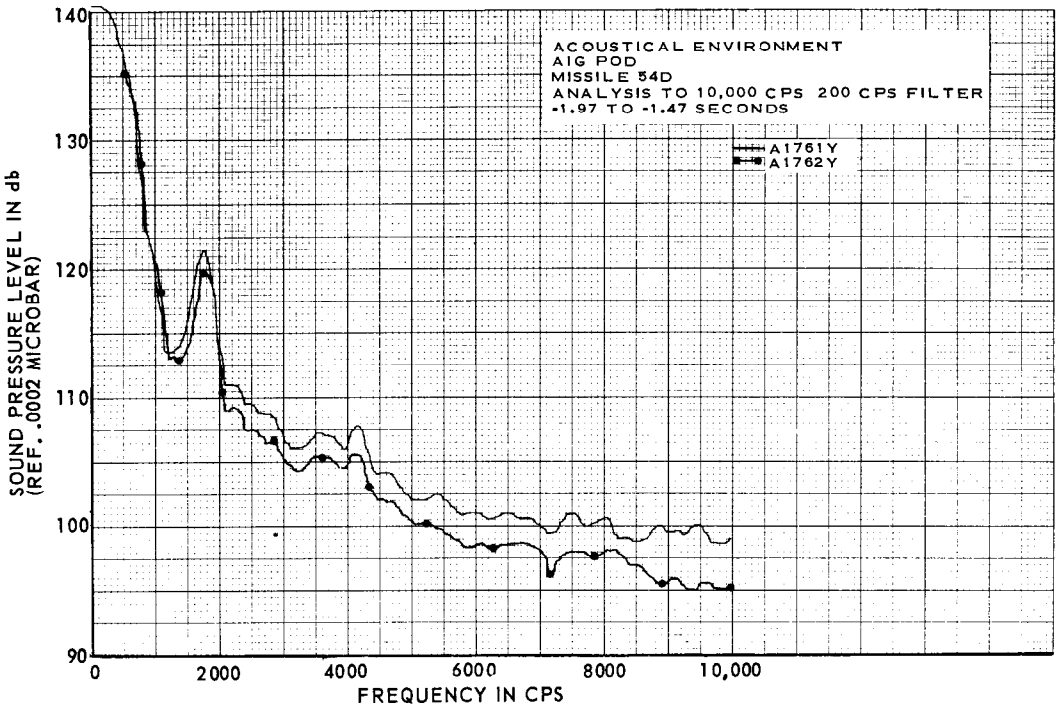

FIGURE 4.1-24 AIG POD ACOUSTICAL ENVIRONMENT, SOUND PRESSURE LEVEL

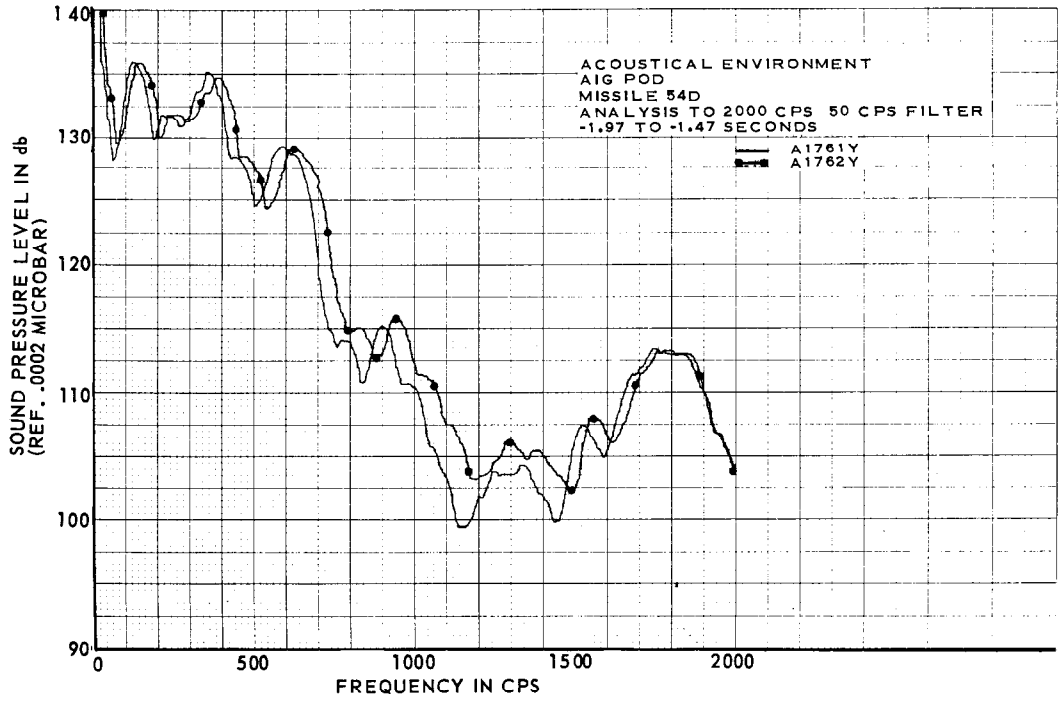

FIGURE 4.1-25 AIG POD ACOUSTICAL ENVIRONMENT, SOUND PRESSURE LEVEL

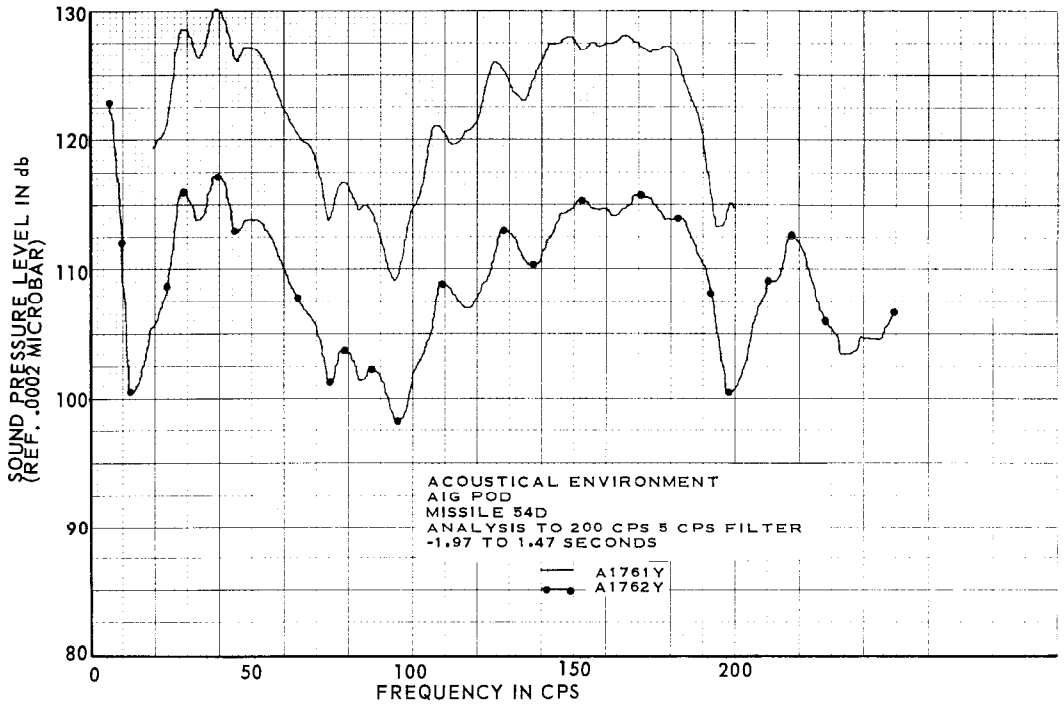

FIGURE 4.1-26 AIG POD ACOUSTICAL ENVIRONMENT, SOUND PRESSURE LEVEL

Flight Vibration Analysis

The vibration measurements obtained within the AIG pod generally displayed moderate vibratory acceleration levels throughout powered flight. The AIG pod maximum intensity period, in flight, occurred earlier than the period of maximum aerodynamic disturbance experienced at the number 1 and 2 equipment pods. The maximum vibration at the equipment pods usually occurred between the time the missile was at Mach 1 and the time of maximum q. The early occurrence of aerodynamic turbulence at the AIG pod may be explained by the irregular shape of the pod. The flight vibration levels appeared to be slightly greater along the Y axis than along either the X or Z axis. Table 4.1-3 presents a summary of the AIG pod section vibration.

TABLE 4.1-3 SUMMARY OF AIG POD VIBRATION DATA

MEAS.	NO.	LOCATION	MISSILE NUMBER 42D 1	42D 2	54D 1	54D 2	60D 1	60D 2	71D 1	71D 2
I560O	3	Binnacle X Axis			0.9	12.5 5.0				
I561O	3	Binnacle Y Axis			0.5	11 130-170	1.5	12 130		
I562O	3	Binnacle Z Axis					0.7	5.3 110 500		
I564O	3	Computer X Axis			1.0	5 50 130-160	0.9	37 170		
I565O	3	Computer Y Axis			2.9	5 50 130	0.8	55 550		
I566O	3	Computer Z Axis			0.9	3.5-4.5 50	0.7	27 65 550		
A643O	4	Outboard Frame, X Axis (Station 1089)	0.8	110						
A644O	4	Outboard Frame, Y Axis (Station 1089)	0.9	55						
A292O	4	Outboard Frame, X Axis (Station 1109)	0.3 to 0.4	40 to 70						
G197O	5	RB-IP Package, Radial							3.0	250 500 525
G587O	5	RB-IP Wave guide, Radial							8.8	700

NOTE:
1. Over-all vibratory acceleration ~ g(rms).
2. Predominant frequency ~ cps.
3. ARMA measurement installation.
4. Astronautics measurement installation.
5. General Electric measurement installation.

Values indicate maximum level during flight.

The AIG platform binnacle and computer vibration levels ranged between 0.2 and 3 g(rms). Frequency components ranging between 5 and 50 cps were intermittently displayed. Predominant components between 110 and 550 cps prevailed throughout flight. Generally, the levels through sustainer stage were not in excess of 0.25 g(rms). Figure 4.1-27 shows an average of the levels at the binnacle and computer, which provides only a display of the vibration trend through booster stage. Power density spectra computations made on the guidance equipment vibration data is shown in Figures 4.1-28 and 4.1-29.

The low frequency vibration measurements on the outboard frame of the AIG pod section indicated levels that were well within the airframe vibration specification limits. The maximum levels occurred between 35 and 45 seconds of flight and ranged between 0.3 to 0.9 g(rms). The predominant frequencies exhibited were between 40 and 110 cps. Vibration levels below 0.5 g(rms) were displayed through most of booster and sustainer stage.

Vibration measurements made on the instrumentation beacon equipment in the No. 1 pod showed normal levels at the rate beacon package and the rate beacon waveguide. The maximum vibration environment was exhibited through the Mach 1 - maximum q period of flight. Table 4.1-3 shows the maximum levels displayed during powered flight. Power density computed for each measurement is shown in Figure 4.1-30.

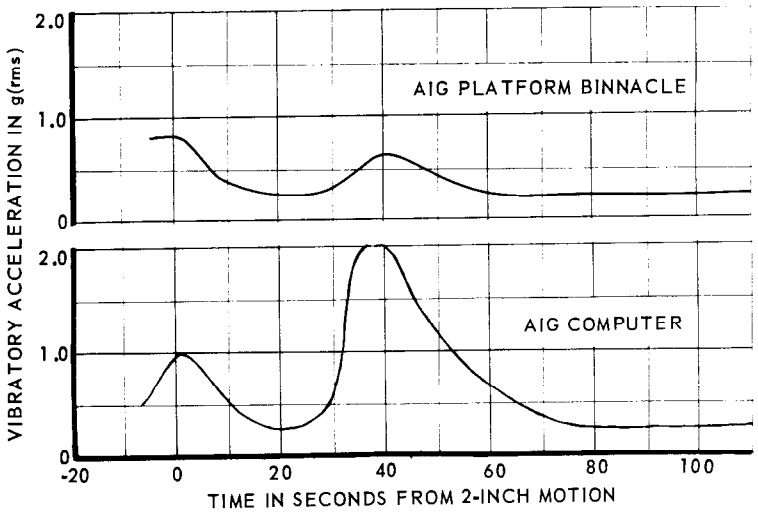

FIGURE 4.1-27 AVERAGE AIG EQUIPMENT POD VIBRATION LEVELS

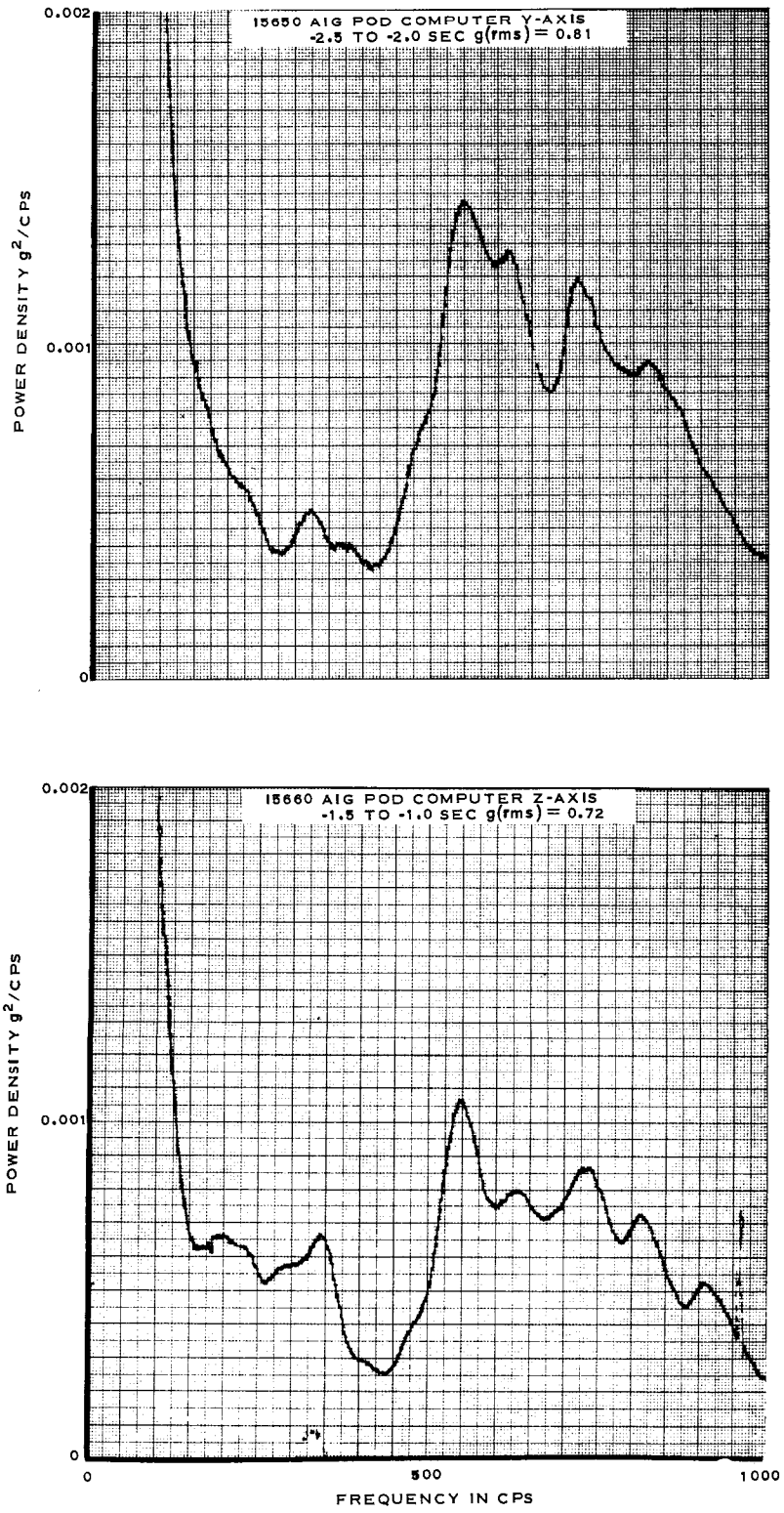

FIGURE 4.1-28 POWER DENSITY SPECTRA, AIG EQUIPMENT POD

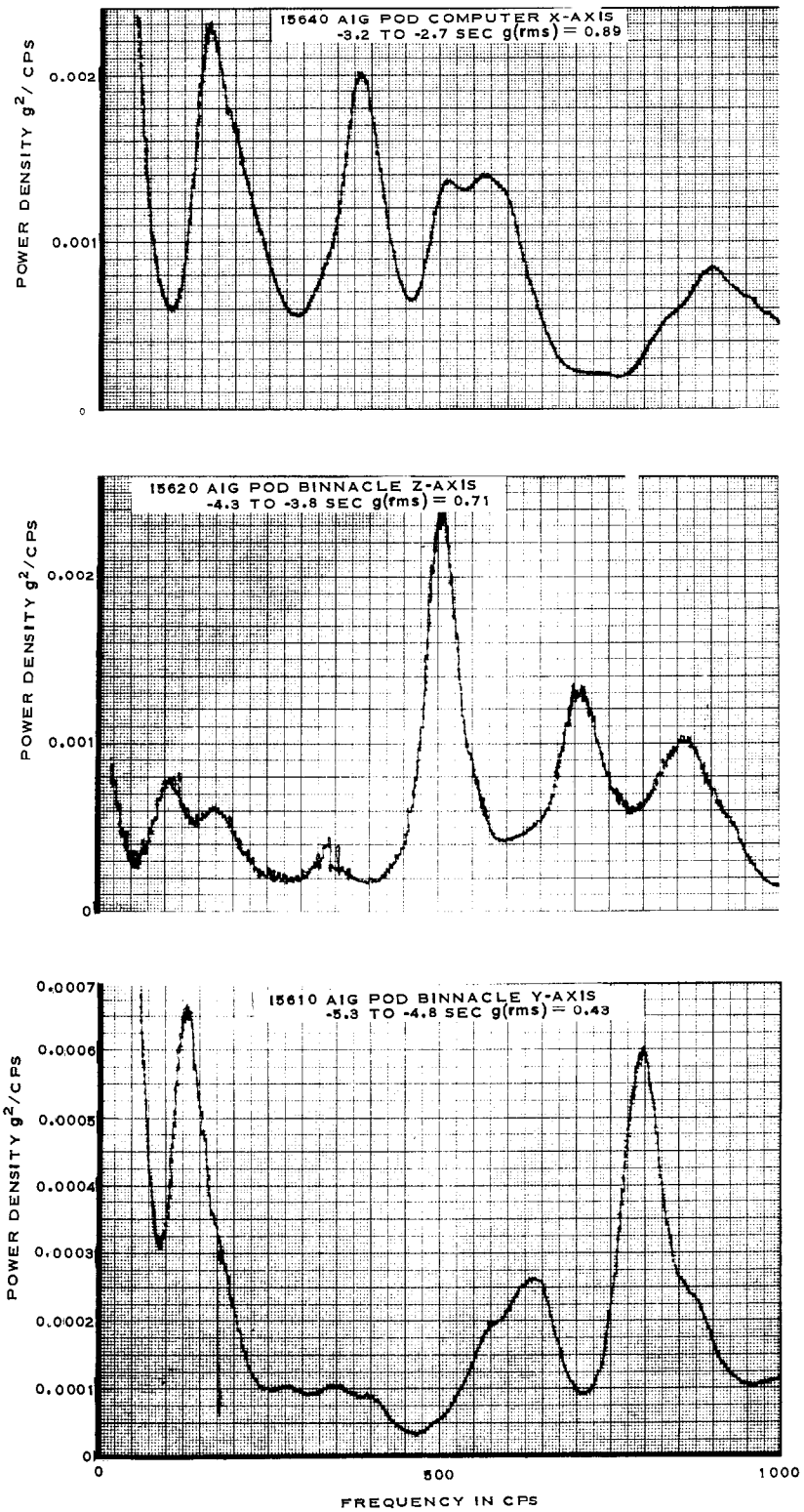

FIGURE 4.1-29 POWER DENSITY SPECTRA, AIG EQUIPMENT POD

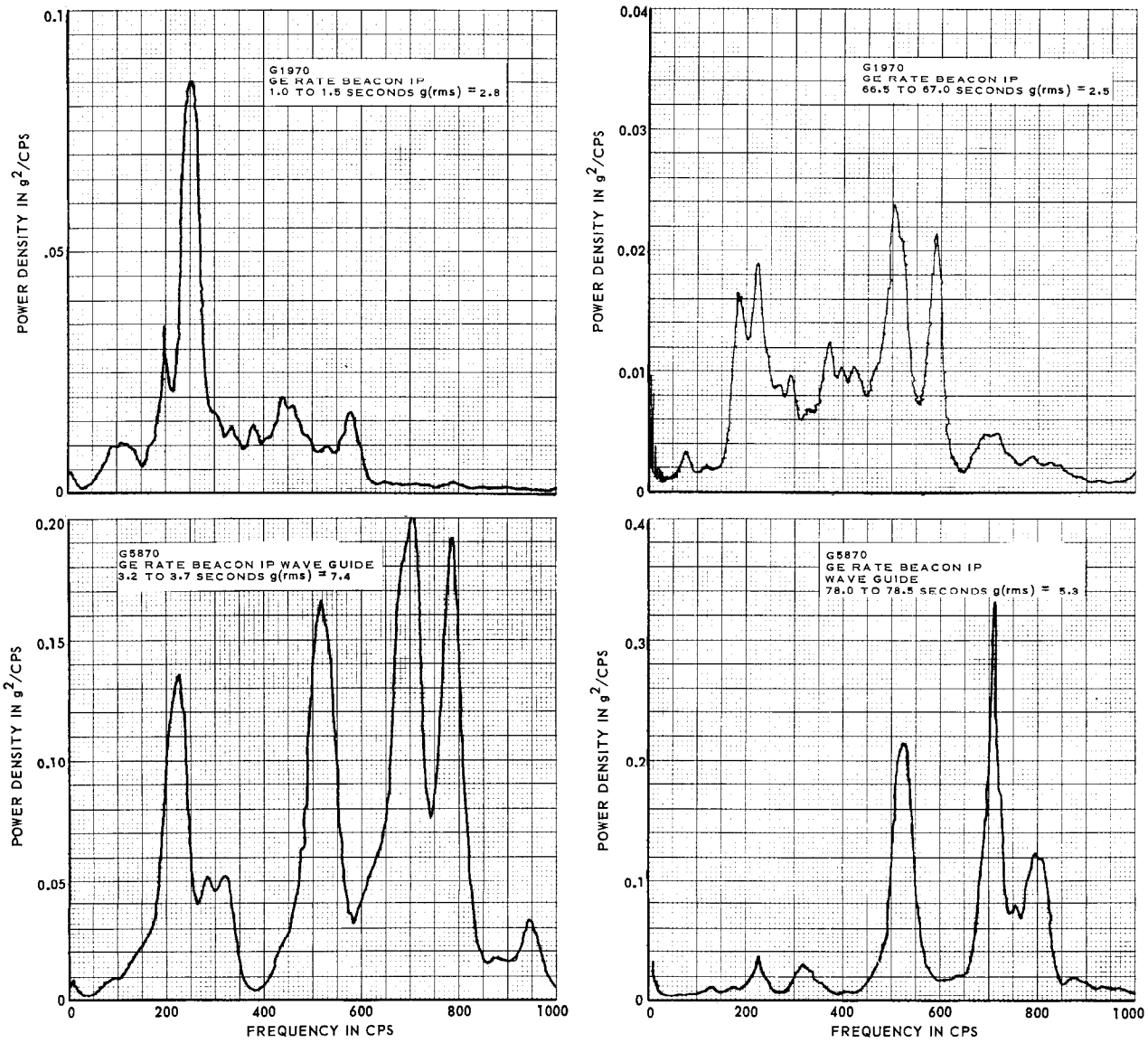

FIGURE 4.1-30 POWER DENSITY SPECTRA, B1 EQUIPMENT POD

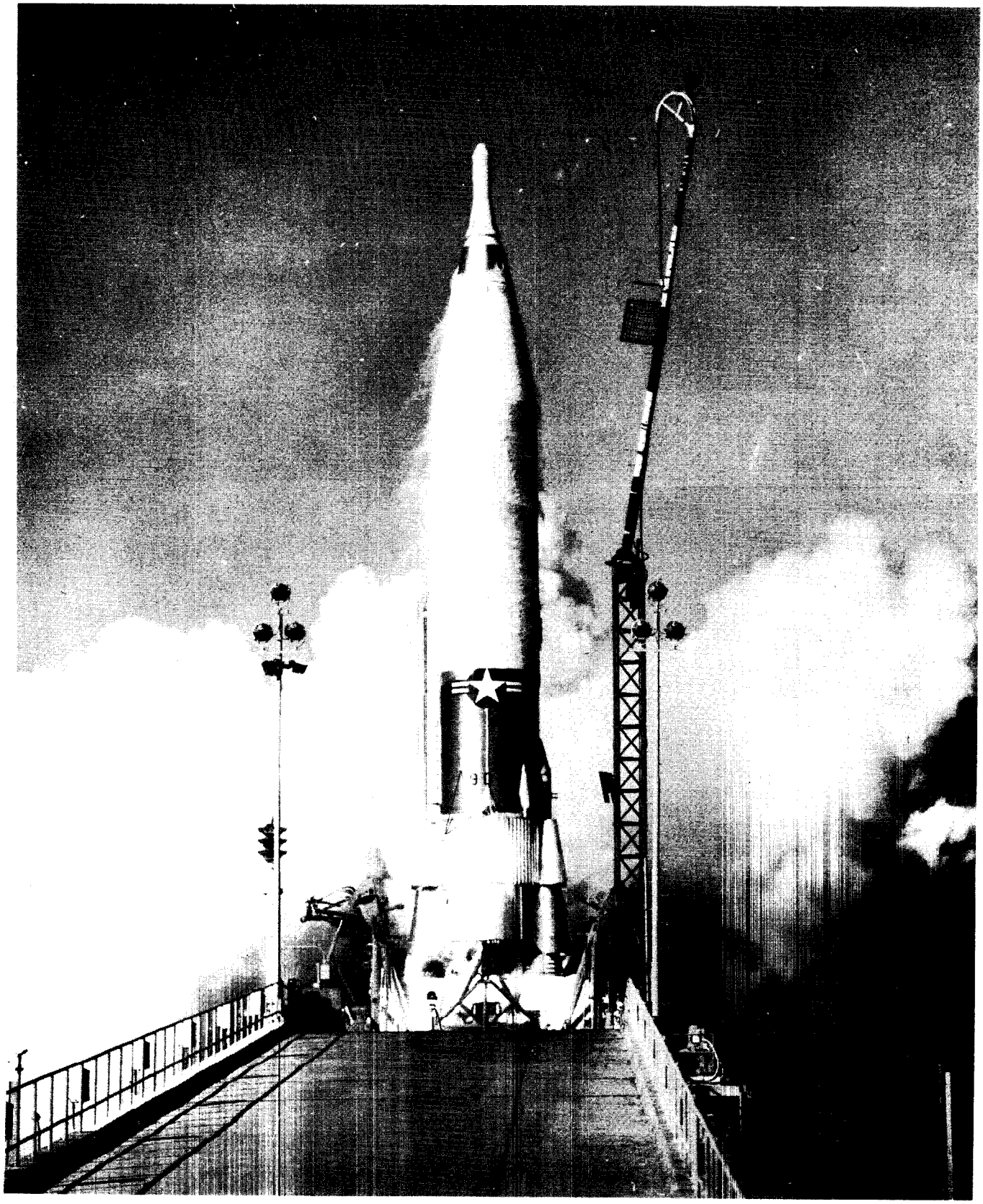

MISSILE 90D, SERIES D/R&D MISSILE

SECTION 4.2 – AERODYNAMIC FORCES

PURPOSE OF TESTING

Aerodynamic forces were determined as part of a continuing effort to obtain data based upon flight test results for comparison with predicted values. Aerodynamic forces so obtained are used to check the input to trajectory calculations in addition to supporting missile structural integrity studies.

TEST RESULTS

The forces determined herein are defined as axial forces and are those forces which act parallel to the missile longitudinal axis. The axial force, equal to the drag force when the missile is flying at zero angle of attack, is determined from the relationship:

$$\frac{T - A}{W} = n_a \tag{1}$$

where: T = thrust, lbs

A = axial force, lbs

W = missile weight, lbs

n_a = axial acceleration, g's

Missile thrust and axial acceleration are readily obtained from telemetry data. Missile weight was determined based upon a linear interpolation between launch weight and the weight just prior to staging. Since the drag term (A) at staging is essentially zero, the above relationship was used to determine the missile weight just prior to staging. A linear interpolation between the two weights is considered valid since the rate of change of the missile weight is essentially linear due to an almost constant propellant flow rate.

Axial force was converted to a coefficient by dividing by the dynamic pressure and a reference area (78.5 sq ft). The coefficient presented in equation form is:

$$C_A = \frac{T - Wn_a}{qS} \qquad (2)$$

where: C_A = axial force coefficient, non-dimensional

T = thrust, lbs

W = weight, lbs

n_a = axial acceleration, g's

q = dynamic pressure, lb/ft^2

S = reference area, ft^2

The axial force coefficient is composed of different types of drag forces (base drag, wave drag, friction drag, etc.). Therefore, the exterior configuration of the missile will affect the axial force coefficient. Considering the missiles discussed in this report, there were four configurations:

1. D/RIG missile with the Mark 3 re-entry vehicle

2. D/AIG missiles with the Mark 3 re-entry vehicle

3. D/AIG missile with the RVX-2A re-entry vehicle

4. D/RIG missile with the Mark 4 re-entry vehicle.

Figure 4.2-1 shows the average coefficient and one standard deviation for all Series D/RIG R&D missiles flown to date with the Mark 3 re-entry vehicle (15 flights). Also shown is the predicted curve for this coefficient. Good agreement is indicated and the standard deviation shows good repeatability.

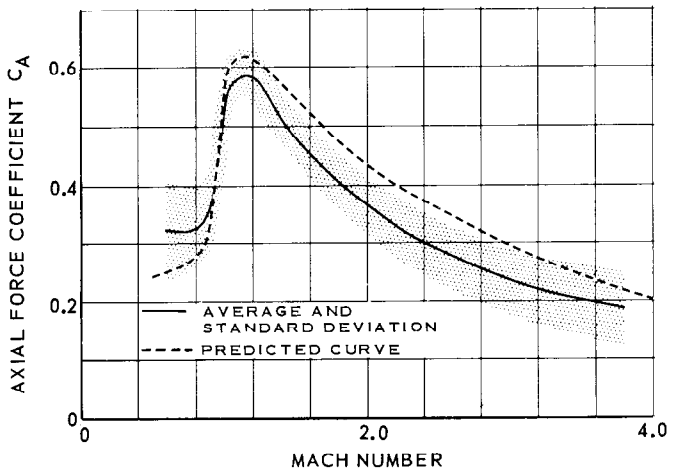

FIGURE 4.2-1 AVERAGE AXIAL FORCE COEFFICIENT, RIG MISSILES WITH MARK 3 RE-ENTRY VEHICLE

Figures 4.2-2 and 4.2-3 present the same comparison for the Series D/AIG R&D missiles flown with the Mark 3 and RVX-2A re-entry vehicles, respectively. No definite conclusions can be established covering the differences between the computed and the predicted data indicated in Figure 4.2-2 due to the limited quantity of data available. Only three D/AIG missiles (42D, 54D, 60D) were flown with the Mark 3 re-entry vehicle aboard.

Similarly, the relatively large scatter of data indicated in Figure 4.2-3 could be the result of the limited quantity of data available. Only three D/AIG missiles (66D, 76D, 71D) were flown with the RVX-2A re-entry vehicle aboard.

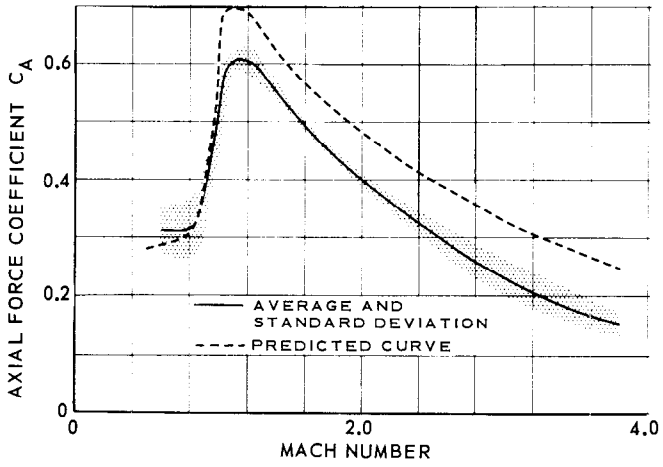

FIGURE 4.2-2 AVERAGE AXIAL FORCE COEFFICIENT, AIG MISSILE WITH MARK 3 RE-ENTRY VEHICLE

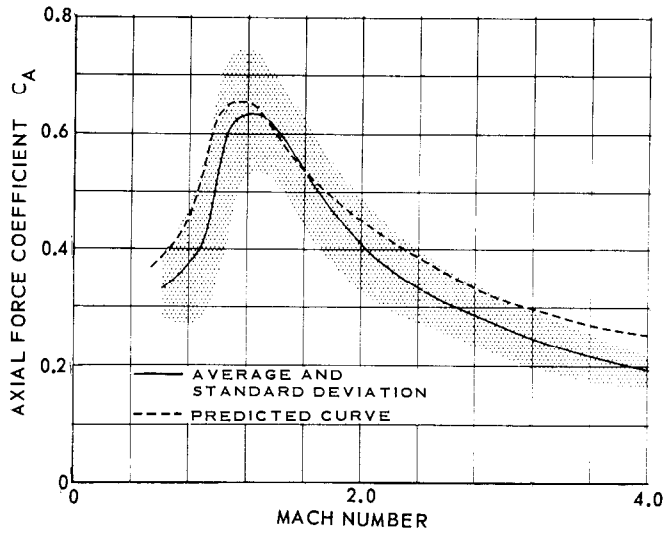

FIGURE 4.2-3 AVERAGE AXIAL FORCE COEFFICIENT, AIG MISSILES WITH RVX-2A RE-ENTRY VEHICLE

Figure 4.2-4 compares the predicted and computed axial force coefficient for the one D/RIG missile flown with the Mark 4 re-entry vehicle aboard.

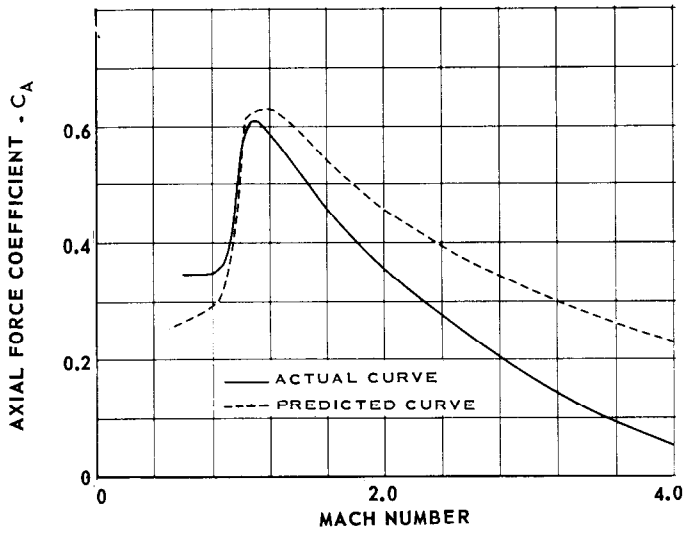

FIGURE 4.2-4 AXIAL FORCE COEFFICIENT, RIG MISSILE WITH MARK 4 RE-ENTRY VEHICLE

ATLAS MISSILE SHORTLY AFTER LIFTOFF

SECTION 4.3–ENGINE COMPARTMENT TEMPERATURES

PURPOSE OF TESTING

Engine compartment temperatures were recorded for a continuing analysis of the abnormal random ambient temperature increases experienced in the engine compartment during the earlier portion of the Series D R&D flight test program. Data from several early Series D flights indicated abnormal temperature increases beginning at about 80 seconds of flight. This anomaly was considered to be of major importance after the flight of Missile 42D which experienced a vernier hydraulic system failure at approximately 100 seconds, with resultant loss of missile attitude control during vernier solo phase. This failure was attributed to an abnormally high temperature environment in the engine compartment. The results of a study to determine the cause of this anomoly are presented in this section.

TEST CONDITIONS

The thrust section configuration and location of components in the engine compartment remained essentially unchanged during the Series D program. The only significant modifications accomplished in the engine compartment area were removal of the sustainer stage pressurization bottle (initiated on Missile 40D) and changing of the heat shield aft surface material from aluminized fiberglass to a refrasil blanket (initiated on Missile 26D). Table 4.3-1 is a configuration resume for the complete Series D R&D flight test program.

The above mentioned minimum configuration changes accomplished during the subject program allows no correlation to be inferred between engine compartment configuration and abnormal temperature environment. Changes in missile exterior configuration therefore become of prime suspect. Series D R&D missiles can be grouped by exterior configuration into four basic groups:

1. RIG missiles flown with the Mark 2 re-entry vehicle aboard.

2. RIG missiles flown with the Mark 3 re-entry vehicle aboard.

3. AIG missiles flown with the Mark 3 re-entry vehicle aboard.

4. AIG missiles flown with the RVX-2A re-entry vehicle aboard.

These four basic configurations constitute the basis for the following discussion.

TABLE 4.3-1 SERIES D/R AND D CONFIGURATION RESUME

MISSILE NO.	RE-ENTRY VEHICLE	AIG POD	BOOT FIX	PROPULSION SYSTEM	HEAT SHIELD	SUS. LOX TANK HELIUM BOTTLE
5D	Mark 2	No	Yes	MA-2	Aluminum honeycomb with aluminized fiberglass covering	Capped off
11D	Mark 2					
14D	Mark 2					
15D	Mark 3		Yes			
17D	Mark 2		No			
18D	Mark 3					
22D	Mark 3					
26D	Mark 3				Aluminum honeycomb with a refrasil blanket in place of the fiberglass	
28D	Mark 3					
31D	Mark 3					Capped off
40D	Mark 2					Removed
43D	Mark 3					
44D	RVX-4A-2					
49D	Mark 3	No	No			
42D	Mark 3	Yes	No			
56D	Mark 3	No	Yes			
54D	Mark 3	Yes	Yes			
62D	Mark 3	No	Yes			
27D	Mark 3	No	Yes			
60D	Mark 3	Yes	No			
32D	Mark 3	No	Yes			
66D(1)	RVX-2A	Yes	Yes			
76D(1)	RVX-2A	Yes	Yes			
79D	Mark 3	No	Yes			
71D(1)	RVX-2A	Yes	Yes			
55D	Mark 3	No	No			
83D	Mk 4 Mod I	No	No			
90D	Mark 3	No	No	MA-2		Removed

NOTE: (1) The configuration includes a heat shield between the forward nacelle doors and the engine fairing on the B2 side.

TEST RESULTS

As a result of abnormal random temperature increases noted in the engine compartment on early Series D missiles, an investigation was initiated to determine the cause and effect, if any, of this anomaly. The abnormal temperature increases were noted to occur beginning at about 80 seconds of flight and were of varying magnitudes. Table 4.3-2 is a tabulation of the differential between maximum temperature and the initial steady-state value prior to 80 seconds. The steady-state values approximate sea level ambient temperature. The data obtained from this initial investigation indicated that the missile exterior configuration associated with the abnormal engine compartment temperature environment was that of the D/RIG missile with the Mark 2 re-entry aboard, whereas the configuration associated with the normal temperature environment was that of the D/RIG missiles with the Mark 3 re-entry vehicle aboard. The Mark 2 re-entry vehicle is blunt, while the Mark 3 re-entry vehicle is streamlined. The exact effect of these two configurations on air flow around the missile has not been determined.

The cause of the abnormal temperature increase could not be definitely established. The entrance of hot exhaust gases into the engine compartment around the boots appears to be the most plausible explanation. It has been determined that, at about 80 seconds, the base pressure of the missile becomes greater than ambient, thus exerting a force on the aft surfaces of the radiation heat shield. Due to the manner by which the booster engine boots are installed, the force on the aft surface of the missile could cause the boots to slip forward on the engines, toward the throat, thus causing an opening between the engine and boots. These openings would vary in size and orientation from missile to missile, thus explaining the inconsistencies in the temperatures recorded in the engine compartment.

On several subsequent flights, a fix was applied consisting of attaching the boots more firmly to the engines in order to eliminate boot deflection. Data obtained from test flights incorporating this fix have been inconclusive.

TABLE 4.3-2 ENGINE COMPARTMENT TEMPERATURE DIFFERENTIAL

MISSILE NO.	PAYLOAD	MEASUREMENT NUMBER						
		P14T	P607T	P671T	A743T	A745T	A746T	A747T
5D	Mark 2			NDp				
11D	Mark 2	10°p	5°p					
14D	Mark 2	35°p	100°(2)p		20°s			
15D	Mark 3	NRs	95°(1)s	25°s	NRs	10°s	10°s	35°(3)s
17D	Mark 2	280°s	85°s	60°s	25°s	100°s	25°s	185°s
18D	Mark 3		10°s	NDp				
22D	Mark 3	NRs		NRs	NRs	NRs	NRs	NRs
26D	Mark 3	NRs		NRs	NRs	NRs	NRs	NRs
28D	Mark 3	NRs		NRs	10°s	NRs	NRs	NRs
31D	Mark 3	5°s		10°s		10°s	NRs	NRs
40D	Mark 2	65°s				20°s	30°s	40°s
43D	Mark 3	NRs				NRs	NRs	NRs
44D	RVX-4A-2	10°s		25°s	10°s	5°s	NRs	NRs
49D	Mark 3	NRs		NRs	5°s	NRs	NRs	NRs
42D	Mark 3	390°(4)s		~200°s	100°s	280°s	350°s	100°s
56D	Mark 3	15°s		20°s	10°s	10°s	10°s	NRs
54D	Mark 3	50°s		10°s	NDs	10°s	NRs	20°s
62D	Mark 3	NRs				5°s	NRs	NRs
27D	Mark 3	15°s		10°s	10°s	10°s	10°s	NRs
60D	Mark 3	160°s		~150°s	30°s	NDs	290°s	~250°s
32D	Mark 3	NRs		NRs	5°s	10°s	NRs	NRs
66D*	RVX-2A	15°s		20°s	10°s	10°s	20°s	NRs
76D*	RVX-2A	NRs		NRs	NRs	NRs	NRs	NRs
79D	Mark 3	NRs				NRs	NRs	NRs
71D*	RVX-2A	5°s		10°s	15°s	NRs	NRs	30°s
55D	Mark 3	5°s				15°s	NRs	NRs
83D	Mk 4 Mod I	15°s				30°(3)s	NRs	NRs
90D	Mark 3	15°s		10°s	20°s	30°(1)s	NRs	NRs

NOTE: (1) Rise starts at zero time.
(2) Out of band at about 200°F.
(3) Rise starts at about 40 seconds.
(4) Out of band at 400°F.
NR - No rise.
ND - No data.
* - Special thermocouple instrumentation added.
Subscript -
s - surface resistance transducer.
p - resistance probe transducer.

During the flight of Missile 42D, a hydraulic system failure occurred, with resultant loss of missile attitude control. The anomaly was apparently caused by an abnormally high temperature environment in the engine compartment, starting at 80 seconds and reaching a maximum at 110 seconds. Figure 4.3-1 is an analog presentation of the temperatures re-

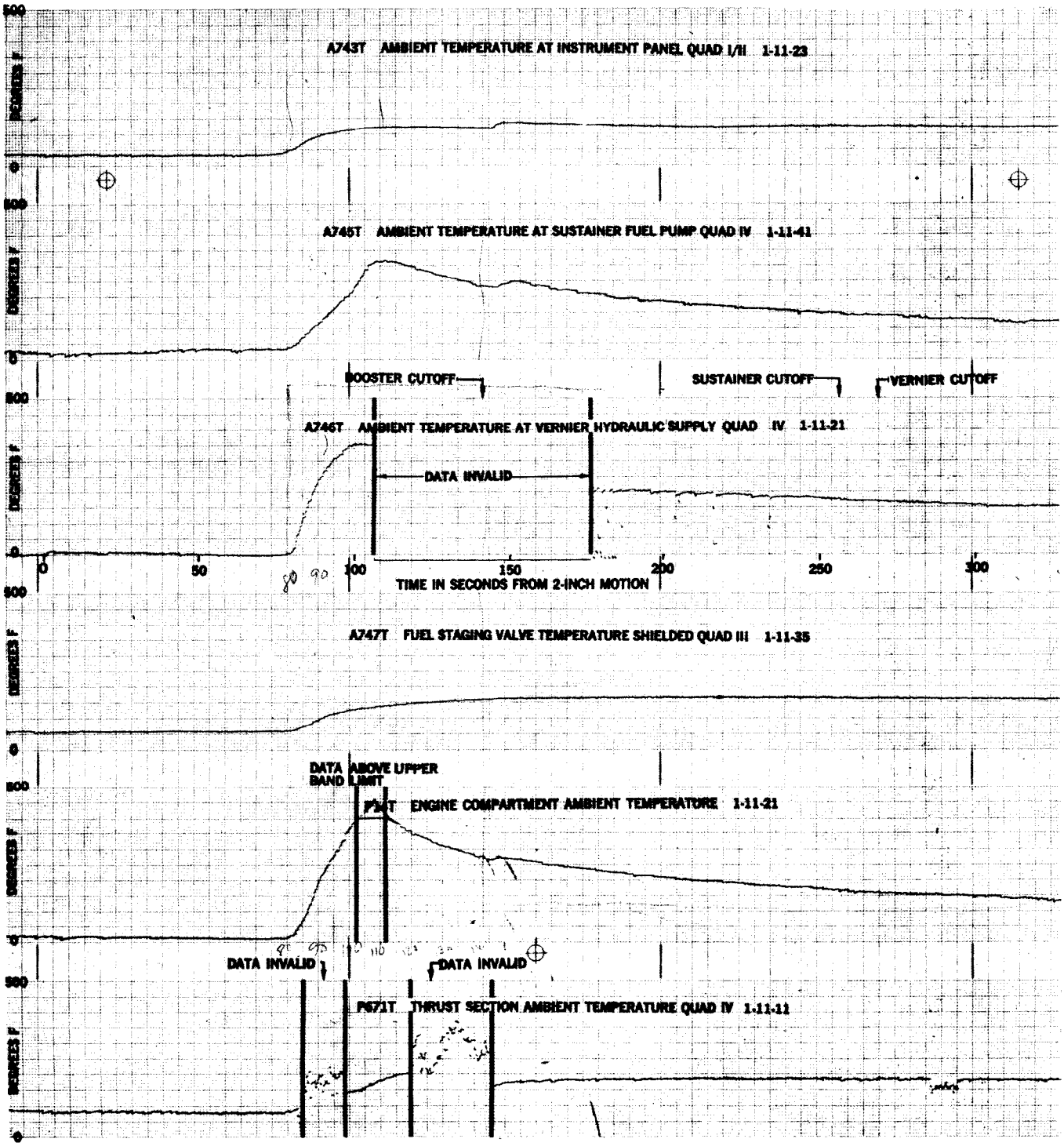

FIGURE 4.3-1 ENGINE COMPARTMENT TEMPERATURE DATA, MISSILE 42D

corded on Missile 42D. It should be noted that Missile 42D was the first Series D R&D missile to be flown with the all-inertial guidance (AIG) system aboard. The exterior configuration of D/AIG missiles differred primarily from that of D/RIG missiles in that the B2 equipment pod was redesigned and enlarged to accommodate the all-inertial guidance system. Figure 4.3-2 illustrates the location of this redesigned pod on a Series D missile. It was felt that the redesigned B2 equipment pod caused a low pressure area to form in the vicinity of the B2 nacelle doors, thereby tending to evacuate the engine compartment, causing a large differential pressure to exist across the boots. This pressure differential displaced the boots, and permitted hot exhaust gases to enter the engine compartment.

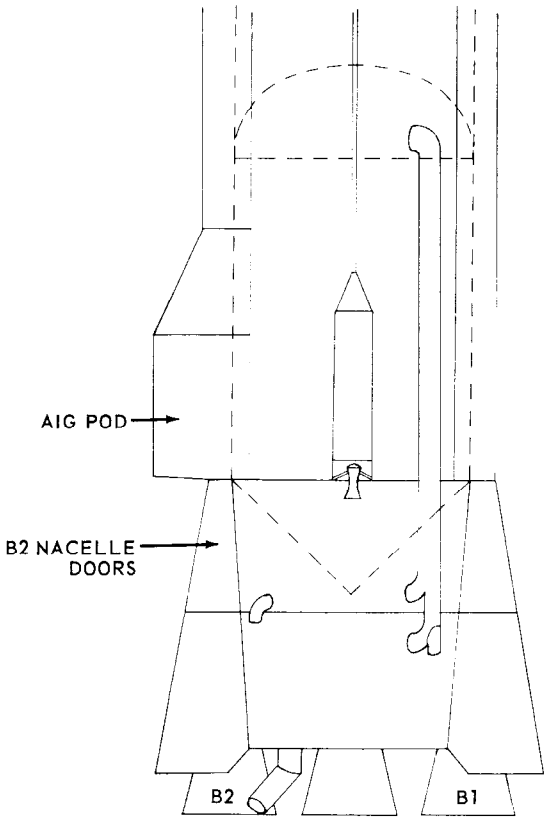

FIGURE 4.3-2 LOCATION OF AIG EQUIPMENT POD

Additional instrumentation was installed on subsequent D/AIG missiles (66D, 71D and 76D) for further study of the engine compartment temperature environment. This instrumentation consisted of 15 thermocouples located at strategic positions within the engine compartment. (See Figure 4.3-3.) In addition, the above mentioned boot fix and an additional heat shield between the nacelle area and the engine compartment was incorporated. (Reference Figure 4.3-4.) These three D/AIG missiles were flown with the RVX-2A re-entry vehicle aboard. The data from these flights indicated results comparable to the D/RIG R&D

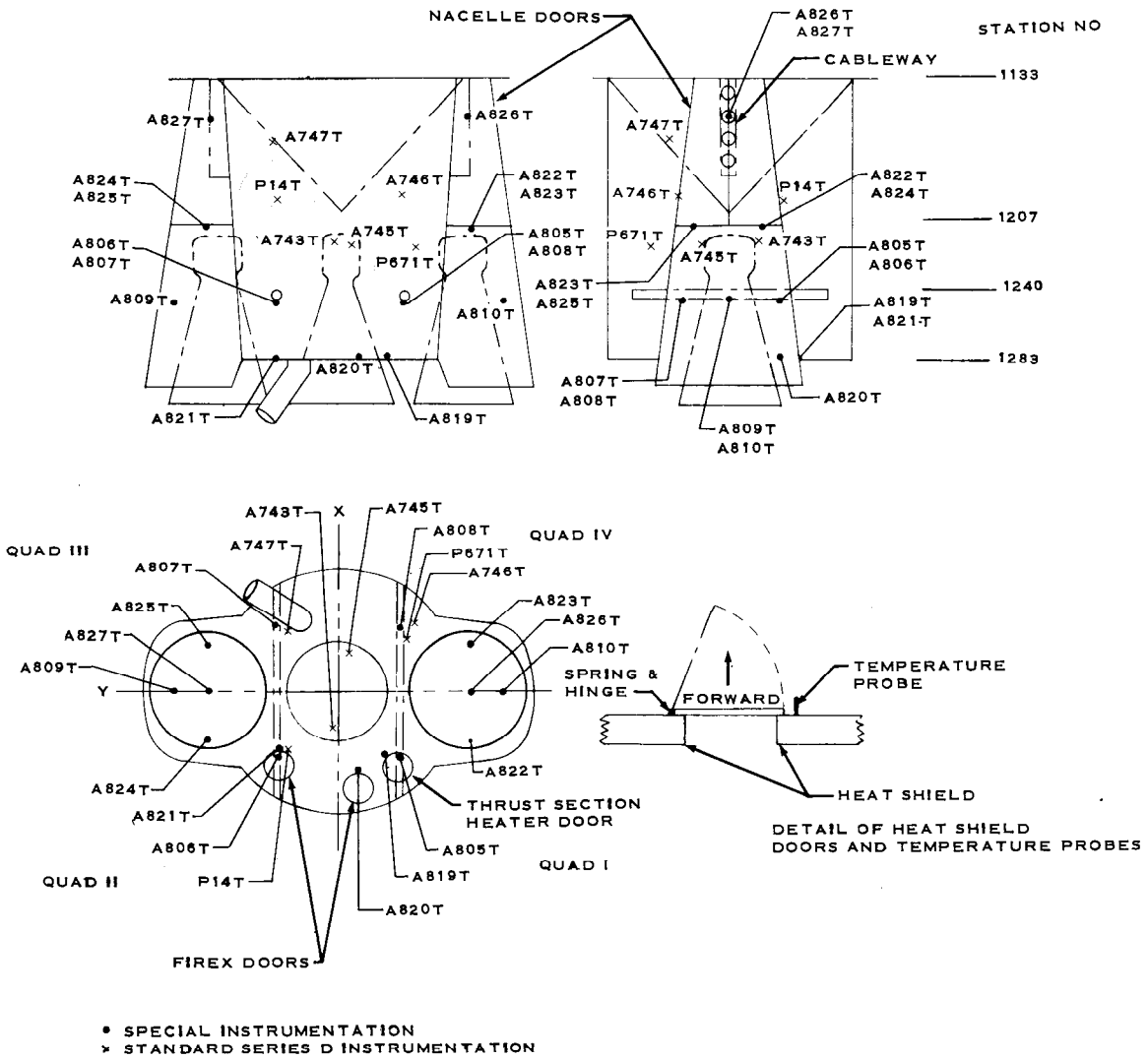

FIGURE 4.3-3 ENGINE COMPARTMENT TEMPERATURE INSTRUMENTATION

~~SECRET~~

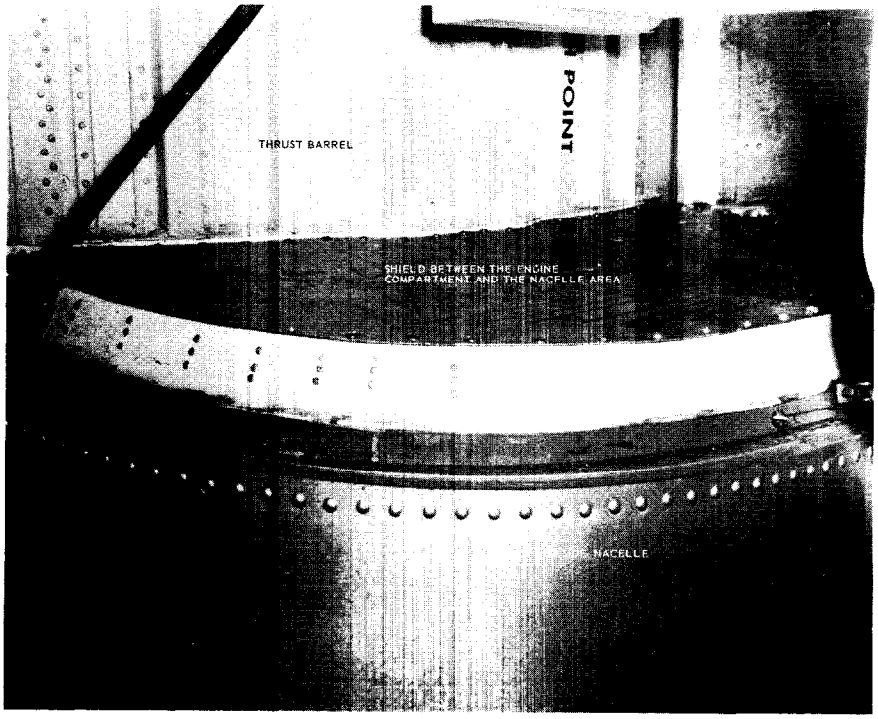

FIGURE 4.3-4 HEAT SHIELD LOCATION

missiles flown with the Mark 3 re-entry vehicle aboard, i.e. no significant temperature rise. Data from the thermocouples indicated temperatures remained at the lower temperature band limit (85°F) except for those measurements located at the firex and heater doors on the heat shield. These measurements indicated in some cases, a sharp rise beginning both just prior to Mach 1 (approx. 50 seconds) and at 80 seconds and, in other cases, a rise beginning at either Mach 1 or 80 seconds. These temperature changes are not considered indicative of a problem because of their location.

Due to the inconsistent external configurations noted above, precise correlation between the data obtained and external configuration is not possible and consequently the exact mechanics causing the abnormal temperature environment cannot be determined.

Since temperature rises of serious proportions appear to be associated mainly with the D/AIG pod-nacelle door area, no external configuration change is planned for Series E missiles since the nacelle doors have been eliminated on these missiles.

~~SECRET~~

SECTION 4.4-STRUCTURAL INTEGRITY

PURPOSE OF TESTING

Flight testing of Series D R&D missiles discussed in this report was partially conducted to demonstrate the structural integrity of the airframe and the functional adequacy of the light weight thrust structure.

TEST CONDITIONS

The missile airframe consists of the re-entry vehicle adapter, propellant tanks, and thrust section.

Two types of re-entry vehicle adapters were used on the Series D flights reported here. One adapter was constructed of corrugated stainless steel and was used on all missiles which incorporated the RVX-2A re-entry vehicle. The other was constructed of aluminum and was used on missiles which carried the Mark 3 and Mark 4 re-entry vehicle.

The propellant tanks consist basically of a thin-walled stainless steel cylinder with an intermediate bulkhead to separate the propellants. The tanks depend on internal pressure to maintain shape and structural integrity. The intermediate bulkhead is concave to the fuel tank and derives structural integrity from differential tank pressures which results in a net forward force on the bulkhead. The intermediate bulkhead is constructed of stainless steel. However, the aft surface is insulated to suppress heat transfer to the lox and thus lox boil-off. The insulation consists of Stafoam sandwiched between the stainless steel bulkhead and a supplementary aluminum liner. This insulation was damaged on Missile 55D and a BMD/STL/Convair decision was made to fly without the insulation. Extensive special instrumentation was installed to provide information on the effect of removing the insulation. Results of this aspect of the 55D flight test are presented in the Pneumatics Section (Section 6.2).

Figure 4.4-1 shows a comparison of the tank skin thickness for the different Series D missiles. The increased skin thicknesses from those of earlier missiles were incorporated to accommodate the added loads imposed by dry starting the booster engines. Dry starting means igniting the engines without an inert fluid leading the fuel into the combustion chambers.

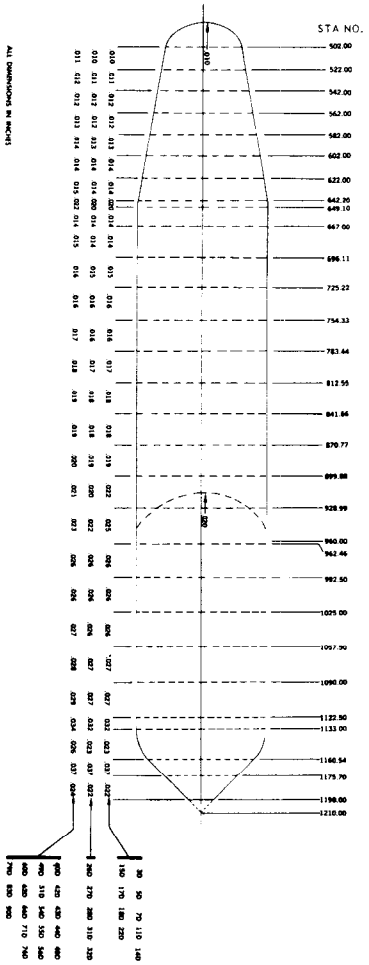

FIGURE 4.4-1 COMPARISON OF SERIES D SKIN THICKNESS

The booster thrust structure on Series D missiles is constructed of corrugated aluminum and laminated fiberglass, with engine fairings constructed of fiberglass. The thrust structure supports the subassemblies of the booster stage propulsion, pneumatic, electrical and hydraulic systems.

TEST RESULTS

Fourteen of the 15 missiles satisfactorily demonstrated the structural integrity of the propellant tanks and light weight booster thrust structure. One missile (48D) was destroyed in the launcher as a result of a propulsion system malfunction which culminated in an engine compartment explosion and subsequent missile destruction. The airframe was in no way responsible for this failure.

This page intentionally left blank.

SECTION 4.5 - ADVANCED GUIDANCE SYSTEM

PURPOSE OF TESTING

Components of the Space Technology Laboratories Advanced Guidance System were flown on Missiles 83D and 90D in order to evaluate their performance under flight environmental conditions. Eight units of the system were installed in a fiberglass pod located between Stations 1050 and 1110 on the dividing line between Quadrants III and IV. Equipment and antenna locations are shown in Figure 4.5-1.

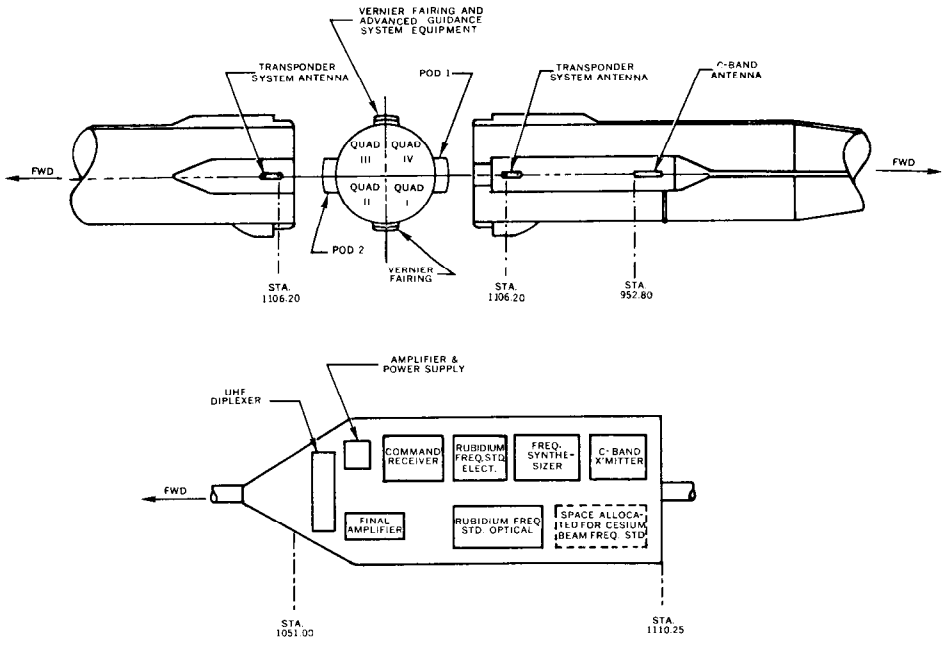

FIGURE 4.5-1 ADVANCED GUIDANCE SYSTEM

TEST RESULTS

Performance of the Rubidium Cell Very Stable Oscillator was monitored by four telemetry measurements: The rubidium cell lamp temperature, the rubidium cell cavity temperature, the rubidium cell second harmonic and the rubidium cell fundamental. Detailed analysis of these data was performed by STL.

SECTION 4.6 - RADIOMETER

PURPOSE OF TESTING

Data on the characteristics of infrared radiation emanating from rocket exhaust plumes during the flight of an Atlas missile were required for the refinement of design criteria for shielding from infrared radiation and for checking theories of after-burning of rocket exhaust gases and jet plume spreading. The information derived from these studies was also intended for use in the design of satellite detection systems. The earth's atmosphere absorbs most infrared frequencies so that any infrared light source seen against an earth background by an orbiting satellite detector would be a probable indication of rocket exhaust above the atmosphere.

TEST CONDITIONS

Air Force Cambridge Research Center and Lockheed Packages

The radiometer package flown on Missiles 27D, 32D, 55D and 56D is shown schematically in Figure 4.6-1. For Missiles 27D and 32D, this unit was referred to as the Air Force Cambridge Research Center (AFCRC) radiometer package and on Missiles 55D and 56D as the Lockheed radiometer package. The different designations refer to the agencies responsible for analysis of test results. The radiometer incorporates five infrared filters which are successively interposed between a port at the end of the B2 equipment pod and a bolometer thermistor detector. The filter wheel rotates at 0.2 rps. The detector responds to the impinging radiation by providing a voltage to the amplifier network and missile telemetry system. The detector output is further modified by a mechanical chopper which assures a square waveform. The measurements telemetered from this apparatus include (1) the five filter outputs, (2) a calibration light to check system continuity and detector operation, (3) three calibration voltages, (4) two temperature measurements, and (5) a reflectance measurement to check sooting or clouding of the filter windows.

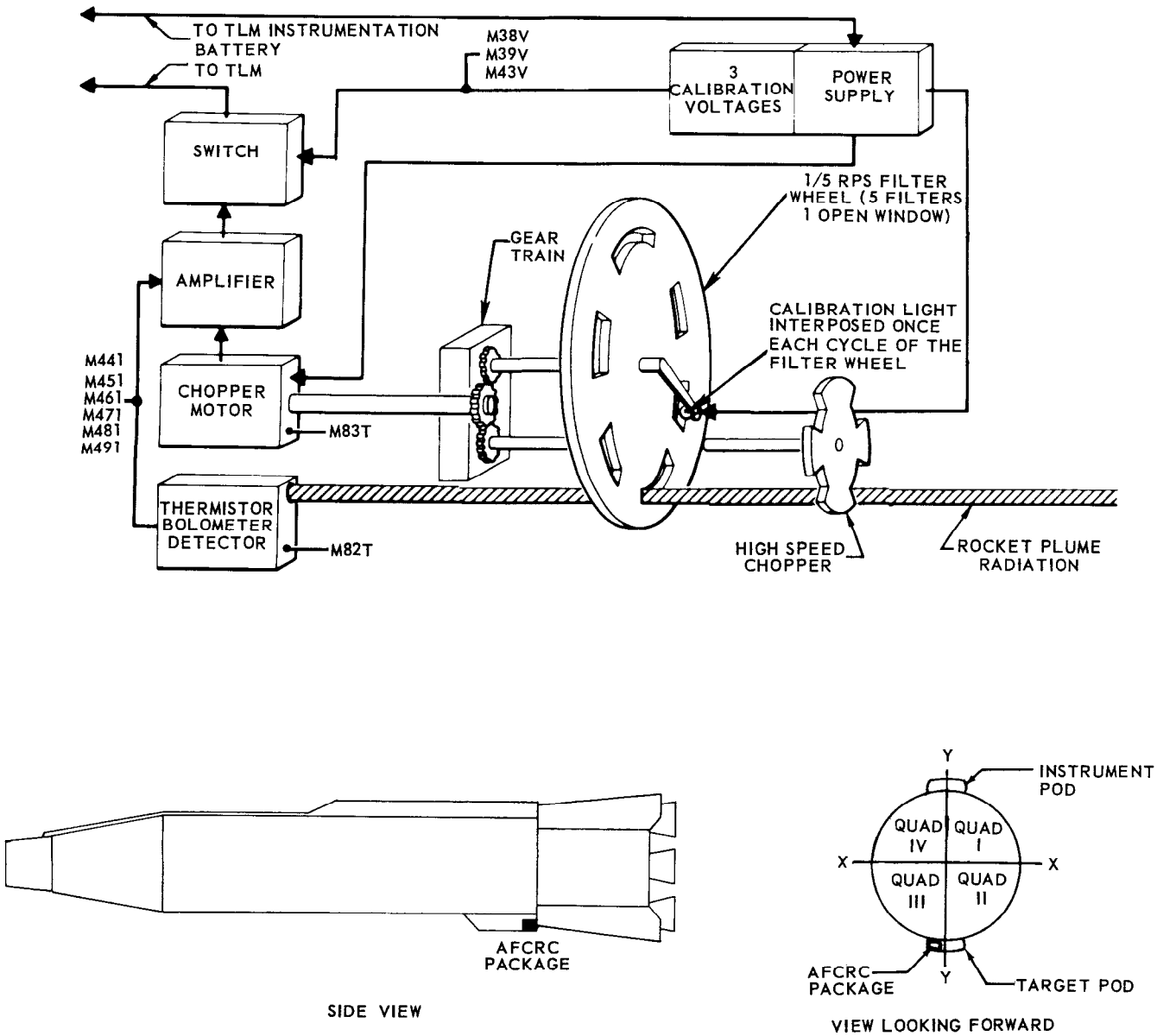

FIGURE 4.6-1 RADIOMETER PACKAGE

Lockheed Spectrometer

The Lockheed spectrometer package flown on Missiles 79D, 83D and 90D is shown schematically in Figure 4.6-2. For Missiles 79D and 83D the unit consisted of two grating monochromators with two separate electronic channels. The resolution of the instrument is 0.1 micron. Two interference filters limit the spectral region received by each monochromator to 1.2 to 2.2 microns and 2 to 4 microns, and to avoid interference from different order spectra. A chopper is placed before the entrance slits of the two monochromators. Each monochromator utilizes an Ebert type grating and mirror system designed so that only one specific frequency impinges upon the lead selenide detector at any one time.

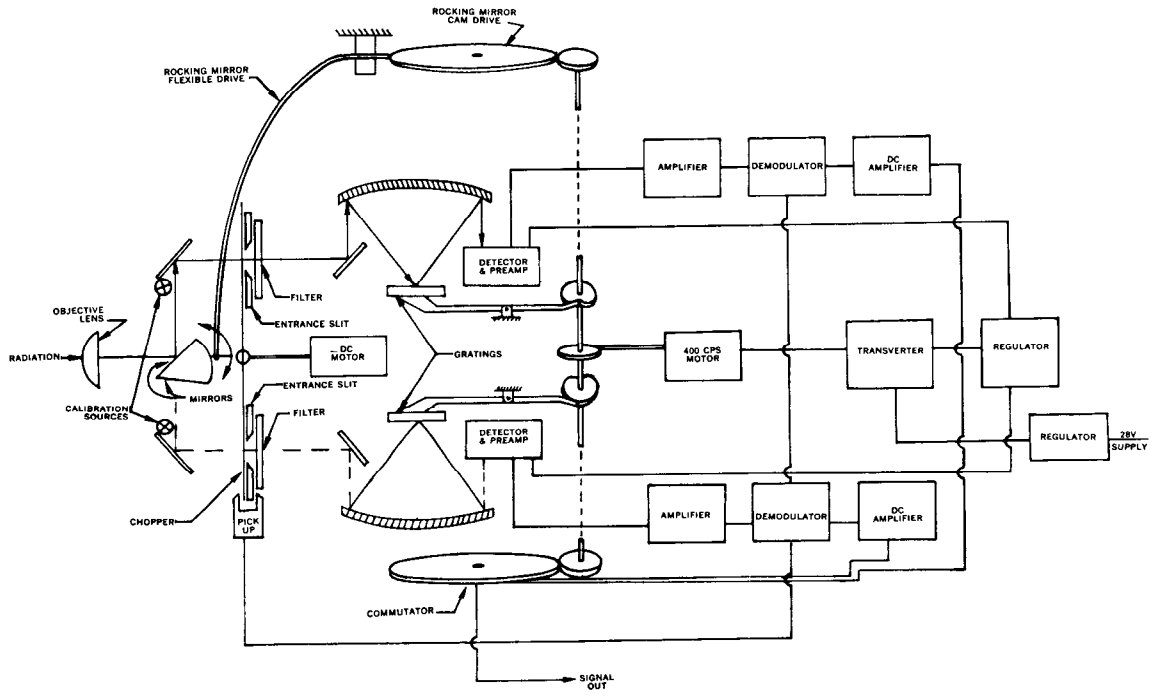

FIGURE 4.6-2 LOCKHEED SPECTROMETER

The package flown on Missile 90D, in contrast to the earlier model with separate channels, consists of one monochromator with one electronic channel. Infrared radiation from the engine exhaust is first separated into two partial wavelength bands of 1.4 to 2 microns and 2 to 4 microns by means of two alternating filters. Light waves within these two wavelength bands then pass to the monochromator, which consists of a collimating mirror and a rocking grating, and then to the lead selenide detector. The detector output is processed by an amplifier, a demodulator and a d-c amplifier from where it is fed to a commutator that switches the output to the telemeter system and adds auxiliary information between the spectral scans.

Test Results

Since test data analysis and system evaluation of the radiometer and spectrometer packages were the responsibility of AFCRC and Lockheed/Burbank, a discussion of test results is outside the scope of this report.

SECTION 5. PROPULSION SYSTEM

SECTION 5.1 - ENGINE PERFORMANCE

PURPOSE OF TESTING

Evaluation of MA-2 propulsion system performance continued to be of major importance on the group of Series D R&D missiles covered in this report. Additional objectives of significance in the test program included the gathering of data for analysis of booster propulsion system combustion characteristics from ignition to 2-inch motion, acquisition of performance data for reliability analysis and the demonstration of satisfactory net positive suction head (NPSH) conditions at the sustainer lox pump inlet at staging. In the discussion which follows, particular attention is also devoted to booster and sustainer engine thrust decay characteristics and propulsion system time interval parameters prior to launch.

TEST CONDITIONS

All the Series D missiles included in the scope of this report employed the Rocketdyne MA-2 propulsion system consisting of one XLR89-NA-3 booster engine package (sea level thrust rating 309,000 lbs), one XLR105-NA-3 sustainer engine (sea level thrust rating 57,000 lbs) and two XLR101-NA-3 vernier engines (sea level thrust rating 1,000 lbs). A schematic diagram of the MA-2 propulsion system is shown in Figure 5.1-1.

~~SECRET~~

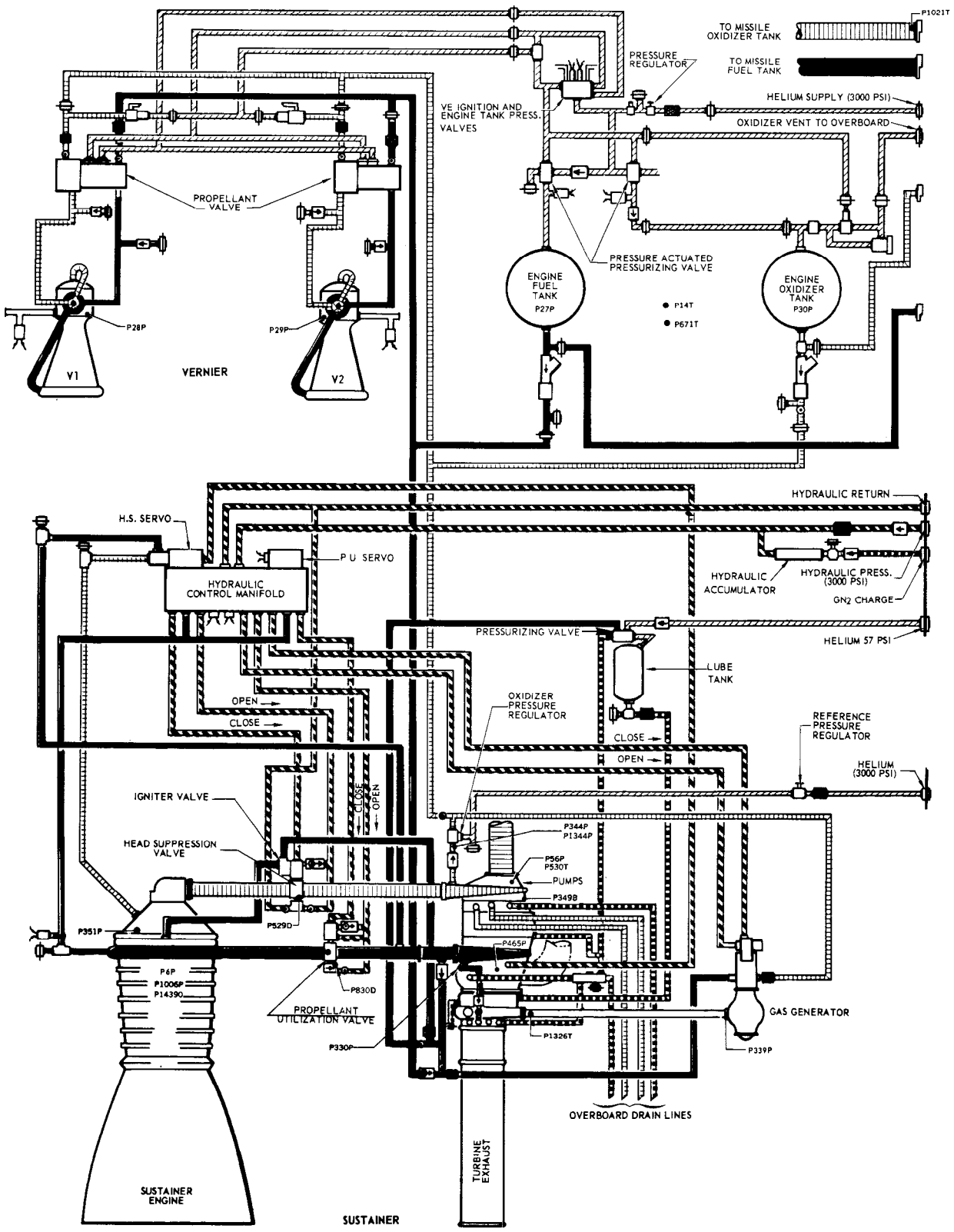

~~SECRET~~

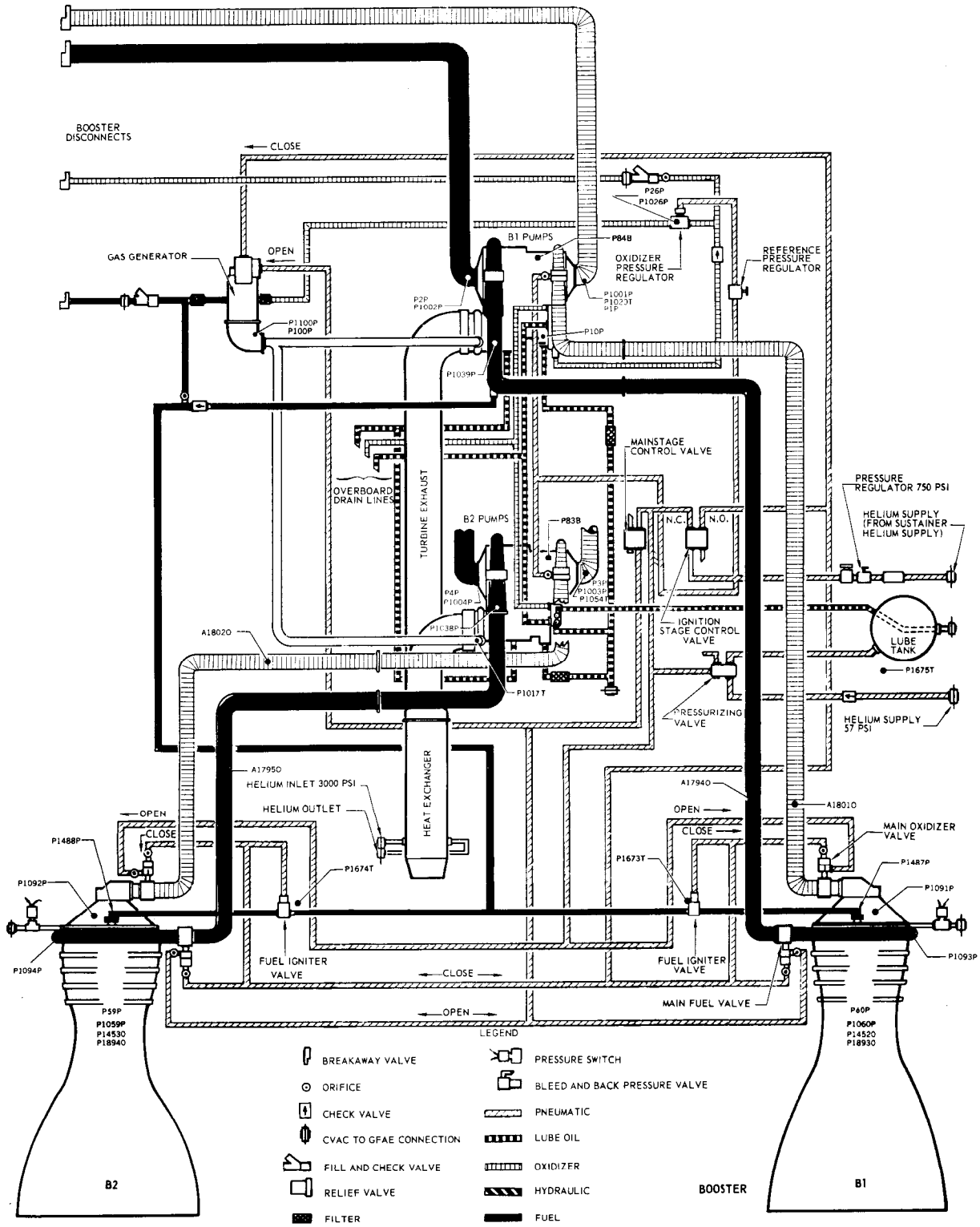

FIGURE 5.1-1 PROPULSION SYSTEM

TEST RESULTS

Engine operating times for the group of Series D missiles covered in this report are shown in Table 5.1-1. System operation was generally satisfactory except for Missile 48D, which was destroyed prior to launch due to booster engine combustion instability, and Missile 60D, on which premature pressurization of the vernier engine propellant tanks produced a severe drop

TABLE 5.1-1 ENGINE OPERATING TIMES

MISSILE NO.	BOOSTER		SUSTAINER		VERNIER	
	ACTUAL	PLANNED	ACTUAL	PLANNED	ACTUAL	PLANNED
42D	141.25	141.0	256.83	257.87	269.40	277.64
48D (2)	-	-	-	-	-	-
56D	136.58	138.96	271.08	279.50	285.00	294.72
54D	137.63	140.12	235.56	246.21	242.83	259.20
62D	117.78	119.04	284.28	285.89	307.70	305.29
27D	132.93	130.98	278.68	282.95	294.03	302.35
60D	141.06	140.12	307.64	246.21	277.45	259.20
32D	131.56	133.27	288.10	285.49	302.01	301.16
66D	136.47	137.62	259.26	267.52	274.46	280.52
76D	138.59	139.12	274.92	272.02	290.93	285.08
79D	138.60	138.08	282.49	286.53	295.23	302.29
71D	139.58	139.62	266.75	273.59	280.73	288.52
55D	135.87	138.06	283.06	287.70	298.14	306.60
83D	137.77	138.76	269.93	276.58	286.35	293.78
90D	137.68	136.27	272.95	277.67	288.77	294.43

NOTE: (1) Times are in seconds from 2-inch motion to start of acceleration decay.
(2) Missile destroyed prior to launch.

in the sustainer engine performance level, particularly following booster cutoff. These and additional discrepancies of a minor nature are discussed further under the Problem Area section of this report. Engine thrust levels, presented as a function of flight time, are depicted graphically in Figures 5.1-2 through 5.1-6 as a mean value of the applicable flights, together with one standard deviation band limits to reflect engine-to-engine thrust variability. Average thrust for all engines was near nominal. An approximation of sustainer specific impulse was calculated for all applicable missiles by plotting the reciprocal of the missile axial acceleration for the time interval between booster and sustainer cutoff and computing the negative reciprocal of the slope of the best straight line through the data points. The resulting values of specific impulse, shown in Table 5.1-2 can be compared with the nominal value of approximately 310 seconds.

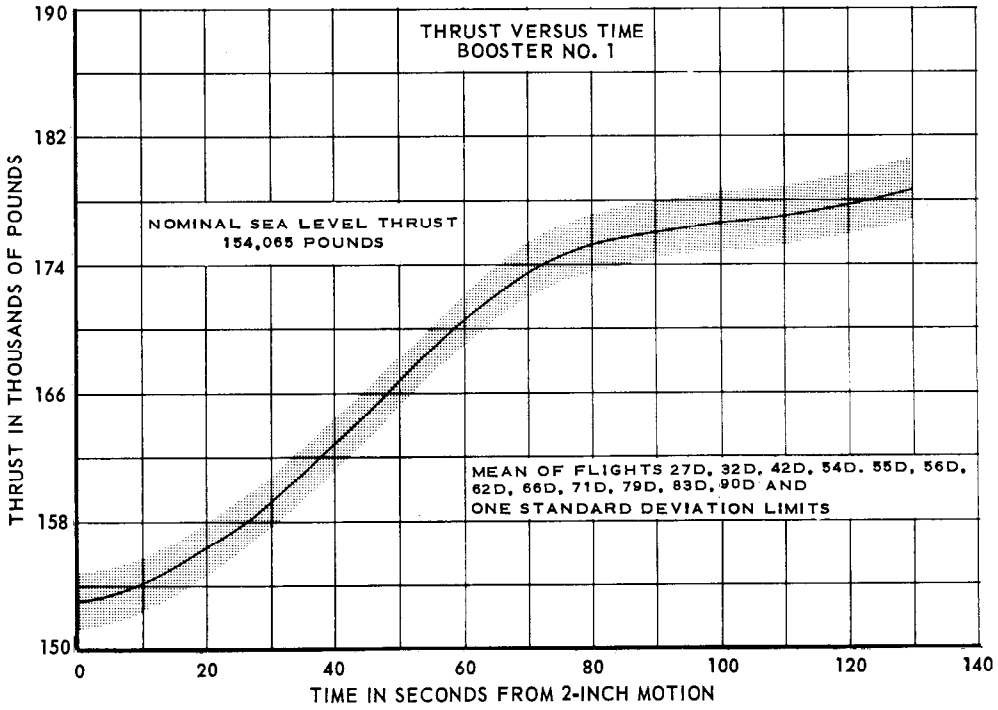

FIGURE 5.1-2 B1 THRUST VS TIME

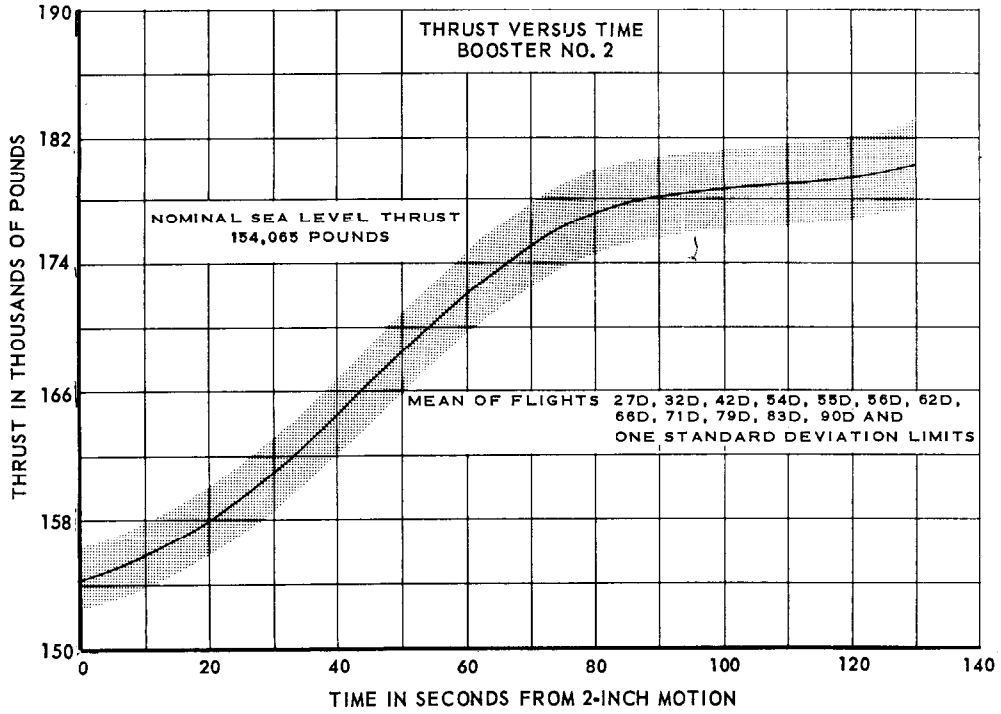

FIGURE 5.1-3 B2 THRUST VS TIME

~~SECRET~~

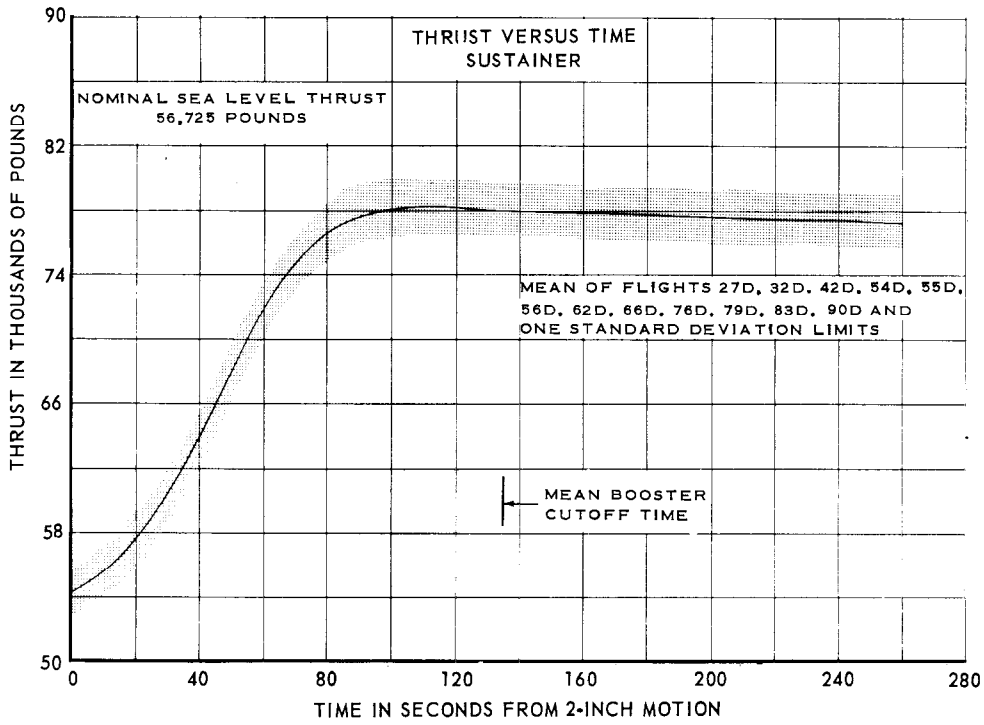

FIGURE 5.1-4 SUSTAINER THRUST VS TIME

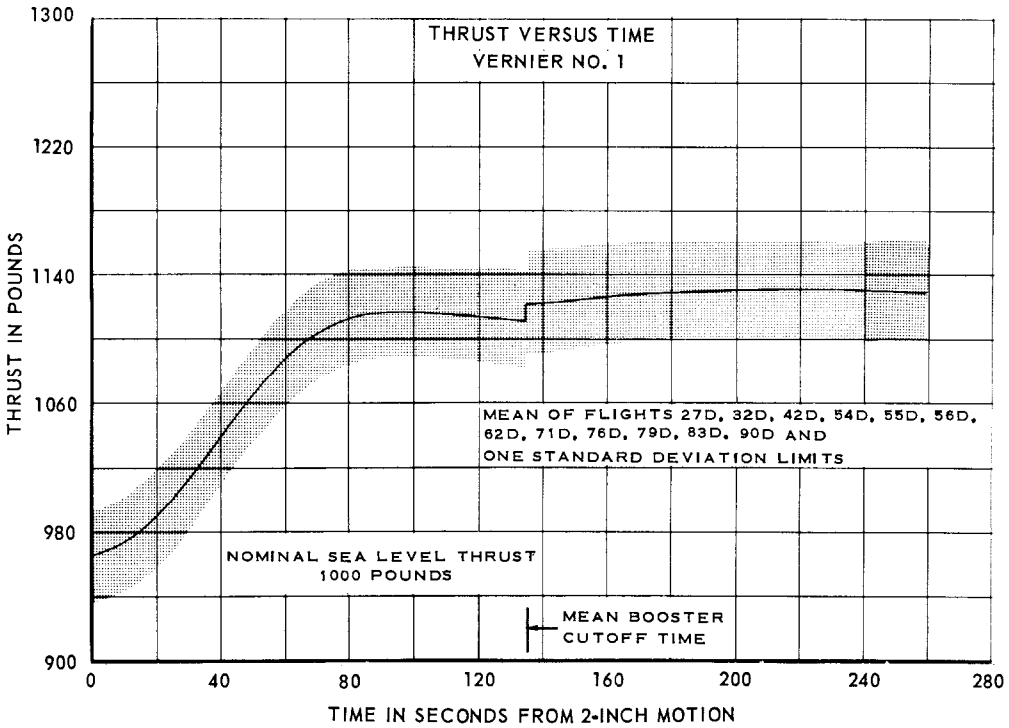

FIGURE 5.1-5 V1 THRUST VS TIME

~~SECRET~~

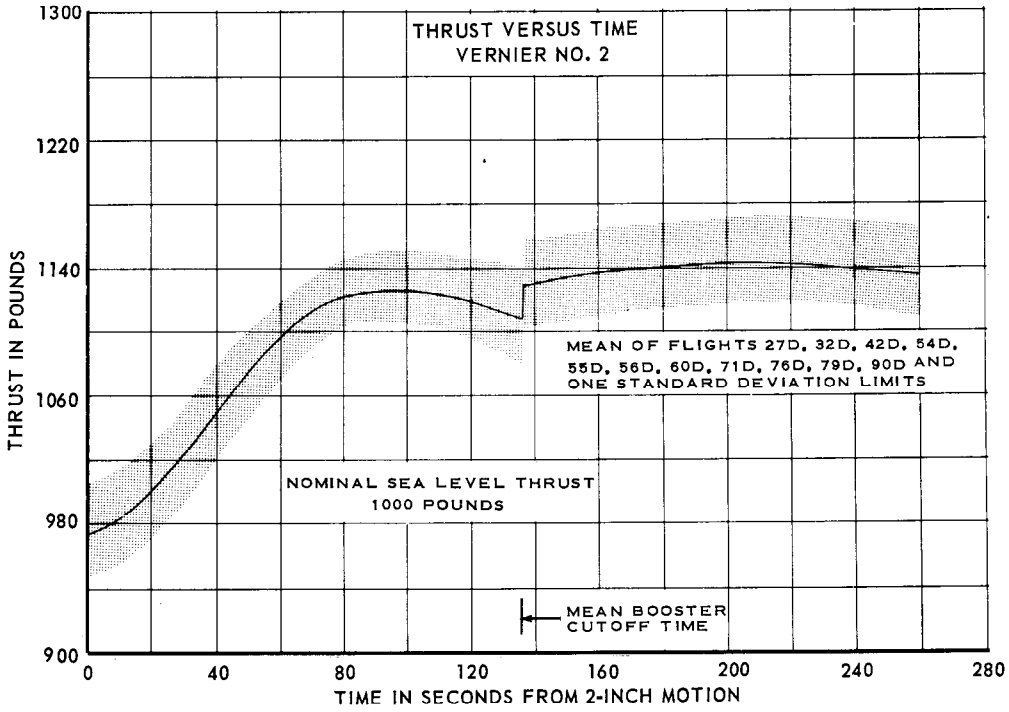

FIGURE 5.1-6 V2 THRUST VS TIME

TABLE 5.1-2 SUSTAINER SPECIFIC IMPULSE

MISSILE NO.	SUSTAINER SPECIFIC IMPULSE (sec)
42D	303
56D	307
54D	305
62D	303
27D	300
32D	300
66D	298
76D	305
79D	296
71D	303
55D	302
83D	305
90D	300
AVERAGE	302

Satisfactory vernier solo operation was achieved in thirteen flights as shown in Table 5.1-1. Combustion chamber pressure difference between pump-fed and tank-fed conditions averaged 41 psi as compared to a nominal of 53 psi.

Except for Missile 71D, in which an apparent obstruction in the main low pressure lox duct adversely affected lox pump inlet pressures (see Problem Area), the sustainer lox pump NPSH immediately after booster cutoff (minimum value during flight) was satisfactory, and no evidence of pump cavitation was observed. The minimum values of NPSH for all flights are shown in Table 5.1-3.

TABLE 5.1-3 MINIMUM NET POSITIVE SUCTION HEAD

MISSILE NO.	MINIMUM SUSTAINER LOX PUMP NPSH (ft of lox)
42D	26
56D	28
54D	26
62D	21
27D	19
60D	28
32D	24
66D	19
76D	15
79D	24
71D	8
55D	26
83D	24
90D	22

A summary of engine thrust decay data is shown in Table 5.1-4. The data include decay impulse and associated time intervals for both booster and sustainer engines. The decay impulse was computed from the time integral of engine thrust, which was calculated from the product of missile axial acceleration and missile weight, minus the axial thrust of engines still operating at the steady-state level.

TABLE 5.1-4 THRUST DECAY

ENGINE	MISSILE (1) NO.	FROM CUTOFF SIGNAL TO START OF THRUST DECAY (2) TIME INTERVAL (sec)	IMPULSE (lb/sec)	NORMALIZED IMPULSE (3)	FROM START OF THRUST DECAY TO 10% OF FULL THRUST TIME INTERVAL (sec)	IMPULSE (lb/sec)	NORMALIZED IMPULSE (3)	TOTAL-FROM CUTOFF SIGNAL TO 10% OF FULL THRUST TIME INTERVAL (sec)	IMPULSE (lb/sec)	NORMALIZED IMPULSE (3)
Boosters	27D	0.35	125,000	0.35	0.28	55,000	0.155	0.63	180,000	0.51
	32D	0.36	130,000	0.36	0.32	57,000	0.158	0.68	187,000	0.52
	55D	0.36	130,000	0.36	0.32	59,000	0.163	0.68	189,000	0.52
	56D	0.35	129,000	0.35	0.31	58,000	0.158	0.66	187,000	0.51
	62D	0.36	130,000	0.36	0.34	62,000	0.171	0.70	192,000	0.53
	79D	0.35	126,000	0.35	0.34	61,000	0.170	0.69	187,000	0.52
	83D	0.28	101,000	0.28	0.33	64,000	0.178	0.61	165,000	0.46
	90D	0.29	103,000	0.29	0.30	56,000	0.159	0.59	159,000	0.45
Sustainer	27D	0.09	7,100	0.09	0.14	5,600	0.072	0.23	12,700	0.16
	32D	0.10	7,800	0.10	0.13	4,900	0.063	0.23	12,700	0.16
	55D	0.11	8,400	0.11	0.12	3,700	0.049	0.23	12,100	0.16
	56D	0.10	8,100	0.10	0.16	6,100	0.076	0.26	14,200	0.18
	62D	0.10	7,700	0.10	0.14	4,700	0.061	0.24	12,400	0.16
	79D	0.09	6,900	0.09	0.14	4,600	0.060	0.23	11,500	0.15
	83D	0.10	7,800	0.10	0.13	4,800	0.062	0.23	12,600	0.16
	90D	0.09	6,900	0.09	0.14	5,400	0.070	0.23	12,300	0.16

(1) Missiles 42D, 54D, 60D, 66D, 71D and 76D are omitted due to high amplitude oscillations in the Arma accelerometer data during engine thrust decay intervals.

(2) Ground guidance discrete command taken as cutoff signal.

(3) Impulse divided by steady-state thrust.

Thus:

$$T_B = (a)\,(W_{BCO}) - T_S - T_V \qquad (1)$$

where: T_B = total booster axial thrust during cutoff transient, lbs

a = axial acceleration, g

W_{BCO} = missile weight during booster cutoff transient, lbs

T_S = sustainer axial thrust at booster cutoff, lbs

T_V = total vernier axial thrust at booster cutoff, lbs.

Similarly:

$$T_S = (a)\,(W_{SCO}) - T_V \qquad (2)$$

where: T_S = sustainer axial thrust during sustainer cutoff transient, lbs

W_{SCO} = missile weight during sustainer cutoff transient, lbs

T_V = total vernier thrust at sustainer cutoff, lbs.

The above formulas make the reasonable assumption that engine gimbal angles and aerodynamic drag are zero.

Booster and sustainer thrust decays during the interval from the 10 percent of full thrust level to zero thrust are shown in Figures 5.1-7 and 5.1-8. The data show that both booster and sustainer thrusts decay to 0.5 percent of steady-state thrust in approximately 2 seconds. The residual decay impulse after the thrust reaches 10 percent of steady-state thrust is approximately 21,000 and 3,600 pound-seconds for the two boosters and sustainer engine, respectively.

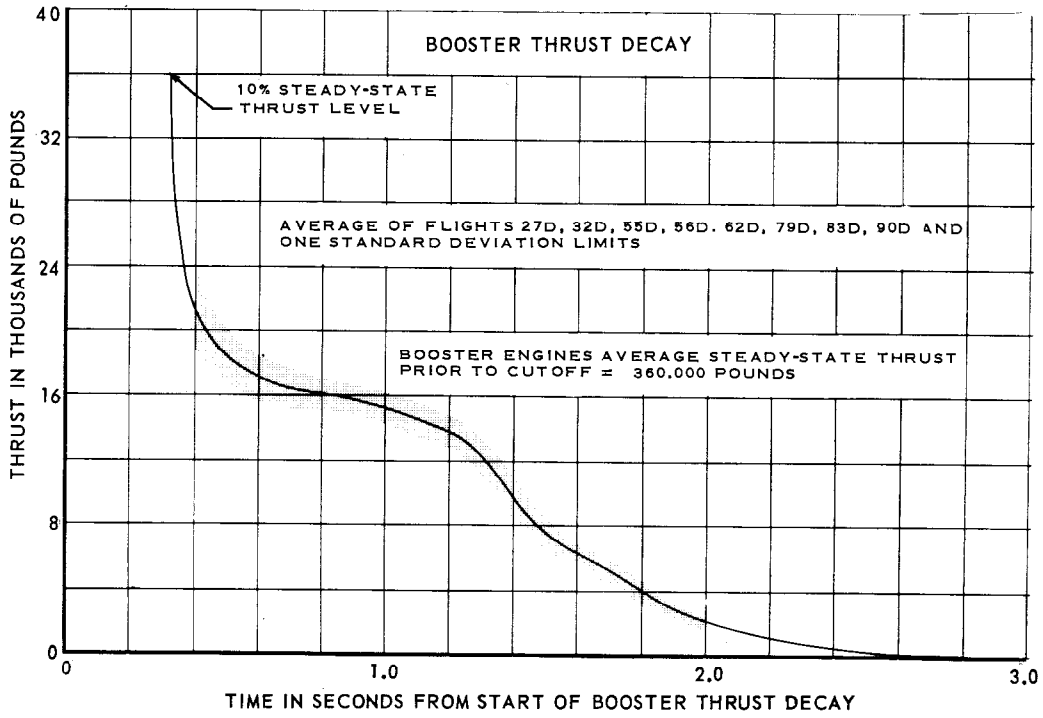

FIGURE 5.1-7 BOOSTER THRUST DECAY CHARACTERISTICS

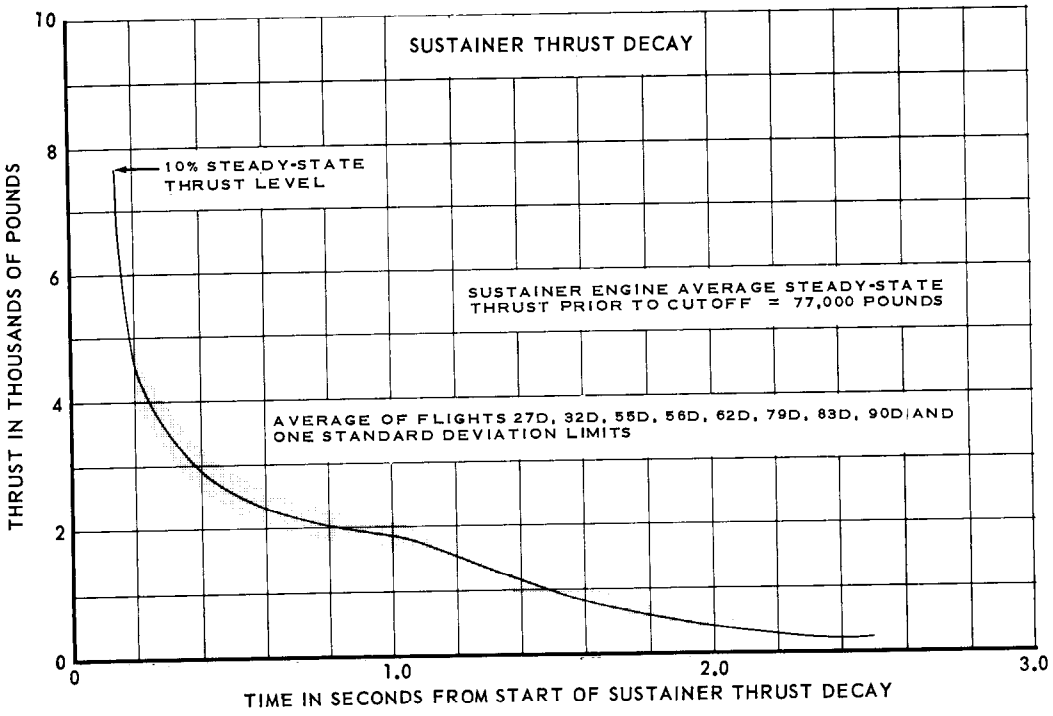

FIGURE 5.1-8 SUSTAINER THRUST DECAY CHARACTERISTICS

A list of significant time intervals during the pre-launch operation is given in Table 5.1-5. Also shown in this table is the pre-launch holddown delay interval which was imposed upon several flights for verification of proper propulsion system operation prior to missile release. This measure was instituted as a result of the loss of Missiles 48D and 51D prior to launch due to booster engine combustion instability. Engine valve operating times are shown in Table 5.1-6.

During the flight of Missile 42D, both vernier engine thrust chamber pressures began to decay 1.37 seconds before activation of the vernier cutoff relay. An abnormal decay rate of the controls helium bottle pressure after engine tank repressurization was also observed, leading to the belief that a leak existed in a vernier propellant feed line, partially depleting the engine tank propellant supply prior to vernier solo operation. The exact nature and cause of this abnormal condition could not be determined.

TABLE 5.1-5 SIGNIFICANT TIME INTERVALS DURING PRELAUNCH OPERATION

MISSILE NO.	TIME IN SECONDS FROM SUSTAINER FLIGHT LOCK-IN TO: MAIN ENGINES COMPLETE	RELEASE SIGNAL	2-INCH MOTION	HOLDDOWN DELAY (seconds) PLANNED	ACTUAL	TYPE BOOSTER ENGINE START
42D	1.19	1.50	2.24	NONE	-	DRY
48D	1.10	1.23	(1)	NONE	-	DRY
56D	1.24	3.13	3.93	1.50	1.76	WET
54D	1.08	6.60	7.28	4.25	5.42	WET
62D	1.15	5.54	6.22	4.25	4.29	DRY
27D	1.04	6.00	6.84	4.25	4.83	WET
60D	1.11	5.81	6.48	4.25	4.59	DRY
32D	1.11	4.02	4.82	2.50	2.77	WET
66D	1.00	3.88	4.56	2.50	2.77	DRY
76D	0.95	1.47	2.21	NONE	-	DRY
79D	1.16	2.79	3.50	1.50	1.52	DRY
71D	1.14	1.46	2.24	NONE	-	DRY
55D	1.08	1.78	2.60	2.50	0(2)	DRY
83D	1.06	1.58	2.24	NONE	-	DRY
90D	1.00	1.46	2.10	NONE	-	DRY

NOTE: (1) Missile destruction occurred prior to 2-inch motion.

(2) Time delay relay malfunctioned.

TABLE 5.1-6 VALVE OPERATING TIMES

MISSILE NO.	BOOSTER GAS GENERATOR BLADE VALVE	BOOSTER LOX VALVE B1	BOOSTER LOX VALVE B2	BOOSTER FUEL VALVE B1	BOOSTER FUEL VALVE B2	SUSTAINER GAS GENERATOR BLADE VALVE	SUSTAINER LOX VALVE	SUSTAINER FUEL VALVE
42D	0.43	0.33	0.31	0.23	0.13	0.45	0.68	0.65
48D	0.43	0.35	0.35	0.12	0.12	0.41	0.68	0.59
56D	0.52	0.35	0.34	0.12	0.12	0.39	0.58	0.60
54D	0.43	0.38	0.39	0.12	0.12	0.41	0.59	0.59
62D	0.45	0.34	0.34	0.12	0.11	0.34	0.70	0.66
27D	0.40	0.33	0.34	0.10	0.12	0.44	0.62	0.62
60D	0.52	0.35	0.36	0.13	0.13	0.43	0.65	0.63
32D	0.42	0.35	0.35	0.12	0.13	0.43	0.66	0.59
66D	0.47	0.38	0.34	0.12	0.13	0.44	0.65	0.60
76D	0.43	0.35	0.33	0.13	0.13	0.38	0.73	0.59
79D	0.44	0.34	0.34	0.10	0.12	0.44	0.61	0.54
71D	0.42	0.34	0.34	0.11	0.13	0.41	0.64	0.60
55D	0.44	0.38	0.35	0.13	0.11	0.37	0.59	0.63
83D	(2)	0.33	0.33	0.12	0.10	0.43	0.58	0.56
90D	0.39	0.35	0.35	0.12	0.11	0.48	0.63	0.60
Average	0.44	0.35	0.34	0.13	0.12	0.42	0.64	0.60

NOTE:

(1) All times given are in seconds from the opening control signal until the valve reached full open.

(2) Data invalid.

PROBLEM AREAS

On Missile 48D, a failure in the booster engine propulsion system occurred prior to liftoff which resulted in explosion of the missile. The failure was the result of high frequency combustion instability in the B2 thrust chamber and was similar in nature to the propulsion system failure on Missile 51D. A holddown delay was incorporated in nine Series D R&D missiles flown subsequent to 48D in order to verify engine performance prior to liftoff. Also, dual rough combustion cutoff (RCC) accelerometers were installed on both the booster and sustainer thrust chambers to provide greater reliability for engine cutoff in the event of accelerometer malfunction. After the failure of Missile 48D, the booster RCC setting was changed from 40 g's for 40 milliseconds to 30 g's for 40 milliseconds. The sustainer setting, 60 g's for 20 milliseconds, remained unchanged.

There were no indications of booster engine combustion instability noted on any flight test conducted subsequent to 48D. However, during the attempted launch of Missile 32D, the sustainer RCC circuitry indicated an instability problem in the sustainer system. The sustainer engine was replaced and a successful launch was achieved.

On Missile 54D, several instances of abnormal sequencing (switch activations) were noted during the holddown period prior to launch, although propulsion system operation during flight was unaffected. Also of significance was the additional unplanned holddown delay time of 1.17 seconds (planned holddown delay time is 4.25 seconds) which resulted in increased missile acceleration during flight and subsequent earlier-than-planned cutoff times. Impact was indicated as being 0.8 NM from the planned target. The discrepancies in the sequence data were possibly caused by a loose umbilical.

On Missile 60D, propulsion system operation was adversely affected by three instances of erroneous activation of the vernier engine propellant tanks pressurizing relay prior to booster cutoff, apparently due to intermittent shorting within the electrical system. Premature pressurization of the vernier fuel tank overcame fuel pump discharge pressure, causing fuel to flow improperly from the tank into the booster gas generator, creating fuel-rich gas generator combustion, a lower gas generator exit temperature, reduced pump speeds and lower booster engine thrust levels. Lox pump discharge pressure was sufficient to keep the vernier lox tank fill and check valve closed throughout.

As a result of these three vernier tank pressurization cycles, the controls helium supply was depleted, with a consequent drop in sustainer gas generator lox regulator reference pressure at 128 seconds after liftoff. At that time, sustainer gas generator pressure began to decrease, causing a corresponding deterioration in sustainer engine thrust levels for the remainder of the flight. The vernier engines operated below nominal levels as a result of the low sustainer pump discharge pressure. At 285 seconds the verniers shut down completely when the vernier propellant valves closed due to spring force when the upstream pressures reached a sufficiently low value. The sustainer engine continued to operate at reduced levels until cutoff was initiated at 308 seconds by the automatic sustainer fuel cutoff signal (ASFCO).

On Missile 71D, abnormal conditions were noted in propulsion system operation during the latter portion of booster stage operation. At approximately 115 seconds after liftoff, the sustainer lox pump inlet pressure dropped off instead of continuing its normal rise until booster cutoff. At staging, the additional decrease in pump inlet pressure, which is normal at booster cutoff, was sufficient to cause partial cavitation as evidenced by momentary transients in pump speed, pump discharge pressures and thrust chamber pressure. Similar erratic behavior was observed in the performance of the B1 engine four seconds prior to staging. Although the cause of this abnormal engine behavior was indeterminate, it was believed that a partial obstruction in the lox line upstream of the staging valve could have caused both difficulties.

On Missiles 32D, 56D, 62D and 66D, the integrated start system (ISS) pneumatic regulator "locked up" between the time of repressurization of the vernier tanks (at booster cutoff) and sustainer cutoff, causing overpressurization of these tanks. The increase in pressure was sufficient to overcome sustainer pump discharge pressure, permitting excess propellant flow to the vernier engines.

No detrimental effects upon propulsion system operation were observed as a result of this condition, although vernier engine chamber pressures were increased slightly.

SECTION 5.2 – PROPELLANT UTILIZATION

PURPOSE OF TESTING

Both Convair and Acoustica propellant utilization systems were tested during the group of Series D flights covered in this report in order to further evaluate their open and closed-loop performance. Extensive testing of the Convair system had already been accomplished in Series B, Series C and earlier Series D flight tests; however, the Acoustica system testing on flight articles was initiated on the Series D missiles and only five closed-loop flights were accomplished prior to the test interval covered in this report.

Propellant tanking using both the Convair propellant loading control unit (PLCU) and the Acoustica propellant loading control monitor (PLCM) was to be accomplished to determine the accuracy of each method in loading propellants into the missile.

TEST CONDITIONS

Both Convair and Acoustica propellant utilization system configurations were similar to those employed on earlier Series D missiles. Schematic diagrams of each are shown in Figures 5.2-1 and 5.2-2. The operational status of both PU systems for all Series D flights included in the scope of this report is summarized in Table 5.2-1.

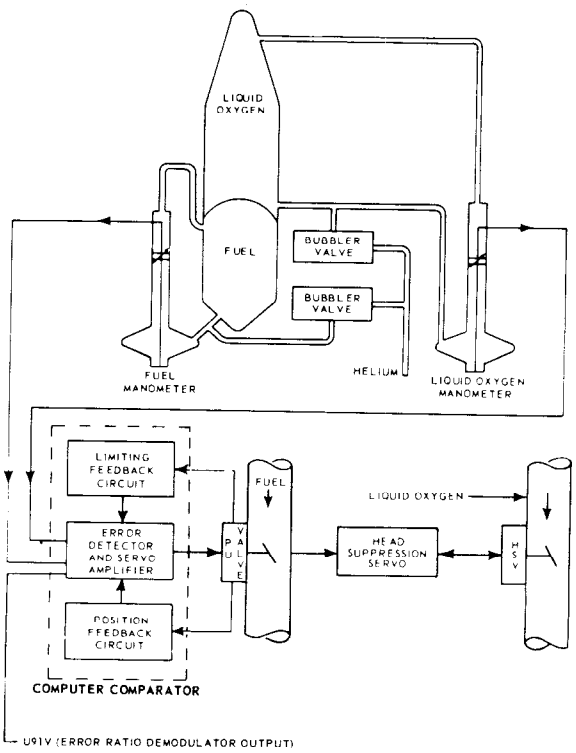

FIGURE 5.2-1 CONVAIR PROPELLANT UTILIZATION SYSTEM

TABLE 5.2-1 OPERATIONAL STATUS OF THE SERIES D PROPELLANT UTILIZATION SYSTEMS

MISSILE NO.	PU SYSTEM			
	CONVAIR		ACOUSTICA (1)	
	Open-loop	Closed-loop	Open-loop	Closed-loop
42D		X		
48D (2)		X		
56D		X	X	
54D				X
62D		X		
27D	X			X
60D				X
32D		X	X	
66D		X		
76D				X
79D		X	X	
71D				X
55D		X		
83D	(3)			X
90D	(3)		X	

(1) Specific gravity matrix was used only on Missiles 27D, 54D, 56D, and 60D.

(2) Missile destroyed prior to liftoff.

(3) Special manometer capacitance monitoring tests. The 6-card computer was used only on Missiles 54D, 60D, 71D, and 76D.

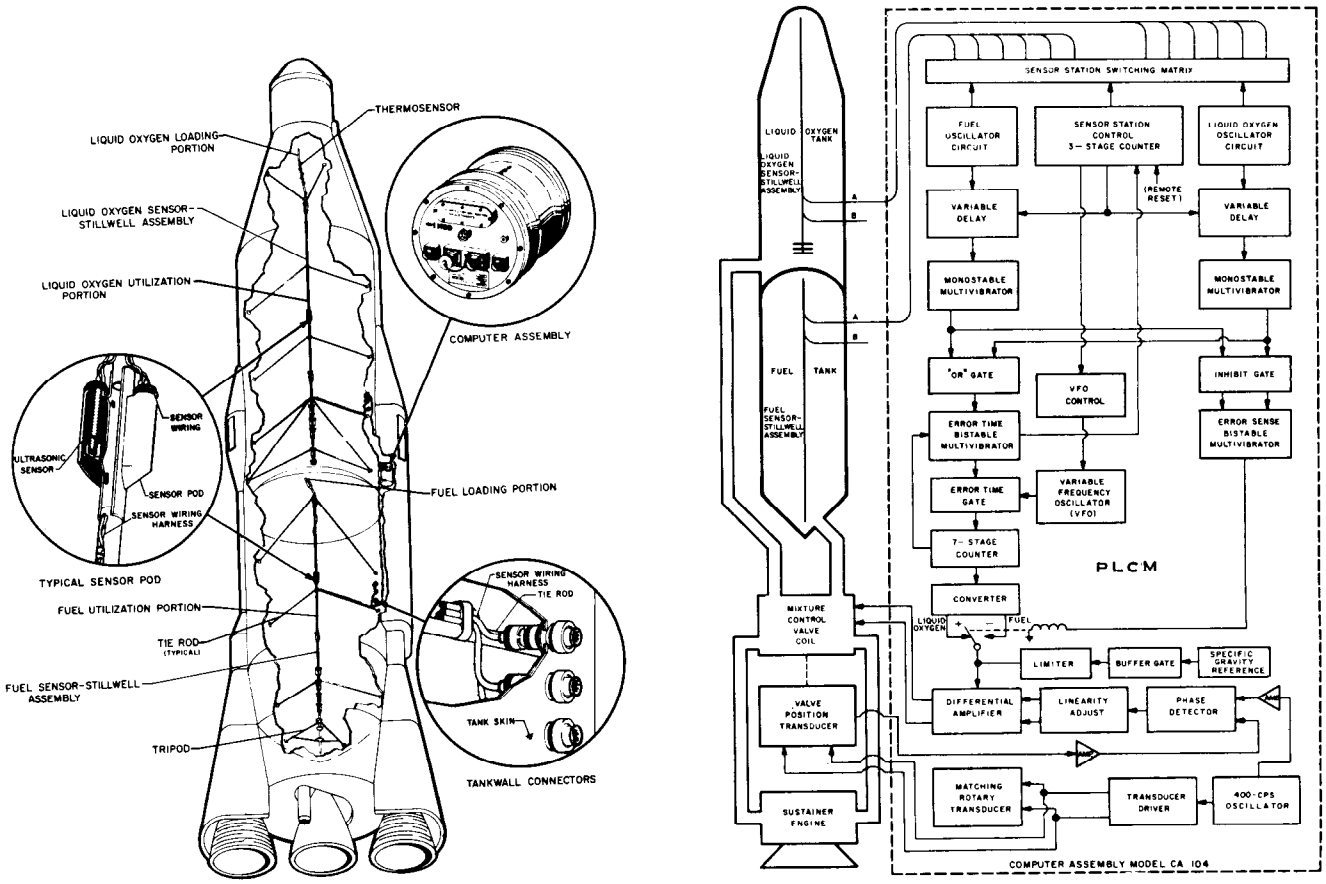

FIGURE 5.2-2 ACOUSTICA PROPELLANT UTILIZATION SYSTEM

TEST RESULTS

The purpose of the propellant utilization system during flight is to maintain the mass ratio of residuals in the main missile propellant tanks at a predetermined value such that the propellants will be exhausted simultaneously. Accomplishment of this objective results in more efficient utilization of the energy potential in the propellants at launch and, thus, greater range for a given payload weight is achieved.

The design specifications for the Convair PU system state that the burnable quantity of one propellant remaining on board when the other propellant is exhausted (assuming the sustainer engine is allowed to continue operation until one propellant is depleted) shall not exceed 0.2 percent of the total weight of propellants on board at ignition. For Series D missiles, this permissible residual error is equivalent to approximately 500 pounds. The allowable tolerance for the Acoustica PU system is 0.05 percent of the propellants on board at ignition, equivalent to approximately 125 pounds.

A summary of propellant residuals and burnable propellant excess at theoretical propellant depletion for all flights is shown in Table 5.2-2. The ability of the propellant utilization system to achieve a burnable propellant excess within the design tolerance could be properly evaluated on only ten of the fifteen flight articles shown in this tabulation. Of these ten flights, five (32D, 55D, 56D, 66D and 79D) were flown with the Convair PU system in closed-loop operation and five with the Acoustica PU system in closed-loop operation. Performance of the Convair PU system was satisfactory and the propellant residual excess at theoretical propellant depletion was within the design tolerance on all five flights.

The propellant residual excess at theoretical propellant depletion, using the Acoustica design tolerance of 125 pounds, was outside the design limits on all five Acoustica PU system closed-loop flights. However, two of the five flights were within the Convair design tolerance of 500 pounds. The five Acoustica closed-loop flights were 27D, 54D, 71D, 70D, and 83D. These are discussed below.

On Missile 27D, the PU valve was not positioned properly at Station 5 to correct for an 800 pound lox-rich residual. As a result, the lox sensor at Station 6 was locked out, the valve was positioned at null, and the lox-rich error increased to approximately 1,900 pounds at theoretical propellant depletion.

On Missile 54D, a fuel-rich residual of 400 to 600 pounds existed at booster cutoff and at Station 5 sensor uncovering time. The error times at both Stations 5 and 6, as indicated by the time shared oscillator activation times, were greater than the error counter operating time. As a result, the computer was locked out and the PU valve was commanded to the null position. Thus, no correction to the fuel-rich error was made in the last 90 seconds of sustainer engine operation. Tank head pressure data at sustainer cutoff showed, in fact, that the fuel-rich error had increased to approximately 1,000 pounds.

TABLE 5.2-2 PROPELLANT RESIDUALS AT SUSTAINER CUTOFF

MISSILE NO.	CLOSED-LOOP OPERATION	RESIDUALS AT SCO (1) (POUNDS)		BURNABLE PROPELLANT (2) EXCESS AT THEORETICAL DEPLETION (POUNDS)		ADDITIONAL SUSTAINER (3) ENGINE OPERATING TIME TO PROPELLANT DEPLETION (SECONDS)
		LOX	FUEL	LOX	FUEL	
42D	Convair	(7)	(7)			
48D (4)	Convair					
56D	Convair	732	217	300		3
54D	Acoustica	2,324	2,082		1,055	13
62D (5)	Convair	2,690	812	565		11
27D	Acoustica	3,797	865	1,937		10
60D	Acoustica	(8)	(8)			
32D	Convair	1,186	528		76	6
66D	Convair	2,694	1,270		243	14
76D	Acoustica	2,899	2,100		848	17
79D	Convair	560	35	490		0.4
71D	Acoustica	2,875	1,097	330		14
55D	Convair	1,333	647		128	7
83D	Acoustica	2,298	947	221		12
90D	(6)	2,910	2,535		1,189	16

NOTES:

(1) Burnable propellants were calculated using propellant tank head pressure data at SCO or, if sensors uncovered prior to SCO, on residuals below head pressure sensor ports less estimated quantity consumed in interval between unporting times and SCO. Burnable propellant is defined as quantity above minimum NPSH level of sustainer pump.

(2) Depletion assumed to occur when either propellant reaches sustainer pump cavitation level. In the interval between SCO and theoritical propellant depletion, the PU valve is assumed to be at the angle corresponding to the EDO signal after SCO (for Convair closed-loop flights) or at the angle commanded at Station 6 (for Acoustica closed-loop flights).

(3) Times calculated on basis of burnable propellants at SCO and flow rates corresponding to valve positions as noted in (2) above.

(4) Missile destroyed prior to liftoff.

(5) Missile tanked lox-rich due to intermediate bulkhead insulation problem.

(6) Neither PU system operated closed-loop.

(7) Not available due to lack of telemetered data.

(8) Not applicable due to subnormal sustainer engine performance.

Acoustica system operation was satisfactory on Missile 71D in that appropriate PU valve positions were commanded at all stations. However, a lox residual of 330 pounds would have resulted at fuel depletion which is greater than the specified residual error of 125 pounds.

On Missile 76D, the PU valve made corrections for an indicated lox-rich residual at both Stations 5 and 6. However, tank head pressure data at sustainer cutoff showed a fuel-rich error of about 800 pounds. Either the probe activation times were incorrect or the propellant flow rates after Station 5 probe activation were not consistent with the valve positions commanded.

On Missile 83D, the residual error was only about 100 pounds fuel-rich at the time of Station 5 uncovering, but became 221 pounds lox-rich at theoretical propellant depletion. As on 76D, valve positionings at both Stations 5 and 6 were proper to minimize the residual error. Thus, again, either probe activation times were incorrect or actual propellant flow rates were inconsistent with the indicated PU valve positions.

The average residual error at theoretical propellant depletion for the five Convair PU system closed-loop flights discussed above was 247 pounds, and for the five Acoustica PU system closed-loop flights, 880 pounds.

The following discussion pertains to the five missiles for which it was not possible to adequately evaluate the closed-loop control capability of the propellant utilization system.

Due to a failure of the lox tank head pressure measurement at liftoff and the absence of the fuel tank head pressure measurement on Missile 42D, it was not possible to determine propellant residuals at sustainer cutoff. The error demodulator output signal was not monitored on this flight nor were the Acoustica system sensors present on the missile, hence no data were available to permit evaluation of either trends in the propellant residual error or PU valve response to changes in EDO signal magnitude and polarity.

Missile 48D, with the Convair PU system in the closed-loop configuration, was destroyed prior to liftoff.

Due to a severe deficiency in the performance level of the sustainer engine after staging, it was not possible to adequately evaluate Acoustica system closed-loop control capability on Missile 60D.

Propellants were deliberately tanked into Missile 62D excessively lox-rich because of a crack in the intermediate bulkhead insulation. As a consequence, the PU valve was held in the full-closed position by the Convair PU system throughout the flight. Based on a desired propellant residual ratio of 2.28 (lox/fuel), a lox excess of approximately 11,000 pounds at launch was reduced to 565 pounds at theoretical propellant depletion.

Neither PU system was in closed-loop control of residual propellants on Missile 90D with the result that 1,189 pounds of excess fuel existed at theoretical propellant depletion. The Acoustica system was on board in the open-loop configuration and the PU valve was held at null throughout the flight.

Open-loop testing of the PU system consisted of one flight for the Convair system and four flights for the Acoustica system (see table under "Test Conditions"). Test results were satisfactory on all flights except 90D (Acoustica open-loop). On this flight the computer was incorrectly restepped at Stations 1, 2, 4, and 5 when the signal from the first of a sensor pair was received by the monostable. Sensor uncovering times correctly indicated the fuel-rich condition of the propellant residual ratio as shown by the tank head pressure sensors.

A summary of propellant tanking data is shown in Table 5.2-3. The Acoustica PLCM system was the primary tanking system on fourteen of the fifteen missiles covered in this report and the Convair PLCU system on the remaining one. Tanking was successfully accomplished in all cases and tanking weights, as determined by the various monitoring systems, were in close agreement with the exception of the PLCU-indicated lox weight on Missile 66D, which differed by approximately 2,000 pounds from the weight shown by PLCM and load cell monitors.

TABLE 5.2-3 SUMMARY OF PROPELLANT TANKING WEIGHTS

MISSILE NO.	POUNDS OF LOX				POUNDS OF FUEL				TOTAL-IZER
	PLANNED	PLCU	PLCM	LOAD CELLS	PLANNED	PLCU	PLCM	LOAD CELLS	
42D	174,744	173,800		172,790	76,672	76,898*		76,640	76,840
48D	174,720	175,983	174,195*	174,545	76,341	76,635	76,635*	76,195	76,560
56D	174,521		175,000*	175,350	76,188	76,430	76,430*	75,850	76,260
54D	174,840		174,720*	174,550	76,297		76,150*	75,975	
62D	166,050	166,410	165,970*	166,190	68,520	68,250	68,250*	68,090	68,432
27D	174,390	175,010	174,640*	174,900	76,190	75,925	75,925*	75,690	75,725
60D	174,390	175,140	174,270*	174,550	76,144	76,000	75,950*	75,640	
32D	174,390	173,997	174,470*	174,900	76,144		75,875*	75,540	75,580
66D	174,390	176,910	174,770*	175,000	76,129	75,810	75,846*	75,540	
76D	174,840		174,921*	174,950	76,083		75,998*	75,540	
79D	174,840		174,770*	175,550	76,320	76,160	76,070*	75,840	75,800
71D	174,390	174,260	174,300*	174,300	76,280	75,970	76,000*	75,500	
55D	174,390	173,560	174,200*	175,050	76,958	76,600	76,690*	76,150	76,470
83D	174,840		174,150*	174,650	76,527		76,325*	75,940	76,075
90D	174,840		174,295*	174,650	76,527		76,570*	76,300	76,960

* Primary tanking system.

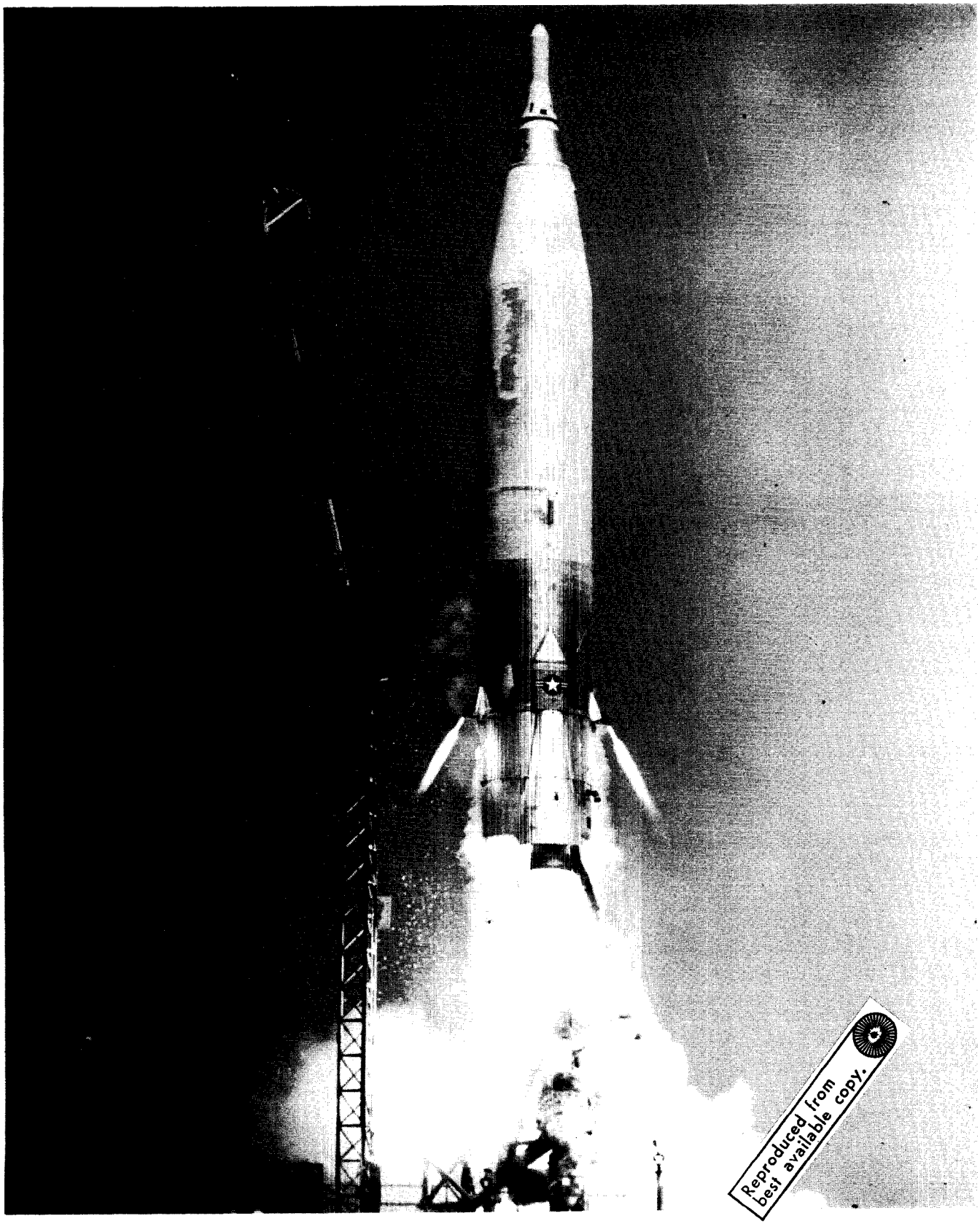

MISSILE 56D, FIRST 9,000 MILE ICBM

SECTION 6. FLIGHT CONTROL

SECTION 6.1 - AUTOPILOT

PURPOSE OF TESTING

Previous flight testing of the autopilot on Series D/RIG R&D missiles has proven the ability of the system to stabilize the missile throughout powered flight, and to properly respond to both the flight programmer outputs and to the radio inertial guidance (RIG) discrete and steering commands. Flight testing of the autopilot on the majority of the Series D/RIG missiles covered in this report was for the purpose of obtaining additional data for reliability analysis of the flight control system. With respect to Missiles 83D and 90D, testing was for the purpose of determining the performance of the "square" type autopilot packages when installed on a D/RIG missile.

Autopilot tests on the seven D/AIG missiles covered in this report were conducted for the purpose of flight testing, for the first time, the "square" type autopilot packages. Of primary interest was the evaluation of the ability of the autopilot to stabilize the D/AIG missile throughout powered flight, to properly execute the pitch and roll programs, to accept and properly execute all-inertial guidance (AIG) steering and discrete commands, and to perform numerous preset switching functions.

DESCRIPTION

Block diagrams of the Series D/RIG and Series D/AIG autopilots, indicating the associated measurement numbers and locations, are shown in Figures 6.1-1 and 6.1-2, respectively. A representative Series D/RIG autopilot flight control circuitry diagram, indicating static gains and programmer switching functions, is shown in Figure 6.1-3. A similar circuitry diagram for the Series D/AIG missile system is shown in Figure 6.1-4.

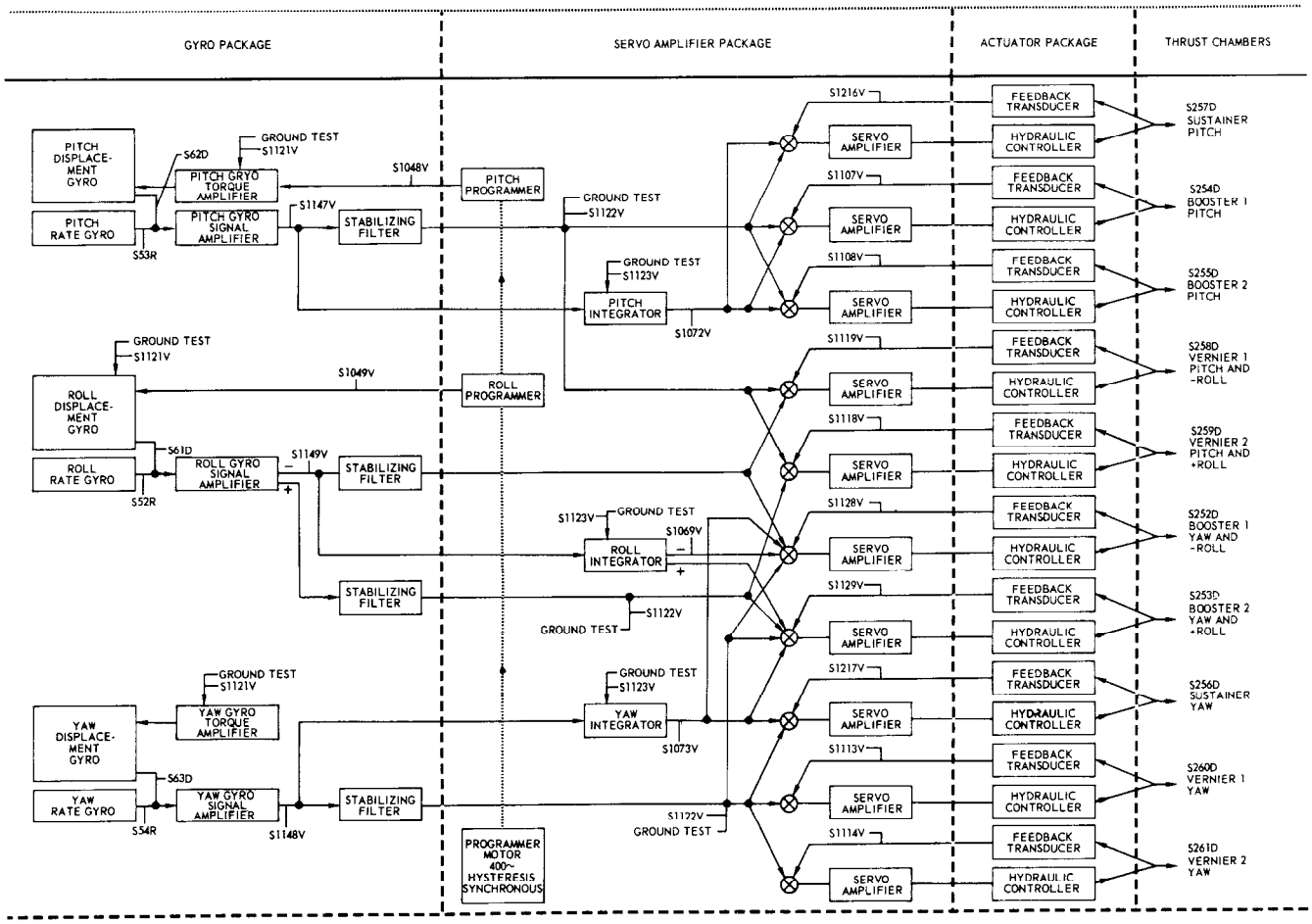

FIGURE 6.1-1 SERIES D/RIG AUTOPILOT SYSTEM, WITH TRANSDUCER LOCATIONS

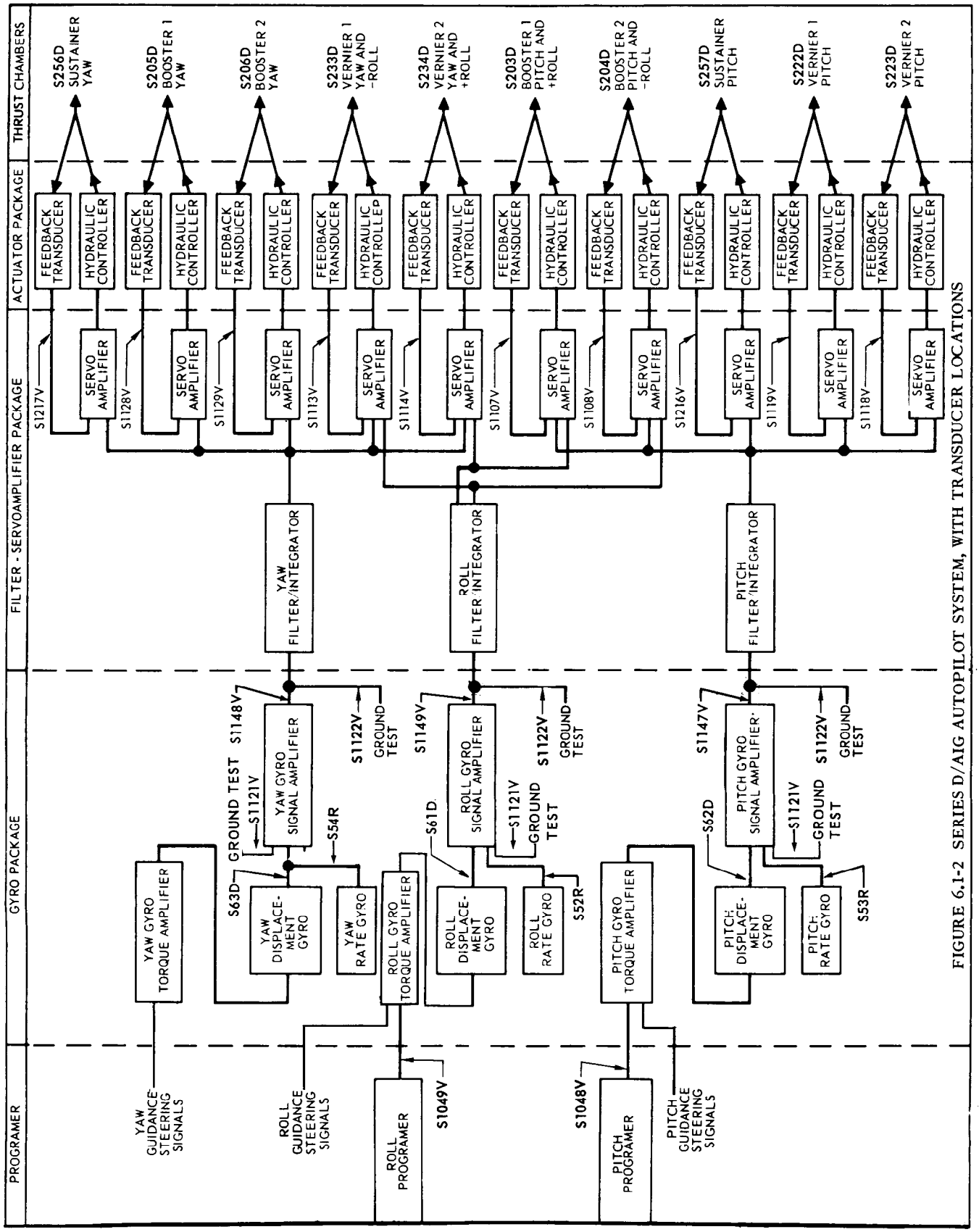

FIGURE 6.1-2 SERIES D/AIG AUTOPILOT SYSTEM, WITH TRANSDUCER LOCATIONS

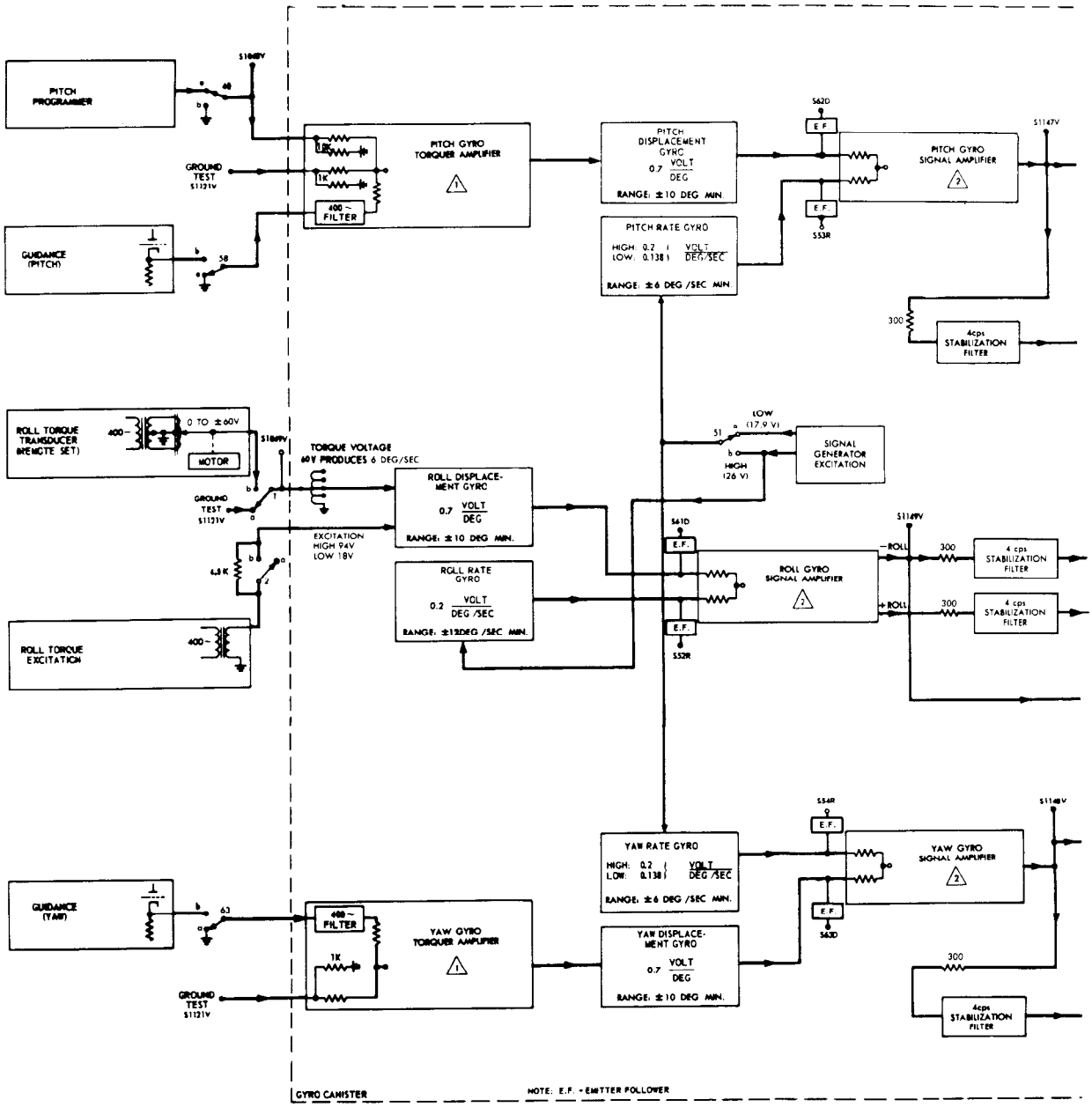

1. TORQUER AMPLIFIER ADJUSTED TO GIVE OVERALL SLAVING SENSITIVITIES AS LISTED IN TABLE 1.

TABLE 1. GYRO PACKAGE SLAVING SENSITIVITIES

INPUT	PITCH	YAW	UNITS
PROGRAM	0.380	—	DEG/SEC VOLT
GUIDANCE	0.1**	0.1**	
GRD TEST	0.380	0.388	

20V PK-TO-PK SIGNAL FROM GUIDANCE PRODUCES 2 DEG/SEC TORQUING RATE

2. SIGNAL AMPLIFIER ADJUSTED TO GIVE RATE & DISPLACEMENT SENSITIVITIES AS LISTED IN TABLE 2.

TABLE 2. GYRO PACKAGE OUTPUT RATE & DISPLACEMENT SENSITIVITIES

GYRO		PITCH	YAW	ROLL	UNITS
DISPLACEMENT		4.5	4.5	1.08	VOLTS/DEG
RATE	HIGH	1.8	1.8	0.43	VOLTS/DEG/SEC
	LOW	1.24	1.24	—	

3. STABILIZATION FILTER TRANSFER FUNCTIONS

PITCH & YAW	+ROLL & -ROLL
$\frac{K}{\frac{S}{2\pi 4}+1}$	$\frac{K}{\frac{S}{2\pi 4}+1}$

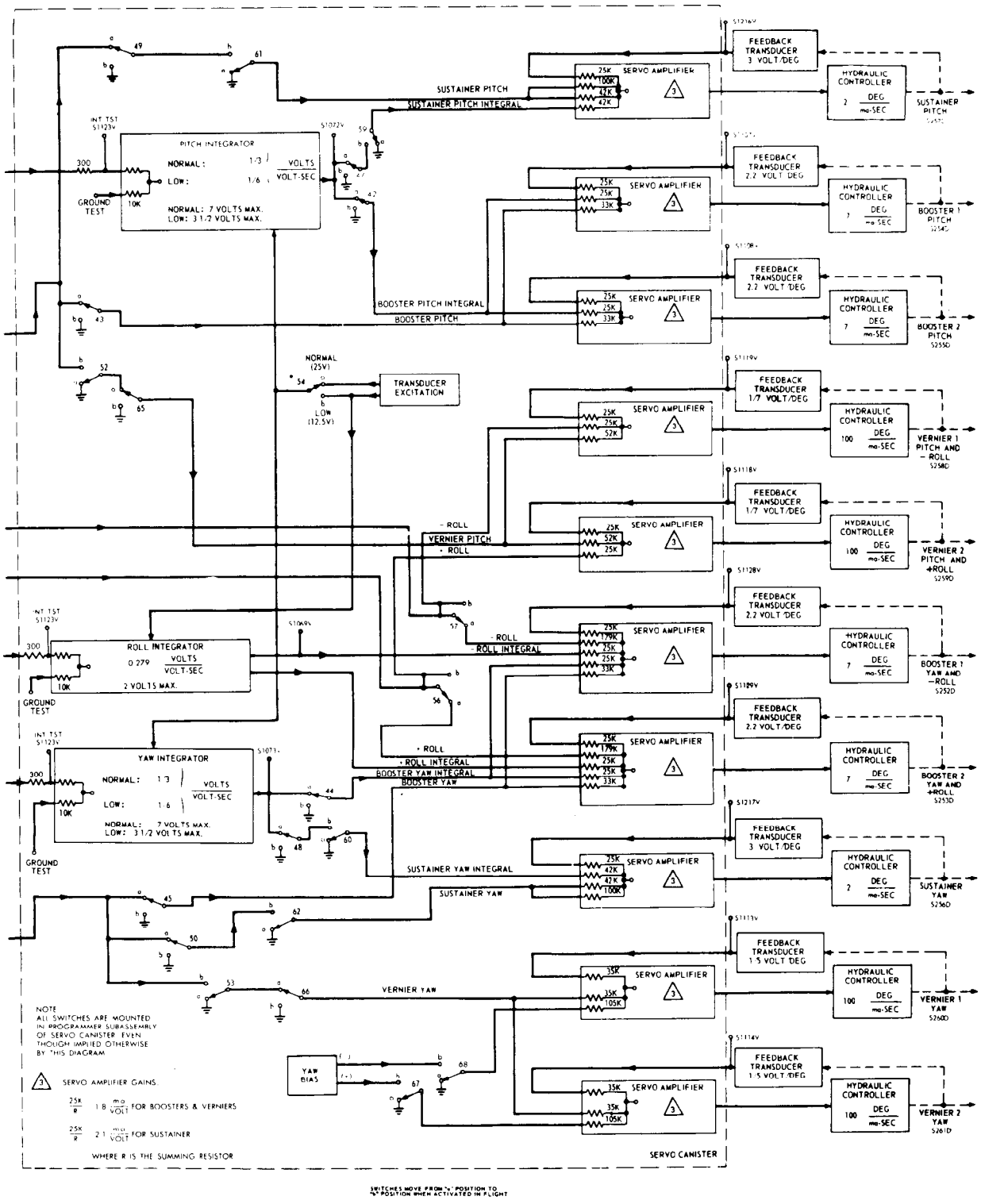

FIGURE 6.1-3 SERIES D/RIG AUTOPILOT CIRCUITRY DIAGRAM

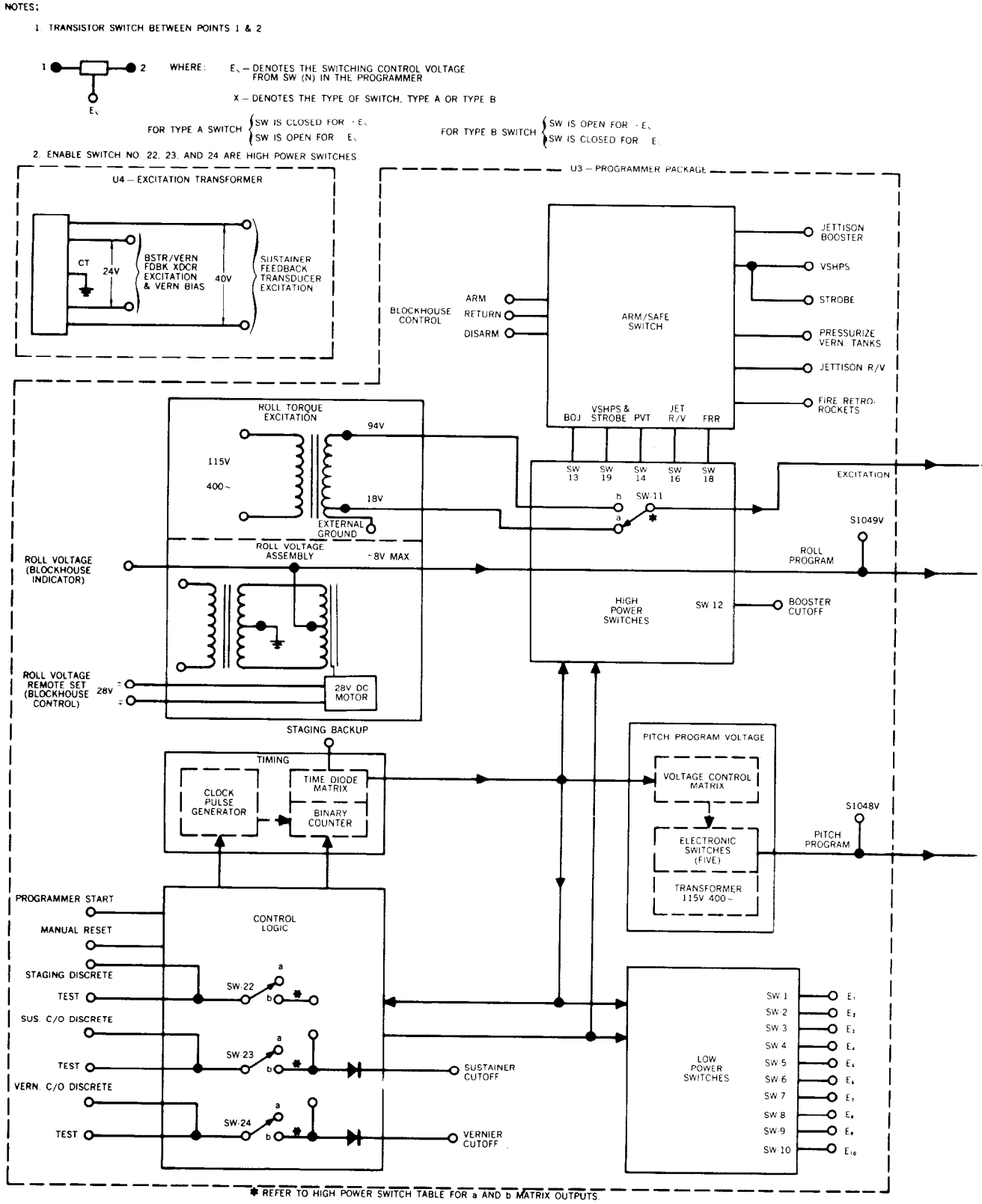

FIGURE 6.1-4 SERIES D/AIG AUTOPILOT CIRCUITRY DIAGRAM

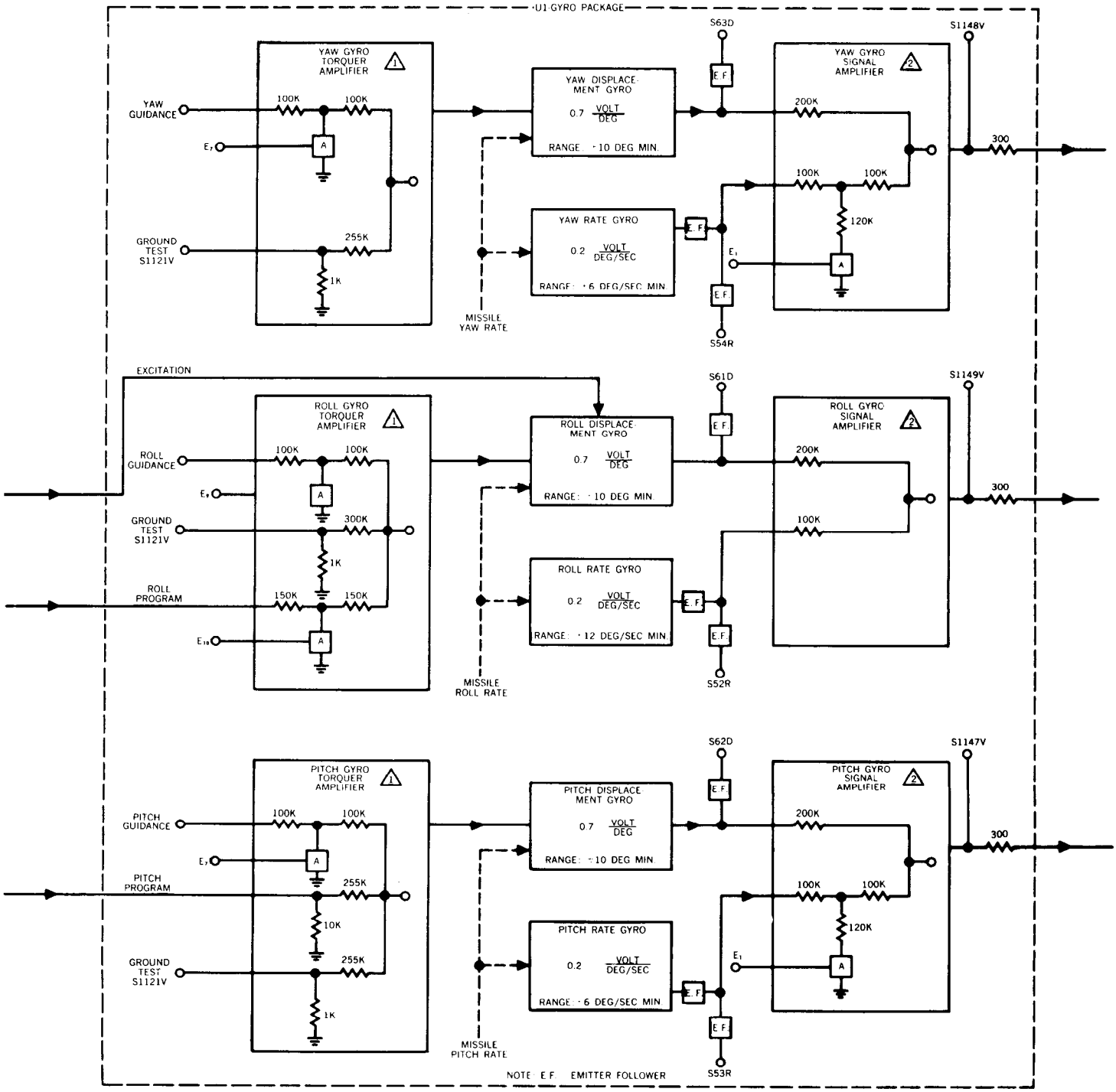

1 TORQUER AMPLIFIER ADJUSTED TO GIVE OVERALL SLAVING SENSITIVITIES AS LISTED IN TABLE 1.

TABLE 1. GYRO PACKAGE SLAVING SENSITIVITIES

INPUT	PITCH	YAW	ROLL		UNITS
			HI EXT.	LO EXT.	
PROGRAM	0.900	–	1.0	–	DEG/SEC / VOLT
GUIDANCE	0.5	0.5	1.5	–	
GRD. TEST	0.900	0.900	1.0	0.19	

2 SIGNAL AMPLIFIER ADJUSTED TO GIVE RATE & DISPLACEMENT SENSITIVITIES AS LISTED IN TABLE 2.

TABLE 2. GYRO PACKAGE OUTPUT RATE & DISPLACEMENT SENSITIVITIES

GYRO		PITCH	YAW	ROLL	UNITS
DISPLACEMENT		3.5	3.5	1.70	VOLT/DEG
RATE	HIGH	1.4	1.4	0.68	VOLT/DEG/SEC
	LOW	0.97	0.97	–	

FIGURE 6.1-4 SERIES D/AIG AUTOPILOT CIRCUITRY DIAGRAM (CONTINUED)

SECRET

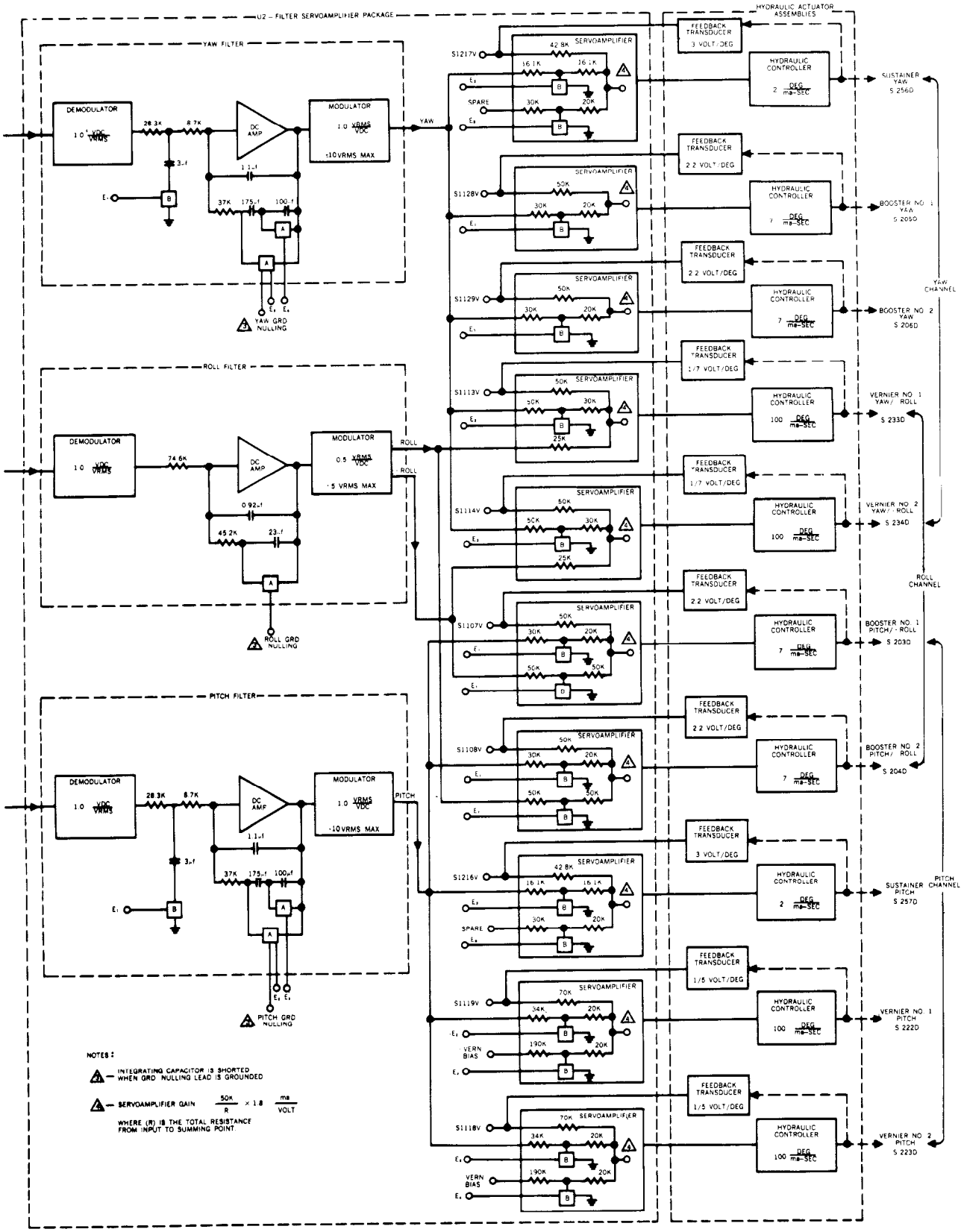

FIGURE 6.1-4 SERIES D/AIG AUTOPILOT CIRCUITRY DIAGRAM (CONTINUED)

SECRET

The Series D/RIG and Series D/AIG autopilot systems basically perform the same functions i.e., stabilization of the missile throughout powered flight, attitude control and steering of the missile, and sequencing of numerous switching functions. The two systems differ considerably, however, with respect to packaging and construction. A comparison of the differences between the two systems is presented in Table 6.1-1.

TABLE 6.1-1 COMPARISON OF THE D/RIG AND D/AIG AUTOPILOTS

SERIES D/RIG	SERIES D/AIG
Packaged in two ground canisters: 1. Gyro canister 2. Servoamplifier-integrator-programmer canister	Packaged in four rectangular (square) canisters: 1. Gyro package 2. Filter - servoamplifier package 3. Electronic programmer package 4. Excitation transformer package
Canisters were located in the B1 equipment pod, with the gyro canister at Station 975.	Canisters were located in the B2 equipment pod, with the gyro canister at Station 974.
The roll gyro torque amplifier was not utilized. Roll program voltages were of sufficient amplitudes to torque the roll displacement gyro directly. No provisions for guidance roll steering commands were incorporated.	A roll gyro torque amplifier was incorporated in the gyro package to permit inertial guidance roll steering commands.
Stabilization filters were located in the gyro canister. Electro-mechanical integrators, located in the servoamplifier-integrator-programmer package, were utilized.	A combined stabilization filter and electronic integrator was located in the filter-servoamplifier package.
An electro-mechanical flight programmer incorporating motors and cam-operated microswitches was utilized. Pitch program was generated by a motor-driven potentiometer.	An electronic flight programmer utilized binary counters, diode matrixes, transistor switching, and controlled silicon rectifier switching. Pitch program was electronically generated.
Construction incorporated printed and wired circuits in wedge-shaped plastic encapsulated units.	Construction incorporated printed circuits on plug-in modules.
A feedback excitation transformer located in the servoamplifier-integrator-programmer canister was incorporated to supply feedback transducer excitation and vernier bias voltage.	A separate feedback excitation transformer was incorporated to supply feedback transducer excitation and vernier bias voltage.
The roll integral signal was not applied to the vernier engines.	The roll integral signal was applied to the vernier engines throughout flight.
Programmer switching functions and subroutines were established to support Series D/RIG configuration requirements and General Electric radio inertial guidance system requirements.	Programmer switching functions and subroutines were established to support Series D/AIG configuration requirements and Arma all-inertial guidance system requirements.

A summary of the flight control system configuration for the Series D research and development missiles covered in this report is presented in Table 6.1-2.

TABLE 6.1-2 SUMMARY OF AUTOPILOT CONFIGURATION

MISSILE NO.	GUIDANCE (TYPE)	RE-ENTRY VEHICLE (TYPE)	AUTOPILOT (TYPE-POD)	RATE GYRO (STATION NO.)	DISPLACEMENT GYRO (STATION NO.)	PITCH/YAW FILTER BOOSTER PHASE (1) (CPS)	PITCH/YAW FILTER SUSTAINER PHASE (CPS)
42D	AIG	MK3 Mod IX	Square - B2	974	974	4	4 & 8
48D	AIG	MK3 Mod IA	Square - B2	974	974	4	4 & 8
56D	RIG	MK3 Mod IB	Round - B1	975	975	4	4
54D	AIG	MK3 Mod IB	Square - B2	974	974	4	4 & 8
62D	RIG	MK3 Mod IIB	Round - B1	975	975	4	4
27D	RIG	MK3 Mod IIB	Round - B1	975	975	4	4
60D	AIG	MK3 Mod IB	Square - B2	974	974	4	4 & 8
32D	RIG	MK3 Mod IB	Round - B1	744	975	4 & 8	4 & 8
66D	AIG	RVX-2A	Square - B2	974	974	4	4 & 8
76D	AIG	RVX-2A	Square - B2	974	974	4, 6, 8 & Quadratic	4, 6, & 8
79D	RIG	MK3 Mod IB	Round - B1	975	975	4	4
71D	AIG	RVX-2A	Square - B2	974	974	4, 6, 8 & Quadratic	4, 6, & 8
55D	RIG	MK3 Mod IIB	Round - B1	975	975	4	4
83D	RIG	AVCO MK4 Mod I	Square - B1	991	991	4, 6, 8 & Quadratic	4, 6, & 8
90D	RIG	MK3 Mod IB	Square - B1	991	991	4, 6, 8 & Quadratic	4, 6, & 8

NOTE: (1) First order lag type filters, with exception of quadratic section which is a lead network.

TEST RESULTS

Mainstage Null Shifts and Transients

Engine position null shifts and transients at mainstage were negligible. Booster and sustainer null shifts, as measured from telemetered engine position data, were within the allowable 0.6 degrees. A summary of engine position null shifts at mainstage is shown in Table 6.1-3. The null shifts continued to indicate the same polarity pattern as has been observed on all Atlas missiles beginning with the A series. This shift is predominantly in a direction away from the appropriate hydraulic actuator, and is caused by application of the engine thrust vector about the moment arm of the thrust chamber actuator outrigger (see Figure 6.1-5). The D/RIG sustainer yaw engine position and the corresponding D/AIG sustainer pitch engine position, however, often shift in the direction of the actuator.

TABLE 6.1-3 TELEMETERED ENGINE POSITION NULL SHIFTS AT MAINSTAGE

MISSILE NO.	TYPE	PITCH (deg)			YAW (deg)		
		B1	B2	SUST	B1	B2	SUST
42D	AIG	-0.20	-0.30	-0.42	+0.39	-0.40	+0.18
48D	RIG	Test terminated prior to liftoff due to a propulsion system malfunction.					
56D	RIG	+0.37	-0.45	+0.20	+0.22	+0.30	-0.60
54D	AIG	-0.20	-0.24	-0.60	+0.40	-0.40	-0.20
62D	RIG	+0.60	-0.30	-0.05	+0.25	+0.30	+0.30
27D	RIG	+0.47	-0.20	+0.05	+0.27	+0.40	+0.65
60D	AIG	-0.30	-0.30	-0.25	+0.30	-0.50	-0.05
32D	RIG	+0.40	-0.40	-0.20	+0.32	+0.25	+0.15
66D	AIG	-0.20	-0.25	-0.55	+0.30	-0.40	-0.25
76D	AIG	-0.17	-0.30	-0.12	+0.46	-0.50	-0.27
79D	RIG	+0.30	-0.60	+0.18	+0.12	+0.15	-0.83
71D	AIG	-0.20	-0.20	+0.30	+0.50	-0.40	-0.30
55D	RIG	+0.45	-0.40	-0.20	+0.25	+0.25	0
83D	RIG	+0.35	-0.25	0	+0.30	+0.10	0
90D	RIG	+0.35	-0.40	0	+0.22	+0.30	-0.18
Series D/RIG Average		+0.41	-0.37	0	+0.24	+0.26	-0.06
Series D/AIG Average		-0.21	-0.26	-0.27	+0.39	-0.43	-0.15

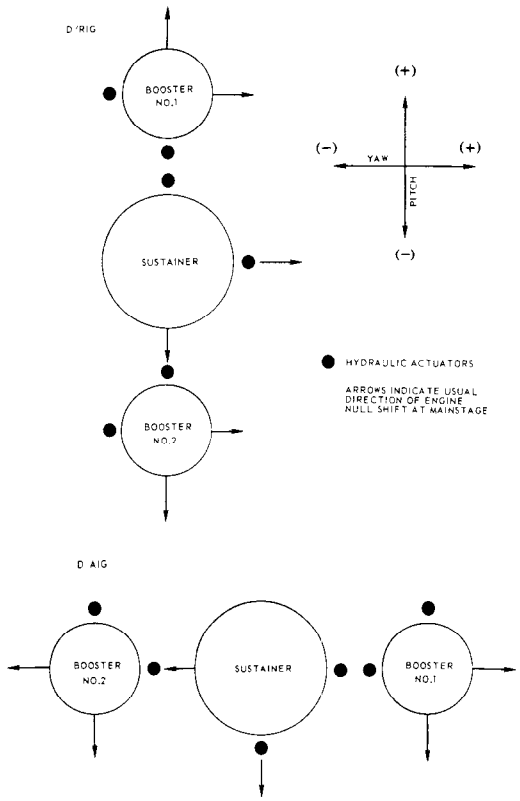

FIGURE 6.1-5 DIRECTION OF ENGINE NULL SHIFTS AT MAINSTAGE

Vertical Flight Phase (Initial Motion)

Figure 6.1-6 defines the flight control system polarity convention and indicates the flight attitude of both D/RIG and D/AIG missiles. It may be seen in this figure that the flight attitude of the D/AIG missiles is rotated 90 degrees from the attitude flown by the D/RIG missiles.

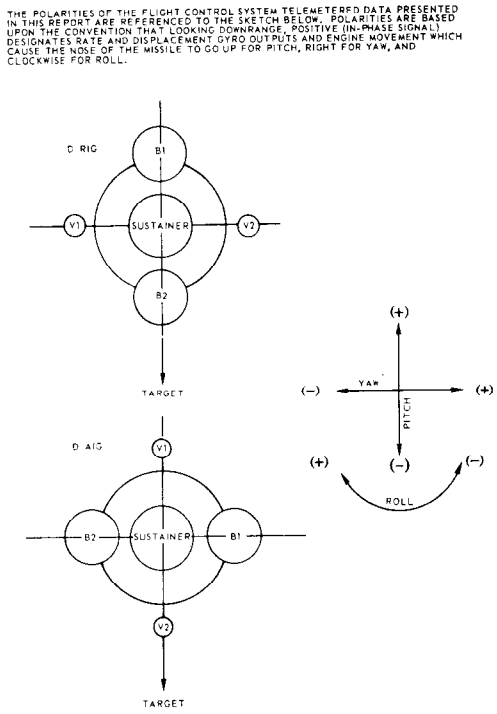

FIGURE 6.1-6 FLIGHT CONTROL SYSTEM POLARITY CONVENTION

There was virtually no engine deflection from mainstage through the initial 42 inches of motion for the subject Series D missiles. This is normal since the outputs of the autopilot gyro signal amplifiers are grounded during this time. The missile, autopilot, and launcher constitute an unstable system with the gyro loop closed, engines firing, and the missile constrained by the launcher. The launching procedure for Series D Atlas missiles therefore allows the missile to rise free of the launcher (approximately 42 inches) before the autopilot is activated. After 42 inches of motion, the grounds are removed from the gyro signal amplifiers, closing the autopilot loop. The autopilot then begins its function of stabilizing the missile, and correcting for any missile displacements and rates which occur during the initial 42 inches of motion.

The maximum booster engine deflection of 42-inch motion did not exceed 0.6 degrees, indicating good thrust alignment, thrust balance, and launcher operation.

Low-amplitude "ringing" of the missile first bending mode of 4.7 cps was evident on the pitch and/or yaw rate gyro trace starting at liftoff on the majority of the subject D/RIG missiles. This "ringing" has been characteristic of practically all Series D launches, and is believed to be a function of launcher operation or booster and vernier engine activation at 42-inch motion. The oscillations were damped out within 12 seconds, and therefore were not considered detrimental. Low-level yaw rate gyro oscillations of approximately 5.0 to 6.0 cps were evident for approximately 14 to 24 seconds following liftoff on all Series D/AIG missiles. The oscillations are attributed to elastic coupling between the rate gyro package, which lies in the yaw plane on D/AIG missiles, and the missile longitudinal mode. These oscillations were also evident on Atlas axial accelerometer data.

Missile clockwise roll transients were observed at liftoff on all subject Series D launches. Peak clockwise roll rates from 1.8 to 6.2 deg/sec were reached. A summary of the liftoff roll transients is presented in Table 6.1-4. Similar roll transients have been observed on practically all previous Series D launches. The roll transients are characterized by 4 to 5 cps oscillations which start in a clockwise direction at approximately +0.2 seconds, and reach a peak clockwise roll rate between 0.1 to 0.4 seconds after 42-inch motion (see Figure 6.1-7). The consistent initial clockwise roll acceleration beginning at approximately +0.2 seconds is attributed to booster turbopump exhaust thrust torque. The exhaust nozzle configuration is such that it imparts a clockwise roll acceleration to the missile. The +0.2-second time referred to above coincides with 7-inch motion, at which time the launcher main support pins are completely retracted from the missile. The missile is still restrained in roll, however, by the launcher kick struts which are not completely disengaged until approximately 42-inch motion. The 4 to 5 cps roll oscillations prior to this time appear to be rigid body motions, with the missile oscillating against the kick struts. The oscillations are in no way detrimental to missile performance.

Missile 62D incorporated a Project Mercury booster engine alignment procedure. This procedure, which utilized the alignment jig (spider) in place of the "bell-bottom level" method, required that the angular difference between both boosters in yaw not exceed 0.25 degrees, in order to prevent excessive roll moments. The clockwise roll transient at liftoff on Missile 62D was higher than usual, reaching a peak rate of 6.2 deg/sec with a corresponding displacement of 2.1 degrees. Missile 67D, a Mercury booster, is included in Table 6.1-4 for comparative purposes. The roll transient at liftoff on this missile was also larger than usual, and identical in rate and displacement magnitude to that observed on Missile 62D.

TABLE 6.1-4 CLOCKWISE ROLL TRANSIENTS AT LIFTOFF

MISSILE NO.	MAXIMUM ROLL RATE (deg/sec peak-to-peak)	MAXIMUM ROLL DISPLACEMENT (degrees peak-to-peak)
42D	4.9	1.4
48D	Test terminated prior to liftoff	
56D	5.2	1.4
54D	4.5	1.4
62D*	6.2	2.1
27D	1.6	0.6
60D	5.2	1.5
32D	2.4	0.5
66D	2.8	0.7
76D	5.0	1.4
79D	2.7	0.9
71D	3.4	1.0
55D	1.8	0.9
83D	1.9	0.3
90D	4.5	0.9
67D*	6.2	2.1
Average**	3.5	1.0

* Incorporated special Project Mercury booster alignment procedures.

** Excludes 62D and 67D.

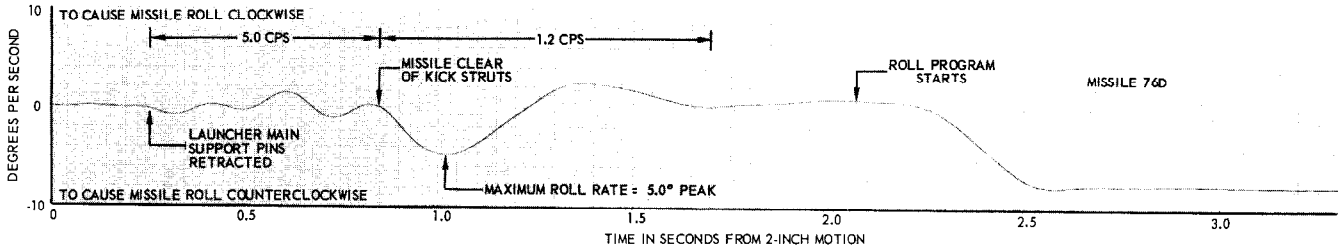

FIGURE 6.1-7 CHARACTERISTIC ROLL TRANSIENTS AT LIFTOFF

With respect to the abort sensing and implementation system (ASIS), the larger than usual clockwise roll transients at liftoff on Missiles 62D and 67D did not result in abort signals. Upon clearing the kick struts, the missile roll oscillation frequency is approximately 1.1 cps. At this frequency, the ASIS primary roll abort level would be approximately 11.8 deg/sec, considerably higher than the recorded 6.2 deg/sec.

Addition of the roll integral signal to the Series D/AIG vernier engines (see Table 6.1-1) was reflected on all AIG flights by an approximate 11-degree offset in roll to compensate for the booster turbopump exhaust thrust torque.

Roll Program

Performance of the roll program was satisfactory for all the subject missiles. None of the missiles incorporated roll attitude gyros to indicate the magnitude of roll. The roll program is performed during the period from 3 to 14 seconds after launch on D/RIG missiles and 2 to 19 seconds after launch on D/AIG missiles. It is during this period that the roll displacement gyro is torqued at a constant rate, causing the missile to roll a predetermined amount.

An indication that the roll program was executed satisfactorily may be obtained by comparing the actual trajectory at booster cutoff with the nominal trajectory. A summary of angular deviations at booster cutoff is shown in Table 6.1-5. The values indicated in this table are not solely an indication of roll program performance since the pitchover program is also performed during the booster phase. In addition, the azimuth at booster cutoff will be affected by cross-winds acting on the missile prior to this time. The allowable azimuth deviation at booster cutoff is in the order of ±3 degrees.

On Missiles 71D and 76D, the roll torquing signal for the nominal 89-degree clockwise (viewed from aft) roll program was generated entirely by the Missile Guidance Set (MGS) azimuth resolver, as planned. On the other D/AIG missiles, the roll torquing voltage was supplied by the roll voltage assembly of the autopilot programmer package, from 2 to 15 seconds after launch, and by the MGS inertial platform azimuth resolver from 15 to 19 seconds after launch. The modification was accomplished within the missile harness by removing the roll gyro torque amplifier input wire (see Figure 6.1-4) from the remote set roll voltage assembly and attaching it to the roll guidance input circuit (which receives its signal from the MGS inertial platform azimuth resolver). With the MGS inertial platform aligned to the nominal flight azimuth prior to launch, the required missile roll angle is equal to the angular difference between the downrange axis of the missile as erected on the launcher (line of centers of the vernier engines) and the platform azimuth alignment. When the azimuth resolver signal is applied to the roll torque amplifier, the missile rolls until the azimuth resolver output is nulled. At this time, the missile has rolled to the predetermined nominal flight azimuth, as required.

TABLE 6.1-5 SUMMARY OF ANGULAR DEVIATIONS FROM NOMINAL FLIGHT PATH AT BOOSTER CUTOFF

MISSILE NUMBER	LAUNCH AZIMUTH (deg)	ROLL[1] ANGLE (deg)	PITCHOVER[1] (deg)	ANGULAR DEVIATION (deg)
42D	195.251	96.626 CW	98.625	0.45 L
48D	195.251	96.626 CW	98.625	(2)
56D	105.031	8.0 CCW	113	0.91 R
54D	195.251	96.626 CW	98.625	0.28 R
62D	104.977	None	105	0.46 R
27D	105.031	None	105	0.84 R
60D	195.251	91.626 CW	103.625	1.16 R
32D	105.031	7.0 CCW	112	0.09 R
66D	195.251	88.988 CW	106.263	0.26 L
76D[3]	195.251	88.988 CW	106.263	0.02 L
79D	104.977	7.0 CCW	112	1.26 R
71D[3]	195.251	88.988 CW	106.263	0.48 R
55D	105.031	7.0 CCW	112	0.40 L
83D	105.031	None	105	0.20 R
90D	105.031	1.27 CCW	106.3	0.30 L

NOTES:

(1) Planned value.

(2) Missile destroyed prior to liftoff.

(3) Roll program generated entirely by the Arma all-inertial guidance system as planned.

CCW Counterclockwise

CW Clockwise

L Left

R Right

Modification of the missile harness to provide roll programming by the MGS azimuth resolver has been incorporated on the majority of Series E/R&D missiles to date and will be incorporated on all Series E and F operational missiles.

Pitchover Program

The booster stage pitchover program was satisfactorily accomplished on all missiles which effected staging. None of the missiles covered in this report utilized a pitch attitude gyro. An indication of satisfactory pitchover program performance was obtained, however, by comparing the indicated pitchover angle at booster cutoff with the expected pitchover angle at this time. Booster cutoff marks the time at which the pitchover torquing signal from the flight programmer to the pitch gyro torque amplifier is removed, thereby ending the pitchover program.

A summary of pitch program deviations at booster cutoff is shown in Table 6.1-6. The indicated pitchover angles were computed from Azusa and General Electric tracking data. The expected pitchover angle was based upon the time of booster cutoff, the nominal pitch program torquing gain, and the volt-second integral of the nominal pitchover program.

The expected accuracy of the pitchover program is approximately ±5%. The accuracy is a function of the volt-second integral of the programmer output voltage, the pitch program torquing gain, 400-cps frequency variations, and 400-cps line voltage variations. It is believed that the 400-cps line voltage variations contribute the most to the pitchover program error. The results indicated in Table 6.1-6 show that the pitchover program was within the expected tolerance, thereby verifying satisfactory pitchover program performance. Missile 71D indicated a pitchover angle 4.88% less than expected. This resulted in a higher than nominal flight trajectory. The higher trajectory had no adverse effect on impact accuracy.

TABLE 6.1-6 SUMMARY OF PITCH PROGRAM DEVIATIONS AT BOOSTER CUTOFF

MISSILE NO.	PITCHOVER ANGLE AT BCO (deg)			DEVIATION FROM EXPECTED (%)
	EXPECTED(1)	INDICATED(2)	DEVIATION(3)	
42D	67.16	65.22	-1.94	2.88
48D	Destroyed on Pad	--	--	--
56D	69.00	67.45	-1.55	2.25
54D	66.29	68.42	+2.13	3.22
62D	61.60	59.42	-2.18	3.54
27D	63.42	62.21	-1.21	1.91
60D	67.13	66.40	-0.73	1.09
32D	63.34	62.14	-1.20	1.89
66D	66.03	66.71	+0.68	1.03
76D	66.56	64.82	-1.74	2.62
79D	69.44	68.18	-1.26	1.81
71D	66.80	63.54	-3.26	4.88
55D	66.88	65.79	-1.09	1.63
83D	64.37	64.58	+0.21	0.33
90D	68.33	66.84	-1.49	2.18

(1) Computed from nominal pitchover program.

(2) Computed from Azusa and GE tracking data.

(3) Minus sign indicates pitchover angle was less than expected. Plus sign indicates pitchover angle was greater than expected.

Booster engine deflections were as expected during the pitchover program, being in the positive (pitch-up) direction as required to balance aerodynamic loads. On the subject D/RIG missiles, maximum deflection occurred between 60 and 70 seconds, the period of maximum dynamic pressure. This is illustrated in Figure 6.1-8 which shows the average B1 engine pitch deflection and standard deviation. Figure 6.1-9 presents the corresponding data for six of the D/AIG missiles. Standard deviation is shown as the shaded area. The aerodynamic pitching moment, which acts to cause the missile to pitch down, increases as the dynamic pressure increases, reaching a peak in the vicinity of maximum dynamic pressure. To stabilize the missile, the booster engines supply a counteracting moment, or pitch-up deflection.

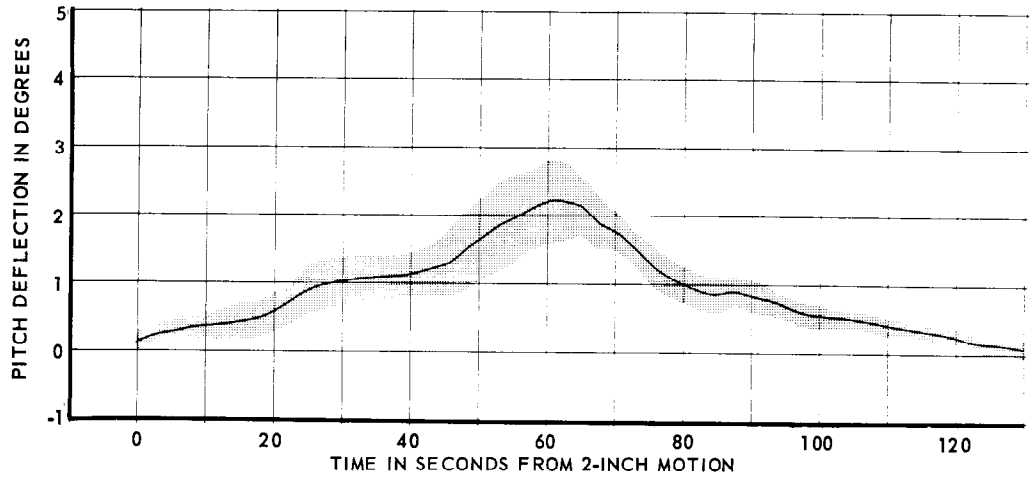

FIGURE 6.1-8 AVERAGE SERIES D/RIG B1 DEFLECTION IN PITCH, AND STANDARD DEVIATION

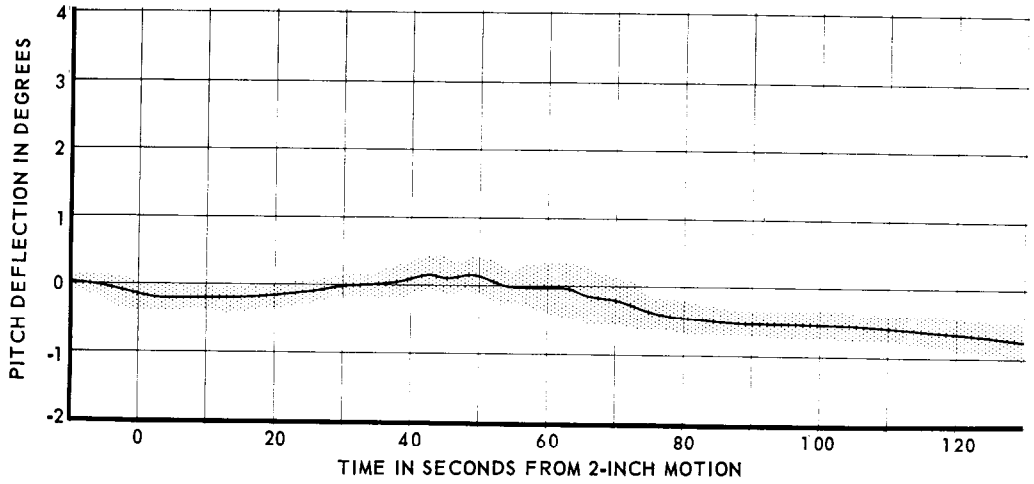

FIGURE 6.1-9 AVERAGE SERIES D/AIG B1 DEFLECTION IN PITCH, AND STANDARD DEVIATION

Comparing Figure 6.1-8 with Figure 6.1-9 it is seen that the maximum pitch deflections for the Series D/AIG missiles were considerably lower than the corresponding deflections for the Series D/RIG missiles. The decreased booster engine pitch deflections during the period of maximum dynamic pressure are attributed to the higher missile stability in the D/AIG pitch plane which results from the booster section fairings and nacelles, and the AIG pod. Similarly, decreased stability in the D/AIG yaw plane was indicated by maximum booster engine yaw deflections, due to wind profile and peak dynamic pressures, substantially higher than corresponding deflections indicated on the D/RIG flights.

Staging Transients

At approximately 0.10 to 0.20 seconds after receipt of the staging discrete signal from either the guidance system or the flight programmer staging backup switch, the boosters are cut off and nulled. This results in transients in the pitch, yaw, and roll planes. The major accelerations occur in the yaw plane on Series D/RIG missiles, and in the pitch plane on Series D/AIG missiles.

The pitch and yaw rate gyro transients indicate a high degree of repeatability during the staging sequence. This is shown in Figure 6.1-10 for the eight D/RIG flights, and in Figure 6.1-11 for the six D/AIG flights. The characteristic pattern for both the Series D/RIG and D/AIG articles is for the missile to pitch-up (positive pitch) and yaw-left (negative yaw) at booster cutoff, and again when the sustainer is nulled prior to jettisoning the booster package. Factors that contribute to the repeatability of the booster cutoff and staging transients are the location of the missile center of gravity (c.g.), booster engine thrust decay time, and the sustainer null position during booster jettison. The yaw rate gyro activity shown in Figure 6.1-10 may be used to analyze the effect of these factors on missile stability.

In Figure 6.1-10 presenting data from RIG missiles it is seen that when the booster engines are cut off and nulled, the yaw rate gyros supply a positive output which would cause the missile to yaw to the right (refer to Figure 6.1-6 for flight control system polarity convention). This indicates that the missile has yawed to the left (negative direction) as viewed from aft. Contributing factors to this negative yaw are the missile c.g. location at booster cutoff, and the relation of the decay time of the booster thrust vector to the time required to null the booster engines. In the yaw plane, the missile c.g. is laterally to the left of the missile longitudinal axis (looking forward). Prior to booster cutoff, the booster engines are deflected in the positive direction (right) to place the thrust vector through the missile c.g. Although the flight programmer switches which cut off and null the booster engines are activated at approximately the same time, the engines are nulled considerably faster than the thrust vector decays. The sudden removal of the booster engine offset for missile c.g. location while the boosters are still supplying thrust, results in a movement which causes the missile to yaw to the left.

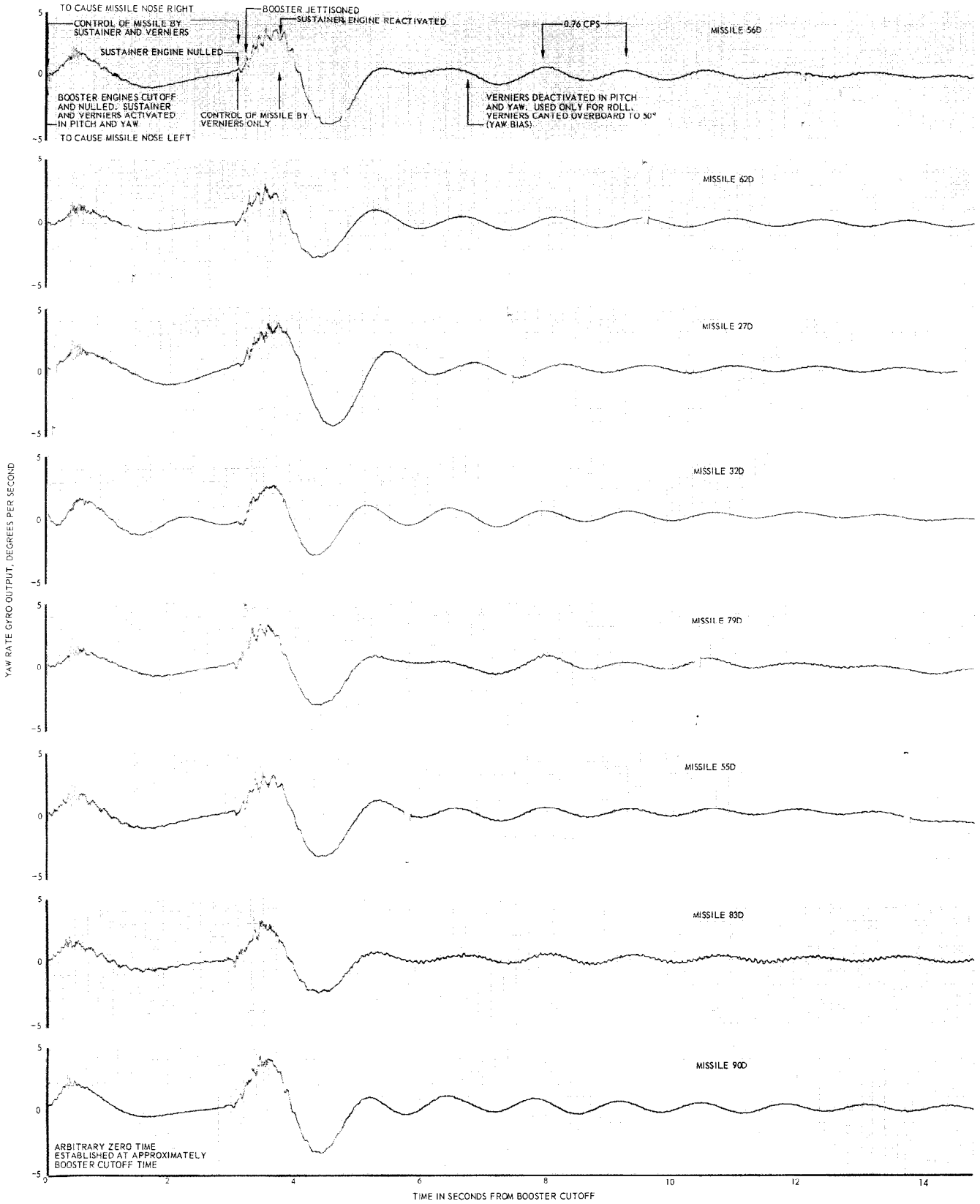

FIGURE 6.1-10 PITCH AND YAW RATE ACTIVITY AT BOOSTER CUTOFF AND STAGING, SERIES D/RIG MISSILES

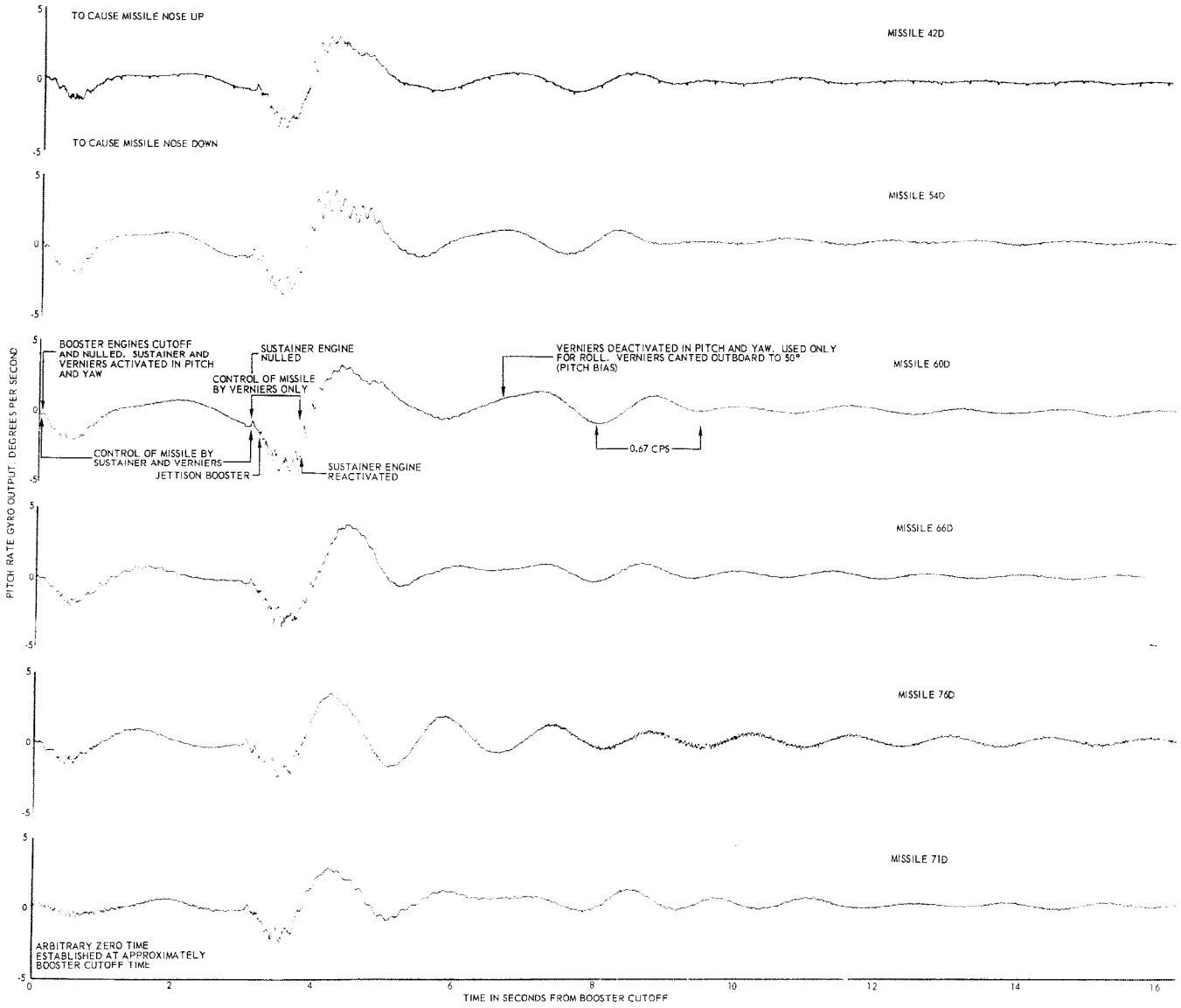

FIGURE 6.1-11 PITCH AND YAW RATE ACTIVITY AT BOOSTER CUTOFF AND STAGING, SERIES D/AIG MISSILES

When the sustainer is nulled in pitch and yaw for the 0.7-second duration at approximately three seconds after booster cutoff, the missile again yaws to the left (as indicated by a positive yaw rate gyro output). This transient is similarly related to the removal of the sustainer engine offset for missile lateral c.g. displacement. It may be observed that this transient is consistently larger than the one occurring at booster cutoff. This is explained by the fact that the missile is stabilized only by the vernier engines during the 0.7-second staging period, and their combined thrust is very small compared to that of the sustainer engine. It should be noted that although the sustainer engine is deactivated in pitch and yaw during this 0.7-second interval, it continues to develop rated thrust and that a moment exists that tends to cause the missile to yaw left.

In the pitch plane, the missile c.g. is vertically displaced above the longitudinal axis (viewed from aft). The tendency, therefore, is for the missile to pitch-up (positive pitch) at booster cutoff and again at sustainer deactivation during booster jettison (see Figure 6.1-11 in which AIG data is presented).

On D/AIG Missiles 42D, 54D, 60D, and 66D, addition of the 8-cps stabilization filters in pitch and yaw at booster cutoff was evident as transient positive sustainer and vernier engine movements in pitch and yaw. Representative sustainer and vernier engine position data, indicating the transients for Missile 54D, are shown in Figure 6.1-12. The transients result from switching in a three microfarad capacitor in the pitch and yaw filter circuitry (see Figure 6.1-4). Addition of this capacitor converts the filter from a 4-cps low-pass type to one representing a combination of a 4-cps and an 8-cps low-pass filter. Prior to addition of the three microfarad capacitor at booster cutoff, the capacitor charges to the transistor switching control voltage (+12 volts) as a result of the transistor collector junction leakage current. At booster cutoff, the switching transistor is programmed to "close" (transistor conducts), providing the capacitor with a discharge path. Subsequent discharge of the capacitor results in the positive engine position transients shown in Figure 6.1-12.

On Mercury boosters 77D and on, which will incorporate "square" type autopilots, a 2.2 megohm resistor will be added in parallel with the transistors that effect the filter change. This will limit the charge buildup on the associated filter capacitors to a fraction of the switching control voltage, and eliminate or significantly reduce the engine transients.

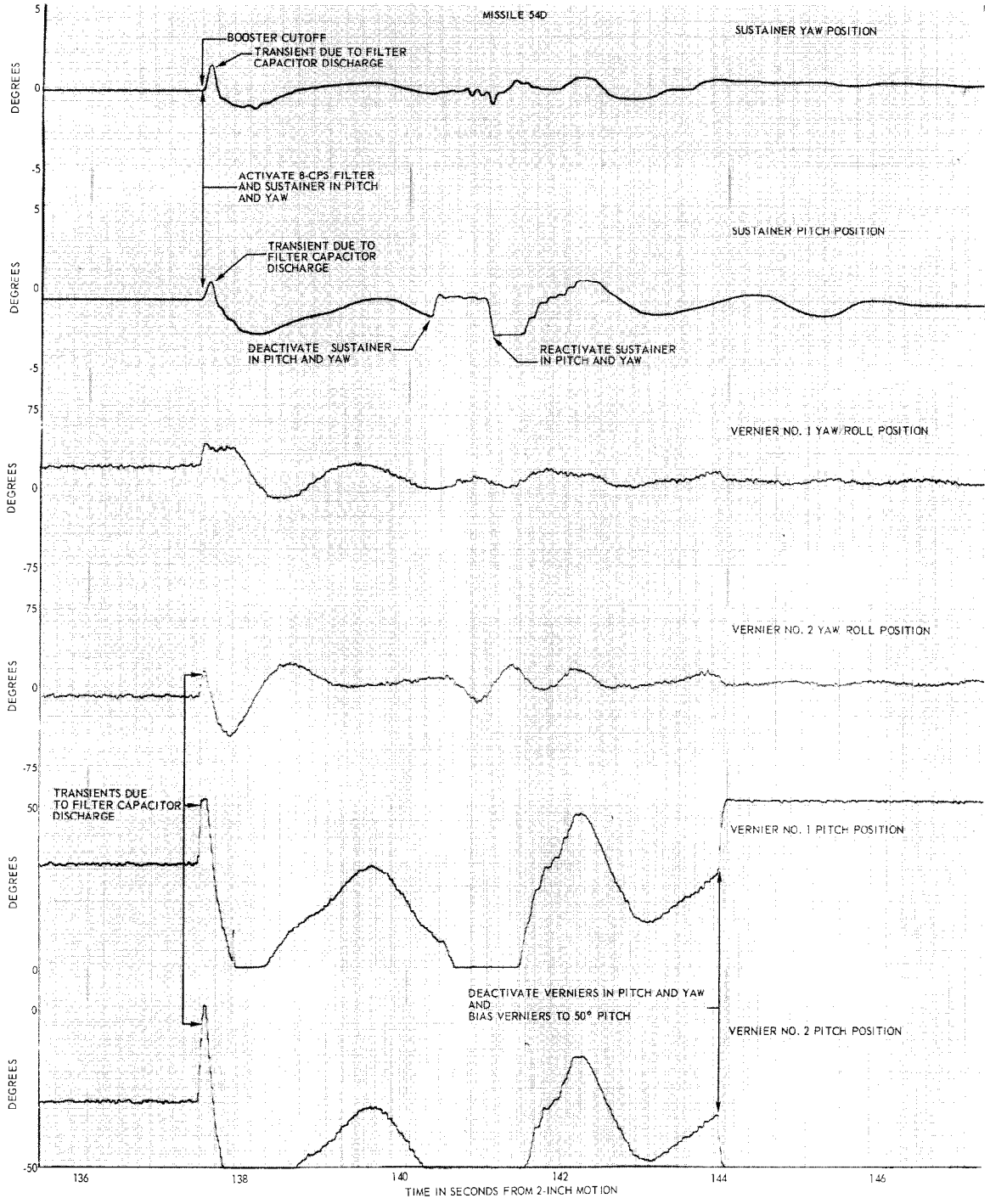

FIGURE 6.1-12 MISSILE 54D ENGINE POSITION DATA AT BOOSTER CUTOFF

Flight Programmer

"Round" Autopilot

Performance of the "round" type autopilot flight programmer, flown on all subject D/RIG missiles except 83D and 90D, was satisfactory. With the exception of a vernier engine cut-off discrete failure on Missile 62D, all guidance discrete commands were properly relayed by the programmer, and associated subroutine switching functions were generated. In addition, all received steering commands were relayed to the pitch and yaw gyro torque amplifiers as required.

A summary of "round" autopilot programmer performance is presented in Table 6.1-7. Representative flight programmer switching sequences and nominal times of switch actuation are shown in Figure 6.1-13.

The majority of switch actuation times shown in Table 6.1-7 were within design tolerances. However, late activation of the sustainer and vernier engines in pitch and yaw was indicated on some flights. This indication of late activation, which has also been observed on earlier missile flights, is not considered to be valid. Since the programmer switches are not instrumented, the time of closure is determined by the resultant event. For example, closure times for switches 61 and 62 (which activate the sustainer in pitch and yaw) are determined by sustainer engine movement, with no time correction made for engine response lag. Where the engine movements are small, due to lack of significant missiles rates and displacements, switch actuation time is not readily discernible. In addition, poor readability of the commutated engine position data often accounts for indications of late switch closures.

SECRET

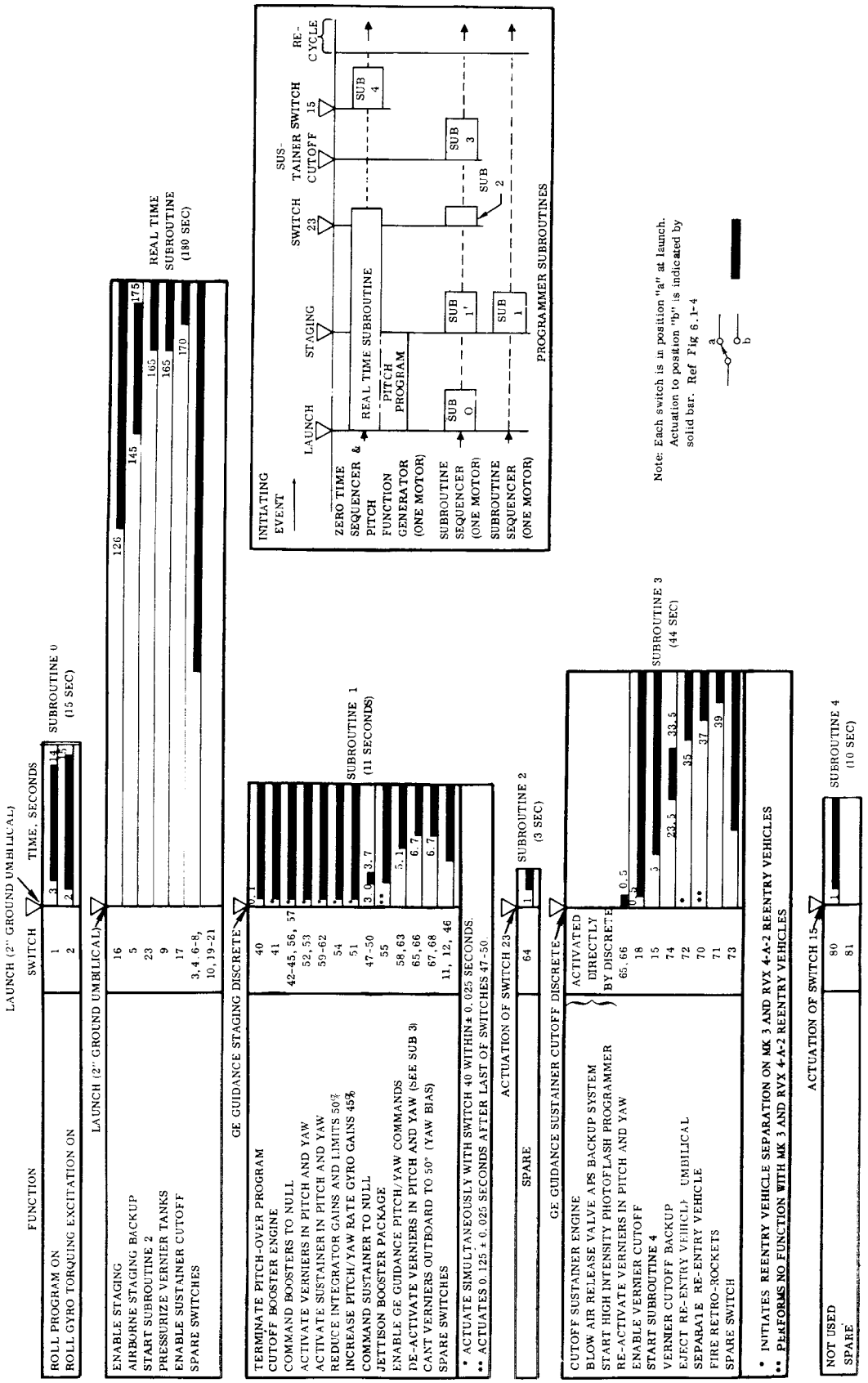

FIGURE 6.1-13 FLIGHT PROGRAMMER SWITCHING SEQUENCE, ROUND AUTOPILOT

SECRET

TABLE 6.1-7 FLIGHT PROGRAMMER PERFORMANCE, ROUND AUTOPILOT

ASSOCIATED SWITCH	FUNCTION	TIME REFERENCE (1)	DESIGN TIME (seconds)	ACTUATION TIME FROM REFERENCE IN SECONDS (2)					
				56D	62D	27D	32D	79D	55D
--	Staging Discrete (3)	Launch	--	136.32	117.49	131.65	131.25	138.37	135.56
5	Staging Backup	Launch	145 ± 0.5(6)	NF	NF	NF	NF	NF	NF
41	Booster Cutoff Relay (P72X)	Staging	$0.1\ ^{+0.1}_{-0.0}$	0.11	0.15	0.13	0.15	0.09	0.16
43	Zero Booster Pitch	Staging	$0.1\ ^{+0.1}_{-0.0}$	0.11	0.13	0.13	0.16	NM	0.17
45	Zero Booster Yaw	Staging	$0.1\ ^{+0.1}_{-0.0}$	0.16	0.35	0.09	0.17	NM	0.17
61	Activate Sustainer Pitch	Staging	$0.1\ ^{+0.1}_{-0.0}$	0.21	0.17	NM	0.20	0.17	0.24
62	Activate Sustainer Yaw	Staging	$0.1\ ^{+0.1}_{-0.0}$	0.20	0.47	NM	0.17	0.15	0.24
52	Activate Vernier Pitch	Staging	$0.1\ ^{+0.1}_{-0.0}$	0.19	0.19	NM	NM	NM	0.14
53	Activate Vernier Yaw	Staging	$0.1\ ^{+0.1}_{-0.0}$	0.17	0.21	0.19	0.21	0.17	0.22
54	Reduce Integrator Gains And Limits	Staging	$0.1\ ^{+0.1}_{-0.0}$	NM	NM	NM	NM	NM	NM
49	Zero Sustainer Pitch	Staging	3.0 ± 0.1	3.11	NM	3.03	3.04	NM	3.04
50	Zero Sustainer Yaw	Staging	3.0 ± 0.1	3.07	2.97	3.07	3.04	2.99	3.04
49	Duration Switch 49 Lockout	Switch 49	$0.7\ ^{+0.1}_{-0.0}$	0.74	NM	0.78	0.72	NM	0.78
50	Duration Switch 50 Lockout	Switch 50	$0.7\ ^{+0.1}_{-0.0}$	0.80	0.76	0.72	0.74	0.72	0.76
55	Jettison Booster Start	(4)	0.125 ± 0.025	--	--	--	--	--	--
55	Axial Acceleration Shows Jettison Start	(4)	0.125 ± 0.025	0.04	0.16	0.13	0.11	0.09	0.10
55	Pitch Rate Vibration Shows Jettison Start	(4)	0.125 ± 0.025	0.04	0.16	0.14	0.11	0.11	0.10
65	Deactivate Vernier Pitch	Staging	6.7 ± 0.5	NM	6.53	NM	6.92	NM	NM
66	Deactivate Vernier Yaw	Staging	6.7 ± 0.5	NM	NM	6.85	NM	NM	NM
67	Bias Vernier No. 1 to -50° Yaw	Staging	6.7 ± 0.5	6.62	6.63	6.85	6.66	6.59	6.78
68	Bias Vernier No. 2 to 50° Yaw	Staging	6.7 ± 0.5	6.62	6.61	6.95	6.87	6.62	6.77
9	Pressurize Vernier Engine Tanks (P27P)	Launch	165 ± 3.0	165.90	165.11	165.37	165.70	164.94	166.2
--	Sustainer Cutoff Discrete	Launch	--	271.09 ± 0.1	284.17 ± 0.1	278.70 ± 0.1	288.00 ± 0.1	282.44 ± 0.1	283.09 ± 0.1
--	Sustainer Cutoff Relay (P347X)	Launch	--	271.02	284.22	278.63	288.04	282.44	283.00
65	Reactivate Vernier Pitch	Sustainer Cutoff	$0.5\ ^{+0.5}_{-0.0}$	0.75	0.83	0.73	0.97	0.82	0.82
66	Reactivate Vernier Yaw	Sustainer Cutoff	$0.5\ ^{+0.5}_{-0.0}$	0.75	0.91	0.67	0.98	NM	0.93
--	Vernier Cutoff Discrete	Launch	--	284.92 ± 0.1	NF	293.90 ± 0.1	301.92 ± 0.1	295.19 ± 0.1	298.09 ± 0.1
--	Vernier Cutoff Relay (P77X)	Launch	--	284.88	307.70	293.92	301.89	295.12	298.01
74	Vernier Cutoff Backup	Sustainer Cutoff	23.5 ± 0.15	23.62	23.36	23.44	23.53	23.51	23.50
72	Pre-Arm Backup (5)	Sustainer Cutoff	35.0 ± 0.5	--	--	--	NF	--	--
72	Re-Entry Vehicle Separation	Sustainer Cutoff	35.0 ± 0.5	34.91	34.92	35.05	--	34.93	35.08
70	Re-Entry Vehicle Separation (5)	Sustainer Cutoff	37.0 ± 0.5	--	--	--	37.15	--	--
71	Fire Retrorockets	Sustainer Cutoff	39.0 ± 0.5	38.89	38.82	38.81	39.06	38.87	39.00

NOTES: (1) Time reference column pertains to the following events except where noted

Launch - 2-inch motion
Staging - Receipt of staging discrete or staging backup actuation, whichever occurs first.
Sustainer Cutoff - Receipt of sustainer cutoff discrete.
Vernier Cutoff - Receipt of vernier cutoff discrete.

(2) Minimum and maximum actuation times indicate commutated data.

(3) The staging discrete command was instrumented on a 5-rps commutated channel. The time given is an approximation chosen for compatibility with the subroutine one switching times as determined from flight data.

(4) Switch 55 actuates 0.125 ± 0.025 seconds after last switch actuation of the 47-50 group.

(5) Missile 32D only.

(6) Design time for staging backup was launch plus 123 ± 0.5 seconds on Missile 62D.

NM - Not measurable from data
NF - Sent or actuated, but performed no function
NA - Not sent or actuated
NP - Not planned

"Square" Autopilot

Performance of the "square" rate autopilot electronic flight programmer was satisfactory on all applicable missiles, with the exception of Missile 54D. The electronic programmer was utilized on all Series D/AIG missiles, and on D/RIG Missiles 83D and 90D. A summary of "square" autopilot programmer performance is presented in Table 6.1-8. Programmer package output voltages for the high and low power switches, and programmer switching sequences are shown in Figure 6.1-14.

The times of switch actuation presented in Table 6.1-8 are sufficiently close to the design times to establish satisfactory electronic programmer performance. Where switch closure times differ from the design time, it is partly attributed to variations in the 400-cps line frequency. Electronic programmer switch timing is accomplished by digitally counting cycles of the 400-cps line voltage, and generating pulses at preset counts which subsequently switch transistors and controlled silicon rectifiers. When the line frequency exceeds 400 cps, the switching times will occur sooner than nominal; when the line frequency is below 400 cps, the switching times will occur later than nominal. Other factors which account for differences between nominal and indicated switching times are lag between switch closure and the resultant event, and poor readability of commutated data.

Slosh

Sloshing of the liquid oxygen in its tank was noted on all subject flights, with similar characteristics to that observed during previous Series D flights. Table 6.1-9 summarizes the maximum missile rates and associated booster engine movements resulting from slosh. The average maximum missile rates were 1.6 deg/sec peak-to-peak in both pitch and yaw, with associated booster engine peak-to-peak movements of 0.8 degrees in pitch and 0.7 degrees in yaw.

Propellant slosh amplitudes on Missiles 71D, 76D, and 90D, which incorporated the Series E double section quadratic stabilization filters, were considerably larger than those encountered on Series D flights without similar filters. Increased propellant slosh with booster engine movements of 3 degrees peak-to-peak had been predicted from studies based upon the additional lag introduced by the Series E double section filter. The higher slosh amplitudes had no known detrimental effect on flight performance.

TABLE 6.1-8 FLIGHT PROGRAMMER PERFORMANCE, SQUARE AUTOPILOT

ASSOCIATED SWITCH	FUNCTION	TIME REFERENCE (1)	DESIGN TIME (SECONDS)	ACTUATION TIME FROM REFERENCE IN SECONDS (2)								
				42D	48D	54D	60D	66D	76D	71D	83D	90D
--	Flight Programmer Start	Launch	0	0	Missile destroyed prior to liftoff	NM	NM	NM	NM	NM	NM	NM
10	Enable Roll Program	Launch	2	2.05		2.22	2.08	2.05	2.06	2.03	NM	NM
11	High Roll Gyro Torque Excitation	Launch	2	NM		NM	NM	NM	NM	NM	NM	NM
10	Disable Roll Program	Launch	15	15.08		15.16	15.02	15.06	NM	NM	NM	NM
9	Enable Roll Guidance (3)	Launch	15	NM		NM	NM	NM	NM	NM	NF	NF
9	Disable Roll Guidance	Launch	19	NM		NM	NM	NM	NM	NM	NF	NF
11	Low Roll Gyro Torque Excitation	Launch	19 (4)	NM		NM	NM	NM	NM	NM	NM	NM
22	Enable Staging Discrete (5)	Launch	134	NM		NM	NM	NM	NM	NM	NM	NM
--	Staging Discrete (6)	Launch	---	NF		137.37	140.78	136.18	138.33	139.34	137.55	137.44
	Staging Backup	Launch	145 (7)	141.0 (8)		NF	NF	NF	NF	NF	NF	NF
12	Booster Cutoff Relay (P72X)	Staging	0.1	NM		NM	NM	0.10	0.10	0.08	0.13	0.14
12	Pressurize Vernier Tanks	Staging	0.1	DA		DA	DA	-0.25/0.15	-0.08/0.32	0.01/0.41	0.13	0.14
1	Zero Booster (Pitch, Yaw, and Roll)	Staging	0.1	0.12		0.10	0.10	0.12	0.16	0.10	0.08	0.08
1	Activate 8 cps Filter (Pitch and Yaw)	Staging	0.1	0.14		0.07	0.15	0.13	DA	DA	DA	DA
1	Deactivate Quadratic Filter (Pitch and Yaw)	Staging	0.1	DA		DA	DA	DA	0.10	NM	DA	DA
1	Increase Pitch and Yaw Rate Gyro Gains	Staging	0.1	0.14		NM	NM	NM	NM	NM	NM	NM
2	Activate Sustainer in Pitch and Yaw	Staging	0.1	0.14		0.10	0.10	0.15	0.16	0.12	0.12	0.17
3	Activate Verniers in Pitch and Yaw	Staging	0.1	0.08		0.07	0.10	0.13	0.10	NM	0.14	0.12
5	Null Integrators - Pitch and Yaw	Staging	0.1	NM		NM	NM	NM	NM	NM	NM	NM
6	Reduce Integrator Gain - Pitch and Yaw	Staging	0.1	NM		NM	NM	NM	NM	NM	NM	NM
2	Zero Sustainer in Pitch and Yaw	Staging	3.0	3.03		2.99	3.03	3.02	3.02	3.02	3.05	3.05
13	Jettison Booster Package (M26D)	Staging	3.1	NM		NM	NM	3.17/3.22	3.12/3.17	3.12/3.17	NM	NM
13	Rate Gyros Indicate Jettison Start	Staging	3.1	3.10		3.08	3.08	3.11	3.10	3.09	3.12	3.12
13	Axial Acceleration Indicates Jettison Start	Staging	3.1	3.16		3.09	3.10	3.09	3.11	3.10	3.10	3.11
2	Reactivate Sustainer in Pitch and Yaw	Staging	3.7	3.72		3.69	3.73	3.72	3.72	3.70	3.75	3.74
7	Enable Guidance Pitch and Yaw Steering	Staging	5.0	NF		4.97	4.97	5.00	4.99	4.98	NM	NM
3	Disable Verniers in Pitch and Yaw	Staging	6.7	6.69		6.66	6.67	6.69	6.68	6.67	NM	NM
4	Bias Verniers to 50 Degrees	Staging	6.7	6.71		6.64	6.67	6.69	6.68	6.67	6.73	6.67
5	Reactivate Integrators - Pitch and Yaw	Staging	10.0	NM		NM	NM	NM	NM	NM	NM	NM
8	Deactivate Quadratic Filter - Pitch and Yaw	Staging	30.0	DA		DA	DA	DA	DA	DA	NM	NM
14	Pressurize Vernier Tanks	Staging	64.0	64.25±0.1		63.73	64.16	NF	NF	NF	NF	NF
23	Enable Sustainer Cutoff Discrete	Staging	80.0	NM		NM	NM	NM	NM	NM	DA	DA
--	Enable Sustainer & Vernier Cutoff Discretes (9)	Staging	80.0	DA		DA	DA	DA	DA	DA	NM	NM
--	Sustainer Cutoff Discrete	Launch	--	NF		235.47	NA	NF	NF	NF	269.82±0.1	271.96±0.1
--	Automatic Sustainer Fuel Cutoff Signal	Launch	--	256.74		NF	307.55	259.18	274.82	266.67	NF	NF
19	Sustainer Cutoff Signal	Sustainer Cutoff	0	DA		DA	DA	DA	DA	DA	NM	NM
19	Start Optical Beacon	Sustainer Cutoff	0	NF		0.02	0.01 (10)	NF	0.0	0.01	DA	DA
--	Sustainer Cutoff Relay (P347X)	Launch	--	256.82±0.1		235.41±0.1	307.52±0.1	259.10±0.1	274.84±0.1	266.60±0.1	269.88	271.90
3	Reactivate Verniers in Pitch and Yaw	Sustainer Cutoff	0	0.03		0.01	NM	0.14	0.0	0.0	0.07	0.04
5	Null Integrators - Pitch and Yaw	Sustainer Cutoff	0	NM		NM	NM	NM	NM	NM	NM	NM
24	Vernier Cutoff Enable	Sustainer Cutoff	0	NM		NM	NM	NM	NM	NM	DA	DA
--	Vernier Cutoff Discrete	Launch	--	NF		242.67	NA	274.30	290.77	280.57	NM	288.58
--	Manual Vernier Cutoff Signal & Pre-Arm R/V	Launch	--	269.24		NF	345.23	NF	NF	NF	NF	NF
--	Programmer Vernier Cutoff Condition (400 Count)	Launch	--	269.24		242.66	340.78 (11)	274.30	290.77	280.57	NM	288.58
20	Vernier Cutoff Signal	Vernier Cutoff	0			DA	DA	DA	DA	DA	NM	NM
--	Vernier Cutoff Relay (P77X)	Launch	--	269.17±0.1		242.64±0.1	NF	274.29±0.1	290.68±0.1	280.57	286.23	288.66
16	Eject Re-Entry Vehicle Umbilical (S246X)	Vernier Cutoff	15	DA		DA	DA	14.98	14.91/15.31	14.63/15.03	DA	DA
16	Re-Entry Vehicle Pre-Arm Backup Signal	Vernier Cutoff	15	DA		DA	DA	DA	DA	DA	NM	NM
16	Re-Entry Vehicle Separation (S248X)	Vernier Cutoff	15	15.03		14.88	14.57	DA	DA	DA	DA	DA
17	Re-Entry Vehicle Separation	Vernier Cutoff	16			DA	DA	15.99	15.97	16.07	16.05	16.02
18	Fire Retrorockets	Vernier Cutoff	17	17.01		MALFUNCTION	16.52	16.95	16.97	16.94	17.07	17.01

NOTES:

(1) Time reference column pertains to the following events except where noted:
Launch - 2-inch motion
Staging - Receipt of staging discrete or staging backup actuation, whichever occurs first.
Sustainer Cutoff - Receipt of sustainer cutoff discrete or automatic sustainer fuel cutoff signal, whichever occurs first.
Vernier Cutoff - Receipt of vernier cutoff discrete, manual vernier cutoff signal (manual fuel cutoff), or programmer vernier cutoff condition, whichever occurs first.

(2) Minimum and maximum actuation times indicate data was commutated.

(3) Switch 9 was not used on Missiles 83D and 90D.

(4) Design time for low roll gyro torque excitation was launch +15 seconds on Missiles 83D and 90D.

(5) On Missiles 83D and 90D, the staging discrete was enabled by a time slot triggered transistor switch, rather than by Switch 22 (magnetic latching relay).

(6) The staging discrete command was instrumented on a 5-rps commutated channel. The times given are approximations chosen for compatibility with the subroutine one switching times as determined from flight data.

(7) Design time for staging backup was launch plus 141 seconds on Missile 42D.

(8) The time of staging backup was not monitored. The value of 141.0 seconds is an approximation chosen for compatibility with the subroutine one switching times as determined from flight data.

(9) On Missiles 83D and 90D, the sustainer and vernier cutoff discretes were enabled by a time slot triggered transistor switch, rather than by switches 23 and 24 respectively (magnetic latching relays).

(10) The value 0.01 is referenced to the manual vernier cutoff signal time of 345.23.

(11) The value 340.78 is an approximation based on the time of staging discrete plus 200 seconds.

NM - Not measurable from data
NF - Sent or actuated, but performed no function
DA - Does not apply
NA - Not sent or actuated
NP - Not planned

HIGH POWER SWITCH TABLE

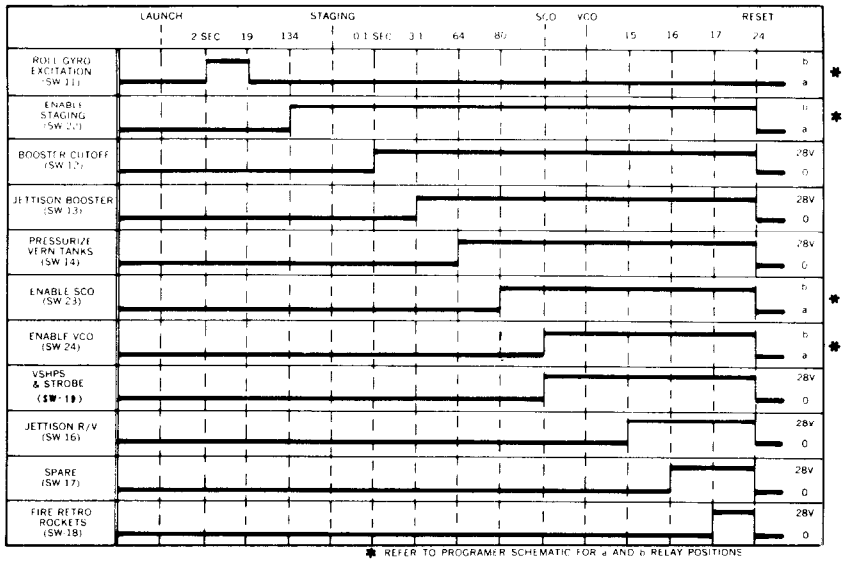

LOW POWER SWITCH TABLE

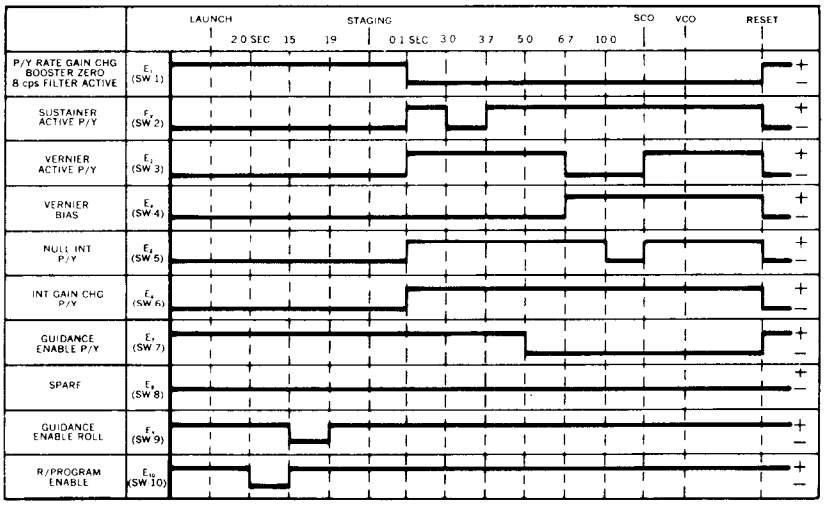

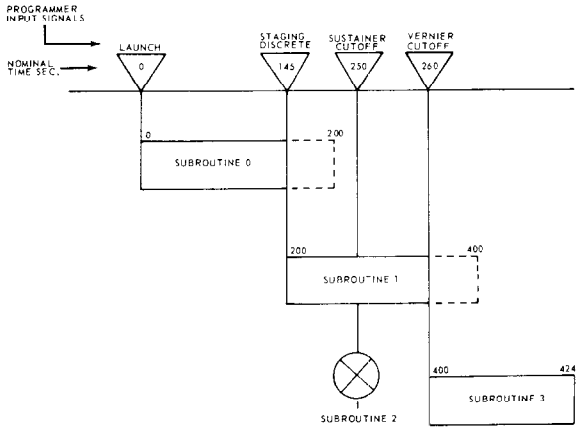

FIGURE 6.1-14 FLIGHT PROGRAMMER SWITCHING SEQUENCE, SQUARE AUTOPILOT

TABLE 6.1-9 PROPELLANT SLOSH CHARACTERISTICS

MISSILE	PLANE	MAXIMUM RATE (deg/sec peak-to-peak)	MAXIMUM BOOSTER ENGINE MOVEMENT (deg peak-to-peak)	TIME FROM LAUNCH (sec)	FREQUENCY (cps)
42D	Pitch	2.2	0.9	97	1.15
	Yaw	1.7	0.9	99	1.15
48D	Pitch	TEST TERMINATED ON PAD			
	Yaw				
56D	Pitch	2.7	1.4	95	1.12
	Yaw	1.5	0.7	95	1.12
54D	Pitch	1.4	0.7	93	1.19
	Yaw	1.7	0.7	93	1.19
62D	Pitch	2.2	1.0	85	1.14
	Yaw	1.7	0.7	85	1.14
27D	Pitch	0.9	0,6	97	1.16
	Yaw	2.5	1.2	97	1.16
60D	Pitch	0.6	0.3	95	1.11
	Yaw	1.3	0.7	95	1.11
32D	Pitch	1.4	0.7	95	1.18
	Yaw	1.7	0.7	94	1.19
66D	Pitch	2.1	0.9	91	1.11
	Yaw	NEGLIGIBLE	NEGLIGIBLE		
76D*	Pitch	7.5	4.0	97	1.03
	Yaw	8.2	4.5	90	0.97
79D	Pitch	1.1	0.6	100	1.12
	Yaw	1.1	0.6	100	1.12
71D*	Pitch	9.0	4.3	94	0.99
	Yaw	4.0	1.8	93	1.00
55D	Pitch	1.8	0.9	99	1.13
	Yaw	1.4	0.7	99	1.18
83D	Pitch	1.2	0.5	98	1.12
	Yaw	1.4	0.5	98	1.12
90D*	Pitch	6.0	2.6	102	1.15
	Yaw	3.9	1.6	96	1.09
Average*	Pitch	1.6	0.8	95	1.14
	Yaw	1.6	0.7	96	1.15

* Excludes 71D, 76D, and 90D

On Missile 83D, which also incorporated a Series E quadratic stabilization filter, propellant slosh amplitudes during booster phase were moderate. The lack of increased propellant slosh on this missile was attributed to the heavier Mark 4 Mod I re-entry vehicle carried on this flight. The slosh amplitudes are observed to decrease with heavier payloads as a result of their effect on the longitudinal location of the missile center of gravity (c.g.). With the heavier payloads, the missile c.g. is shifted forward, and the sloshing moments are reduced. This effect was previously demonstrated during the flights of Missiles 20D and 80D (Able boosters). The slosh amplitudes on both flights were relatively low, as expected, as a result of the heavier upper stages. Maximum booster engine movements resulting from slosh did not exceed 0.2 degrees peak-to-peak in either plane on both flights.

Figure 6.1-15 shows a representative example of the booster engine movements that occurred during the flight of Missile 42D as a result of propellant slosh. It may be seen that the phase angle between the pitch and yaw engine position traces gradually shifts. This indicates that the plane of oscillation of the equivalent lox pendulum* is slowly rotating.

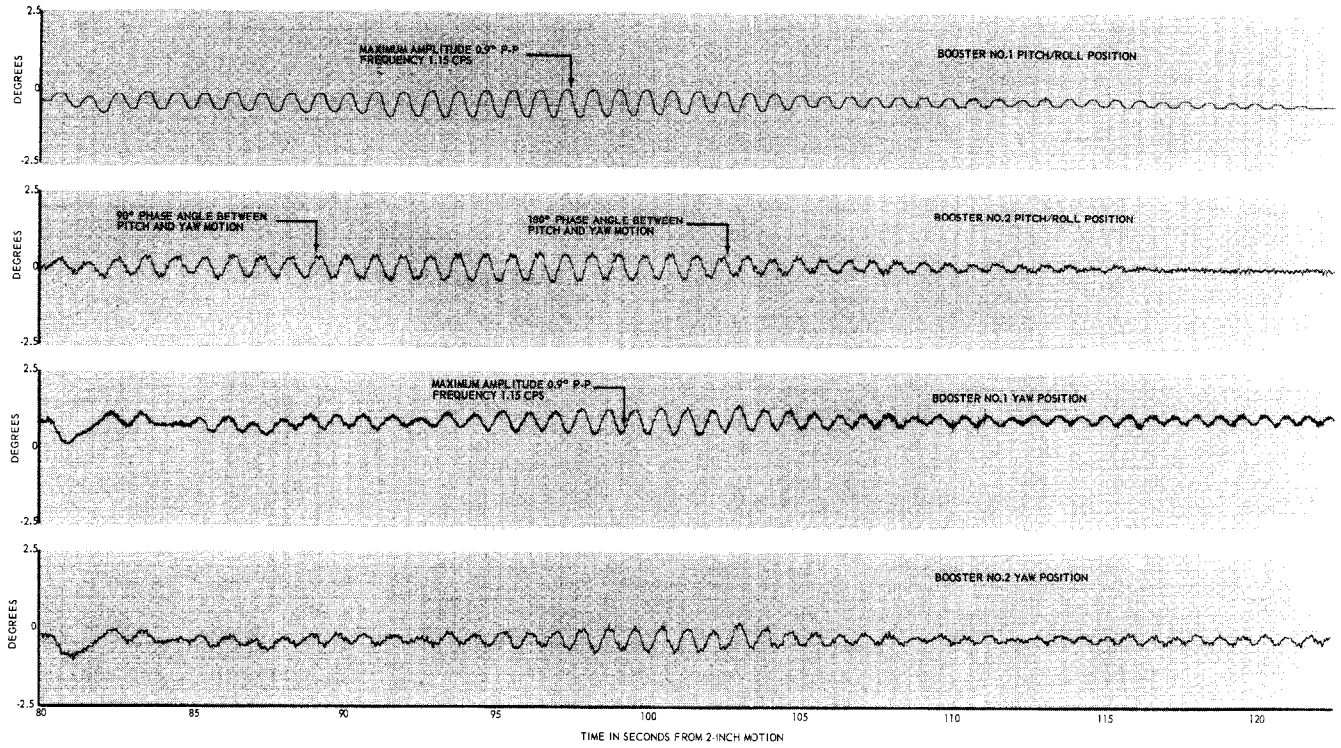

FIGURE 6.1-15 CHARACTERISTIC BOOSTER ENGINE MOVEMENT DURING SLOSH PERIOD

For the Series D missiles, rate gyro output data indicated that sloshing started during the period from 50 to 70 seconds after launch. It is during this period that maximum aerodynamic disturbances are acting on the missile, tending to excite slosh. After sloshing is excited, it builds up to a peak amplitude, then decays, and is usually damped out prior to booster cutoff. On Missile 32D, however, sloshing was sustained up to booster cutoff. Similar slosh characteristics were previously indicated during the flights of Missiles 15D and 31D.

The sustained propellant slosh on Missile 32D was the result of additional lag introduced by the 8-cps pitch and yaw stabilization filters which were incorporated throughout the flight. The filters were required for bending mode stability with the remote rate gyro package at Station 744. Pitch and yaw end-to-end rate gains were increased 14.75 percent to compensate for the additional lag (see Table 6.1-2). The sustained slosh did not constitute a problem as it had no detrimental effect on flight performance or booster separation.

The subject Series D missiles were equipped with 11 four-inch wide anti-slosh baffles and four triangular baffles in the liquid oxygen tank (see Figure 6.1-16).

* The equivalent lox pendulum is a term used in the pendulum analogy of sloshing. In this analogy, the mass of the sloshing fluid is considered to be a pendulum swinging about on imaginary hinge point.

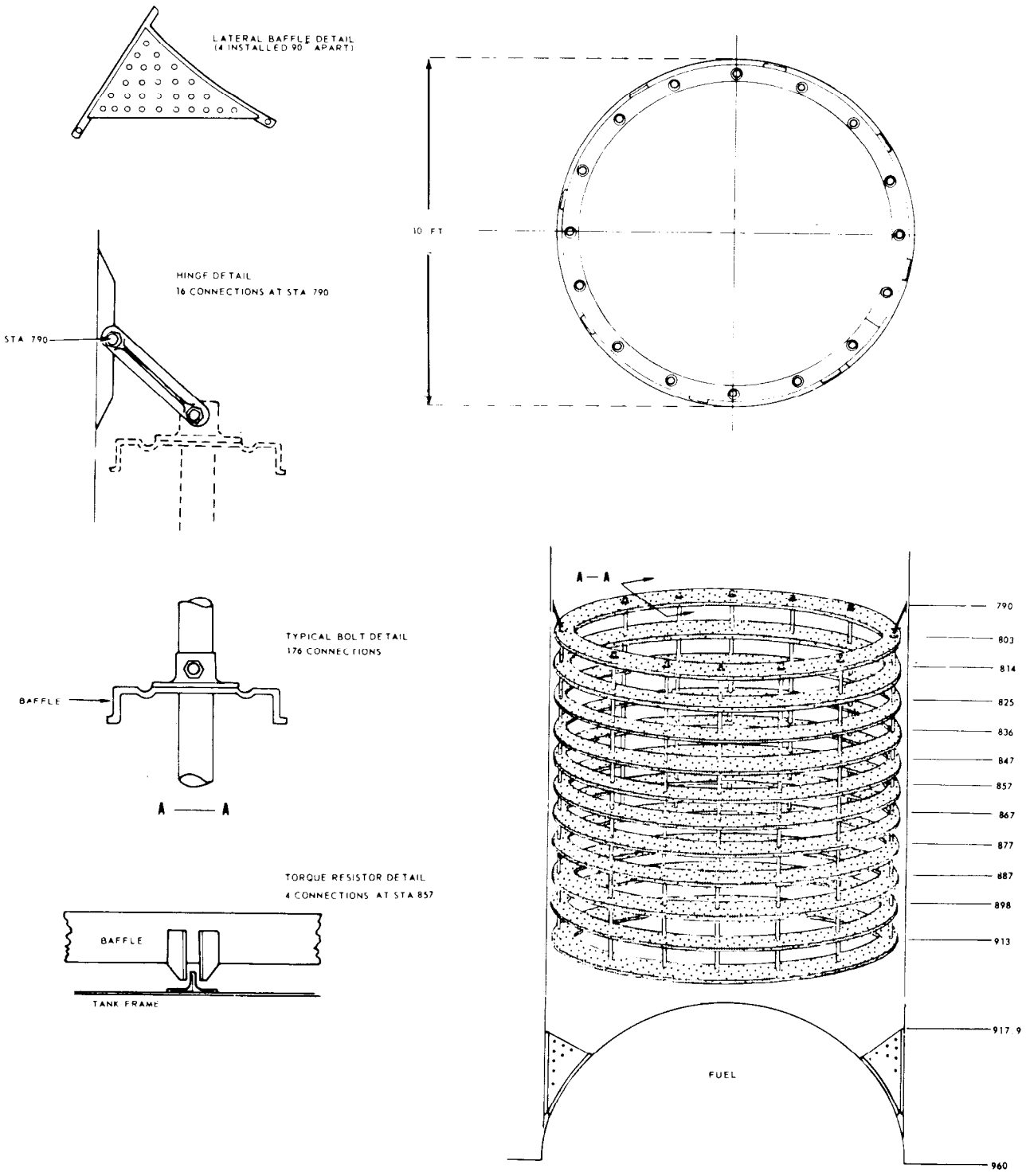

FIGURE 6.1-16 LOX TANK BAFFLE CONFIGURATION

Guidance Steering Commands

Missile guidance is accomplished, in pitch and yaw only, by guidance steering commands. The D/RIG missiles are steered by commands transmitted from the ground guidance system. The D/AIG missiles are steered by commands received from the airborne missile guidance set (MGS). Steering commands are enabled by the flight programmer at staging discrete plus 5.1 seconds nominal on D/RIG articles, and at staging discrete plus 5.0 seconds nominal on D/AIG articles. In conjunction with the autopilot, they function to place the missile on the desired trajectory.

The steering commands, when applied to the autopilot, electrically torque the pitch and yaw displacement gyros (which provide the inertial reference attitude for the missile). With the displacement gyros displaced with respect to the missile, the autopilot positions the engines in order to realign the missile with the gyro reference axes. In this manner the missile is steered.

Ability of the autopilot to accept and properly execute D/RIG and D/AIG steering commands is indicated in Figures 6.1-17A and B, respectively. Figure 6.1-17A illustrates the response of Missile 32D to a planned positive 92% (yaw right) RIG steering command which was required to accomplish a "dogleg" trajectory. Figure 6.1-17B illustrates the response of Missile 71D to a maximum positive 4.8 volt (yaw right) AIG steering command. In both figures, the guidance yaw command (steering signal or decoder analog output) and the yaw displacement gyro output are plotted on the same time scale. It is seen that torquing of the yaw displacement gyro, as indicated by the displacement gyro output, followed closely the guidance yaw command. Response of the missile to the steering command is indicated by the yaw rate gyro output trace, which indicates the missiles angular rate of movement.

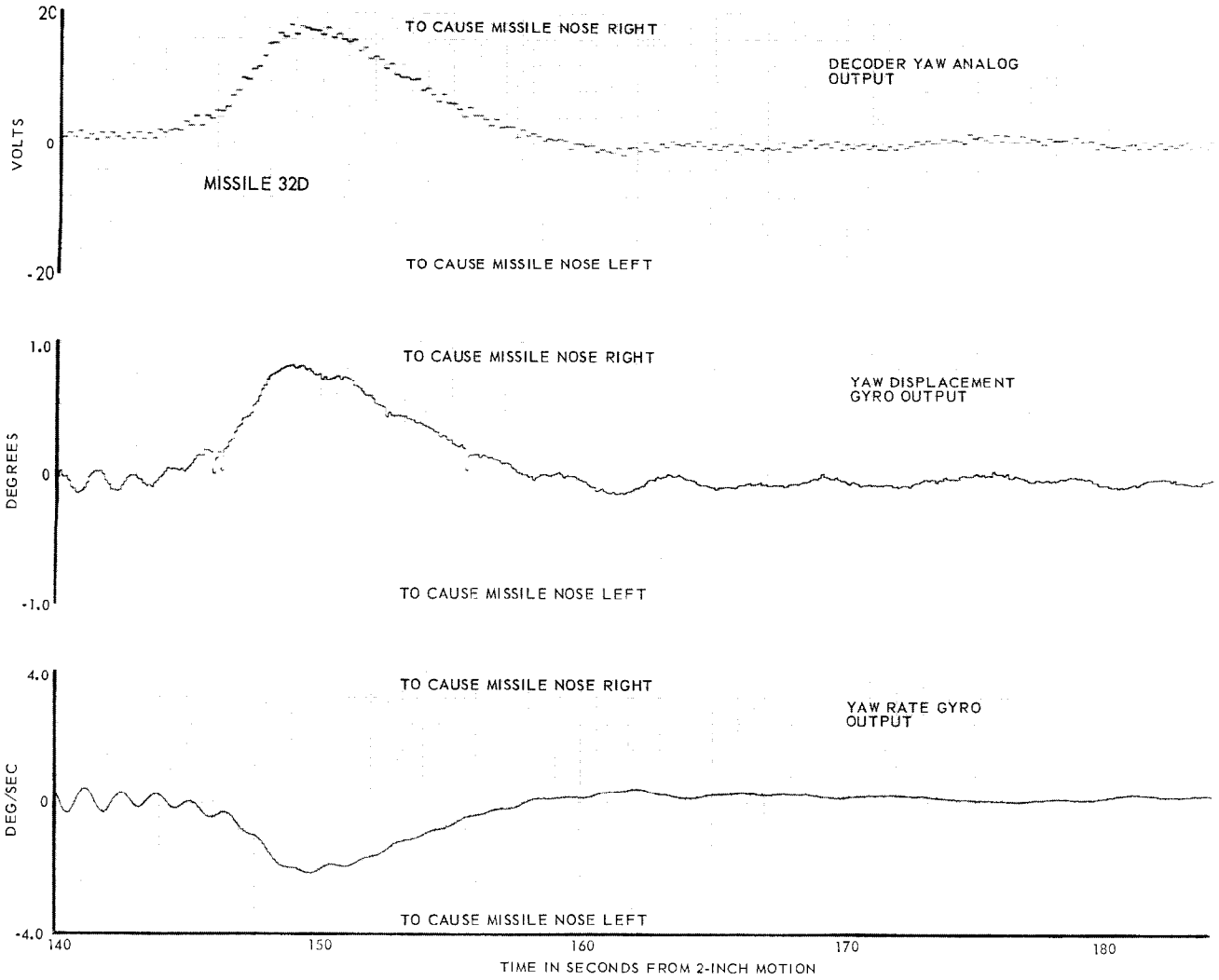

FIGURE 6.1-17A AUTOPILOT RESPONSE TO RADIO-INERTIAL GUIDANCE YAW STEERING COMMANDS

The yaw rate gyro and yaw displacement gyro traces are also plotted in Figures 6.1-17A and 6.1-17B on the same time scale. It may be noted that the two signals are always of opposite polarity during steering, with the rate gyro output tending to cancel out the displacement gyro signal. The reason for this is that the rate gyro output is always of such phase as to oppose the missile motion that is causing the output.

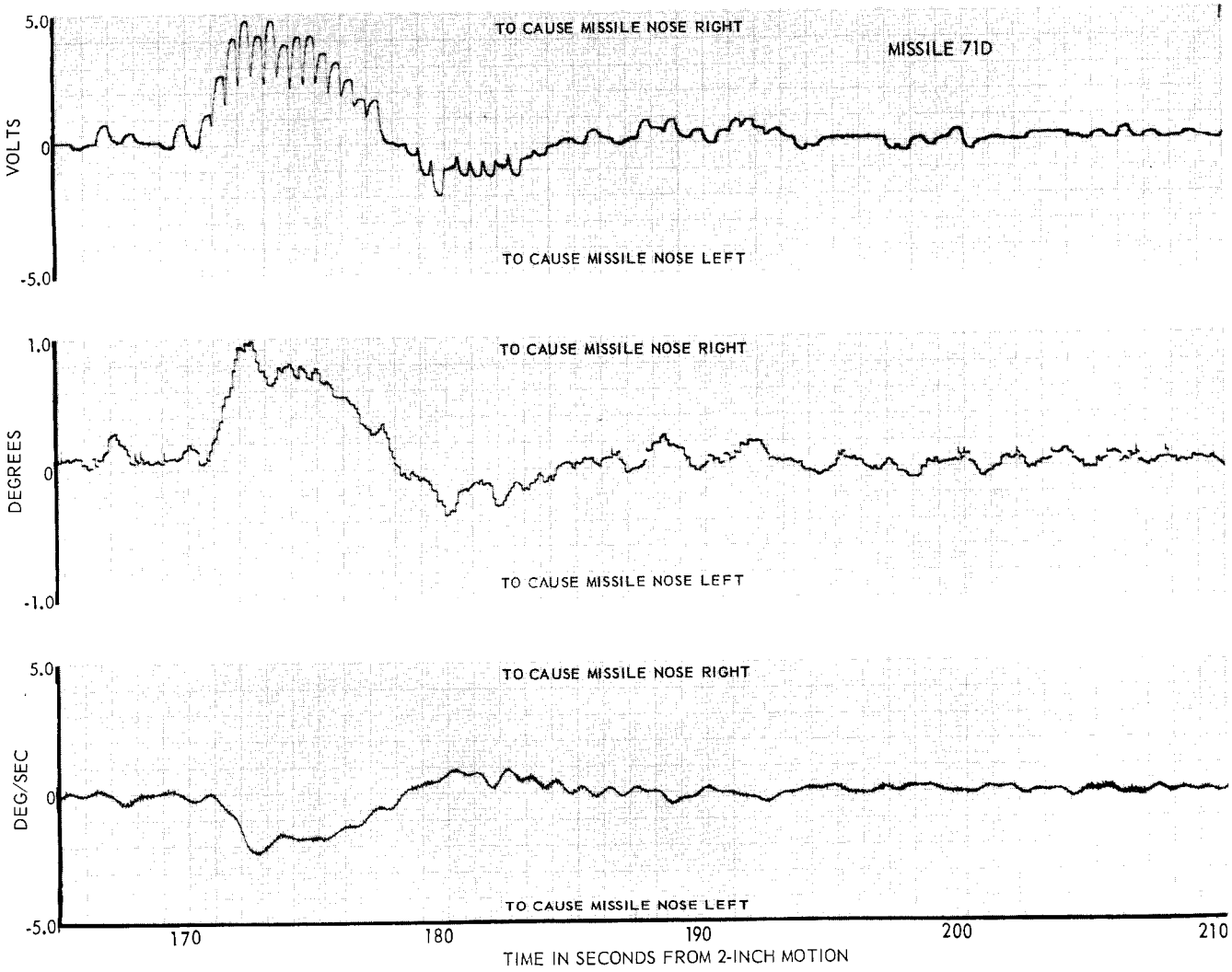

FIGURE 6.1-17B AUTOPILOT RESPONSE TO ALL INERTIAL GUIDANCE YAW STEERING COMMAND

Mark 3 Re-entry Vehicle Separation

The effect of Mark 3 re-entry vehicle separation on missile stability is shown in Figure 6.1-18 for five of the subject missiles. It may be seen that separation of the re-entry vehicle imparts a counterclockwise missile roll rate of 0.6 to 0.8 deg/sec. The counterclockwise missile roll rate is a characteristic of Mark 3 re-entry vehicle separation, and results from re-entry vehicle torque bar reaction. The Mark 3 re-entry vehicle is spin stabilized at separation by the action of the energy stored in the torque bar.

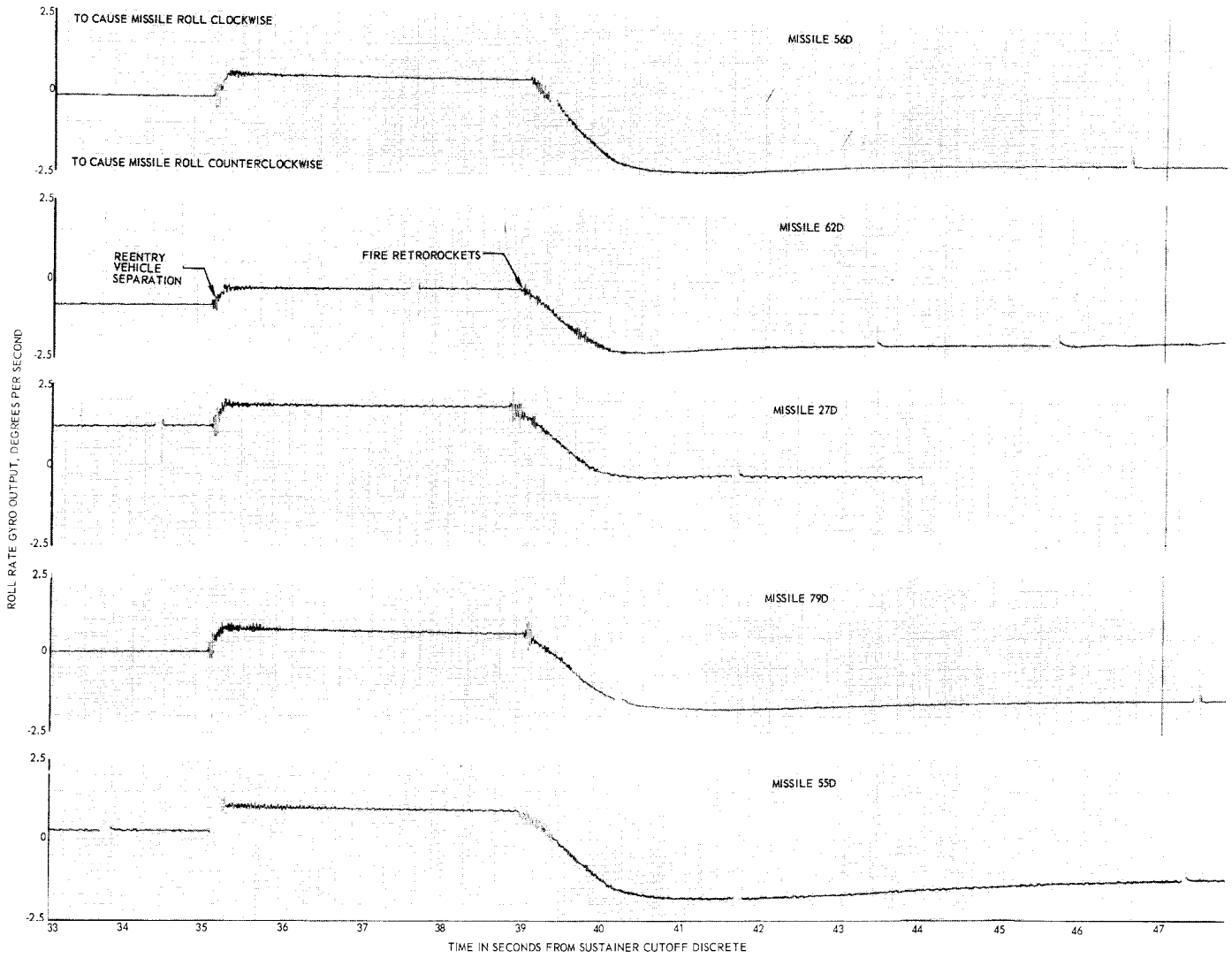

FIGURE 6.1-18 EFFECT OF RE-ENTRY VEHICLE SEPARATION ON MISSILE STABILITY

Bending Oscillations

First mode bending oscillations at frequencies between 10 and 12 cps were observed during the latter portion of the sustainer phase on the majority of the subject Series D/RIG missiles. There were no undesirable effects noted on missile or flight control system performance as a result of the oscillations. Missile first bending mode oscillations have also been observed on most Series B, C and previous D flights. A potential problem inherent in missile airframe bending oscillations concerns elastic coupling of these oscillations into the autopilot rate gyros. If amplified sufficiently and applied to the flight control system in proper phase, they can cause missile instability and possible destruction.

There was little evidence of the usual sustainer phase 10 to 12-cps bending mode oscillations on the Series D/AIG flights, apparently as a result of sufficient filtering in the pitch and yaw channels of these frequencies. Four Series D/AIG flight missiles (42D, 54D, 60D, and 66D) incorporated 8-cps low-pass filters (pitch and yaw only), which were switched in at booster cutoff, in addition to the regular 4-cps low-pass filters.

PROBLEM AREAS

During the flight of Missile 62D, the vernier engine cutoff discrete (VECO), generated by the ground guidance computer at 299.7 seconds, failed to initiate vernier cutoff. The verniers were subsequently cutoff by the flight programmer vernier cutoff backup (switch No. 74) at 307.7 seconds (23.5 seconds after sustainer cutoff relay activation).

Failure of the VECO discrete to effect vernier engine cutoff on Missile 62D was isolated to a discontinuity in the electrical harness between the GE Mod III guidance decoder and the autopilot flight programmer. An examination of preflight test data indicated that the discontinuity had existed prior to launch. Post-flight examination of data from both the autopilot-Mod III guidance integrated checkout test and the flight acceptance composite test indicated that vernier cutoff was not effected when the VECO discrete was transmitted. Also, re-examination of landline data obtained during the countdown data link test, conducted between T-10 and T-5 minutes, confirmed a discontinuity in the vernier cutoff circuitry between the guidance decoder and the autopilot flight programmer.

The most probable point for signal loss between the guidance decoder and the flight programmer on Missile 62D was believed to be at plug P303. This plug was potted at AMR prior to running the Autopilot-Guidance Integrated Test, and it is possible that an open circuit resulted from this process.

There were no hardware changes made as a result of the VECO failure on 62D. It was determined that a valid end-to-end test from the guidance system to the propulsion relays could be accomplished with the countdown procedure then in effect.

On Missile 54D, a flight programmer malfunction resulted in failure of the retrorockets to fire at vernier cutoff (VCO) plus 17 seconds as required. This failure was indicated by the absence of the usual vibration and acceleration on the rate gyro and inertial guidance accelerometer traces. In addition, the programmer failed to recycle at VCO plus 24 seconds, as indicated by the absence of vernier engine tank venting, and the absence of re-entry vehicle jettison signal dropout (switch 16, measurement No. S248X). Performance of the programmer was normal during the countdown when two autopilot-inertial guidance integrated tests were performed.

During the FACT test conducted on Missile 54D on 27 May 1960, the booster engines failed to null at the time of booster cutoff. This problem was traced to a 40-volt peak-to-peak inductive surge on the 28-vdc missile source, resulting from the closure of the main booster propellant valves in the NAA propulsion system. This surge caused the booster nulling programmer switch function to drop out. To alleviate this condition, a 28-vdc filter was added to the missile harness at the flight programmer input. A second FACT test was conducted with satisfactory programmer performance. A similar programmer timing malfunction occurred on a subsequent special test in which fuses were substituted for the pyrotechnic squibs. A re-examination of records showed that the re-entry vehicle jettison signal dropped out after two seconds. This signal normally remains activated for nine seconds, from VCO plus 15 seconds to programmer recycle (VCO plus 24 seconds).

The programmer malfunction on Missile 54D was attributed to ringing of the 28-vdc programmer filter, which resulted from firing the re-entry vehicle jettison and umbilical eject squibs at 257.55 seconds. These latter events, and the retrorockets firing function, are accomplished during subroutine 3 which begins at VCO, at which time the programmer count is advanced to 400 (see Figure 6.1-14). Ringing of the programmer filter caused the internal programmer power supply voltages to ring. This in turn caused the S-100 binary in the programmer logic to flip, advancing the programmer digital clock counter to a 200-second count (staging discrete) condition, thus bypassing the "fire retrorockets" function. The programmer then ran for 200 seconds to a count of 400 seconds (VCO condition) and approximately 17 seconds later fired the retrorockets.

In order to prevent recurrence of the problem encountered on Missile 54D, a redesigned 28-vdc programmer filter with built-in damping was installed on subsequent D/AIG missiles, with satisfactory results.

Another problem, external to the flight programmer, occurred during the flights of Missiles 54D, 66D, and 90D, and adversely affected programmer performance. This was shorting of the retrorockets wiring during retrorockets firing, and consequent burn-out of a programmer printed circuit board. A similar failure was also experienced during factory testing of Missile 2E, due to shorting of the retrorockets squib wiring to shield ground. The short on Missile 54D appeared to be unrelated to the previously discussed failure of the retrorockets to fire. Flight programmer circuit board burnout on Missiles 54D and 66D caused loss of the 28-vdc power within the programmer, premature resetting of the programmer (as indicated by the dropout of all high power switches), and subsequent programmer cycling with a 24-second period.

The above malfunctions had no adverse effect on flight performance, as the "fire retrorockets" event is the final programmer function. A possible short of other high power switch functions could however, have serious consequences if the normal programmer switching sequence is disrupted. In order to prevent such an occurrence, current limiters will be added to all programmer high power switch outputs on all Series E and F operational missiles, and on Series E research and development flight missiles (12E, 17D, and on).

Intermittent shorting of the retrorockets wiring was also indicated on Missile 76D during retrorockets firing as evidenced by slight drops in the programmer 28-vdc input trace, and larger drops in two of the instrumented high power switch output traces (switches 12 and 14). The shorting was not severe enough to cause burnout of the programmer printed circuit board, as the programmer recycled normally at approximately 24 seconds after receipt of the vernier cutoff discrete.

During the flight of Missile 60D, shorting in the missile electrical system produced repeated pressurization and venting of the vernier engine start tanks (see Electrical Section of this report). Normally, the vernier engine start tanks are pressurized by flight programmer high power switch No. 14 at 64 seconds after receipt of the staging discrete. Examination of flight data, and subsequent ground tests gave no indication that the erroneous "pressurize vernier tank" (PVT) signal originated in the flight programmer.

On Missiles 66D, 71D, and 76D, special instrumentation and modification of the PVT circuitry were incorporated (see Figure 7.3-3, Electrical Section). This was done for failure analysis and to isolate any recurrence of an erroneous PVT signal. The missile circuitry was modified so that the PVT signal was provided by programmer switch No. 12 at booster cutoff (staging discrete plus 0.1 second nominal). The normal PVT circuitry was modified by routing the PVT relay (K32C) output signal through umbilical 305-P1 (autopilot 42-inch motion umbilical) to the engine tanks pressurizing control valve. This allowed the PVT circuitry to function as designed during preflight checks, but to operate only open-loop during flight for instrumentation purposes. Special PVT circuitry instrumentation data obtained from Missiles 66D, 71D, and 76D were normal, with no recurrences of erroneous PVT signals.

On Missile 66D, excessive missile bending was recorded on the yaw rate gyro and re-entry vehicle rate and acceleration measurements during the booster phase of flight, with the yaw bending mode beginning at approximately 80 seconds. A peak maximum rate gyro output of 4.67 degrees/second at a frequency of 4.8 cps was reached at 112.3 seconds. Associated booster engine displacement in yaw reached 1.38 degrees peak, while sustainer engine yaw fluctuations indicated 0.41 degrees peak. At 112.515 seconds, the rate gyro data indicated a shock due to an impulse type disturbance, with an abrupt reduction in peak yaw rate gyro output to 1.2 degrees/second.

The initial buildup of yaw bending on Missile 66D was attributed to the RVX-2A re-entry vehicle configuration, and the associated latch clearances. The abrupt drop in the magnitude of the bending mode oscillations at 112.515 seconds was attributed to yielding of the upper right (Quad IV) re-entry vehicle separation latch. The RVX-2 latch configuration consists of three non-tension latches with an allowable clearance of from 0.010 to 0.050 inch.

In order to prevent similar bending mode oscillations on Missiles 71D and 76D, which also flew with RVX-2A re-entry vehicles, latch clearances were reduced to 0.010 and 0.014, and 0.018 inch. In addition, both missiles incorporated the Series E type quadratic-lead, triple-lag stabilization filter in the pitch and yaw channel in order to phase stabilize the 4.8 cps modal problem. The flight tests of both missiles indicated the changes were successful, as there was no evidence of first bending mode oscillations during booster phase. Bending mode oscillations during booster phase were experienced on 44D (RVX-2A) 49D (MK3 Mod IX) and 56D (MK3 Mod IB). However, maximum amplitude on these flights were significantly smaller than on 66D.

On Missile 90D flown with the Mark 3 Mod IB re-entry vehicle aboard, excessive pitch rate gyro output oscillations began to buildup at 29 seconds, being first evident at 25.0 cps. A pitch rate gyro output of approximately 10.6 degrees/second peak-to-peak at 25.3 cps was reached by 36 seconds and was maintained at essentially this amplitude until 38 seconds. The oscillation then began a gradual decay and died out by approximately 42 seconds, reaching a frequency of 26.5 cps. The B1 pitch engine position trace indicated low level movement of approximately 0.1 degree peak-to-peak at these frequencies. Coupling of the oscillation into the yaw and roll planes resulted in maximum gyro output rates of 0.9 and 5.3 deg/sec peak-to-peak, respectively.

The pitch oscillations on Missile 90D appeared qualitatively similar to those that occurred during the booster phase of flight on Missiles 80D (Able booster) and 3E. The use of the quadratic-lead, triple-lag stabilization filters for pitch and yaw in the "square" autopilot packages may have resulted in insufficient attenuation near 25 cps for the Missile 90D configuration. It should be noted that with the exception of different pitch program torquing gains and re-entry vehicles, the autopilot configuration of 90D was identical to that of 83D. Both missiles were flown with Moog booster hydraulic actuators. Missile 83D flew with the MK4 Mod I re-entry vehicle aboard. There was no oscillation buildup noted during the flight of Missile 83D.

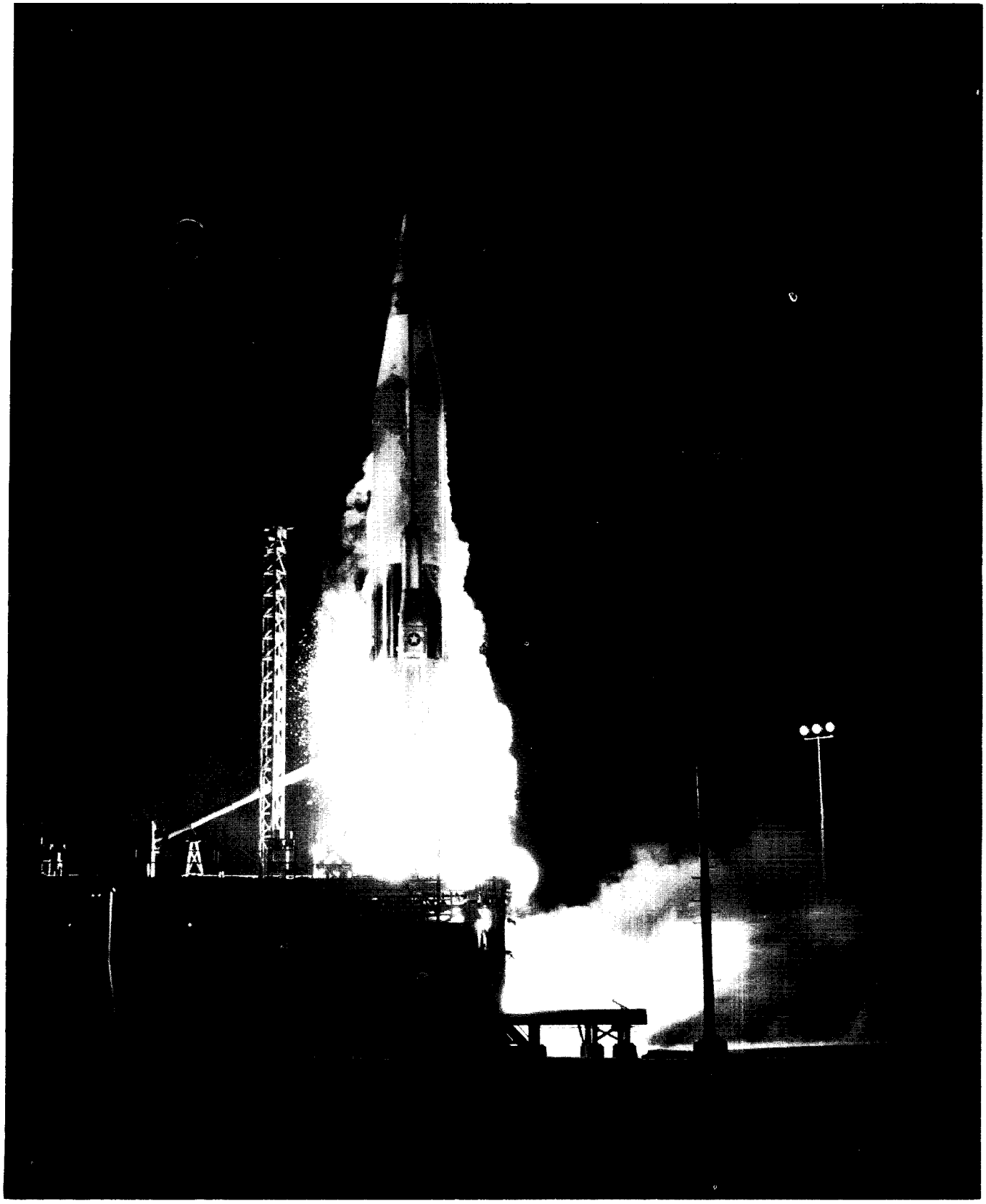

MISSILE 71D AT LIFTOFF

SECTION 6.2 - GUIDANCE SYSTEM

The section of this report analyzing the performance of the Radio Guidance System was prepared in its entirety by the General Electric Co. Certain portions of the subject section treat problems and test procedures not immediately related to the summary analysis of Series D Atlas missile testing. These portions have been retained, however, for their value and interest in the subject area.

The treatment of impact data in the GE analysis of the Mod III guidance system differs slightly in method from that used in the Astronautics prepared trajectory analysis section. The differences in numerical answers obtained for impact miss distance are very small and due entirely to the reference used. The method of calculation of weapon system CEP, although different from that used in the Astronautics treatment, yields approximately the same results when data for the same missiles are used in the computation. The apparent discrepancy between the GE and Astronautics CEP's, as presented, is due to the selection of a different set of missiles for inclusion in each case.

The precision of the GE Mod III system in providing both a guidance and an instrumentation function has been capably demonstrated by the Series D missile tests. Also useful in indicating the system's accuracy, are aircraft tests which assist in determining tracking errors, and the self-consistency program which has been invaluable in determining velocity errors. The self-consistency program uses internal system data only, subtracting integrated rates from the position data transformed to hyperbolic coordinates. Any bias in the rates then appear as a linear slope in the residuals.

An estimate of the probable real-time guidance rms errors is given in Table 6.2-1. Table 6.2-2 shows the probable instrumentation rms errors. These tables include both random and systematic errors.

TABLE 6.2-1 ESTIMATE OF PROBABLE REAL-TIME GUIDANCE RMS ERRORS, MOD III SYSTEM 1

FUNCTION	ϕ = 0.7° (or above) RMS error
RANGE	25.0 ft
AZIMUTH	0.003°
ELEVATION	0.005°

NOTE: Values include refractive uncertainties.

The assumption is made here that the bias errors, or systematic errors, have been removed; therefore, only the uncertainty in the bias estimate remains to contribute to the total RMS error.

Estimates taken from Aircraft Test General Electric 1504, dated 19 January 1961.

TABLE 6.2-2 ESTIMATE OF PROBABLE INSTRUMENTATION RMS ERRORS, MOD III SYSTEM 1

FUNCTION	ϕ = 0.7° (or above) RMS error
RANGE	20.0 ft
AZIMUTH	0.002°
ELEVATION	0.003°

NOTE: The above figures could be improved by using integrated rate data to replace the position data.

Estimates taken from Aircraft Test General Electric 1504, dated 19 January 1961.

Accelerometer and Keplerian ellipse comparisons have yielded useful estimates of low frequency random noise errors in the lateral rate velocity measurements. The low frequency noise is probably of atmospheric origin and is caused by inhomogeneities of the troposphere, i.e., wave front shimmer caused by varying index of refraction*. This effect is characteristic of radio tracking interferometer systems and is a ~~direct~~ function of baseline length. It would be a critical limitation in shorter baseline interferometer systems. The low frequency

* Reference, Low Frequency Noise in Range Instrumentation Systems, R. A. Bain, Nov. 1960, STL-TM60-0000-19102 (Conf.)

noise is the most serious factor in the degradation of lateral rate data. Because of the geometric dilution of precision (GDOP) introduced by the transformation to a Cartesian coordinate set, the sensitivity to low frequency noise on P-dot and Q-dot tends to degrade the quality of the transformed data. For an instrumentation function, this effect is a limitation of the present Mod III system; however it should be emphasized that this is not an equipment malfunction nor does it seriously compromise the missile guidance function for which the Mod III was originally designed.

Table 6.2-3 gives a summary of current estimates of various lateral rate errors. Real-time and post-flight data processing effects are considered. These estimates of lateral rate errors were summarized from past Series C and D missile flight tests.

TABLE 6.2-3 ESTIMATES OF LATERAL RATE ERROR, MOD III SYSTEM 1

ERROR	P-DOT (ft/sec)	Q-DOT (ft/sec)	PERIOD	REAL-TIME EFFECTS	POST-FLIGHT EFFECTS	HOW DETERMINED	COMMENTS
Systematic Bias Error	-0.0014	-0.0014	Long Term	Currently not removed during real-time guidance or IIP.	Removed during post-flight processing.	Hyperbolic track to rate self-consistency during actual missile flights.	A very long term systematic bias error consistently observed on each AMR Atlas C, D, and E series missile flight tests. Seems to be characteristic of Mod III System I rate subsystem. Number shown is mean of past D series tests. An improved error model is under investigation.
Uncertainty in Systematic Error	±0.0003	±0.0003	Long Term	Cannot be removed.	Cannot be removed.	One sigma standard deviation of systematic error observed during D series flights.	One sigma of above mean.
High Frequency Random Errors	±0.0009 (2PPS) Data ±0.003 (10PPS) Data	±0.0009 (2PPS) Data ±0.003 (10PPS) Data	8 seconds or less	Nearly 50% removed in Burroughs computer smoothing (guidance).	Up to 80% removed during data processing (instrumentation).	Standard deviation of residuals between smoothed and raw data.	Average noise merit figure observed on D series flights between BCO and VCO.
Low Frequency Random Errors	±0.0010 to ±0.0016	±0.009 to ±0.0013	10 seconds or more	Cannot be removed.	Cannot be removed.	Estimated from GE/ARMA P and Q comparisons; also free flight comparisons.	Due to atmospheric inhomogeneities; serious limitations in short baseline interferometer system (see text).
Total Real Time RMS	±0.0018 to ±0.0022	±0.0018 to ±0.0020	NA	Measurement uncertainty as "seen" by Burroughs computer.	Can be significantly reduced during data processing.	RMS sum of random and systematic errors.	None.
Total RMS Post-Flight Data Processing	±0.0010 to ±0.0016	±0.0009 to ±0.0013	NA	Not available as real-time capability.	Measurement uncertainty in post-flight best estimate trajectory data supplied to various contractors.	All systematic and random error removed during data processing except low frequency noise.	Measurement accuracy limited by atmospheric effect direct function of baseline length.

The estimate of probable rms error in range rate amounts to 0.1 ft/sec. This includes random and systematic errors.

Noise merit figures are tabulated for each missile test. Standard deviations between raw and smoothed data were examined in exactly the same manner for each test, and in this way a consistent noise figure characteristic for the flight is determined. Noise merit figures are estimated by averaging the standard deviations during the period between BCO and nosecone separation. Excessive tracking noise during launch is not considered, nor are isolated noise bursts which occur at BCO and SCO. An average of noise standard deviations for Series D 2/pps data is shown in Table 6.2-4. The data was smoothed using a 67-point weighted numerical filter with a 0.25 cps cutoff frequency and zero velocity, acceleration and jerk error coefficients

TABLE 6.2-4 AVERAGE OF NOISE STANDARD DEVIATION, SERIES D 2 PPS DATA

Range (feet)	8.0
Azimuth (deg)	0.002
Elevation (deg)	0.002
Range Rate (ft/sec)	0.08
Pitch Rate (ft/sec)	0.0009
Yaw Rate (ft/sec)	0.0009

During the period covered by this report, the GE Mod III, System 1 radar participated in 15 R&D flight tests of the Atlas D Series missile. Eight of the 15 missiles utilized the radio command guidance provided by the Mod III system, while the remaining 7 missiles carried the all-inertial guidance system. The Mod III system provided range safety and instrumentation data on the AIG flights.

Table 6.2-5 presents the Mod III impact data for the eight successful missiles with radio command guidance. The Mod III impact data for the six successful AIG missiles are listed in Table 6.2-6.

TABLE 6.2-5 MOD III GUIDANCE SYSTEM IMPACT DATA, SERIES D RIG FLIGHTS

MISSILE	GE/SYRACUSE (1) MOD III	GE/SYRACUSE (1) MOD I	BURROUGHS COMPUTER (2) MOD III	BURROUGHS COMPUTER (2) MOD I
56D	40.9445 S	40.9885 S	40.9319 S	40.9997 S
	37.9814 E	37.9826 E	37.9752 E	37.9802 E
	0.81 LEFT	0.98 LEFT	1.11 LEFT	1.18 LEFT
	2.74 SHORT	0.66 SHORT	3.37 SHORT	0.15 SHORT
62D	8.2219 S	8.2159 S	8.2351 S	8.2355 S
	14.5128 W	14.5105 W	14.4941 W	14.4992 W
	0.15 LEFT	0.51 LEFT	0.20 LEFT	0.12 LEFT
	16.33 LONG	16.25 LONG	17.90 LONG	17.59 LONG
27D	8.0690 S	8.0611 S	8.0733 S	8.0813 S
	14.7519 W	14.7499 W	14.7537 W	14.7295 W
	0.11 LEFT	0.57 LEFT	0.15 RIGHT	0.26 LEFT
	0.56 SHORT	0.72 SHORT	0.54 SHORT	0.94 LONG
32D	33.5124 S	33.4982 S	33.5048 S	33.5000 S
	10.3553 E	10.3542 E	10.3327 E	10.3911 E
	0.23 LEFT	0.99 LEFT	0.16 LEFT	1.62 LEFT
	2.38 LONG	1.99 LONG	1.16 LONG	3.87 LONG
79D	38.5071 S	38.4950 S	38.5108 S	38.4987 S
	41.0290 E	41.0614 E	40.9878 E	41.0808 E
	0.28 RIGHT	0.61 LEFT	0.70 RIGHT	0.42 LEFT
	1.40 LONG	2.84 LONG	0.55 SHORT	3.85 LONG
55D	33.5111 S	33.4876 S	33.5003 S	33.4837 S
	10.3641 E	10.3303 E	10.3237 E	10.3237 E
	0.47 LEFT	1.09 LEFT	0.24 LEFT	1.20 LEFT
	2.75 LONG	0.63 LONG	0.67 LONG	0.41 LONG
83D	8.0777 S	8.0908 S	8.0842 S	8.0767 S
	14.7493 W	14.7165 W	14.7495 W	14.7395 W
	0.21 RIGHT	0.19 LEFT	0.55 RIGHT	0.15 LEFT
	0.16 SHORT	1.90 LONG	0.03 LONG	0.28 LONG
90D	8.2000 S	8.2074 S	8.2062 S	8.1973 S
	14.7028 W	14.6885 W	14.7077 W	14.7090 W
	0.94 RIGHT	0.01 RIGHT	0.58 RIGHT	0.17 RIGHT
	0.14 SHORT	0.81 LONG	0.19 SHORT	0.56 SHORT

NOTES: (1) Post-flight trajectory intregration. (2) Real time impact prediction.

The ability of a missile system to impact at a desired target is commonly measured in terms of a statistical quantity designated Circular Error Probability (CEP). The CEP is defined as the radius of a circle, centered at the target, within which the re-entry vehicle will impact with 50 percent probability.

TABLE 6.2-6 MOD III GUIDANCE SYSTEM IMPACT DATA, SERIES D AIG FLIGHTS

MISSILE	GE/SYRACUSE (1)	BURROUGHS COMPUTER (2)
42D	2.0068 S	1.9900 S
	10.8233 W	10.8433 W
	17.76 LEFT	19.11 LEFT
	1.40 LONG	0.45 LONG
54D	1.3921 S	1.3849 S
	12.1908 W	12.1808 W
	0.93 RIGHT	0.51 RIGHT
	1.20 SHORT	0.68 SHORT
60D	1.0676 S	1.1102 S
	12.7979 W	12.7850 W
	2.88 RIGHT	4.69 RIGHT
	42.24 SHORT	40.28 SHORT
66D	8.1521 S	8.1470 S
	14.7387 W	14.7537 W
	1.38 LEFT	1.18 LEFT
	2.74 LONG	1.81 LONG
71D	8.1300 S	8.1255 S
	14.7803 W	14.7885 W
	0.95 LEFT	1.10 LEFT
	0.06 SHORT	0.61 SHORT
76D	8.2211 S	8.2236 S
	14.7713 W	14.7703 W
	3.14 RIGHT	3.18 RIGHT
	3.36 LONG	3.40 LONG

NOTES:
(1) Post-flight trajectory integration.
(2) Real time impact prediction.

Utilizing MILS post analysis data from eight Series D missiles, including previous tests not subject to this report, the Atlas total weapon system CEP was computed.

Weapon System CEP (4,400 NM Range) = 0.58 NM

Only RIG missiles that successfully impacted within the MILS hydrophone pentagon (11D, 14D, 18D, 22D, 31D, 44D, 27D and 83D) were considered in the above calculation. The equation used for the CEP calculations is:

$$CEP = 0.588 \left[\sqrt{\frac{\Sigma (CM)^2}{N-1}} + \sqrt{\frac{\Sigma (DM)^2}{N-1}} \right] \quad (1)$$

where:

CM = Crossrange miss of MILS results from target
DM = Downrange miss of MILS from target
N = Number of missiles.

The weapon system CEP is indicative of the accuracy of the Atlas missile with Mod III radio inertial guidance for 4,400 nautical mile targets, and includes all weapon system errors, i.e., nosecone dispersion, model errors, targeting errors, measurement or tracking errors, etc.

On Atlas AIG flights where the Mod III system is used in an instrumentation capacity, two impact points are computed - namely, a Quick-Look impact from the outputs of the Burroughs computer and a GE/Syracuse Trajectory Integration impact point.

In order to demonstrate the impact prediction capabilities of the Mod III system, two CEP's have been determined using the Quick-Look and GE/Syracuse impact data. These CEP circles are centered on the MILS post analysis impact point and indicate that the two Mod III impact points will lie within these circles with 50 percent probability.

Quick-Look Impact Prediction CEP = 0.62 NM
GE/Syracuse Impact Prediction CEP = 0.41 NM

The above calculations were made from data collected on six Series D missiles that impacted in the MILS pentagon, namely 18D, 22D, 31D, 44D, 27D, and 83D. All six missiles carried ablating nosecones. The same equation was used for IP CEP calculations as was used for the calculation of the Weapon System CEP.

During the Series D/RIG test program, special investigations were performed to evaluate acquisition and memory performance and ripple-fire capability. The results of these tests are documented in GE Report Number SE-ER-91, "R&D Final Evaluation Report of the Mod III Radio Guidance System on WS107A-1 Test Program", dated 30 September 1960.

Recent tests (1) in the Mod III rate subsystem have confirmed the presence of a systematic bias error in the lateral rate functions, P-dot and Q-dot. As a result of these tests and an analysis (2) of the rate loops, a new error model has been developed which results in a significant improvement in the instrumentation data supplied to associate contractors.

Reference: (1) Informal Communications, D. Bissell, GE/AMR, March 1961.

(2) An explanation of the observed bias error in the WS107A-1 rate system, 31 March 1961, Report Number SE-ER-103, E. R. Schulz, Range Systems Analysis, MSS/DSD, General Electric Company.

Transformation effects are especially critical in the period after SCO. The GE-to-Arma coordinate transformation is especially sensitive to P-dot and to a lesser degree, Q-dot. On a long range flight the transformation (GDOP) effects are more severe than those experienced on the MILS net targeted AIG Atlas missiles. Any random or systematic errors associated with these functions result in transient discrepancies in the GE/Arma comparisons. An unexplained bias error was observed in the GE/Arma comparisons starting at SCO and continuing through the vernier and free-flight phase until lock was lost with the missile. The magnitude of this error was about 10 ft/sec in Arma's Z-dot depending on transformation sensitivity. The bias error seemed to be a constant step velocity error starting at SCO. Besides the GE/Arma comparisons, a similar velocity error was observed in GE/free-flight comparisons. As the vernier and free-flight phase is of special interest in inertial guidance analysis, the bias errors in the GE instrumentation data were very disturbing. In an effort to improve the quality of the GE Mod III instrumentation data a series of tests were conducted at AMR to determine if any errors existed in the rate data.

For the past year a consistent and repeatable systematic bias error in P-dot and Q-dot has been observed in all Atlas and Titan flights in which the Mod III system participated. This was detected by means of the hyperbolic self-consistency check. This is a comparison of the track and integrated rate data in rate's hyperbolic coordinate set. This comparison results in a series of P and Q residuals (Note: Not P-dot or Q-dot residuals) with respect to time. Plots were published in each missile report showing this check. The long term slope of these residuals is a velocity error and has been commonly referred to as the lateral rate bias error. At least 150 seconds of data (usually between BCO and SCO) was necessary to calculate a slope. The velocity errors so detected were -0.0014 ± 0.0003 ft/sec (one sigma). As the period between SCO and VCO was only 20 seconds or so it was impossible to detect any velocity errors during this period. Consequently the nominal lateral rate bias of -0.0014 ft/sec was assumed to be in the P-dot and Q-dot data throughout the flight and the data was so corrected during Syracuse Data Processing. This was the crude error model used on all past missile flights including the AIG series. Furthermore, it was impossible to detect any velocity errors in comparisons with other range instrumentation systems. It has been only recently that such meaningful velocity comparisons as GE/Arma and GE/free-flight have been available. Prior to this the only means of checking the rate system was by self-consistency comparisons with the track position data. The self-consistency residuals told us little about velocity errors during the vernier or free-flight phase. Ballistic camera strobe data (position only) on missile flight tests was of little use for velocity comparisons. Ballistic camera data from aircraft tests when compared with integrated rates over long test runs of 200 seconds or more failed to reveal the bias errors observed during missile flights as determined from the track-to-rate self-consistency. Systematic bias errors observed during ballistic camera aircraft tests were usually about -0.0005 ft/sec for outbound runs and close to zero on incoming runs. Of course, the aircraft never approached $\dot{R}$ accelerations typical of missile flight tests.

The hyperbolic self-consistency residuals have indicated a velocity error throughout the AMR missile test program. During this time it was annoying to observe such an error and not be able to explain it satisfactorily. Thus, this is the status of the lateral rate bias problem up to March 1961. The AMR Mod III test results opened the door to a satisfactory explanation and correction of this error.

Briefly, the test set up at GE/AMR simulated a missile ($\dot{R}$) velocity of up to 25,000 ft/sec and $\dot{R}$ accelerations of about 200 ft/sec. This was done by a precision motor driven variable frequency oscillator used to simulate increasing and decreasing $\dot{R}$. By injecting this signal in the lateral rate loops and establishing a RF link between the P/Q pads and the central rate station, $\dot{R}$ and $\ddot{R}$'s were simulated while true P-dot and Q-dot were zero.

Lateral rate errors were then determined by measuring P-dot and Q-dot digital data. This was then plotted as a function of time and compared with the simulated R-dot. This conclusively showed that the lateral rates did experience a systematic error as a function of $\ddot{R}$. From this an estimate of delays in the local oscillator waveguide could be established. The time delay so measured showed very close agreement with theoretical calculations of the LO waveguide run. The waveguide itself, runs between the central station and the out-lying pads. The LO + delta f from the central station are transmitted down the waveguide where mixing occurs at the P or Q station.

From analytical investigations of the lateral rate phase lock loops an expression for the lateral rate acceleration correction term was derived as follows:

$$\text{Delta } \dot{P} = \frac{2\ddot{R}}{C}(P + Tx).$$

A similar expression for Q-dot correction also applies. Tx is determined experimentally from the above tests.

This correction was then applied to several recent AIG missile test data and the resulting GE trajectory compared with Arma data. It was interesting to note that the large velocity error, especially in Z-dot after SCO, had been removed. Residuals after SCO were more consistent with data trends prior to this discontinuity. As $\ddot{R}$ is close to zero and may even be slightly negative during vernier or free-flight, the bias correction would be very small. Previously, a correction of + 0.0014 ft/sec had been applied during this phase. Consequently, the P-dot and Q-dot data was being over corrected by about 0.0014 ft/second. This resulted in the large Arma and free-flight residuals observed after SCO. The use of the new error model as a function of $\ddot{R}$ will remove this difficulty.

The investigation of the velocity errors is continuing and modifications to the error model will be made as required. It is important to understand what effect the lateral rate acceleration correction has on the missile test program. Its effect is insignificant during real-time guidance or impact prediction. This is because the nominal 0.0014 ft/sec correction was not used in the real-time Burroughs computer. So, over correction during the vernier phase was not done. As $\ddot{R}$ is close to zero during the vernier phase, so the acceleration error is very small. Post flight instrumentation will be effected. Prior to the acceleration correction the data was being over corrected during the vernier phase. The new error model will eliminate this.

SUPPLEMENTAL INFORMATION

The test results considered in this section are based upon data obtained from the Mod III Radio Inertial Guidance, Mod I Downrange Impact Predictor and Mod III-E Instrumentation Beacon Systems. This analysis was performed by Astronautics to obtain a characteristic signal strength curve for both the airborne pulse beacon and rate beacon in each system.

The data were averaged together by system to show the typical general trend of the signal strengths obtained on the Atlas missile receivers. The maximum and minimum signals for each measurement were time correlated to give a better indication of the total dispersion from an average mean signal. During the first stage of Atlas powered flight, when the maximum signal attenuation occurs, the best correlation between signal strength and trajectory was found to occur just prior to booster cutoff.

There was no evidence of signal strength loss due to malfunctions of the airborne beacon units and associated missile equipment. System operation was generally normal during the entire flight. Both received and transmitted signal levels of the pulse and rate beacons were strong and steady throughout powered flight, with only the usual signal fluctuations at liftoff, during early part of booster phase, and at booster jettison. Some fluctuations and dropout of signal levels also occurred beyond missile powered flight due to loss of missile stability at this time.

On three AIG missiles (54D, 60D and 76D) unusual track and rate beacon signal disturbances were encountered; these disturbances did not occur on later tests. Studies into the possible causes of these disturbances were centered about the AIG airborne boom mounted antenna and waveguide installation. Corrections were made for discrepancies noted during the study which provided a subsequent trouble-free flight on Missile 71D.

Guidance System Mod III

The agc signal strengths associated with the Number 1 and Number 2 guidance rate beacons and the guidance pulse beacon are shown in Figure 6.2-1 as a function of time and slant range. These signal strengths showed adequate values for the reception of discrete and steering commands on each radio-inertially guided flight.

The adequacy of these signals gave good results of position and velocity on the ground, thus obtaining a final impact prediction of the re-entry vehicle during the freefall period.

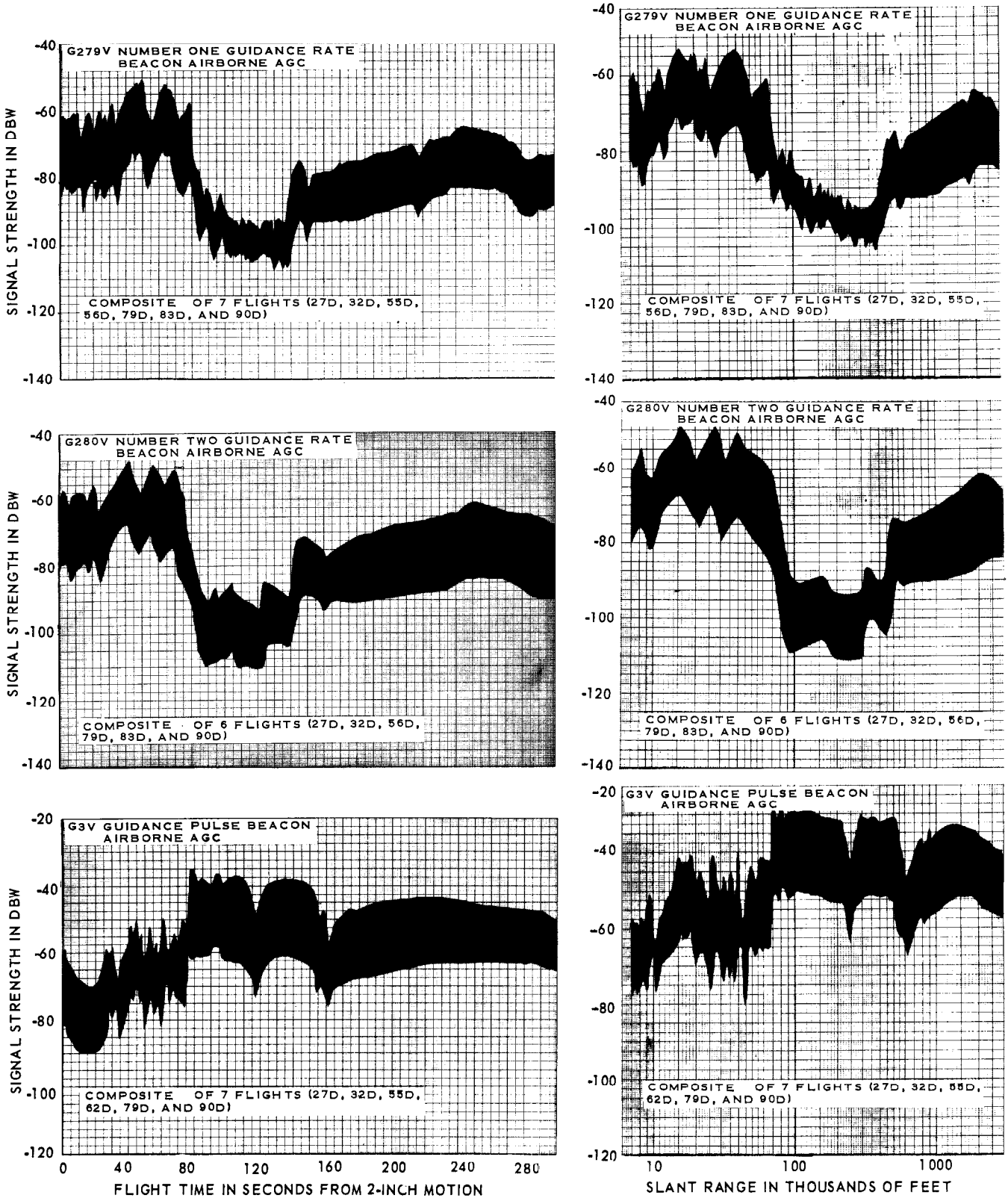

FIGURE 6.2-1 GUIDANCE SYSTEM SIGNAL STRENGTH

The data shows that no excessive dropouts of signals occurred during the guided portion of powered flight (from BECO to VECO). Small signal dropout due to wave attenuation, as on earlier Series C and D Atlas flights, was recorded during the first stage of powered flight (from launch to BECO).

Impact Predictor Mod I

The rate beacon and pulse beacon agc signal strengths are shown in Figure 6.2-2 as a function of time. Figure 6.2-3 shows the geometrical relationship of the San Salvador transmitter station and missile trajectory. As noted on the signal strength plots, there were no signals received until the San Salvador station acquired the missile, which took place at approximately 104 seconds for the rate beacon and 116 seconds for the pulse beacon (from a two-inch motion time reference).

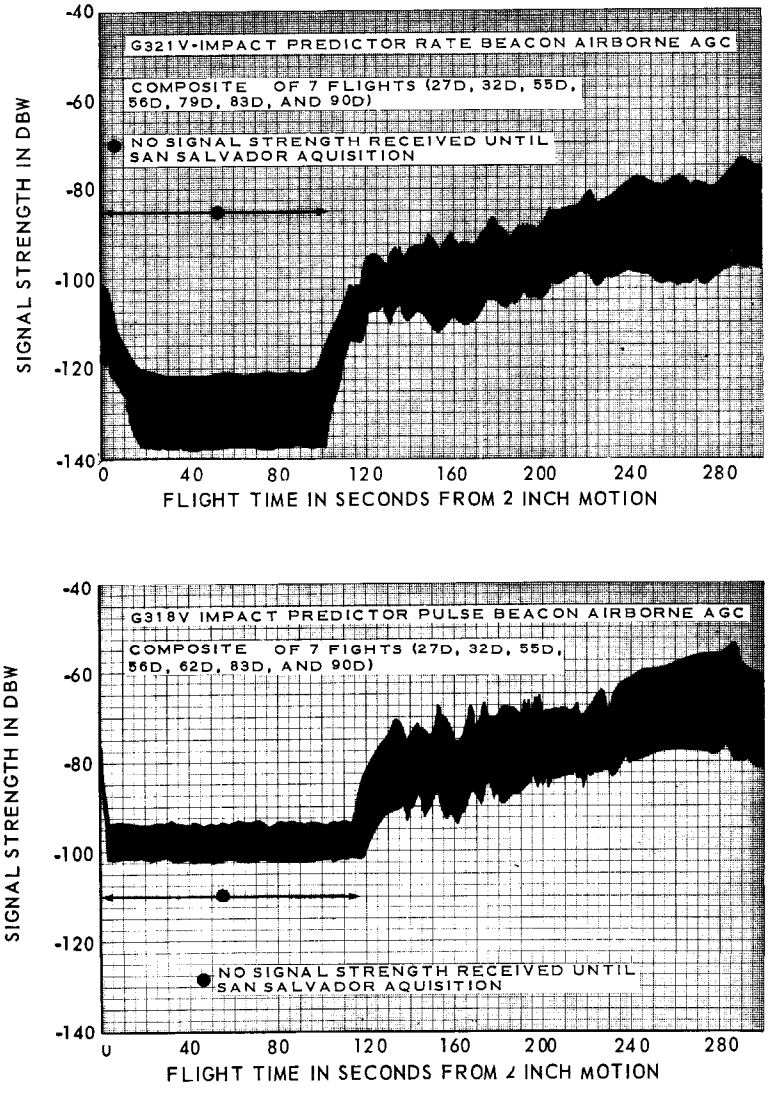

FIGURE 6.2-2 IMPACT PREDICTOR AIRBORNE SIGNAL STRENGTH

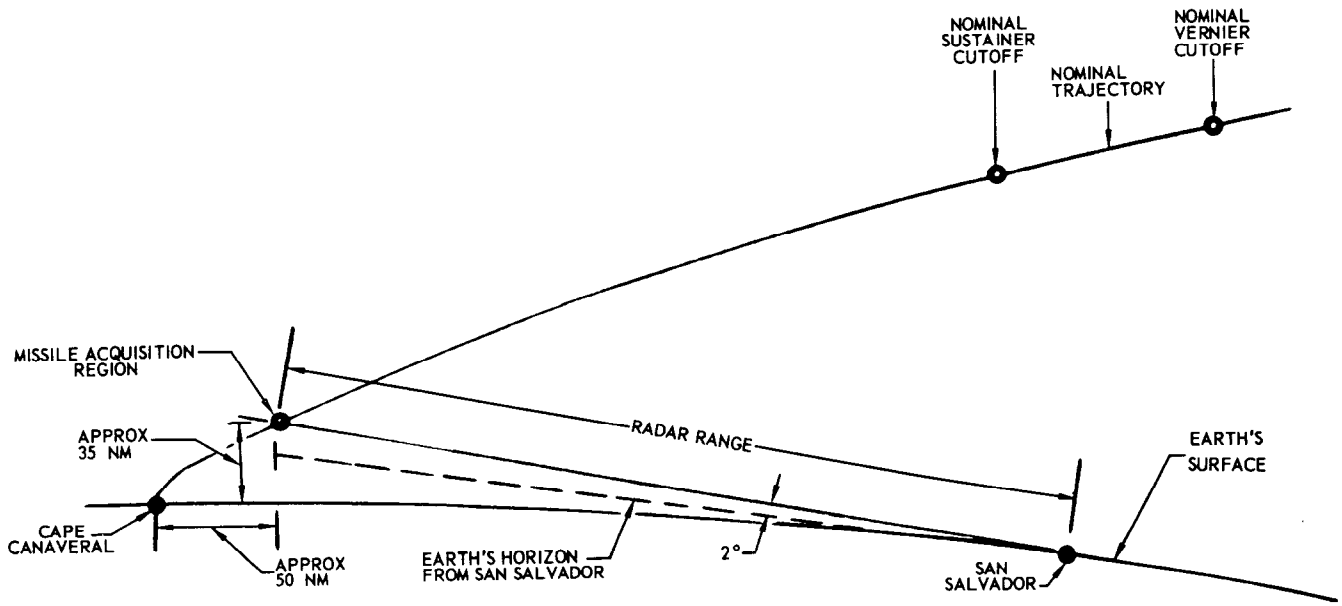

FIGURE 6.2-3 MISSILE AQUISITION FROM SAN SALVADOR

The adequacy of these signals presented satisfactory information to determine the position and velocity of the missile during second stage and the freefall periods. These periods are needed to obtain a final accurate impact prediction of the re-entry vehicle during freefall and to receive real time missile position and velocity data for range safety purposes during the second stage of powered flight.

Instrumentation Beacon Mod III-E

This system is used in place of the Mod I system on the AIG flights. The rate and pulse beacon agc signal strengths are seen in Figure 6.2-4 as a function of time and slant range.

These signal strengths showed adequate results in obtaining data during second stage and freefall periods. No extensive dropouts of signal strength occurred at these times.

Since this instrumentation beacon operated as a tracking system for position and velocity, it provided accurate data to compare with the all-inertial guidance system.

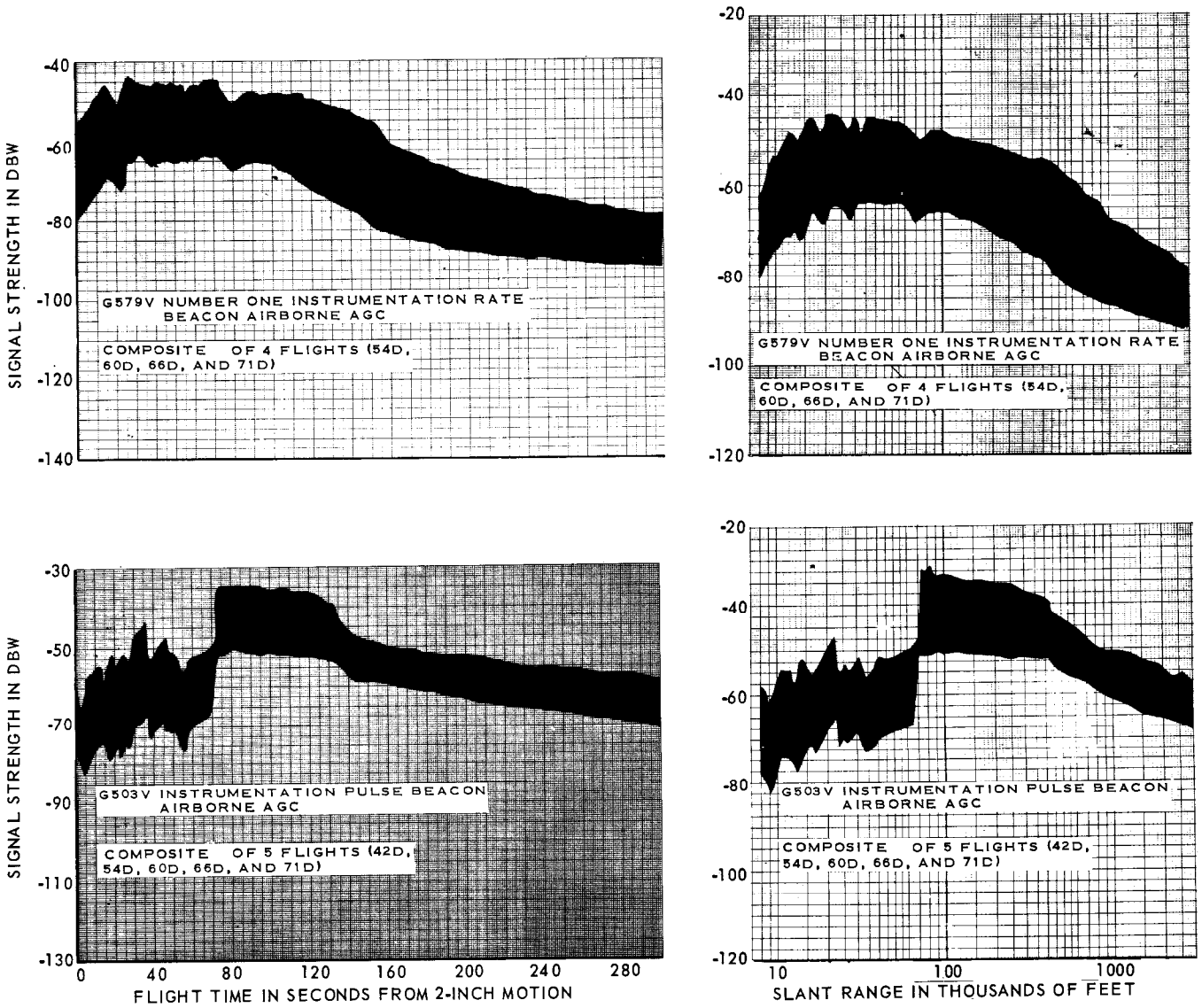

FIGURE 6.2-4 INSTRUMENTATION BEACON MOD II-E AIRBORNE SIGNAL STRENGTH

The Arma Division, American Bosch Arma Corporation, Garden City, New York, has prepared and published summary report DAG 7479 "Arma Inertial Guidance System, Atlas Series D Missile Flight Tests" in accordance with Contract No. AF04(645)-21. This report is available from Arma. The following is an abstract of its contents.

Complete compatibility of the inertial guidance system with all associated airborne systems, and with the entire 107A-1 Weapon System, was clearly demonstrated. All guidance missile control functions were properly executed. Roll guidance commands performed either as corrections to the flight programmer roll program or to generate the entire roll program (as on Missiles 71D and 76D), were executed smoothly and accurately. Pitch control, assumed by the guidance system after staging, was executed in a minimum of time, and maintained the missile in the correct pitch orientation with excellent stability throughtout powered flight. Yaw steering, derived from the missile guidance digital computer, was effected properly with stability in every case, verifying the capability of digital computer control of an analog missile steering loop. Inertial guidance system and missile compatibilty was also demonstrated by correct response to all computer discretes generated to effect shutdown of the various engines during flight.

A high degree of accuracy was demonstrated on the D/AIG flights. Based on four flights for which the Circular Probable Error (CEP) could properly be determined (54D, 66D, 71D and 76D), the IGS showed a guidance accuracy of 2.0 nautical miles CEP. Based on other techniques to include the other two flights, average radial error was determined to be 1.7 nautical miles. These numbers include certain errors in the radar tracking system since external data were used to determine the IGS miss. The detailed results also served to verify the adequacy of the basic design of the IGS as well as to demonstrate its inherent and ultimate capabilities.

The reliability of the inertial guidance system was clearly demonstrated. There were no in-flight failures of the IGS during any of the flight tests. On Missile 60D, however, the computer output digital data indicated a circuit in the Z channel of the computer was inoperative. This resulted in an error in the value of the Range Error Function (REF) calculated by the computer, and a small error in the yaw steering signal. Analysis of flight test data indicated the circuit probably had failed before launch. At the time of this flight, pre-launch computer checks would not have detected this failure. To prevent recurrence of this situation on future flights, a new test problem, which included exercising of this circuit, was included in subsequent field test procedures. No other flight tested guidance computer exhibited this type of malfunction.

In other areas, the D/AIG flight tests demonstrated the high reliability of the guidance flight test instrumentation. Virtually complete data were obtained on all flights through the analog signal converter (ASC) and the digital signal converter (DSC). Not a single failure of the DSC was experienced. There were, however, some ASC malfunctions. These had no adverse effect on MGS flight evaluation since the analog signals affected were of secondary importance and used primarily for backup information.

The compatibility of the IGS with ground operations was demonstrated by these tests. The adequacy of the basic countdown procedure for IGS tests was confirmed. No significant flight delays attributable to the IGS, ground equipment, or procedures were encountered.

This page intentionally left blank.

SECTION 7. SUPPORTING SYSTEMS

SECTION 7.1 - HYDRAULIC SYSTEM

PURPOSE OF TESTING

The primary area of interest for the testing conducted on the hydraulic system during this portion of Series D flight testing was concerned with both evaluation of the basic system design and of any modifications leading toward the development of a more reliable system. Of significance was the continued evaluation of the 25 cubic-inch vernier solo accumulator system. This system replaced the GN_2 powered vernier solo hydraulic power supply unit (VSHPS) primarily used during the first portion of the Series D flight test program.

Specific hydraulic system requirements during the portion of Series D flight tests reported here are listed in Section 2 under Test Objectives.

TEST CONDITIONS

The hydraulic system configuration utilized during this phase of the Series D flight test program was the standard Series D installation as illustrated in Figure 7.1-1. The only significant modification of the system was the incorporation of a 25 cubic-inch accumulator to supply hydraulic fluid for the nominal 20-second vernier solo period. This change in design represents a considerable savings in weight as compared to the previously used VSHPS system.

~~SECRET~~

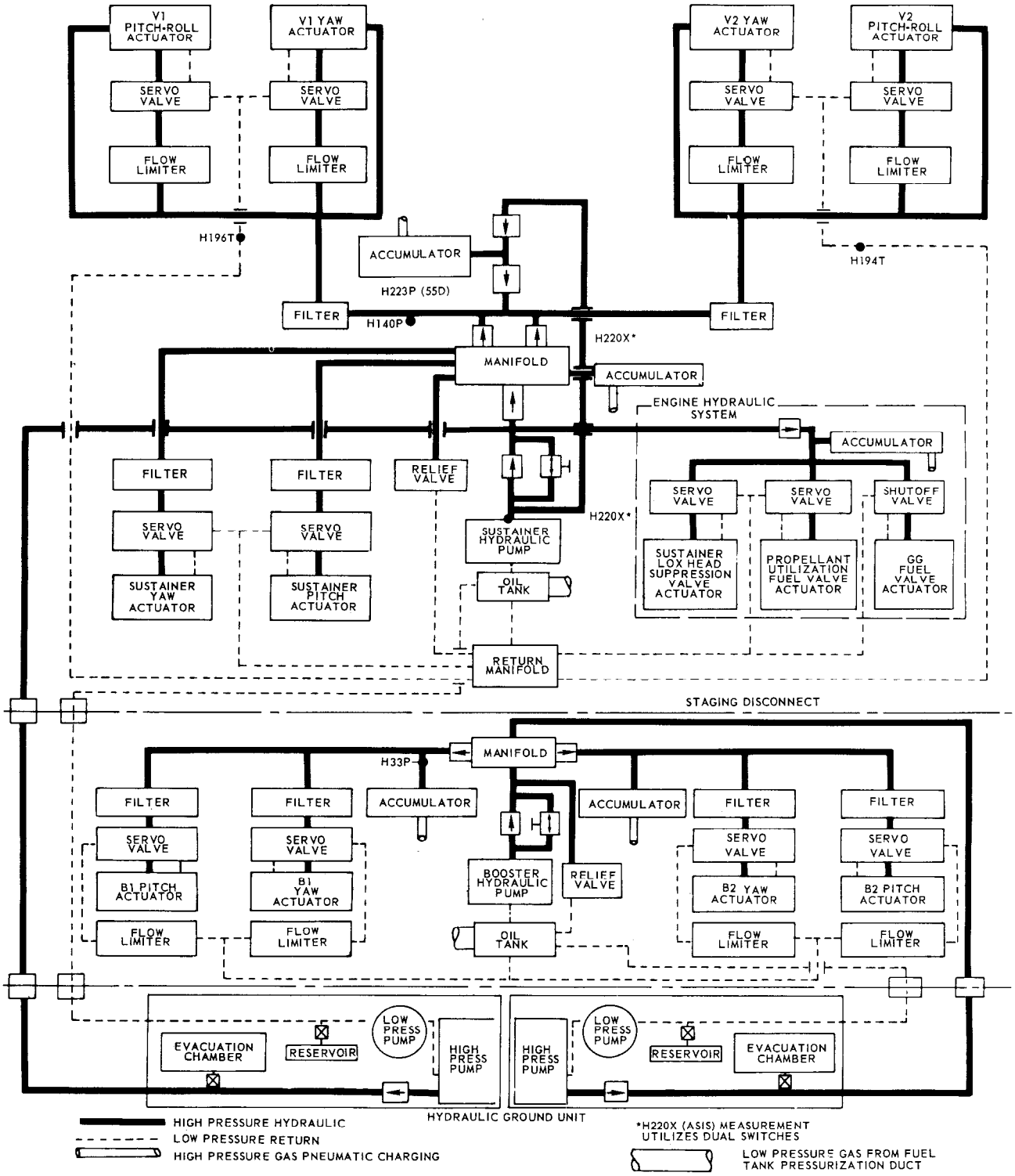

FIGURE 7.1-1 HYDRAULIC SYSTEM, SERIES D

~~SECRET~~

TEST RESULTS

Performance of the hydraulic system during this phase of Series D flight testing was as required. (Reference Table 7.1-1) With the exception of Missile 42D, hydraulic system operation was without incident. During this flight, the sustainer/vernier hydraulic supply pressure dropped from a steady-state value of 3,100 psig to 280 psig within 3.5 seconds after sustainer engine cutoff. As the pressure did not recover during the vernier solo phase, missile attitude control was lost. This anomaly will be discussed in detail in the problem areas section of this analysis.

Booster System Operation

Booster hydraulic system performance was satisfactory. Ground supplied power was maintained at an average of 1,916 psig (nominal 2,000 psig) by the hydraulic pumping unit (HPU). During pre-launch operations on Missile 71D a ground supplied pressure of 2,860 psig was indicated. This reading was considered to be in error, as the HPU pressure switch data confirmed that, prior to engine ignition, hydraulic pressure had been less than 2,500 psig. Switchover from ground to airborne hydraulic supply for the booster system was adequate, requiring an average time of 0.7 seconds (Reference Figure 7.1-2). Steady-state airborne pressures averaged 3,090 psig.

Sustainer System Operation

Sustainer hydraulic system performance was satisfactory. Ground supplied hydraulic pressure averaged 1,993 psig as compared to a nominal 2,000 psig. Switchover from ground to airborne hydraulic power required between 0.3 and 0.7 seconds longer for the sustainer system than for the booster system (Reference Figure 7.1-2). Airborne steady-state pressures were maintained at an average of 3,070 psig.

TABLE 7.1-1 SUMMARY OF HYDRAULIC SYSTEM PERFORMANCE

MISSILE NO.	DATE	ENGINE CUTOFF TIME SECONDS FROM 2-INCH MOTION BOOSTER	SUSTAINER	VERNIER	BOOSTER SYSTEM PRESSURE (psig) GROUND SUPPLY	STEADY STATE	SUSTAINER SYSTEM PRESSURE (psig) GROUND SUPPLY	STEADY STATE	VERNIER SOLO PERFORMANCE PRECHARGE GN_2 (psig)	OPERATION FROM SCO (seconds)	BOTTOM PRESSURE (psig)	TEST RESULTS	COMMENTS
42D	2/8/60	141.25	256.83	269.17	1930	2850	1945	3115	1000			Booster system performance was satisfactory. Sustainer/vernier system operation was satisfactory until SCO, at which time vernier solo stage pressure started to decay reaching 280 psig within 3.5 seconds. Pressure did not recover and as a result missile attitude control was lost. An ambient temperature of 400°F was noted in the engine compartment coincident with an unusual pressure transient in the S/V system at 97.2 seconds. Impact was within one mile of the target.	Supporting tests established loss of the GN_2 charge line which supplies pressure to the verniers solo accumulator. This failure was partially due to the excessive engine compartment temperature.
47D	4/7/60											Hydraulic system performance was satisfactory prior to missile destruction at 1.8 seconds. This was the last Series D R&D flight vehicle to utilize the VSHPS which, due to the premature cutoff, was not activated.	
56D	5/20/60	136.58	271.08	284.89	2000	3170	2190	3080	1000	26.7	560	System performance was satisfactory. However, the normal pressure surges at fluid evacuation (X-30 seconds) appeared heavily damped on both the flight and previous flight attempt. No explanation is apparent.	Status of the HPU will be varied earlier in the countdown on future launches.
54D	6/11/60	137.62	235.55	242.79	1960	3150	2030	3080	1000	20.0	630	Satisfactory	
62D	6/22/60	147.77	284.26	307.69	1850	3175	1860	3080	1000	26.6	788	Hydraulic system performance was adequate. The ASIS switch in the sustainer hydraulic manifold failed to indicate sustainer cutoff.	The hydraulic sensing line was blocked by frozen fluid due to metal-to-metal contact with the lox sensing line to P30P. The lines were re-oriented on subsequent flights.
27D	6/27/60	131.93	278.68	294.03	1940	3110	2085	3080	1000	33	683	Satisfactory	
60D	7/2/60	141.03	307.55	277.45	1965	3105	1925	3005	1000	20	740	Satisfactory	
32D	8/9/60	131.56	288.10	301.89	1835	3010	2040	3010	1000	19.4	796	Satisfactory	
66D	8/12/60	136.45	259.24	274.43	1935	3070	1980	3010	1000	17.4	770	Satisfactory	
76D	9/16/60	138.59	274.92	290.68	1930	3105	2015	3080	1000	22.9	735	Satisfactory	
79D	9/19/60	138.59	282.44	295.12	1875	3185	1855	3060	1000	37.1	720	Satisfactory	
71D	10/3/60	140.0	267.38	280.67	2860	3125	1995	3100	1000	25.7	735	Performance was satisfactory, although a ground system pressure of 2860 psig was indicated. The data was considered invalid and incompatible with other data.	Prelaunch test records confirmed the 2,000 psig nominal setting of the HPU pressure compensator. No action was required.
55D	10/22/60	135.86	283.04	298.13	1860	3090	1820	3118	1000	42.6	665	Satisfactory	
83D	11/15/60	137.77	269.93	286.23	1865	3055	2015	3140	1000	32.3	560	Satisfactory	
90D	1/23/61	137.66	271.93	288.77	1835	3100	2050	3065	1000	21.3	718	Satisfactory	
				AVERAGE	1915	3090	1990	3070		25.7	698		

Vernier System Operation

With the exception of 42D, performance of the vernier solo accumulator system was satisfactory. Adequate hydraulic pressure was provided above 680 psig as shown in Figure 7.1-2, for an average duration of 25.7 seconds (42.6 seconds during the flight of Missile 55D).

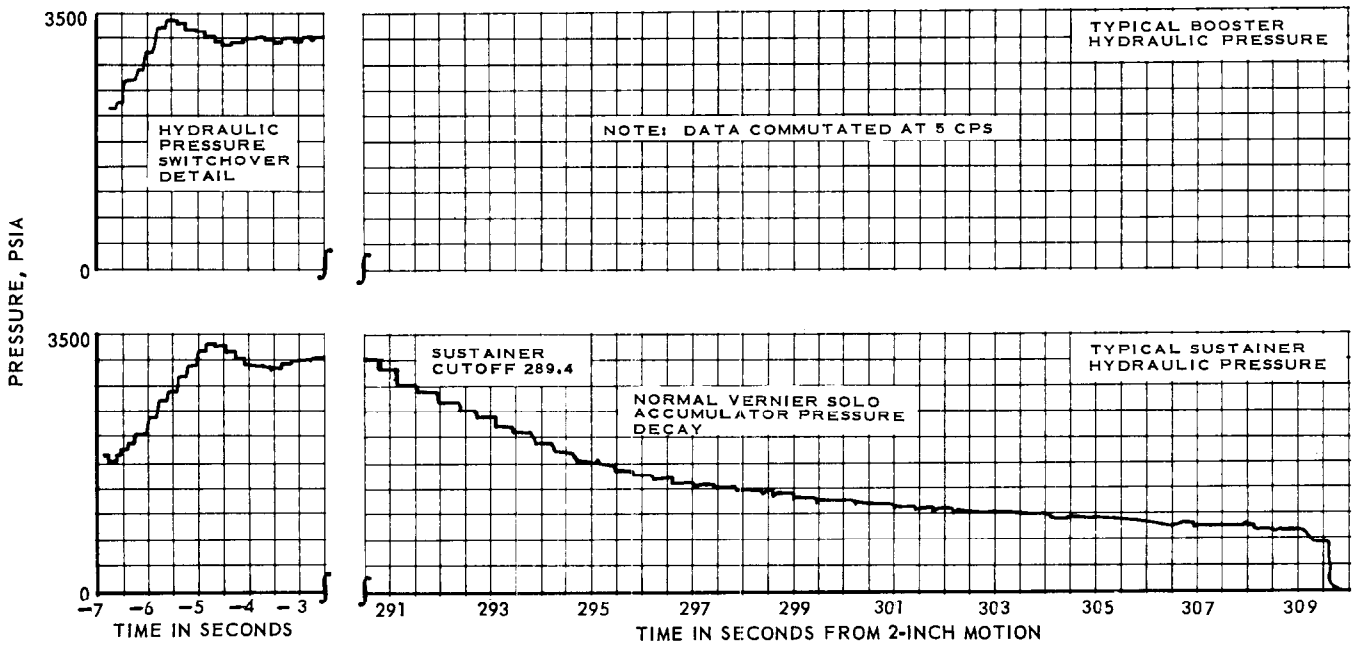

FIGURE 7.1-2 VERNIER SOLO HYDRAULIC ACCUMULATOR PRESSURE

The vernier solo accumulator installation, Figure 7.1-3, is now scheduled for all future flight missiles. Certain special space boosters will utilize a 50 cubic-inch capacity vernier solo accumulator unit (either two 25 cubic-inch units or one 50 cubic-inch unit) to provide additional vernier solo pressurization.

~~SECRET~~

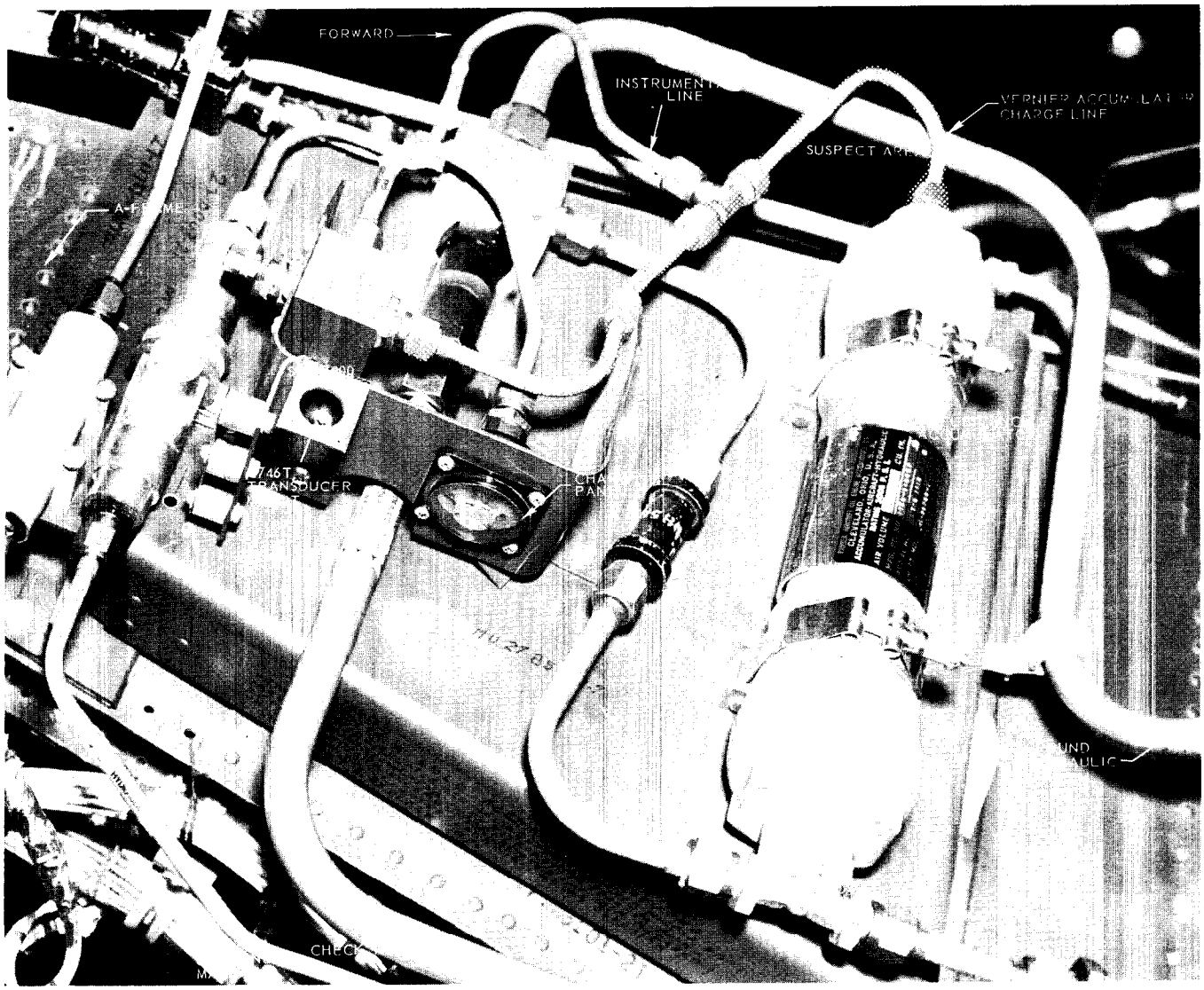

FIGURE 7.1-3 INSTALLATION OF THE VERNIER SOLO HYDRAULIC ACCUMULATOR

PROBLEM AREAS

The sharp decrease in sustainer/vernier supply pressure noted during the flight of Missile 42D, indicated a complete loss of vernier solo accumulator pressure at sustainer cutoff. Figure 7.1-3 shows a typical vernier solo hydraulic supply installation.

~~SECRET~~

The rate of pressure build-up at engine start indicated that the system was functioning properly. A short-duration heavy fluid demand period was indicated at 97.2 seconds by an unusual pressure transient of 300 psig. Subsequent investigation revealed that a pressure transient of this type could be closely simulated by abruptly venting the accumulator GN_2 charge line to atmosphere. It is therefore assumed that, at 97.2 seconds, the aluminum GN2 charge line (as shown in Figure 7.1-3) ruptured, venting the 3,000 psig GN2 pressure and causing subsequent loss of accumulator pressure.

The exact reason for this line failure is unknown, but several contributing factors have been isolated. One of these is the abnormal engine compartment temperature increase noted at 80 seconds during the Missile 42D flight. At the time of the assumed charging line failure, data indicated that the temperature in the vicinity of that line reached 370°F.

Laboratory tests were subsequently performed on the GN_2 charging line assembly. This type assembly was pressurized to 3,000 psig and subjected to temperatures between 400 and 600°F. Of the resultant failures, only one was similar in manner to that which is assumed to have occurred on Missile 42D. This failure occurred when an assembly was subjected to a 400°F environment for a period of 30 seconds. However, further investigation of the failed item revealed that a faulty connection between the charge line and the accumulator flared coupling had contributed to the failure. Other assemblies developed only minor leaks after being subjected to temperatures between 500 and 600°F for period of 1 to 3 minutes.

These results indicate that tube damage during production and/or installation deficiencies in combination with environmental conditions must be considered as probable causes of a failure of this nature.

The Series D internal safe release ladder circuitry required hydraulic pressures to exceed 2,500 psig prior to activation of the Main Engine Thrust Complete signal (P1627X). This requirement has not been met for the sustainer system on the vehicles utilizing the vernier solo accumulator system which requires an additional 18 cubic-inches of fluid at engine start. Refer to Table 7.1-2. The only consequence of this problem is a momentary (0.1 to 0.5 seconds in duration) no-go redlight indication on the TCC panel. This has not constituted a major problem particularly since the circuitry has been deleted on Series E missiles and other subsequent installations.

TABLE 7.1-2 HYDRAULIC SYSTEM HIGH PRESSURE SWITCH ACTIVATION TIMES

MISSILE NO.	TIME IN SECONDS FROM SUST FLT LOCK-IN TO BOOST HI PRESS SW	SUST HI PRESS SW	MAIN ENGINE THRUST COMPLETE SWITCH	LAG TIME (sec) SUST PRESS CHANGE OVER TO MAIN ENG BUILDUP COMPLETE
42D	0.68	1.34	1.21	0.13
48D	0.67	0.99	(1)	(1)
56D	0.74	1.37	1.23	0.14
54D	0.64	1.31	1.09	0.22
62D	0.76	1.48	1.15	0.33
27D	1.03	1.38	1.03	0.35
60D	0.70	1.34	1.10	0.24
32D	0.63	0.75	1.11	0.36
66D	0.65	1.30	1.00	0.30
76D	0.59	1.32	0.94	0.38
79D	0.75	1.40	1.16	0.24
71D	0.72	1.32	1.14	0.18
55D	1.14	1.62	1.08	0.54
83D	0.66	1.42	1.04	0.38
90D	0.60	1.30	0.99	0.31
Average	0.73	1.29	1.09	

NOTE: (1) Missile destroyed prior to liftoff, no data received.

SECTION 7.2 - PNEUMATICS

PURPOSE OF TESTING

The pneumatics system was evaluated in a continued program to determine the over-all performance characteristics of the Series D propellant tank and control pressurization systems, and to obtain data for reliability analysis of the pneumatic system hardware. Of particular interest was determination of the booster jettison bottle pressure history during the booster phase, and the ability of the Hadley Series D regulator to provide proper propellant tank ullage pressures.

Also of interest was the effect of removal of the insulation bulkhead on lox boiloff and helium requirements to the main propellant tanks. Missile 55D was the only missile flown without an insulation bulkhead.

TEST CONDITIONS

The standard Series D pneumatics system configuration is shown in Figure 7.2-1. Basically the pneumatic system is composed of two subsystems; the propellant tank pressurization system and the engine controls pressurization system.

The propellant tank pressurization system provides helium regulated at the proper levels to pressurize the propellant tanks and also to provide pressure to the pneumatic side of the hydraulic and lube oil tanks during the booster stage of flight. Major components include five 7,365 cubic-inch helium storage bottles subcooled prior to launch by a shroud of liquid nitrogen, a heat exchanger located in the booster turbine exhaust duct to raise the required helium to desired temperatures, and two main propellant tank pressure regulators, one for the fuel tank and one for the lox tank. Figure 7.2-1 shows schematically the location of each component. All components except the lox tank regulator are jettisoned with the booster section at staging.

~~SECRET~~

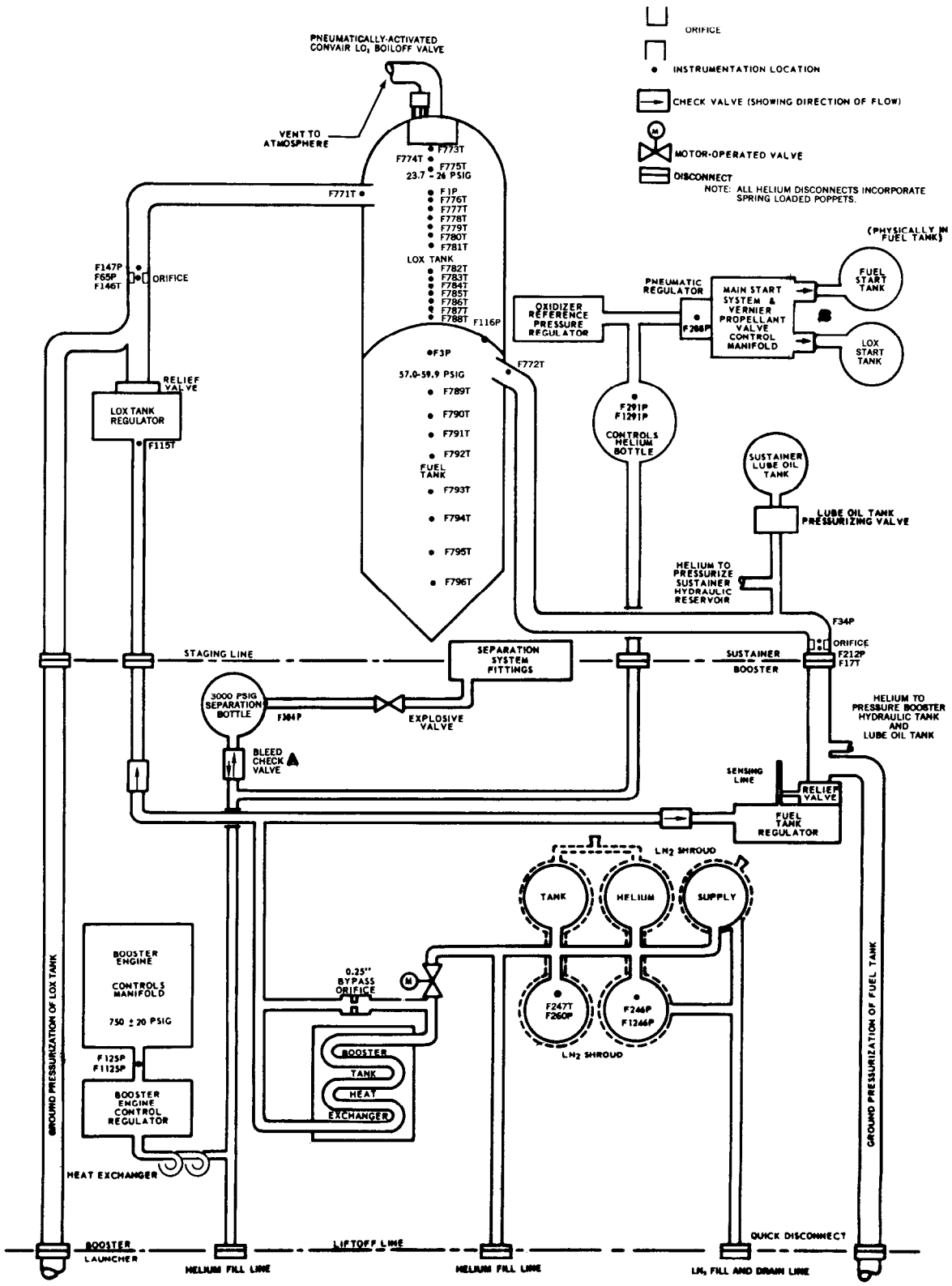

FIGURE 7.2-1 SERIES D PNEUMATIC SYSTEM

~~SECRET~~

The engine controls system is composed essentially of a sustainer and a booster section. A 4,650 cubic-inch controls helium storage bottle, an integrated start system (ISS) regulator and an oxidizer reference pressure regulator are the components which constitute the sustainer section. The booster section, composed of a booster controls regulator, an 870 cubic-inch fiberglass booster separation bottle and ten pneumatically actuated separation fittings, is jettisoned at booster staging.

No major pneumatic system modifications were initiated after the flight of Missile 42D, the first of 15 flight tests covered by this report. A tabulation of major system components is included in Table 7.2-1. This lists, for comparative purposes, modifications made throughout the entire Series D R&D test program. The sustainer stage tank pressurization system

TABLE 7.2-1 COMPARISON OF PNEUMATIC SYSTEM COMPONENT MODIFICATION, SERIES D R&D

	FIRST SUMMARY TEST PERIOD																SECOND SUMMARY TEST PERIOD													
	MISSILE NO.																													
	3D	5D	7D	11D	14D	15D	17D	18D	22D	26D	28D	31D	40D	43D	44D	49D	51D	42D	48D	56D	54D	62D	27D	60D	32D	66D	76D	79D	71D	55D	83D	90D
Steel Helium Storage Bottles	X																													
Titanium Helium Storage Bottles		X	X	X	X	X	X	X	X	X	X	X	X	X	X	X	X	X	X	X	X	X	X	X	X	X	X	X	X	X
Second Stage Lox Tank Pressurization	X	X	X																											
Removal of Sustainer Tank Pressurization Hardware													X	X	X	X	X	X	X	X	X	X	X	X	X	X	X	X	X	X
Fiberglass Booster Separation Bottle													X	X	X	X	X	X	X	X	X	X	X	X	X	X	X	X	X	X
Hadley Series C Regulator	X	X	X	X	X	X	X	X																						
Hadley Series D Regulator									X	X	X	X	X	X			X	X	X	X	X	X	X	X	X	X	X	X	X	X
F and G Regulator																X														
Stratos Regulator															X															
"Backward" Plumbing to Controls Helium Bottle															X	X	X	X	X	X	X	X	X	X	X	X	X	X	X	X
Series C Pneumatic Actuated Boiloff Valve	X	X	X	X	X																									
Electrically Actuated Boiloff Valve						X	X	X	X	X			X																	
Series D Pneumatic-Activated Boiloff Valve (blowdown ring installed on 31D and succeeding assemblies)											X	X		X	X	X	X	X	X	X	X	X	X	X	X	X	X	X	X	X
Controls Heat Exchanger (25-ft coiled, 1/4 in. line)				X	X	X	X	X	X	X	X	X	X	X	X	X	X	X	X	X	X	X	X	X	X	X	X	X	X	X
Controls Pressurization Switchover During Riseoff													X	X	X	X	X	X	X	X	X	X	X	X	X	X	X	X	X	X

hardware was deleted after the flight of Missile 32D. Sustainer stage lox tank pressurization has been accomplished by lox boiloff since early in the Series D program. A fuel tank pressurization system is not necessary during sustainer stage.

On Missile 55D the insulation bulkhead, normally installed on the fuel side of the intermediate bulkhead, was damaged during prelaunch operations. A joint BMD/STL/CVA decision was made to remove the bulkhead and launch the missile with special instrumentation in order to evaluate the effects of anticipated increase in heat transfer between the two main propellant tanks on helium usage and lox boiloff during flight. The main propellant tanks internal temperature environment was also determined in support of this objective.

Pneumatic system instrumentation is presented in Figure 7.2-1. For applicability of particular measurements refer to the Telemetry Analysis.

TEST RESULTS

Propellant Tank Pressurization

A tabular summary of pneumatic system performance data is presented in Table 7.2-2. The ability of the Series D tank pressurization system to provide properly regulated helium pressure to the missile lox and fuel tanks was demonstrated on each of the long-duration flights accomplished during the subject test period. The pneumatic system installed on Missile 48D was functioning properly when the test was terminated prematurely prior to liftoff.

Two of the more significant parameters measured in flight are the ullage pressures in the main lox and fuel tanks. These measurements provide information for use in analysis of missile structural integrity, propellant pump net positive suction head (NPSH), liquid oxygen boiloff, and aerodynamic heating. In order to maintain necessary structural strength during periods of maximum aerodynamic loading and to provide necessary pump NPSH during critical periods, tank pressures were optimized at 26.0 psig in the lox tank and 59.9 psig in the fuel tank. Pressure regulators were set to maintain a range of 23.4 to 26.0 psig in the lox tank and 55.0 to 60.0 psig in the fuel tank during booster stage. Hadley Series D regulators, used on all subject test flights, maintained ullage pressure in the propellant tanks within these ranges, free of undue pressure fluctuations during flights.

TABLE 7.2-2 SUMMARY OF PNEUMATIC SYSTEM PERFORMANCE

MISSILE	FUEL TANK PRESSURES (psig)			LOX TANK PRESSURE (psig)			BOOSTER CONTROLS REGULATOR PRESS		INTEGRATED START SYST REG PRESS		CONTROLS BOTTLE PRESS (psig)				SEPARATION HELIUM BOTTLE PRESSURE	
	LIFTOFF	BCO	SCO	LIFTOFF	BCO	SCO	LIFTOFF	BCO	MEAN	MAX	LIFTOFF	BCO	SCO	VCO	LIFTOFF	BCO
42D	61.7	59.5	49.6	25.2	24.9	23.0	740	745	585	640	3,130	2,615	2,000	1,200	3,150	3,040
48D*	61			25.6			754		600		3,085				3,110	
56D	60.5	61.4	48.5	24.4	24.0	22.0	750	752	607	705	3,060	2,390	2,390	1,560	3,240	2,695
54D	59.3	57.5	49.0	24.3	24.0	22.5	760	740	580	660	3,100	2,400	2,125	1,700	3,150	3,025
62D	60.0	59.3	49.2	25.1	25.0	22.6	754	752	585	675	2,940	2,550	2,225	840	3,240	3,045
27D	59.0	56.9	45.4	23.9	24.2	22.2	761	764	621	680	2,860	2,595	2,250	1,340	3,275	3,010
60D	58.7	59.8	52.3	25.0	24.9	22.9	770	580	erratic	795	3,100				3,180	3,010
32D	59.8	59.5	46.6	24.1	24.4	21.8	753	753	589	654	3,065	2,710	2,350	1,465	3,250	2,900
66D	61.9	61.5	51.6	25.3	24.9	22.7	750		590	675	3,005	2,675	2,400	1,500	3,135	2,940
76D	57.9	58.8	47.9	25.3	24.8	22.8	752	752	569	589	3,065	2,655	2,400	1,475	3,065	2,905
79D	58.8	58.5	48.5	24.0	24.5	22.2	750	750	600	690	3,145	2,600	2,250	1,400	3,150	2,900
71D	59.6	58.8	48.4	25.4	24.3	22.1	745	753	589	670	3,100	2,710	2,500	1,600	3,085	2,940
55D	58.2	56.5	39.2	24.8	24.8	23.0	745	745	595	650	3,235	2,775	2,450	1,550	3,310	3,130
83D	59.9	59.7	48.9	24.8	25.0	23.0	753	753	591	703	3,140	2,840	2,125	1,700	3,240	3,010
90D	56.6	55.9	45.9	24.2	24.0	21.7	741	744	600	640	3,095	2,235	2,100	1,000	3,150	2,240

NOTE: *The values quoted were taken just prior to liftoff.

Average lox tank pressures were 24.7 psig at liftoff and 24.5 psig at booster cutoff. Lox tank ullage pressure at engine start exhibited small fluctuations with peak pressures averaging 26.1 psig and minimum pressures averaging 23.8 psig. These fluctuations are the normal result of severe demands on the pressure regulator at engine start due to effects of small ullage space combined with the sudden start of the propellant pumps.

Although the propellant tanks do not receive supplemental helium pressure during the sustainer stage, the decrease in pressure level was small in the lox tank due to the self-pressurization effects of lox boiloff. Lox tank ullage pressures at sustainer cutoff on fourteen flights averaged 22.5 psig, representing a decrease in pressure during sustainer stage of 2.0 psig. This average pressure was well above the minimum specification level of 18 psig.

Minor buildups in lox tank pressure were noted during periods of unusually high propellant slosh during the booster phase of flight on two Series D/AIG missiles. The lox tank pressures on Missiles 71D and 76D were observed to increase slowly by one or two psi (4 to 8%) then return to the steady-state level over a time interval of approximately 25 seconds. Correlation of these pressure buildups with flight control system data indicated that they were due to excessive lox boiloff resulting from the unusually high propellant slosh activity. The pressures did not reach undesirable levels.

Fuel tank pressures were maintained within specifications (55.0 to 60.0 psig) except for two flights (Missiles 56D and 66D) during which steady-state pressures were indicated to be in excess of 60 psig. However, the amount of overpressurization in each case was less than the accepted accuracy range of the telemetry loop (3%, or 1.8 psi) and was therefore not considered significant.

Since pressurization of the fuel tank is not continued after booster cutoff, fuel tank ullage pressure is expected to decrease during sustainer stage in proportion to the amount of fuel evacuated. The average fuel tank pressure was 47.9 psig at sustainer cutoff representing a decrease of 10.9 psi during sustainer stage. The pressure decrease in the fuel tank was greater than that in the lox tank (2.0 psi) because fuel lacks the self-pressurization effects of lox boiloff during sustainer stage.

Controls Pressurization

Performance of the controls pressurization system was adequate. Telemetry data indicated the existence of helium leakage in the area of the vernier propellant tanks on Missile 42D, and in the separation subsystem on Missile 56D and 90D. The leakage rate was not great enough to deplete controls regulator output pressure below the specification requirements of 750 ± 20 and 600 ± 15 psig in the booster engine control manifold and the integrated start system manifold, respectively. Significant data are summarized in Table 7.2-2. The controls pressurization system on two flights reflected the effects of anomalies which occurred in other missile systems. Also during the flight of Missile 60D, the repeated pressurization and venting of the vernier engine tanks caused the premature depletion of controls helium bottle pressure. Refer to Problem Areas for a detailed discussion of these anomalies.

Capacity of the 4,650 cubic-inch controls helium storage bottle was sufficient on all flights except that of Missile 42D, to maintain pressure above 1,000 psig. Average controls bottle pressures were 3,075 psig at liftoff when the ground pneumatic supply to the missileborne helium bottles was discontinued. Normal usage of controls helium during flight had reduced average bottle pressures to 2,595, 2,275 and 1,410 psig at booster, sustainer and vernier cutoff, respectively.

Operation of the booster stage separation system was satisfactory on all flight tests except for Missiles 56D and 90D. A discussion of these two missiles is presented in Problem Areas. Adequate pressure was available at staging on all flight tests to properly actuate the ten separation fittings which effect booster jettison.

Separation helium bottle pressure, exclusive of that noted on Missiles 56D and 90D, averaged 2,975 psig at booster cutoff. For Missiles 56D and 90D, booster separation bottle pressures at booster cutoff were 2,695 and 2,245 psig, respectively.

Helium Consumption and Flow Rates to the Propellant Tanks

The quantity of helium required to maintain proper propellant tank ullage pressures is dependent upon the propellant evacuation rate, lox boiloff rate and the thermal characteristics of the gaseous mixture in the ullage spaces. The ullage gas thermal characteristics and lox boiloff rates are in turn affected by aerodynamic heating, heat exchanger efficiency and heat transfer across the intermediate bulkhead.

With the removal of the insulation bulkhead on Missile 55D it was expected that an increase in heat transfer across the intermediate bulkhead would chill the fuel tank ullage space and significantly increase the amount of helium required to maintain proper tank pressure. A graph of helium requirements for Missile 55D propellant tank pressurization is presented in Figure 7.2-2. Also shown are data from previous Series D flights, included for comparison. From Figure 7.2-2, it is evident that the helium requirements on Missile 55D were greater than normal, but not excessive. Total helium used during the booster phase of flight, calculated from the time history of pressure, temperature and volume data in the five helium storage bottles, was found to be 79.8 lbs or 12% greater than the average 71 lbs required on previous Series D flights. Refer to Figure 7.2-3. Approximately 55 lbs of usable helium, or 42% of the total available at liftoff, remained at booster cutoff. At staging, this helium along with all tank pressurization system hardware, with the exception of the lox tank regulator, was jettisoned along with the booster thrust section.

Calibrated orifices were located in the helium supply lines to the propellant tanks for determining helium flow rates. Resulting flow rates to the fuel and lox tanks calculated from recovered data indicated that helium flow to the fuel tank was significantly greater on Missile 55D than the average noted on six previous Series D flights. Refer to Figure 7.2-2. Approximately 10 to 15% more helium was required for fuel tank pressurization during booster stage, most of which was assumed to be the result of removal of the insulation bulkhead.

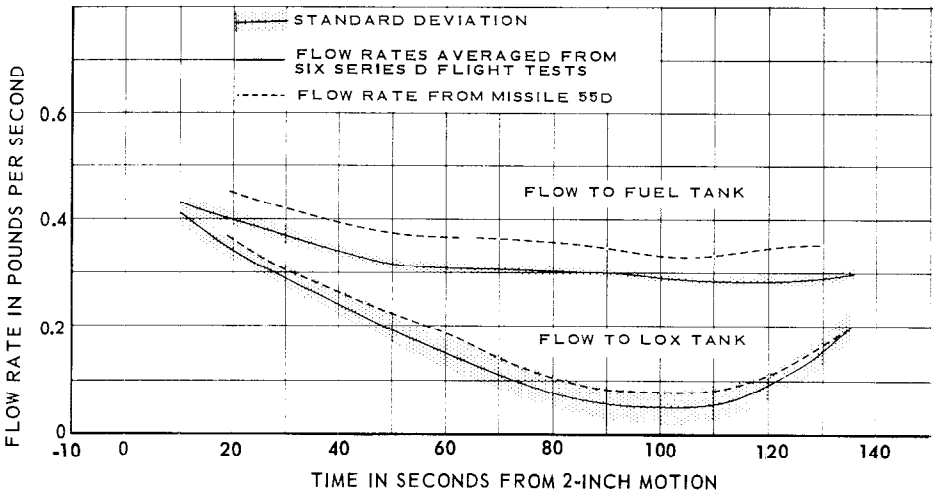

FIGURE 7.2-2 COMPARISON OF PROPELLANT TANKS HELIUM REQUIREMENTS

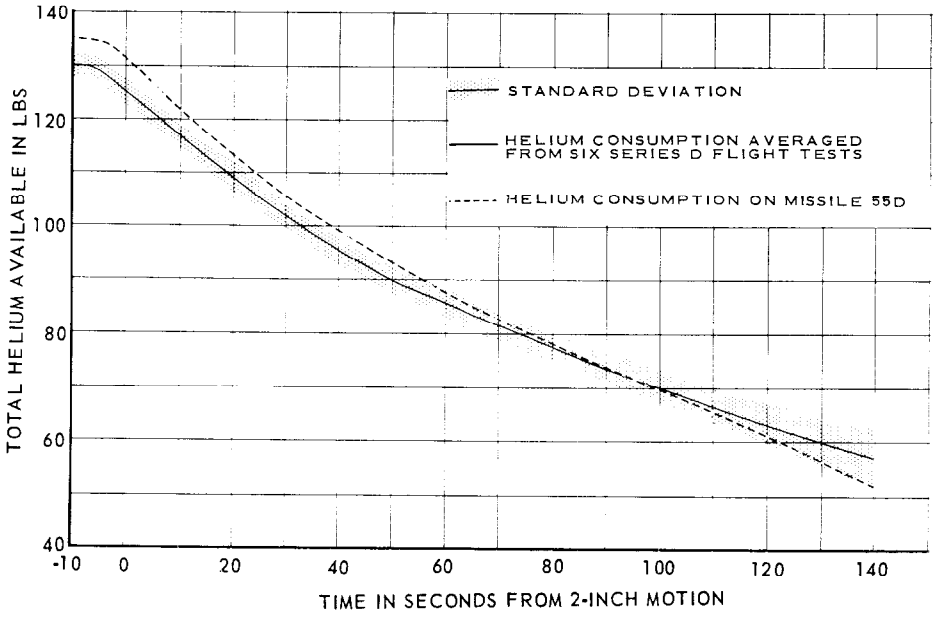

FIGURE 7.2-3 COMPARISON OF PROPELLANT TANKS HELIUM CONSUMPTION

Helium flow to the lox tank on Missile 55D appeared to be normal, falling on the high side of the standard deviation spread. Flow decreased from 0.4 lbs per second shortly after liftoff to a minimum of approximately 0.08 lbs per second at 100 seconds. At this time, a high level of propellant slosh and resulting increased lox boiloff rates reduced helium flow to the lox tank to a minimum. By booster cutoff, helium flow to the lox tank had increased to 0.2 lbs per second.

Tank Pressurization Regulators

All of the missiles flown in this test series utilized the Hadley Series D regulator, as noted in the pneumatic system configuration history given in Table 7.2-1. Performance of the Hadley Series D regulators was entirely satisfactory. Pressure remained stable during flight, with the steady-state levels consistently within the design nominal range. Pressure oscillations at engine start, discussed previously under propellant tank pressurization, were relatively small.

Integrated Start System (ISS) Regulator

The integrated start system regulator provided adequate pressure to the main engine start system and vernier engine propellant valve control manifold. On six flights (56D, 62D, 32D, 66D, 79D and 83D) regulator discharge pressures increased after vernier start tank repressurization, attaining pressures as high as 705 psig prior to sustainer cutoff. After the start of tank-fed vernier solo operation at sustainer cutoff, pressures recovered to nominal levels (600 ± 15 psig). Refer to Table 7.2-2 for a summary of steady-state and maximum pressure levels encountered on individual flight tests. On all flights, other than the six noted above, the maximum pressures tabulated in Table 7.2-2 are the normal transient pressure peak at repressurization. No detrimental effects were noted as a result of these overpressurizations. This anomaly is treated in detail under Problem Areas.

Missile 55D Special Instrumentation

With the removal of the insulation bulkhead on Missile 55D, special instrumentation was installed to establish the effect of this configuration change on lox boiloff rates, helium usage and internal temperature environment of the propellant tanks. The parameters monitored were helium temperatures at the inlet to the lox and fuel tank, and ullage temperatures in the main propellant lox and fuel tanks. The data obtained from ullage temperature measurements are summarized in Table 7.2-3. Using this data, a study was conducted to establish the quantity of lox boiloff which had occurred during the Missile 55D flight. Results indicated that approximately 114.8 and 251.3 lbs of lox had boiled off by booster cutoff and sustainer cutoff, respectively.

SECRET

TABLE 7.2-3 SUMMARY OF ULLAGE TEMPERATURE DATA, MISSILE 55D

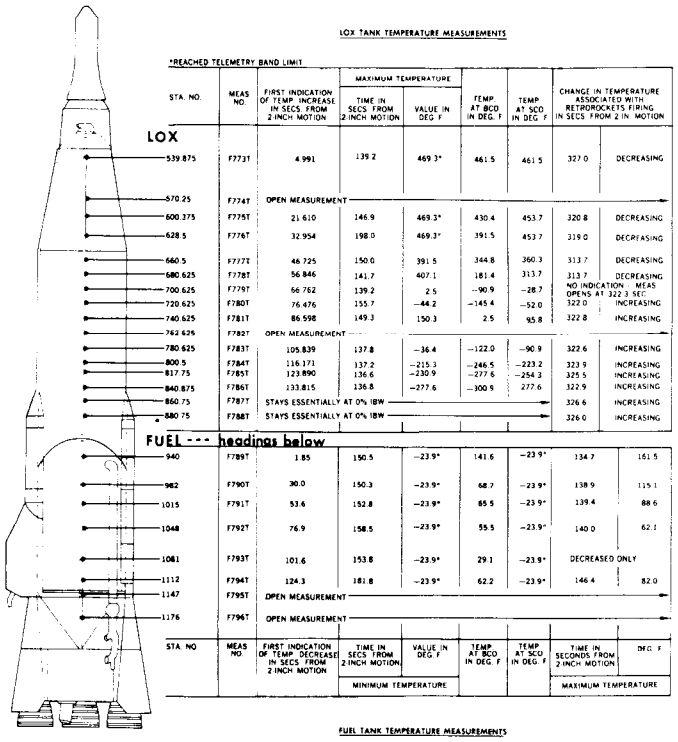

LOX TANK TEMPERATURE MEASUREMENTS

*REACHED TELEMETRY BAND LIMIT

STA. NO.	MEAS NO.	FIRST INDICATION OF TEMP. INCREASE IN SECS. FROM 2 INCH MOTION	MAXIMUM TEMPERATURE: TIME IN SECS. FROM 2 INCH MOTION	MAXIMUM TEMPERATURE: VALUE IN DEG. F	TEMP. AT BCO IN DEG. F	TEMP. AT SCO IN DEG. F	CHANGE IN TEMPERATURE ASSOCIATED WITH RETROROCKETS FIRING IN SECS. FROM 2 IN. MOTION	
LOX								
539.875	F773T	4.991	139.2	469.3*	461.5	461.5	327.0	DECREASING
570.25	F774T	OPEN MEASUREMENT						
600.375	F775T	21.610	146.9	469.3*	430.4	453.7	320.8	DECREASING
628.5	F776T	32.954	198.0	469.3*	391.5	453.7	319.0	DECREASING
660.5	F777T	46.725	150.0	391.5	344.8	360.3	313.7	DECREASING
680.625	F778T	56.846	141.7	407.1	181.4	313.7	313.7	DECREASING
700.625	F779T	66.762	139.2	2.5	−90.9	−28.7	NO INDICATION MEAS OPENS AT 322.3 SEC	
720.625	F780T	76.476	155.7	−44.2	−145.4	−52.0	322.0	INCREASING
740.625	F781T	86.598	149.3	150.3	2.5	95.8	322.8	INCREASING
762.626	F782T	OPEN MEASUREMENT						
780.625	F783T	105.839	137.8	−36.4	−122.0	−90.9	322.6	INCREASING
800.5	F784T	116.171	137.2	−215.3	−246.5	−223.2	323.9	INCREASING
817.75	F785T	123.890	136.6	−230.9	−277.6	−254.2	325.5	INCREASING
840.875	F786T	133.815	136.8	−277.6	−300.9	277.6	322.9	INCREASING
860.75	F787T	STAYS ESSENTIALLY AT 0% IBW					326.6	INCREASING
880.75	F788T	STAYS ESSENTIALLY AT 0% IBW					326.0	INCREASING
FUEL --- headings below								
940	F789T	1.85	150.5	−23.9*	141.6	−23.9*	134.7	161.5
982	F790T	30.0	150.3	−23.9*	68.7	−23.9*	138.9	115.1
1015	F791T	53.6	152.8	−23.9*	65.5	−23.9*	139.4	88.6
1048	F792T	76.9	158.5	−23.9*	55.5	−23.9*	140.0	62.1
1081	F793T	101.6	153.8	−23.9*	29.1	−23.9*	DECREASED ONLY	
1112	F794T	124.3	181.8	−23.9*	62.2	−23.9*	146.4	82.0
1147	F795T	OPEN MEASUREMENT						
1176	F796T	OPEN MEASUREMENT						

STA. NO.	MEAS NO.	FIRST INDICATION OF TEMP. DECREASE IN SECS. FROM 2 INCH MOTION	MINIMUM TEMPERATURE: TIME IN SECS. FROM 2 INCH MOTION	MINIMUM TEMPERATURE: VALUE IN DEG. F	TEMP. AT BCO IN DEG. F	TEMP. AT SCO IN DEG. F	MAXIMUM TEMPERATURE: TIME IN SECONDS FROM 2 INCH MOTION	MAXIMUM TEMPERATURE: DEG. F

FUEL TANK TEMPERATURE MEASUREMENTS

Approximate lox boiloff values were obtained by application of the equation-of-state of a gas (PV = WRT).

The equation was applied in the following manner.

The lox tanks ullage space was divided into incremental volumes with a homogeneous mixture of helium and oxygen assumed to exist within each. The equation could then be written:

$$P_T V_T = (WR)_{mix} T_g \qquad (1)$$

SECRET

where:

P_T = tank pressure

T_g = temperature of the gas mixture

W = weight of the gas mixture

V_T = tank ullage volume

R = gas mixture constant.

The term $(WR)_{mix}$ may be written as $(W_{ox} R_{ox} + W_{He} R_{He})$ where:

W_{ox} = total weight of oxygen at a given time

W_{He} = total weight of helium at a given time

R_{ox} = oxygen gas constant

R_{He} = helium gas constant.

Substituting into equation (1):

$$P_T V_T = (W_{ox} R_{ox} + W_{He} R_{He}) Tg \qquad (2)$$

This was solved for W_{ox}, the weight of oxygen in gas mixture.

$$W_{ox} = \frac{P_T}{R_{ox}} \left(\frac{V_T}{T_g}\right) - \frac{R_{He}}{R_{ox}} W_{He} \qquad (3)$$

Gas pressure, P_T, was assumed to be constant throughout the tank. The remaining parameters on the right side of equation (3) were obtained from flight data and from standard gas tables. Total weight of helium in the lox tank was determined from helium supply line flow data or from helium supply bottles pressure and temperature data.

Temperature in the tank was not constant at anytime but existed as a gradient (refer to Table 7.2-3). This gradient was established by the data obtained during flight, and temperatures representative of particular volumes could be substituted:

$$\frac{V_T}{T_g} = \sum_{i=1}^{i=n} \frac{V_i}{T_{gi}} = \frac{V_1}{T_{g1}} + \cdots\cdots \frac{V_n}{T_{gn}} \tag{4}$$

and equation (3) becomes

$$W_{ox} = \frac{P_T}{R_{ox}} \sum_{i=1}^{i=n} \frac{V_i}{T_{gi}} - \frac{R_{He}}{R_{ox}} W_{He} \tag{5}$$

Gaseous oxygen weights and lox boiloff values were thus obtained.

This method of estimating lox boiloff had not been used previously, therefore, no data for comparison are available.

It was expected that omission of the insulation bulkhead would not significantly affect lox boiloff rate, and the calculated weights noted previously are believed to be representative of normal boiloff rates.

PROBLEM AREAS

Although the pneumatic system satisfied all normal missile requirements during this test period, minor problems were noted in some areas. These are discussed in the following paragraphs.

Lox Tank Orifice Differential Pressure Increase

A transient increase to the upper telemetry band limit occurred in the lox tank orifice differential pressure measurement, 0.4 seconds after booster cutoff on Missile 56D. This would normally be indicative of an increase in lox tank helium flow. However, no lox tank demand is expected after booster cutoff and none was indicated by flight data. One event noted at this same time, as indicated by the pitch rate gyro data, was a shock to the missile which normally occurs as a result of booster engine shutdown characteristics. It is probable that this shock may have affected the lox tank orifice pressure sensor, resulting in a false transient in the data.

Lox Tank Pressure Buildup

An unusual increase in lox tank ullage pressure was noted on AIG Missiles 71D and 76D and a similar pressure buildup was noted during the Project Mercury flight of Missile 67D.

Pertinent data is summarized in Table 7.2-4.

TABLE 7.2-4 UNUSUAL LOX TANK PRESSURE INCREASES

MISSILE NO.	START OF PRESSURE CUSP (seconds from 2-inch motion)	MAXIMUM INCREASE ABOVE STEADY-STATE PRESSURE (psi)	RESUME STEADY-STATE PRESSURE (seconds)
71D	97.9	2.0	121.5
76D	93.6	3.1	125.3
67D	85.5	2.6	122.6

Two possible causes of an increase in lox tank pressure during this time interval are:

1. Momentary opening of the lox tank pressure regulator. This regulator is normally closed at this time because normal lox boiloff due to propellant slosh has greatly reduced the quantity of helium required to maintain tank pressure.

2. An unusually high lox boiloff rate sufficient to increase tank pressure.

Performance characteristics of the pressure regulator could not be determined directly due to insufficient instrumentation. The measurement on which helium demands are normally reflected, helium storage bottles pressure, indicated no unusual changes at this time. However, the pressure change in the helium storage bottle resulting from a helium flow sufficient to cause the observed increase in ullage pressure would be difficult to distinguish.

The change would be relatively small and would extend over a 10 to 25-second time interval. Therefore, an anomalous momentary opening of the lox tank pressure regulator on these flights could not be definitely established.

These pressure buildups can be attributed to abnormal propellant sloshing effects. Propellant slosh amplitudes on Missiles 76D, 67D and 71D which were two or more times as great as that noted on previous Series D flights, are the result of additional flight control system phase lag introduced by the Series E type double section quadratic filter used on these missiles. It was established that the buildup and decay of propellant slosh, indicated by missile pitch, yaw and roll rate gyro data, occurred over the same time interval as the observed lox tank pressure buildups. Apparently abnormal high slosh amplitudes permitted sufficient lox to contact the hot forward tank section resulting in abnormal lox boiloff and a subsequent rise in tank pressures.

On the flight of Missile 90D, abnormally high rate gyro oscillations, indicative of excessive propellant sloshing, were also noted but without a corresponding increase in the lox tank ullage pressure. Further examination of Missile 90D data, however, indicated that the rate oscillations were most prominent about the roll axis, with less motion in the pitch and yaw planes than that noted on Missiles 76D, 71D and 67D. The effect of propellant slosh about the roll axis, on lox boiloff, may have been insufficient to increase lox tank pressure above the steady-state level.

Pressure buildups of this nature are not considered to constitute a problem at this time and no remedial actions have been initiated.

Integrated Start System (ISS) Regulator Overpressurization

The integrated start system (ISS) pneumatic regulator did not maintain the expected pressure levels (600 ± 15 psig) after vernier engine tanks repressurization, on six flights (Missiles 56D, 62D, 32D, 66D, 70D and 83D). Regulator discharge pressure failed to recover properly after the normal overpressurization transient and exhibited a gradual increase to a pressure of approximately 700 psig. Refer to Table 7.2-2 for maximum pressures reached on these flights. The pressure remained at this level until sustainer cutoff when it abruptly returned to the nominal level. There were no apparent detrimental effects.

Configuration records were examined to determine if any modifications had been accomplished on these six missiles which could account for this anomaly. It was subsequently established that an ISS regulator modification was initiated on these vehicles which incorporated an "O" ring (gasket) in the groove of the regulator piston causing tighter dimensions and tolerances than those used previously. The new "O" ring could possibly bind against the cylinder wall causing the piston to stick and move erratically, thereby causing the pressure buildup noted.

Another possible cause of this anomaly is a malfunction of the vernier solo lox tank helium checkvalve in the ISS manifold identified for the purposes of this discussion as checkvalve "B" in Figures 7.2-1 and 7.2-4. A malfunctioning of this valve would permit pressure in the ISS manifold to build up to the level in the vernier solo lox tank. This pressure buildup

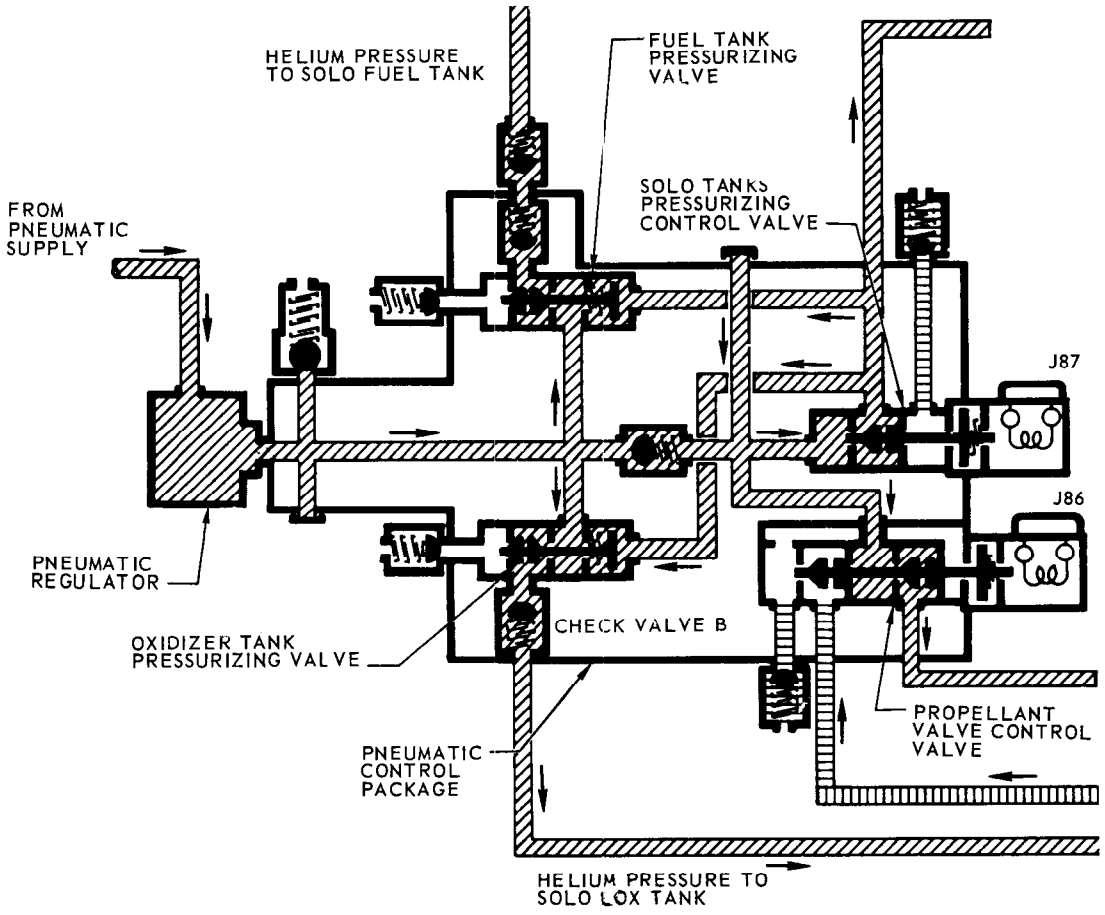

FIGURE 7.2-4 INTEGRATED START SYSTEM MANIFOLD

could begin after initiation of the pressurize vernier tanks (PVT) function had positioned the solenoid-operated tank pressurization valves in the open position (Refer to Figure 7.2-4). During operation of the sustainer lox pump, pressure in the lox solo tank is approximately 670 psig. The suspect checkvalve normally remains closed from engine start until sustainer cutoff when the vernier engines begin tank-fed operation.

Neither possibility can be firmly established as the cause of this anomaly. Investigation of this problem is being continued.

Abnormal Decay of Controls System Storage Bottle Pressure

Data on one flight (42D) indicated an abnormal decay rate in controls helium bottle pressure after vernier start tank repressurization. Separation bottle pressure data on two other flights (56D and 90D) indicated system leakage in the area of the separation bottle prior to staging. These anomalies will be discussed separately.

Controls bottle pressure on Missile 42D began to decay at 5.4 psi/second (ten times the normal rate) after initiation of the Pressurize Vernier Tanks (PVT) function (BCO plus 64 seconds). This abnormal decay continued until the start of vernier solo operation. Any abnormality in the decay rate during the vernier solo period was obscured by the normal high depletion rate during tank-fed vernier engine operation. Controls helium bottle pressure normally stabilizes following vernier cutoff. However, on Missile 42D pressure decayed at 25 psi/second from VCO until the start tanks were vented 24 seconds later.

It was evident from these characteristics that there was a high pressure leak in the controls system after the start tank and associated system were pressurized. This correlation locates the suspect area downstream of the integrated start system manifold in the area of the propellant start tanks. The most plausible explanation for the change in decay rates after VCO is that during the vernier solo phase the escaping media had changed from a liquid to a gas. It is noted that a gas would escape more rapidly than a liquid. The change in pressure decay rate after vernier cutoff could be accounted for by considering that the leak existed in a propellant line and that a propellant was escaping after start tanks pressurization and until the propellant was evacuated during the vernier solo phase. Thereafter, helium gas would continue to escape but at an accelerated rate. The existence of a propellant leak could not be definitely established from other flight data. However, it was noted that vernier engine thrust decayed prior to VCO, which suggests that one of the propellants had been prematurely depleted, possibly as a result of propellant leakage in the manner described above.

Prelaunch leak check procedures were reviewed in both the propulsion and the pneumatic controls pressurization systems to prevent a recurrence of the problem.

The separation bottle exhibited abnormal pressure decay rates prior to staging on Missiles 56D and 90D (and also on the Atlas-Able flight of Missile 80D, not covered in this report). Data indicated that between liftoff and booster cutoff, separation bottle pressure decayed 545 and 910 psig on Missiles 56D and 90D, respectively. The normal pressure loss during this period has averaged 198 psig for 12 flights. Helium pressures in the interconnected controls pressurization system decayed in approximately the same manner during this period. On Missile 90D, controls bottle pressure decreased abruptly by 160 psig as a result of helium demands to pressurize the vernier start tanks at booster cutoff. Separation bottle pressure decay rate increased from 5 psi/second prior to booster cutoff, to 40 psi/second between BCO and staging. On Missile 56D, vernier tank pressurization was initiated after staging and the pressure data indicated no change in decay rate at booster cutoff. On both flights all separation fittings functioned normally at staging and the separation pressure data trace dropped abruptly to the zero bandwidth. Controls system pressure resumed normal decay characteristics during the remainder of both flights.

A brief review of the inter-relation between the separation and controls subsystems is desirable prior to the following discussion. Pressure from the separation bottle is used only to actuate the ten separation system fittings. This circuit is connected to the booster controls subsystem by a two-way check/bleed valve (identified in Figure 7.2-1 by the notation "A") in order that the separation and controls bottles may be serviced prior to launch from common charge and bleed lines. With this configuration, helium could flow rapidly from the controls system to the separation system through checkvalve A, but is limited in the reverse direction to a flow corresponding to a nominal pressure decay of 200 psi in the separation bottle during booster stage.

The return to normal pressure decay in the controls system after booster staging indicated that on both flights the cause of the anomaly was located in the jettisoned booster section.

A study was initiated to approximate the sizes of leaks required to cause the abnormalities described above. The quantity of helium ($\dot{W}$) used from the respective bottles, was first calculated based upon a time history application of the equation-of-state of a gas;

$$PV = WRT \tag{6}$$

where PV and T are pressure, volume and temperature, respectively, of the bottle, and R is the gas constant for helium. The amount of helium normally used for control functions was calculated from data of a previous flight where no leakage was evident. The difference was considered to represent helium lost through leakage. The result, expressed as a flow rate ($\dot{W}$) was applied to the orifice flow equation:

$$\dot{W} = \frac{8.02\ C_d A(0.513P)}{\sqrt{ZRT}} \qquad (7)$$

where:

A = equivalent orifice diameter

C_d = 0.83, the orifice coefficient

P = helium pressure at the orifice

T = helium temperature at the orifice

Z = 1.1, compressibility factor for gas

R = 386, the gas constant for helium.

Equivalent orifice diameters were computed in this manner for the helium leakage evident during booster stage, and were found to be 0.0088 and 0.0299 inches, respectively, for Missiles 56D and 90D. Since the bleed orifice "A" has a nominal diameter of 0.0035 inches it was evident that helium was escaping from the separation system faster than it could normally flow into the controls system through bleed orifice "A". This indicated that either the leak was located in the area of the separation bottle, or a faulty bleed valve ("A") permitted excessive helium flow into the booster portion of the controls system, with the helium subsequently escaping to atmosphere via a leak existing in that area. A similar calculation was performed to determine the leak size to account for the aforementioned accelerated separation bottle pressure decay between BCO and staging on Missile 90D. The equivalent diameter was found to be 0.0328 inches. This value implies that helium was leaking to atmosphere through the leak and also to the controls side through the bleed orifice to equalize pressure after the 160 psi pressure loss at BCO. When it is noted that the nominal size of the bleed orifice (0.0035 inches) and the 0.0299 inch leak size assumed to exist prior to BCO equals approximately 0.0328 inches, it is evident that one leak of 0.0299 inches diameter can account for separation bottle pressure decay anomalies observed on Missile 90D. A leak in the booster controls system could account for the data on both flights (56D and 90D) only if a failure of the bleed check valve "A" occurred. A similar failure of this valve on two vehicles is considered unlikely. Therefore, the abnormal separation bottle pressure decays observed on Missiles 56D and 90D is concluded to be result of helium leakage in the separation system.

A general review of prelaunch leak check procedures was initiated to prevent the recurrence of anomalies of this type on future flights.

SECTION 7.3 - ELECTRICAL

PURPOSE OF TESTING

Primary objectives for the flight testing of the electrical system included the following:

1. Obtain data for system reliability studies.

2. Determine the performance of the battery-inverter power supply using the remotely-activated main missile battery in conjunction with either the Bendix or Leland rotary inverter.

3. Determine the characteristics of the 28 vdc power supply at the autopilot programmer input, after vernier cutoff.

This latter objective was initiated in support of a circuitry problem which caused a discontinuity in an electrical harness between the guidance decoder and the flight control programmer on Missile 62D.

TEST CONDITIONS

The airborne electrical system, shown schematically in Figure 7.3-1, included the following major components:

1. A power changeover switch for selection of the proper combination of ground or airborne a-c and d-c power.

2. A rotary inverter, essentially a motor-generator driven by 28 vdc power, to produce 115 vac, three phase 400-cycle power.

3. A remotely-activated, one-shot, silver-zinc battery with an electrolyte canister assembly (activated from the blockhouse at T-140 seconds).

~~SECRET~~

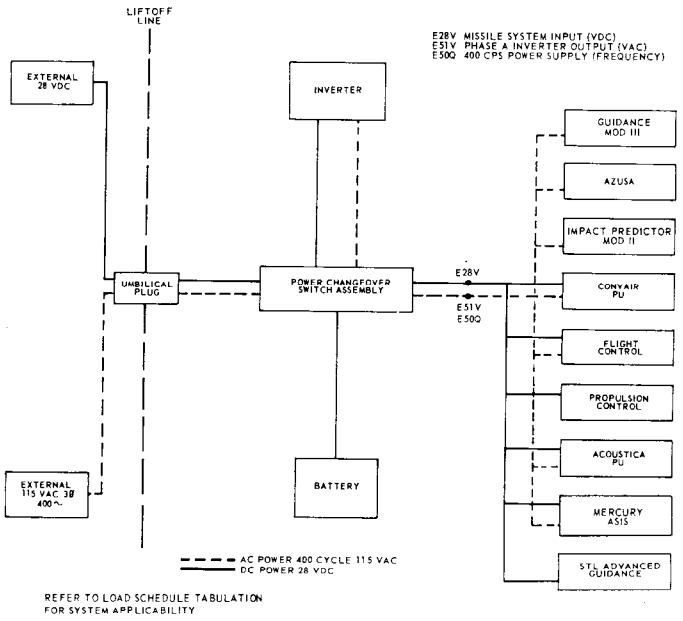

FIGURE 7.3-1 ELECTRICAL SYSTEM

The Leland rotary inverter flight tested for the first time on Missiles 79D and 83D, was planned as a back-up for the standard Bendix unit. This component utilizes similar armature and control mechanisms but is designed to minimize weight requirements for missile use. The Leland inverter is square in shape and smaller in size and also, less sensitive to abrupt changes in missile motion than the Bendix inverter. The Bendix rotary inverter utilized on all other Series D flights is an adaption of an inverter designed for aircraft. It is cylindrical in shape and weighs 71 lbs, ten pounds more than the Leland.

A tabulation of the electrical system load schedule is shown in Table 7.3-1.

TEST RESULTS

Performance of the battery-inverter electrical system was satisfactory on all 15 Series D flights reported here. Battery and inverter outputs were within specifications as indicated by user systems performance. On some flights, minor transients were noted in the inverter

~~SECRET~~

output parameters at the time of booster, sustainer, and vernier cutoff, and retrorocket firing. These were evidently a result of changes in electrical load or missile acceleration and had no detrimental effect on system operation. Electrical power transients which occurred during flight as a result of problems in the system are discussed under Problem Areas.

TABLE 7.3-1 ELECTRICAL SYSTEM LOAD SCHEDULE

MISSILE NO.	PU SYSTEM		GUIDANCE		IMPACT PREDICTOR		OPTICAL	MERCURY
	CONVAIR	ACOUSTICA	RIG	AIG	DOWNRANGE IP	MOD. III INST. REAC.	BEACON	ASIS
42D	CL			OL		X		
48D	CL			X		X	X	
56D	CL	OL	X		X			X
54D		CL		X		X	X	
62D	CL		X		X		X	X
27D	OL	CL	X		X		X	
60D	OL	CL		X		X	X	
32D	CL	OL	X		X			X
66D	CL			X		X		
76D		CL		X		X	X	
79D	CL	OL	X		X			X
71D		CL		X		X	X	
55D	CL	CL	X		X		X	X
83D			X		X		X	
90D		OL	X		X		X	

NOTE: The STL Advanced Guidance System was installed on Missiles 83D and 90D.

CL = Closed-loop operation
OL = Open-loop operation

The following is a summary of performance of the two major electrical components, the main missile battery and the rotary inverter. Performance of the power changeover switch was satisfactory on all flights. Refer to Table 7.3-2.

Main Missile Battery Performance

Missile systems input (d-c) voltage, measured between the power changeover switch and the user system boss, was within 1.5 volts of the average 27.4 vdc at liftoff. The voltage level in each case either remained constant or exhibited a small gradual increase until the battery life was expended (700 to 800 seconds).

TABLE 7.3-2 SUMMARY OF ELECTRICAL SYSTEM PERFORMANCE

MISSILE NO.	LAUNCH DATE	ENGINE DURATION (sec)			INVERTER		BATTERY OUTPUT (vdc)
		BOOSTER	SUSTAINER	VERNIER	FREQ. (cps)	VOLTAGE (vac)	
42D	2-8-60	141.35	256.83	269.17	400	115.2	28.9
48D	4-7-60	DESTROYED PRIOR TO LIFTOFF			398.8	114.7	28.2
56D	5-20-60	136.58	271.08	284.89	399	114.0	27.1
54D	6-11-60	137.62	235.55	292.79	400	114.6	28.6
62D	6-22-60	117.77	284.26	307.69	400	113.8	26.7
27D	6-27-60	131.93	278.68	294.03	400	114.6	26.1
60D	7-2-60	141.03	307.55	277.45[1]	402.2	113.6	27.3
32D	8-9-60	131.56	288.10	301.89	400	114.6	28.8
66D	8-12-60	136.45	259.24	274.43	401.2	114.6	27.4
76D	9-16-60	138.59	274.92	290.68	401.2	115.2	27.5
79D	9-19-60	138.59	282.47	295.22	400	115.1	27.3
71D	10-13-60	140.00	267.38	281.31	From 401 to 402.4	115.7 115.1	27.0 28.2
55D	10-22-60	135.86	283.04	298.13	400.6	114.6	27.1
83D	11-14-60	137.77	269.93	286.23	399.4	115.8	25.8
90D	1-23-61	137.66	271.93	288.77	399	114.0	27.0
AVERAGE					400	114.6	27.4

(1) Vernier engine shutdown occurred when pressure in the propellant feed system decayed below minimum valve spring tension levels because of depleted pneumatic pressure.

Inverter Performance

Two three-KVA rotary inverter models were tested during the period covered in this report. These were the Series D Bendix inverter and the Leland inverter developed as a back-up component. Both performed satisfactorily, with the Leland inverter being slightly more stable during periods of sudden changes in missile acceleration and electrical loading.

Inverter output parameters showed unusual transients of as much as 1.2 vdc accompanied by similar fluctuations in battery voltage, at retrorockets firing on Missiles 66D, 71D, 83D and 90D. Refer to Table 7.3-3. These transients appear to have been the result of partial electrical short circuits, associated with retrorocket firing sequence, either in the firing squibs or the electrical harness. (See Problem Areas for further discussion.)

Transients in inverter output not accompanied by shifts in battery voltage were considered to result from changes in missile acceleration and/or electrical loads. These transients were generally less prominent than those noted in earlier Series D and C flights and were not of sufficient magnitude or duration to affect user system operation.

TABLE 7.3-3 ELECTRICAL SYSTEM TRANSIENTS

MISSILE NO.	MEAS. NO.	UNITS	TRANSIENTS BCO	SCO	VCO	OTHER	CHANGE
56D	E50Q	cps		1			
	E51V	vac		0.3			
54D	E50Q	cps				84.0 sec	0.7
	E51V	vac	0.4	0.4		142.0 sec	1.2
62D	E51V	vac		0.4			
27D	E50Q	cps	2.0	2.0	2.0	Staging	3.0
32D	E50Q	cps	1.2	1.2			
66D	E50Q	cps	0.7	1.5		112.5 sec	1.2
						RRF	1.8
	E28V	vdc				RRF	0.6
	E51V	vac				RRF	0.5
76D	E50Q	cps	2.6	3.3	1.5	RRF	1.3
79D	E50Q	cps				RRF	1.0
	E51V	vac	0.3				
71D	E50Q	cps	0.6	4.5	1.2	RRF	1.8
	E28V	vdc		0.5		RRF	0.5
	E51V	vac		0.5		RRF	0.4
55D	E50Q	cps	0.9			33 sec	1.5
						159 sec	1.0
	E51V	vac	0.5	0.5		33 sec	0.4
83D	E28V	vdc				RRF	0.7
	E51V	vac				RRF	0.4
90D	E50Q	cps				RRF	1.0
	E28V	vdc				RRF	1.2
	E51V	vac				RRF	0.6

NOTE: RRF = Retrorockets Firing

Inverter outputs remained within specifications even during the power transients noted above. Phase A voltage, in each case, assumed a steady-state level after liftoff within one volt of the average 114.6 vac. Steady-state Phase A 400-cycle frequency was maintained within 2.2 cps of the average 400 cps.

PROBLEM AREAS

Electrical system problems which occurred during flight tests covered in this report were located in the power distribution circuitry rather than in the power generating or regulating components. Flight performance was affected by the following two discrepancies in system operation.

Circuitry Discontinuity

During the flight of Missile 62D, a discontinuity in electrical system circuitry between the guidance decoder and the flight programmer prevented initiation of vernier cutoff (VCO) by guidance discrete. The VCO signal, sent at 299.7 seconds was not acted upon and VCO was accomplished at 307.69 seconds by the flight programmer back-up signal. This extended vernier operation caused the re-entry vehicle to impact 18 NM beyond the planned target point. Post flight examination of records taken during the countdown revealed that the discontinuity had existed prior to launch (refer to Section 6.1 - Autopilot, for further details). It was resolved, that on subsequent launches the monitoring of the landline records would be included in the countdown procedures to confirm integrity of the circuit and thereby prevent recurrence of a similar problem.

Electrical Short Circuit

During booster stage operation on the flight of Missile 60D, an intermittent electrical short circuit erroneously energized the Pressurize Vernier Tanks (PVT) relay K32C. This resulted in alternate pressurization and venting of the vernier engine tanks, and subsequent depletion of helium supply pressure to the propellant feed system by 128 seconds. This lack of pressure affected the propulsion system causing a loss of thrust and subsequently an impact 40 NM short of the assigned target point.

Prior to launch, during the vernier engine leak test, the 600J3 umbilical (refer to Figure 7.3-2) was found to contain water. This caused a problem similar to that which occurred during the flight. The umbilical was removed, dried out and reinstalled. This was apparently sufficient, as the problem did not occur again during preflight checks. The recurrence of this problem during flight made it evident that the true cause had not been established. This fact was given more credence as a result of laboratory tests during which a similar umbilical was doused with salt water. Results of this testing were negative, as the umbilical did not short out across the pins.

After detailed review of the events which occurred during ground checkout and flight and thorough analysis of the system circuitry, it was determined that an electrical short circuit between the PVT relay (K32C) and the vernier propellant valves control relay (K44C) would cause a malfunction of the type which occurred during the flight. However, the reason for the existence of this short could not be established from the data available.

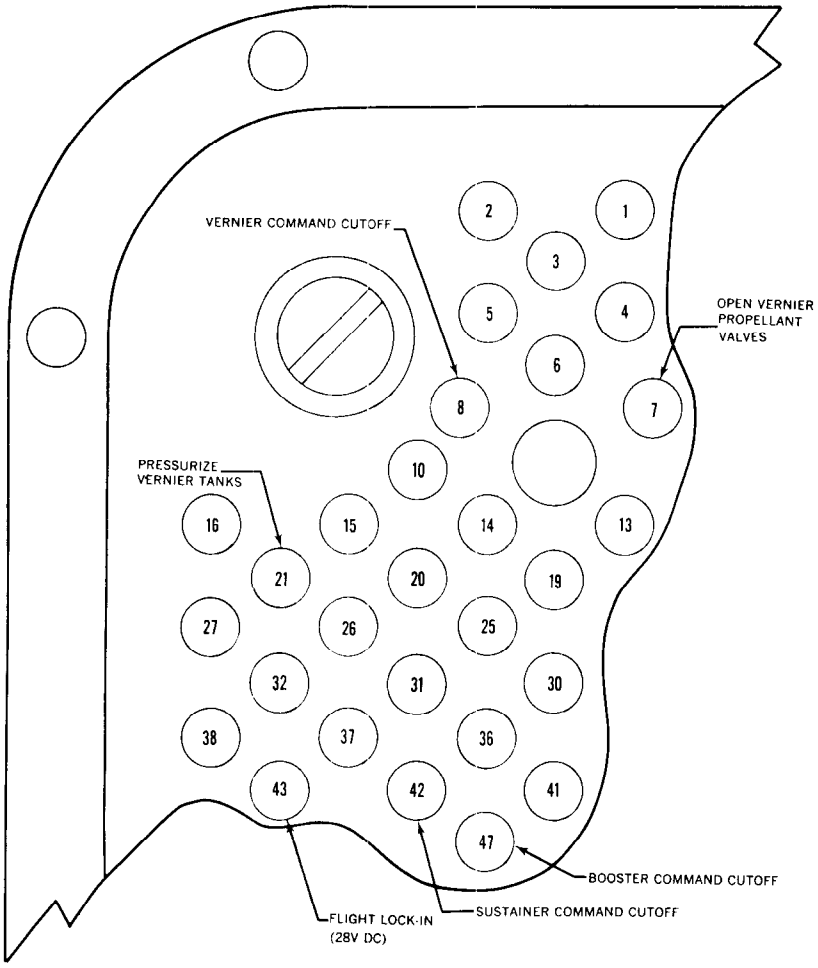

FIGURE 7.3-2 600J3 UMBILICAL RECEPTACLE

On Missiles 66D, 71D and 76D, additional instrumentation was added to monitor the vernier tanks pressurization circuitry and the booster cutoff circuitry. The electrical circuitry, on all missiles subsequent to 60D, was modified in that the PVT sequence was initiated by the booster cutoff relay (K92C) at booster cutoff rather than the programmed PVT relay (K32C) at 165 seconds (BCO plus 64 seconds on vehicles utilizing the square autopilot). The programmed PVT relay sequence was operated open-loop to monitor spurious signals, short circuits or other anomalies. Figure 7.3-3 shows this modified circuitry and location of the additional instrumentation.

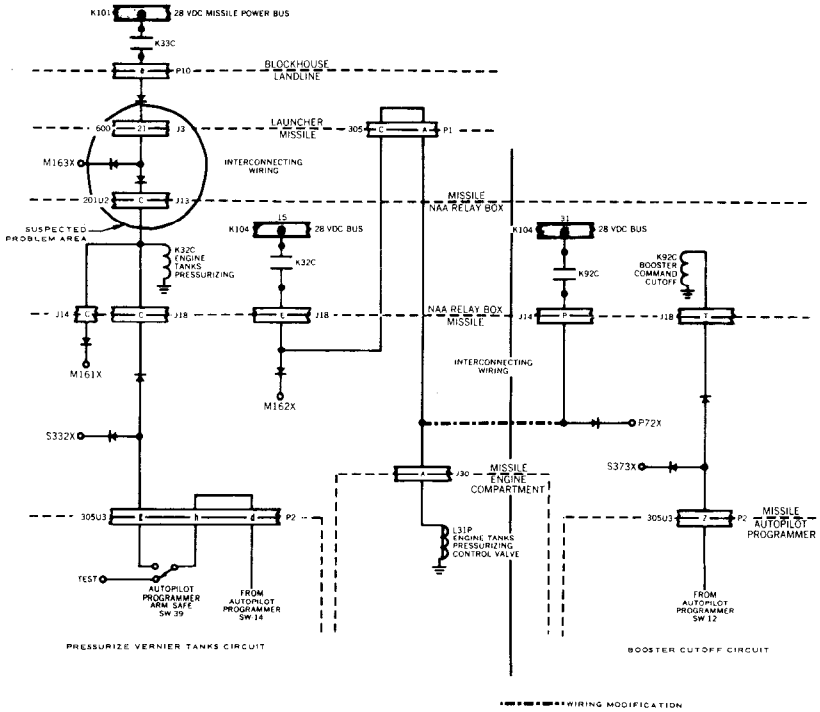

FIGURE 7.3-3 PRESSURIZE VERNIER TANKS CIRCUITRY, SHOWING SUSPECT PROBLEM AREA

Results of data obtained during the flight testing of Missiles 66D, 76D and 71D, indicated normal operation of relays K32C and K92C. No recurrence of the 60D problem has been evidenced on any subsequent Atlas flight.

Discrepancies which occurred in the electrical system, during the flight test period covered in this report, which did not seriously affect flight performance are as follows.

Transients at Retrorockets Firing

Data obtained on four flights (66D, 71D, 83D, and 90D) indicated minor transients in inverter outputs accompanied by similar fluctuations in battery voltage, at retrorockets firing. These transients are characteristic of inverter control reaction to an a-c or d-c power overload not occurring as a result of missile acceleration. Refer to Table 7.3-3. Sufficient data was not available with which to establish the cause of these transients. However, the retrorocket squibs which utilize 28 vdc power, were ignited at the time the transients occurred. It is possible that momentary short circuits in the squibs or associated circuitry were sufficient to cause a d-c overload without affecting the squib ignition sequence.

Electrical System Transients

Unusual transients were noted in the inverter output measurements on Missile 54D at 5, 84 and 142 seconds. These transients did not correlate with any known system demand or event and as they were small in magnitude, user system performance was not affected.

Laboratory tests simulated these transients by inducing an a-c overload on the inverter, but due to the lack of sufficient flight data, the existence or location of such an overload could not be established.

During the flight of Missile 83D, an a-c voltage shift of 1.8 volts occurred prior to booster cutoff. This shift did not correlate with any known flight event and was not accompanied by a change in output frequency which is normally expected during periods of abrupt change in inverter output voltage. Since these conditions were not apparent in the flight data the voltage shift was disregarded.

Missile 55D exhibited unusual inverter output shifts during flight. Both inverter frequency and Phase A voltage maintained the levels which were assumed at liftoff for 33 seconds at which time data indicated abrupt shifts (refer to Table 7.3-3). At booster cutoff both frequency and a-c voltage exhibited the normal transients often accompanying abrupt changes in electrical load and missile acceleration at this time. However, rather than recovering immediately to the steady-state levels as usual, both parameters remained at the displaced level for twenty-one seconds, recovering abruptly to 399.1 cps and 115.0 volts a-c at 159 seconds.

Available data on user system performance, flight control programmer switch activations, missile motion, and telemetry system performance were closely examined for contributing factors. Nothing which might have contributed to the observed electrical system anomalies was found. No conclusions as to the cause of the observed electrical parameter shifts appear possible based on available data.

This page intentionally left blank.

SECTION 7.4 - AZUSA

PURPOSE OF TESTING

The objective assigned to the Azusa system during a flight test is to supply real-time impact prediction data in order to maintain range safety, in addition to providing satisfactory data for post-flight trajectory analysis.

Two outstanding changes in the Azusa system and in the related airborne instrumentation occurred during the latter portion of the Atlas Series D test program discussed here. These changes were:

1. The use of the Mark II Azusa system for real-time range safety purposes.
2. Use of the tilted beam antenna on the missile.

The effect of these changes on the ability of the system to perform its range safety function was of prime interest.

TEST CONDITIONS

The primary function of the Azusa system is to furnish tracking data for use as input to the range safety impact prediction system. The real-time impact points are displayed on plots and indicate where the missile would impact if the flight were terminated at any given instant. In order to furnish a continuous impact prediction display, the Azusa system must maintain radio frequency lock between the airborne and ground station antennas.

A second function of the Azusa system is to furnish data for computing a "Quick-Look" impact point. Directly after vernier cutoff, a "Quick-Look" impact point is computed from each of the available tracking systems and transmitted to the downrange tracking systems for use in acquiring track on the re-entry vehicle. Since this data is needed by the downrange tracking stations five minutes before impact, there is insufficient time to correct the data for ambiguities. It is therefore necessary to maintain non-ambiguous tracking during the free-fall period (between vernier cutoff and the firing of retrorockets) in order to fulfill this second requirement of the system.

Data for post-flight trajectory computations are furnished by the Azusa system. Ambiguous tracking can be compensated for by correcting the data after the flight. The data, however, is invalid during periods of signal dropout. A final impact point is also computed using Azusa data obtained during part of the free-fall period. For continuous post-flight meteric trajectory data and a final impact point, it is necessary to maintain lock during powered flight and immediately thereafter.

The two criteria used in the test results section to determine if satisfactory operation of the Azusa system has been accomplished are as follows:

1. Maintenance of radio frequency lock throughout powered flight.

2. Maintenance of non-ambiguous tracking during at least part of the free-fall period.

The geometry of Azusa parameters is shown in Figure 7.4-1.

GEOMETRY

R = slant range (best value from refraction corrected r_m or r_{cc} data)

α = direction angle with respect to X axis

β = direction angle with respect to Y axis

γ = direction angle with respect to Z axis

MEASURED PARAMETERS

$\ell = \cos \alpha = \frac{X}{R}$

$m = \cos \beta = \frac{Y}{R}$

r = uncorrected slant range (either r_m or r_{cc})

r_m = modulation slant range (nonambiguous)

r_{cc} = incrementally derived range

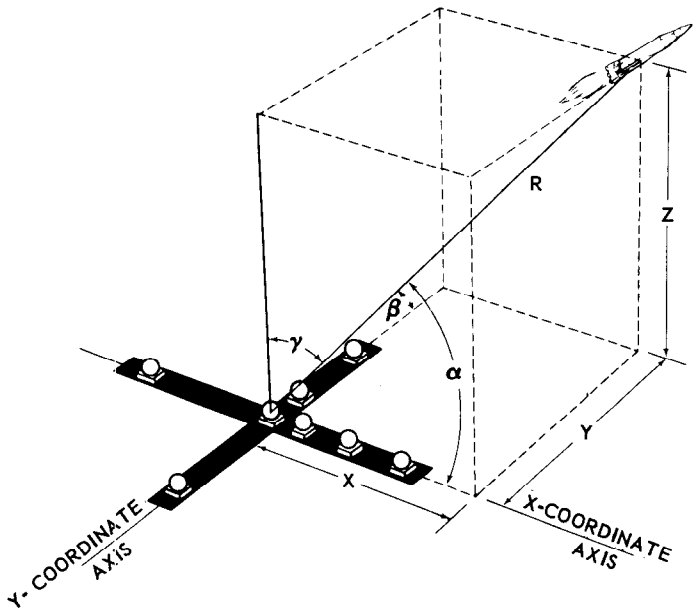

FIGURE 7.4-1 GEOMETRY OF AZUSA PARAMETERS

TEST RESULTS

Of the fifteen Series D missiles summarized in this report, the Azusa system completely satisfied range safety requirements on ten. These were: Missiles 42D, 56D, 54D, 60D, 66D, 76D, 79D, 71D, 55D, and 83D. Azusa data on these flights were available for use in the real-time impact prediction range safety system not later than 65 seconds after launch. The actual time period in which Azusa data was used is presented in Figure 7.4-2. It will be noted that both Mark I and Mark II systems actively tracked Missile 71D. According to the test plan, radar data would be used for range safety when the Mark II system became active at 145 seconds. The Azusa Mark I system fulfilled range safety requirements by furnishing data until 145 seconds.

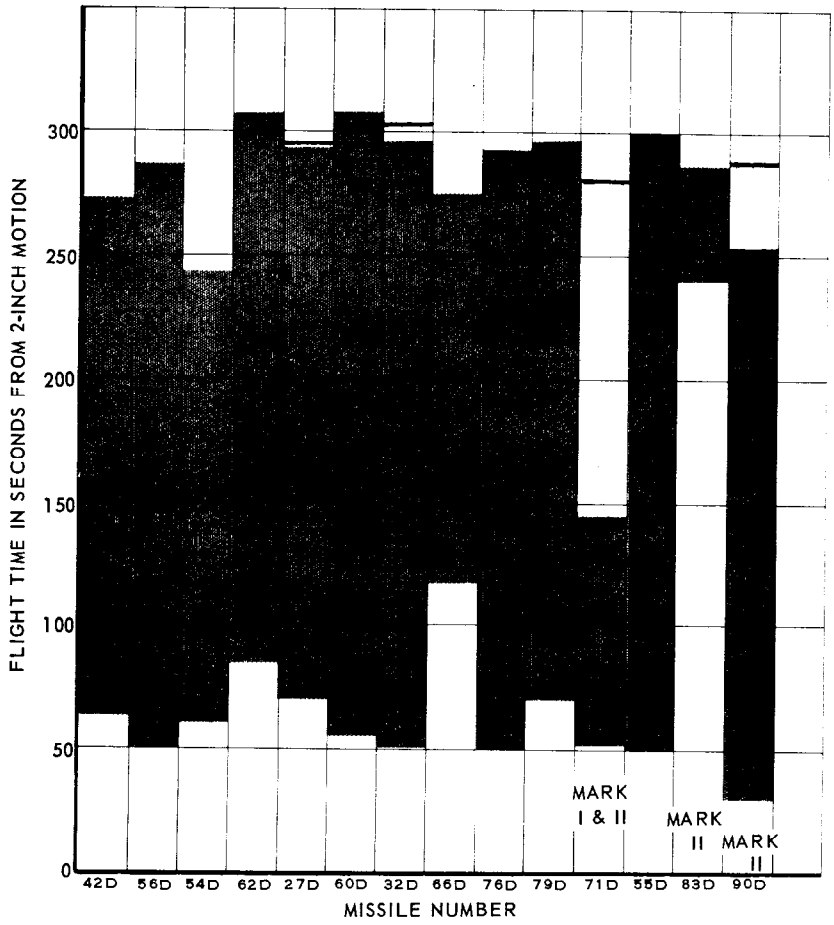

FIGURE 7.4-2 USE OF AZUSA DATA FOR IMPACT PREDICTION

Azusa system operation was partially satisfactory on Missile 62D. Poor look angles resulted from placing the airborne antenna in Quadrant IV instead of Quadrant I, causing a brief loss of lock between 41.2 and 42.1 seconds. During the loss of lock period, the ℓ cosine channel incurred a one fine cycle ambiguity which was not resolved until 150.4 seconds. However, real-time impact point determination was furnished by Azusa from 85 seconds to the end of powered flight along with a valid quick-look impact point. Table 7.4-1 summarizes the performance of the Azusa system during each flight.

TABLE 7.4-1 SUMMARY OF AZUSA SYSTEM PERFORMANCE

MISSILE NO.	POWERED FLIGHT TIME (sec)	END OF AZUSA TRACKING (sec)	METRIC TRAJECTORY DATA AVAILABLE (sec)	SLANT RANGE AT ENGINE SHUTDOWN (feet)	SLANT RANGE AT END OF AZUSA TRACKING (feet)	ANTENNA	SYSTEM	TRANSPONDER
42D	269.17	303.8	302.898	2,374,687	3,067,008	Elliptical Horn	Mark I	B-1
56D	284.98	323.72	318.316	2,820,013	3,722,376	Elliptical Horn	Mark I	B Coherent
54D	242.79	360.635	323.231	2,056,240	4,348,702	Elliptical Horn	Mark I	B-1
62D	307.688	341.66	341.66	2,859,824	3,544,460	Elliptical Horn	Mark I	B Coherent
27D	294.027	261.65	259.948	N/A	2,022,198	Elliptical Horn	Mark I	B Coherent
60D	307.550	351.107	349.403	3,057,919	3,894,892	Elliptical Horn	Mark I	B-1
32D	301.187	351.33	351.33	2,872,681	3,972,884	Elliptical Horn	Mark I	B Coherent
66D	274.43	347.44	345.736	2,458,231	3,889,150	Elliptical Horn	Mark I	B-1
76D	290.91	333.511	332.207	2,639,361	3,485,686	Elliptical Horn	Mark I	B-1
79D	295.22	348.801	337.401	2,888,969	4,127,838	Elliptical Horn	Mark I	B Coherent
71D	280.71	149.96	149.96	2,493,616	526,696	Elliptical Horn	Mark I	B-1
	280.71	323.31	323.31	2,493,616	3,313,336	Elliptical Horn	Mark II	
55D	298.125	347.43	339.330	2,876,608	3,958,098	Elliptical Horn	Mark I	B Coherent
83D	286.34	315.34	313.490	2,582,349	3,158,495	Tilted Beam	Mark II	B Coherent
90D	288.77	252.00	250.45	N/A	N/A	Tilted Beam	Mark II	B Coherent

Azusa tracking data was not obtained on Missile 48D due to an incident which occurred prior to liftoff resulting in the destruction of the missile. Preflight Azusa operation, however, appeared to be normal.

MARK II CONFIGURATION

The Mark II Azusa system was utilized on Missiles 83D, and 90D and partially on 71D. This system employs the same basic electronic measuring configurations as the Mark I system, however it has the added advantage of a longer baseline cosine system. This longer baseline affords the system a resolution of 2×10^{-7}, or 0.2 parts per million, in the extended baseline direction cosine data. Further up-grading of data quality has been achieved in the Mark II system in the following manner:

1. New range logic,
2. New cosine logic,
3. Narrow banding of data channels,
4. Inclusion of battle shorting equipment,
5. Thermal stability in antenna pads,
6. More accurate surveying of antenna field,
7. Multiple tower and reference waveguide zero setting and equipment calibration,
8. Improved basic hardware.

A schematic of the Mark II ground station configuration is shown in Figure 7.4-3. In addition to the improved resolution of the extended baseline 500-meter cosine parameters (ℓ_e and m_e), these parameters yield higher quality angular rate information than the 50-meter cosines (ℓ and m cosine). Anomalies in the tropospheric refractive profile cause rather severe angular rate disturbances which can be decreased only by using a longer baseline system. Comparisons of data obtained from the 50 and 500-meter cosine systems have shown that the disturbances can be decreased almost inversely with an increase in the baseline length. This improved angular rate accuracy allows the Azusa data to be compared with precise guidance systems, such as the all-inertial system, for guidance evaluation purposes.

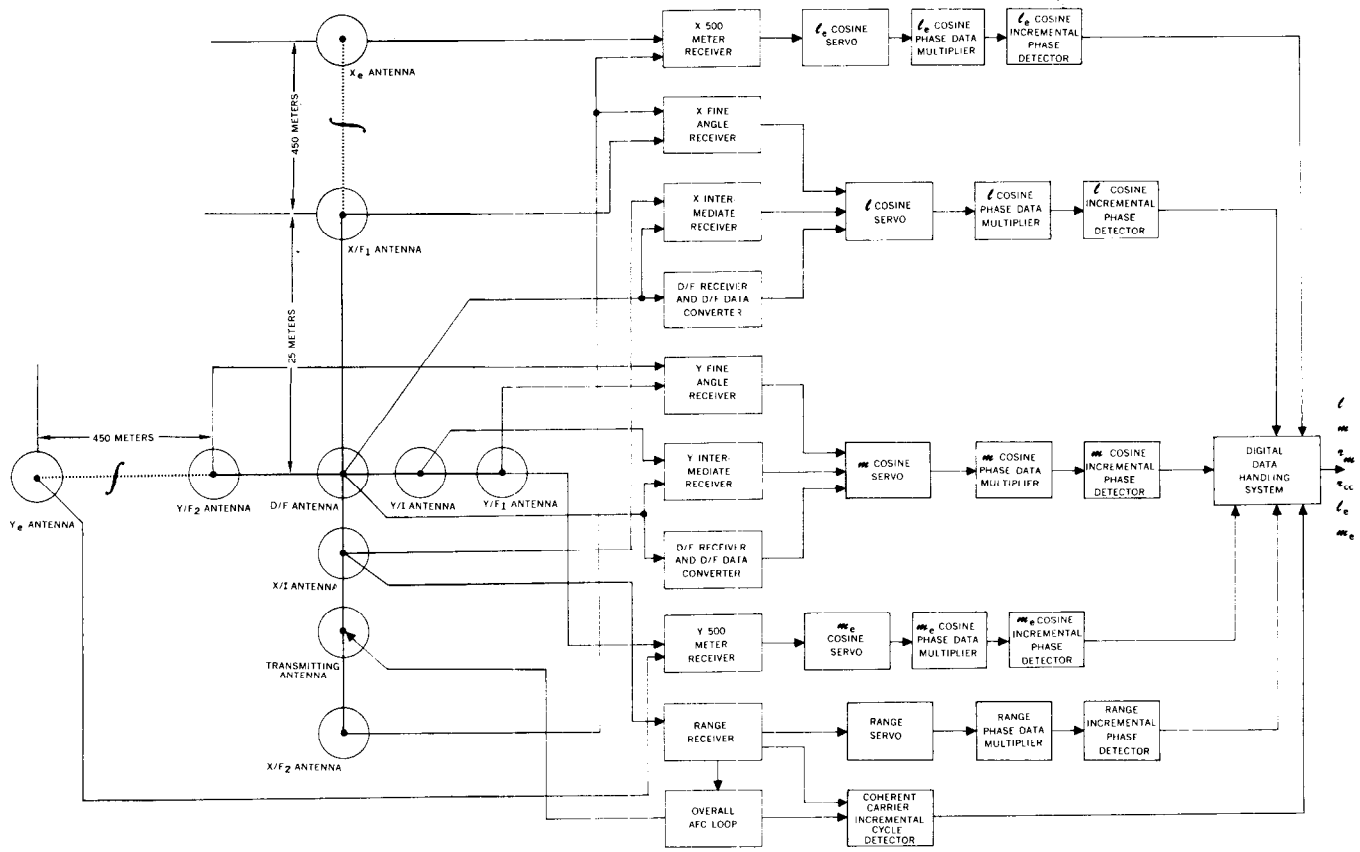

FIGURE 7.4-3 AZUSA SYSTEM GROUND STATION, MARK II

Data Quality Comparison

Dispersions in the 500-meter extended baseline system and the 50-meter baseline system for Mark II are presented for Missile 90D. Although the Azusa system did not satisfy the range safety requirements after 252 seconds of flight, data representative of the Mark II system was acquired to this time. The reduction of data dispersions between 50-meter data and extended baseline data, and between the modulation range (r_m) and carrier range (r_c) data can be seen in Figure 7.4-4 through 7.4-6.

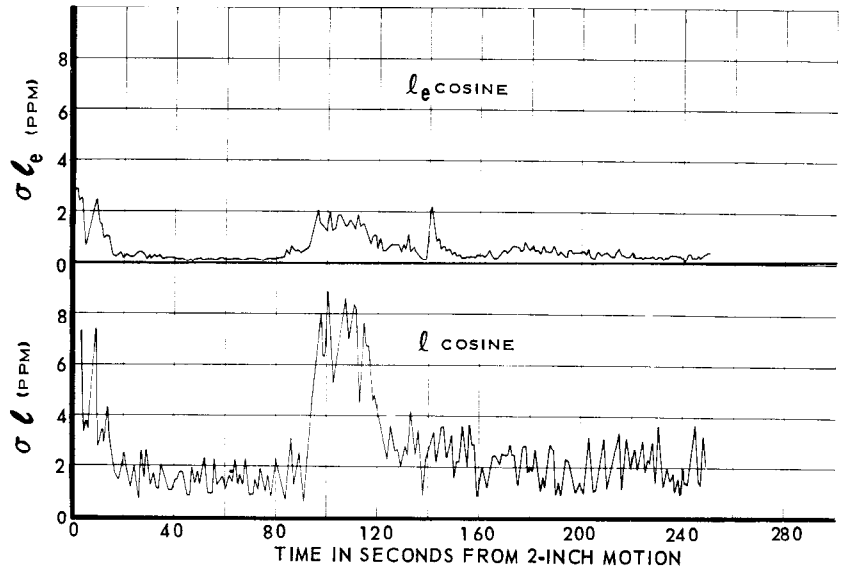

FIGURE 7.4-4 DISPERSION OF ℓ COSINE DATA

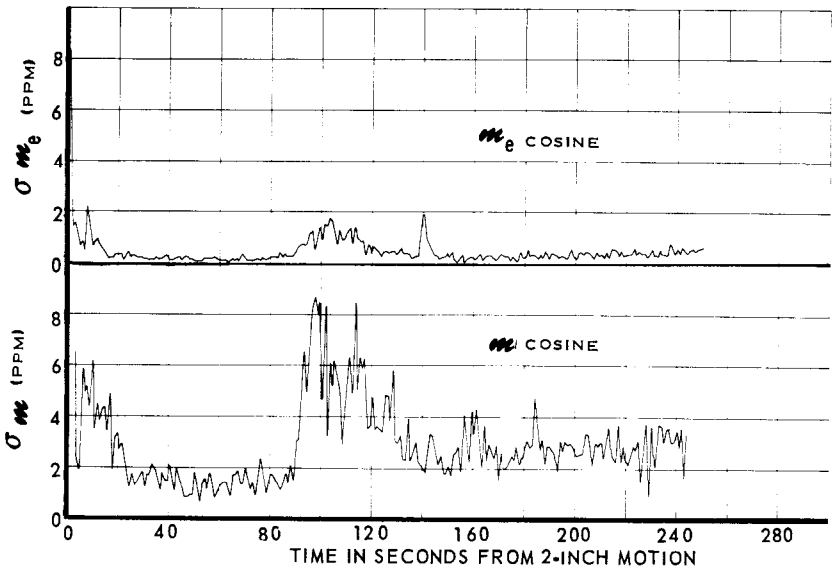

FIGURE 7.4-5 DISPERSION OF m COSINE DATA

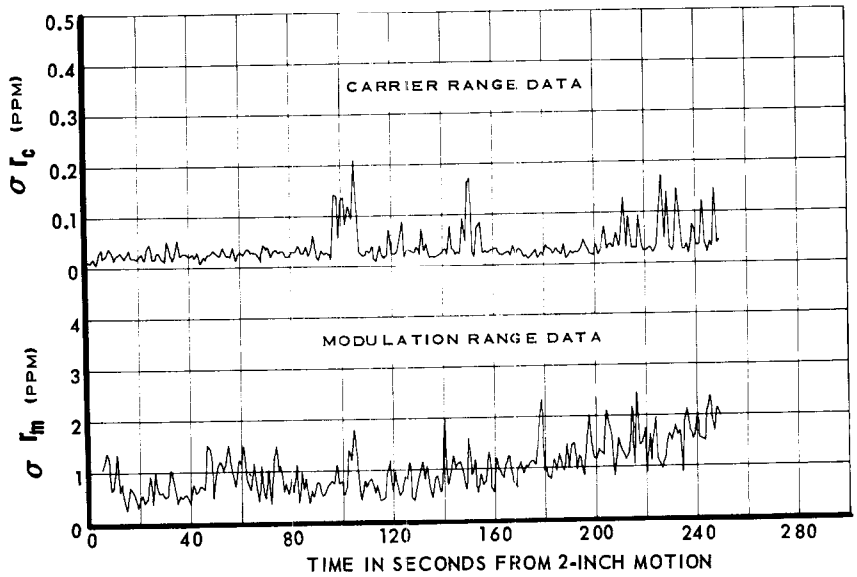

FIGURE 7.4-6 DISPERSION OF RANGE DATA

Antenna Configuration

The airborne antenna configuration for the Atlas missile is a horn type antenna mounted on either a tripod which extends 40 inches from the missile or a boom extending 32 inches from the missile frame. This particular arrangement was found to be suitable for overcoming problems in excess reflected energy from the airframe itself and in yielding better look angles to the Azusa ground station. The elliptical horn antenna was used on all the Series D missiles discussed in this report with the exception of Missiles 83D and 90D which were flown with the tilted beam antenna installed. The advantage of the elliptical horn antenna is its high gain; however, during the early portion of flight (0 to 60 seconds) the pattern of the antenna is such as to yield lobing effects on the data. Multiple lobes are inherent to antennas of this type due to constructive and destructive interference caused by reflected energy. These lobes, when viewed by the Azusa ground station become phase disturbances in the received radiated data and consequently induce a severe noise condition on the final parameters of ℓ and ∞ cosine and range data. The tilted beam antenna was designed to overcome the lobing effects in the early portion of flight. This antenna has the advantage of a broader pattern but the disadvantage of lower gain. As the name implies, the antenna tilts the radiation away from the booster fairing, thus reducing reflection. Plots of the patterns of both the elliptical horn and the tilted beam antenna, which show the difference in lobe structure and beam width, are presented in Figure 7.4-7.

SECRET

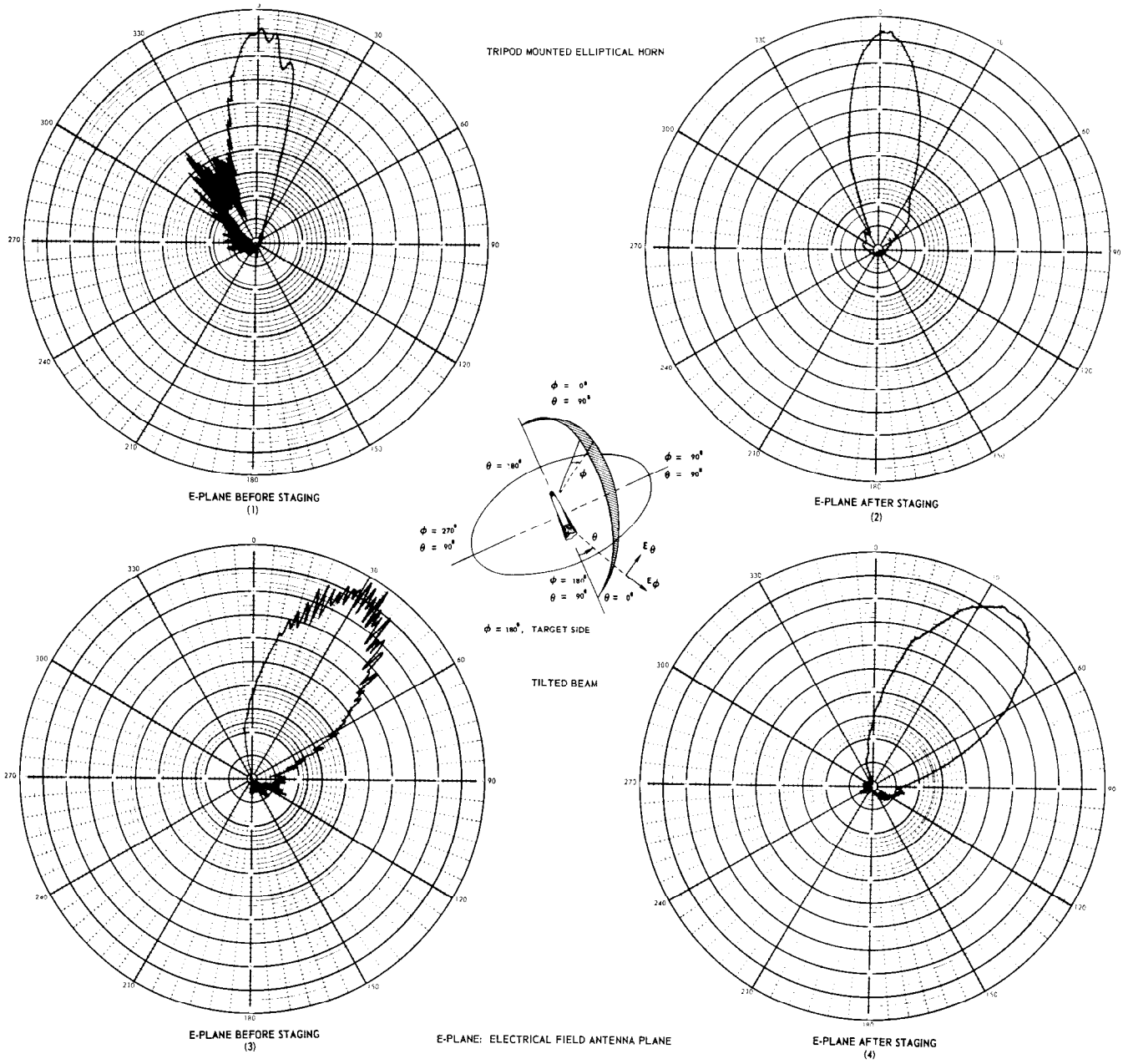

FIGURE 7.4-7 AZUSA ANTENNA PATTERNS

SECRET

Antenna Comparison

Signal strength received at the airborne transponder and at the ground antennas during the flight of Missile 54D are compared with the 90D signal strength data. The elliptical horn antenna was utilized on 54D whereas the tilted beam was used on 90D. The automatic gain control plots on Missile 54D, as shown in Figure 7.4-8, show erratic dips in signal strength due to antenna lobing for the first 40 seconds of flight. The plots for Missile 90D, as shown in Figure 7.4-9, indicate the improvement obtained when lobes are reduced in quantity and severity.

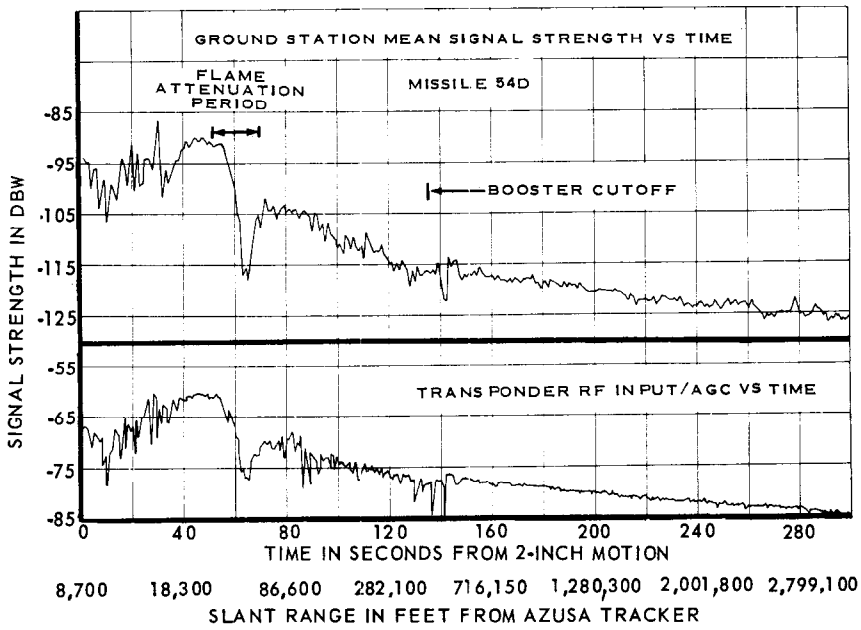

FIGURE 7.4-8 AUTOMATIC GAIN CONTROL, MISSILE 54D

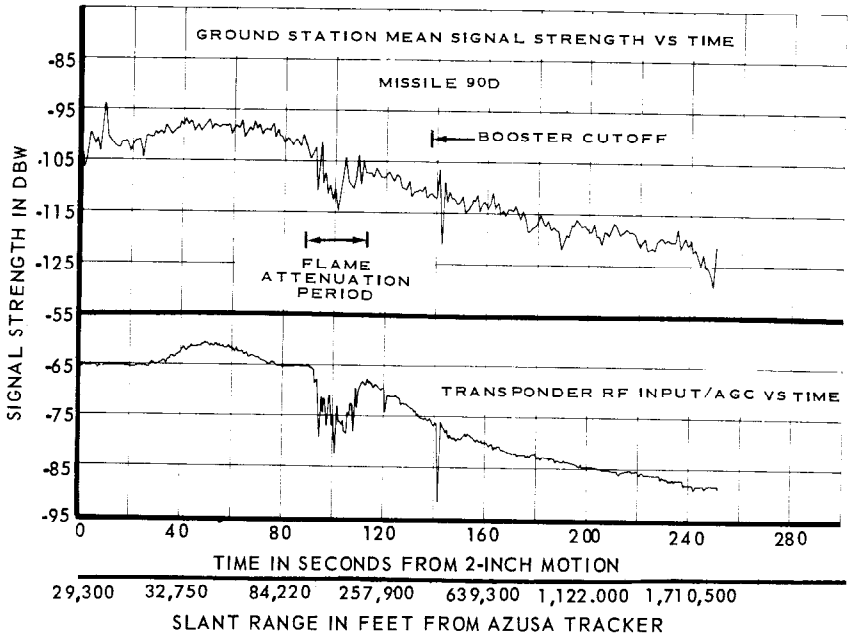

FIGURE 7.4-9 AUTOMATIC GAIN CONTROL, MISSILE 90D

Flame attenuation of signal strength occurred between 55 and 72 seconds on Missile 54D and between 92 and 112 seconds on Missile 90D. Flame attenuation occurs whenever the trajectory path of the missile places the airborne antenna in a position such that the expanding exhaust gases interfere with the signals. Neither antenna configuration tended to lessen the effects of the flame attenuation phenomena significantly.

After booster jettison, the problem of energy being reflected from the booster fairing is no longer present and both antennas produce relatively smooth lobe patterns. It will be noted, however, that the signal strengths recorded on the 90D flight decrease more rapidly after booster cutoff than do the signals of the 54D flight. This is due to the elliptical horn antenna's advantage of high gain during the latter portions of a flight. The tilted beam antenna, although it has a lower maximum gain, receives and radiates sufficient signals to remain within the theoretical limits of the transponder and ground station receivers during powered flight and the free-fall period.

ELLIPTICAL HORN MAXIMUM GAIN

Before Staging: 14.4 db

After Staging: 15.5 db

TILTED BEAM MAXIMUM GAIN

Before Staging: 13.0 db

After Staging: 10.09 db

Impact Prediction Accuracy

The Azusa system furnished real-time impact predictions for range safety on the 14 Series D flights. The extent to which Azusa data was used for range safety impact prediction is graphically illustrated in Figure 7.4-2. The quality of the data used for impact determination, however, is presented in Figure 7.4-10. The σ_X is the standard deviation of the semi-major axis of the miss ellipse while σ_Y refers to the semi-minor axis. A miss ellipse is formed by computing impacts from a succession of data points (usually 5 to 10 seconds of data) during the free-fall period. This gives a measure of the dispersions present in the data and hence is a representation of data quality.

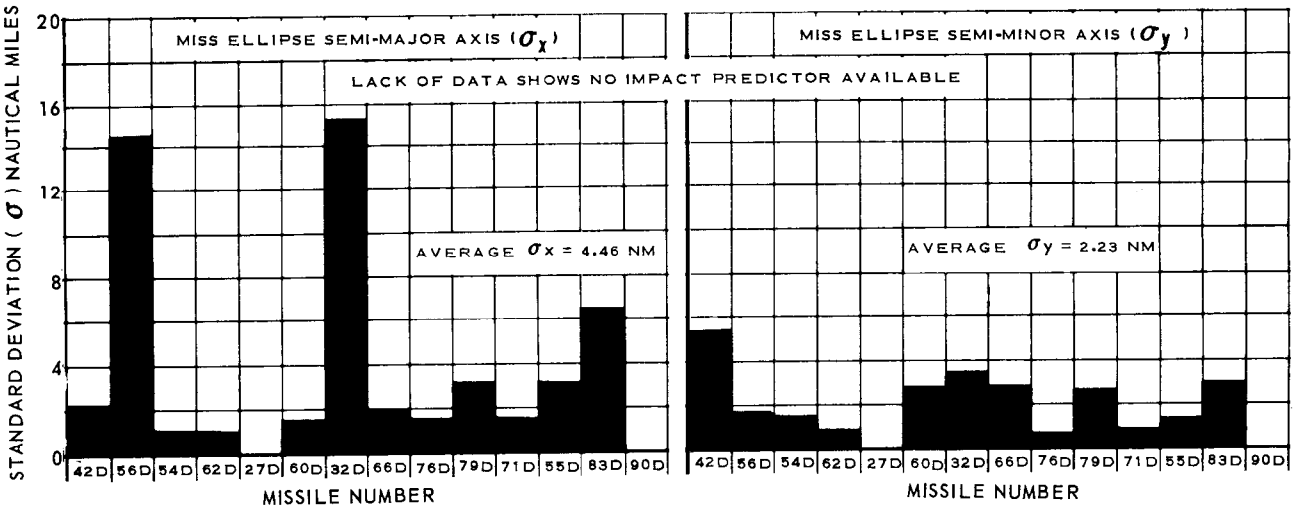

FIGURE 7.4-10 AZUSA DATA QUALITY FOR IMPACT DETERMINATION

Errors in the final impact point can be predicted using the errors in position and velocity at engine cutoff. Figures 7.4-11 and 7.4-12 show the errors in the downrange and cross-range position of impact if position errors of 1,000 feet and 1,000 PPM were present in the range and cosine data after vernier cutoff. Similarly, velocity errors of 1 ft/sec and 1 PPM/sec were transformed into errors in impact position and displayed in Figures 7.4-13 and 7.4-14. These values were chosen for their ease of computation and display. Expected error in position and velocity are presented in Table 7.4-2. Impact errors using any desired Azusa parameter error can be determined from the appropriate graph by dividing the points on the curve by the above rated errors and considering the answer as a partial derivative. For example, if it is necessary to know what kind of downrange error will result from an input range error of 100 feet at a 300-nautical mile cutoff range, simply multiply the downrange error on the graph at 300 NM by 100/1000 or by 0.1. The same procedure is true for the cosine and rate errors.

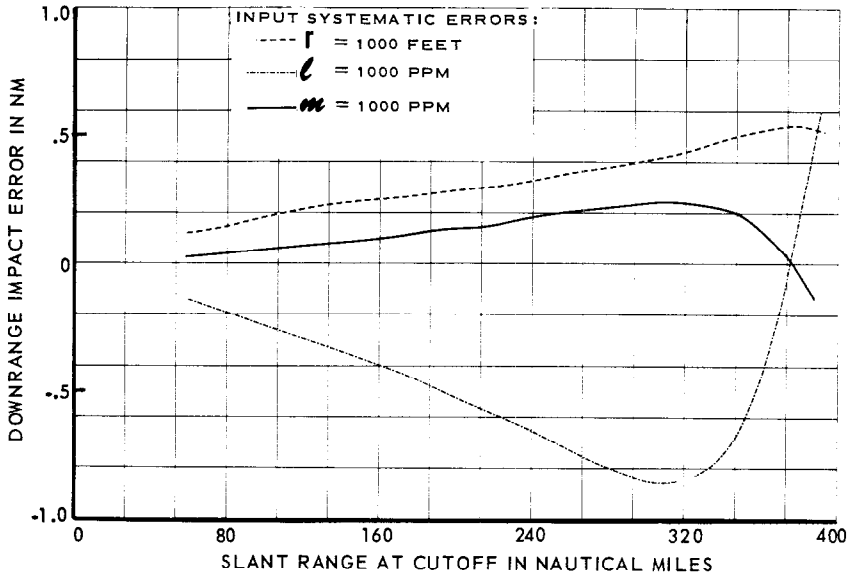

FIGURE 7.4-11 DOWNRANGE IMPACT ERROR VS SLANT RANGE AT CUTOFF (SYSTEMATIC)

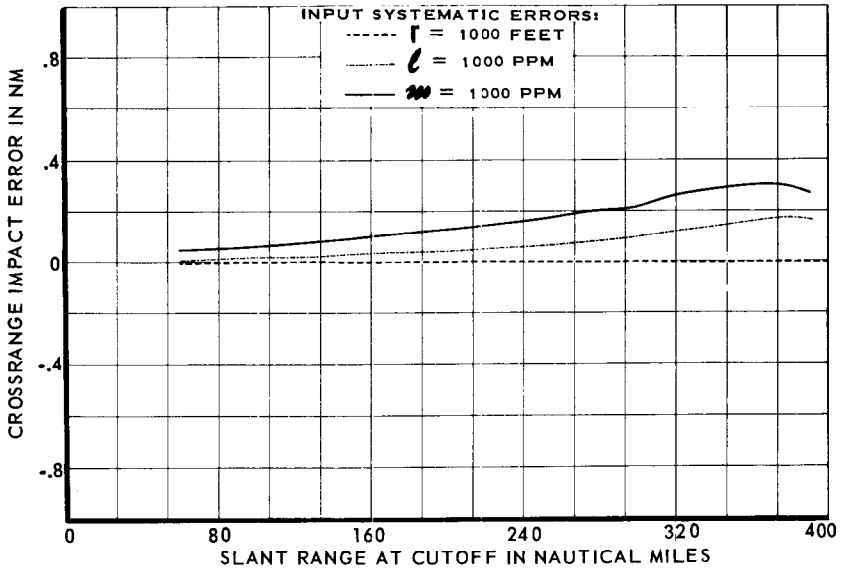

FIGURE 7.4-12 CROSSRANGE IMPACT ERROR VS SLANT RANGE AT CUTOFF (SYSTEMATIC)

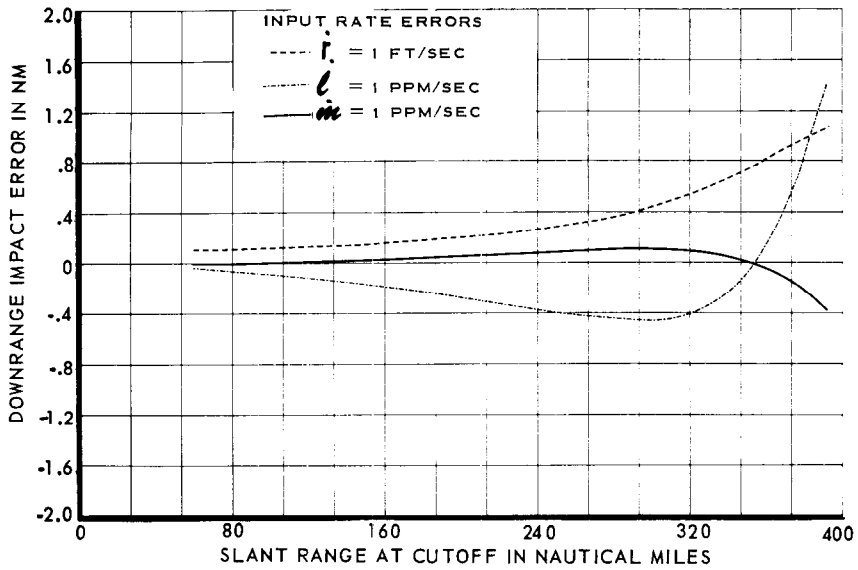

FIGURE 7.4-13 DOWNRANGE IMPACT ERROR VS SLANT RANGE AT CUTOFF (RATE)

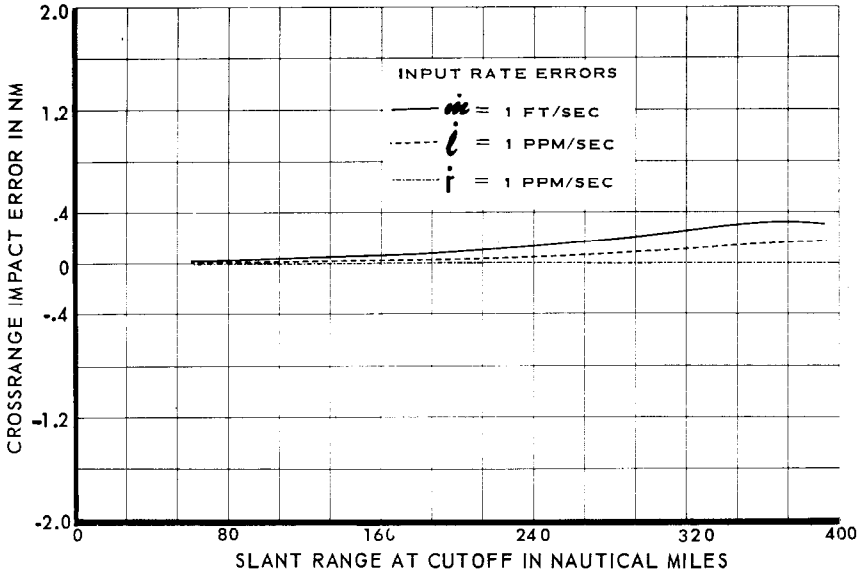

FIGURE 7.4-14 CROSS RANGE IMPACT ERROR VS SLANT RANGE AT CUTOFF (RATE)

Azusa Accuracy

Two sets of position and velocity error plots are included and are considered representative of the Mark I and Mark II data quality (Figure 7.4-15 through 7.4-18). These errors, normally referred to as GDOP or Geometric Dilution of Precision, included the Azusa systematic bias errors, expected cosine and range rate errors, and random errors which arise out of quantizing electronic data handling, and external noise. Table 7.4-2 is a list of the errors used to compute these error functions.

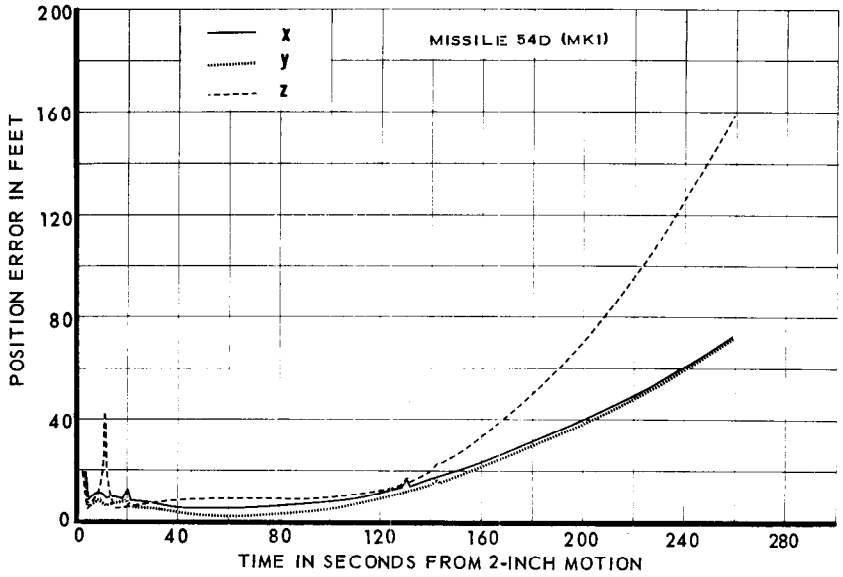

FIGURE 7.4-15 POSITION ERROR VS TIME, MARK I SYSTEM

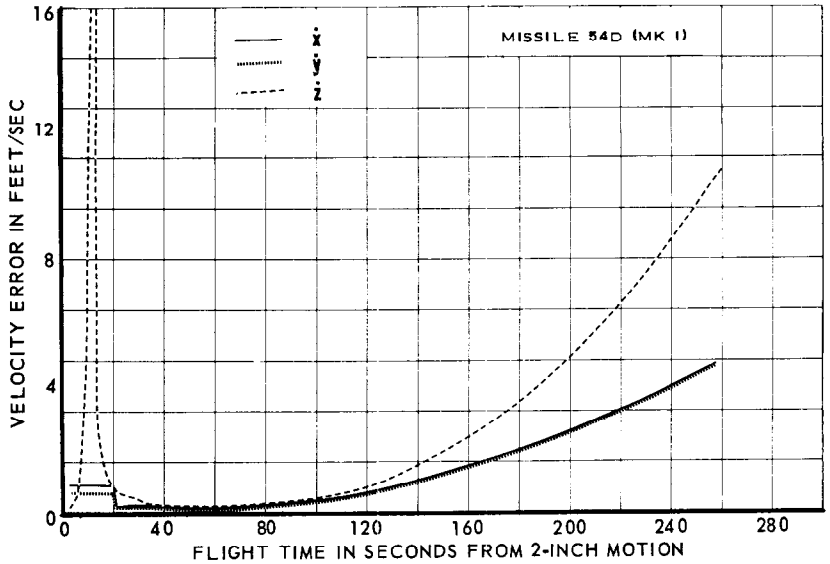

FIGURE 7.4-16 VELOCITY ERROR VS TIME MARK I SYSTEM

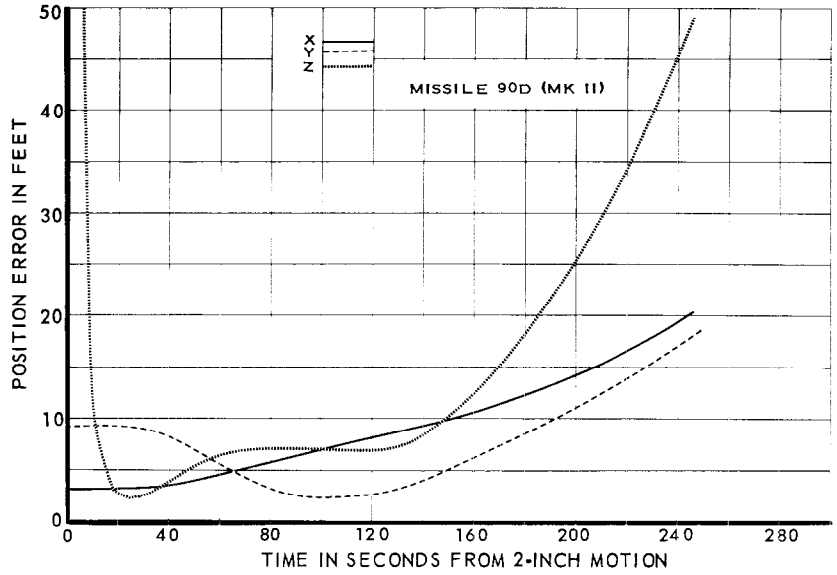

FIGURE 7.4-17 POSITION ERROR VS TIME, MARK II SYSTEM

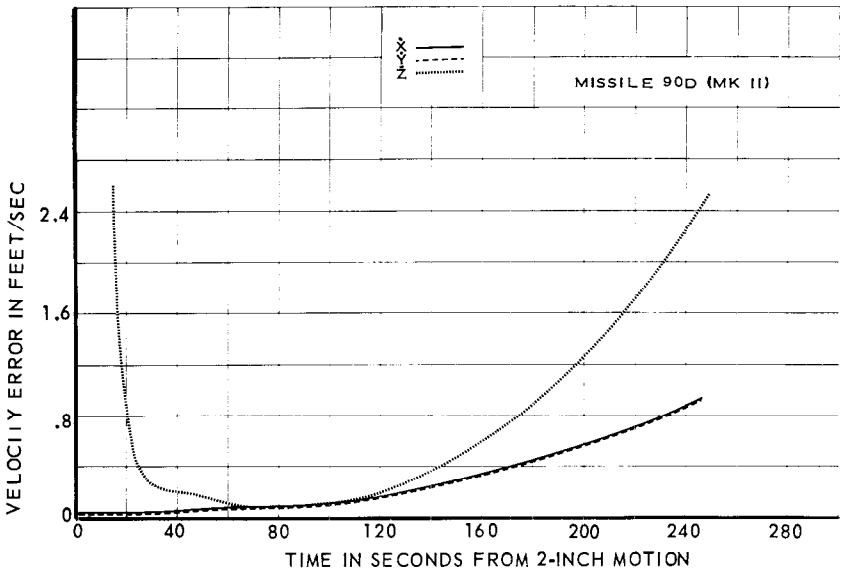

FIGURE 7.4-18 VELOCITY ERROR VS TIME, MARK II SYSTEM

TABLE 7.4-2 SYSTEM ERRORS FOR ERROR FUNCTION COMPUTATIONS

	SYSTEM	
	MARK I	MARK II
Systematic Errors		
$\sigma\ell$	30×10^{-6}	10×10^{-6}
σm	30×10^{-6}	10×10^{-6}
σr_m	35 ft	10 ft
σr_c	35 ft	10 ft
$\sigma \ell_e$		10×10^{-6}
σm_e		10×10^{-6}
Rate Errors		
$\sigma \dot{\ell}$	2×10^{-6} 1/sec	2×10^{-6} 1/sec
$\sigma \dot{m}$	2×10^{-6} 1/sec	2×10^{-6} 1/sec
$\sigma \dot{r}_m$	1.0 ft/sec	1.0 ft/sec
$\sigma \dot{r}_c$	0.1 ft/sec	0.1 ft/sec
$\sigma \dot{\ell}_e$		0.4×10^{-6} 1/sec
$\sigma \dot{m}_e$		0.4×10^{-6} 1/sec

PROBLEM AREAS

On Missile 27D, a malfunction in the RF system at the transponder caused premature loss of tracking at 261.65 seconds.

A transponder malfunction on 32D caused loss of lock between 289.3 and 294.8 seconds in all channels, and between 304.7 and 305.4 seconds in the ℓ and m channels. A final impact point was computed using Azusa free-fall data after 305.4 seconds.

The Azusa system on Missile 90D lost lock at 252 seconds when the ground station D/F antenna slewed completely off of its null position. By 285.55 seconds lock had been reacquired in all channels and by 315.45 seconds the system was producing non-ambiguous tracking data. However, an impact point could not be obtained from Azusa data since the system was invalid between vernier cutoff (288.58 seconds) and the time of retrorockets firing (305.67 seconds).

This page intentionally left blank.

SECTION 7.5 - RANGE SAFETY COMMAND

PURPOSE OF TESTING

Testing of the range safety command system was continued during the Series D flight test program reported here to demonstrate the reliability and capability of the system to fulfill range safety requirements. The range safety system is designed to protect personnel and property from the danger of possible missile impact outside of the target area.

TEST CONDITIONS

Protection for areas outside the target area is effected by the range safety system when necessary, either by cutting off the engines thereby restricting missile range or by destroying the missile. The range safety officer (RSO) is responsible for determining if the missile constitutes a hazard. He observes an instantaneous plot of the predicted missile impact point, based upon termination of thrust and instantaneous plots of the missiles position compared to its predicted position. The RSO may send either the manual fuel cutoff (MFCO) or the missile destruct command at any time for safety reasons. The MFCO signal shuts off the propellants to all five rocket engines. The destruct command explodes the missile by igniting a small charge located at the junction of the lox and fuel tanks.

The RSO may also use MFCO as a backup for the vernier cutoff discrete command which is normally sent by the guidance system. For additional safety, the sustainer cutoff (SCO) guidance discrete is followed by an automatic sustainer fuel cutoff (ASFCO) command from the impact prediction system. Since the impact point is moving too fast at this time for the RSO to take effective action, the ASFCO signal is sent automatically about 0.18 seconds after the SCO guidance discrete or when the locus of instantaneous impact points crosses a predetermined safety line (Refer to Figure 7.5-1). During vernier solo operation, the impact point moves at approximately 3 NM per second and there is sufficient time for the RSO to exercise effective manual control by use of either the MFCO or destruct commands.

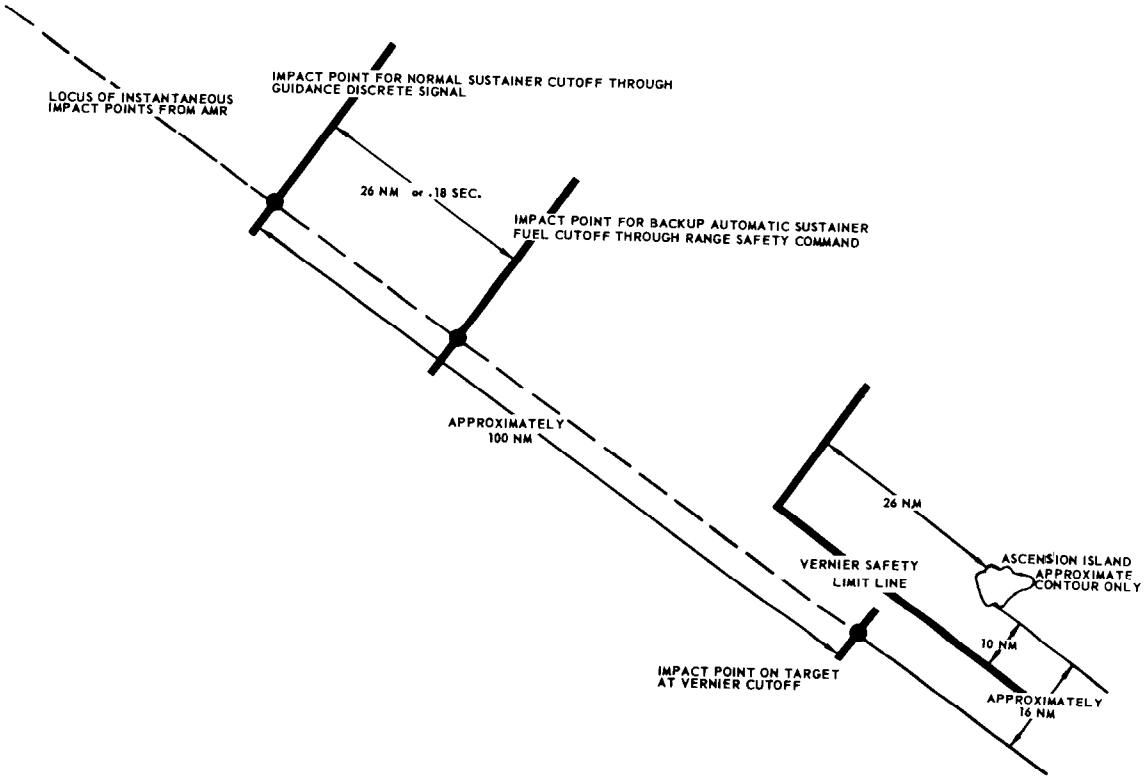

FIGURE 7.5-1 AUTOMATIC SUSTAINER FUEL CUTOFF PROTECTION FOR ASCENSION ISLAND NEAR TARGET AREA

The ground portion of the range safety system consists of the impact predictor system, automatic plotting boards and UHF transmitters. The operation of the impact predictor system is discussed in the Azusa section of this report. The UHF transmitters are located at each of three locations: Cape Canaveral, San Salvador and Grand Turk Island.

The airborne system (Figure 7.5-2) receives the commands transmitted by the pertinent ground station (Figure 7.5-3) and relays the signal directly to the engine relay box for cutoff or to the destructor package for flight termination.

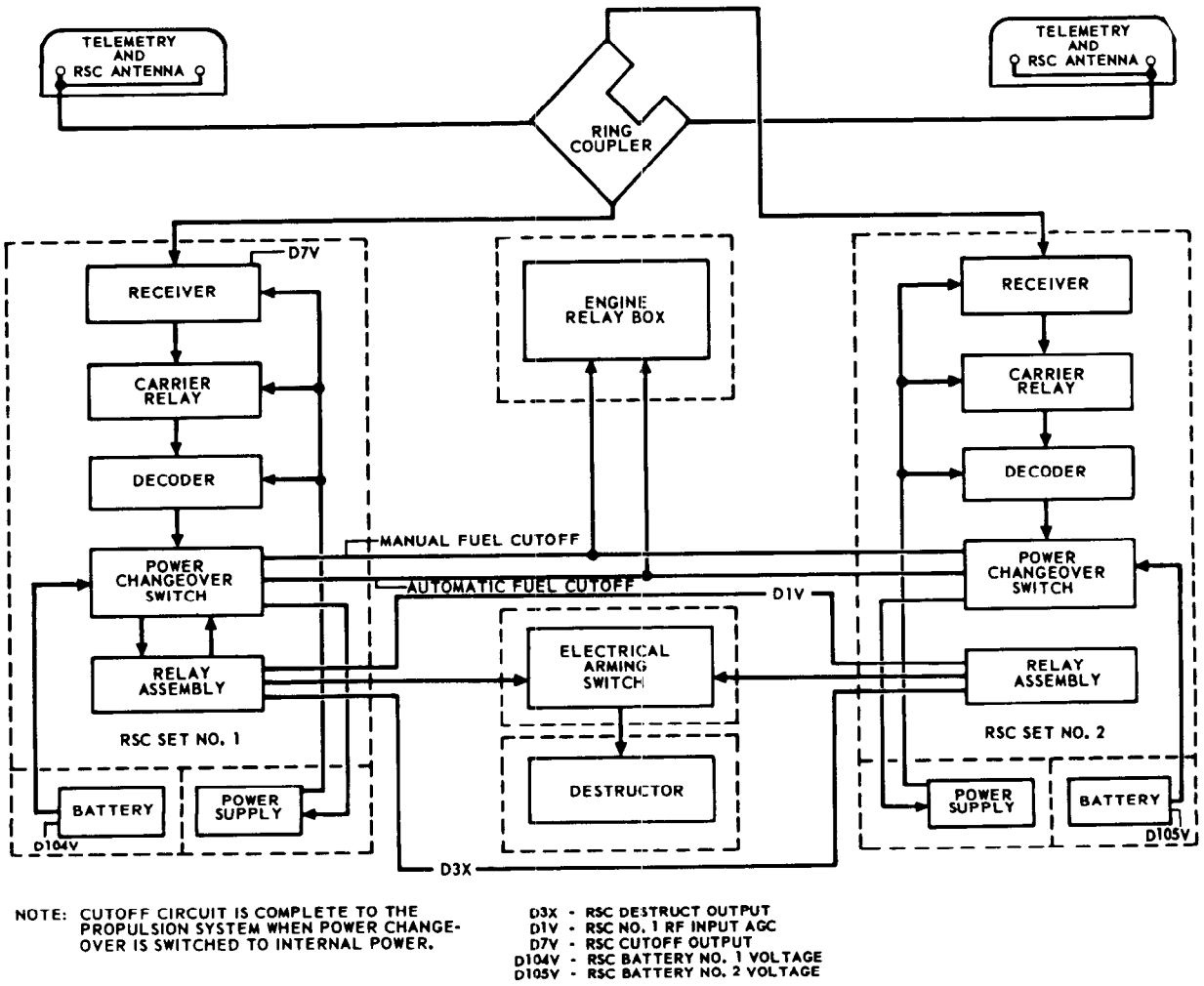

NOTE: CUTOFF CIRCUIT IS COMPLETE TO THE PROPULSION SYSTEM WHEN POWER CHANGE-OVER IS SWITCHED TO INTERNAL POWER.

D3X - RSC DESTRUCT OUTPUT
D1V - RSC NO. 1 RF INPUT AGC
D7V - RSC CUTOFF OUTPUT
D104V - RSC BATTERY NO. 1 VOLTAGE
D105V - RSC BATTERY NO. 2 VOLTAGE

FIGURE 7.5-2 AIRBORNE RANGE SAFETY COMMAND SYSTEM

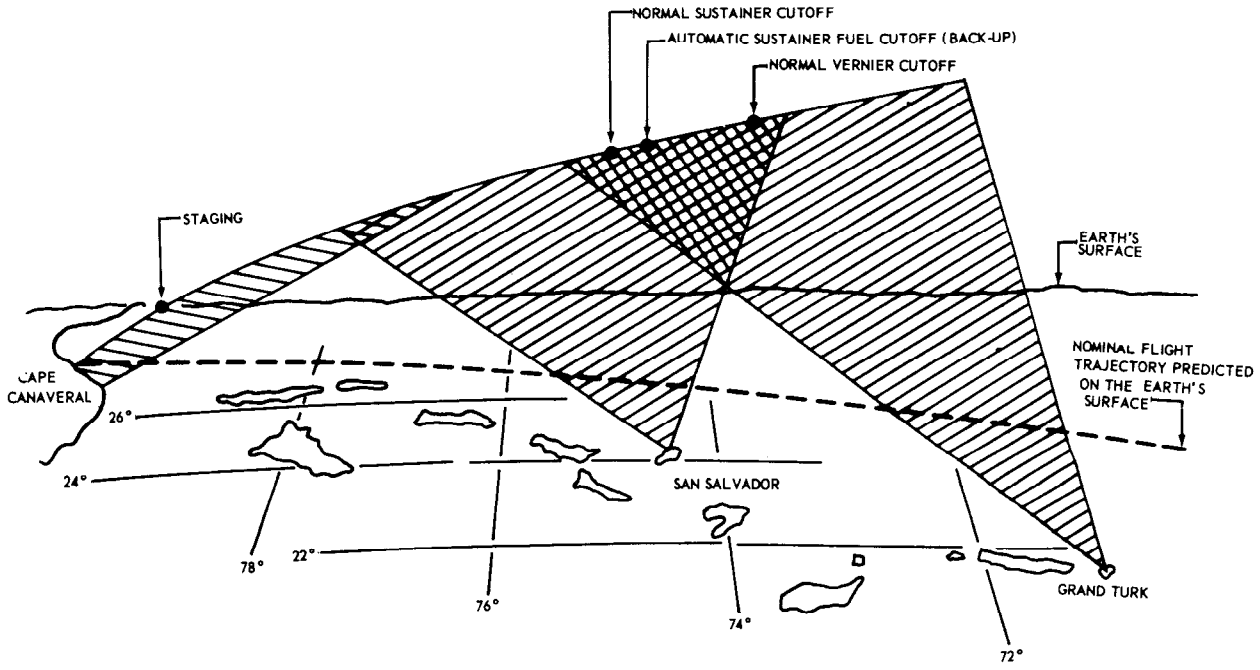

FIGURE 7.5-3 DOWNRANGE COVERAGE BY RANGE SAFETY COMMAND ULTRA-HIGH FREQUENCY TRANSMITTERS

CONFIGURATION CHANGES

The RSC system used for these tests was essentially the same as that used for the earlier Series D test program. The only major changes were in the weight and the amperage consumption of the airborne receiver. The weight of the airborne receiver was reduced from 55 lbs to 12 lbs, and the amperage requirement was reduced from approximately 3 amps to 1.2 amps. The former receiver is identified as ARW 59. The new receiver is called ARW 62.

TEST RESULTS

The performance of the range safety system was determined to be satisfactory during all of the fourteen flights covered in this report. Signal strength received at the missile was more than adequate during all flights. All range safety commands sent were received by the airborne sets. The messages were decoded, and the resulting cutoff signals were properly generated in the missile circuitry. A resume of RSC system operation including commands sent to the missile is presented in Table 7.5-1.

TABLE 7.5-1 SUMMARY OF RANGE SAFETY COMMAND SYSTEM PERFORMANCE

MISSILE NO.	FLIGHT DATE	RECEIVER	RECEIVED SIGNAL STRENGTH(1)	ASFCO DECODED	MFCO DECODED	RE-ENTRY VEHICLE SEPARATION	COMMENTS
42D	3-8-60	ARW-62	25 mv	256.74	269.24	284.4	Satisfactory. First flight test of the ARW-62 receiver. The RSC system initiated SCO and VCO via the ASFCO and MFCO signals, respectively, since the all-inertial guidance system was operated open-loop.
48D	4-7-60	ARW-62					The missile was destroyed prior to liftoff.
56D	5-20-60	ARW-59	40 mv		330.33	305.92	Satisfactory. ASFCO was not planned for this flight. Antenna lobing caused three dropouts during MFCO.
54D	6-11-60	ARW-62	10 mv	237.65	300.73	257.55	Satisfactory.
62D	6-22-60	ARW-62	100 mv	284.28	327.50	319.1	Satisfactory. All range safety functions were properly generated and received.
27D	6-27-60	ARW-62	5 mv	278.68	326.44	313.7	Satisfactory. Due to a short in the RSC No. 1 receiver at the time of transmission of the MFCO signal only the No. 2 receiver acted upon the signal.
60D	7-2-60	ARW-62	10 mv	307.55	345.20	355.35	Satisfactory. The ASFCO signal initiated SCO due to a guidance hardware failure. Re-entry vehicle separation was effected by the programmer.
32D	8-9-60	ARW-62	(2)	288.14	335.26	325.1	Satisfactory. Signal strength was greater than 85 IBW to at least 320 seconds.
66D	8-12-60	ARW-62	40 mv	259.18	320.22	290.27	Satisfactory. The ASFCO signal preceded the SCO guidance discrete by 0.12 seconds.
76D	9-16-60	ARW-62	100 mv	274.82	320.10	306.7	Satisfactory. The ASFCO signal preceded the SCO guidance discrete by 4 milliseconds.
79D	9-19-60	ARW-62	25 mv	282.92	330.24	317.5	Satisfactory. Two range safety functions were planned and accomplished. Signal strength was more than adequate.
71D	10-13-60	ARW-62	30 mv	266.675	320.70	297.6	Satisfactory. The ASFCO signal preceded the SCO guidance discrete by 15 milliseconds.
55D	10-22-60	ARW-59	100 mv	283.15	330.35	318.1	Satisfactory.
83D	11-15-60	ARW-62	40 mv	269.90	320.40	302.2	Satisfactory.
90D	1-23-61	ARW-62	50 mv	271.99	330.10	304.68	Satisfactory.

NOTES: (1) The values listed are the minimum signal strength recorded during each test.
(2) The calibration for this measurement was not available.

System performance could not be determined for one missile (48D) since this missile was destroyed on the launcher prior to liftoff. RSC system operation was considered satisfactory during the flight of Missile 27D, even though one of the two airborne receivers was inoperative during the time of MFCO transmission. However, the RSC system properly received MFCO via the alternate receiver. Subsequent laboratory tests confirmed the diagnosis of the difficulty as a probable short to ground between the decoder and the signal control unit in the MFCO circuit of the number one command set.

Three signal dropouts, each of 0.2 to 0.4 seconds duration, during transmission of MFCO to 56D were caused by antenna lobing effects. This condition was not serious since the alternate receiver was decoding the message throughout each dropout period. Continuous communication at this time (330 seconds) is difficult since the missile is beyond the controlled portion of the flight, and as a result tumbling and unfavorable look angles may occur. Random missile gyrations can temporarily bring into view "holes" in the radiation pattern due to antenna lobing. The presence of a hole in the antenna pattern causes a decrease in the strength of the signal to one receiver, but an increase in the strength of the signal to the other. This counter-balancing of signal strength is advantageous since it insures continuous reception. The phenomenon is due to the fact that the two antennas are ring coupled (Figure 7.5-2).

Requirements for the operation of the range safety system ordinarily are terminated at vernier cutoff which occurs prior to the time the MFCO signals were transmitted during these tests. With the exception of Missile 42D (Refer to Table 7.5-1), MFCO was sent during these flight tests only as a backup to insure re-entry vehicle separation. It also provided data on the operation of the equipment. It was not necessary to send the signal for range safety reasons during these tests.

Signal Strength

Signal strength received at the missile was evaluated for each test, out to 350 seconds of flight. The intensity was found to have been more than adequate during each test. Signal strength received at the missile at all times, except as previously mentioned, was greater than 10 microvolts during all fourteen flights. Five microvolts is a satisfactory minimum level.

Average signal strength (in dbw) vs time and slant-range is shown in Figure 7.5-4. The increase in signal strength noted at 80 seconds is due to switching from a 500 watt to a 10 kilowatt transmitter at Cape Canaveral. The other two pronounced increases in signal are caused by switching to the next downrange station (Reference Figure 7.5-3). The relatively large but temporary drop in signal strength at BCO is believed to be due to attenuation by the sustainer exhaust flame, which "splashes" from the booster section during jettison. The booster section itself can cause momentary reflection of the signal during separation.

The apparent difference in signal strength shown between the respective curves for the ARW-59 and ARW-62 receivers in Figure 7.5-4 may be semi-quantitative only; since the calibration curve for the new receiver is saturated for the signal levels attained in these tests. While this condition affects the quantitative evaluation of the signal strength, it is not serious from an operational standpoint, because the general signal level (greater than 50 microvolts or greater than -100 dbw) is well above the required minimum of 5 microvolts or -120 dbw.

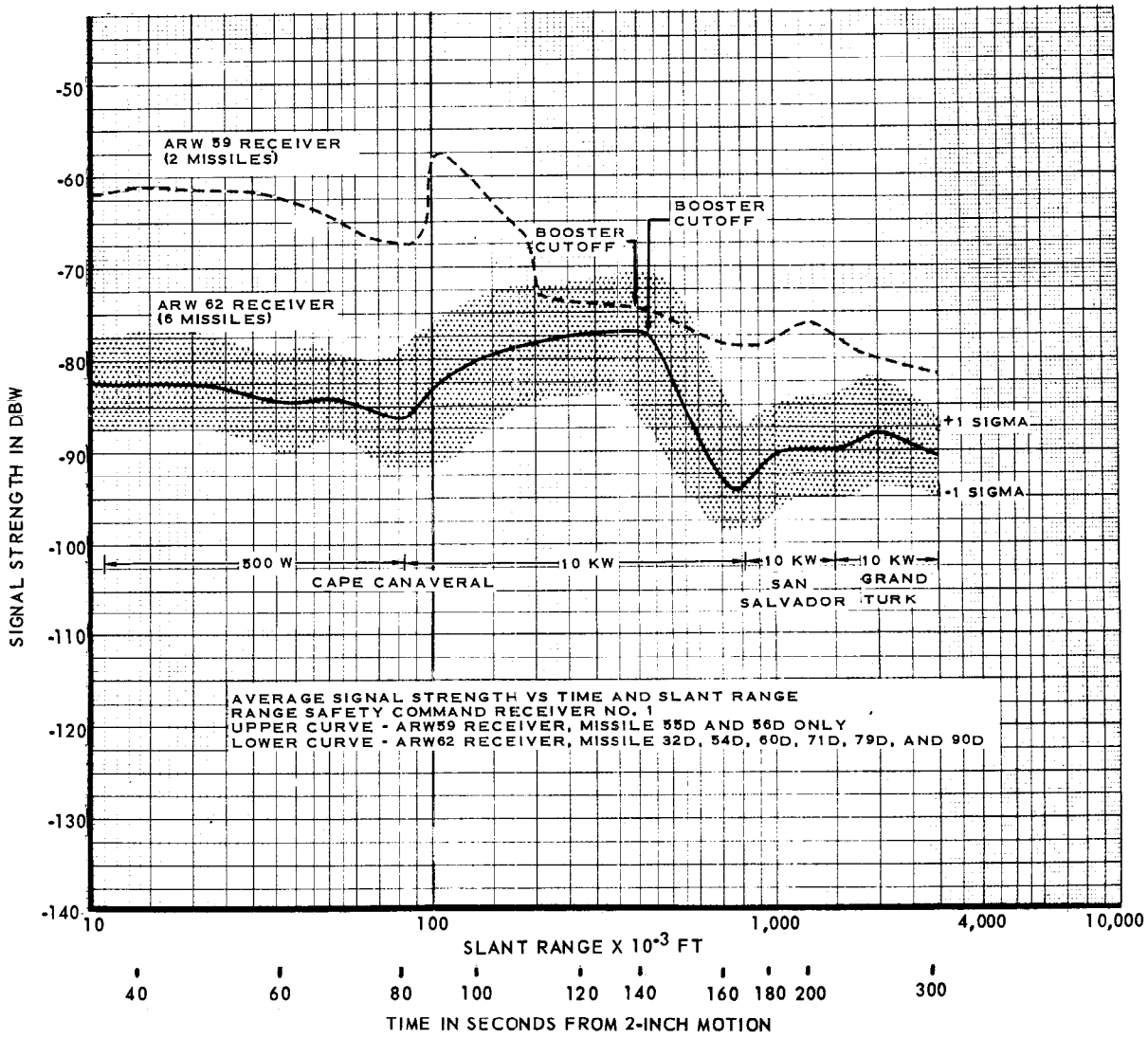

FIGURE 7.5-4 AIRBORNE RECEIVED SIGNAL STRENGTH

PROBLEM AREAS

Unusual ASFCO's

Ordinarily ASFCO lags the guidance SCO by approximately 0.18 seconds. However, ASFCO preceded the guidance SCO command on three AIG flights 66D, 76D, and 71D by 0.12, 0.004 and 0.015 seconds, respectively. These small amounts of lead in sustainer cutoff were insufficient to seriously affect the accuracy of the impact points. These ASFCO signals were sent from the computer at Cape Canaveral rather than from the San Salvador impact predictor. This procedure is common to all AIG missiles. Two of these Missiles 66D and 71D fell short of the assigned impact point by 1.6 and 3.5 NM, respectively, according to splash-net data. The third missile (76D) impact point was 0.86 NM long, as computed from the same type of data. While the slightly early cutoff times are not serious, a small difference between the impact prediction and the AIG system is indicated.

For Missile 60D, ASFCO initiated sustainer cutoff because of low thrust and velocity limiting features of the computer. For 42D, ASFCO was utilized as planned for sustainer engine cutoff since the AIG system was operating in the open-loop configuration. ASFCO was not planned for Missile 56D.

SECTION 7.6 - LAUNCHER

PURPOSE OF TESTING

One objective of this test series was the demonstration of satisfactory operation of the launcher. Determination of the performance of the Benbow holddown cylinder pressure release valve was also of primary interest for two missiles of this group.

TEST CONDITIONS

The only major change in the launcher system configuration from that of the earlier Series D tests, discussed in Report No. AE60-0131-1, was the use of the Benbow release valve, instead of the Barksdale release valve, for the launch of Missiles 83D and 90D. The release valves provide a controlled release of pressure from the holddown cylinder (Figure 7.6-1) during the launching operation.

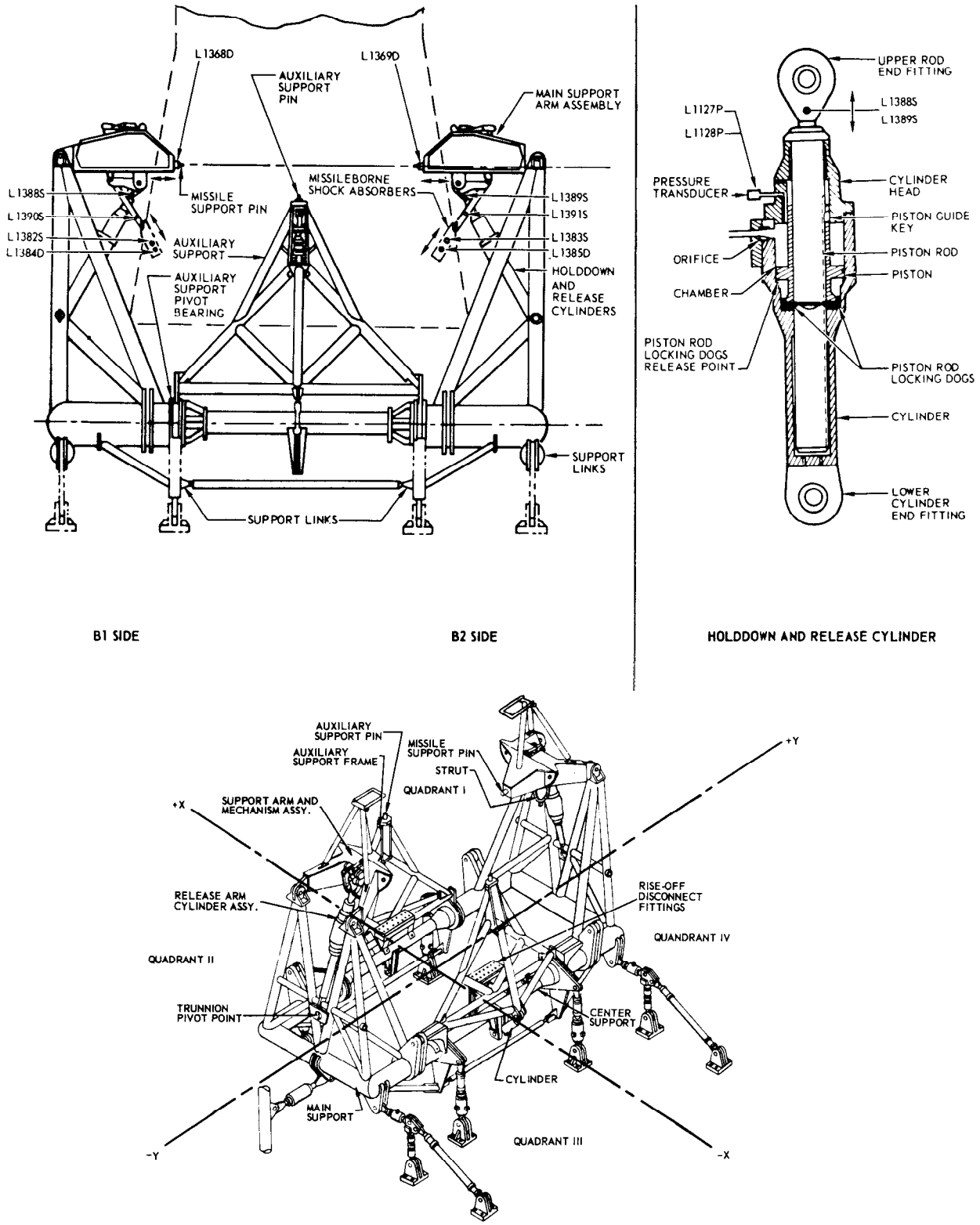

FIGURE 7.6-1 SERIES D LAUNCHER CONFIGURATION

The Benbow valve uses a poppet actuated by an integral hydraulic cylinder. The Barksdale valve uses a rotor which is actuated by an external hydraulic cylinder. Figure 7.6-2 shows the type of pressure release system employed by both valves. The Benbow valve was designed for the purpose of maintaining a small differential holddown pressure between the two holddown cylinders and also for lowering residual pressures in the holddown cylinders. The valve is to operate within the launcher design criteria over a full operational temperature range of -30 to +160°F.

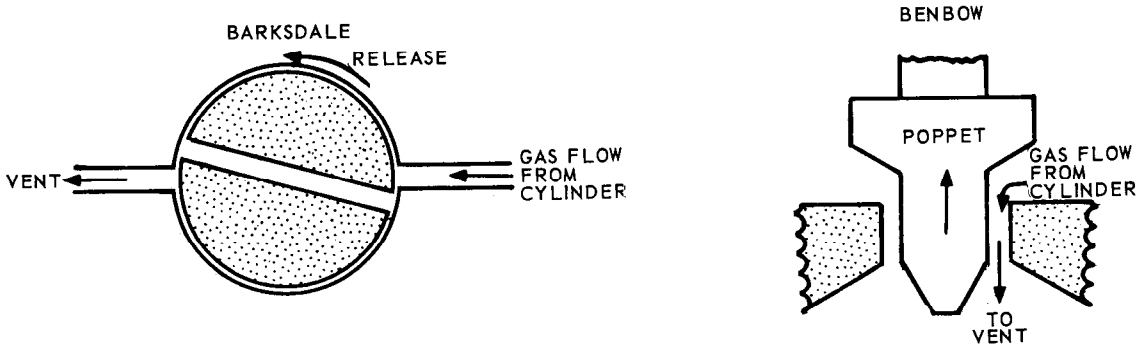

FIGURE 7.6-2 COMPARISON OF LAUNCHER RELEASE VALVES

High residual pressures are undesirable since they may cause damage to the missile due to the application of excessive loads via the kick struts during release. High differential pressure between cylinders is to be avoided since it creates unbalanced side loads on the missile.

The use of the buggy spring, as shown in Figure 7.6-3, was continued in an effort to minimize the loads imposed by the kick struts on the engine nacelles during the launch.

The use of additional leaf springs which were added to the buggy spring (effective on Missile 44D) to insure proper lockup of the kick struts was also continued for this series of tests.

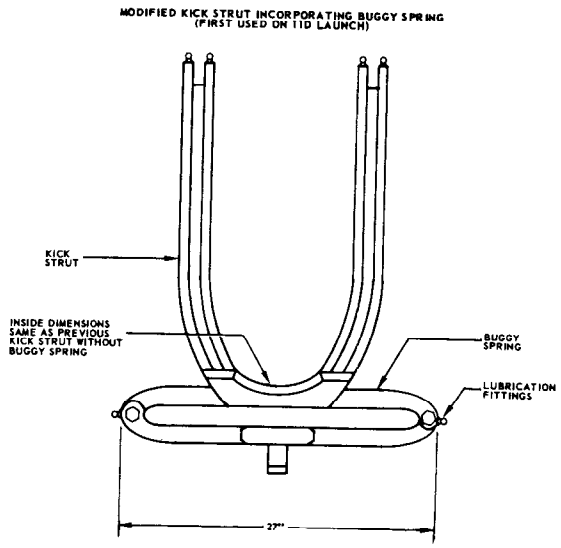

FIGURE 7.6-3 BUGGY-SPRING MODIFICATION OF LAUNCHER KICK STRUT

The operation of the launcher is as follows:

The launcher restrains the missile during the short period from engine ignition to initiation of the controlled launch. The missile is permitted to rise while partially restrained due to forces exerted by the holddown cylinders. The rising missile causes the launcher heads to rotate to the outboard side of the launcher via forces exerted on the launcher kick struts by the missile engine nacelles. The rate and smoothness of missile release is largely governed by the pressure decay characteristics in the holddown cylinders.

To insure proper missile release, specifications have been established for the performance of the holddown cylinders. These are:

1. The holddown cylinder pressure shall decay below 2,550 psig 0.5 seconds after release signal activation for Series D missiles through 66D. The corresponding criteria for Missile 76D and on are 2,480 psig and 0.45 seconds.

2. Differential pressure between the two cylinders shall be less than 440 psig after the pressure has decayed below 2,550 psig for missiles through 66D, and below 2,480 psig for Missile 76D and on.

3. The rate of pressure decay shall be less than 23,200 psi per second for missiles up to 66D. The corresponding value for Missile 76D and on is 22,500 psi per second.

4. The residual pressure measured 0.5 seconds after the 2,550 or 2,480 psig level is reached shall be less than 350 psig nominal. (Maximum allowable is 440 psig due to instrumentation tolerance.)

TEST RESULTS

The launcher system operated satisfactorily in releasing the fourteen missiles which attained liftoff. One flight test, 48D, was terminated prior to liftoff due to a propulsion system malfunction. Complete launcher system operation was not evaluated due to loss of engine thrust before holddown pressures had decayed sufficiently to allow missile motion. However, the holddown and release system properly released the holddown pneumatic force after automatic sequencing of the release signal. Pressure blowdown characteristics in both cylinders were satisfactory and indications are that a satisfactory controlled missile release would have been effected if propulsion system performance had been satisfactory.

The four holddown cylinder criteria were determined to be completely satisfied for nine tests, including Missile 48D, as shown in Table 7.6-1. During the successful launches of two missiles (54D and 60D) the performance of only one holddown cylinder (B1) could be determined. Data was not obtained from the other holddown cylinder due to an instrumentation malfunction. Qualitative holddown cylinder pressure data was obtained during the launch of Missile 71D, due to instrumentation calibration difficulties.

During the launching of Missiles 27D and 55D at AMR (Complex 12), criterion 1 (See Test Conditions) was not satisfied. This was due to a peculiarity in the Complex 12 circuitry which caused a slightly longer (0.05 seconds) time lapse between initiation of the release signal and the start of pressure decay. This characteristic is not considered serious since the only undesirable feature is an extended holddown delay which causes a slight additional propellant consumption.

TABLE 7.6-1 SUMMARY OF LAUNCHER SYSTEM PERFORMANCE

MISSILE NO.	TIME FROM RELEASE SIGNAL TO 2" MOTION (SEC) LAUNCHER COMPLEX 11	12	14	CYLINDER PRECHARGE PRESSURE (psig) B1 SIDE	B2 SIDE	LAUNCHER SYSTEM CRITERIA* SATISFACTION 1	2	3	4	CYLINDER RESIDUAL PRESSURE (350 psig MAX) B1 SIDE	B2 SIDE	COMMENTS
42D	0.76			6,420	6,250	Y	Y	Y	Y	310	350	Launcher operation was satisfactory as indicated by film coverage and landline holddown cylinder pressure data.
48D				6,310	6,310	Y	Y	Y	Y	365	300	Launcher system performance was satisfactory. However, the missile was not released due to loss of engine thrust before the holddown cylinders had decayed sufficiently.
56D		0.80		6,150	6,030	Y	Y	Y	Y	270	300	The launcher system operated satisfactorily in providing a controlled missile release as indicated by film coverage and landline data.
54D	0.66			5,880	(1)	B1 Y B2 See Comments	B1 Y	B1 Y	B1 Y	320	(1)	Launch was satisfactory according to motion pictures. Malfunction in B2 instrumentation system precluded evaluation of B2 holddown cylinder operation.
62D			0.69	6,280	6,200	Y	Y	Y	Y	260	280	Launcher performance was satisfactory. No problem with the auxiliary pin support A-frame due to rework after 45D.
27D		0.84		6,140	6,250	N	Y	Y	Y	380	350	Launch was successful. However, criterion 1 was not satisfied due to excessive time required prior to start of pressure decay.
60D	0.67			6,200	(1)	B1 Y B2 See Comments	B1 Y	B1 Y	B1 Y	315	(1)	Launch was satisfactory as indicated by motion picture coverage. Quantitative data was not obtained on B2 holddown cylinder due to an instrumentation malfunction.
32D		0.80		6,180	5,980	Y	Y	Y	Y	400	300	Launcher system performance was satisfactory. However, B1 residual pressure was marginal due to a slightly slow rate of pressure decay and a slightly (.05 sec) slow decay start.
66D	0.67			5,920	6,020	Y	Y	Y	N	580	485	Launch satisfactory as indicated by film coverage. Residual holddown pressures were high, but the buggy spring tends to compensate for this difficulty.
76D	0.73			6,050	6,120	Y	Y	Y	Y	240	270	Launcher performance was satisfactory.
79D			0.72	6,390	6,130	Y	Y	Y	Y	325	335	Launcher performance was satisfactory.
71D	0.78			(2)	(2)	(2)	(2)	(2)	(2)	(2)	(2)	Launch was satisfactory as indicated by film coverage. Holddown cylinder pressure data appeared normal but was qualitative only due to calibration difficulties.
55D		0.82		5,980	6,100	N	Y	Y	Y	280	275	Launch was satisfactory. However, slow (by .05 sec) start of pressure decay caused criterion 1 not to be satisfied.
83D		0.65		5,600	5,660	Y	Y	Y	Y	60	30	Launcher operation was satisfactory. The Benbow release valve was first used in this test. Desired low residual pressures obtained.
90D		0.63		5,300	5,970	Y	Y	Y	Y	75	30	Launcher operation was satisfactory. Second launch with the Benbow release valve. Desired low residual pressures obtained.

NOTES: Launcher Criteria* - See Test Conditions.
N = No; criterion not satisfied.
Y = Yes; criterion satisfied.

(1) Instrumentation malfunction.
(2) Calibration difficulty in the system.

Criteria 2 and 3 were satisfied during all launches, except for Missiles 54D, 60D and 71D which had launcher instrumentation problems as previously explained. Condition 4 was met during all tests, except 54D, 60D, 71D and 66D. The high residual pressure during release of Missile 66D, and the marginal residual pressures during four other launches (42D, 48D, 27D, 32D) were caused by a slow rate of pressure decay after the holddown cylinder pressure attained the 2,480 psig level. Satisfaction of criterion 4 could not be determined for the B2 holddown cylinder pressures during the launching of Missiles 54D, 60D, and 71D due to instrumentation system discrepancies in the B2 cylinder.

With the newer Benbow release valve, installed for the launches of Missiles 83D and 90D, residual pressures were much lower as desired, ranging from 30 to 75 psig for the B2 and B1 side cylinders, respectively, as shown in Table 7.6-1. These pressures are well below the 350 psig maximum. Residual pressures with the Barksdale valve ranged from 240 (76D) to 580 psig (66D). A low residual pressure is desirable since it minimizes the force exerted on the missile by the kick struts near the completion of missile release. The significantly smaller residual pressures, when utilizing the Benbow valve, are due to the larger gas exit orifice incorporated in this valve.

One reason for the start of qualification testing of the Benbow valve was that the Barksdale valve was not available in a large enough orifice size to provide a sufficiently low residual pressure (pressure at 0.45 seconds after 2,480 psig). Also, the mere insertion of a larger exit orifice in the valve would not in itself solve the problem. An excessively large orifice would cause the holddown cylinder pressure to be released too fast. This condition would allow too great an acceleration to the missile during first motion, and would result in excessive main propellant tank stresses.

Pressure Differentials Between the Holddown Cylinders

Criterion 2, relating to a maximum pressure differential between the B1 and B2 holddown cylinders, was determined to be satisfied during all tests for which data was obtained.

Graphic presentations (refer to Figure 7.6-4) of the average B1 and B2 cylinder pressures versus time using the Barksdale release valve show a very small pressure differential between the two cylinders. The greatest difference (approximately 100 psig) between the two curves appears at 2,480 psig plus 0.5 seconds. Another group of Series D missiles, related because they were launched when the 2,550 psig pressure reference was in effect, shows an even smaller differential between the B1 and B2 pressure curves as illustrated in Figure 7.6-5. A minimum pressure differential between the B1 and B2 holddown cylinders means that the side loads exerted on the nacelles by the kick struts are well balanced.

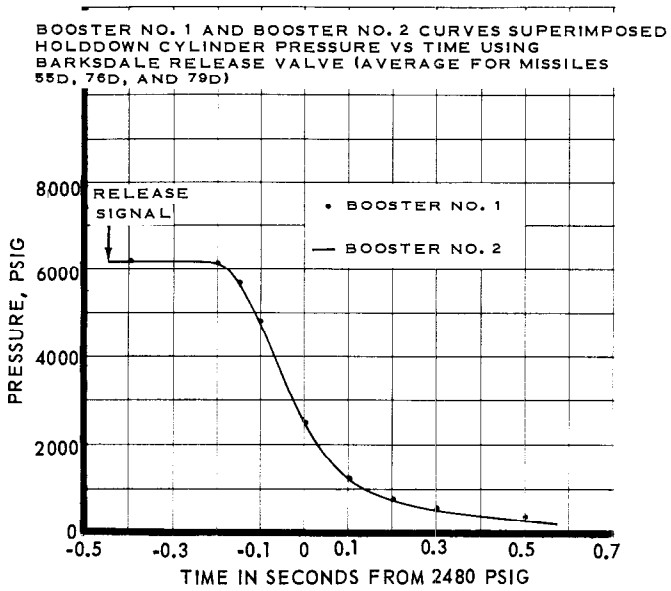

FIGURE 7.6-4 AVERAGE HOLDDOWN AND RELEASE CYLINDER PRESSURE, USING THE 2,480 PSIG PRESSURE REFERENCE

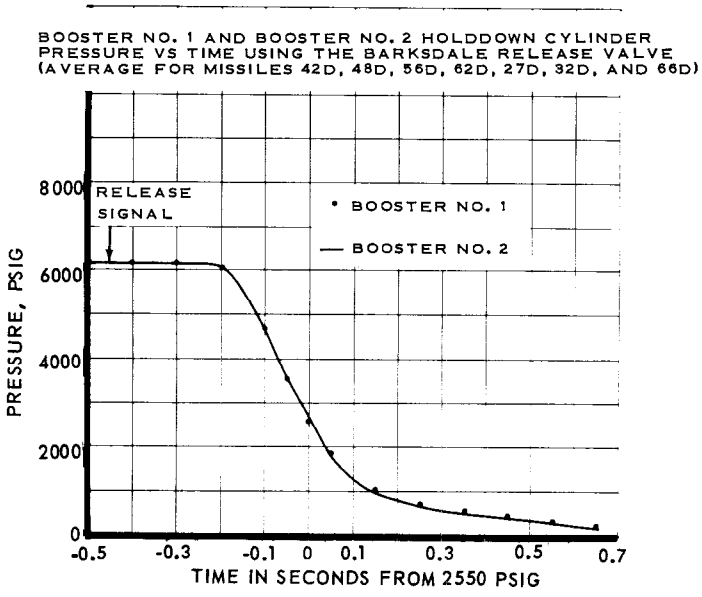

FIGURE 7.6-5 AVERAGE HOLDDOWN AND RELEASE CYLINDER PRESSURE, USING THE 2,550 PSIG PRESSURE REFERENCE

Comparable curves for missile launches wherein the launcher incorporated the Benbow release valve are presented in Figure 7.6-6. These curves show a maximum pressure differential of approximately 150 psig between the B1 and B2 holddown cylinders. However, this condition may not be representative since this comparison comprises data from only two tests (83D and 90D).

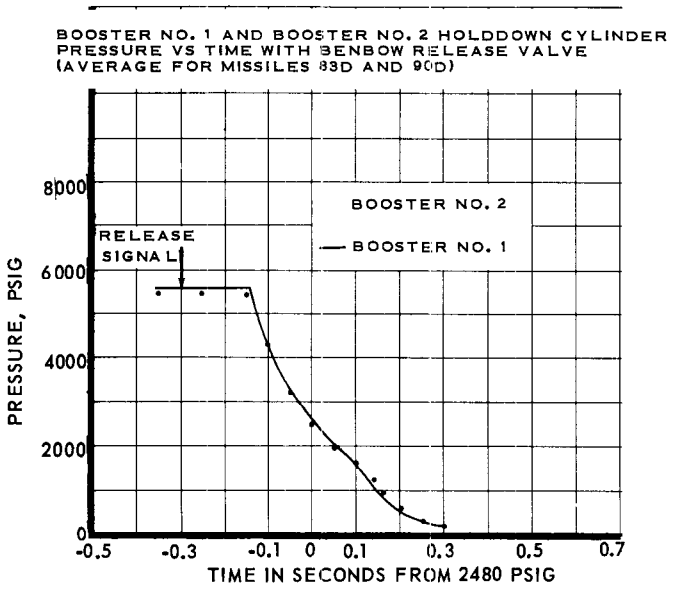

FIGURE 7.6-6 AVERAGE HOLDDOWN AND RELEASE CYLINDER PRESSURE, BENBOW RELEASE VALVE

It is interesting to note that the B1 and B2 holddown cylinder pressure decay curves for the individual missile launches show significantly larger, but not excessive, pressure differentials than do the average pressure decay curves. (For all launches the pressure differentials were below the 440 psig criteria.) This indicates that there are cases where the individual B1 pressure curve was higher than the corresponding B2 curve, and vice versa, so that in the averaging process, the high curve cancels the effect of the low curve. The fact that the differential pressure between the B1 and B2 holddown cylinder average pressure decay curve is less than the differential for individual flights can be due to random decay characteristics and instrumentation inaccuracies. The determination of the exact reason will be the subject of further study.

Comparison of Holddown Cylinder Pressure Decay Characteristics

Pressure decay starts 0.07 seconds sooner (after the initiation of the release signal) with the Benbow valve, than with the Barksdale valve as shown in Figure 7.6-7. The faster response is due to the fact that the Benbow actuator contains a larger hydraulic orifice which permits greater fluid flow and thus faster action. Rapid response is desirable from a weapons system standpoint. Also, there is some saving in propellants, in this case approximately 105 lbs, due to a slightly shortened holddown time. The pressure decay rate from the start of pressure decay down to 3,000 psig is almost equal for the two valves. The Benbow decay rate is slightly less than the Barksdale decay rate from 3,000 psig to 1,620 psig. Thereafter, the Benbow decay rate exceeds the Barksdale rate, and the holddown cylinder pressure drops below the 350 psig upper limit at 2,480 psig plus 0.235 seconds. Comparable decay time for the Barksdale valve is plus 0.48 seconds. The faster decay rate shown by the Benbow valve after 1,600 psig is due to larger orificing for the exit of the pressurizing gas.

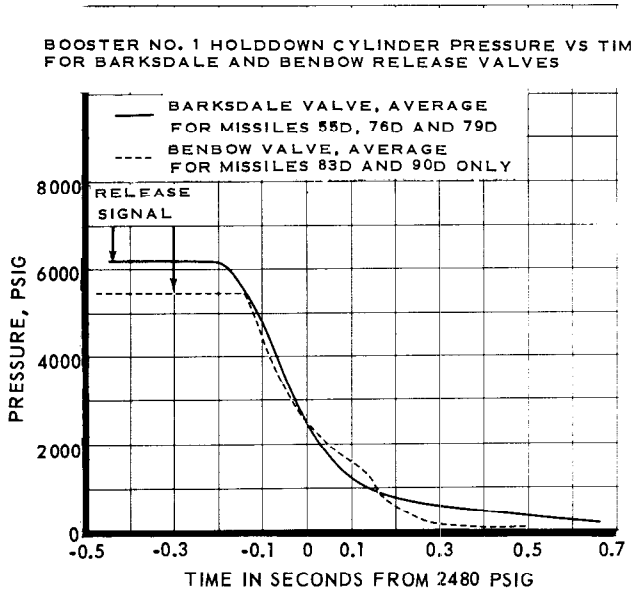

FIGURE 7.6-7 COMPARISON OF BENBOW AND BARKSDALE RELEASE VALVE PRESSURE DECAY CHARACTERISTICS

The outstanding differences between the curves shown in Figure 7.6-7 are the faster rate of pressure release by the Benbow valve 0.10 seconds after the 2,480 psig level is reached and the characteristic changes in slope which occur at 0.10 and 0.14 seconds after the 2,480 psig pressure level. The two irregularities in the curves are due to abrupt changes in effective orifice diameter when different diameter portions of the poppet shaft pass the exit orifice (Figure 7.6-2). The abrupt changes in slope of the release curve are not considered to be detrimental to proper launcher operations.

The Benbow valve has demonstrated two desirable features: (1) Faster start of pressure decay after initiation of the release signal; and (2) Lower residual pressure. However, further testing will be necessary to establish a definite pattern of operation.

SECTION 7.7 - FACILITY AND SITE

PURPOSE OF TESTING

Test objectives pertaining to facility and site were primarily concerned with the launchings of the Series D/AIG missiles and consisted of establishing operational checkout of pre-launch and launch procedures, and demonstrating compatibility of blockhouse and launch equipment. These objectives were met for the Series D/RIG missiles during the earlier portion of the Series D R&D flight test program. (Ref. Report No. AE60-0131-1)

TEST RESULTS

The objectives for launch procedures and compatibility between blockhouse and launch control were successfully met where specified for all missiles covered by this report.

In order to reduce checkout time and pre-launch activities, a dry start was employed on the booster engines for the first time on Missile 40D and repeated on the subsequent flights of Missiles 43D, 44D, 49D, and 42D without adverse effects. Engine dry start means that the thrust chamber walls are void of any fluid prior to engine ignition. However, with the unsuccessful launchings of Missiles 51D and 48D, both of which exploded on the launch pad after experiencing propulsion system combustion instability problems, the wet start procedure was reinstated as a matter of precaution. In addition, the pre-release holddown time was extended 1.5 to 4.25 seconds (see Table 7.7-1) to insure the rough combustion cutoff circuitry adequate time to detect combustion instability and to shut down the engines prior to releasing the missile for flight.

TABLE 7.7-1 SUMMARY OF ENGINE START AND HOLDDOWN TIMES

MISSILE NO.	ENGINE START WET	ENGINE START DRY	HOLDDOWN TIME PLANNED	HOLDDOWN TIME ACTUAL	REMARKS
42D		X	0	0	Satisfactory
51D		X	0	0	Exploded due to combustion instability.
48D		X	0	0	Exploded due to combustion instability.
56D	X		1.50	1.76	Satisfactory
54D	X		4.25	5.42(2)	Satisfactory
62D		X	4.25	4.29	Satisfactory
27D	X(1)		4.25	4.83	Satisfactory
60D		X	4.25	4.59	Satisfactory
32D	X(1)		2.50	2.77	Satisfactory
66D		X	2.50	2.77	Satisfactory
76D		X	0	0	Satisfactory
79D		X	1.50	1.52	Satisfactory
71D		X	0	0	Satisfactory
55D		X	2.50	0(3)	Satisfactory
83D		X	0	0	Satisfactory
90D		X	0	0	Satisfactory

NOTE:

(1) These missiles were planned for wet starting prior to the 51D and 48D incidents as the missile skin thicknesses were insufficient to support dry starting.

(2) Reason for additional 1.17 second delay not established.

(3) Time delay relay malfunctioned.

With the successful launching of Missiles 56D and 54D, the dry start procedure was again employed. No recurrence of the propulsion system malfunction experienced on Missiles 51D and 48D have been noted.

With the exception of Missile 42D, all missiles discussed in this report were launched without a flight readiness firing (FRF). The average erection-to-launch period for these missiles was 27.9 days. The erection-to-launch period for Missile 42D was 78 days. It should be noted that Missile 42D had one unsuccessful FRF and two attempted launches.

A tabulation of the countdown holds required during FRF's and launches is presented in Table 7.7-2. The hold times are presented graphically in Figure 7.7-1. This figure presents the accumulated hold times and the number of launch countdown aborts attributed to a given missile subsystem. Equipment failures were responsible for the largest number of aborts (64%).

TABLE 7.7-2 SUMMARY OF HOLDS AND ABORTS

MISSILE	FLIGHT READINESS FIRING (FRF) AT-TEMPTED	FRF SUCCESS-FUL	LAUNCH AT-TEMPTED	LAUNCH SUCCESS-FUL	COUNTDOWN (Minutes) PLANNED	COUNTDOWN (Minutes) ACTUAL	TOTAL HOLD & RECYCLE TIME (Minutes)	HOLD (Minutes) START	HOLD (Minutes) DURA-TION	RECYCLE TIME (Minutes)	ABORT TIME (Minutes)	CAUSE OF HOLD OR ABORT AREA	CAUSE OF HOLD OR ABORT TYPE	CAUSE OF HOLD OR ABORT SYSTEM	REMARKS
42D (Complex 11)	2/4/60*				180	329	149	X-180	25			Ground	Pro-cedure	Guidance	Arma's precount was incomplete.
								X-120	91			Missile	Equip	Range Safety	Faulty range safety command battery.
								X-45	11			Missile	Engr	Guidance	Arma guidance not ready for GAP test.
								X-35	17			Ground	Equip	LS&T	To replace the safety vent rupture disc in the lox storage tank.
								X-15	5			Ground	Engr	Autopilot	To conduct a rate gyro response test at Stage III pressurization.
		2/23/60			180	243	63	X-135	30			Missile	Equip	Range Safety	No. 2 RSC battery voltage below redline.
								X-35	5			Ground	Equip	Pneumatics	Erratic pressure control of liquid nitrogen trailer.
								X-1	22	6		Ground	Equip	Pneumatic	Pneumatic internal permit light failed to light during Stage III pressurization sequence.
			3/2/60		180		78	X-85	63			Missile	Equip	Instrumen-tation	Fluctuating missile lox tank pressure on land-line instrumentation.
								X-35	10			Ground	Equip	Instrumen-tation	Instrumentation problem concerning lox tank overfill light.
								X-7	1			Missile	Equip	Guidance	Low pulse beacon output.
								X-3	0	4		Missile	Equip	Telemetry	Telemetry remotely activated battery filament voltage failed at switch to internal.
								X-7	Abort		X-7	Missile	Equip	Range Safety	Instrumentation pulse beacon power output was low; required replacement.
			3/4/60		180		382	X-2	4	5		Ground	Engr	Instrumen-tation	Pneumatic pressure readings were doubtful.
								X-2	279	68		Missile	Equip	Propulsion	Integrated start system regulator indicated erratic operation.
								X-35	7			Ground	Human	Guidance	Guidance required additional time to prepare for start of GAP test.
								X-1	3	6		Ground	Engr	Pneumatic	Lox panel meter was oscillating.
								X-0	10		X-0	Ground	Human	Facility	Ignition was achieved, but test was terminated by test conductor because of inadvertent hold call-out from blockhouse.
				3/8/60	180	190	10	X-1	4	6		Ground	Equip	Pneumatic	Pneumatics internal permit light did not come on.
48D (Complex 11)				4/7/60	150	156	6	X-4	6			Ground	Engr	LS&T	To complete lox tanking.
56D (Complex 12)			5/10/60		150		406	X-70	50			Range	Human	Range Safety	Late delivery of range safety plotting charts and required setup time.
								X-35	356		X-35	Range	Engr	Logistics	Range lost contact with ships and aircraft in impact area.
			5/12/60		150		456	X-45	131	25		Range	Engr	Logistics	To re-establish downrange communications.
								X-45	132			Missile	Equip	Autopilot	To replace a faulty B1 pitch actuator servovalve.
								X-45	132			Ground	Equip	Launcher	To replace a piston in the launch booster unit.
								X-42	12			Ground	Equip	Instrumen-tation	To allow ground guidance to prepare for a second loop test rerun which was required due to an autopilot instrumentation discrepancy during first rerun.

* Unsuccessful because of ARMA AIG problem after ignition

TABLE 7.7-2 SUMMARY OF HOLDS AND ABORTS (CONTINUED)

MISSILE	FLIGHT READINESS FIRING (FRF) AT-TEMPTED	FRF SUCCESS-FUL	LAUNCH AT-TEMPTED	LAUNCH SUCCESS-FUL	COUNTDOWN (Minutes) PLANNED	COUNTDOWN (Minutes) ACTUAL	TOTAL HOLD & RECYCLE TIME (Minutes)	HOLD (Minutes) START	HOLD (Minutes) DURATION	RECYCLE TIME (Minutes)	ABORT TIME (Minutes)	CAUSE OF HOLD OR ABORT AREA	CAUSE OF HOLD OR ABORT TYPE	CAUSE OF HOLD OR ABORT SYSTEM	REMARKS
79D (Complex 14) (Cont)								X-5	Same Hold As Above	30		Ground	Engr / Pro-cedure	Facility	To complete replenishment of the lox supply in the storage tank.
								X-0:19	1	4:41		Ground	Equip	Nose Cone Tracking	To rectify ground station inability to receive nose cone data.
71D (Complex 11)			10/7/60		150		250	X-7	32			Range	Equip	TLM	To replace generator at Elysse site.
								X-7	10			Range	Equip	Guid	Arma required time to rerun guidance problem.
								X-7	131	63		Range	Equip	Facility	To re-carbon the searchlights.
								X-3	7			Ground	Human	Prop	B1 backup RCC was inadvertently switched result cutoff was generated.
								X-3	7 (Abort)		X-3	Missile	Equip	Nose Cone	Nose cone recorder failed.
				10/13/60	150	304	154	X-15	120	30		Ground	Equip	LS&T	Wrong plug was inserted in LC pump power receptacle.
								X-7	2			Range	Pro-cedure	RSC	Hold called to allow ship to clear the down-range area.
								X-3:30	2			Range	Pro-cedure	RSC	
55D (Complex 12)				10/22/60	150	403	253	X-35	7			Ground	Equip	Facility	Thrust section heater required.
								X-35	173	35		Missile	Equip	A/P	Broken wire in P901 to gyro caused absence of sustainer response in yaw.
								X-40	15			Range	Equip	Guidance	Tube replacement required in Mod DI guidance GMCF No. 1 (track).
								X-40	10			Range	Equip	RSC	San Salvador - adjusted the range tracker vernier counter (IP).
								X-31	13			Ground	Equip	LS&T	Rupture disc in lox storage tank required replacement.
83D (Complex 14)			11/10/60		150			X-40	Abort		X-40	Missile	Equip	Pneumatic	Decision made to change F&G regulators to Hadley D because of problem at MSTS 1-4.
				11/15/60	150	444	294	X-11	41			Ground	Human	Launcher	Wiring between Benbow valve switch and connector were not completely installed - was jumpered.
								X-7	151	63		Ground	Equip	LS&T	Rupture discs in lox storage area had to be replaced.
								X-7	25			Range	Equip	RSC	San Salvador - problem in voltage control of system 4 track mode relay.
								X-6	5	1		Range	Equip	RSC	Hold called to warm up the tube filaments of system 4 - SS to allow SS to perform an automatic track range check.
								X-4	5	3		Range	Pro-cedure	RSC	
90D (Complex 12)			1/11/61		150			X-35	220	35		Missile	Human	Airframe	GE downrange antenna fairing was not in place, part had to be made.
								X-35	13			Missile	Human	Airframe	To finish installing the fairing.
								X-34:33	Abort		X-34:33	Range	Pro-cedure	Weather	Downrange weather would not allow optical tracking.
			1/12/61		150			X-35	22 (Abort)		X-35	Range	Pro-cedure	Weather	Downrange weather problems.
			1/13/61		150			X-7	22 (Abort)		X-7	Range	Pro-cedure	Weather	Downrange weather problems.
			1/16/61		150			X-35	37 (Abort)		X-35	Range	Pro-cedure	Weather	Downrange weather problems.
				1/23/61	150	167	18	X-7	18			Range	Equip	Facility	FPS-16 radar at station 12 was experiencing problems.

TABLE 7.7-2 SUMMARY OF HOLDS AND ABORTS (CONTINUED)

MISSILE	FLIGHT READINESS FIRING (FRF) ATTEMPTED	FRF SUCCESSFUL	LAUNCH ATTEMPTED	LAUNCH SUCCESSFUL	COUNTDOWN (Minutes) PLANNED	COUNTDOWN (Minutes) ACTUAL	TOTAL HOLD & RECYCLE TIME (Minutes)	HOLD (Minutes) START	HOLD (Minutes) DURATION	RECYCLE TIME (Minutes)	ABORT TIME (Minutes)	CAUSE OF HOLD OR ABORT AREA	CAUSE OF HOLD OR ABORT TYPE	SYSTEM	REMARKS
56D (Complex 12) (Cont)								X-1	18	6	X-7	Ground	Equip	Radio Frequency	Azusa ground system difficulties.
				5/20/60	150	150	0	None							NO HOLDS
54D (Complex 11)				6/11/60	150	390	240	X-55	21			Range	Human	Range Safety	Noise and low sensitivity in the track receiver at GMCF No. 1.
								X-40	19			Range	Human	Range Safety	To allow GMCF No. 1 to reach -40 minute countdown status; track receiver problem delayed testing.
								X-40	7			Ground	Equip	Pneumatic	To repair a leak in the Haskell compressors.
								X-40	5			Ground	Equip	Facility	To re-carbon the searchlights.
								X-15	158	30		Ground	Equip	LS&T	Lox tanking problem; pump LA had blown gasket on outlet flange.
62D (Complex 14)			6/20/60		150		284	X-70	284		X-70	Range	Equip	Range Safety	Station No. 5 had lost range gate and automatic tracking capability mandatory for test. Problem could not be resolved.
				6/22/60	150	199	49	X-45	36			Ground	Equip	Instrumentation	To replace a malfunctioning audio warning amplifier in the landline system.
								X-3:30	2:30	3:30		Range	Equip	Range Safety	Loss of communications to the ground station at San Salvador.
								X-2	2	5		Missile	Procedure	Electrical	To resolve a discrepancy in missile inverter power.
27D (Complex 12)			6/24/60		150		50	Data Unobtainable	50			Range	Procedure	Logistics	Range supporting another operation.
								X-70	Abort		X-70	Missile	Equip	Nose Cone	Nose cone had zero telemetry output on external power.
				6/27/60	150	150	0	None							NO HOLDS
60D (Complex 11)			6/30/60		150		189	X-139	34			Missile	Equip	Telemetry	To change telemetry RF No. 2 canister; noisy link.
								X-70	28			Ground	Equip	Guidance	To rerun GAP test due to poor functioning of data checker.
								X-54	127		X-54	Missile	Equip	Guidance	An improper frequency output for accelerometer String 1 of the inertial guidance system on Channel 5 of the analog signal converter could not be resolved.
				7/2/60	150	328	178	X-45	6			Ground	Equip	Instrumentation	To replace an RCC audio warning amplifier.
								X-12	114	33		Missile	Equip	Electrical	To replace the main missile battery.
								X-30	25			Ground	Equip	LS&T	To replace a ruptured disc in the lox topping line.
32D (Complex 12)			8/2/60		150		40	X-70	40			Range	Equip	Range Safety	A control wiring problem at GMCF No. 1.
								X+0:01.53	Abort		X+0:01.53**	Missile	Procedure	Range Safety	Engine cutoff due to an accumulation of RCC count on the sustainer engine.

** See history of Atlas flight tests

TABLE 7.7-2 SUMMARY OF HOLDS AND ABORTS (CONTINUED)

MISSILE	FLIGHT READINESS FIRING (FRF) AT-TEMPTED	FRF SUCCESS-FUL	LAUNCH AT-TEMPTED	LAUNCH SUCCESS-FUL	COUNTDOWN (Minutes) PLANNED	COUNTDOWN (Minutes) ACTUAL	TOTAL HOLD & RECYCLE TIME (Minutes)	HOLD (Minutes) START	HOLD (Minutes) DURATION	RECYCLE TIME (Minutes)	ABORT TIME (Minutes)	CAUSE OF HOLD OR ABORT AREA	TYPE	SYSTEM	REMARKS
32D (Complex 12) (Cont)				8/9/60	150	218:05	68:05	X-50	13			Ground	Engr	Guidance	To rerun the autopilot-guidance loop test.
								X-1	20	6		Ground	Equip	Instrumentation	GE guidance station had a recording problem.
								X-3:30	16	3:30		Ground	Equip	Radio Frequency	Azusa dropouts at the ground station.
								X-0:25	5	4:35		Ground	Equip	Instrumentation	The blockhouse AM and FM recorders stopped running.
66D (Complex 11)			7/22/60		150		Data Unobtainable	X-144	Data Unobtainable			Missile	Equip	Autopilot	The pitch program output voltage failed to properly step from 1.7 to 1.9 volts at 39 seconds of programmer run time during GAP test.
								X-70	Abort		X-70	Missile	Engr	Instrumentation	Discrepancy in the sustainer RCC accelerometer circuitry due to water in the coaxial cable plug.
			7/25/60		150		182:58	X-25	80	20		Missile	Equip	Radio Frequency	To replace the Azusa canister.
								X-0:40	7	6		Ground	Engr	Launch Control	There was no Acoustica ready light on the prestart ladder. The hold fire override switch was used to obtain a range ready light.
			7/25/60		150		182:58	X-0:02	Abort	69:58		Ground	Engr	Launch Control	No Arma computer reset had occurred due to a late Arma computer reset because sequencer timing was off from previous hold.
								X-0:02	Abort		X-70	Missile	Equip	Pneumatic	Inadvertent pressurization of the engine fuel tank occurred.
			8/8/60		150		3:30	X-3:30	Abort	3:30	X-7	Missile	Equip	Nose Cone	GE nose cone reported a NO-GO due to loss of telemetry link 4 modulation.
				8/12/60	150	150	0	None							NO HOLDS
76D (Complex 11)				9/16/60	150	328	178	X-150	174			Ground	Human	Guidance	To replace Arma computer, to complete an Arma precount operation, and to check out the Go Inertial Pulse (GIP) wiring between the blockhouse and the GMCF No. 1.
								X-7	4			Ground	Engr	LS&T	To complete lox tanking.
79D (Complex 14)			9/15/60		150		69:35	X-80	60			Missile	Engr	Instrumentation	Sustainer fuel valve position (P830D) transducer wiring was intermittent.
								X-0:25	3	6:35		Ground	Procedure	Range Safety	To allow the range to complete launch preparations.
								Note (1)	Abort		Note (1)	Missile	Engr	Electrical	Terminated due to absence of a release signal.
				9/19/60	150	481:22	331:22	X-3:30	3			Missile	Procedure	Pneumatic	To allow the booster tanks helium bottle temperature to stabilize at a low enough temperature.
								X-0:19	90	34:41		Missile Ground	Equip	Nose Cone Facility	To remove the nose cone umbilical after the lanyard broke.
								X-7	10			Ground	Equip	Pneumatic	To complete pneumatics helium bottle pressurization as one Haskell compressor failed and pressurization had to be completed with the remaining compressor.
								X-4	157	1		Ground	Engr Equip	Facility LS&T	To replenish the lox supply in the storage tank.

Note (1): Engines were cut off 5.45 seconds after sustainer flight lockin by the engine cutoff timer.

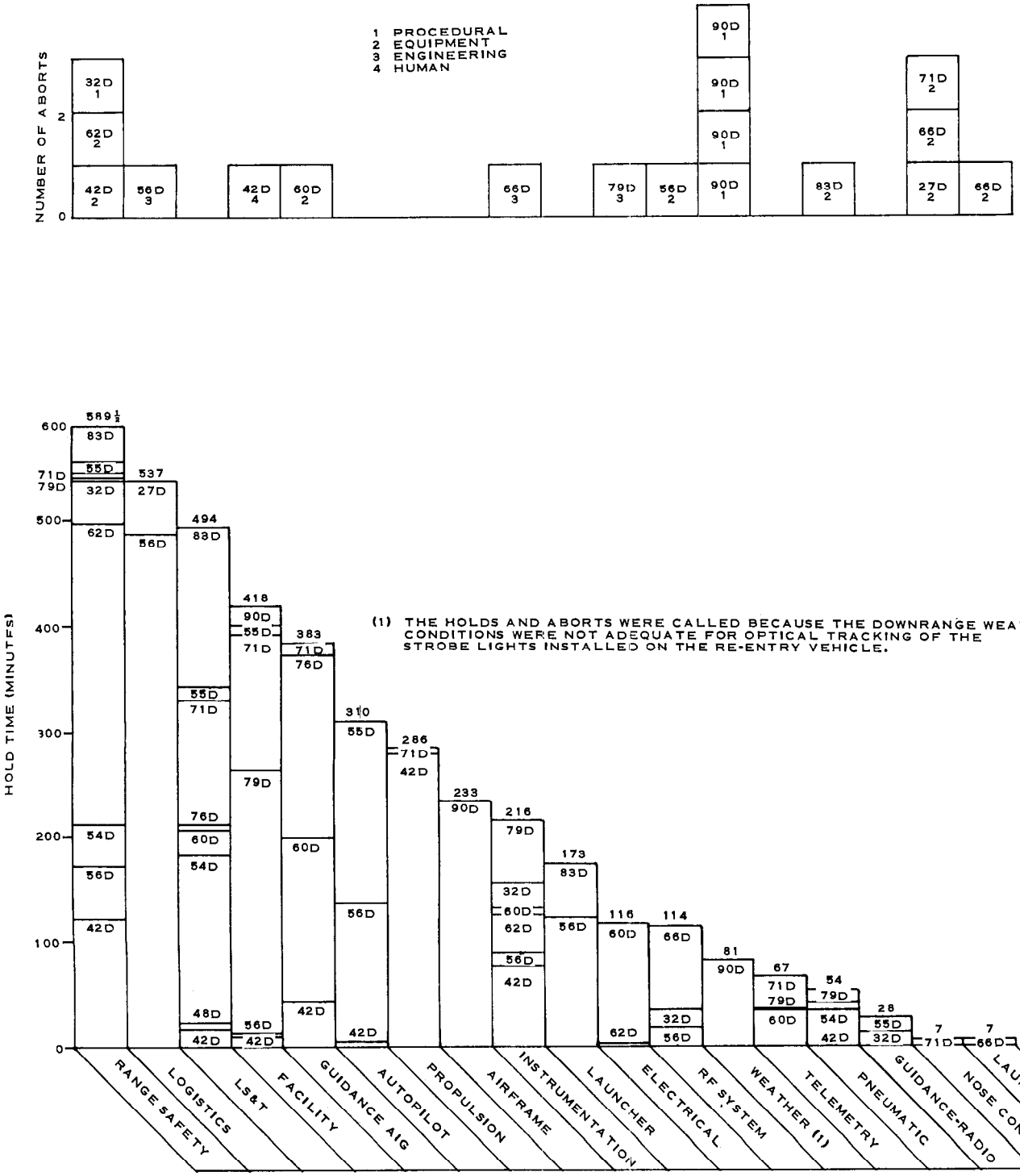

FIGURE 7.7-1 CUMULATIVE HOLD TIME AND ABORTS, WITH AFFECTED MISSILE INDICATED

This page intentionally left blank.

SECTION 7.8 – INSTRUMENTATION SYSTEM

(TELEMETRY)

PURPOSE OF TESTING

Performance evaluation of the telemetry system in conjunction with the Series D AIG missiles was of primary concern during this phase of Series D flight testing. However, system performance was evaluated for all Series D R&D missiles discussed in this report.

TEST CONDITIONS

Two telemetry configurations were utilized during this phase of testing. These were: (1) the configuration installed on the RIG missile consisting of a telemetry package, a transverter power supply, transducers, accessory package, a T coupler, two antennas, a transducer transverter power supply, and a telemetry battery (Reference Figure 7.8-1) and (2) the configuration installed on the AIG missile consisting of three telemetry packages, three telemetry transverter power supplies, transducers, a ring coupler, a diplex coupler, two antennas, two transverter power supplies, and three batteries. (Reference Figure 7.8-2)

A separate telemetry system was installed in the re-entry vehicle for evaluation of the re-entry vehicle functions and environmental conditions to which it is subjected. Since reduction and evaluation of this data is the responsibility of the appropriate contractors, results will not be discussed in this section.

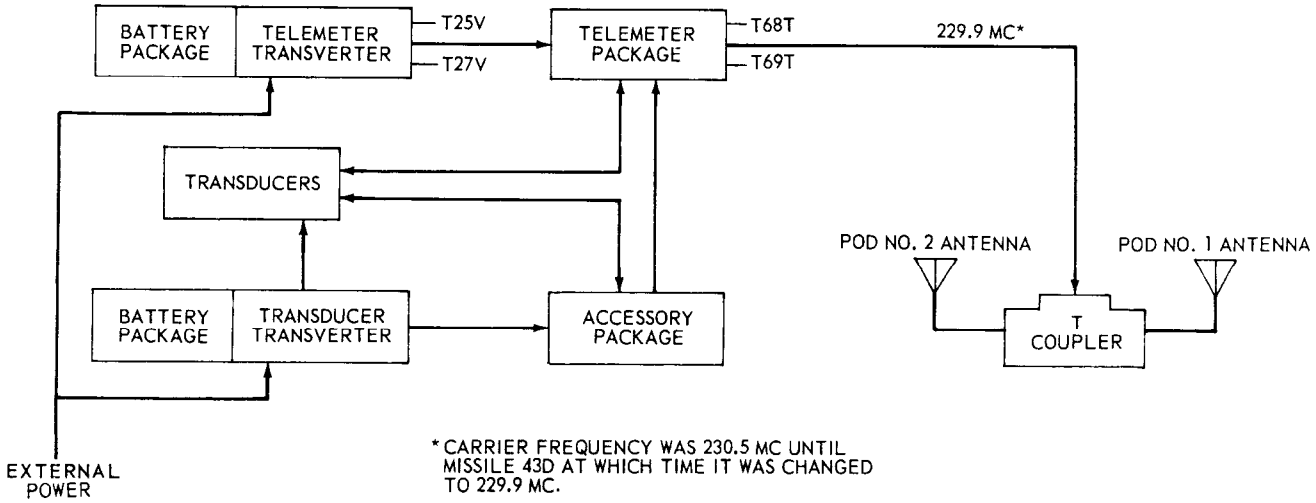

FIGURE 7.8-1 INSTRUMENTATION SYSTEM FOR SERIES D/RIG MISSILES

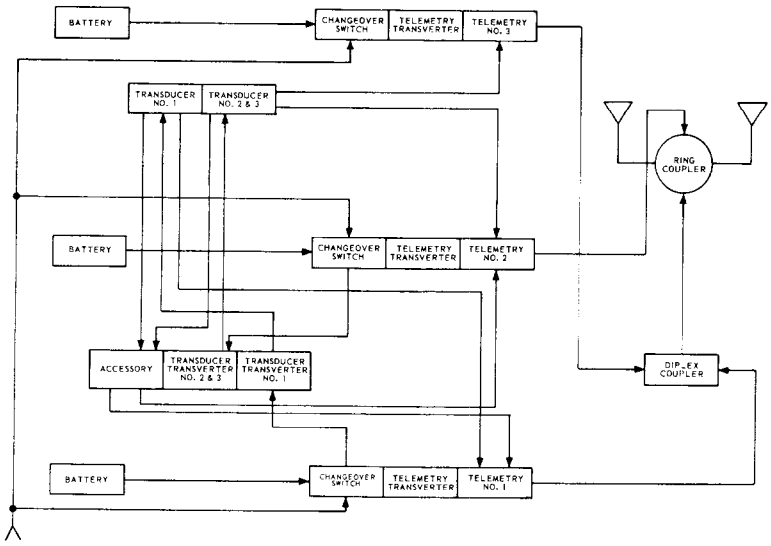

FIGURE 7.8-2 INSTRUMENTATION SYSTEM FOR SERIES D/AIG MISSILES

TEST RESULTS

Telemetry system performance during the fifteen Series D R&D flights, discussed herein, was satisfactory. A total of 2,172 measurements were attempted; of these, 59 failed to yield satisfactory data, for a percentage recovery of 97.3%. Table 7.8-1 lists the measurements attempted, by missile, on both the telemetry and landline systems. The unsatisfactory measurements are also listed in this table. Table 7.8-2 lists the distribution of the unsatisfactory measurements by type. As shown, vibration type instrumentation yielded the least desirable results (percentage failure of 21.1%).

(LANDLINE)

PURPOSE OF TESTING

There were no formal objectives assigned to the landline instrumentation system. The instrumentation failure survey presented here is for general information only.

TEST RESULTS

A total of 2,814 measurements were attempted, 48 of which were considered unsatisfactory, for a percentage recovery of 98.3%. Table 7.8-1 contains a tabulation of the landline measurements attempted including those considered unsatisfactory. Table 7.8-3 lists the distribution of the unsatisfactory measurements by type. Again, as in the telemetry system, vibration type instrumentation yielded the least desirable results (percentage failure of 17.6%).

TABLE 7.8-1 INSTRUMENTATION OF SERIES D FLIGHT MISSILES

MEASUREMENT NUMBER	DESCRIPTION	MISSILE NUMBER														
		27D	32D	42D*	48D*	54D*	55D	56D	60D*	62D	66D*	71D*	76D*	79D	83D	90D
		KEY: O Telemetry; X Landline; □ Telemetry Failure; ○ Landline Failure														
A295D	AIG POD COVER Q11				O	O										
A296D	AIG POD COVER Q111				O	O										
A815D	QUAD II DOOR POSITION											O	O			
A816D	QUAD III DOOR POSITION											O	O			
A622I	TH SECT LIGHT QUAD IV	□	O	O	O	O	O	O	O	O	O	O	O	O	O	□
A287O	FWD GUID PLAT RAD				O	□										
A288O	FWD GUID PLAT TAN				□											
A289O	A/P GYRO CAN PCH AX				O											
A290O	A/P GYRO CAN YAW AX				O											
A291O	AFT GUID PLAT RAD				O	□										
A292O	AFT GUID PLAT TAN				O	O										
A643O	OUTBOARD FRAM Q3X-X			O												
A644O	OUTBOARD FRAM Q3Y-Y			O												
A794O	B1 HI PRESS FUL LINE	X	X			○	X	X	X	X	○	X		○		
A795O	B2 HI PRESS FUL LINE	X	X			X	X	○	X	○	○	X		○		
A801O	B1 LOX HI PRESS DUCT	X	X			X	X	X	○	○	X	X		○	X	X
A802O	B2 LOX HI PRESS DUCT	X	X			X	X	X	○	X	X	X		○	○	X
A803O	B LOX LO PRESS DUCT	X	X			X	X	X	X	X	X	X		○	X	X
A804O	B FUEL LO PRESS DUCT	X	X			X	X	X	X	X	X	X		○	○	○
A646T	DUMMY HYD VLV INBD							O		□				O		
A647T	DUMMY HYD VLV OUTBD							O		O				O		
A666T	ADAPT SKIN FWD														O	
A667T	ADAPT SKIN CTR														O	
A743T	AMB AT S INST PANEL	O	O	O	O	□	O	O	O		O	O	O			O
A745T	AMB AT S FUEL PUMP	O	O	O	O	O	O	O	□	O	O	O	O	O	O	O
A746T	AMB AT V HYD SUPPLY	O	O	□	O	O	O	O	O	O	O	O	O	O	O	O
A747T	F STG VLV SHIELDED	O	O	O	O	□	O	O	O	O	O	O	O	O	O	□
A764T	AMB NEAR B2 BOOT QIII															O
A765T	AMB NEAR B2 BOOT QII															O
A766T	AMB NEAR B2 BOOT QI															O
A767T	AMB NEAR B2 BOOT QVI															O
A805T	AMB AT STANCHION QI										O	O	O			
A806T	AMB AT STANCHION QII										O	O	O			
A807T	AMB AT STANCHION QIII										O	O	O			
A808T	AMB AT STANCHION QVI										O	O	O			
A809T	B1 AFT NACELLE AMB										O	O	O			
A810T	B2 AFT NACELLE AMB										O	O	O			
A819T	AMB AT HEATER DOOR										O	O	O			
A820T	AMB AT FIREX DOOR QI										O	O	O			
A821T	AMB AT FIREX DOOR QII										O	O	O			
A822T	B1 FWD NACELLE QI										O	O	O			
A823T	B1 FWD NACELLE QVI										O	O	O			
A824T	B2 FWD NACELLE QII										O	O	O			
A825T	B2 FWD NACELLE QIII										O	O	O			
A826T	B1 NACELLE CABLEWAY										O	O	O			
A827T	B2 NACELLE CABLEWAY										O	O	O			
A811X	QUAD II DOOR FWD MSW										□					
A812X	QUAD III DOOR FWD MSW										□					
A813X	QUAD II DOOR AFT MSW										○					
A814X	QUAD III DOOR AFT MSW										□					
A761Y	AIG POD SOUND INT			X		X			X							
A762Y	AIG POD SOUND INT			X		X			X							
D 1V	RSC CUTOFF OUTPUT	O	O	O	O	O	O	O	O	O	O	O	O	O	O	O
D 7V	NO 1 RSC RF INPUT/AGC	O	O	O	O	O	O	O	O	O	O	O	O	O	O	O
D 3X	RSC DESTRUCT OUTPUT	O	O	O	O	O	O	O	O	O	O	O	O	O	O	O
D110X	MSL DESTRUCT SIGNAL															
D357X	TCC RS INT AND ARMED	X	X				X	X		X				X	X	X
E 43C	CRITICAL POWER A			X	X	X			X		X	X	X			
E 44C	CRITICAL POWER B			X	X	X			X		X	X	X			
E 45C	CRITICAL POWER C			X	X	X			X		X	X	X			
E 50Q	400-CYCLE AC PWRSUP	O	O	O	O	O	O	O	O	O	O	O	O	O	O	O
E 6V	INVERTER PHASE A											X	X			
E 7V	INVERTER PHASE B														X	X
E 8V	INVERTER PHASE C														X	X
E 28V	MSL SYSTEMS INPUT	O	O	O	O	O	O	O	O	O	O	O	O	O	O	O
E 51V	400-CYCLE AC PHASE A	O	O	O	O	O	O	O	O	O	O	O	O	O	O	O
E 53V	400-CYCLE AC PHASE C			O	O	O			O		O	O	O			
E 34X	AC LOW VOLTAGE		O					O		O						
E 49X	TCC INTL PWR RDY LT	X	X				X	X		X	X	X	X	X	X	X

* Series D/AIG missile.

TABLE 7.8-1 INSTRUMENTATION OF SERIES D MISSILES (CONTINUED)

MEASUREMENT NUMBER	DESCRIPTION	MISSILE NUMBER														
		27D	32D	42D*	48D*	54D*	55D	56D	60D*	62D	66D*	71D*	76D*	79D	83D	90D
F 1P	LOX TANK HELIUM	OX	OX	OX	OX	OX	OX	OX	OX	OX	OX	OX	OX	OX	OX	OX
F 3P	FUEL TANK HELIUM	OX	OX	OX	OX	OX	OX	OX	OX	OX	OX	OX	OX	OX	OX	OX
F 34P	FUEL PRESS ORFC DP						O	O								
F 65P	LOX TK HE LINE AT ORFC						O									
F 90P	LO_2 ORFC DP REVERSE															
F 91P	FUEL ORFC DP REVERSE													O		
F116P	DP ACROSS BULKHEAD	O	O				O	O		O						
F125P	B CTL PNEU REG OUT	OX	OX	OX	OX	OX	OX	OX	OX	OX	OX	OX	OX	OX	OX	OX
F147P	LOX PRESS ORFC DP						O	O								
F194P	FACILITY GN_2 SUPPLY	X	X	X	X	X	X	X	X	X	X	X	X	X	X	X
F212P	FUEL PRESS ORFC IN						O									
F246P	B TK HE BTL HI	OX	OX	OX	OX	OX	OX	OX	OX	OX	OX	OX	OX	OX	OX	OX
F260P	B TK HE BTL LO						O									
F288P	ST PNEU REG OUT	OX	OX	OX	OX	OX	OX	OX	OX	OX	OX	OX	OX	OX	OX	OX
F291P	S CTL HE BTL	OX	OX	OX	OX	OX	OX	OX	OX	OX	OX	OX	OX	OX	OX	OX
F304P	SEPARATION BTL DISCH	O	O	O	O	O	O	O	O	O	O	O	O	O	O	O
F 17T	FUEL PRESS ORFC IN						O									
F115T	LOX PRESS REG IN	O	O				O	O		O				O	O	O
F146T	LOX PRESS ORFC IN						O									
F247T	B TK HE BTL	O	O				O	O		O				O	O	O
F771T	LOX TANK ULLAGE						O									
F772T	LOX TANK ULLAGE						O									
F773T	LOX TANK ULLAGE						O									
F774T	LOX TANK ULLAGE						O									
F775T	LOX TANK ULLAGE						O									
F776T	LOX TANK ULLAGE						O									
F777T	LOX TANK ULLAGE						O									
F778T	LOX TANK ULLAGE						O									
F779T	LOX TANK ULLAGE						O									
F780T	LOX TANK ULLAGE						O									
F781T	LOX TANK ULLAGE						O									
F782T	LOX TANK ULLAGE						O									
F783T	LOX TANK ULLAGE						O									
F784T	LOX TANK ULLAGE						O									
F785T	LOX TANK ULLAGE						O									
F786T	LOX TANK ULLAGE						O									
F787T	LOX TANK ULLAGE						O									
F788T	LOX TANK ULLAGE						O									
F789T	FUEL TANK ULLAGE						O									
F790T	FUEL TANK ULLAGE						O									
F791T	FUEL TANK ULLAGE						O									
F792T	FUEL TANK ULLAGE						O									
F793T	FUEL TANK ULLAGE						O									
F794T	FUEL TANK ULLAGE						O									
F795T	FUEL TANK ULLAGE						O									
F796T	FUEL TANK ULLAGE						O									
F132X	LOX TK PRESS SW		O				O	O		O						
F133X	DELTA P SWITCH		O				O	O		O						
F152X	BCO-LOX TK PRESS SW		O				O	O		O						
F207X	TCC IN PNEU P LITE	X	X				X	X		X				X	X	X
G 4C	PB MAGNETRON AVERAGE	O	O				O	O		O				O	O	O
G301C	PB-IP MAGNETRON AVG	O	O				O	O		O				O	O	O
G302C	PB-IP MODULATOR AVG											O	O			
G504C	MOD III MAGNETRON			O	O	O			O		O	O	O			
G 82E	RB RF OUTPUT	O	O				O	O		O				O	O	O
G324E	RB-IP RF OUTPUT	O	O				O	O		O				O	O	O
G582E	MOD III RB RF OUTPUT			O	O	O			O		O	O	O			
G 94O	BOOM ANTENNA											O				
G197O	RB-IP RADIAL											O				
G587O	POD WAVEGUIDE											O				
G 3V	PB AGC	O	O				O	O		O				O	O	O
G 26V	PITCH ANALOG	X	X				X	X		X				X	X	X
G 27V	YAW ANALOG	X	X				X	X		X				X	X	X
G279V	RB AGC NO. 1	O	O				O	O		O				O	O	O
G280V	RB AGC NO. 2	O	O				O	O		O				O	O	O
G281V	RB REFLECT SET											O	O			
G282V	RB PHASE DETR NO. 1	O	O				O	O		O				O	O	O
G283V	RB PHASE DETR NO. 2	O	O				O	O		O				O	O	O
G287V	D PITCH OUTPUT	O	O				O	O		O				O	O	O
G288V	D YAW OUTPUT	O	O				O	O		O				O	O	O
G289V	D MESSAGE READ	O	O				O	O		O				O	O	O
G318V	PB-IP AGC	O	O				O	O		O				O	O	O
G321V	RB-IP AGC	O	O				O	O		O				O	O	O
G503V	MOD III PB AGC			O	O	O			O		O	O	O			
G579V	MOD III RB AGC NO. 1			O	O	O			O		O	O	O			
G290X	D CONTACTS NO. 1 & NO. 2	O	O				O	O		O				O	O	O
G291X	D CONTACTS NO. 3 & NO. 4	O	O				O	O		O				O	O	O
G292X	D CONTACTS NO. 5 & NO. 6	O	O				O	O		O				O	O	O
G549X	D CONTACT NO. 1	X	X				X	X		X				X	X	X

TABLE 7.8-1 INSTRUMENTATION OF SERIES D MISSILES (CONTINUED)

MEASUREMENT NUMBER	DESCRIPTION	MISSILE NUMBER													
		27D	32D	42D*	48D*	54D*	55D	56D	60D*	62D	66D*	71D*	76D*	79D	83D	90D
G550X	D CONTACT NO. 2	X	X				X	X		X				X	X	X
G551X	D CONTACT NO. 3	X	X				X	X		X				X	X	X
G552X	D CONTACT NO. 5	X	X				X	X		X				X	X	X
G553X	D CONTACT NO. 6	X	X				X	X		X				X	X	X
G554X	D CONTACT NO. 7	X	X				X	X		X				X	X	X
H 33P	B1 HYD ACCUMULATOR	O	O	O	O	O	O	O	O	O	O	O	O	O	O	O
H140P	S/VERN HYD PRESS	O	O	O	O	O	O	O	O	O	O	O	O	O	O	O
H211P	VERN AIR FLASK PRESS													O	O	O
H223P	VRN HYD ACM PS-GAS						O									
H194T	SUR AL TUBING TO V2						O									
H196T	SUR AL TUBING TO V1						O									
H101X	TCC INT HYD PRESS SW	X	X				X	X		X	X	X	X	X	X	X
H146X	B HYD HI PRESS SW	X	X				X	X		X	X	X	X	X	X	X
H147X	S HYD HI PRESS SW	X	X				X	X		X				X	X	X
H187X	BSTR OIL EVACUATION	X	X				X	X		X	X	X	X	X	X	X
H188X	SUST OIL EVACUATION	X	X				X	X		X	X	X	X	X	X	X
H210X	SIG TO V HYD SQUIB													O	O	O
H220X	S HYD P SW		O				O	O		O				O		
I513A	ACCEL XF1 DIRECT			O	O	O			O		O	O	O			
I514A	ACCEL XF2 DIRECT			O	O	O			O		O	O	O			
I515A	ACCELEROMETER XF1			X	X	X			X		X	X	X			
I516A	ACCELEROMETER YF1			OX	OX	OX			OX		OX	OX	OX			
I517A	ACCELEROMETER ZF1			OX	OX	OX			OX		OX	OX	OX			
I518A	ACCELEROMETER XF2			X	X	X			X		X	X	X			
I519A	ACCELEROMETER YF2			OX	OX	OX			OX		OX	OX	OX			
I520A	ACCELEROMETER ZF2			OX	OX	OX			OX		OX	OX	OX			
I591C	PITCH GYRO TORQUE			X	X	X			X		X	X	X			
I592C	ROLL GYRO TORQUE			X	X	X			X		X	X	X			
I593C	YAW GYRO TORQUE			X	X	X			X		X	X	X			
I549D	PITCH SERVO ERROR			O	O	O			O		O	O	O			
I550D	ROLL SERVO ERROR			O	O	O			O		O	O	O			
I551D	AZIMUTH SERVO ERROR			O	O	O			O		O	O	O			
I552D	REDNDT GYRO PICK-OFF			O	O	O			O		O	O	O			
I594D	PENDULUM NO. 1 NULL			X	X	X			X		X	X	X			
I595D	PENDULUM NO. 2 NULL			X	X	X			X		X	X	X			
I596D	OPTIC SIGNAL			X	X	X			X		X	X	X			
I505H	COMPUTER POSITION X			OX	OX	OX			OX		OX	OX	OX			
I506H	COMPUTER POSITION Y			OX	OX	OX			OX		OX	OX	OX			
I507H	COMPUTER POSITION Z			OX	OX	OX			OX		OX	OX	OX			
I508H	RANGE ERROR FUNCTION			OX	OX	OX			OX		OX	OX	OX			
I509H	AZM ERROR FUNCTION			OX	OX	OX			OX		OX	OX	OX			
I502L	COMPUTER VELOCITY X			OX	OX	OX			OX		OX	OX	OX			
I503L	COMPUTER VELOCITY Y			OX	OX	OX			OX		OX	OX	OX			
I504L	COMPUTER VELOCITY Z			OX	OX	OX			OX		OX	OX	OX			
I560O	BINNACLE X AXIS			O	O	O			O							
I561O	BINNACLE Y AXIS			O	O	O			O							
I562O	BINNACLE Z AXIS			O	O	O			O							
I564O	COMPUTER X AXIS			O	O	O			O							
I565O	COMPUTER Y AXIS			O	O	O			O							
I566O	COMPUTER Z AXIS			O	O	O			O							
I572P	BINNACLE			O	O	O			O		O	O	O			
I531T	GYRO 1			O	O	O			O		O	O	O			
I532T	GYRO 2			O	O	O			O		O	O	O			
I533T	BINNACLE			O	O	O			O		O	O	O			
I534T	ANALOG SIG CONVERTER			O	O	O			O		O	O	O			
I535T	COMPUTER			O	O	O			O		O	O	O			
I528V	YAW STEERING SIG			O	O	O			O		O	O	O			
I529V	ROLL RESOLVER SIG			O	O	O			O		O	O	O			
I530V	PITCH RESOLVER SIG			O	O	O			O		O	O	O			
I540V	CONTROL 115 PHASE B			O	O	O			O		O	O	O			
I541V	CONTROL M22.5 PSUP			O	O	O			O		O	O	O			
I543V	COMPUTER M50 PSUP			O	O	O			O		O	O	O			
I544V	COMPUTER M16.5 PSUP			O	O	O			O		O	O	O			
I545V	COMPUTER M10 PSUP			O	O	O			O		O	O	O			
I547V	COMPUTER 4 PSUP			O	O	O			O		O	O	O			
I548V	COMPUTER 38 PSUP			O	O	O			O		O	O	O			
I580V	AZM RESOLVER SIG			O	O	O			O		O	O	O			
I601V	400 CPS REFERENCE			X	X	X			X		X	X	X			
I510W	ELAPSED TIME			OX	OX	OX			OX		OX	OX	OX			
I581W	TIME T			O	O	O			O		O	O	O			
I521X	VERN ENGINE COF SIG			OX	OX	OX			OX		OX	OX	OX			
I522X	S ENGINE COF SIG			OX	OX	OX			OX		OX	OX	OX			

TABLE 7.8-1 INSTRUMENTATION OF SERIES D MISSILES (CONTINUED)

MEASUREMENT NUMBER	DESCRIPTION	MISSILE NUMBER														
		27D	32D	42D*	48D*	54D*	55D	56D	60D*	62D	66D*	71D*	76D*	79D	83D	90D
I523X	S&V COF RELAYS			O	O	O			O		O	O	O			
I525X	PRE-ARM SIGNAL 1			O	O	O			O		O	O	O			
I526X	PRE-ARM SIGNAL 2			O	O	O			O		O	O	O			
I527X	PRE-ARM RELAY CLOS			O	O	O			O		O	O	O			
I537X	COMPUTER REDUNDANCY			O	O	O			O		O	O	O			
I570X	STAGING SIGNAL			OX	OX	OX			OX		OX	OX	OX			
I603X	WORD GATE FIVE				X	X			X		X	X	X			
I604X	MULT GATE SIX				X	X			X		X	X	X			
I605X	112 CPS GATE				X	X			X		X	X	X			
L127P	HOLDDOWN CYL B1 SIDE	X	X	X	X	X	X	X	X		X	X	X		X	X
L128P	HOLDDOWN CYL B2 SIDE	X	X	X	X	X	X	X	(X)		X	X	X		X	X
M 79A	MSL AXIAL ACCEL FINE								O		[O]	O	O			
M 26D	JET SECT SEPARATION	O	O	[O]	O	O	O	[O]	O	[O]	[O]	O	[O]	[O]	[O]	[O]
M 44I	IR FILTER NO. 1 OUTPUT	O	O				O	O		O				O	O	O
M 45I	IR FILTER NO. 2 OUTPUT	O	O				O	O		O				O	O	O
M 46I	IR FILTER NO. 3 OUTPUT	O	O				O	O		O				O	O	O
M 47I	IR FILTER NO. 4 OUTPUT	O	O				O	O		O				O	O	O
M 48I	IR FILTER NO. 5 OUTPUT	O	O				O	O		O				O	O	O
M 49I	IR CALIBRATION LIGHT	O	O				O	O		O				O	O	O
M 81I	REFLECTANCE	O	O				O	O		O				O	O	O
M 82T	BOLOMETER TEMP	O	O				O	O		O				O	O	O
M 83T	CHOPPER TEMP	O	O				O	O		O				O	O	O
M135T	AGS RB CELL LAMP														O	O
M136T	AGS RB CELL CAVITY														O	O
M 38V	IR CALIBRATION NO. 1	O	O				O	O		O				O	O	O
M 39V	IR CALIBRATION NO. 2	O	O				O	O		O				O	O	O
M 43V	IR CALIBRATION NO. 3	O	O				O	O		O				O	O	O
M137V	AGS RB CELL 2ND HARM														O	O
M138V	AGS RB CELL FUND														O	O
M 28X	ABORT SYSTEM SIGNAL		O					O		O				O		
M 30X	MSL TWO-INCH MOTION	X	X	X	X	X	X	X	X	X	X	X	X	X	X	X
M 50X	MSL 42-INCH MOTION			X												
M 78X	STROBE LIGHT OCCUR	O	O		O	O		O	O	O		O	O	O	O	O
M145X	BOOSTER ABORT READY	O	O					O		O				O		
M161X	PVT RELAY SIGNAL										O	O	O			
M162X	PVT RELAY OUTPUT										O	O	O			
M163X	GROUND PVT SIGNAL										O	O	O			
M165X	A/P BCO DISCRETE										O					
N342T	POD AIR DUCT	X	X	X	X	X	X	X	X	X	X	X	X	X	X	X
N344T	TRANSFER ROOM	X	X	X	X	X	X	X	X	X	X	X	X	X	X	X
N353T	THST SECT HTR OUTPUT	X	X	X	X	X	X	X	X	X	X	X	X	X	X	X
N343X	POD AIR DUCT VALVE	X	X	X	X	X	X	X	X	X	X	X	X	X	X	X
N354X	KECO AIRFLOW SAIL SW	X	X	X	X	X	X	X	X	X	X	X	X	X	X	X
N969X	AA 90% PROBE						X					X	X			
N970X	AA FUEL 95% PROBE											X	X			
N971X	AA 99.8% PROBE	X	X				X	X		X		X	X	X	X	X
N972X	AA 100.2% PROBE	X	X				X	X		X		X	X	X	X	X
N973X	AA LOX RAPID SIG						X					X	X			
N974X	AA LOX BU RAPID SIG											X	X			
N975X	AA LOX FINE SIG						X				X	X	X			
N976X	AA LOX BU FINE SIG						X									
N977X	AA LOX TOPG COF SIG	X	X				X	X		X	X	X	X	X	X	X
N978X	AA LOX EM SIG	X	X				X	X		X		X	X	X	X	X
P 83B	B2 PUMP SPEED	O	O	O	O	O	O	O	O	O	O	[O]	O	O	O	O
P 84B	B1 PUMP SPEED	O	O	O	O	O	O	[O]	O	O	O	O	O	O	O	O
P349B	S PUMP SPEED	O	O	O	O	O	O	O	O	O	O	O	O	O	O	O
P314C	LOX TOPPING SIGNAL	X	X				X	X		X				X	X	X
P529D	S MAIN LOX VALVE	O	O	O	O	O	O	O	O	O	O	[O]	O	O	O	O
P830D	SUST FUEL VLV POS	O	O			O	O	O	O	O	O	O	O	[O]	O	O
P439O	S NAA RCC ACCEL	X	X		X	X	X	X	X	X	X	X	X	(X)	X	X
P452O	B1 NAA RCC ACCEL	X	X		X	(X)	X	X	(X)	X	X	X	X	X	X	X
P453O	B2 NAA RCC ACCEL	X	X		X	X	X	X	X	X	X	X	X	(X)	X	X
P893O	B1 NAA ACCEL BK U	X	X			X	X	X	X	X	X	X	X	X	(X)	X
P894O	B2 NAA ACCEL BK U	X	X			X	X	X	X	X	X	X	X	X	(X)	(X)
P 1P	B1 LOX PUMP INLET	OX	OX			X	OX	OX	X	OX	X	X	X	OX	OX	OX
P 2P	B1 FUEL PUMP INLET	OX	OX			X	OX	OX	X	OX	X	X	X	OX	OX	OX
P 3P	B2 LOX PUMP INLET	OX	OX			X	OX	OX	X	OX	X	X	X	OX	OX	OX
P 4P	B2 FUEL PUMP INLET	OX	OX			X	OX	OX	X	OX	X	X	X	OX	OX	OX
P 6P	S THRUST CHAMBER	OX	OX	OX	OX	OX	OX	OX	OX	OX	OX	OX	OX	OX	OX	[OX]
P 10P	B1 LUBE OIL INJ MAN	O	O				O	O		O				O	O	O
P 26P	B LOX REG REFERENCE	OX	OX	OX	OX	OX	OX	OX	OX	OX	OX	OX	OX	OX	OX	OX
P 27P	VERNIER FUEL TANK	O	O	O	O	O	O	O	O	O	O	O	[O]	O	O	O

TABLE 7.8-1 INSTRUMENTATION OF SERIES D MISSILES (CONTINUED)

MEASUREMENT NUMBER	DESCRIPTION	MISSILE NUMBER													
		27D	32D	42D*	48D*	54D*	55D	56D	60D*	62D	66D*	71D*	76D*	79D	83D	90D
P 28P	V1 THRUST CHAMBER	O	O	O	O	O	O	O	O	O	O	O	O	O	O	O
P 29P	V2 THRUST CHAMBER	O	O	O	O	O	O	O	O	O	O	O	O	O	O	O
P 30P	VERNIER LOX TANK	O	O	O	O	O	O	O	O	O	O	O	O	O	O	O
P 38P	B2 FUEL PUMP OUTLET	X	X			X	X	X	X	X	X	X	X	X	X	X
P 39P	B1 FUEL PUMP OUTLET	X	X			X	X	X	X	X	X	X	X	X	X	X
P 56P	S LOX PUMP INLET	O	O	O	O	O	O	O	O	O	O	O	O	O	O	O
P 59P	B2 THRUST CHAMBER	OX	OX	OX	OX	OX	OX	OX	OX	OX	OX	OX	OX	OX	OX	OX
P 60P	B1 THRUST CHAMBER	OX	OX	OX	OX	OX	OX	OX	OX	OX	OX	OX	OX	OX	OX	OX
P 91P	B1 LOX INJ MANIFOLD	X	X			X	X	X	X	X	X	X	X	X	X	X
P 92P	B2 LOX INJ MANIFOLD	X	X			X	X	X	X	X	X	X	X	X	X	X
P 93P	B1 FUEL INJ MANIFOLD	X	X			X	X	X	X	X	X	X	X	X	X	X
P 94P	B2 FUEL INJ MANIFOLD	X	X			X	X	X	X	X	X	X	X	X	X	X
P100P	B GG COMBUSTION CHM	OX	OX	O	O	OX	OX	OX	OX	OX	OX	OX	OX	OX	OX	OX
P330P	S FUEL PUMP DISCH	O	O	O	O	O	O	O	O	O	O	O	O	O	O	O
P339P	S GAS GEN DISCH	O	O	O	O	O	O	O	O	O	O	O	O	O	O	O
P344P	S LOX REG REFERENCE	OX	OX	OX	OX	OX	OX	OX	OX	OX	OX	OX	OX	OX	OX	OX
P351P	S LOX INJ MANIFOLD	O	O	O	O	O	O	O	O	O	O	O	O		O	O
P465P	S LO PR LUB OIL MAN	O	O				O	O		O				O	O	O
P487P	B1 IGN FUEL INJECTOR	X	X			X	X	X	X	X	X	X	X	X	X	X
P488P	B2 IGN FUEL INJECTOR	X	X			X	X	X	X	X	X	X	X	X	X	X
P721P	S FUEL JACKET PURGE	X	X			X	X	X	X	X	X	X	X	X	X	X
P847P	B1 THST CHM-LIM RNG						O									
P848P	B2 THST CHM-LIM RNG						O									
P850P	S LOX PUMP IN LO RNG						O	O		O						
P899P	LOX DOME PURGE	X	X			X	X	X	X	X	X	X	X	X	X	X
P901P	B FUEL JACKET PURGE	X	X			X	X	X	X	X	X	X	X	X	X	X
P 14T	ENGINE COMP AMBIENT	O	O	O	O	O	O	O	O	O	O	O	O	O	O	O
P 17T	B2 TURBINE INLET	X	X	X	X	X	X	X	X	X	X	X	X	X	X	X
P 20T	B1 LOX PUMP INLET	X	X			X	X	X	X	X	X	X	X	X	X	X
P 21T	LOX AT BREAKAWAY VLV	X	X	X	X	X	X	X	X	X	X	X	X	X	X	X
P 54T	B2 LOX PUMP INLET	X	X			X	X	X	X	X	X	X	X	X	X	X
P326T	S TURBINE INLET	X	X	X	X	X	X	X	X	X	X	X	X	X	X	X
P530T	S LOX PUMP INLET	O	O	O	O	O	O	O	O	O	O	O	O	O	O	O
P671T	TH SECT AMB QUAD 4	O	O	O	O	O	O	O	O		O	O	O			O
P673T	B1 FUEL IGN VLV AMB	X	X	X	X	X	X	X	X	X	X	X	X	X	X	X
P674T	B2 FUEL IGN VLV AMB	X	X	X	X	X	X	X	X	X	X	X	X	X	X	X
P675T	ENG CTL PNEU MAN	X	X	X	X	X	X	X	X	X	X	X	X	X	X	X
P437W	S RCC BINARY COUNTER	X	X			X	X	X	X	X	X	X	X	X	X	X
P454W	B1 RCC BINARY COUNT	X	X			X	X	X	X	X	X	X	X	X	X	X
P455W	B2 RCC BINARY COUNT	X	X			X	X	X	X	X	X	X	X	X	X	X
P897W	B1 RCC BIN CNT BK U	X	X			X	X	X	X	X	X	X	X	X	X	X
P898W	B2 RCC BIN CNT BK U	X	X			X	X	X	X	X	X	X	X	X	X	X
P 67X	B2 LOX VLV CLSD MSW	OX	OX	X	X	X	OX	OX	X	OX	X	X	X	OX	OX	OX
P 68X	B1 LOX VLV CLSD MSW	OX	OX	X	X	X	OX	OX	X	OX	X	X	X	OX	OX	OX
P 69X	B2 FUEL VLV CLSD MSW	OX	OX	X	X	X	OX	OX	X	OX	X	X	X	OX	OX	OX
P 70X	B1 FUEL VLV CLSD MSW	OX	OX	X	X	X	OX	OX	X	OX	X	X	X	OX	OX	OX
P 71X	BGG VLV CLOSED MSW	X	X	X	X	X	X	X	X	X	X	X	X	X	X	X
P 72X	BOOSTER CUTOFF RELAY	OX	OX	OX	OX	OX	OX	OX	OX	OX	OX	OX	OX	OX	OX	OX
P 73X	V1 PV CLOSED MSW	X	X	X	X	X	X	X	X	X	X	X	X	X	X	X
P 74X	V2 PV CLOSED MSW	X	X	X	X	X	X	X	X	X	X	X	X	X	X	X
P 77X	VERNIER CUTOFF RELAY	OX	OX	OX	OX	OX	OX	OX	OX	OX	OX	OX	OX	OX	OX	OX
P137X	ETP PREP COMPLETE LT	X	X	X	X	X	X	X	X	X	X	X	X	X	X	X
P147X	B GG VLV OPEN MSW	X	X	X	X	X	X	X	X	X	X	X	X	X	X	X
P154X	TCC B ENGINE COF SW	X	X	X	X	X	X	X	X	X	X	X	X	X	X	X
P155X	OBSERVER CUTOFF	X	X	X	X	X	X	X	X	X	X	X	X	X	X	X
P157X	B2 TBN OVRSPEED TRIP	X	X	X	X	X	X	X	X	X	X	X	X	X	X	X
P158X	PREP INCOMPLETE COF	X	X	X	X	X	X	X	X	X	X	X	X	X	X	X
P161X	TCC START SWITCH	X	X	X	X	X	X	X	X	X	X	X	X	X	X	X
P164X	TCC VERN ENG COF SW	X	X	X	X	X	X	X	X	X	X	X	X	X	X	X
P169X	B2 LOX VLV OPEN MSW	X	X	X	X	X	X	X	X	X	X	X	X	X	X	X
P170X	B1 LOX VLV OPEN MSW	X	X	X	X	X	X	X	X	X	X	X	X	X	X	X
P172X	V1 PV OPEN MSW	X	X	X	X	X	X	X	X	X	X	X	X	X	X	X
P174X	V2 PV OPEN MSW	X	X	X	X	X	X	X	X	X	X	X	X	X	X	X
P192X	B1 ROUGH COMB COF	X	X	X	X	X	X	X	X	X	X	X	X	X	X	X
P193X	B2 ROUGH COMB COF	X	X	X	X	X	X	X	X	X	X	X	X	X	X	X
P194X	B1 FUEL VLV OPEN MSW	X	X	X	X	X	X	X	X	X	X	X	X	X	X	X
P195X	B2 FUEL VLV OPEN MSW	X	X	X	X	X	X	X	X	X	X	X	X	X	X	X
P198X	S LOX HSV OPEN MSW	X	X	X	X	X	X	X	X	X	X	X	X	X	X	X
P199X	S LOX HSV CLOSED MSW	X	X	X	X	X	X	X	X	X	X	X	X	X	X	X
P202X	S FUEL PUV OPEN MSW	X	X	X	X	X	X	X	X	X	X	X	X	X	X	X
P203X	S FUEL PUV CLSD MSW	X	X	X	X	X	X	X	X	X	X	X	X	X	X	X
P300X	B1 INJ MAN P SW		O				O	O		O				O		
P311X	90% FUEL LVL IND	X	X	X	X	X	X	X	X	X	X	X	X	X	X	X
P313X	B2 INJ MAN P SW		O				O	O		O				O		
P335X	SGG VLV CLSD MSW	X	X	X	X	X	X	X	X	X	X	X	X	X	X	X
P347X	S COF RELAY LOCKIN	OX	OX	OX	OX	OX	OX	OX	OX	OX	OX	OX	OX	OX	OX	OX
P357X	TCC R/S INT P ARMED									X	X	X	X	X		
P438X	S ROUGH COMB COF	X	X	X	X	X	X	X	X	X	X	X	X	X	X	X
P441X	IGNITION STAGE TIMER	X	X	X	X	X	X	X	X	X	X	X	X	X	X	X
P445X	B FUEL PRE VLV OPEN	X	X	X	X	X	X	X	X	X	X	X	X	X	X	X
P446X	B FUEL PRE VLV CLSD	X	X	X	X	X	X	X	X	X	X	X	X	X	X	X
P499X	SGG VLV OPEN MSW	X	X	X	X	X	X	X	X	X	X	X	X	X	X	X

TABLE 7.8-1 INSTRUMENTATION OF SERIES D MISSILES (CONTINUED)

MEASUREMENT NUMBER	DESCRIPTION	MISSILE NUMBER													
		27D	32D	42D*	48D*	54D*	55D	56D	60D*	62D	66D*	71D*	76D*	79D	83D	90D
P566X	DC GND PWR FAIL COF	X	X	X	X	X	X	X	X	O	X	X	X	O	X	X
P574X	S INJ MAN P SW		O				O	O		X				X		
P575X	PRE START READY	X	X	X	X	X	X	X	X	X	X	X	X	X	X	X
P577X	RELEASE SIGNAL	X	X				X	X		X	X	X	X	X	X	X
P580X	S FUEL PRE VLV CLSD	X	X	X	X	X	X	X	X	X	X	X	X	X	X	X
P581X	S FUEL PRE VLV OPEN	X	X	X	X	X	X	X	X	X	X	X	X	X	X	X
P588X	S TBN OVERSPEED TRIP	X	X	X	X	X	X	X	X	X	X	X	X	X	X	X
P592X	BOOSTER ENG CUTOFF	X	X	X	X	X	X	X	X	X	X	X	X	X	X	X
P593X	SUSTAINER ENG CUTOFF	X	X	X	X	X	X	X	X	X	X	X	X	X	X	X
P594X	TCC SUSTAINER COF SW	X	X	X	X	X	X	X	X	X	X	X	X	X	X	X
P596X	PRE-RLS COF DISARM	X	X	X	X	X	X	X	X	X	X	X	X	X	X	X
P598X	VERNIER ENG CUTOFF	X	X	X	X	X	X	X	X	X	X	X	X	X	X	X
P608X	ENG TANKS PRES	X	X	X	X	X	X	X	X	X	X	X	X	X	X	X
P609X	ENG FUEL TK PRESD	X	X	X	X	X	X	X	X	X	X	X	X	X	X	X
P610X	ENG LOX TK PRESD	X	X	X	X	X	X	X	X	X	X	X	X	X	X	X
P611X	MAIN IGNITION START	X	X	X	X	X	X	X	X	X	X	X	X	X	X	X
P612X	GG IGN LINK PILOT	X	X	X	X	X	X	X	X	X	X	X	X	X	X	X
P613X	V1 P CHM SWITCH ON	X	X	X	X	X	X	X	X	X	X	X	X	X	X	X
P614X	V2 P CHM SWITCH ON	X	X	X	X	X	X	X	X	X	X	X	(X)	X	X	X
P616X	B FLIGHT LOCKIN	X	X	X	X	X	X	X	X	X	X	X	X	X	X	X
P617X	MAIN STAGE LIMITER	X	X	X	X	X	X	X	X	X	X	X	X	X	X	X
P618X	B1 FUEL MAN P SW ON	X	X	X	X	X	X	X	X	X	X	X	X	X	X	X
P619X	B2 FUEL MAN P SW ON	X	X	X	X	X	X	X	X	X	X	X	X	X	X	X
P621X	IGN STAGE VLVS	X	X	X	X	X	X	X	X	X	X	X	X	X	X	X
P622X	S FLIGHT LOCKIN	X	X	X	X	X	X	X	X	X	X	X	X	X	X	X
P623X	S FUEL MAN P SW ON	X	X	X	X	X	X	X	X	X	X	X	X	X	X	X
P624X	MAIN ENGS COMPLETE	X	X	X	X	X	X	X	X	X	X	X	X	X	X	X
P627X	MAIN ENG TH COMPLETE	X	X	X	X	X	X	X	X	X	X	X	X	X	X	X
P628X	IGN STAGE LIM COF	X	X	X	X	X	X	X	X	X	X	X	X	X	X	X
P630X	MAIN STAGE LIM COF	X	X	X	X	X	X	X	X	X	X	X	X	X	X	X
P631X	LOX F&D VLV AIRB OPN	X	X				X	X		X	X	X	X	X	X	X
P632X	LOX F&D VLV AIRB CLS	X	X				X	X		X	X	X	X	X	X	X
P633X	LOX F&D VLV GND OPEN	X	X				X	X		X				X	X	X
P634X	LOX F&D VLV GND CLSD	X	X				X	X		X				X	X	X
P635X	FUL F&D VLV AIRB OPN	X	X				X	X		X	X	X	X	X	X	X
P636X	FUL F&D VLV AIRB CLS	X	X				X	X		X	X	X	X	X	X	X
P637X	FUL F&D VLV GND OPN	X	X				X	X		X				X	X	X
P638X	FUL F&D VLV GND CLS	X	X				X	X		X				X	X	X
P639X	ENGINE RESET	X	X				X	X		X				X	X	X
P686X	B&S GG LOX PURGE	X	X	X	X	X	X	X	X	X	X	X	X	X	X	X
P687X	B&S GG FUEL PURGE	X	X	X	X	X	X	X	X	X	X	X	X	X	X	X
P688X	VERNIER ENGINE PURGE	X	X	X	X	X	X	X	X	X	X	X	X	X	X	X
P975X	B1 RCC BACK-UP RELAY	X	X			X	X	X	X	X	X	X	X	X	X	X
P976X	B2 RCC BACK-UP RELAY	X	X			X	X	X	X	X	X	X	X	X	X	X
P987X	FUEL OVER-FILL PROBE			X	X	X			X		X	X	X			
P988X	LOX 95% LVL EMER COF	X	X	X	X	X	X	X	X	X	X	X	X	X	X	X
P997X	MSL FUEL 95%	X	X	X	X	X	X	X	X	X	X	X	X	X	X	X
P998X	LOX O/FILL EMER COF	X	X	X	X	X	X	X	X	X	X	X	X	X	X	X
P999X	MSL FUEL 100%	X	X	X	X	X	X	X	X	X	X	X	X	X	X	X
S 61D	ROLL DISPL GYRO SIG	O	O	O	O	O	O	O	O	O	O	O	O	O	O	O
S 62D	PITCH DISPL GYRO SIG	O	O	O	O	O	O	O	O	O	[O]	O	O	O	O	O
S 63D	YAW DISPL GYRO SIG	O	O	O	O	O	O	O	O	O	O	O	O	O	O	O
S203D	B1 PITCH ROLL			O	O	O			O		O	O	O			
S204D	B2 PITCH ROLL			O	O	O			O		O	O	O			
S205D	B1 YAW			O	O	O			O		O	O	O			
S206D	B2 YAW			O	O	O			O		O	O	O			
S222D	V1 PITCH			O	O	O			O		O	O	[O]			
S223D	V2 PITCH			O	O	O			O		O	O	O			
S233D	V1 YAW ROLL			O	O	O			O		O	O	O			
S234D	V2 YAW ROLL			O	O	O			O		O	O	O			
S252D	B1 YAW ROLL	O	O				O	O		O				O	O	O
S253D	B2 YAW ROLL	O	O				O	O		O				O	O	O
S254D	B1 PITCH	O	O				O	O		O				O	O	O
S255D	B2 PITCH	O	O				O	O		O				O	O	O
S256D	SUSTAINER YAW	O	O	O	O	O	O	O	O	O	O	O	O	O	O	O
S257D	SUSTAINER PITCH	O	O	O	O	O	O	O	O	O	O	O	O	O	O	O
S258D	V1 PITCH ROLL	O	O				O	O		O				O	O	O
S259D	V2 PITCH ROLL	O	O				O	O		O				O	O	O
S260D	V1 YAW	O	O				O	O		O				O	O	O
S261D	V2 YAW	O	O				O	O		O				O	O	O
S 52R	ROLL RATE GYRO SIG	O	O	O	O	O	O	O	O	O	O	O	O	O	O	O
S 53R	PITCH RATE GYRO SIG	O	O	O	O	O	O	O	O	O	O	O	O	O	O	O
S 54R	YAW RATE GYRO SIG	O	O	O	O	O	O	O	O	O	O	O	O	O	O	O
S 48V	PROGRAMMER PITCH SIG	X	X	X	X	X	X	X	X	X	X	X	X	X	X	X
S 49V	PROGRAMMER ROLL SIG	X	X	X	X	X	X	X	X	X	X			X	X	X
S 69V	ROLL INT OUTPUT SIG	X	X				X	X		X				X	X	X
S 72V	PITCH INT OUTPUT SIG	X	X				X	X		X				X	X	X
S 73V	YAW INT OUTPUT SIG	X	X				X	X		X				X	X	X
S107V	B1 PCH ACTR FEEDBACK	X	X	X	X	X	X	X	X	X	X	X	X	X	X	X
S108V	B2 PCH ACTR FEEDBACK	X	X	X	X	X	X	X	X	X	X	X	X	X	X	X
S113V	V1 YAW ACTR FEEDBACK	X	X	X	X	X	X	X	X	X	X	X	X	X	X	X
S114V	V2 YAW ACTR FEEDBACK	X	X	X	X	X	X	X	X	X	X	X	X	X	X	X
S118V	V2 PCH ACTR FEEDBACK	X	X	X	X	X	X	X	X	X	X	X	X	X	X	X

TABLE 7.8-1 INSTRUMENTATION OF SERIES D MISSILES (CONTINUED)

MEASUREMENT NUMBER	DESCRIPTION	MISSILE NUMBER														
		27D	32D	42D*	48D*	54D*	55D	56D	60D*	62D	66D*	71D*	76D*	79D	83D	90D
S119V	V1 PCH ACTR FEEDBACK	X	X	X	X	X	X	X	X	X	X	X	X	X	X	X
S121V	GYRO TEST SIG	X	X	X	X	X	X	X	X	X	X	X	X	X	X	X
S122V	SERVO TEST SIG	X	X	X	X	X	X	X	X	X	X	X	X	X	X	X
S123V	INTEGRATOR TEST SIG	X	X				X	X		X				X	X	X
S128V	B1 YAW ACTR FEEDBACK	X	X	X	X	X	X	X	X	X	X	X	X	X	X	X
S129V	B2 YAW ACTR FEEDBACK	X	X	X	X	X	X	X	X	X	X	X	X	X	X	X
S147V	PITCH GYRO AMP OUT	X	X	X	X	X	X	X	X	X	X	X	X	X	X	X
S148V	YAW GYRO AMP OUT	X	X	X	X	X	X	X	X	X	X	X	X	X	X	X
S149V	ROLL GYRO AMP OUT	X	X	X	X	X	X	X	X	X	X	X	X	X	X	X
S216V	S PCH ACTR FEEDBACK	X	X	X	X	X	X	X	X	X	X	X	X	X	X	X
S217V	S YAW ACTR FEEDBACK	X	X	X	X	X	X	X	X	X	X	X	X	X	X	X
S368V	28V INPUT TO PROGRAM										O	O	O			
S179X	BCO SYSTEM OUTPUT		O					O		O				O		
S235X	PROGRAMMER RUN TIME	X	X	X	X	X	X	X	X	X	X	X	X	X	X	X
S244X	PRE-ARM SIGNAL	X	X	X	X	X	X	X	X	X	X	X	X	X	X	X
S248X	RELEASE PAYLOAD	O	O	O	O	O	O	O	O	O	O	O	O	O	O	O
S332X	PRESSURIZE VERN TANK										O	O	O			
S356X	TCC A/P READY SW	X	X				X	X		X	X	X	X	X	X	X
S373X	BOOSTER CUTOFF										O	O	O			
S380X	PROGRAMMER PVT OUT										X	X	X			
U101A	AXIAL ACCELERATION	O	O				O	O		O				O	O	O
U 80P	LOX TANK HEAD	O	O	O	O	O	O	O	O	O	O	O	O	O	O	O
U 81P	FUEL TANK HEAD	O	O	O	O	O	O	O	O	O	O	O	O	O	O	O
U191T	AA INSTN CAN TEMP	X	X				X	X								
U 91V	ERROR RATIO DEMOD OP	OX	OX	X	OX	X	OX	OX	OX	OX	OX			OX	OX	OX
U112V	ACOUSTIC COUNTER OTP	O	O			O	O	O	O	O		O	O	O	O	O
U113V	ACOUSTIC VLV POS FB	O	O			O	O	O	O	O		O	O	O	O	O
U134X	AA TIME SHARD OSC OP	O	O			O	O		O			O	O			
U135X	ACOUSTICA SNSRS SIG	O	O			O	O	O	O	O		O	O	O	O	O
Y102L	EJECTION VELOCITY															O
Y122L	D1 VELOCITY						O	O		O				O	O	
Y132L	D6 VELOCITY						O	O		O				O	O	
Y137L	D8 VELOCITY						O	O		O				O	O	
Y119P	ADF POD PRESSURE						O	O		O				O	O	
Y112T	TUBE TEMP @ SQUIB													O	O	
Y114T	TEMP-UNDER FAIRING						O	O		O				O	O	
Y116T	TUBE OUTSIDE SURFACE													O	O	
Y118T	BATTERY SURFACE-TOP													O	O	
Y117V	ADF CALIB VOLTAGE						O	O		O				O	O	
Y156V	BATTERY VOLTAGE															O
Y 1X	SEPARATION SIG														O	O
Y103X	BAROMETRIC SW						O	O		O				O	O	O
Y104X	TIMER START SIGNAL						O	O		O				O	O	O
Y105X	BOOSTER ACCEL CYCLE						O	O		O				O	O	O
Y106X	SUSTAINER HALF CYCLE						O	O		O				O	O	O
Y120X	D1 UNLATCH						O	O		O				O	O	
Y121X	D1 EJECT						O	O		O				O	O	
Y123X	D1 INFLATION						O	O		O				O	O	
Y124X	D2 UNLATCH & EJECT						O	O		O				O	O	
Y125X	D3 UNLATCH						O	O		O				O	O	
Y126X	D3 EJECT						O	O		O				O	O	
Y128X	D4 UNLATCH & EJECT						O	O		O				O	O	
Y129X	D5 UNLATCH & EJECT						O	O		O				O	O	
Y130X	D6 UNLATCH						O	O		O				O	O	
Y131X	D6 EJECT						O	O		O				O	O	
Y134X	D7 UNLATCH & EJECT						O	O		O				O	O	
Y135X	D8 UNLATCH						O	O		O				O	O	
Y136X	D8 EJECT						O	O		O				O	O	
Y138X	D8 INFLATION						O	O		O				O	O	
Y141X	EJECT SURE TUBE 1						O	O		O				O	O	O
Y142X	EJECT SURE TUBE 6						O	O		O				O	O	
Y143X	EJECT SURE TUBE 8						O	O		O				O	O	
Y144X	D1 UNLATCH ORIENT						O	O		O						
Y145X	D6 UNLATCH ORIENT						O	O		O						
Y146X	D8 UNLATCH ORIENT						O	O		O						
Y150X	FAIRING RELEASE SIG															O
Y151X	UNLATCH SIGNAL															O
Y152X	MOTOR START SIGNAL															O
Y153X	EJECT SIGNAL															O
Y154X	TUBE ORIENTATION															O
Y155X	TUBE UNLATCH															O
Z 2E	KLYSTRON PWR OUTPUT	O	O	O	O	O	O	O	O	O	O	O	O	O	O	O
Z 3E	XPONDR RF INPUT/AGC	O	O	O	O	O	O	O	O	O	O	O	O	O	O	O
Z 13T	TRANSPONDER CAN GAS			O	O	O			O		O	O	O			
Z 4V	KLYSTRON BEAM			O	O	O			O		O	O	O			

TABLE 7.8-2 TELEMETRY SYSTEM PERFORMANCE

MEAS. TYPE	ATTEMPTED	FAILURES	% OF ATTEMPTED
Intensity (I)	71	2	2.8
Vibration (O)	38	8	21.1
Temperature (T)	275	15	5.5
Discrete Position (X)	416	7	1.7
Pressure (P)	456	10	2.2
Power (E)	53	2	3.8
Acceleration (A)	54	1	1.8
Deflection (D)	274	12	4.4
Rotation Rate (B)	45	2	4.4
Remaining	490	0	0
Total	2172	59	2.7

TABLE 7.8-3 LANDLINE SYSTEM PERFORMANCE

MEAS. TYPE	ATTEMPTED	FAILURES	% OF ATTEMPTED
Vibration (O)	136	24	17.6
Pressure (P)	414	15	3.6
Temperature (T)	165	7	4.2
Discrete Position (X)	1525	2	0.1
Remaining	574	0	0
Total	2814	48	1.7

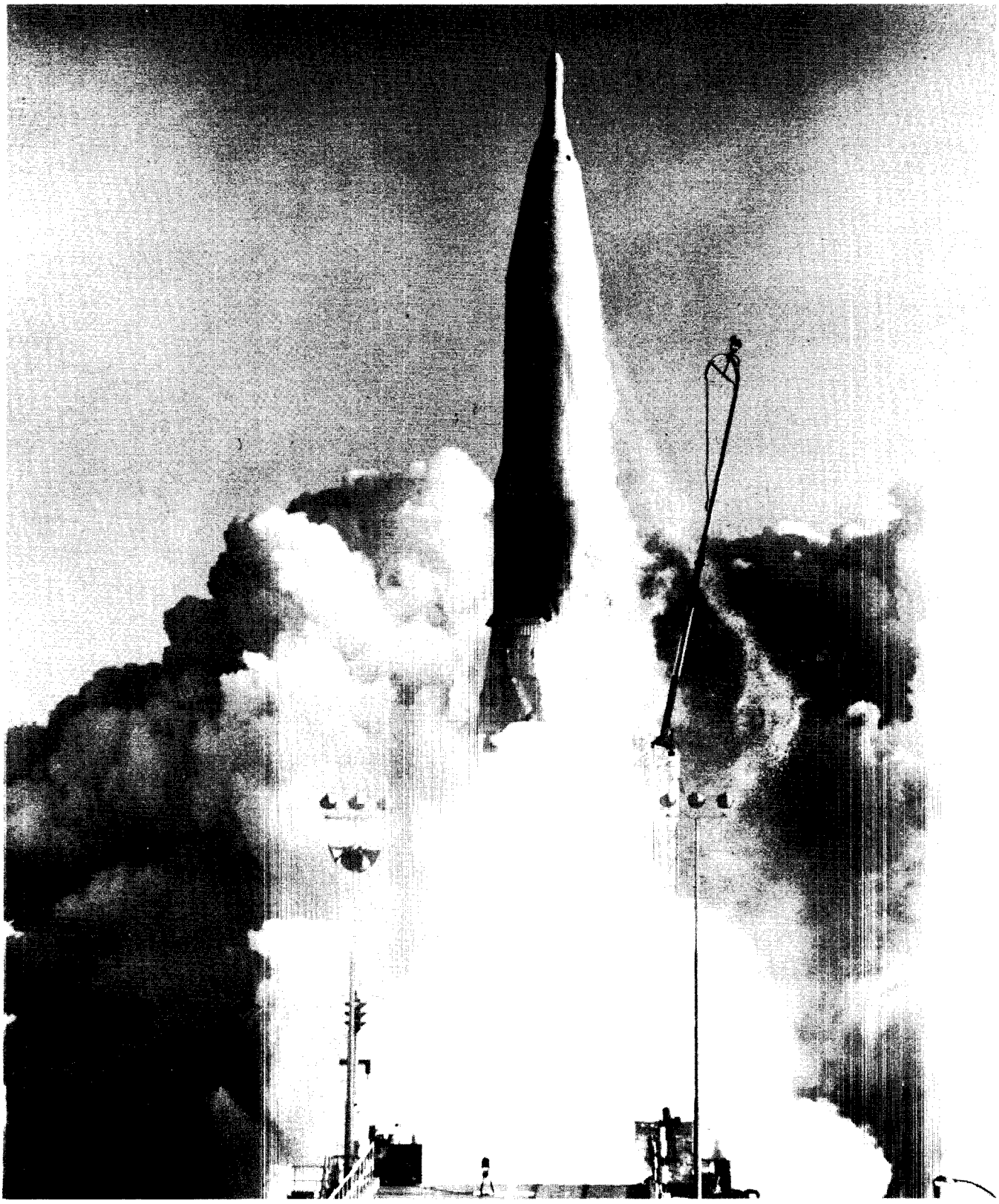

MISSILE 42D, TYPICAL AIG MISSILE WITH MARK 3 RE-ENTRY VEHICLE

SECTION 8 PAYLOAD

The Atlas Series D missile has carried re-entry vehicles of different types and configuration as well as research satellites and probes. The space vehicles are discussed briefly in the opening sections of this report. A total of 15 re-entry vehicles, carried by Series D missiles on research and development flights employing radio-inertial guidance (RIG) and all-inertial guidance (AIG) systems are discussed in this section. This is followed by a discussion of the decoy system which is being developed to increase penetration capabilities of the Atlas weapon. Since system evaluation of the re-entry vehicles and decoy system are the responsibilities of their respective manufacturers, the following discussions are largely of a descriptive and comparative nature.

SECTION 8.1 - RE-ENTRY VEHICLE

PURPOSE OF TESTING

The objectives for the re-entry vehicles discussed here are listed in Section 2 of this report.

INTRODUCTION

A summary of re-entry vehicles carried by Series D R&D missiles discussed in this report is presented chronologically in Table 8.1-1. Table 8.1-2 groups these re-entry vehicles by type with pertinent comments concerning general performance.

TABLE 8.1-1 SUMMARY OF RE-ENTRY VEHICLE TYPES TESTED

MISSILE NO.	LAUNCH DATE	R/V TYPE	RANGE	COMMENTS
42D*	3/8/60	Mk 3 Mod IX	4,395 NM	Impact in the target area. AIG system installed open-loop.
48D*	4/7/60	Mk 3 Mod IA		Exploded prior to liftoff.
56D	5/20/60	Mk 3 Mod IB	7,859 NM	Impact on target.
54D*	6/11/60	Mk 3 Mod IB	4,306 NM	Impact on target.
62D	6/22/60	Mk 3 Mod IIB	4,389 NM	Impact in target area.
27D	6/27/60	Mk 3 Mod IIB	4,389 NM	Impact on target.
60D*	7/2/60	Mk 3 Mod IB	4,306 NM	Impact in target area.
32D	8/9/60	Mk 3 Mod IB	6,350 NM	Impact on target.
66D*	8/12/60	RVX-2A	4,389 NM	Impact on target.
76D*	9/16/60	RVX-2A	4,389 NM	Impact on target.
79D	9/19/60	Mk 3 Mod IB	7,863 NM	Impact on target.
71D*	10/13/60	RVX-2A	4,389 NM	Impact on target.
55D	10/22/60	Mk 3 Mod IIB	6,350 NM	Impact on target.
83D	11/15/60	Mk 4 Mod I	4,389 NM	Impact on target.
90D	1/23/61	Mk 3 Mod IB	4,389 NM	Impact on target.

*Denotes all inertial guidance system employed.

TABLE 8.1-2 GENERAL RE-ENTRY VEHICLE PERFORMANCE

TYPE	MOD. NO.	SERIAL NO.	MISSILE NO.	COMMENTS
Mark 3 (eleven flown)	IX	211	42D	Satisfactory separation and performance.
	IA	216	48D	Missile exploded prior to liftoff.
	IB	220	56D	Satisfactory separation and performance. First R/V flown with modified flare (biconic-2), providing 10% greater base area. Thicker heat shield on biconic flare.
	IE	221	54D	Satisfactory separation and performance.
	IB	223	60D	Satisfactory separation and performance.
	IB	224	32D	Satisfactory separation and performance.
	IB	226	79D	Satisfactory separation and performance.
	IB	218A	90D	Satisfactory separation and performance. Dummy Sandia "C" center section. Two stroboscopic lights on aft face.
	IIB	219	62D	Satisfactory separation and performance.
	IIB	213B	27D	Satisfactory separation and performance.
	IIB	222	55D	Satisfactory separation and performance.
RVX-2A (three flown)		421	66D	Satisfactory separation and performance. Cast ablative coating. Recoverable R/V, recovery not effected.
		422	76D	Abnormal separation caused by failure of inflight disconnect. Restraint produced abnormal motions upon separation. Performance of R/V satisfactory except as noted. Vehicle was not recovered.
		423	71D	Satisfactory separation and performance. Ablation material. Special experiments and biospecimens carried. R/V recovered as planned.
Mark 4 (one flown)	I	11	83D	Satisfactory separation and performance. Data "cassette" ejected and recovered as planned.

The re-entry vehicles installed on the 15 Series D R&D missiles reported here, consisted of; eleven Mark 3 (Mod I, IX, IA, IB, or IIB) vehicles, one Mark 4 Mod I vehicle, and three RVX-2A vehicles. All of these re-entry vehicles were of the ablative type with high ballistic parameters, capable of both shallow and high velocity re-entry.

The flight test data quoted herein for each re-entry vehicle, as well as design and performance considerations, were based on individual General Electric and AVCO Flight Test Evaluation Reports. Data on the Missile 83D Mark 4 re-entry vehicle was obtained from an AVCO preliminary flight test report. General Electric data on the Mark 3 Mod IB re-entry vehicle flown on Missile 90D was not available at the time of the preparation of this report.

Table 8.1-3 is a listing and definition of symbols used in the discussion which follows. For information and clarity, Figures 8.1-1 and 8.1-2 pictorially define (1) the re-entry vehicle reference axes (X, Y, Z), and angular motions (Θ, ϕ, ψ) about these axes, and (2) the re-entry vehicle angle of attack (α) and flight path angle (β).

TABLE 8.1-3 DEFINITION OF SYMBOLS

SYMBOL	DEFINITION	UNITS
A	Characteristic cross section area	ft^2
a	Acceleration	g's
α	Angle of attack	degrees
β	Flight path angle w/respect to the local horizontal	degrees
C_D	Drag coefficient at zero angle of attack	non-dimensional
η	Depth of material ablated	feet
γ	Flight path angle w/respect to the local vertical	degrees
H,h	Altitude	feet
He	Heat of ablation	BTU/lb
Φ	Roll angle ($\dot{\Phi}$ = rate, deg/sec)	degrees
Ψ	Yaw angle ($\dot{\Psi}$ = rate, deg/sec)	degrees
q	Dynamic pressure	lbs/H^2
q	Heat flux	BTU/ft^2 sec
ρ	Density of the air	lbs sec^2/ft^4
ρ	Density of ablative material	lbs/ft^3
θ	Pitch angle ($\dot{\theta}$ = rate, deg/sec)	degrees
W	Weight	lbs
X	Re-entry vehicle longitudinal (roll) axis	
Y	Re-entry vehicle transversal (pitch) axis	
Z	Re-entry vehicle vertical (yaw) axis	

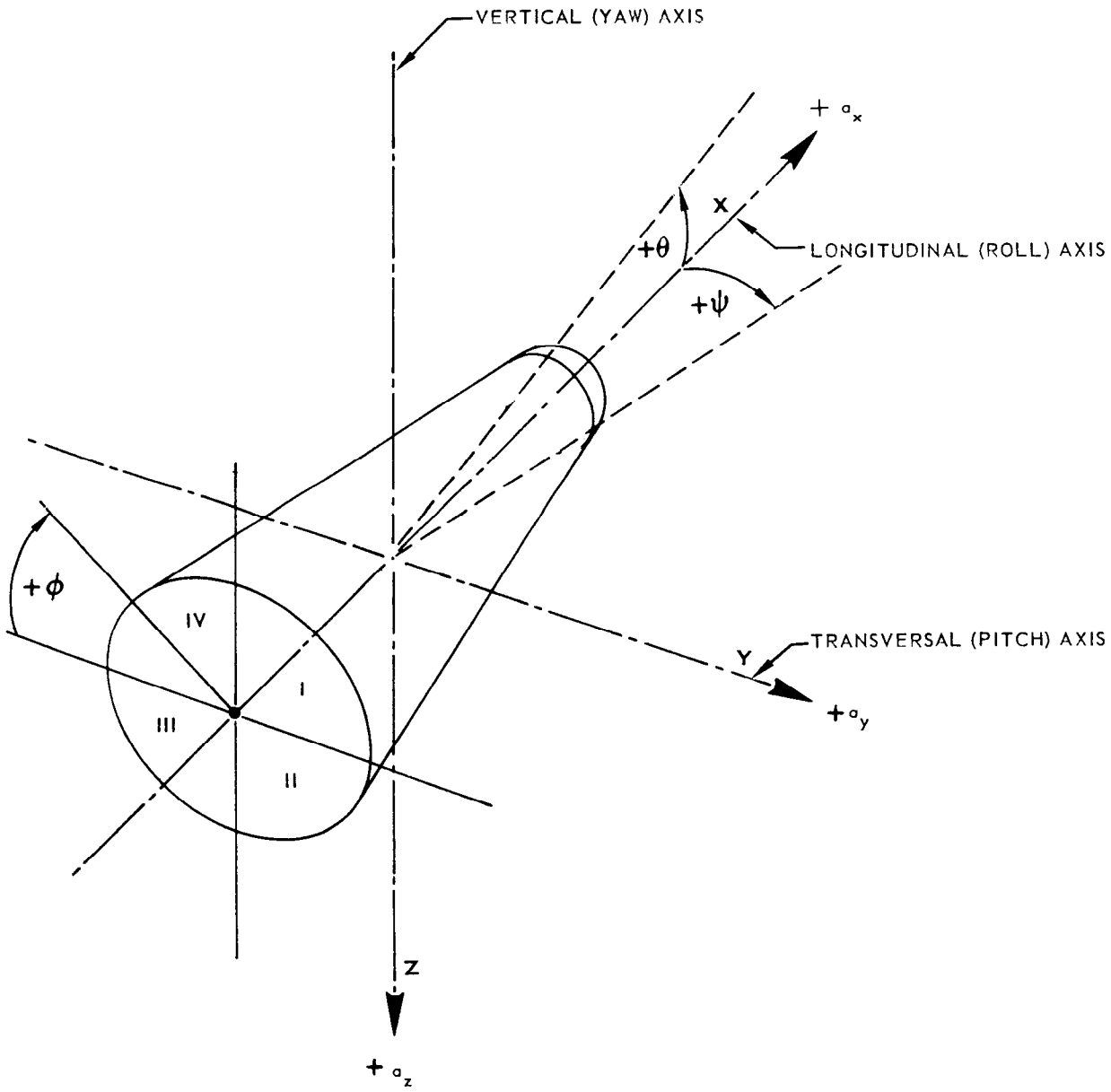

FIGURE 8.1-1 RE-ENTRY VEHICLE REFERENCE AXES AND PLANES OF ANGULAR MOTION

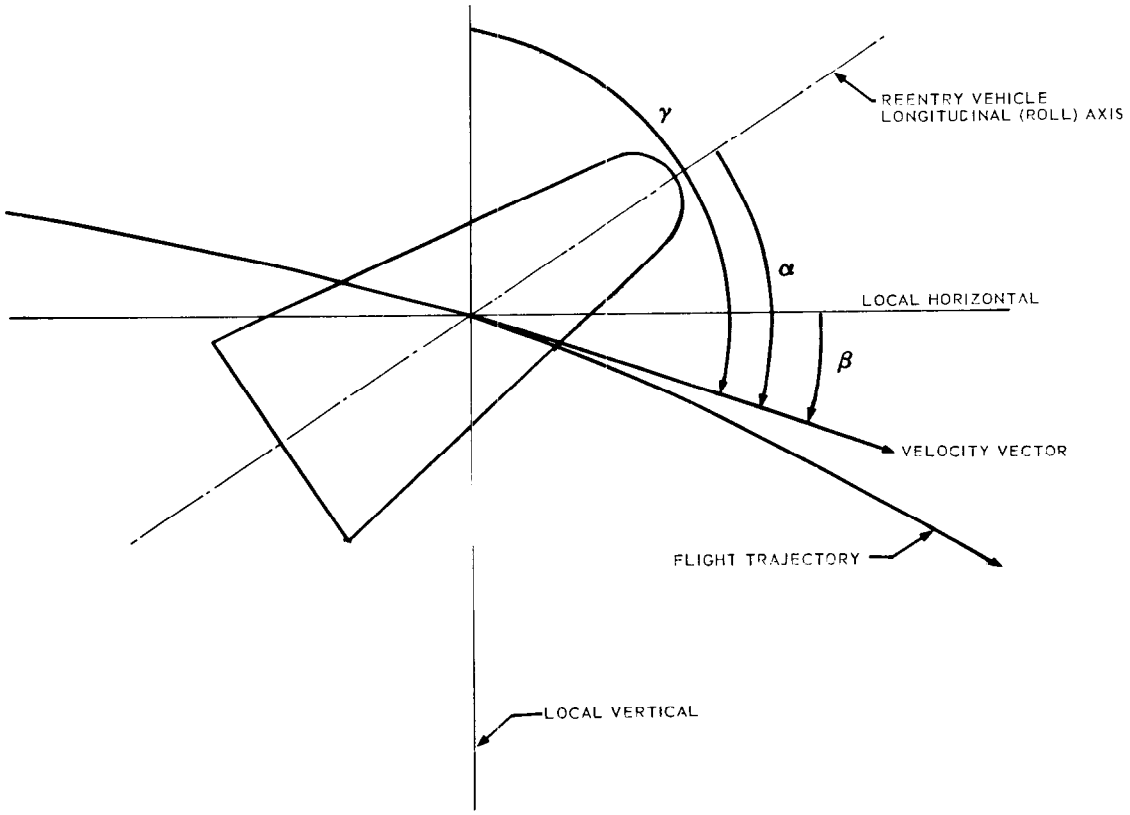

γ = ANGLE BETWEEN THE LOCAL VERTICAL AND THE VELOCITY VECTOR ($90° + \beta$)
α = ANGLE BETWEEN THE LONGITUDINAL AXIS AND THE VELOCITY VECTOR = ANGLE OF ATTACK (AFTER REENTRY)
β = ANGLE BETWEEN THE LOCAL HORIZONTAL THE VELOCITY VECTOR = FLIGHT PATH ANGLE

FIGURE 8.1-2 RE-ENTRY VEHICLE ANGLE OF ATTACK AND FLIGHT PATH ANGLE

MARK 3 RE-ENTRY VEHICLE

DESCRIPTION

The Mark 3 re-entry vehicles (R/V) included in this report were, with exception of those carried by Missiles 42D and 48D, of the configuration defined as "biconic-2" and designated as Mod IB and Mod IIB.

Missiles 42D and 48D carried Mk 3 Mod IX and Mk 3 Mod IA vehicles, respectively. The Mod IX vehicle had a conical flare of constant angle and was flown with its c.g. displaced forward of the usual location for the Mod I type, for the purpose of obtaining greater stability during flight through the atmosphere. Table 8.1-4 shows the weight and balance characteristics of the Mk 3 vehicle. The Mod IA vehicle, that was to be flown on Missile 48D, had a biconic flare similar to R/V 217 aboard Missile 51D (see 1st Series D Atlas Flight Summary Report). Neither 51D nor 48D was successfully flown.

The first Mark 3 re-entry vehicle with a biconic flare tested on an Atlas missile was No. 212 flown on Missile 49D. Missile 56D carried the first "biconic-2" of the group of missiles being discussed in this report. Externally, there is considerable difference in configuration between the Mk 3 Mod I and IX and the Mods IA, IB and IIB vehicles incorporating biconic flare sections. Figure 8.1-3, although not to scale, depicts these differences. Figures 8.1-4 and 8.1-5 depict the internal configurations of Mk 3 Mods IB and IIB vehicles, respectively.

It may be observed that the nose section, of a spherical-conical configuration, as well as the cylindrical midsection are common to all models of the Mk 3 vehicle. The aft face of these vehicles is a portion of a sphere of 30 inches radius plus a cone sector extending from the edge of the flare, tangential to the spherical portion of the mentioned aft face, on Mods IA, IB and IIB.

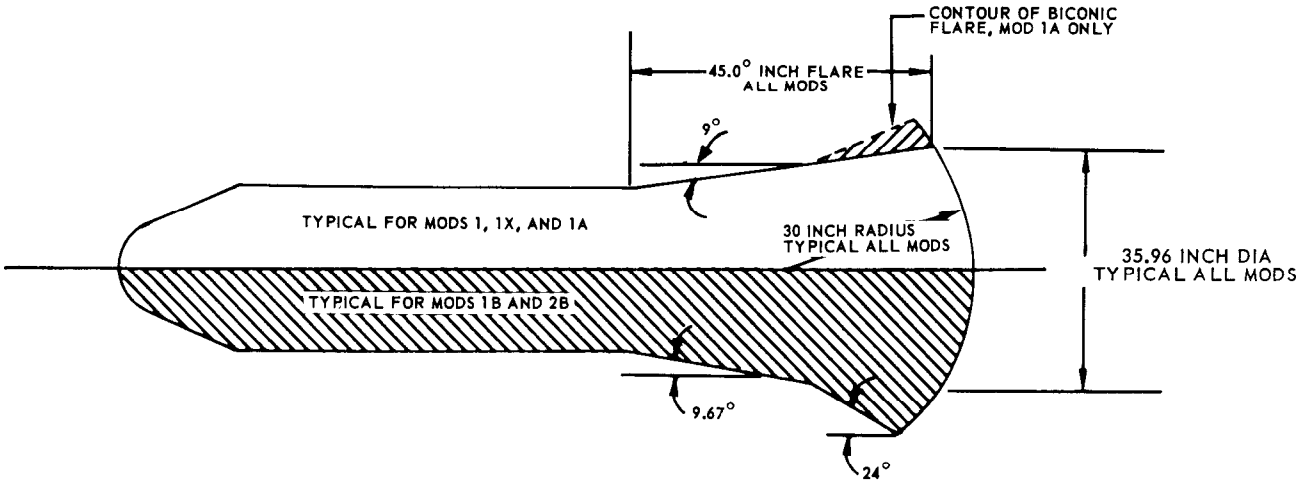

FIGURE 8.1-3 COMPARISON OF MARK 3 EXTERNAL CONFIGURATIONS

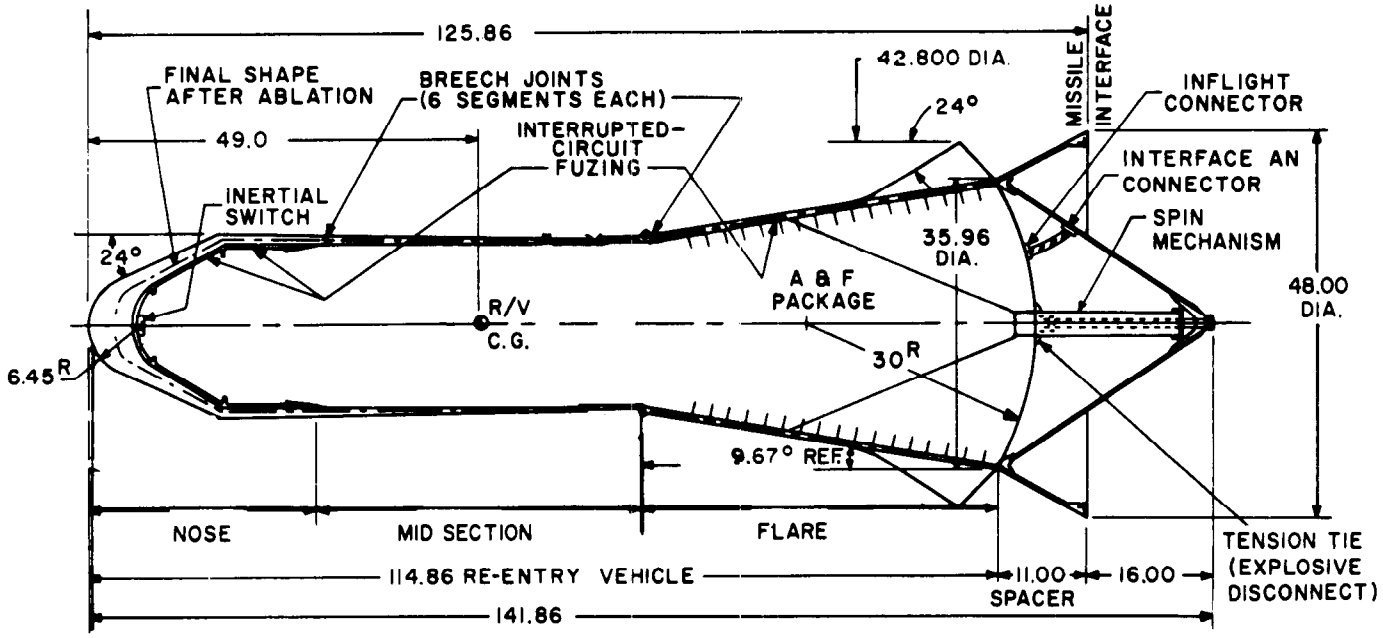

NOTE: ALL DIMENSIONS ARE IN INCHES.

FIGURE 8.1-4 CUTAWAY OF MARK 3 MOD IB RE-ENTRY VEHICLE

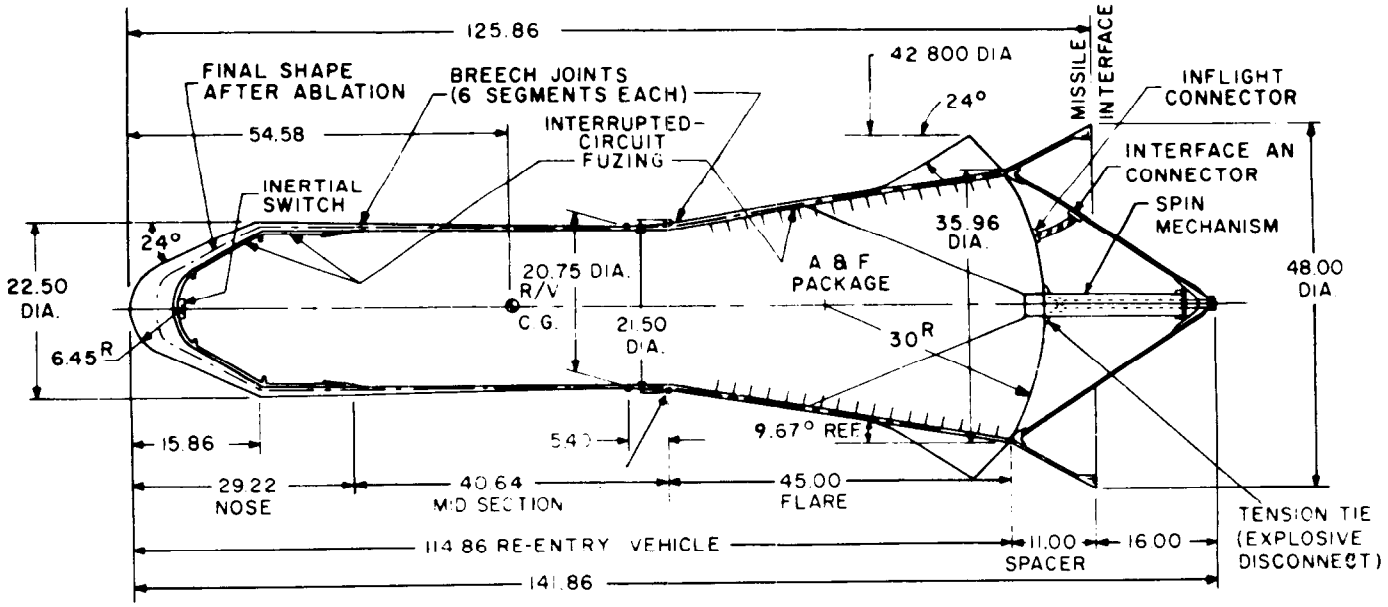

NOTE: ALL DIMENSIONS ARE IN INCHES.

FIGURE 8.1-5 CUTAWAY OF MARK 3 MOD IIB RE-ENTRY VEHICLE

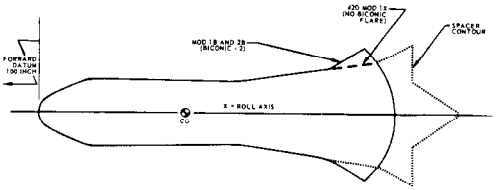

TABLE 8.1-4 MARK 3 WEIGHT AND BALANCE DATA

ITEM	MSL NO. R/V MOD.	42D MOD IX	48D MOD IA	56D MOD IB	54D MOD IB	62D MOD IIB	27D MOD IIB	60D MOD IB	32D MOD IB	79D MOD IB	55D MOD IIB	90D MOD IIB
1												
	A	2206.20	2211.0	2339.50	2369.61	2419.29	2399.26	2371.15	2352.87	2343.41	2413.22	
	B	2293.15	NDA	2425.10	2454.58	2504.26	2483.09	2457.53	2432.29	2429.43	2499.97	
2												
	A	148.50	151.08	153.35	153.75	154.58	145.57	153.71	153.49	153.62	154.51	
	B	151.33	NDA	155.84	156.16	156.92	156.89	156.15	155.96	156.08	156.89	
3												
	A	0.046	0.0071	0.052	-0.05	-0.005	0.061	-0.049	0.0505	-0.001	0.015	
	B	0.032	NDA	0.057	-0.04	-0.013	0.028	-0.037	0.0387	0.010	0.007	
4												
	A	-0.011	0.0075	0.001	-0.01	-0.004	-0.032	0.003	0.0138	-0.010	0.021	
	B	0.008	NDA	-0.007	0.00	0.003	-0.046	0.002	0.0158	-0.010	0.021	
5												
	A	0.048	0.0104		0.05	0.007	0.069	0.050	0.0523	0.010	0.026	
	B	0.033	NDA		0.04	0.013	0.054	0.037	0.0418	0.014	0.022	
6												
	A	35.06	36.40	45.27	47.63	45.43	45.06	47.34	46.61	44.35	44.83	
	B	41.32	NDA	51.49	53.85	51.69	51.24	53.68	52.87	50.64	51.17	
7												
	A	399.37	439.37	497.78	508.66	437.48	433.87	506.95	496.93	496.13	435.98	
	B	503.56	NDA	588.65	598.18	525.50	520.96	597.52	588.106	586.39	525.12	
8												
	A	398.51	436.61	498.64	509.47	437.76	434.15	507.56	495.45	498.48	436.17	
	B	502.72	NDA	589.50	599.00	525.77	521.22	598.11	586.55	588.76	525.29	

KEY TO ITEMS ON CHARTS:

1) Gross weight. (lbs)
2) CG position, longitudinal from forward datum roll axis X. (inches)
3) CG position, vertical from roll axis, along yaw axis Z. (inches)
4) CG position, lateral from roll axis, along pitch axis Y. (inches)
5) CG total offset from roll axis (X). (inches)
6) Moment of inertia about roll axis (I_x). (slug-ft^2)
7) Moment of inertia about pitch axis (I_y). (slug-ft^2)
8) Moment of inertia about yaw axis (I_z). (slug-ft^2)

A Denotes value less spacer.
B Denotes value with spacer.
NDA No data available.

The incorporation of the biconic flare was done for the purpose of increasing the cross-section area toward the rear of the vehicle. During penetration through the atmosphere, this change results in a further displacement of the aerodynamic center of pressure toward the rear of the vehicle, when compared with the constant cone flare of Mod I and Mod IX vehicles. This provides a greater stabilizing moment that tends to reduce oscillations and minimize the vehicles angle of attack. A summary of over-all performance of the Mk 3 re-entry vehicle is presented in Table 8.1-5.

STRUCTURE

Nose Section

The structural portion of the nose section is a single piece magnesium casting. Its thermal shield is constructed of moulded phenolic nylon.

Midsection

The midsection structure consists of the steel warhead case, thermally protected by tape-wound phenolic nylon.

Flare Section

The structural portion of the flare section is a magnesium casting, thermally protected by tape-wound phenolic nylon.

Spacer

The spacer, which remains with the Atlas airframe after separation, is an aluminum structure which contains the separation rate monitors.

TABLE 8.1-5 SUMMARY OF MARK 3 RE-ENTRY VEHICLE PERFORMANCE

TEST CONDITIONS AND EVENTS DURING FLIGHT	MISSILE 42D	MISSILE 48D	MISSILE 56D	MISSILE 54D	MISSILE 62D
TEST DATA					
TEST DATE AND TIME	8 MARCH 1960-0810:16 EST-AMR	7 APRIL 1960-2106 EST-AMR	20 MAY 1960-1000:26 EST-AMR	11 JUNE 1960-0130:18 EST-AMR	22 JUNE 1960-0940.33 EST-AMR
PLANNED RANGE, NM	4395	4306	7859	4306	4389
RE-ENTRY VEHICLE DESCRIPTION AND CONFIGURATION					
TYPE, MODEL AND SERIAL NUMBER	GE MK 3 MOD IX S/N 211	GE MK 3 MOD IA S/N 216	GE MK 3 MOD IB S/N 220	GE MK 3 MOD IB S/N 221	GE MK 3 MOD IIB S/N 219 (XXI BC-2)
WEIGHT (UNABLATED, LESS SPACER), lbs	2206.2	2211	2339.5	2369.61	2419.29
WARHEAD TEST PACKAGE	STEEL TEST UNIT, INSTRUMENTED FIRING SET	STEEL TEST UNIT, INSTRUMENTED FIRING SET	SANDIA STU AIRBORNE INSTRUMENTATION SUBSYSTEM	STEEL TEST UNIT, INSTRUMENTED FIRING SET	SANDIA INSTRUMENTED WARHEAD SYSTEM
TRACKING BEACON	C-BAND, INTERR. 5480 MC REPLY 5555 MC	C-BAND	C-BAND, INTERR. 5480 MC REPLY 5555 MC	C-BAND, INTERR. 5480 MC REPLY 5555 MC	NO TRACKING BEACON CARRIED
SOFAR BOMBS	TWO, NON-EJECTABLE ALUMINUM CASES	TWO, NON-EJECTABLE ALUMINUM CASES	NONE CARRIED	TWO, NON-EJECTABLE ALUMINUM CASES	NONE CARRIED
SPECIAL EQUIPMENT	NONE	NONE	NONE	NONE	NONE
COUNTDOWN HOLDS DUE TO RE-ENTRY VEHICLE	NONE	NONE	NONE	NONE	NONE
MISSILE AND RE-ENTRY VEHICLE EVENTS					
TELEMETRY START, flt/time - sec	0.00	LAUNCHING FAILED, MISSILE EXPLODED AFTER BURNING FOR APPROXIMATELY 60 SECONDS. THE RE-ENTRY VEHICLE DROPPED INTO THE LAUNCH STAND EXHAUST DEFLECTOR AND WAS RECOVERED IN WORKING ORDER	0.00	0.00	0.00
PREARM LOCKOUT SWITCH CLOSURE, sec	79.80		80.32	78.14	73.66
BOOSTER ENGINE CUTOFF, sec	141.29		136.57	137.62	117.77
SUSTAINER ENGINE CUTOFF, sec	256.80		271.06	235.55	284.26
VERNIER ENGINE CUTOFF, sec	269.17		285.00	242.79	307.69
PREARM SIGNAL, sec	269.10		286.42	243.66	314.26
BATTERY ACTIVATION, sec	269.10		286.42	243.66	314.26
SEPARATION SIGNAL, sec	284.20		NOT MONITORED	257.55	319.06
INFLIGHT DISCONNECT SEPARATION, sec	284.26		305.98	257.67	NOT MONITORED
START SPIN AND SEPARATION, sec	284.35		306.05 (PREDICTED)	257.79	SEPARATION SWITCH 319.16
SEPARATION CONDITIONS	SATISFACTORY		SATISFACTORY	SATISFACTORY	SATISFACTORY
SEPARATION RATE, in/sec	5.11 AVERAGE		4.13	4.77 ±0.7	NOT MONITORED
MEASURED ROLL RATE, deg/sec	88		ROLL RATE GYRO FAILED	58	68 (BASED ON TELEMETRY SIGNAL STRENGTH NULLS)
RETROROCKETS IGNITION, sec	286.25		309.92	473.24 (RATE GYRO AND AIG ACCEL. DATA. ELECTRICAL MALFUNCTION SUSPECTED)	323.00
RE-ENTRY TIME (300,000 FT), sec	1831.97		3260.4 (PREDICTED)	1846.04	1989.51
RE-ENTRY ANGLE (300,000 FT) deg	23.52		21.06	25.27	27.3 (CALCULATED)
RE-ENTRY VELOCITY (300,000 FT), ft/sec	21,326.0		24,500	21,132	21,402 (CALCULATED)
TELEMETRY BLACKOUT START, sec	1835.60		3258.02	1846.94	1991.76
ALTITUDE FUZING SEQUENCE START, sec	1856.43		LIMITED RE-ENTRY DATA RECEIVED	1868.42	2010.12
WARHEAD ARMING, sec	1859.21		LIMITED RE-ENTRY DATA RECEIVED	1871.16	2013.36
MAX. INT. TEMP. DURING RE-ENTRY, °F	85.5		LIMITED RE-ENTRY DATA RECEIVED	NOT INSTRUMENTED	75
MAX. SHIELD TEMP. DURING RE-ENTRY, °F/time			LIMITED RE-ENTRY DATA RECEIVED	2240° @ 1879 SECONDS	NOT MONITORED
TELEMETRY BLACKOUT END, sec	1855.6		3289.08	1876.24	2016.26
ALTITUDE FUZING, ft/time	5005/1871.77		LIMITED RE-ENTRY DATA RECEIVED	7393/1883.79	8200/2024.31
IMPACT TIME, sec	1874.95		3315.72 (PREDICTED)	1891.54	2030.0
EVENTS EXTERNAL TO RE-ENTRY VEHICLE PERFORMANCE					
R/V TRACKING	TRACKING BEACON RESPONDED TO ALL STATIONS		PARTIAL TRACKING OBTAINED FROM ALL STATIONS EXCEPT ASCENSION	SATISFACTORY FROM 3 STATIONS. NO TERMINAL TRACKING REPORTED	MISSILE TRACKED BY GE MOD III, GE IP AND AZUSA DURING POWERED FLIGHT
R/V TELEMETRY COVERAGE	BOTH REAL TIME AND PLAYBACK WERE SATISFACTORY		NO REAL TIME RCVD. AFTER 90 SEC. PLAYBACK RECEPTION GOOD	VERY SATISFACTORY REAL TIME AND PLAYBACK DATA OBTAINED	COMPLETE FROM SHIP, AIRCRAFT ASCENSION. PARTIAL FROM OTHER STATIONS
R/V VISUAL SIGHTING	NOT REPORTED		AVCO	NOT REPORTED	NOT REPORTED
R/V PHOTO AND CINE' COVERAGE	NOT REPORTED		AVCO CORP. FILMS REVEALED 2 FLASHES AT APPROXIMATELY 40,000 FT. A SPECTROGRAPHIC ANALYSIS WAS PERFORMED, ITS RESULTS BEING INCONCLUSIVE.	NOT REPORTED	NOT REPORTED
SOFAR BOMB REPORT	NO DETONATIONS DETECTED		NO SOFAR BOMBS CARRIED	TWO DETONATIONS DETECTED	NO SOFAR BOMBS CARRIED
REMARKS			FIRST BICONIC - 2 CONFIGURATION FLOWN	NO ACCURATE IMPACT LOCATION DETERMINATION SINCE ASSIGNED TARGET WAS NOT WITHIN AN INSTRUMENTED AREA	

TABLE 8.1-5 SUMMARY OF MARK 3 RE-ENTRY VEHICLE PERFORMANCE (CONT)

MISSILE 27D	MISSILE 60D	MISSILE 32D	MISSILE 79D	MISSILE 55D	MISSILE 90D
27 JUNE 1960-2130:54 EST-AMR	2 JULY 1960-0158:22 EST-AMR	9 AUGUST 1960-1309:33 EST-AMR	19 SEPT. 1960 1331:27 EST-AMR	22 OCTOBER 1960-0:13:20 EST-AMR	23 JANUARY 1961-1602 EST-AMR
4389	4306	6350	7860	6350	4389
GE MK 3 MOD IIB S/N 213B	GE MK 3 MOD IB S/N 223	GE MK 3 MOD IB S/N 224	GE MK 3 MOD IB S/N 226	GE MK 3 MOD IIB S/N 222	GE MK 3 MOD IB
2399.26	2371.15	2352.87	2343.41	2413.22	
SANDIA INSTRUMENTED WARHEAD SYSTEM	STEEL TEST UNIT, INSTRUMENTED AIMING AND FIRING SET	STEEL TEST UNIT, INSTRUMENTED ARMING AND FIRING SET	SANDIA INSTRUMENTED PACKAGE	SANDIA INSTRUMENTED PACKAGE	SANDIA "C" MIDSECTION DUMMY WARHEAD
	C-BAND, INTERR. 5480 MC REPLY 5555 MC	C-BAND, INTERR. 5481.7 MC REPLY 5555 MC	"C-BAND" BEACON WAS REMOVED FROM R/V	NO RADAR BEACON CARRIED ON R/V	C-BAND
NONE CARRIED	TWO, NON-EJECTABLE, ALUMINUM CASES	NONE CARRIED	NO SOFAR BOMBS CARRIED	NO SOFAR BOMBS CARRIED	
NONE	NONE	NONE	NONE	NONE	STROBOSCOPIC LIGHTS ON REARFACE FOR TERMINAL OPTICAL TRACKING
NONE	NONE	NONE	UMBILICAL LANYARD AND GROUND STATION DIFFICULTIES 91 MINUTES	NONE	NONE
0.00	0.00	0.00	0.00	0.00	0.00
NO TIME DATA AVAILABLE	80.61	79.83	80.6	82.68	
131.93	141.03	131.55	138.59	135.856	137.66
278.68	307.55	288.09	282.47	283.040	271.93
294.03	277.45	301.99	295.22	298.125	288.77
308.50 (MSL TLM)	365.46	318.23	312.65	313.19	
308.50 (MSL TLM)	355.46	318.53	312.65	313.19	
313.65	355.36	NOT MONITORED	317.5	318.11	
NOT MONITORED	355.36	325.21	317.3	NOT MONITORED	
NOT MONITORED	355.46	325.21	N.D.A.	318.75	
SATISFACTORY	SATISFACTORY	SATISFACTORY	SATISFACTORY	SATISFACTORY	
NOT MONITORED	4.91	5.4	4.36 ± 0.10	NOT MONITORED	
NO GRYOS ON BOARD, 66 (BASED ON TLM SIGNAL STRENGTH NULLS)	60	66 (BASED ON TLM SIGNAL STRENGTH NULLS)	ROLL RATE GYRO = 56 ANTENNA NULLS 60.06	68 (ANTENNA NULLS)	
317.40	357.30	327.10	321.32	322	305.67
1925.95 (CALCULATED)	1845.59	2753.23	3204.4	2666.10	
26.1 (CALCULATED)	25.31 (CALCULATED)	24.49 (CALCULATED)	20.4	23.27	
21,333 (CALCULATED)	21,186 (CALCULATED)	23,532 (CALCULATED)	24,400	23,438.37	
1926.95	1847.51	2752.73	3200.4	2669.47	
NOT MONITORED ON MOD 2 VEHICLES	1869.31	2775.03	3224.83	NOT MONITORED ON MOD II VEHICLES	
NOT OBTAINED	1871.96	2777.83	3228.23	NOT OBTAINED	
78	118°F @ 1869.81	136°F @ 2796.23	90°F	74°F	
NOT MONITORED	280°F UPON IMPACT	1540°F @ 2786.73	1320°F	NOT MONITORED	
1954.45	1877.16	2783.23	3233.2	2695.10	
8300/1962.55	8425/1884.04	4265/2791.88	11,900/3243.21	2705.50	
1969.27	1892.61	2796.48	3259.82	2713.27	
		NOTE: TIMES AFTER SEPARATION ARE UNRELIABLE			
			A/F, FROM AZUSA AND GE FOR IMPACT LOCATION		
SATISFACTORY FROM CAPE AND SHIP. PARTIAL FROM OTHER STATIONS	PARTIAL, FROM CAPE AND ASCESSION	PARTIAL FROM CAPE, GRAND BAHAMA, SAN SAL., ASC. ISL.	EXCELLENT THROUGHOUT FLIGHT	GOOD EXCEPT AFTER TLM BLACKOUT	
NOT REPORTED	NOT REPORTED	NOT REPORTED	INFORMATION NOT AVAILABLE	NOT REPORTED	
NOT REPORTED	NOT REPORTED	NOT REPORTED	INFORMATION NOT AVAILABLE	NOT REPORTED	
NO SOFAR BOMB CARRIED	TWO DETONATIONS REPORTED	NO SOFAR BOMBS CARRIED CONVERTED IOC ATLAS MISSILE	NO SOFAR BOMBS CARRIED	NO SOFAR BOMBS CARRIED	STROBOSCOPIC LIGHTS DID NOT ACTIVATE

SUBSYSTEM OPERATION

Separation and Spin

Mark 3 re-entry vehicles begin spinning about their longitudinal axes upon separation by using the energy stored in a torsion member mounted on the center of the adapter. Average separation time for the Mk 3 vehicles included here was 33.36 seconds after sustainer cutoff.

Retrorocket ignition, an airframe event which ensures positive separation, occurred at an average of 2.99 seconds after separation. Spin and separation occur simultaneously since at the same time the re-entry vehicle is allowed to rotate about its longitudinal axis by the action of an explosive bolt, compression members impart a forward motion to the vehicle.

With the exception of Missiles 67D, 27D and 55D, separation rates were monitored on all Mk 3 flights by means of linear potentiometers mounted on the rear face of the vehicle. The average of the three outputs received by telemetry provided a rate of separation of 4.78 inches per second for the six missiles considered.

Arming and Fuzing Subsystem

The warhead functions are controlled by the arming and fuzing subsystem shown in Figure 8.1-6.

Safing Functions

Premature operation of the arming and fuzing circuits is prevented by a prearm lockout baroswitch and a prearm switch. The prearm baroswitch closes during powered flight between 50,000 and 100,000 feet altitude, completing part of the arming circuit. At the end of powered flight, when the missile has attained a velocity compatible with its instantaneous position for an accurate impact, a signal originated in the guidance system closes the prearm switch. On R&D missiles, a backup prearm signal is sent at the time of re-entry vehicle separation switch closure, ensuring arming and fuzing capability in the event either the baroswitch or prearm circuits fail.

Safing Events

The prearm signal is locked-out at range zero. The prearm lockout switch is barometrically closed between altitudes of 50,000 to 100,000 feet.

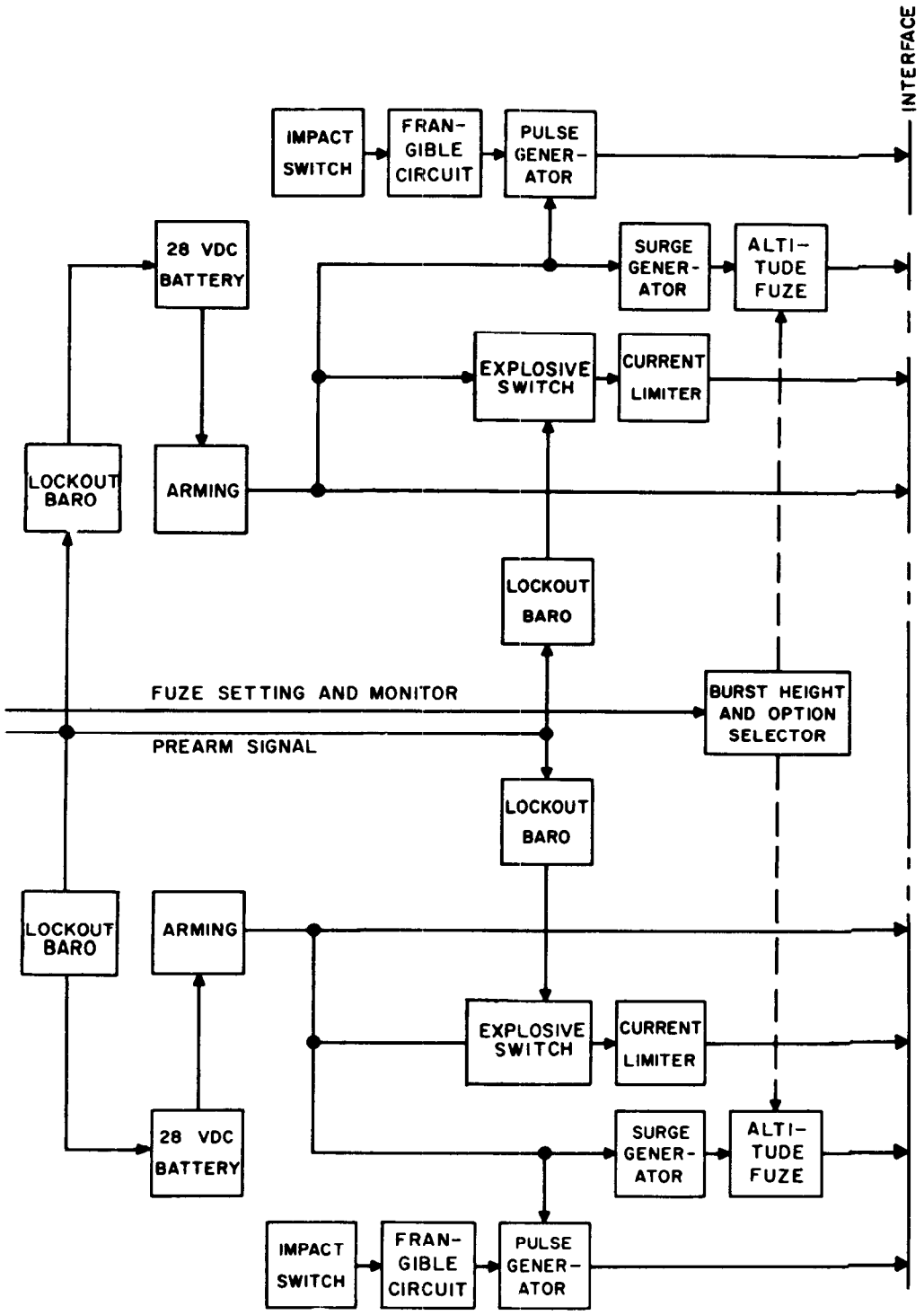

FIGURE 8.1-6 MARK 3 ARMING AND FUZING SUBSYSTEM

Arming and Fuzing

The prearm signal is received by the re-entry vehicle at the end of powered flight, activating the fuzing batteries and firing the arming-enabling explosive switches.

Arming is accomplished by means of deceleration sensitive switches during re-entry, upon reaching a deceleration value of 22-1/2g.

Fuzing is normally accomplished through a compensating g-timer, set for a desired altitude, or by impact through either of two inertial switches (installed in parallel) or by interrupting frangible circuits in the nose or flare sections of the vehicle. Fuzing occurs between 5 and 90 seconds after the arming event. Following impact fuzing, an interval of about 70 micro-seconds elapses before 1/2 inch warhead deformation occurs.

Post Flight Determination of Altitude Fuzing Occurrence

Height of burst is calculated by General Electric, on the basis of flight test data, by means of the following equation:

$$HOB = \left[\int_{t_o}^{t_1} a \sin \beta \, dt + \dot{h}_1 - g\,(t_1 - t_o)\right](t_2 - t_o) - \iint_{t_o}^{t_2} a \sin \beta \, dt + 1/2g\,(t_2 - t_o)^2 \qquad (1)$$

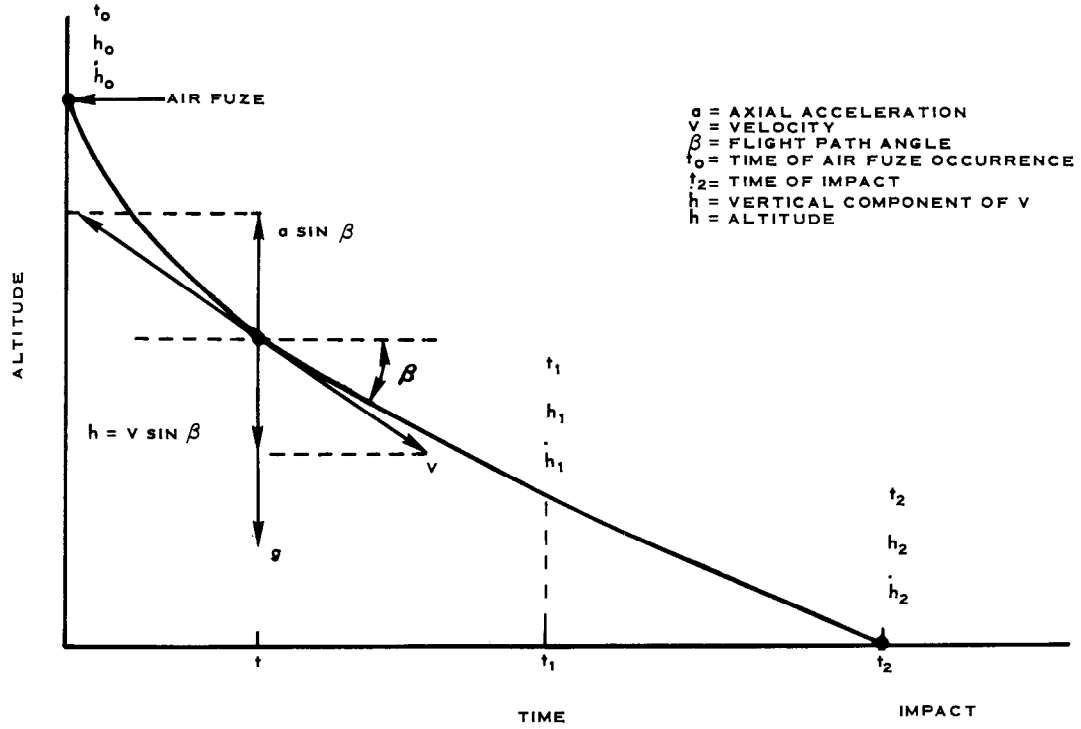

Equation (1) defines the height of burst in terms of measured acceleration, gravity and altitude h at any time t. All quantities in the equation are either known or obtained from test data, with the exception of h which must be calculated.

Electrical Power and Distribution Subsystem

The instrumentation subsystem, the arming and fuzing subsystem and the missile/re-entry vehicle inflight disconnect receive electrical power from two different sources.

Instrumentation Subsystem

This subsystem is powered by a 28 vdc, 15 ampere-hour, silver-zinc rechargeable battery and three semiconductor power supplies, one delivering 185 vdc and the other two delivering 300 vdc.

Arming and Fuzing Subsystem and Inflight Disconnect

This subsystem contains two 28 vdc, 15 ampere-hour, remotely activated silver-zinc batteries connected to two separate parallel circuits. Electrical power is supplied through the current-limiting and surge-generator circuits for air burst and through the pulse generator for surface fuzing. This circuit also energizes the four ejection squibs for the 24-pin inflight disconnect plug. The plug is ejected from the aft face of the vehicle just prior to separation.

Figure 8.1-7 shows interface and ground connections for the arming and fuzing system as well as a schematic representation of impact-sensing fuzes.

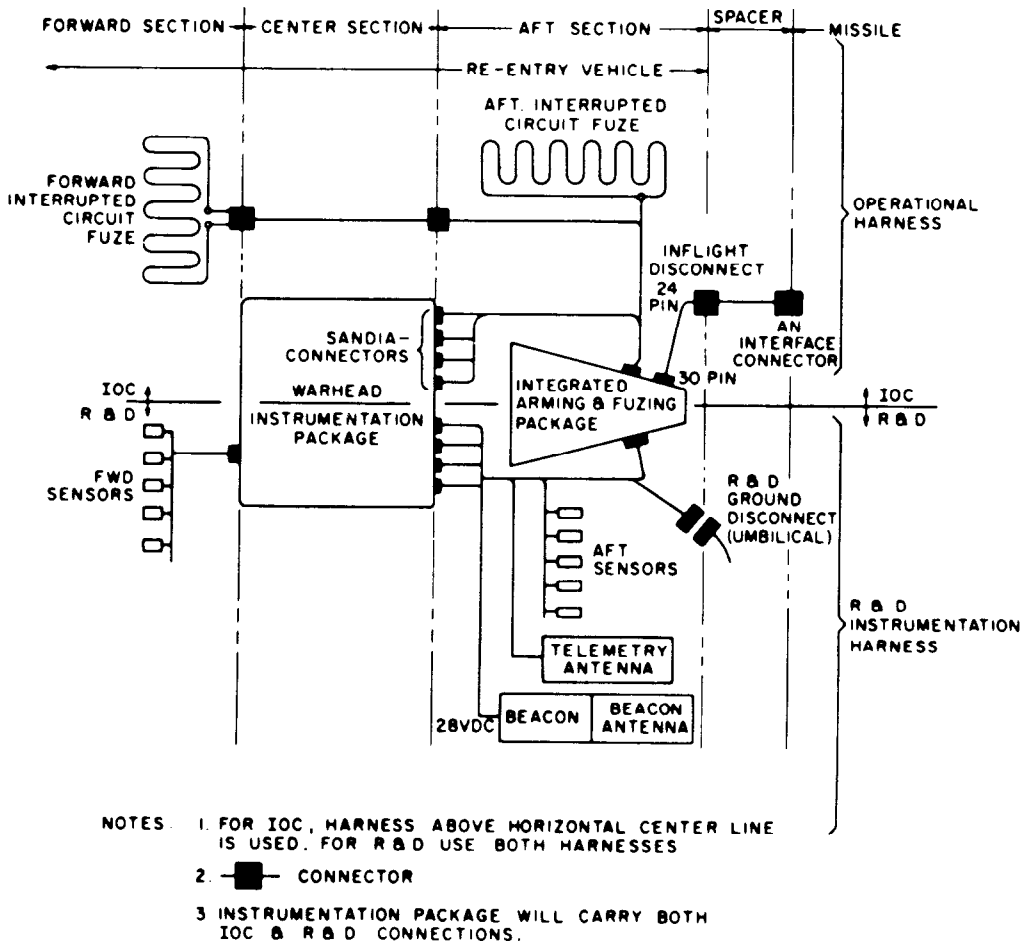

FIGURE 8.1-7 ARMING AND FUZING SUBSYSTEMS, INTERFACE AND GROUND CONNECTIONS

PROTECTION FROM AERODYNAMIC HEATING

Previous Atlas missiles carried re-entry vehicles on which aerodynamic heating protection was provided by thick copper alloy "heat sink" shields (on the low impact velocity Mk 2 vehicles) and by ablative shields (Mk 3, RVX-2A and AVCO vehicles).

The missiles included in this report carried, without exception, ablative re-entry vehicles.

Ablation, when applied to protection against aerodynamic heating, is a process by which the intense heat generated in surfaces exposed to a high velocity airstream, is absorbed by a meltable coating. A great amount of heat is absorbed by the melting process which permits separation of layers of melted material thereby avoiding a high heat transfer rate into the vehicle. This ablative coating dissipates heat that would otherwise reach critical values for the re-entry vehicle structure and its internal equipment, rendering the weapon inoperative.

Different shield materials have been employed, such as phenolic nylon, Refrasil, RAD 58E, and AVCOAT.

The Atlas flights being discussed permitted thorough testing of the effectiveness of heat protection shields on Mk 3 vehicles.

Ablation sensors, installed at different locations on the ablative surfaces, provided data on ablation depth. Re-entry vehicles utilized on long range flights require a thicker ablative coating, as aerodynamic heating is more severe. The suitability of the heat shields employed on long range flights (7,860 NM for 56D and 79D and 6,350 NM for 32D) was verified through telemetered data. Actual depth of ablation at different stations was compared with corresponding predicted values obtained by means of the equation:

$$\eta = \int \frac{\dot{g}_{net}\, dt}{\rho\, H_e} \qquad (2)$$

where: η = material ablated, feet

$\dot{g}_{net}$ = net heat flux, BTU/ft^2 second

ρ = density of ablative material, lb/ft^3

H_e = heat of ablation, BTU/pound.

The net heat flux to the body was determined by the use of an IBM 7090 ablating re-entry vehicle program, incorporating an integral turbulent heating equation.

The integrated heat of ablation, H_e, was determined from the equation:

$$H_e = \int \frac{\dot{g}_{net}\, dt}{\rho\, \eta} \qquad (3)$$

where the symbols are the same as in equation (2). The value of this thermodynamic parameter for similar re-entry vehicle stations on three flights of different ranges is shown in Table 8.1-6.

TABLE 8.1-6 INTEGRATED HEAT OF ABLATION*

STA. NO.**	MISSILE NO. 79D (7,860NM)	32D (6,350NM)	54D (4,300NM)
103.8	2,500	2,200	2,500
109.4	2,800	2,600	3,000
114.8	3,100	2,800	3,000
121.0	3,600	3,700	4,400

NOTE: * Heat of ablation values given in BTU/lb.

** Station numbers apply to the re-entry vehicle only.

The thermal shields used on long range flights demonstrated their adequacy during the re-entry conditions attained on these flights. A comparison of the re-entry parameters corresponding to different ranges is provided by Figures 8.1-8 through 8.1-10.

In the mentioned graphs, it may be observed that re-entry flight paths are much shallower for long ranges than for 4,400 NM flights. Re-entry velocities are higher and times from re-entry to impact longer, exposing the re-entry vehicle to thermoaerodynamic conditions much more severe than in shorter ranges.

AIRBORNE INSTRUMENTATION

The Mark 3 re-entry vehicles were extensively instrumented in order to gather data on all relevant aspects of their performance. This data was transmitted to ground stations via one or two telemetry links, according to the type of instrumentation system employed.

With exception of R/V 222 (Missile 55D) all Mk 3 vehicles were equipped with data recorders to provide data coverage during the phase of re-entry flight defined as "telemetry blackout" of "re-entry fade." This phenomenon, due to ionization of the airflow enveloping the re-entry vehicle, has for most flights an approximate duration of 30 seconds and prevents radio signals originated in the telemetry transmitters from reaching receiving stations.

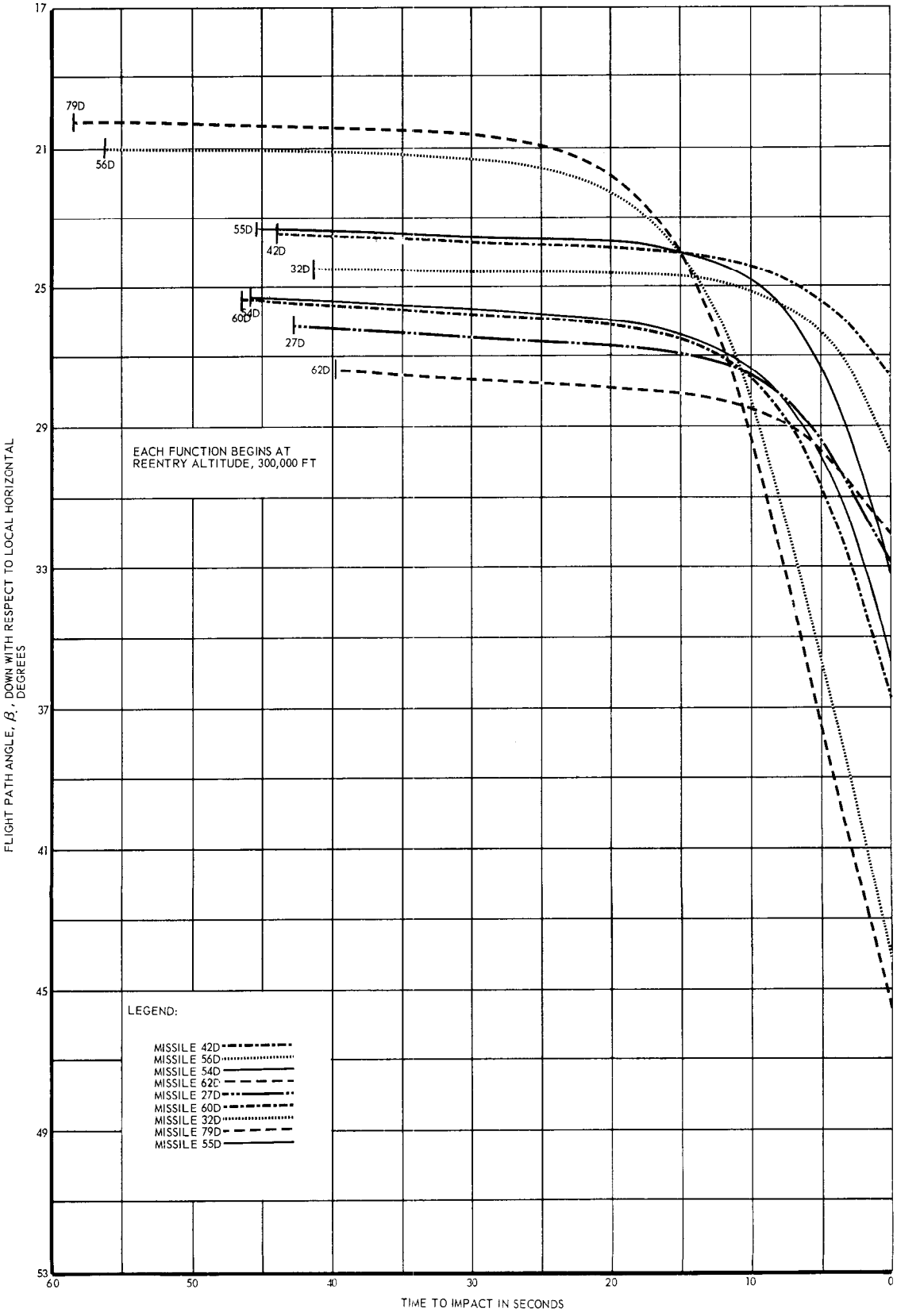

FIGURE 8.1-8 RE-ENTRY VEHICLE FLIGHT PATH ANGLE AS A FUNCTION OF TIME TO IMPACT

SECRET

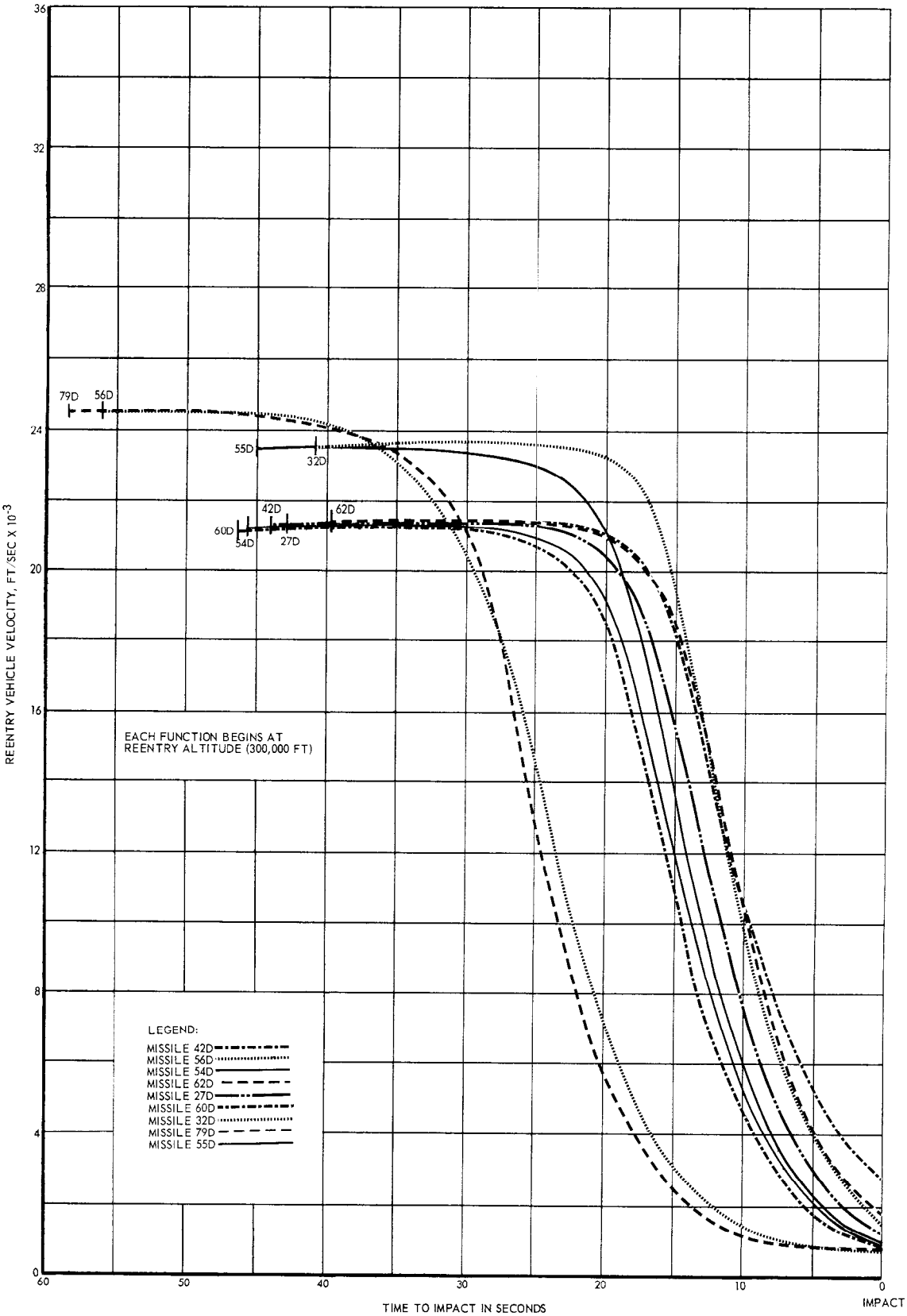

FIGURE 8.1-9 RE-ENTRY VEHICLE VELOCITY AS A FUNCTION OF TIME TO IMPACT

SECRET

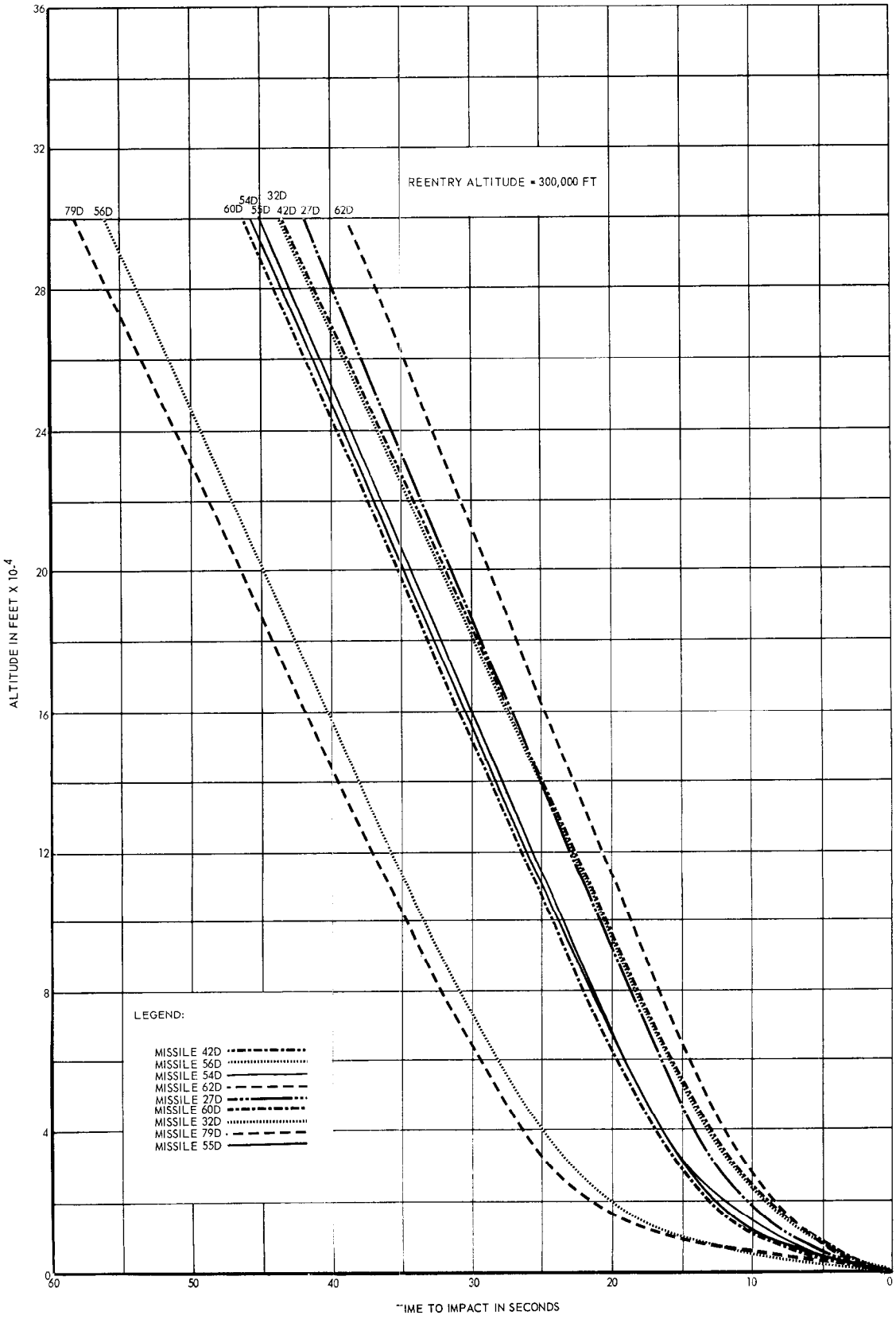

FIGURE 8.1-10 RE-ENTRY VEHICLE ALTITUDE AS A FUNCTION OF TIME TO IMPACT

Collection of data during this period is nevertheless effected by the instrumentation system and stored in a tape recorder. Since Mk 3 vehicles are not recoverable, this data is transmitted with reference to real time through the playback link after the velocity of the vehicle has diminished to a value at which ionization no longer occurs.

The airborne instrumentation subsystem may be described according to the functions it performs, as follows:

1. Sensing elements;

2. Telemetry collection and transmission of data.

The sensing elements employed on Mk 3 vehicles are briefly described below:

1. Dynamic sensors: These are accelerometers and rate gyros aligned with each one of the reference axes of the vehicle, providing data on acceleration motions about the axes and vibrations. Post flight analysis of the data collected permits obtaining a comprehensive evaluation of the aerodynamic behavior of the vehicle and its ability to align its longitudinal axis with velocity vector. Accelerometers also provide useful data for the determination of warhead functions and serve to energize the inflight data recorders. Periodicity of signal strength nulls has been used in some flights to determine separation roll rates.

2. Thermal and ablation sensors: These elements provide data on the ability of the ablative thermal shield to protect the vehicle and its internal equipment from the aerodynamic heating encountered during re-entry. Internal temperatures measured at critical points have proved the adequacy of the heat shields on Mk 3 vehicles (see protection from aerodynamic heating).

3. Separation rate monitors: Linear potentiometers mounted on the rear face of the R/V provided data on the relative attitudes of airframe and re-entry vehicle upon separation.

4. Acoustic Sensors: These sensors were installed for the purpose of collecting acoustic noise data.

5. Pressure Sensors: Internal pressure sensors provide data on the environment of the instrumentation, warhead and equipment contained in the vehicle. External pressure sensors serve an additional purpose by supporting motion instrumentation for determining angle of attack.

Monitoring Functions

The instrumentation subsystem also monitors its own functions and those of the arming and fuzing subsystem, transmitting signals representing occurrence of events via the telemetry system.

Collection and Transmission of Data

Vehicles employing two telemetry links (Mod IX and Mod IB) had two transmitters located in the forward section of the steel warhead case.

Operating frequencies were: (1) Playback link 237.8 mc;

(2) Real-time link 244.3 mc.

Vehicles not employing the inflight data recorder (Mod IIB) relayed data through the real-time telemetry link on 244.3 mc.

Instrumentation System Differences

The airborne instrumentation of the Mk 3 vehicles may be grouped into three main configurations, namely Mod I and Mod II types 1 and 2. Block diagrams depicting these three instrumentation subsystems are shown on Figures 8.1-11, 8.1-12 and 8.1-13. The SANDIA Corporation is responsible for the instrumentation of Mk 3 Mod II vehicles.

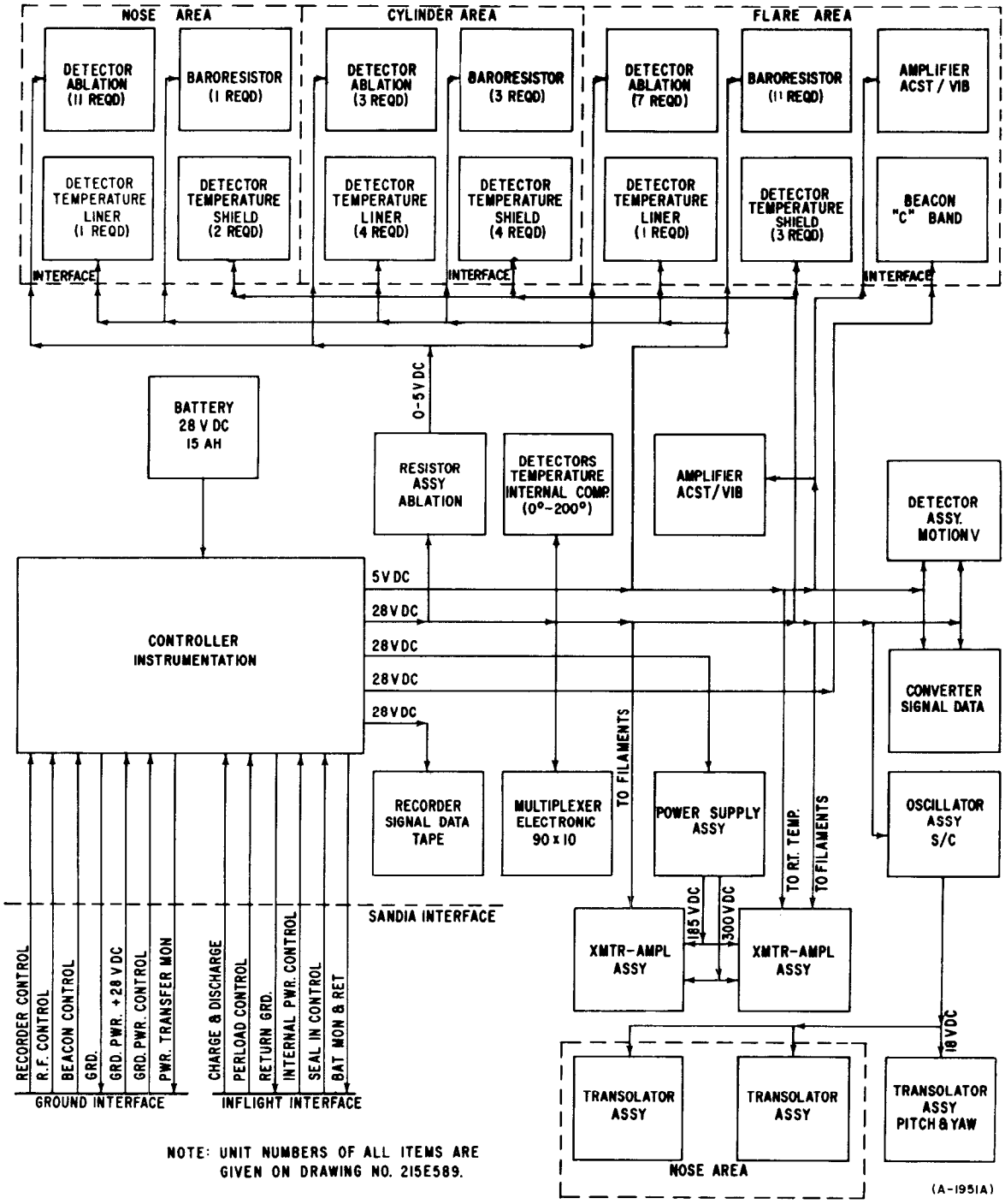

FIGURE 8.1-11 MARK 3 MOD IB AIRBORNE INSTRUMENTATION SUBSYSTEMS

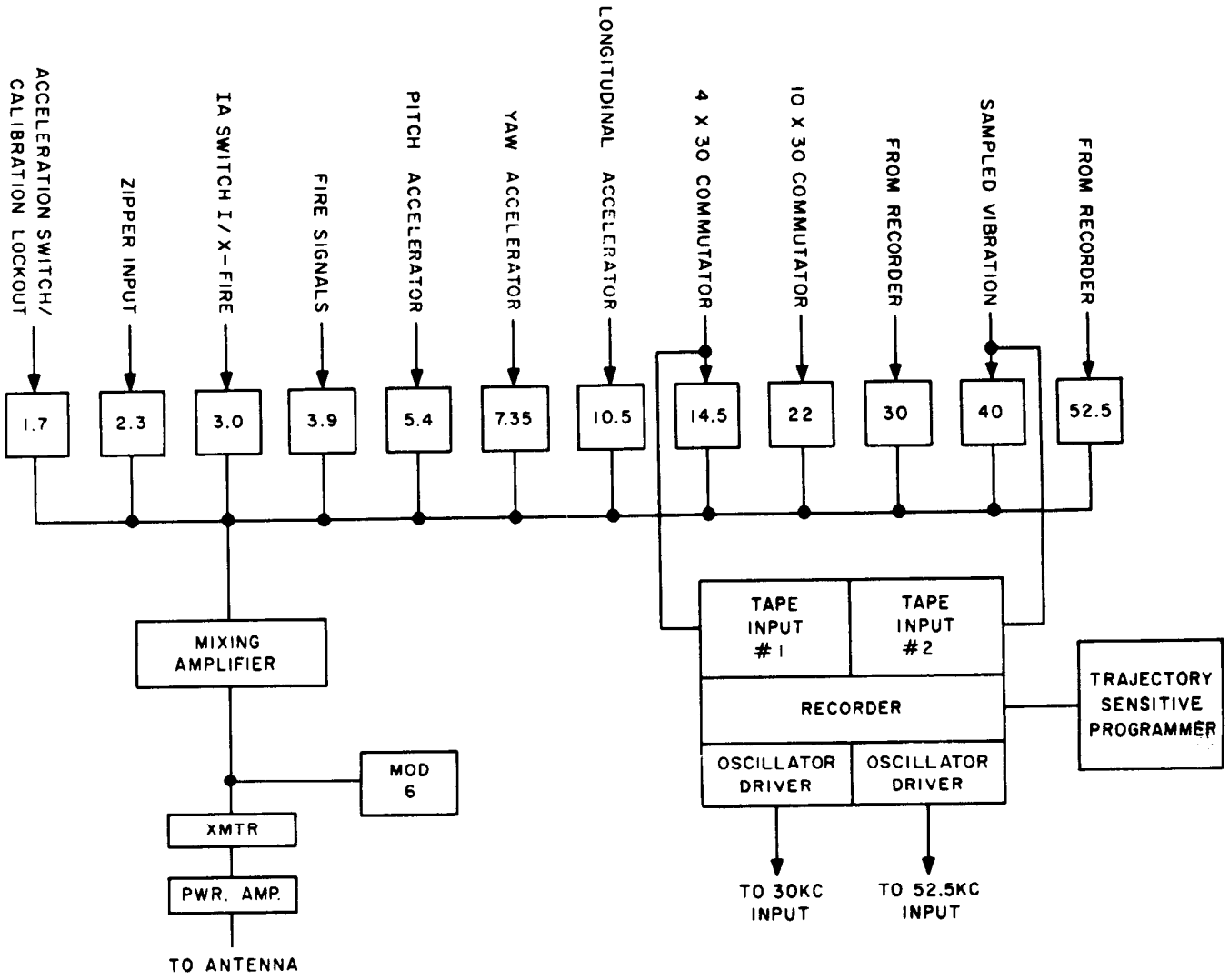

FIGURE 8.1-12 MARK 3 MOD II, TYPE 1 AIRBORNE INSTRUMENTATION SUBSYSTEM

SECRET

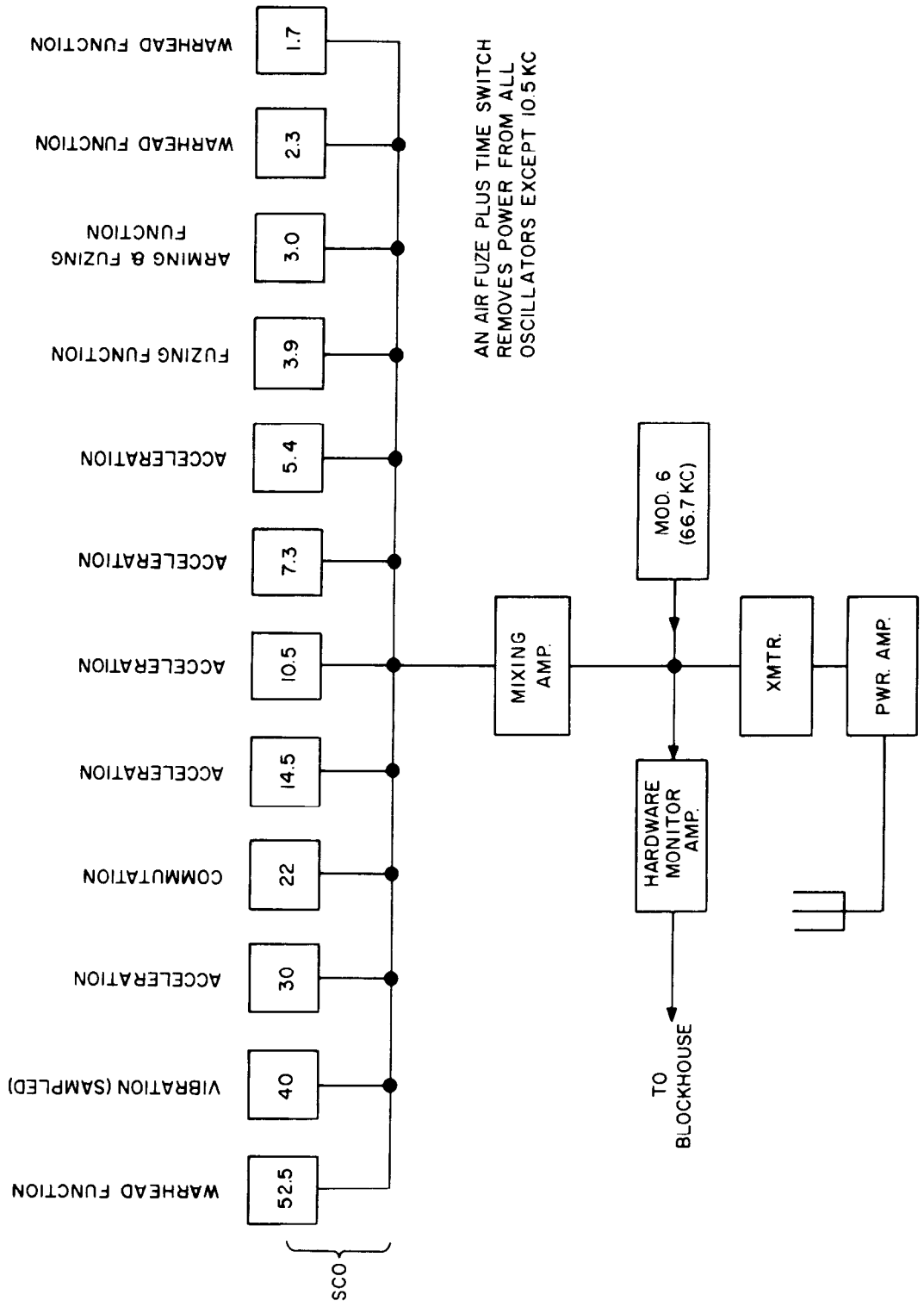

FIGURE 8.1-13 MARK 3 MOD II, TYPE 2 AIRBORNE INSTRUMENTATION SUBSYSTEM

SECRET

Mod I Instrumentation

This configuration was employed in the Mod IX flown on Missile 42D and on all Mod I vehicles. Mod I instrumentation included ablation, thermal, pressure, and acoustic sensors, accelerometers and rate gyros as well as monitoring circuits for the arming and fuzing system. Linear potentiometers were also utilized to determine separation rates and attitudes with respect to the airframe. All data was relayed through two telemetry links, one in real-time and the other playing back the data collected during the telemetry blackout period.

Mod II Type 1 Instrumentation

This instrumentation arrangement was employed in Mod IIB vehicles flown on Missiles 27D, 62D and 79D. This configuration carried no ablation sensors. The motion sensing instrumentation included accelerometers and rate gyros. There was no inflight data recorder to collect data during telemetry blackout and therefore no playback telemetry link was employed, only the transmitter relaying real-time data on a frequency of 244.3 mc. This transmitter was cleared at air-fuze plus 14 seconds for the transmission of SANDIA Mod VI warhead information.

Mod II Type 2 Instrumentation

This instrumentation configuration was carried by R/V No. 222 (Missile 55D) only. This vehicle carried no ablation sensors. Rate gyros were not installed, the vehicles motion sensing instrumentation being limited to accelerometers. Roll rate upon separation was measured by the periodicity of telemetry signal nulls, since the two telemetry antennae were placed at dimetrically opposed locations.

SANDIA Mod VI warhead information was transmitted at air-fuze plus 1 second through the real-time telemetry link. The inflight data recorder was not employed.

AERODYNAMIC CHARACTERISTICS

To attain maximum penetration efficiency as a weapon, a re-entry vehicle such as the Mk 3, not equipped with any means of attitude control during the ballistic flight prior to re-entry, must depend on aerodynamic stabilization. The angle of attack upon re-entry may reach considerably high values (Reference Table 8.1-7). It is therefore desirable that the transition between that initial angle of attack to a value of α approaching zero occur early during re-entry, with rapid damping of oscillations about the Y and Z axes compatible with the structural characteristics of the vehicle.

TABLE 8.1-7 SUMMARY OF RE-ENTRY CONDITIONS

	FUNCTION	UNITS	MISSILE NO. 42D MOD IX	56D MOD IB	54D MOD IB	62D MOD IIB	27D MOD IIB	60D MOD IB	32D MOD IB	79D MOD IB	55D MOD IIB	90D MOD IB
(1)	Planned Range	NM	4,395*	7,859	4,306	4,389*	4,389	4,306*	6,350	7,863	6,350	4,389
(2)	Total Flight Time to Impact	sec from 2-in. motion	1874.95	3315.72	1891.54	2030.0	1969.27	1892.61	2796.48	3259.82	2713.27	
(3)	Re-entry Time**	sec from 2-in. motion	1831.97	3260.40	1846.04	1989.51	1925.95	1845.59	2753.23	3204.40	2666.10	
(4)	Re-entry to Impact Time**	sec	42.98	55.32	45.50	40.49	43.32	47.02	43.25	55.42	47.17	
(5)	Re-entry to Impact Range**	NM	110	125	102	94	97	101	NDA	130	94	
(6)	Re-entry Velocity**	ft/sec	21,326	24,500	21,132	21,402	21,186	21,186	23,532	24,400	23,438	
(7)	Re-entry Flight Path Angle β **	degs	23.52	21.06	25.27	27.40	26.11	25.31	24.49	20.40	23.27	
(8)	Re-entry Angle of Attack α***	degs	65	180	NDA	113	115	100	NDA	148	150	
(9)	Peak Dynamic Pressure Time**	sec from 2-in. motion	1863.40	3291.65	1876	2017	1954.5	1875	2782	3232.4	2695	
(10)	Peak Dynamic Pressure Altitude**	ft	37,500	40,000	40,000	36,500	37,500	40,100	36,016	40,100	35,000	
(11)	Peak Dynamic Pressure q **	lbs/ft^2	71,388	68,732	68,808	75,700	71,840	68,417	88,326	75,765	78,913	
(12)	Mach Number at Peak q **		NDA	15.65	15.00	14.61	14.50	15.07	15.68	16.30	15.09	
(13)	Angle of Attack α at Peak q ***	degs	2	1	0.2	1	0	0	NDA	0.5	0	
(14)	Flight Path Angle at Impact**	degs	27.57	43.87	35.53	32.00	32.77	36.38	29.72	45.37	32.87	
(15)	Angle of Attack at Impact***	degs	0	0	3.6	0	0	0	NDA	6.5	0	
(16)	Velocity at Impact**	ft/sec	2,800	768	981	1,899	1,310	967	1,497	773	1,022	

NOTES:

* Denotes impact in target area, all other missiles reached their assigned targets.

** Items 3 through 7, 9 through 12, 14 and 16 were obtained from GE post flight 3-degree-of-freedom simulations, included GE Flight Evaluation Reports for each missile, and prepared with actual flight parameters as initial input conditions.

*** Items 8, 13 and 15 were obtained from rate gyro data.

NDA No data available.

To fulfill this requirement, successive changes were introduced in the Mk 3 vehicles having achieved, through Atlas Series D missile testing, results which appear to be quite adequate for the purpose and capabilities of the 107A-1 Weapon System. The comments that follow briefly describe these changes while Table 8.1-7 will supplement the discussion with an outline of the re-entry behavior of the individual vehicles tested.

Of the eleven Mk 3 re-entry vehicles discussed, nine are "B" vehicles, of the configuration designated as "biconic-2."

Figure 8.1-3 depicts the essential configurational differences that characterize Mods I and IX, IA, IB and IIB. It may be observed that Mods I, IX and IA vehicles differ from Mods IB and IIB in the taper ratio of the initial conical flare beginning at the aft end of the cylindrical midsection (warhead case). Mod IB and IIB vehicles have flares with a half-cone angle of 9.67 degrees compared with the 9.0-degree angle of previous Mk 3 vehicles.

Mod IB and IIB vehicles have a further divergence of the flare, changing from 9.67 degrees to 24 degrees. This change constitutes the "biconic-2" flare. Previous Mk 3 vehicles designated Mod IA also had a 24-degree "biconic" flare originating in the initial 9-degree flare.

The "B" vehicles have a maximum flare diameter of 42.80 inches which results in a base cross section area of 9.99 ft^2. This change in base area represents more than a 7% increase over the previous constant cone flare Mk 3 re-entry vehicles, which had a base cross section area of 9.334 ft^2. This increase in initial unablated base cross-section area results in a further displacement of the aerodynamic center of pressure towards the rear of the vehicle. The effect of this change is to produce a greater stabilizing moment which is a function of dynamic pressure, tending to diminish the amplitude of oscillations about the Y and Z axes. This permits attaining a smaller angle of attack and consequently a higher penetration velocity to impact.

An attempt to obtain analogous results was made with R/V 211 flown on Missile 42D by displacing forward the center of gravity of the vehicle.

Rate gyro and pressure distribution data from the tests of the re-entry vehicles discussed here have permitted performance analysis of re-entry vehicle motions and attitude changes during flight through the atmosphere.

Re-Entry Vehicle Drag

The most relevant aerodynamic parameter as to the penetration potentialities of a re-entry vehicle is defined by the expression $\frac{W}{C_D A}$. The value of this parameter varies with the

changes introduced during re-entry flight by the ablation phenomena, since both base cross section area and re-entry vehicle weight are continually affected by degradation of the heat shield. These changes cease when the vehicle has decelerated to a velocity at which ablation no longer occurs and $\frac{W}{C_D A}$ may be considered only a function of Mach number. However, this condition applies only from low altitudes, of the order of 20,000 feet, to impact. The value of $\frac{W}{C_D A}$ at any instant of the flight may be expressed as follows:

$$\frac{W}{C_D A} = \frac{W_o \left(\frac{W}{W_o}\right)}{C_D A_o \left(\frac{A}{A_o}\right)} \tag{4}$$

where the subscripts o denote initial unablated conditions of weight and area.

Figure 8.1-14, "Drag Coefficient vs. Mach Number," illustrates this function for three different re-entry velocities and re-entry flight path angles (β) ranging from 20.6 to 22.6 degrees.

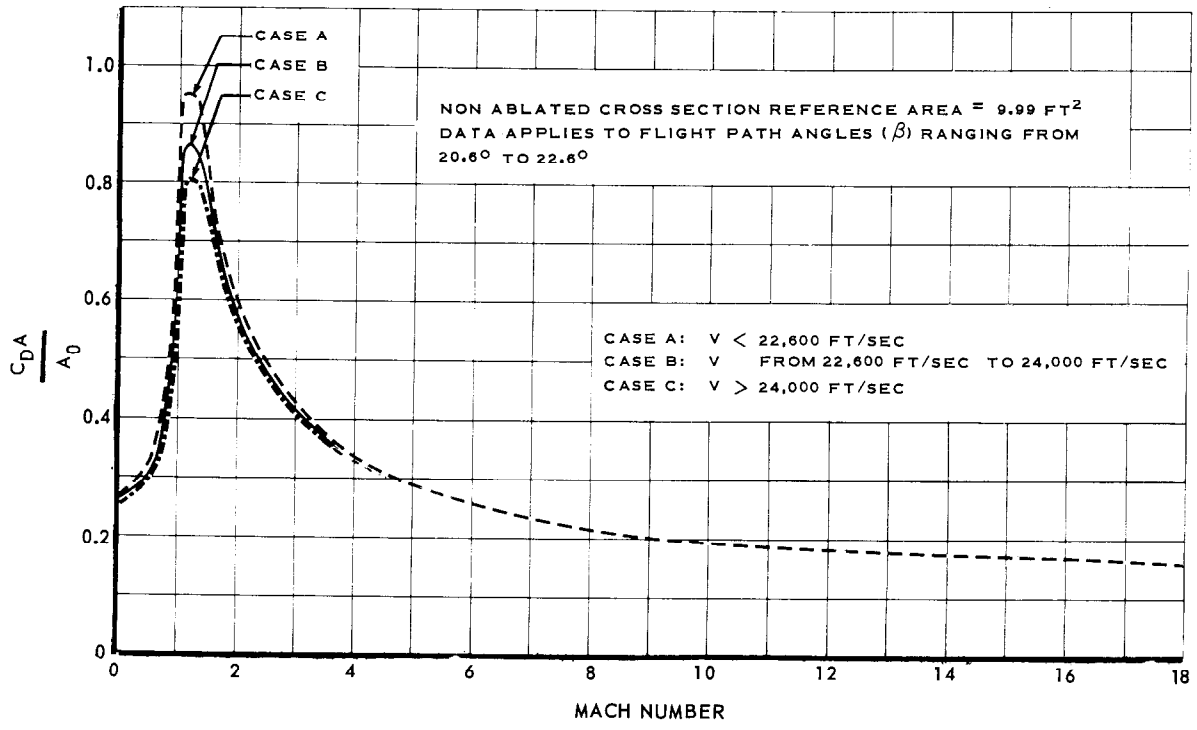

FIGURE 8.1-14 DRAG COEFFICIENT VS MACH NUMBER

Figure 8.1-15, "Re-entry Vehicle Weight Reduction as a Function of Altitude", depicts this function based on the same three cases illustrated in Figure 8.1-14.

These two graphs, permit approximate determination of the parameter $\frac{W}{C_D A}$ corresponding to the Mk 3 Mod IB or IIB re-entry vehicle, for different conditions of re-entry.

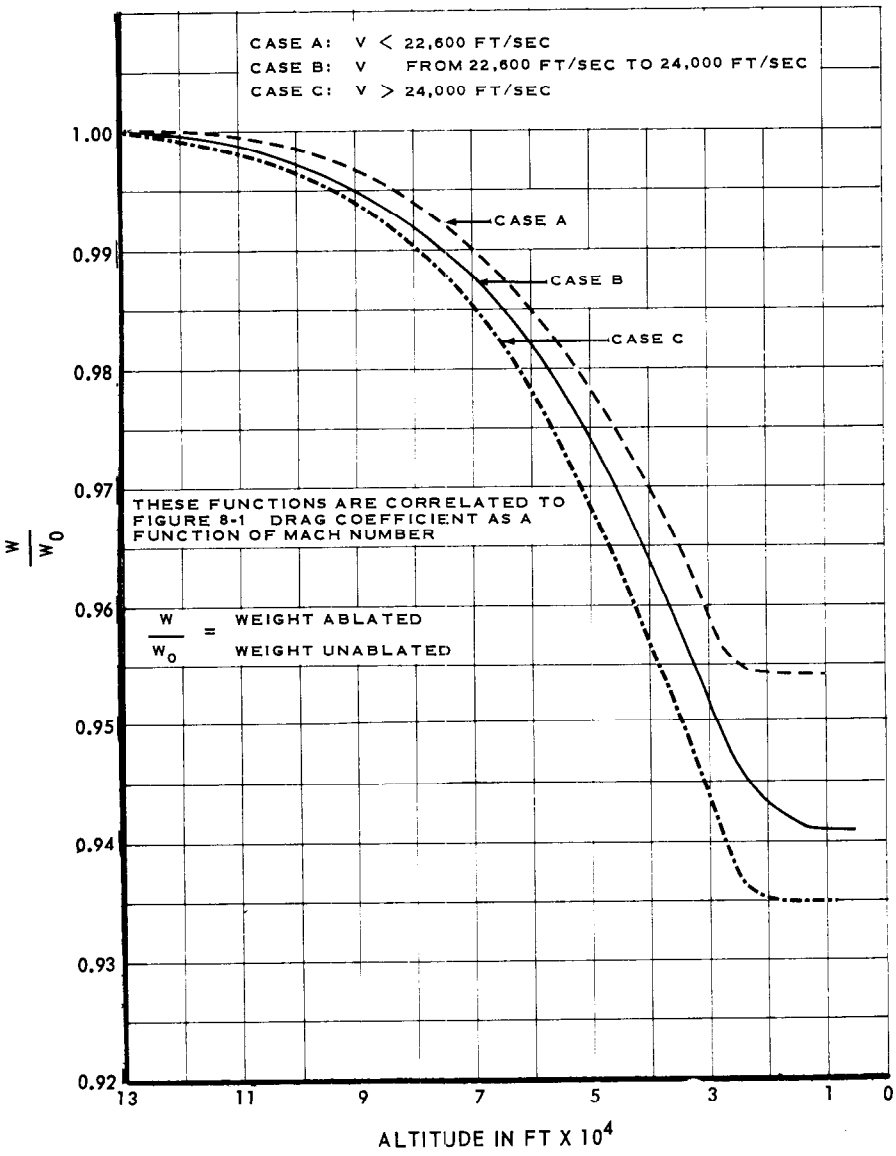

FIGURE 8.1-15 RE-ENTRY VEHICLE WEIGHT REDUCTION AS A FUNCTION OF ALTITUDE

VEHICLE PERFORMANCE

Figures 8.1-8, 8.1-9 and 8.1-10, respectively, depict the variation of R/V flight path angle (β), velocity and altitude with time to impact from the instant the vehicle reaches the boundary of the atmospheric envelope, assumed to be at an altitude of 300,000 feet.

Although the flights considered differ in range and trajectory development, which results in dissimilar re-entry conditions, the expedient of employing a common zero (impact) time permits a comparison of the respective functions, $\beta = f(t)$, and $H = f(t)$. Correlation of these figures will provide an indication of the re-entry to impact performance of the nine missiles considered.

The sources of these functions are the post flight trajectory simulations included in the General Electric Flight Evaluation Reports for each individual flight.

Data was not available for the preparation of functions corresponding to R/V 218A (Missile 90D) at the time this report was written.

A summary of the performance of 10 Mk 3 re-entry vehicles carried on 11 of the 15 missiles considered in this report is presented in Table 8.1-7. The one exception is Missile 48D, which was destroyed prior to liftoff.

MARK 4 RE-ENTRY VEHICLE

DESCRIPTION

The Mk 4 Mod I re-entry vehicle flown by Missile 83D is a vehicle of a sphere-cone-cylinder-flare configuration as shown in Figure 8.1-16.

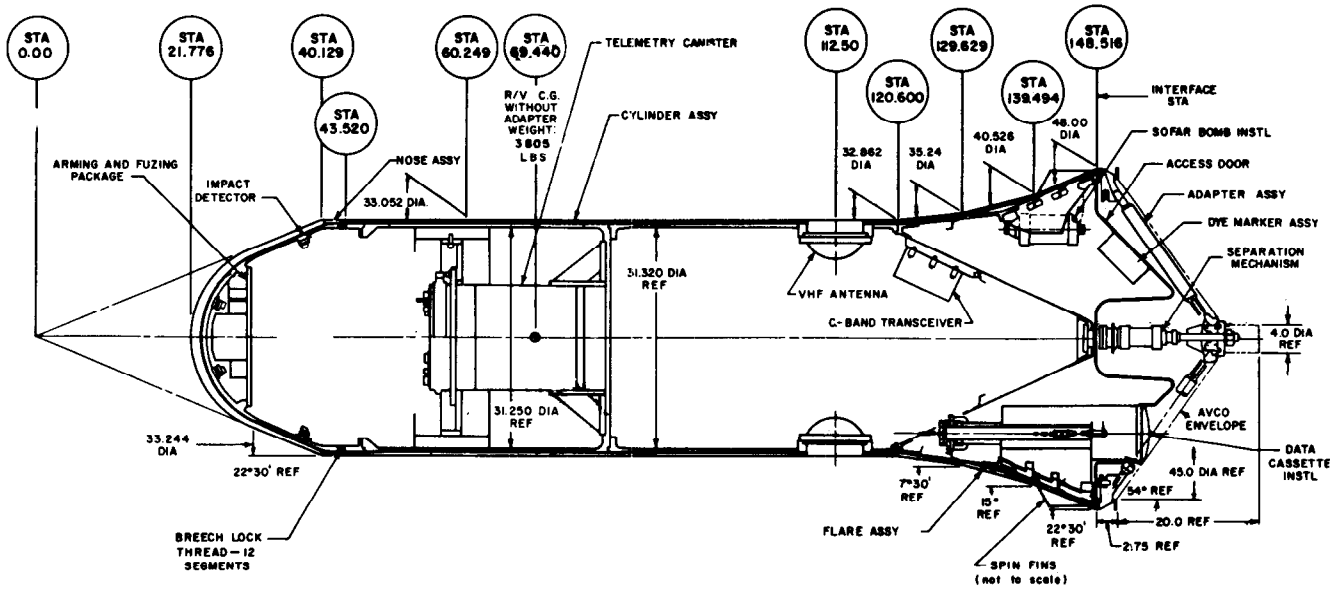

Figure 2 INBOARD PROFILE, MARK 4, MOD 1-11
60-412A

FIGURE 8.1-16 CUTAWAY SHOWING INTERNAL CONFIGURATION OF MARK 4 MOD I RE-ENTRY VEHICLE

This vehicle carried an instrumented canister in place of a warhead package. Its structure was coated with ablation materials for heat protection. The distribution of ablative material is shown in Figure 8.1-17. This vehicle employed an ejectable data cassette to record information during the period of telemetry blackout, instead of the playback telemetering arrangement used on Mk 3 vehicles.

The vehicle is equipped with complete instrumentation to obtain data on the thermodynamics of re-entry, and motion-sensing elements for the determination of the behavior of the vehicle during re-entry. In addition, monitoring circuits provided data on the warhead functions. The Mk 4 vehicle is not equipped for terminal trajectory or attitude control, except for its aerodynamic characteristics that tend to minimize angle of attack and two small fins to induce roll by aerodynamic reaction. This vehicle is considerably heavier than the Mk 3, its weight being of the order of 3,800 pounds. Reference Table 8.1-8, which presents weight and balance data for the Mark 4 Mod I re-entry vehicle.

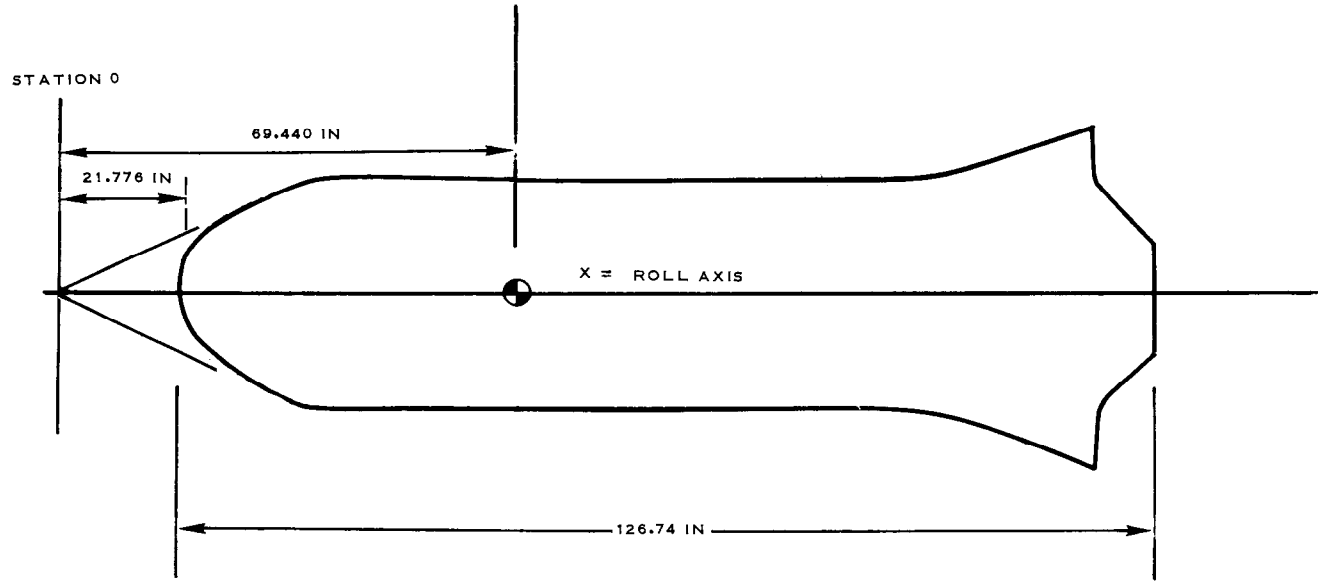

TABLE 8.1-8 MARK 4 MOD I WEIGHT AND BALANCE DATA

ITEM	UNITS	MSL 83D
Gross Weight	lbs	3805.0
CG Location, From Forward Datum:		
Along X (roll axis)	inches	69.440
Along Z (yaw axis)	inches	- 0.012
Along Y (pitch axis)	inches	+ 0.054
Moments of Inertia:		
About Roll Axis (I_x)	slugs-ft^2	143.55
About Yaw Axis (I_z)	slugs-ft^2	940.055
About Pitch Axis (I_y)	slugs-ft^2	936.95

Tracking Beacon

A C-band tracking beacon was installed on the Mark 4 vehicle.

Impact Location

The vehicle carried a SOFAR bomb and dye marker powder.

Data Cassette

An ejectable, recoverable data cassette was carried at the rear compartment of the vehicle. This cassette contained a recorder to gather and retain data during the telemetry blackout period caused by ionization. Ejection of the cassette from the R/V was effected by means of a rocket unit.

SUBSYSTEM OPERATION

Arming and Fuzing Subsystem

The Mark 4 vehicle carried an arming and fuzing system capable of performing the sequence of functions necessary for the detonation of a warhead. It consisted of lockout and arm-safe switches, post separation arming circuit with its two independent batteries, an airburst fuzing system also with two independent batteries, and a set of impact-sensing switches.

Warhead functions as well as the voltages of the batteries powering the system were monitored through 14 telemetry channels.

VEHICLE PERFORMANCE

Telemetry

Over-all telemetry reception was satisfactory; overlap between records obtained from the Cape, Grand Bahama Island, Antiqua, Ascension, TLM Ship Lima, and Aircraft 630 permitted the preparation of a composite record.

Arming and Fuzing

The arming and fuzing system performed all its functions satisfactorily, including the redundant RAD airburst switch. Detailed analysis of records indicate that the impact switches operated successfully.

Heat and Ablation Data

The heat shield adequately protected the R/V and its internal components. Internal temperatures were as expected, with a rise at the time of data cassette ejection, caused by the ejection rocket exhaust. Figure 8.1-17 shows the distribution of ablation material constituting the Mk 4 heat shield.

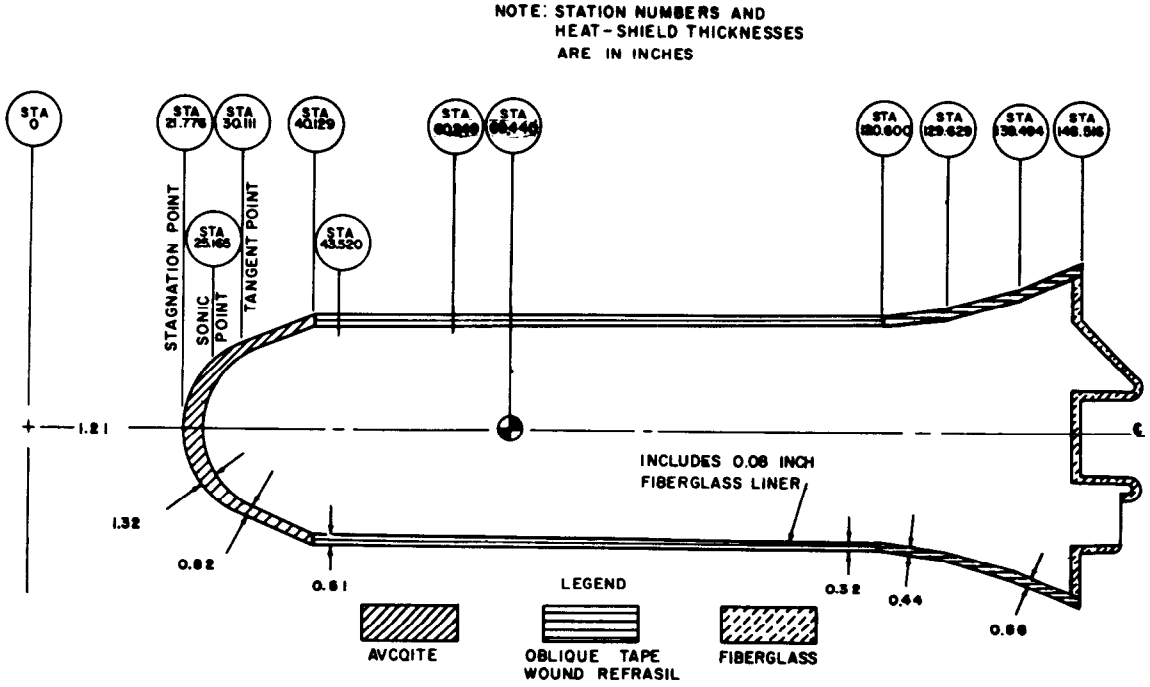

FIGURE 8.1-17 RE-ENTRY VEHICLE PROFILE AND ABLATION MATERIAL CONFIGURATION

AERODYNAMIC ANALYSIS

Peak deceleration occurred at 1909 seconds with a value of 60g. Maximum trim acceleration was -12.5g at 1908.8 seconds for the pitch axis and 10.4g at 1909 seconds for the yaw axis.

Separation occurred normally without any undue motions being imparted to the vehicle. Pitch-yaw motions about the axes, which were essentially zero at 350,000 feet, increased to amplitudes of about 30 degrees/second near 1893 seconds, becoming convergent after that time. Roll rate, induced by the spin-fins, built up to about 450 degrees/second at peak g loading (1908.1 seconds) increasing to a maximum value of 740 degrees/second at 1930 seconds. A summary of flight event times is shown in Table 8.1-9.

Angle of attack, established to be about 70 degrees at re-entry diminished to about 9 degrees at impact, as indicated by the envelopes of oscillation amplitudes.

TABLE 8.1-9 SUMMARY OF MARK 4 FLIGHT EVENTS

TEST CONDITIONS AND EVENTS DURING FLIGHT	
Test Date	11/15/60
Planned Range (NM)	4389
R/V Serial Number	11
Radar Tracking Beacon	C-Band
Countdown Holds Due to Re-entry Vehicle	None
Telemetry Start	0.00
Booster Engine Cutoff	137.75
Sustainer Engine Cutoff	269.91
Vernier Engine Cutoff	286.34
R/V Separation	302.24
First Telemetry Reception From Ascension Island	1117.44
Loss of Telemetry Signal at Antigua	1419.64
Telemetry Blackout Start	1883.54
Cassette Recording Start	1884.58
Maximum Axial Deceleration	1908.54
Telemetry Blackout Ends	1909.24
Cassette Ejection	1928.14
Loss of Telemetry Signal	1938.74
Impact Time	1938.74

REMARKS:

The signal of the data cassette's SARAH beacon was received immediately after impact and the cassette was recovered about 2 hours after launch. Good radar tracking coverage except after blackout. Radar chaff was ejected at the time of cassette ejection and detected by terminal area detection and tracking facilities.

NOTE: All times given in seconds from two-inch motion.

RVX-2A RE-ENTRY VEHICLE

DESCRIPTION

The following, unless otherwise specified, applies to all three RVX-2A vehicles flown on Missiles 66D, 76D and 71D.

The RVX-2A is a research test vehicle designed to be flown to ICBM ranges. It is equipped with elaborate instrumentation and a complete recovery subsystem to permit retrieving the entire vehicle for post-flight inspection and analysis.

The sequence of events that leads to the placement of the RVX-2A vehicle into a ballistic trajectory is similar to that of any other re-entry vehicle of the types flown by Atlas missiles.

The RVX-2A does not employ attitude or trajectory control devices and is designed to describe a ballistic path to re-entry. Within the atmosphere, the deceleration caused by aerodynamic drag steepens the trajectory and reduces the velocity to a point at which parachute deployment is effected, attaining a slow descent, nominally vertical.

The re-entry vehicle, depicted in Figure 8.1-18, is approximately 174 inches long. It is thermally protected by a shield of ablative material.

All RVX-2A vehicles described herein carried a number of special experiments on the basis of minimum interference with the main objectives of the flights.

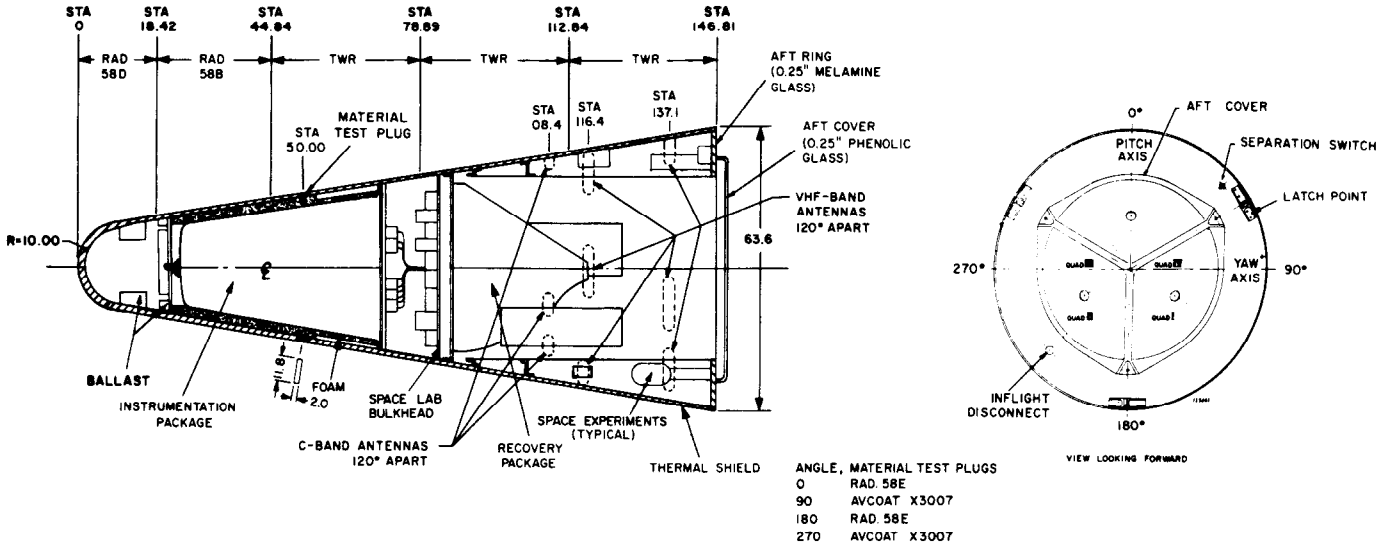

FIGURE 8.1-18 RVX-2A RE-ENTRY VEHICLE, INTERNAL CONFIGURATION

STRUCTURE

Nose Section

The nose section, which is a portion of a sphere, is made of stainless steel and has a radius of 10 inches.

Conical Section

The conical section, from the nose cap to the aft bulkhead, consists of four semimonocoque sections made of aluminum sheet. The conical shell is reinforced at the aft section by three longerons that distribute the loads from the missile attachment points.

The vehicle structure contains ballast, instrumentation, recovery package, antennae and various sensors. RVX-2A vehicles incorporated neither simulated warheads nor warhead instrumentation. Therefore, none of the functions of the arming and fuzing set common to Mk 3 vehicles, will be found on the Flight Events Summary table (Table 8.1-10) corresponding to RVX-2A vehicles. Table 8.1-11 shows weight and balance data for each of the three RVX-2A vehicles flown.

TABLE 8.1-10 SUMMARY OF RVX-2A FLIGHT PERFORMANCE

TEST CONDITIONS AND EVENTS DURING FLIGHT	MISSILE 66D	MISSILE 76D	MISSILE 71D
Test Date	8/12/60	9/16/60	10/13/60
Planned Range (NM)	4,387	4,387	4,387
R/V Serial Number	421	422	423
Radar Tracking Beacon	C-Band	C-Band	C-Band
Countdown Holds Due to Re-entry Vehicle	None	None	None
Telemetry Start	0.00	0.00	0.00
Recovery System Arming	NDA	NDA	NDA
Booster Engine Cutoff	136.45	138.59	139.56
Sustainer Engine Cutoff	259.24	274.89	266.73
Vernier Engine Cutoff	274.43	290.91	280.71
Separation Switch Closure	281.04	NDA	NDA
Inflight Disconnect Separation	289.34	309.84	296.20
Separation Time and Conditions	Normal @ 290.34	306.7 (1)	Normal @ 297.60
Retrorockets Ignition	291.24	NDA	297.51
Switch Motion Sensors to Coarse	NDA	NDA	1874.84
Recovery Timer Cocked	NDA	NDA	NDA
Switch Motion Sensors to Fine	(2)	NDA	1890.00
De-energize Record - Erase Record Head	(2)	NDA	1890.00
Recovery Timer Start	1921.54	NDA	1896.66
Re-entry Time at 400,000 ft	1867.94	286,908 ft at 1,809.24	1841.61
Re-entry Velocity (ft/sec)	21,220.00	21,371.00	21,205.00
Re-entry Flight Path Angle β (deg)	24.69	22.72	23.90
Re-entry Angle of Attack (deg)	72.00	38.00	90.00
Parachute Cover Ejection	1927.14	NDA	1902.36
Parachute Deployment	1929.34	NDA	1904.30
Parachute Open (reefed)	1929.84	NDA	1905.60
Parachute Disreefed	1932.94	NDA	1908.36
Recovery Basket Separation	1944.34	NDA	1919.20
0.4 kc Tone	1944.54	NDA	1919.30
SOFAR Bomb Ejection and Chaff	NDA	NDA	NDA
Balloon Inflation	NDA	NDA	NDA
Balloon Tether Cut	NDA	NDA	NDA
Impact Switch Arming	(2)	NDA	NDA
Water Landing (with parachute)	1993.74	NDA	1958.20
De-energize Instrumentation	(2)	NDA	NDA
Activate Recovery Aids	(2)	NDA	NDA
Water Impact (no parachute)	(2)	NDA	(2)

NOTES:

All times given in seconds from two-inch motion.

(1) Inflight disconnect did not eject properly imparting extraneous motions to the R/V.

(2) Event did not occur.

NDA No data available.

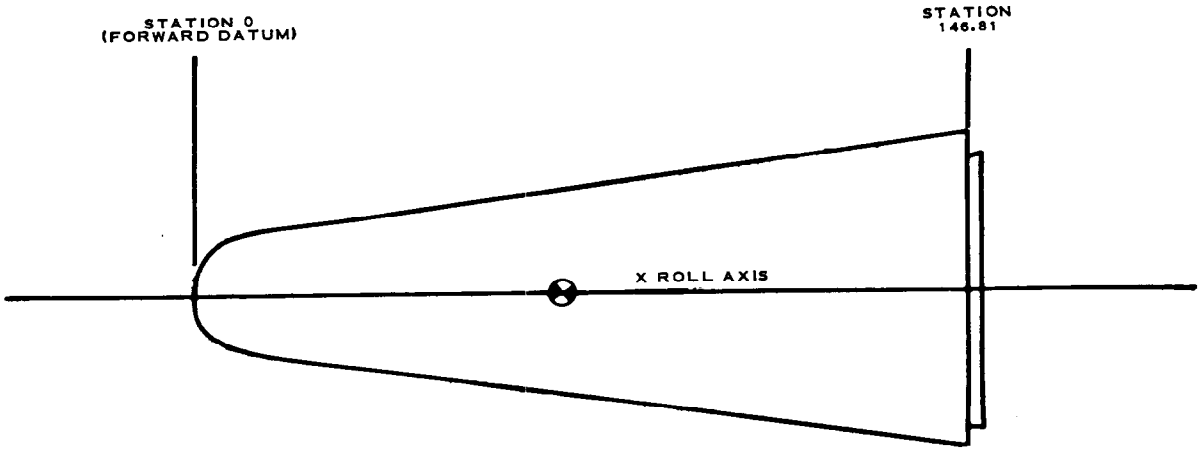

TABLE 8.1-11 RVX-2A WEIGHT AND BALANCE DATA

ITEM	UNITS	MISSILE NO. 66D	76D	71D
Gross Weight	lbs	2,715	2,723.54	2,796.6
CG Location:				
Longitudinal, Along X Axis	inches	75.4	75.43	76.1
Radial, Along Y and Z Axes	inches	0.5	0.113	0.5
Moments of Inertia:				
About X Axis, I_x (roll)	slugs-ft^2	178.0	175.9	190.0
About Y Axis, I_y (pitch)	slugs-ft^2	1,330.0	1,419.2	1,358.6
About Z Axis, I_z (yaw)	slugs-ft^2	1,325.0	1,410.9	1,352.4

NOTE:

Gross weights quoted correspond to vehicles "as launched," i.e., unablated.
Location of CG is quoted with respect to R/V Station 0 (stagnation point).

PROTECTION FROM AERODYNAMIC HEATING

The RVX-2A vehicle (S/N 422) carried by Missile 76D was thermally protected by ablative materials of two different types; RAD 58E covering the nose and first conical frustum and tape-wound Refrasil over the remainder of the conical body. In addition, material test plugs were inserted in the tape wound Refrasil of the second conical frustum (Sta. 50), spaced at 90 degrees. The test plugs consisted of two RAD 58E and two AVCOAT X3007 strips 2 inches wide and 12 inches long, inserted circumferentially into the Refrasil coating and bonded to the body. Since there are no structural or geometrical discontinuities in these vehicles the expressions "first frustum," "fourth frustum" and so on are conventional and serve merely to define areas of the heat shield between specific vehicle stations for the purpose of locating different types of ablation materials and facilitate thermodynamic studies.

The nose cap extends between Sta. 0 (stagnation point) and Sta. 18.42; the frustums are defined as follows:

1st between Sta. 18.42 and Sta. 44.84,

2nd between Sta. 44.84 and Sta. 78.89,

3rd between Sta. 78.89 and Sta. 112.84,

4th between Sta. 112.84 and Sta. 146.81.

Heating and ablation data on R/V 422 (Missile 76D) were not obtained due to loss of intelligible telemetry data at the beginning of re-entry fade. The vehicle was not recovered. On vehicle No. 421 (Missile 66D) re-entry heating and ablation data objectives were partially satisfied. Final ablation depths were received after re-entry fade. The vehicle was not recovered.

On vehicle No. 423 (Missile 71D) re-entry heating and ablation data objectives were satisfied. Post-flight inspection and analysis of the recovered vehicle together with telemetered data permitted GE to effect a thorough study of re-entry thermodynamic phenomena and of the adequacy of the ablative materials employed.

Re-entry vehicles No. 421 and 423 (Missiles 66D and 71D, respectively) were thermally protected by ablative materials developed and produced by General Electric and distributed over the vehicles' exposed area as follows:

Nose cap - GE Type 123, pigmented-opaque;

1st frustum - GE Type 124, pigmented-opaque;

2nd frustum to Sta. 68.89 GE Type 125 clear,

remainder of 2nd frustum GE Type 525 opaque;

3rd frustum - GE Type 125 clear;

4th frustum - GE Type 124 clear.

The thorough analysis performed by GE and presented in the form of numerous graphs is too extensive and beyond the scope of this report. Conclusions of the analyses for vehicles 421 and 423 by General Electric are summarized as follows:

> The thermal shields of the vehicles adequately protected the structural and equipment components from excessive temperatures during the critical phases of re-entry flight. The maximum internal temperatures reached by vehicles No. 421 and 423 were 90 and 100°F, respectively, well below the maximum allowable of 350°F.
>
> Ablation sensors measured greater shield degradation depths than anticipated, particularly on the nose cap of both R/V 421 and 423.
>
> On R/V 423, degradation of the GE-series material on the skirt regions was comparable to what would be predicted for phenolic nylon. Performance results of the heat shields were approximately simulated by a computer program in an analogue solution.
>
> Transmission of radiative energy through the transparent GE material was found to be negligible on the skirt region of R/V 423.

INSTRUMENTATION

The RVX-2A instrumentation subsystem provides data on the operation of the vehicle throughout the flight. The outputs of the sensing elements measuring all significant parameters, as well as the outputs of subsystem operation monitors, are converted and transmitted by two FM/FM VHF transmitters. The instrumentation subsystem uses thirteen subcarrier oscillators (SCO) and a 52.5 kc reference oscillator. Five of the SCO's are translator-type assemblies. Two 8-watt, phase-modulated transmitters are used; one operating at a frequency of 244.3 mc transmits real-time data from range zero to impact; the other, transmitting at a frequency of 237.8 mc, continuously plays back the mixed SCO signal from a storage recorder. The storage recorder is of the continuous-loop type with a time delay of 40 seconds. The recording and erasing heads of the storage recorder are de-energized during re-entry when the decreasing deceleration reaches 25g. This makes possible the playback of data recorded during the period of telemetry blackout due to ionization of the air flow enveloping the vehicle.

The recorded re-entry data is also available on the recorder magnetic tape after recovery. Re-entry vehicle No. 423 (71D) incorporated a second recorder as a backup unit, for the purpose of retaining the re-entry data.

A flight programmer is used to switch the accelerometers and rate gyros from fine to coarse ranges during re-entry in order to obtain as much data as possible from the continuous channels at the highest attainable accuracy. The programmer also switches the motion sensors back to fine range during the final phase of re-entry, de-energizes the recorder erasing and recording heads and starts a 65 second timer which arms an impact switch. Power to the instrumentation subsystem is interrupted at impact by actuation of the impact switch, thus providing impact data as a positive loss of signal. This impact cutoff switch was not included in the programmer functions of R/V 423 (Missile 71D).

Instrumentation Sensors

The opening and closing of printed circuits was employed on R/V 421 (66D) for measuring depth of ablation, or thermal shield degradation.

Circuits imbedded at different depths in the ablation material provided step voltages as different circuits were broken due to ablation. On R/V 423 a different type of degradation sensor was employed in the nose cap to overcome the excessive ablation caused by the bonding of sensing elements. Holes were drilled from the inside surface of the nose cap, at different depths. Some of these holes were connected to pressure sensing elements by means of teflon tubing. When ablation of the nose cap heat shield reached the depth of one of these holes, the value of pressure initially read (the re-entry vehicle internal ambient pressure,) changed to the value of the external pressure. The time at which a pressure change was sensed for a particular pressure measurement indicated the time at which a definite depth of ablation was reached.

Other holes were fitted with "make-break" type ablation sensors, each having only one depth of wire, which produce a single voltage step for each depth.

The sensing elements employed on RVX-2A vehicles are as follows:

1. Shield Temperature Sensors: Intra-plastic shield temperature sensors with ranges of either 500 to 1,500°R or 500 to 2,000°R were used.

2. Temperature Sensing Elements: Calorimeters were employed in different locations of the vehicle for measuring wake heating flux to the afterbody at several radial stations.

3. Liner Compartment and Aft Ring Temperature Sensors: These were thermistors with nominal temperature ranges of 32 to 300°F. The sensing element is a ceramic bead whose resistance varies inversely with temperature. These units were fitted by means of brackets, in contact with the area to be studied.

4. Transmissibility Plugs: These plugs, made of transparent shield material, were installed for the purpose of determining the transmissibility of radiative energy through re-entry vehicle shield material and were placed at points of comparable heat flux.

5. Surface Temperature Sensors: R/V 423 had surface temperature sensors installed in the heat shield at selected depths to measure ablation temperature. A thermocouple and a breakwire were installed at the same shield depth. The thermocouple read temperature continuously and, when the surface ablated to thermocouple depth, the breakwire opened causing a voltage step. At this time, the thermocouple temperature and the surface temperature coincide.

6. Baroresistors: These sensors consist of a pressure port, made of graphite, connected to a pressure transducer by means of teflon tubing.

7. Acoustic Sensors: Noise sensing devices were installed on the aft ring of RVX-2A vehicles. Two independent filtering systems separated high frequency from low frequency noise. The amplitude range of these sensors and associated circuit is 120 to 160 db with a sampling rate of 600 per minute.

8. Motion Sensing Elements: In addition to the instrumentation described above, RVX-2A vehicles carried motion sensing elements in the form of rate gyros and accelerometers to gather data on the aerodynamic performance of the vehicle through the analysis of motions during free flight through the atmosphere.

AERODYNAMIC ANALYSIS

The analysis of aerodynamic performance is based on accelerometer and rate gyro data. These instruments provide acceleration and motion rate histories in terms of real-time.

Pressure data is also obtained in order to verify the distribution of pressure over the re-entry vehicle. All this information is relayed, through the instrumentation telemetry system, to ground stations.

Quality of Motion Analysis

The data obtained from the flight of R/V 421 (66D) was limited due to failure of the playback transmitter and the rate data power supply. The switching of the motion sensors to fine range did not occur because of improper mounting of the programmer.

On vehicle No. 422 (76D), data was obtained until 166,000 feet (t = 1824 seconds). Failure of the inflight disconnect plug to release properly, imparted extraneous motions to the vehicle which reached re-entry with sinusoidal motion rates in pitch and yaw of about 6 to 7 degrees/second. Actual motion data was obtained until 1824 seconds when the telemetry signal was lost. The remaining data for this flight was calculated on the basis of known initial conditions.

Complete acceleration and motion rate histories were obtained during the flight of vehicle No. 423, flown on Missile 71D.

Conditions at the Beginning of Re-Entry

Roll rate was effectively zero. A natural frequency oscillation began, which damped out as peak dynamic pressure was approached. This is considered normal and the effect of oscillations of minor magnitude on the gross motion of the vehicle is negligible.

Pitch and yaw rates exceeded predicted values, although they did not reach magnitudes considered excessive.

The envelopes of pitch and yaw accelerations show converging oscillations which damped out at an altitude of approximately 20,000 ft. The data on R/V 423 (71D) shows consistency with that of R/V 421 (66D). Differences between measured and calculated values are attributable to the choice of initial re-entry parameters in the calculated 3-degree-of-freedom-trajectories.

Angle of attack upon re-entry was derived from measured motion data with the following values:

Vehicle No. 421; 72 degrees at 400,000 ft, with a rate of 0 deg/sec.

Vehicle No. 423; 112 degrees at 310,000 ft, with a rate of -2 deg/sec.

Static pitching moment and normal force coefficients as functions of angle of attack, for vehicles 421 and 423, were very close to predicted values.

Studies of pressure distribution conducted on re-entry vehicles 421 and 423 supported motion instrumentation and calculated data on the determination of R/V angle of attack.

RECOVERY SUBSYSTEM

The recovery subsystem, functionally depicted on Figure 8.1-19, performs the following basic functions:

1. It decelerates the re-entry vehicle from ICBM velocities to about 100 ft/second.
2. It ensures water flotation for a period of up to 36 hours to provide adequate time for recovery.
3. It provides location data and a homing signal to aid recovery.

The sequence of recovery events is programmed by an electro-mechanical timer and associated pyrotechnic and thermal relays. An arming subsystem is activated at an axial acceleration of +5g during powered flight. After an increasing deceleration of 10g is reached during re-entry, a deceleration switch closes several pyrotechnic relays, and the timer circuit starting motor becomes energized. The re-entry vehicle aft face cover is then ejected and a reefed parachute is mortared out of its container. After 3.5 seconds the reefing line is released and the parachute deployed, decelerating the velocity of the vehicle to a descent rate of 100 feet/second. A prima cord is then fired inside the vehicle, freeing the recovery basket from the re-entry vehicle. The basket is attached to the parachute to separate the flotation balloon from the hot surfaces of the R/V. At this time, the SOFAR bomb, radar chaff and aluminum powder are ejected.

The buoyancy of R/V 423 (71D) was improved by addition of foam material in empty areas. After the flotation balloon is inflated its line is lengthened so it can trail above the parachute. Upon immersion of the vehicle into the water, a salt-water-activated battery energizes the SARAH (search and rescue and homing) beacon and the beacon light. Dye marker powder and shark repellent are allowed to dissolve in the water. The second SOFAR bomb sinks to a

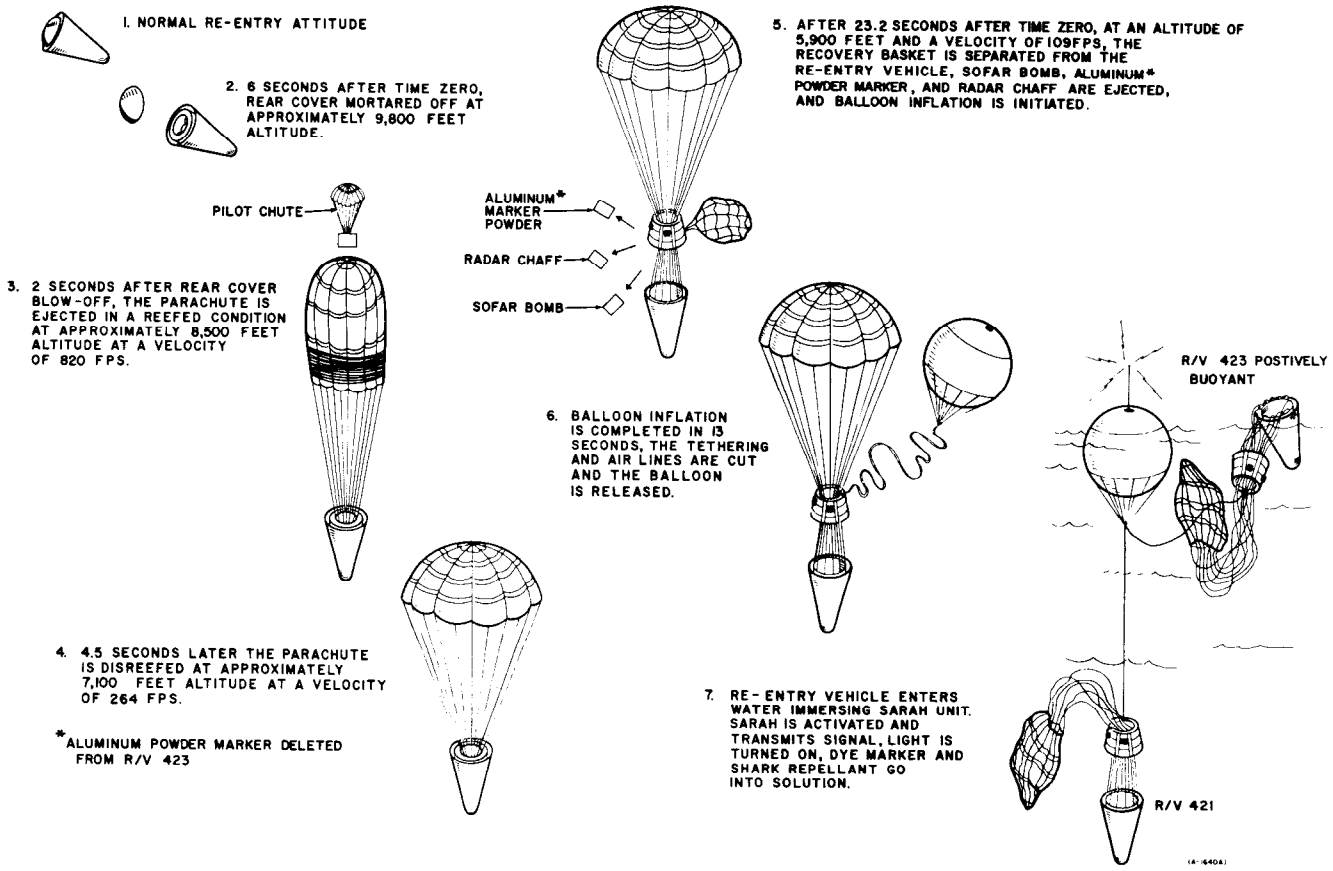

FIGURE 8.1-19 SEQUENCE OF RVX-2A RECOVERY OPERATIONS

selected depth and detonates, providing an acoustical fix. Radar chaff creates a radar image equivalent to that of a large aircraft. The SARAH beacon continually transmits a signal used by the recovery party to "home-in" on the balloon. Location of the R/V is further facilitated by a flashing beacon and dye marker-powder.

RECOVERY SYSTEM PERFORMANCE

Re-entry vehicle No. 421 (Missile 66D): The recovery system accomplished all the operational events up to balloon inflation. A malfunction in the flotation system caused the vehicle to sink making recovery impossible.

Re-entry vehicle No. 422 (Missile 76D): Performance of the recovery system during re-entry is not available due to loss of all telemetry during this period. Ascension Island Mod II radar detected radar chaff at an altitude of 38,000 feet and tracked it, for 28 minutes, to 400 feet. (Normal tracking time for this type of chaff and this altitude should exceed one hour.) The R/V was not recovered.

Re-entry vehicle No. 423 (Missile 71D): All the events in the recovery system operational sequence occurred as planned. The vehicle was recovered within one hour from impact.

SPACE LABORATORY EXPERIMENTS

All three RVX-2A re-entry vehicles carried a series of experiments for the purpose of obtaining a variety of data on the effect of ballistic flight extra-atmospheric environment and re-entry conditions on different test specimens and devices.

Vehicle No. 241 flown by Missile 66D carried 12 experiments from which meaningful data was received for three. Loss of re-entry data and failure to recover the vehicle prevented post flight analysis.

Missile 76D was launched with vehicle No. 242, carrying a total of 12 experiments. Data was gathered only on two of the experiments; most of the others would have required post flight analysis, but the vehicle was not recovered.

Vehicle No. 243 was launched by Missile 71D and carried 14 space laboratory experiments. Data was obtained from 13 of these, the exception being an emulsion package which was missing when the vehicle was recovered.

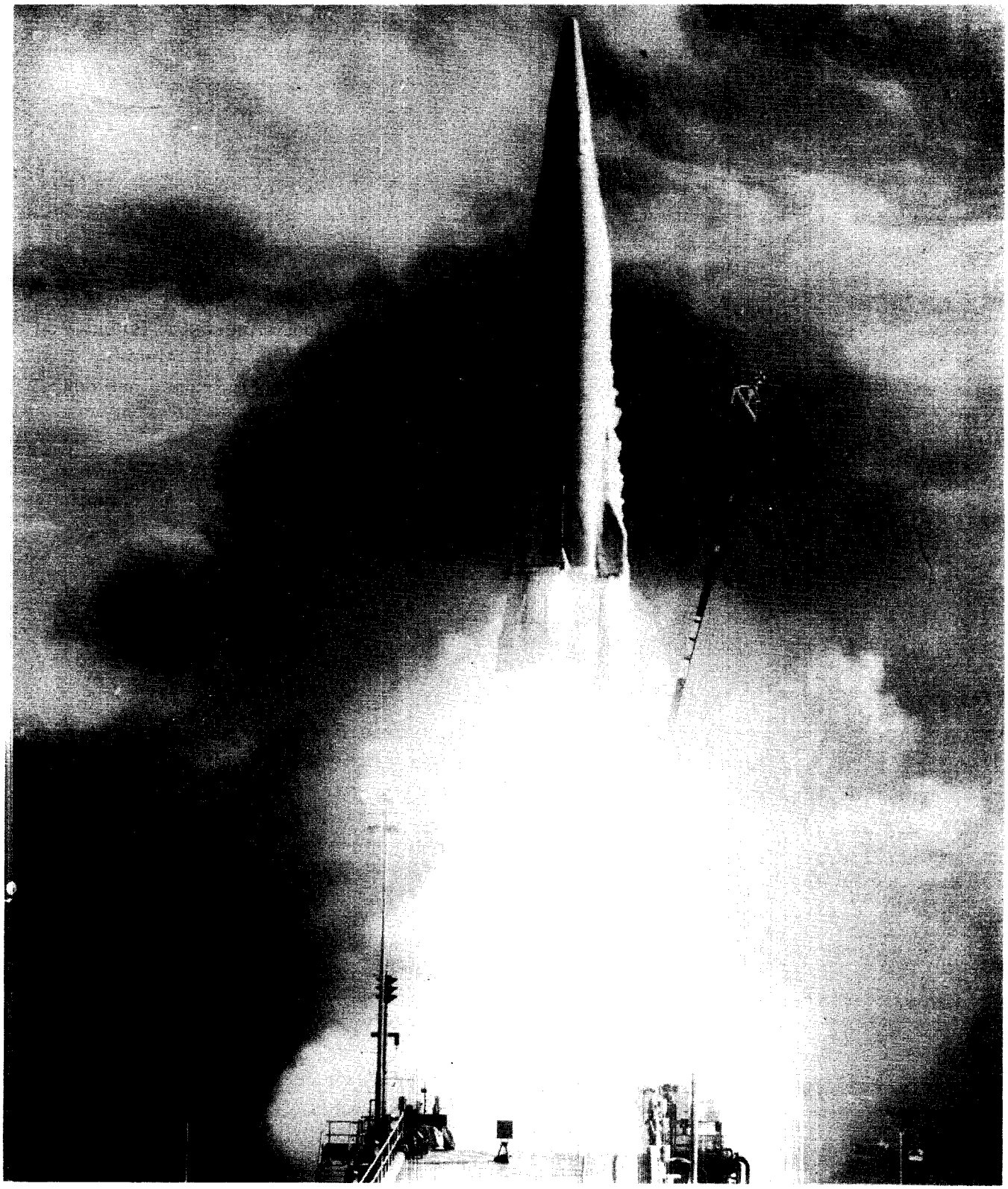

MISSILE 66D, TYPICAL AIG MISSILE WITH RVX-2A RE-ENTRY VEHICLE

SECTION 8.2 - DECOY SYSTEM

PURPOSE OF TESTING

The purpose of the decoy system is to reduce the probability of enemy destruction of the Atlas warhead before it reaches the target. The ADF system is designed to accomplish this by ejection of dummy shapes from the missile after the powered phase of the flight thereby confusing enemy radar detection facilities which would be unable to distinguish these shapes from the warhead re-entry vehicle.

Specific objectives of these flight tests were to demonstrate the performance of the safety, arming and timing system, to demonstrate satisfactory ejection of canisters and inflation of decoy balloons, to investigate decoy pod environmental conditions, and to determine graphite dart and balloon trajectory characteristics.

Aeronutronics is responsible for the evaluation of data gathered on this system.

TEST CONDITIONS

A decoy pod was flown on four of the missiles included in the scope of this report. Missiles 55D, 62D and 83D carried the 4-tube version of the R&D pod as shown in Figure 8.2-1. Launch tubes 1, 3, 6 and 8 were installed, each containing decoys planned for ejection. Tubes 1 and 8 each contained a prototype nosecone balloon and tubes 3 and 6, a graphite dart with arms. Missile 90D carried the Mod I pod shown in Figure 8.2-2 which carried a single launch tube containing a ring-augmented dart.

Instrumentation was provided to monitor system arming steps and programmed functions including tube unlatching, tube orientation, ejection squib firing, canister ejection, and ejection velocities.

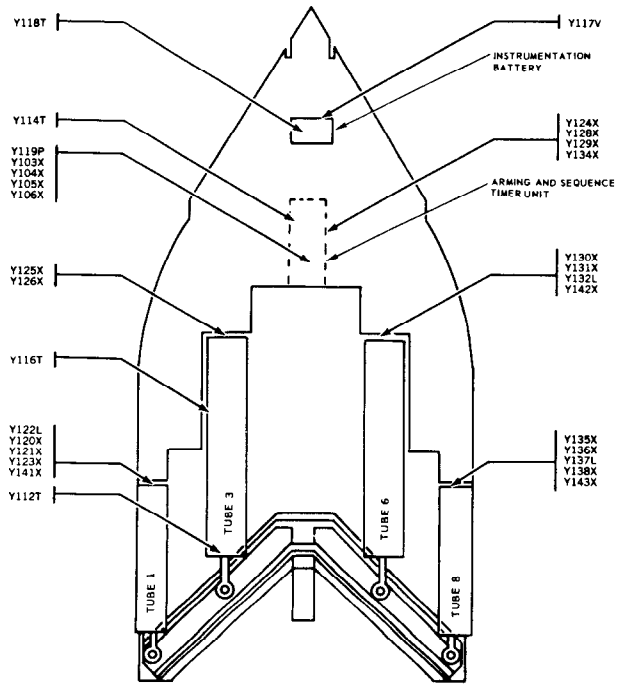

RESEARCH AND DEVELOPMENT INSTALLATION

FIGURE 8.2-1 RESEARCH AND DEVELOPMENT FOUR TUBE DECOY POD

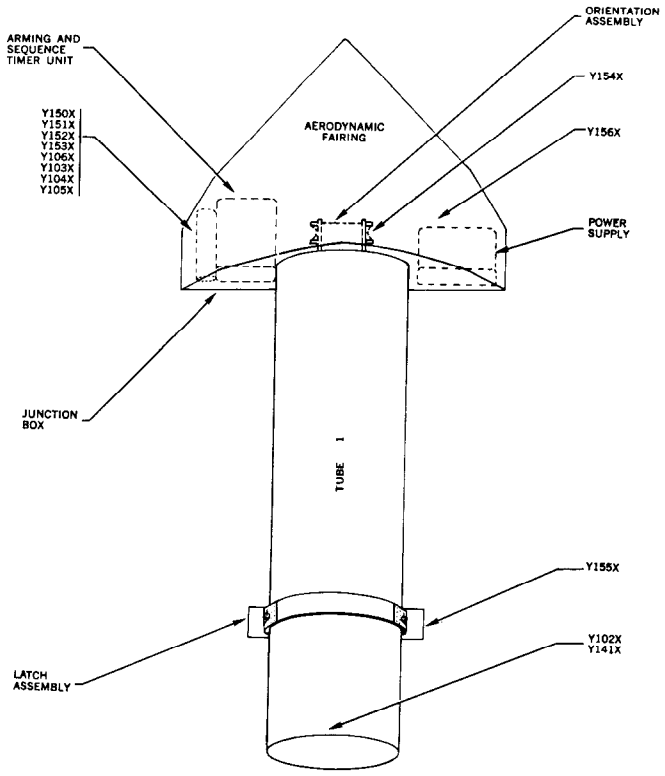

FIGURE 8.2-2 MOD I SINGLE TUBE DECOY POD

TEST RESULTS

Since Aeronutronics is responsible for data evaluation and analysis of the decoy system, the following discussion is intended only as a brief resume of individual flight test results.

Missile 55D

Operation of the decoy system was completely satisfactory. All arming and sequence timer functions were completed within the required time intervals and all four decoys were ejected. Tube unlatch, orientation and canister ejection signals were all generated as programmed. Ejection velocities of 30, 90 and 41 ft/sec were recorded for tubes 1, 6 and 8, respectively.

Missile 62D

Arming and programmed sequence timer outputs were properly generated. However, telemetered data indicated that tubes 1 and 8 did not unlatch and their respective canisters were not ejected. An ejection velocity of 12 ft/sec was recorded for tube 6. Tube 3 ejection was not monitored.

Laboratory tests conducted after the flight indicated that the failure of tubes 1 and 8 was probably due to an interference with the proper action of the pin puller which unlatches the launch tube. Design modifications were effected to prevent a recurrence of the failure.

Missile 83D

No telemetry data were recorded due to a malfunction which prevented activation of the decoy system instrumentation circuits. However, system operation appeared to have been satisfactory in that successful ejection of all four decoys was indicated by disturbances observed in the guidance radar RF link. Decoy ejections were in the proper order and at the programmed times.

The pod instrumentation system power supply was separate from the pod electrical system so that a failure of the former would not preclude proper operation of the latter.

Missile 90D

Operation of the arming and timing unit was satisfactory; however, the telemetry data indicated that the single launch tube did not orient properly and the decoy canister was not ejected. Post-test investigation revealed a possible malfunction of the launch tube latch assembly, resulting in failure to orient the tube properly. Failure to eject the decoy canister was attributed to an open circuit between the timing unit and the ejection mechanism.

SECTION 8.3 - ABORT SENSING AND IMPLEMENTATION SYSTEM

PURPOSE OF TESTING

The Project Mercury abort sensing and implementation system (ASIS) was tested in open-loop configuration in a continuing effort to insure highly reliable system operational capability when installed on the missiles assigned to the Project Mercury mission. In support of this objective, data was obtained on the performance of sensors proposed for the Project Mercury ASIS and installed on five Series D R&D missiles. These sensors monitored various critical parameters of Atlas Systems performance.

TEST CONDITIONS

The function of the ASIS is to sense the development of critical malfunctions in the Mercury/Atlas booster, and generate an "Abort Command" which activates the Mercury capsule escape system prior to the time the capsule occupant would be placed in jeopardy.

In operation, correct performance of Atlas systems permits a redundant 23 vdc signal to reach the capsule. A failure in any system monitored by ASIS results in loss of the 23 vdc signals to the capsule and activation of the capsule abort system. The system is enabled from 2-inch motion to sustainer/vernier cutoff.

The ASIS is designed to monitor the over-all Atlas flight performance through selected points in five missile subsystems as follows:

1. Flight Control System

   (a) Pitch, yaw and roll rates;

2. Tank Pressurization System

   (a) Liquid oxygen tank pressure

   (b) Differential pressure across the intermediate bulkhead;

3. Propulsion System

   (a) Sustainer and booster engine fuel injection manifold pressures;

4. Hydraulic System

   (a) Sustainer engine controls hydraulic pressure;

5. Electrical System

   (a) 115-volt, 400-cps voltage

   (b) Atlas/Capsule interface continuity.

The respective abort levels for Project Mercury Atlas boosters are as follows.

Pitch, Yaw and Roll Rates

During the interval when the flight control system is operating (2-inch motion to sustainer cutoff) the rate gyro outputs are monitored through a single section linear first-order lag filter, with a time constant of 225 $^{+50}_{-25}$ milliseconds. Pitch and yaw rates exceeding 3.0 ±0.15 deg/sec and roll rates greater than 6.4 ±0.3 deg/sec will cause an abort signal to be initiated, except during the period of Atlas booster engine cutoff plus 30 ±0.5 seconds. During this interval, the pitch and yaw rate thresholds are doubled (±12.5%) in order to prevent activation of the capsule escape system due to possible excessive but not hazardous Atlas booster staging transients.

To insure that missile stability will be monitored at all times, a backup rate gyro package is installed to also sense missile rates in three axes. Pitch and yaw rates as monitored by this redundant "backup" gyro group, exceeding 4.75 ±0.25 deg/sec and roll rates greater than 9.4 ±0.40 deg/sec will cause an abort signal to be initiated. The redundant pitch and yaw rate gyro thresholds are also doubled during the Atlas booster staging interval. A single section linear first-order lag filter with a time constant of 80 ±20 milliseconds is used in the sensor system for this set of gyros.

Liquid Oxygen Tank Pressure

During Atlas booster phase, lox tank pressure must remain above 21.5 ±0.5 psig to support the capsule under Atlas booster accelerations and maximum aerodynamic loading. During sustainer stage, the abort level is 11.0 ±0.5 psig. It is noted that, on a normal flight the lox tank pressure will always be greater than 21.5 psig although it is unnecessary to maintain this pressure after booster cutoff for structural integrity. The abort level of 11.0 ±0.5 psig was chosen to prevent an inadvertent abort due to a non-hazardous malfunction after staging.

Differential Pressure Across Intermediate Bulkhead

The pressure differential required to avoid reversal of the liquid oxygen tank/fuel tank intermediate bulkhead should not fall below 2.5 ±0.5 psid during Atlas flight. During six of the seven flights with the ASIS system installed, the differential pressure switches were set to abort at 4.0 ±0.5 psid. As a result of testing, the value was determined to be conservative and was changed to the lower value of 2.5 ±0.5 for future flights. Refer to Table 8.3-1. On Missiles 62D and 79D, oscillations were noted in the Δp measurement beginning at liftoff, a pneumatic filter was added to the Δp sensor plumbing.

TABLE 8.3-1 SUMMARY OF ASIS PERFORMANCE

MISSILE NO.		56D	62D	50D	32D	79D	55D	67D
FLIGHT DATE		5-20-60	6-22-60	7-29-60	8-9-60	9-19-60	10-22-60	2-21-61
CANISTER SERIAL NUMBER		-	-	005-0004	3	006-0006(8)	-	006-0005
CLOSED-LOOP		No	No	No	No	No	No	Yes
ABORT GENERATED DURING FLIGHT		Yes	Yes (Δ P)	Yes (Elec)	No	Yes (Δ P)	No	No
SYSTEM PERFORMANCE		Marginal	Satisfactory	Satisfactory	Satisfactory	Satisfactory	Satisfactory	Satisfactory
ABORT SYSTEM PARAMETERS AND PERFORMANCE								
Pitch Rate Abort Criteria		NA	NA				NA	
Primary (Prior to Staging/During Staging/Post Staging)	(deg/sec)			3.0/6.0/3.0	3.0/6.0/3.0	3.0/6.0/3.0		6.0/6.0/6.0
Backup (Prior to Staging/During Staging/Post Staging)	(deg/sec)			4.75/9.5/4.75	4.75/9.5/4.75	NA		9.5/9.5/9.5
Actual Maximum Recorded Pitch Rate (Primary/Backup)	(deg/sec)			0.6/2.0 at 0.5 cps	2.9/NI at 0.65 cps	3.2/NA @ 0.8 cps		2.9/3.1 at 1 cps
Required Rate to Provide Abort (Including Time Constants) (2)	(deg/sec)			3.55-3.95/4.85-5.0	3.88-4.48/4.94-5.17	4.23-5.08/NA		9.6-12.0/10.2-11.2
Yaw Rate Abort Criteria		NA	NA				NA	
Primary (Prior to Staging/During Staging/Post Staging)	(deg/sec)			3.0/6.0/3.0	3.0/6.0/3.0	3.0/6.0/3.0		6.0/6.0/6.0
Backup (Prior to Staging/During Staging/Post Staging)	(deg/sec)			4.75/9.5/4.75	4.75/9.5/4.75	NA		9.5/9.5/9.5
Actual Maximum Recorded Yaw Rate (Primary/Backup)	(deg/sec)			1.1/1.3 at 0.5 cps	2.9/NI at 0.65 cps	5.9/NA @ 8 cps**		2.4/2.4 @ 1 cps
Required Rate to Provide Abort (Including Time Constants) (2)	(deg/sec)			3.55-3.95/4.85-5.0	3.88-4.48/4.94-5.17	4.23-5.08/NA		9.6-12.0/10.2-11.2
Roll Rate Abort Criteria		NA	NA					
Primary	(deg/sec)			5.7	5.7	5.7		6.4
Backup	(deg/sec)			7.0	7.0	NA		9.4
Actual Maximum Recorded Roll Rate (Primary/Backup)	(deg/sec)			4.9/7.0 at 1.6 cps	3.1/NI at 1.5 cps	5.0/NA @ 5 cps		6.8/6.9 @ 1 cps
Required Rate to Provide Abort (Including Time Constants) (2)	(deg/sec)			12.8-16.5/8.15-9.65	12.1-15.6/8.05-9.4	6.75-7.5/NA		10.2-12.8/10.1-11.1
Lox Tank Pressure Abort Level (Prior to Staging/After Staging)	(psig)	21.5/11.0	21.5/11.0	21.5/11.0	21.5/11.0	21.5/11.0	21.5/11.0	21.5/11.0
Actual Minimum Lox Tank Pressure (Prior to Staging/Atlas Staging)	(psig)	24.0(A)/21.8(A,	25.0/22.3	26/NA	25/22.5	25.0/23.0	25.5/23.5	ND/23.3
Lox/Fuel Tank Δ Pressure Abort Level	(psid)	4.0	4.0	4.0	4.0	4.0	4.0	2.5
Actual Minimum Measured Lox/Fuel Δ P Level (Standard/Backup)	(psid)	10.0/NA	6.5/NA(A)	8/NA	6/NA	7.5/NA(A)	8/NA	6.9/11.0
Booster Fuel Manifold Pressure Abort Level*	(psia)	470	470	470	470	470(1)	470	470
Actual Minimum B Thrust Chamber Pressure, B1/B2	(psia)	542/558	547/540	545/555	542/544	540/538	552/558	544/544
Sustainer Fuel Manifold Pressure Abort Level*	(psia)	560	560	560	560	560	560(1)	560
Actual Minimum S Thrust Chamber Pressure	(psia)	684	640	690	650	641	660	665
Sustainer Hydraulic Pressure Abort Level	(psia)	2,000	2,000	2,000	2,000	2,000	2,000	2,000
Actual Minimum Sustainer Hydraulic Pressure	(psia)	3,050(A)	3,050(1)	3,100	3,000	3,100	3,100	3,100
Phase A 400 cps Voltage Abort Level	volts	NA	80 ± 10	80 ± 10	80 ± 10	80 ± 10	NA	80 ± 10
Measured Phase A 400 cps Voltage	volts		113.3	Below 110(A)	114.4	114.5		115

NOTES:

* Not directly instrumented, however chamber pressures are good indications of actual manifold pressure

** Data recorded during staging

NI Not Instrumented

NA Not Applicable

ND No Data

(A) Abort signal from the given parameter (see text)

(AP) Possible Abort - Data inconclusive

(1) See text for description of missiles

(2) Since the data is presented for a given frequency the abort limits have been calculated using filter attenuation at this frequency. The data is present primary/backup with the range (filter range).

Fuel Injection Manifold Pressures

Pressure sensor monitoring of the booster and sustainer fuel injection manifold pressures allows detection of abnormal engine performance. These sensors are set at 470 ±10 psia for the booster engines and 560 ±10 psia for the sustainer engine. The actual manifold pressures are not normally monitored during flight. These pressures are reflected in the chamber pressure measurements for sensor evaluation. A level of 355 psia in the B1 and B2 thrust chambers is equivalent to a normal pressure in the manifold. An equivalent sustainer chamber pressure is 445 psia.

Sustainer Engine Controls Hydraulic Pressure

The pressure must remain above 2,000 ±40 psia to provide a safe pressure for engine gimbaling and for valve closure to shut down the sustainer and vernier engines.

Electrical System A-C Phase A Voltage

This sensor monitors the 115-volt, 400-cycle Phase A inverter output and is set to generate an "Abort Command" when the voltage drops below 80 ±10 vac (rms).

Loss of Atlas/Capsule Interface Continuity

Should continuity of the redundant 23-volt "hot wire" between the capsule and booster vehicle be broken during flight, the ASIS will sense an abort condition and cause automatic activation of the capsule escape system.

For system reliability, the ASIS is designed with parallel circuitry for each pressure sensor with the exception of the lox tank pressure sensor that is used after booster cutoff.

Instrumentation is provided such that the origin of an abort signal and the reliability of the vernier components may be determined. Telemetered signals from the pressure switch instrumentation have four levels of approximately 0, 40, 80, and 100% of bandwidth indicating, respectively, normal operation, one sensor in abort condition, the sensor is parallel in abort condition, and both sensors in an abort condition. Both sensors must indicate an abort condition before the capsule is aborted.

During the test program reported here, two missiles (32D and 79D) were flown with the complete ASIS configuration (open-loop) except that the backup rate gyro package was not installed on Missile 79D. Missiles 55D and 56D were flown with only the pressure switches installed. Missile 62D was flown without the excessive rate ("over-rate") threshold detectors. For continuity purposes the discussion which follows also includes an analysis of the performance of the ASIS installed aboard Project Mercury Atlas boosters 50D and 67D.

Missile 50D was flown with the complete system in the open-loop configuration. Missile 67D was flown with the system in the closed-loop configuration for the first time. Figure 8.3-1 is a functional block diagram of the Project Mercury abort sensing and implementation system.

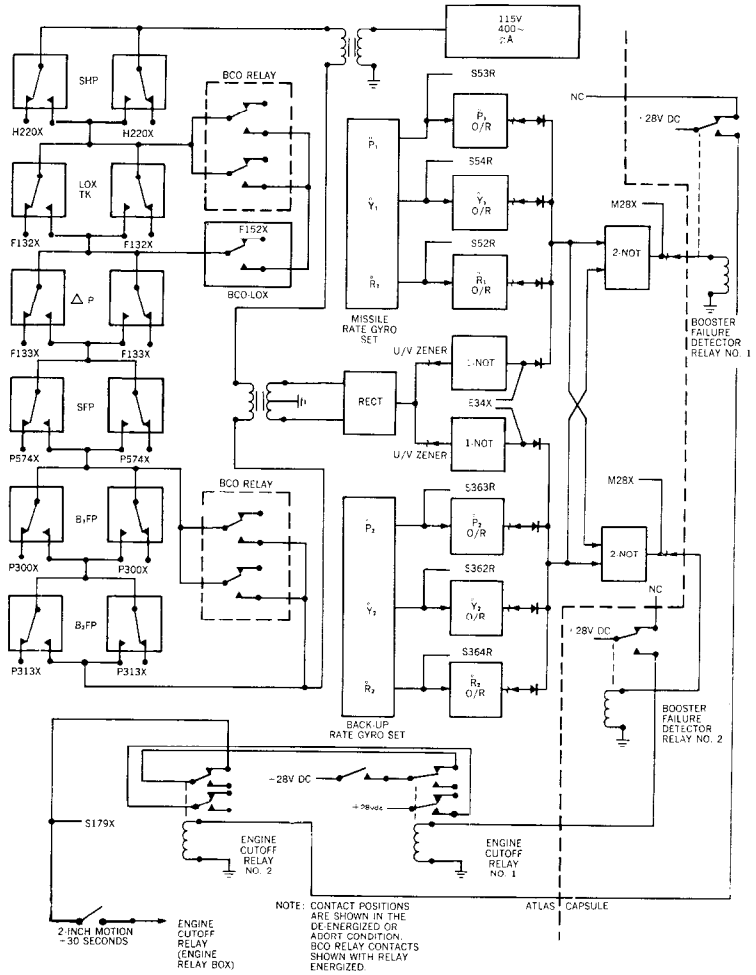

FIGURE 8.3-1 ABORT SENSING AND IMPLEMENTATION SYSTEM

TEST RESULTS

The ASIS configuration, as carried on the five Series D R&D flight vehicles (See Test Conditions), performed satisfactorily. Abort parameters were not exceeded and with the exceptions noted below, no abort conditions were indicated by ASIS sensors during powered flight.

For the two Atlas/Mercury Missiles, 50D and 67D, flown during the test series discussed in this report, the ASIS was installed in the open and closed-loop configuration, respectively. The open-loop ASIS performed satisfactorily during the Missile 50D flight which culminated at 58.995 seconds with loss of Atlas telemetry and destruction of the Atlas booster. The abort system signal (M28X) was generated between 57.56 and 57.66 seconds, a minimum of 1.335 seconds before missile destruction, based upon loss of 400-cycle a-c voltage to ASIS. The abort signal was generated in adequate time for capsule escape to be effected prior to development of a condition which would have been hazardous to the capsule occupant.

The ASIS, operating closed-loop for the first time during the successful flight of Missile 67D, performed satisfactorily. No abort conditions were present and no abort command was generated during powered flight. System readiness was demonstrated by post-sustainer cutoff abort commands when the sustainer fuel injection pressure and the sustainer hydraulic pressure decayed below their abort levels.

Data, pertinent to the ASIS, obtained from the seven aforementioned Series D flights are summarized in Table 8.3-1. Also included are the abort levels for all ASIS parameters. It is noted that the abort system parameters were changed for Missile 67D flight. Specifically, the pitch and yaw over-ride levels for the pre-staging and post-staging phases were doubled. The change was accomplished to prevent a unintentional abort in the event the dynamics of

the Atlas/Mercury configuration was not as expected. A primary objective of this flight was to determine the actual dynamic characteristics of this vehicle.

The following is a discussion of ASIS sensors performance, by systems monitored for the five applicable Series D R&D missiles (56D, 62D, 32D, 79D and 55D).

Flight Control System - Rate Gyro Outputs

One Series D R&D flight missile (32D) carried the ASIS excessive ("over-rate") pitch, yaw and roll rate detectors. No over-rate conditions existed at any time during this flight. Maximum pitch, yaw and roll rates were considerably less than that required to cause abort and the ASIS over-rate gyro detectors performed satisfactorily. No abort signals were generated during powered flight.

Tank Pressurization System - Lox Tank Pressure

The pressure switches that monitor lox tank pressure performed satisfactorily on four of the five Series D R&D flight vehicles on which these switches were installed. During the flight of Missile 56D, the two lox tank pressure monitor switches (the pre- and post-staging switches) both indicated an abort condition, although analog measurements of pressures which activate these switches indicated proper tank pressure levels throughout flight. A subsequent investigation of Missiles 53D and 62D at AMR disclosed that the atmospheric pressure sensing ports on these transducers were inadvertently left capped for missile flight. Laboratory tests of pressure switches with these ports capped indicated this condition probably occurred on Missile 56D and caused activation of the switches. In effect, capping off the atmospheric sensing line biases the tank pressure sensors causing the pressure switches to sense and activate at pressures somewhat higher than the normal setting.

Tank Pressurization System - Intermediate Bulkhead Differential Pressure

The switches which monitor the differential pressure across the lox tank/fuel tank intermediate bulkhead were installed on five Series D R&D missiles. Switch operation was proper on three of these five flights. During the flights of Missiles 62D and 79D, these switches indicated erroneous abort conditions. The analog measurement of the pressure which activates these switches indicated a non-critical condition. This condition was resolved to be the result of a momentary pressure surge resulting from lox being forced into the sensing

UNCLASSIFIED

line at liftoff and flashing into vapor as a result of contact with the relatively warmer sensing line. A modification was satisfactorily accomplished on Atlas/Mercury Missiles 50D and 67D. The abort signals were being sensed by an incompatible sensing technique; the sensing line being in common with the propellant utilization manometer line. Consequently, the modification effected included installations of a separate boss (at Station 937) and a sensing line independent of the PU system, incorporating a high rate bubbler, to sense pressure for the differential pressure switch.

The oscillations noted in the Δp measurements, at liftoff, which were a contributing factor to the abort signals generated on Missiles 62D and 79D, were attenuated on Missile 67D by the addition of a pneumatic filter in the lox sensing line. The Δp on Missile 67D was monitored by two transducers, one filtered and the other unfiltered. The results indicated that the filter attenuated the oscillation from 8 psi peak-to-peak unfiltered to 2 psi filtered. The abort switches are installed in the filter section of the plumbing.

Propulsion System-Fuel Injection Manifold Pressures

Proper operation of the fuel injection pressure switches was indicated on all but one of the five Series D R&D missiles on which these switches were installed. Erratic operation of the B1 fuel injection pressure switch No. 2 was noted in the telemetered data during the booster phase of Missile 79D flight. Booster engine performance was normal during the flight. Intermittent shorting within the switch instrumentation is believed to have caused this anomaly. Investigation revealed that moisture in the system resulting from weather condition existing at AMR prior to launching Missile 79D was the source of the trouble.

Hydraulic System - Sustainer Engine Controls Hydraulic Pressures

Erroneous activation of the dual sustainer hydraulic pressure switch occurred at 207 seconds during the flight of Missile 56D. Normal pressure levels were indicated by the analog measurement of the pressure which activates this switch. Proper switch operation was noted throughout powered flight on the remaining four Series D R&D missiles flown with the switch aboard. The cause of the anomaly on Missile 56D was resolved to be a configuration problem peculiar to Missile 56D. The sensing lines to the pressure switch were attached to the sustainer gas generator lox line at three points. It is believed that, due to the close proximity of lox, this caused freezing of the hydraulic oil in the sensing line which subsequently lowered the pressure in the line and caused an erroneous activation. Under a normal Mercury configuration, the sensing line to the pressure switch is routed differently and redundancy in switches and corresponding lines is provided.

UNCLASSIFIED

After sustainer cutoff, when sustainer hydraulic pressure decays below 2,000 psig, an abort condition should be indicated by the dual sustainer hydraulic pressure switch during normal switch operation. (This does not abort the capsule because the system is deactivated at SCO.) During the flight of Missile 62D, the sustainer hydraulic pump discharge switch indicated an abort condition. The remaining switch of this parallel pair, which is sensed at the sustainer hydraulic high pressure manifold, did not go to the abort condition until 453 seconds. (Sustainer cutoff occurred at 284.26 seconds.) It is believed that the vernier lox tank pressure transducer sensing line, which is clamped to the sensing line of the switch which failed to operate properly, may have had a minor leak thereby chilling the pressure switch sensing line through the metal to metal clamp, permitting the oil to freeze locally and block the line. Leakage of oil past the block or sudden collapse of the block would permit pressure decay and eventual activation of the switch. To prevent recurrence of this incident the sensing lines and clamps associated with the hydraulic pressure switches will be insulated on all missiles equipped with ASIS.

Electrical System

The electrical system a-c Phase A source voltage was monitored on 3 Series D R&D flight articles. (See Table 8.3-1.) Voltage levels did not fall below the abort level of 80 ±10 volts rms and, properly, no signal was initiated for activation of the capsule escape system as a direct result of a-c low voltage. However, as a consequence of the spurious differential pressure abort signal experience during the flight of Missile 79D (discussed previously under Tank Pressurization System) the a-c low voltage signal, as well as the abort system signal and the booster abort ready signal, indicated abort conditions at liftoff, as expected.

[redacted]

UNCLASSIFIED

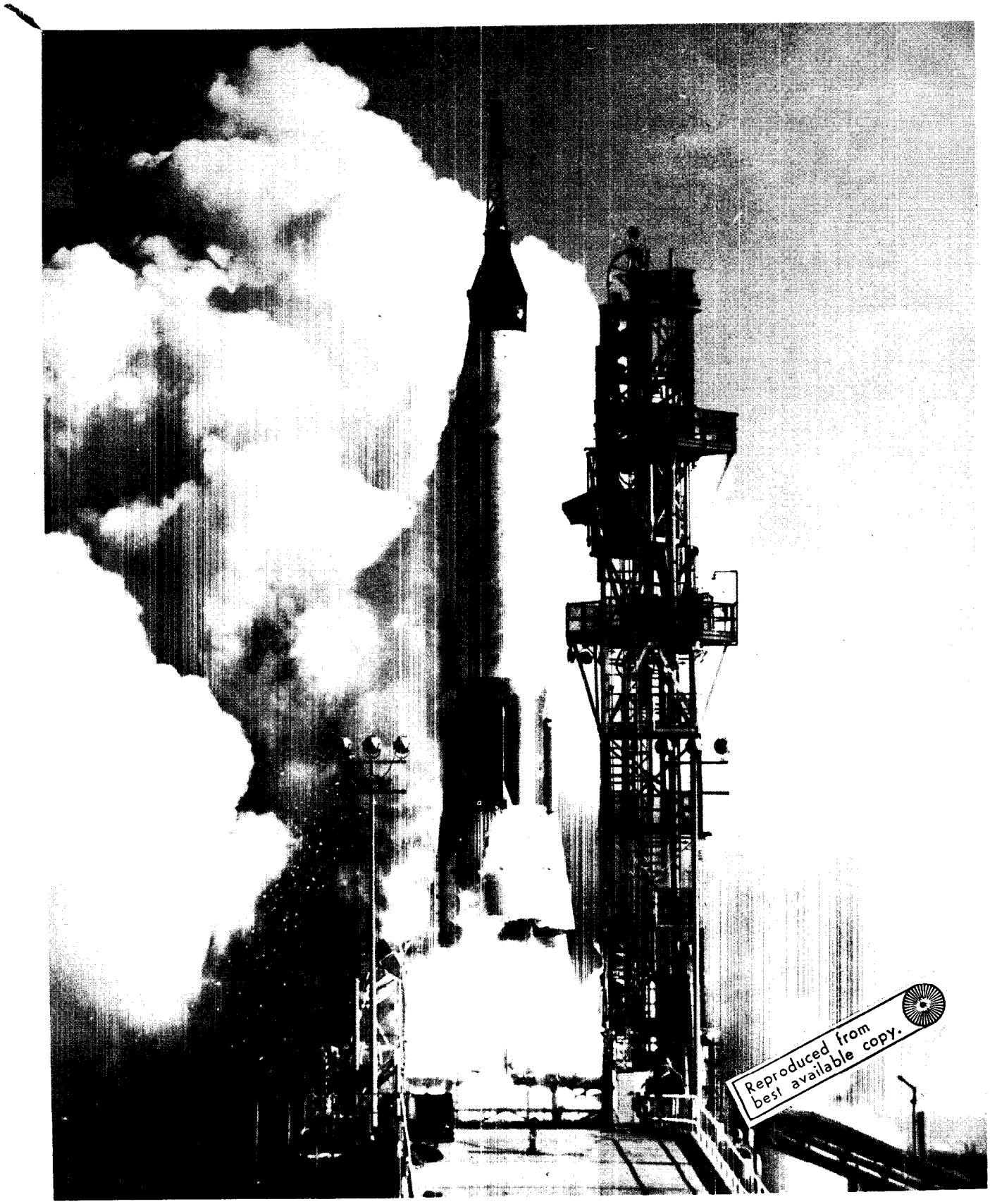

MISSILE 67D, ASSIGNED TO PROJECT MERCURY

[redacted] UNCLASSIFIED